bulletin 22

state-of-art report

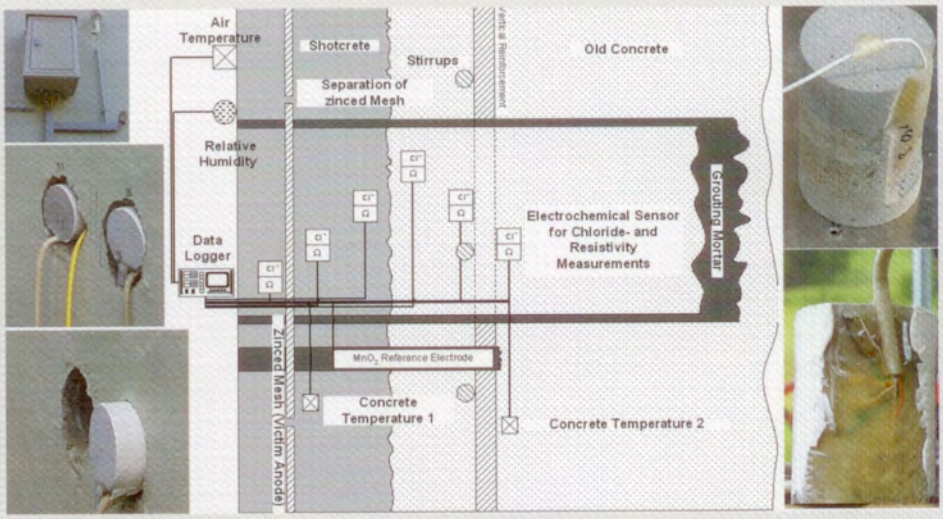

Monitoring and safety evaluation of existing concrete structures

Monitoring and safety evaluation of existing concrete structures

State-of-art report prepared by

Task Group 5.1

March 2003

Subject to priorities defined by the Steering Committee and the Praesidium, the results of *fib*'s work in Commissions and Task Groups are published in a continuously numbered series of technical publications called 'Bulletins'. The following categories are used:

category	minimum approval procedure required prior to publication
Technical Report	approved by a Task Group and the Chairpersons of the Commission
State-of-Art report	approved by a Commission
Manual or Guide (to good practice)	approved by the Steering Committee of *fib* or its Publication Board
Recommendation	approved by the Council of *fib*
Model Code	approved by the General Assembly of *fib*

Any publication not having met the above requirements will be clearly identified as preliminary draft.

This Bulletin N° 22 has been approved as a *fib* State-of-art report in autumn 2002 by *fib* Commission 5 *Structural service life aspects*

The report was drafted by *fib* Task Group 5.1 *Monitoring and safety evaluation of existing concrete structures*:

Konrad Bergmeister (Convenor, Austria)
A. Emin Aktan (USA), Christian Bucher (Germany), Luis Dorfmann (Austria), Ekkehard Fehling (Austria), Rudolf P. Frey (Switzerland), Roman Geier (Austria), Olaf Huth (Switzerland), Daniele Inaudi (Switzerland), Johannes E. Maier (Switzerland), Ulrich Santa (Austria), Peter Schwesinger (Germany), Volker Slowik (Germany), Helmut Wenzel (Austria)

Full affiliation details of Task Groups members may be found in the *fib* Directory or on *fib's* website http://fib.epfl.ch.

In addition to the above, the following contributed to chapter 11: Annex (case studies) :
F. N. Catbas, Vladimir Cervenka, James M. Cutts, J. Degrieck, G. De Roeck, W. De Waele, Eva M. Eichinger, Branko Glisic, K. A. Grimmelsman, S. Jacobs, Johann Kolleger, Stijn Matthys, W. Moerman, Drahomir Novak, Jerome P. O'Connor, Carlton A. Olson, M. Pervizpour, Radomir Pukl, Benny Raphael, Yvan Robert-Nicoud, Ian F. C. Smith, Alfred Strauss, Luc Taerwe, Samuel Vurpillot, Gregory R. Yates

Cover picture: Corrosion sensor unit developed by Zimmermann, Schiegg, Elsener and Böhni

First published 2003 by the International Federation for Structural Concrete (*fib*)
Post address: Case Postale 88, CH-1015 Lausanne, Switzerland
Street address: Federal Institute of Technology Lausanne - EPFL, Département Génie Civil
Tel +41 21 693 2747, Fax +41 21 693 5884, E-mail fib@epfl.ch, web http://fib.epfl.ch

ISSN 1562-3610
ISBN 2-88394-062-2

Printed by Sprint-Digital-Druck Stuttgart

Preface

The condition assessment of aged structures is becoming a more and more important issue for civil infrastructure management systems. The continued use of existing systems is, due to environmental, economical and socio-political assets, of great significance growing larger every year. Thus the extent of necessary repair of damaged reinforced concrete structures is of major concern in most countries today. Monitoring techniques may have a decisive input to limit expenditures for maintenance and repair of existing structures.

Modern test and measurement methods as well as computational mechanics open the door for a wide variety of monitoring applications. The need for quantitative and qualitative knowledge has led to the development and improvement of surveillance techniques, which already have found successful application in other disciplines such as medicine, physics and chemistry. The design of experimental test and measurement systems is inherently an interdisciplinary activity. The specification of the instrumentation to measure the structural response will involve the skills of civil engineers, electrical and computer engineers.

The main aim of *fib* Commission 5 is to provide a rational procedure to obtain an optimal technical-economic performance of concrete structures in service and to ensure a feedback of experience gained to design, execution, maintenance and rehabilitation. Against this background *fib* Task Group 5.1 "Monitoring and Safety Evaluation of Existing Concrete Structures" had been established to evaluate worldwide the existing practice.

The objective of this state-of-art report is to summarize the most important inspection and measuring methods, to describe the working process and to evaluate the applicability to structural monitoring. Particular emphasis is placed upon non-destructive systems, lifetime monitoring, data evaluation and safety aspects.

Thanks are due to the contributing members of the task group and to a lot of researchers around the world in this field. Special thanks go to Ulrich Santa and Claudia Honeger, who did the tremendous work of assembling the various papers and examples.

Konrad Bergmeister
Convenor *fib* TG 5.1

January 2003

Steen Rostam
Chairman *fib* Commission 5

Contents

1 Introduction to monitoring concepts and safety evaluation of existing concrete structures

The stock of structures such as bridges, tunnels, retaining walls, and many others has been accumulating in developed countries over the years of civilization, especially in the last decades of our century. Despite the many years of maintenance-free operation, the inherent level of safety of many in-service structures can be shown to be inadequate relative to current design documents. Owners and maintenance authorities are therefore in a difficult position in a world where public safety is paramount and the financial and other consequences of failure are great. So far, the most commonly applied concept of maintenance includes the periodical inspection, which usually starts with a visual inspection. One main scope of this report is to focus on methods and techniques for monitoring with instruments that can be used with a high degree of automation. Modern transducer and information technologies allow more complex surveillance tasks to be realized with good cost effectiveness. Today we can monitor highly instrumented structures continuously, or remotely, with a high degree of versatility and flexibility.

The fundamental of structural integrity and durability aspects is to develop continuous monitoring concepts for structural components and for the global behavior. A structure is said to have general structural integrity if localized damage does not lead to widespread collapse. Structural integrity has to be guaranteed by the structural safety under ultimate and serviceability conditions and by ductility as well as redundancy of load paths.

An effective management system for structures is a crucial point in the development of a life extension or replacement strategy for structures within normative and budgetary constraints. A key component of such a system is a means of monitoring and determining the condition of an existing structure. In order to gather information about the structures and their performance over a period of several years, an adequate instrumentation and surveillance concept has to be realized. Determining the condition of a structure includes the measurement of the physical quantities that are of interest and, in a second step, the evaluation and interpretation of the measured data. The advances in today's hard- and software technologies, in sensor and communication technologies appear to offer a convenient way to implement highly flexible and complex instrumentation and monitoring applications by the use of computer based components.

A central issue is the identification of the different types of measurement that should be implemented for a global monitoring system. The following figure shows a classification of the main quantities that might be of interest.

The installation of sensing elements and of an automated data acquisition system to collect measured data is only the start of monitoring field performance. Interpretation of the acquired data is equally important. A crucial point of an interpretation is the comparison of measured and calculated data in order to validate the model assumptions or to verify the effectiveness and efficiency of the monitoring system. The results of all measurements should be the basis for the condition assessment and the safety evaluation of a bridge. Therefore a comparison of measured and analytically modeled behavior may be necessary.

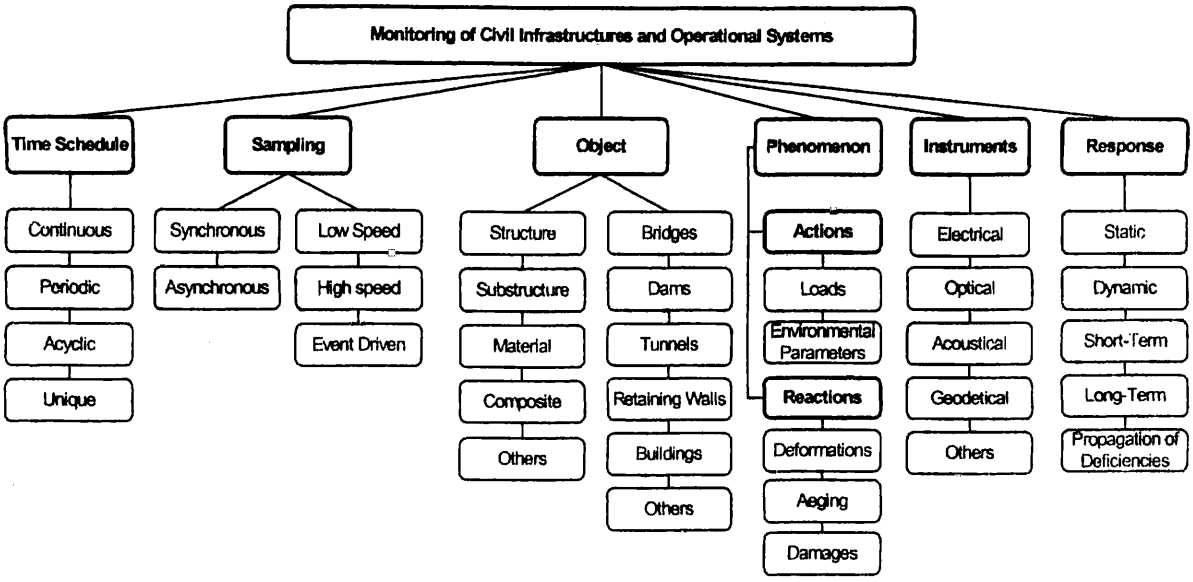

Fig. 1-1: Classification of surveillance techniques and objectives

Finally, all observations should yield some safety ranges in order to facilitate replacement and/or repair decisions.

In the following sections we will try to provide an outline for a global monitoring concept for concrete structures such as bridges by the discussion of the different types of measurements that can be made.

1.1 Terminology

Terms and definitions according to ISO 2394 and ISO 13822:

Assessment
set of activities performed in order to verify the reliability of an existing structure for future use

Damage
unfavorable change in the condition of a structure that can affect structural performance

Deterioration
process that adversely affects the structural performance, including reliability over time due to

- naturally occurring chemical, physical or biological actions
- repeated actions such as those causing fatigue,
- normal or severe environmental influences,
- wear duc to use, or
- improper operation and maintenance of the structure

Deterioration model
mathematical model that describes structural performance as a function of time, taking deterioration into account

Inspection
on-site non-destructive examination to establish the present condition o the structure

Investigation
collection and evaluation of information through inspection, document search, load testing and other testing

Load testing
test of the structure or part thereof by loading to evaluate its behavior or properties, or to predict its load-bearing capacity

Maintenance
routine intervention to preserve appropriate structural performance

Material properties
mechanical, physical or chemical properties of structural materials

Monitoring
frequent or continuous, normally long-term, observation or measurement of structural conditions or actions

Reference period
chosen period of time, which is used as a basis for assessing values of variable actions, time-dependent material properties, etc. (NOTE: The remaining working life or the minimum standard period for safety of an existing structure can be taken as reference period).

Rehabilitation
work required to repair, and possibly upgrade, an existing structure

Remaining working life
period for which an existing structure is intended/expected to operate with planned maintenance

Repair, verb
(of a structure) improve the condition of a structure by restoring or replacing existing components that have been damaged

Safety evaluation
The set of activities performed in order to verify the safety (reliability) of an existing structure for future use.

Safety plan
plan specifying the performance objectives, the scenarios to be considered for the structure, and all present and future measures (design, construction, or operation, such as monitoring) to ensure the safety of the structure

Structural performance
qualitative or quantitative representation of the behavior of a structure (e.g. load-bearing capacity, stiffness) in terms of its safety and serviceability

Target reliability level
level of reliability required to ensure acceptable safety and serviceability

Upgrading
modifications to an existing structure to improve its structural performance

Utilization plan
plan containing the intended use (or uses) of the structure, and listing the operational conditions of the structure including maintenance requirements, and the corresponding performance requirements

1.2 Safety evaluation

Different methods, such as global or semi-probabilistic partial safety factor formats as well as reliability or decision theory based methods, are used to determine the reliability of an existing structure and to define structural safety. Using reliability formats the stress S applied and the resistance R describing the strength of the structural element are described by stochastic variables because their values are not perfectly known. If the verification of the criterion related to the limit-state results in the inequality

$$S \leq R$$

the structure is considered safe. The difference of R-S is called safety margin M. Fig. 1-2 shows this problem with the three normally distributed variables R, S and M. As the sum of two variables the safety margin M is also a variable and is normally distributed if the variables R and S are normally distributed. β is the so-called reliability index and is determined as $\beta = \mu_M/\sigma_M$.

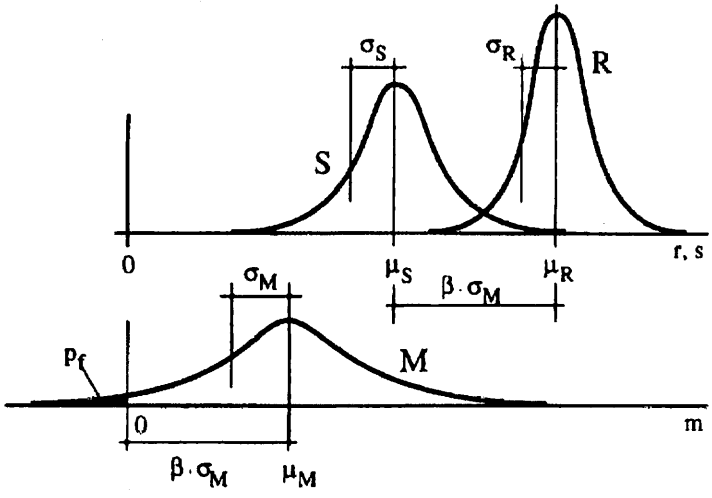

Fig. 1-2: Distributions of resistance R, stress S and safety Margin M = R - S

The safety margin M distinguishes three states:

- the safe state or safety domain with $M \geq 0$,
- the limit state with $M = 0$ and
- the unsafe state or failure domain with $M \leq 0$.

The probability of failure p_f of $S \leq R$ characterizes the reliability level of a structure with regard to the limit state considered:

$$p_f = P(R - S \leq 0) = P(M \leq 0)$$

In Fig. 1-3 R and S are plotted as marginal probability density functions on the r and s axes. The limit state equation M = R-S separates the safe from the unsafe region dividing the hump into two parts. The volume of the part cut away and defined by s > r corresponds to the probability of failure p_f. The design point (r*,s*) lies on the line defined by R-S=0 where the joint probability density is greatest. If failure occurs it is likely to be there.

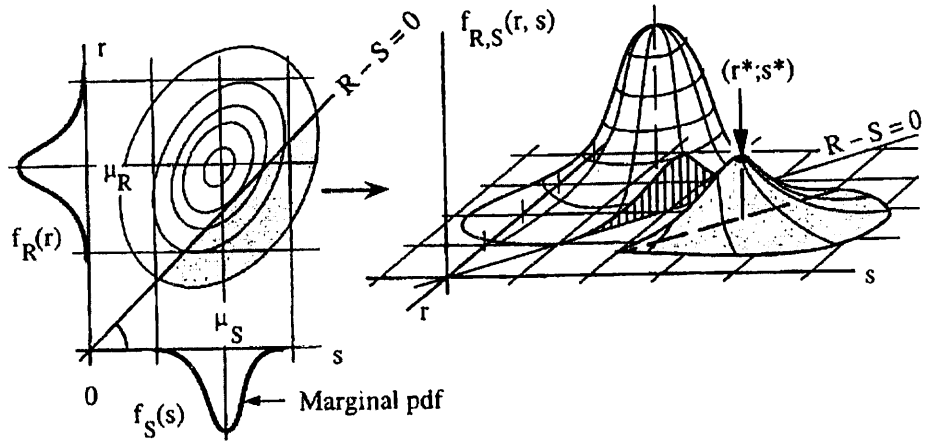

Fig. 1-3: Two-dimensional probability density functions

If more than two variables are considered and if the safety margin is expressed by a non-linear function of the different variables, the probability of failure is:

$$p_f = \int_{M \le 0} f_x(x_1,....,x_n)dx_1...dx_n \qquad (1\text{-}1)$$

with M being the safety margin composed of n variables resumed in the vector x and $M \le 0$ representing the failure domain.

Reliability methods taking into account uncertainties of variables are main criteria for a realistic safety assessment. Thus, reliability formats using probabilistic methods are an important alternative to semi-probabilistic approaches. Reliability formats are based on:

- the definition of a limit-state criterion
- the identification of all variables influencing the limit-state criterion
- the statistical description of these variables and the consideration of stochastical (in)dependency
- the derivation of the probability density and its moments for each basic variable
- the calculation of the probability that the limit-state criterion is not satisfied
- the comparison of the calculated probability to a target probability

If the assumptions on the variables are not based on adequate data, estimates of reliability can be misleading. Therefore, it is essential to ensure the quality of data and validity of assumptions when using probabilistic methods to make a decision on the reliability of a specific structure. This can be assured by standardising the approach and by setting requirements on how to use data with it. When modelling the variables it is also very important to take into account what design codes, design methods and assumptions the engineer has used during the original design of the structure. Furthermore, old codes and standards are often a valuable source of information when parameters of the distributions have to be determined.

The evaluation of eq. (1-1) is a very difficult task, except for linear limit states and Gaussian variables. A direct analytical solution or numerical integration are often not

possible. Thus, two methods, i.e. the reliability index methods and simulation methods, are introduced which allow the calculation of the probability of failure even for complicated functions.

1.2.1 Reliability index method

Reliability index methods such as FORM (First Order Reliability Method) or SORM (Second Order Reliability Method) approximate the calculus of the probability of failure. Using FORM the limit-state surface is linearized in the design point. The procedure to determine the probability of failure is straight forward even for non-linear limit-state functions and non-Gaussian random variables. It is a quite robust method and difficulties might only arise in very extreme cases where the linearization of the transformed limit state equation leads to inaccurate results. The first step of a FORM analysis consists of transforming the problem into a space of standard normal distributions (Fig. 1-4). In the standardized space the nearest point form the origin to the transformed limit state is called design point and its distance form the origin is the reliability index β.

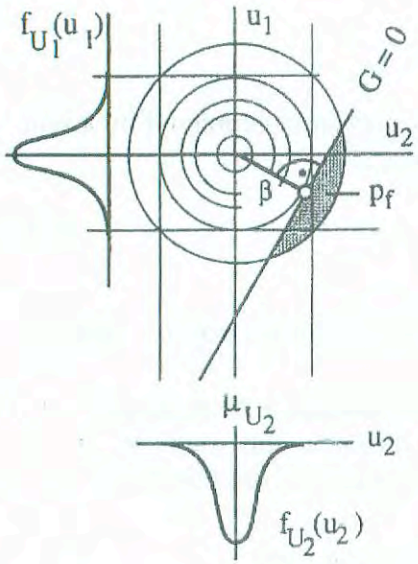

Fig. 1-4: Transformation to the standardized space

In FORM the failure surface is approximated by a tangent hyperplane in the design point and the probability of failure can be approximated by

$$p_f = \Phi(-\beta)$$

where Φ is the probability function of the standard normal variable.

FORM uses the derivatives of the limit-state function. For simple examples the derivatives can be expressed explicitly. But when the limit-state function is complex and depending on structural behavior or analysis other numerical procedures are necessary which increases the computational effort as the number of basic variables increases.

1.2.2 Simulation methods

The most important sampling methods are Monte-Carlo sampling where the probability density function and the associated statistical parameters of the safety margin are estimated approximately employing random sampling. This method is very time-consuming for the solution of real engineering problems.

Advanced simulation methods such as importance or directional sampling try to reduce computational time by reducing the sample size required for the estimation of the probability of failure. These methods can be used instead of or together with reliability index methods especially in cases where it becomes important to check the accuracy of reliability index methods, such as multi-mode or multi-component failure.

1.3 Economic considerations

The condition assessment of aged structures is becoming a more and more important issue for civil infrastructure management systems. The continued use of existing systems is, due to environmental, economical and socio-political assets, of great significance growing larger every year. The performance of many of these in-service structures has decayed over the years of utilization and the inherent level of safety might be inadequate relative to current design documents. Structural integrity has to be guaranteed by the structural safety under ultimate and serviceability conditions in order to ensure the safety of the structure and its users. For the purpose of developing adequate life extension and replacement strategies, issues such as whole-life performance assessment rules, target safety levels and optimum maintenance strategies must be formulated and resolved from a lifetime reliability viewpoint and lifecycle cost perspective (Frangopol 2000, [45]).

In order to maintain the health of a structure up to a given time into the future, a cost-effective maintenance strategy has to be used. The optimal maintenance strategy will correspond to the minimum expected life-cycle criterion. The optimization problem for existing structures consists of minimizing the total expected cost under the reliability constraints as follows (Frangopol 2000, [45]):

$$C_E = C_{PM} + C_{INS} + C_{REP} + C_{FAIL}$$

$$\min (C_E) = f(\beta \geq \beta^*)$$

C_E ... total expected cost
C_{PM} ... preventive maintenance cost
C_{INS} ... inspection and monitoring cost
C_{REP} ... repair cost
C_{FAIL} ... failure cost
β, β^* ... structural and target reliability index

As indicated in Fig. 1-5, we can mainly differentiate between two types of interventions, namely preventive and essential maintenance. While preventive maintenance is undertaken when the structural performance is above the target reliability, essential maintenance is undertaken when the performance has violated the target value.

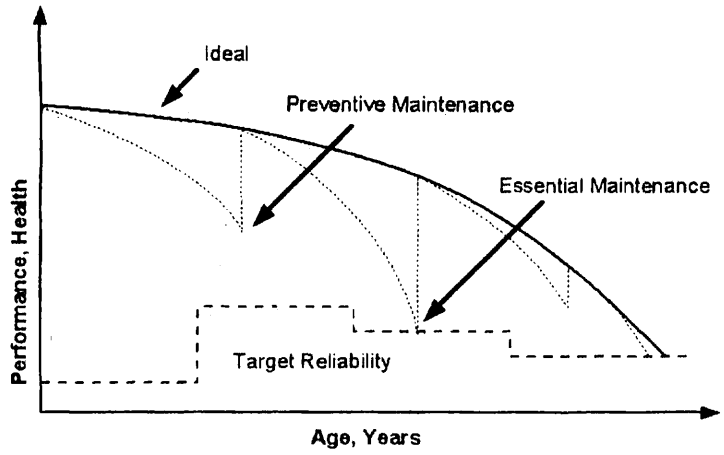

Fig. 1-5: Maintenance options and reliability, (Santa, Bergmeister 2000, [119])

Structure-related life-cycle costs can be reduced at all levels of engineering work as follows (Yanev 2000, [160]):

- Design (by eliminating components requiring labor-intensive or complex maintenance)
- Construction (by improving quality)
- Inspection (by more conclusive structural evaluation)
- Maintenance (by improving service and extending the structure useful life)
- Management (by accurate needs assessment, strategy selection and implementation)

Non-destructive testing and evaluation techniques can contribute in all of the above and, as a result, is incorporated in current bridge management considerations (Yanev 2000, [160]). A visual inspection may yield a first qualitative, maybe purely intuitive impression. A better judgment would be based on the evaluation of acquired quantitative information. Recent progress in the development of sensing technologies and material/structure damage characterization combined with current data processing techniques have resulted in a significant interest in diagnostic tools to monitor structural integrity and to detect structural degradation. Adequate monitoring techniques provide qualitative and quantitative knowledge that facilitates more precise condition assessments and resulting maintenance interventions. This includes the observation of mechanical parameters such as loads, strains, displacements and deformations as well as environmentally induced processes such as corrosion (Santa, Bergmeister 2000, [119]). The significant current development is the transition from incidental to continual mode of operation. "On-line" sensor systems, capable of continued remote monitoring of certain structure condition indicators, are becoming part of modern structural design (Yanev 2000, [160]).

In all of these cases the added "first" cost of the monitoring system and the perpetual cost of its maintenance are expected to protect the much greater investment in the bridge construction and user costs. The Health Monitoring of Structures international initiative can contribute greatly to this process by integrating the growing variety of methods, techniques and research topics into a coherent and comprehensive tool (Yanev 2000, [160]).

1.3.1 Cost-reliability interaction

In general, the present value of cost is evaluated based on the assumption that the maintenance cost is independent on its effect on the system reliability level. However, in reality, cost varies according to the maintenance method selected and the improvement in

system reliability level. Maintenance expenses invested in the past influence the current system reliability and the maintenance cost requested in the future. Thus interaction between maintenance cost and system reliability over lifetime is considered in Fig. 1-6 by using three different relationships between the unit rehabilitation cost and system reliability improvement.(Frangopol 2000, [45])

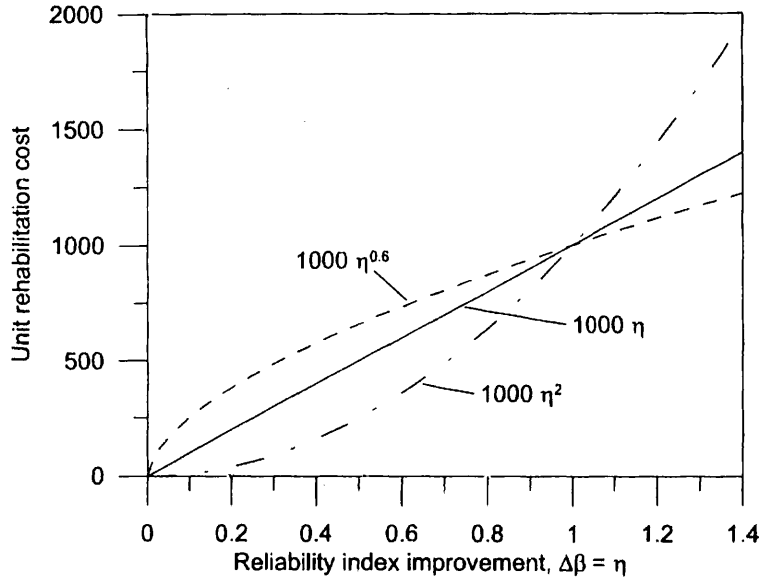

Fig. 1-6: Unit rehabilitation cost versus reliability improvement, (Frangopol 2000, [45])

Fig. 1-7 shows the present value of the expected cumulative and rehabilitation cost for the case in which only one essential maintenance is applied during the service life of a bridge group. It is clear that the present value of the expected cumulative unit rehabilitation cost is dependent on the cost function selected (Frangopol 2000, [45]).

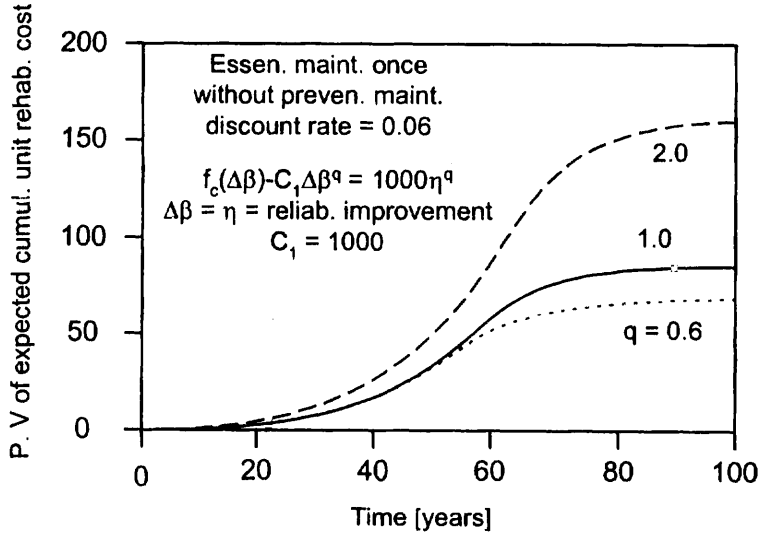

Fig. 1-7: Present value of expected cumulative unit rehabilitation cost: Essential maintenance applied once during the service life of a bridge group, (Frangopol 2000, [45])

1.4 Technical concepts and performance

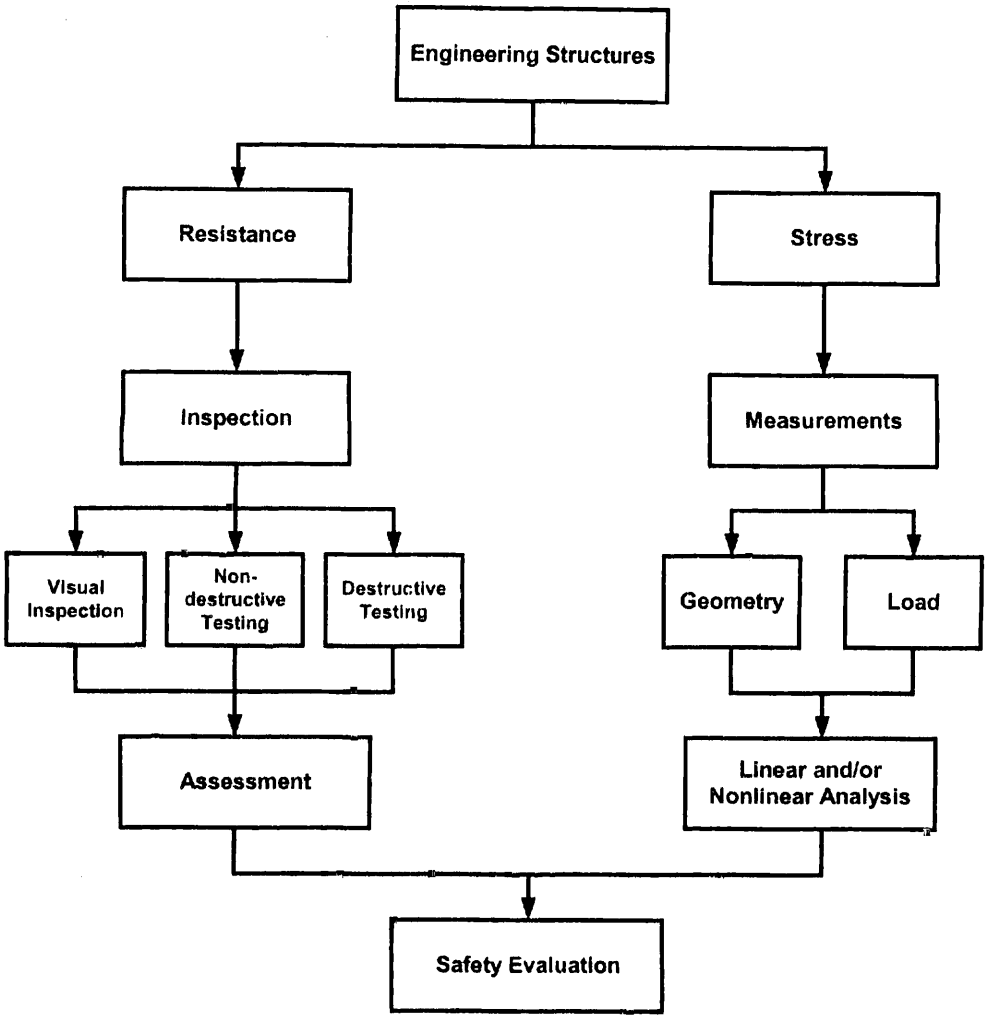

Fig. 1-8: Structural assessment

Typically the assessment process for an existing structure will consist of the following steps (Santa, Bergmeister 2000, [119]):

- Preliminary on-site inspection (to ascertain location, condition, loadings, environmental influences, necessity for further testing)
- Recovery and review of all relevant documentation, including loading history, maintenance and repair and alterations
- Specific on-site testing and measurements, (e.g. proof loading)
- Analysis of collected data to refine the probabilistic models for structural resistance
- Accurate (re-)analysis of the structure with updated loading and resistance parameters
- Structural reliability analysis
- Decision analysis

1.4.1 Typical test methods for concrete structures

Property under investigation	Test
Material properties	Cores Pull-out Pull-off Break-off Internal fracture Penetration resistance Rebound hammer Maturity
Concrete quality, durability and deterioration, reinforcement	Surface hardness Ultrasonic pulse velocity Radiography Radiometry Neutron absorption Relative humidity Permeability Absorption Petrography Sulphate content Expansion Air content Cement type and content Abrasion resistance
Corrosion	Half-cell potential Resistivity Linear polarization resistance A.C. Impedance Cover depth Carbonation depth Chloride concentration
Integrity and performance	Tapping Pulse-echo Dynamic response Acoustic emission Thermoluminescence Thermography Radar Strain or crack measurement Load test

Element dimensions	Reinforcement location Electromagnetic cover meters Ultrasonics
Deformation and displacement	Extensometer Dial gages Potentiometer LVDT Fiber optic sensors Geodetic measurements GPS Laser Strain measurement Heave or settlement of supports Deflection Liquid leveling systems Slope measurement
Loads	WIM systems Load cells
Dynamic response	Velocity and acceleration measurement Dynamic load tests

Table 1-1: Test methods for concrete structures (Bungey, Millard 1996, [19])

1.4.2 Performance levels

The International Standard ISO 13822 (2001, [66]) defines the following 3 structural performance levels for the assessment of an existing structure in terms of its required future structural performance.

- Safety performance level,
  which provides appropriate safety for the users of the structure.
- Continued function performance level,
  which provides continued function for special structures such as hospitals, communication buildings or key bridges, in the event of an earthquake, impact, or other foreseen hazard.
- Special performance requirements of the client related to property protection (economic loss) or serviceability. The level of this performance is generally based on life cycle cost and special functional requirements.

2 Structures and materials

The next Chapter gives an overview of the structural systems and corresponding elements as well as for their most frequent and relevant defects.

2.1 Structural systems

2.1.1 Buildings

In the following the most common defects in buildings made of reinforced or prestressed concrete are summarized. It has to be stated that most of the problems in building construction are related to serviceability, some influence the durability and finally a small number of defects actually affects the load carrying capacity of the structure. Depending on the loading (live loads, dead loads, impact loads etc.) and the type of structural system excessive deflection, cracking and spalling may be caused on different parts of the structure.

A wide variety of factors influences the behavior of the concrete. These factors include design, materials, construction, service loads, service conditions and exposure conditions.

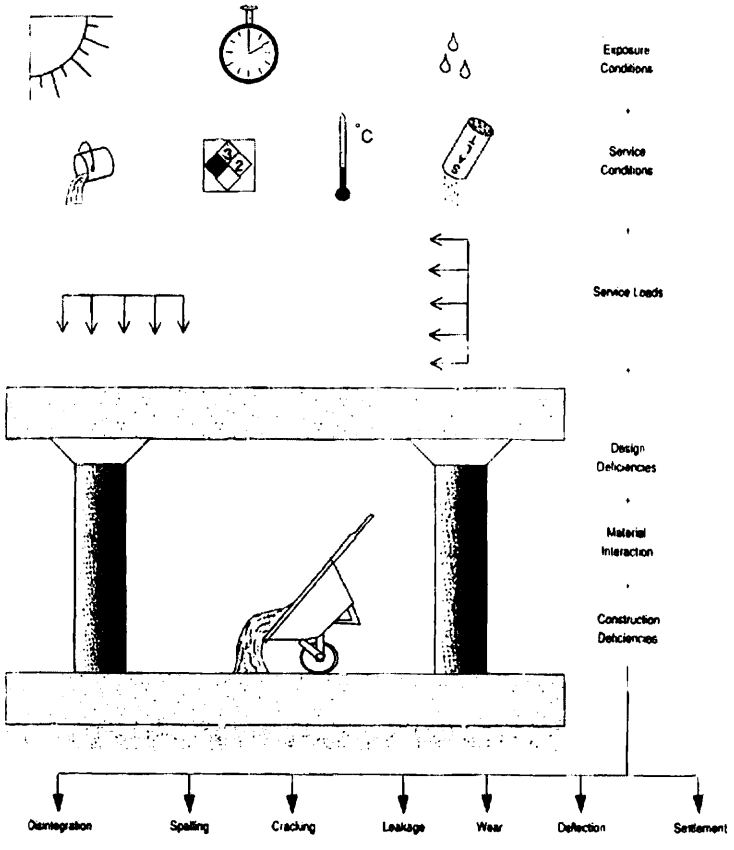

Fig. 2-1: Factors influencing concrete durability

Most of the observed problems in concrete structures are the results of a combination of these factors working together. The main problems are disintegration, spalling, cracking, leakage, wear, deflection or settlement.

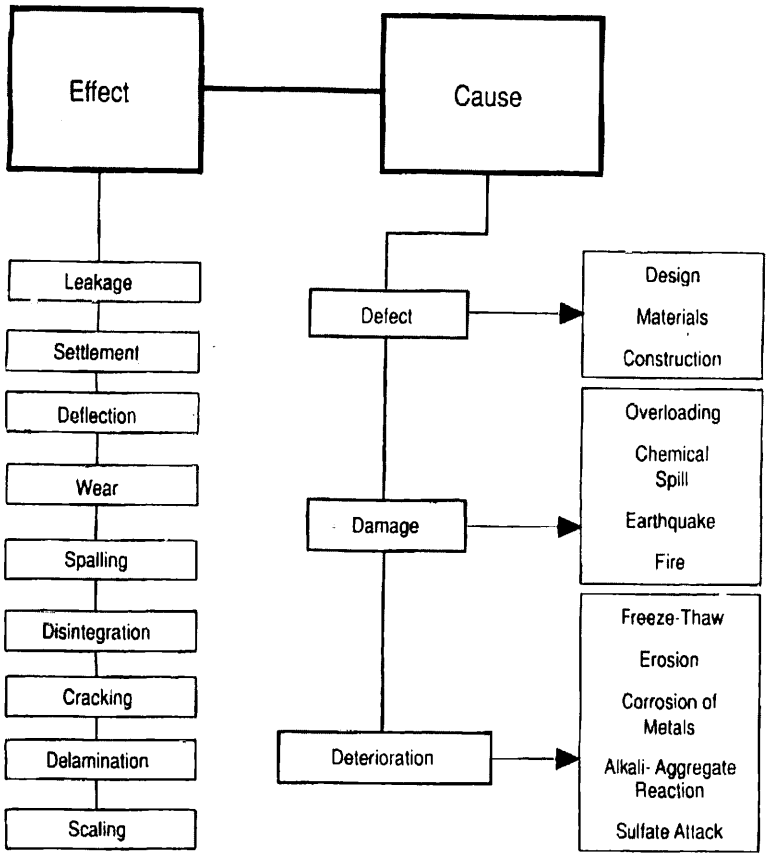

Fig. 2-2: Effects and causes of deterioration

As far as embedded metal corrosion is concerned corrosion-induced cracking and spalling as well as a reduction in structural capacity due to loss of section might cause problems. In this context the presence of chlorides which can penetrate from the outside (e.g. de-icing salts in parking structures) or may be introduced deliberately during the construction process as an accelerator or in the form of natural ingredients found in some aggregates are of importance. Furthermore, carbonation which reduces the pH value of the concrete and therefore leads to a loss of concrete protection of the reinforcing steel has to be considered.

Disintegration mechanisms are also of importance as depending on the type of attack, the concrete – in part or in whole - can soften or completely disintegrate. Disintegration of concrete is initiated by exposure to aggressive chemicals, freeze-thaw cycles, alkali-aggregate reactions, sulfate attack or erosion due to cavitation or abrasion.

Moisture effects also play an important role as far as defects of concrete structures are concerned. In the case of young concrete drying shrinkage, which might lead to dry shrinkage cracking has to be mentioned. If the surfaces of a structural member are subject to different levels of relative humidity moisture vapor transmission might cause problems. For slabs cast on grade curling which is caused by uneven moisture and temperature gradients across the thickness of the slab is a common problem.

Thermal effects, such as thermal volume changes or uneven thermal loads create stresses when the concrete is restrained and can lead to cracks, spalling or excessive deflections. In this context also early thermal cracking of freshly cast concrete has to be mentioned.

Finally faulty workmanship of designers, detailers and contractors is an important source for structural defects. There are so many variables affecting the design and construction of a building that there is always a potential for something to go wrong. Often structural members are cast out of tolerance which may lead to eccentric loading of columns or with improper grades of slab surfaces causing standing water with the potential of saturation and the worst condition for freeze-thaw cycles. The main problems influencing serviceability (cracking,

deflections), durability or in the extreme case load carrying capacity (collapse) are improper reinforcing steel placement, premature removal of formwork or improper column form placement which is especially critical for cardboard cylinder forms. Furthermore cold joint, segregation, honeycomb and rock pockets which often lead to durability problems fall into this category.

2.1.2 Bridges

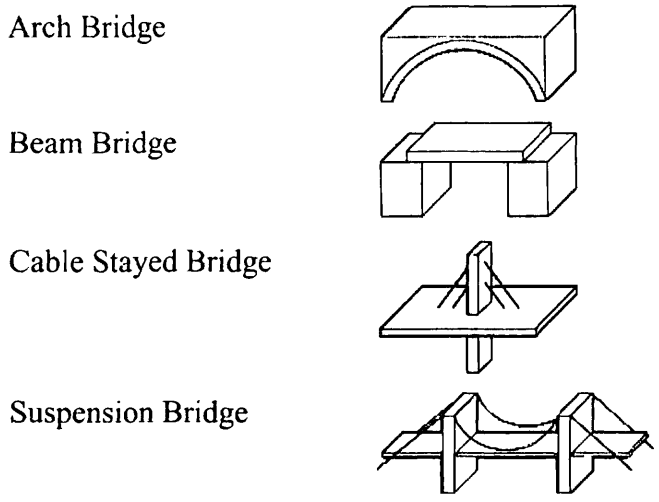

Fig. 2-3: Bridge types

Arch bridges use a curved structure, which provides a high resistance to bending forces. Unlike beam bridges, both ends of an arch are fixed in the horizontal direction (i.e. no horizontal movement is allowed in the bearing). Thus when a load is placed on the bridge horizontal forces occur in the bearings of the arch and as a result arches can only be used where the ground or foundation is solid and stable. The lighter weight of the cable-stayed bridge, though a disadvantage in a heavy wind, is an advantage during an earthquake. However, should uneven settling of the foundations occur during an earthquake or over time, the cable-stayed bridge can suffer damage. Long span suspension bridges are strong under normal traffic loads, but vulnerable to wind forces. Thus special measures have to be taken to assure that the bridge does not vibrate or sway excessively under heavy winds.

Basically, there are three subsystems used by bridge engineers that serve to divide a bridge into distinct sections. These major subsystems are the foundation, the substructure, and the superstructure. The *foundation* consists of the footings and piles used to distribute the load to the ground elements. For single span bridges, the *substructure* consists of the bridge *bearings*, which are the components that serve to transfer forces from the superstructure to the substructure, and the *abutments*, which are a particular type of retaining wall that transfer forces from the superstructure to the foundations (Barker and Puckett 1997). A bridge's abutments are often integrated with the foundation elements. Continuous or multi-span bridges have piers included in the substructure. The bridge *superstructure* is referred to as the structural make-up of the bridge above the bearings. The superstructure could consist of different types of details depending on the particular bridge design. The superstructure often refers to the *girders*, which are the longitudinal supporting members, the *deck*, and the diaphragms. *Diaphragms* are components that are transverse to the main longitudinal members and serve to transfer lateral wind loads to the deck, transfer dead and live load to the girders, and support the girders during construction of the deck. (Prince 1998, [109])

For condition rating assessment a structure may be divided into the following sections and corresponding elements (Bevc, Mahut, Grefstad 1999, [11]):

Components	Sub-elements
Superstructure	Slabs, voided slabs, girders, box girders, transverse beams, etc...
Substructure	Piers, columns
Prestressing elements	Cords and cables
Foundations	Single or strip footings, piles, pile caps, caissons, ground and rock anchors
Bearings	Roller bearings, fixed bearings, reinforced elastomeric bearings, pot bearings, etc...
Road Joints	Modular joints, rubber joints, waterproofing membrane, etc...
Carriage-way surface	Sidewalk, curbs, sealing joints, etc...
Caps (Bridge concrete surface)	Slab, longitudinal girders, transverse beams, cantilever slab; waterproofing layers, facings, etc.
Protective facilities	Safety barriers, parapet walls, etc...
Miscellaneous items	Tailings, drainage systems, signs, etc...

Table 2-1: Structural components and elements

2.1.2.1 Classification of defects

Bridge structures accumulate damage during their service life. Whether this damage consists of cracking, loss of prestress, pile scour, material fatigue or creep, or other factors, the outcome is the same: the actual structure's response to loading is changed (degraded) from the predicted design performance.

A review of the most frequent and relevant defects on the elements of a bridge structure is given in this section, taken from (Bevc, Mahut, Grefstad 1999, [11]). These defects have a more or less great impact on the bridge condition, and on the assessment of the condition. The review was made after examination of documents on this subject from different countries. To some types of damages also a classification of intensity or severity is suggested without any numerical values. This gradation would mostly depend on the experience of inspection and condition assessment personnel as well as on national regulations (Bevc, Mahut, Grefstad 1999, [11]).

Riverbanks, riverbed, embankments	Erosion of riverbank Erosion of riverbed Erosion of embankments Abrasion, deterioration of slope protection structures in riverbank Abrasion, deterioration of riverbed protection structures Abrasion, deterioration of slope protection structures on embankments Scoured area beneath pier/abutment Vegetation in riverbed and on riverbed and embankment slopes under and in the near vicinity of the bridge structure
Substructure	Lateral movements Tilt, rotations Differential settlements
Superstructure	Excessive vertical displacements
Concrete	Poor workmanship (surface porosity, honeycomb, stratification,...) Mechanical damages (abrasion, delamination and spalling due to impact load; delamination and spalling due to excessive load from temperature effects, differential movements of closely spaced elements, post-tensioning; small distance of the bearings from the free edge;) Cracks and open joints between the segments (structural and non-structural; with or without presence of water, exudation, efflorescence); width of the cracks should be graded into three or four grades) Deterioration (peeling, spalling and delamination of concrete cover due to freezing and thawing, corrosion of the reinforcement, ASR, leakage through concrete, constant presence of dirt, moss and other vegetation...;); to be graded with respect to the thickness of the spalled concrete into three or four grades; Wetting (wet exposed concrete surface in the tidal zone and in the splashing zone of waves and driving cars, or, exposure to the marine environment, leakage of water through concrete element due to the damaged or missing waterproofing membrane, damaged joint sealings on the sidewalk or edge beams,...); to be graded into three or four grades; Concrete cover depth defects; to be graded into three or four grades with the respect to the required minimum concrete cover depth for certain environmental conditions. Carbonation front in the concrete cover: to be graded into three or four grades with reference to the concrete cover depth and the level of the stirrups, main reinforcement and prestressed reinforcement. Chloride penetration depth: to be graded into three or four grades regarding total chloride content threshold level and with reference to the concrete cover depth and the position of the stirrups, main reinforcement and prestressed reinforcement. It is based on some measurements performed on site or in the laboratory.

Reinforcement	Corrosion of the stirrups and main reinforcement: to be graded into three or four grades with reference to the reduced cross section of the reinforcement with regard to typical dimension of the element cross section. The assessment is made on the basis of special investigation. Corrosion of the prestressed and post-tensioned tendons: to be graded into three or four grades with reference to the amount and depth of the pits of the prestressing steel and as the ultimate stage, the broken wires or strands. The assessment is made on the basis of special investigation. Corrosion of the ducts for post-the tensioned tendons: to be graded into three or four grades with the respect to the amount of corrosion and amount of the total chloride content in the grout. The assessment is made on the basis of special investigation and measurements. Corrosion of the anchorage elements and deviators for external prestressing and for stay cables (including the deterioration of the protective paint). Damage of the protective cover of external tendons and stay-cables. Ungrouted ducts
Bearings (steel, reinforced concrete, reinforced elastomeric, pot bearings, ...)	Excessive deformations (displacements, rotations) Deterioration (reinforced concrete, rubber) Corrosion and/or deterioration of the protective coatings (steel bearings, steel elements of the pot bearings, reinforced elastomeric bearings, fixing bolts,...) Mechanical damage (broken bolts, broken or deformed steel elements, cracked welds due to impact load, damaged sliding surface, malfunction of the bearings due to specific causes - dirt, uncleanliness, lack of grease on sliding bearings,...) Construction defects (missing bolts, thin welds, welding imperfections,...)
Expansion joints	Corrosion and/or deterioration of the protective coatings of steel elements Mechanical damage (broken fixing bolts, broken or deformed steel elements, cracked welds due to impact load, damaged rubber surface, malfunction of the expansion joints due to specific causes - dirt, cleanliness,...) Construction defects (missing fixing bolts, thin welds, welding imperfections, missing waterproofing membrane, missing or malfunction of expansion joint drainage system,...) Deterioration (rubber membrane - leakage; sealant along the expansion joint; surface rubber; expansion joint sealant;...)

Pavement with waterproofing membrane (asphalt and concrete pavement of carriage ways and sidewalks)	Cracks (single, several, congested) Crushed surface (with or without visible reinforcement - sidewalk) Wheel tracks: to be graded into three or four grades with the reference to the width and/or depth of the track) Damaged or missing waterproofing membrane (leakage through concrete element) Uneven approach on the bridge and/or over expansion joint
Curbs (made of concrete or stone)	Crushed surface (with or without visible reinforcement - concrete curbs) Deformations (transverse or vertical displacements) Missing elements of the curbs (stone, concrete, steel edge profiles)
Safety barriers (steel and concrete, on the bridge and on the approach ramps)	Deterioration of concrete elements (due to freezing and thawing, presence of de-icing salts,...) Deformations (transverse or vertical displacements) Corrosion of steel elements Mechanical damages due to impact loads (concrete and steel elements)
Joint sealing (between: curb - sidewalk; sidewalk - edge beam; on sidewalk; between edge beam and safety barrier sections)	Deterioration (light cracks, severe cracks, spalled sealing, totally damaged; presence of vegetation in the cracks,...) Missing sealant
Protective devices (steel railings, noise barriers with steel or concrete support elements and metal, plastic or wooden filling panels)	Corrosion Deterioration of the protective paint (steel, plastic, wood) Deterioration of concrete elements Mechanical damages due to impact load Missing elements
Drainage systems	Mechanical damage, corrosion of the pipelines or fasteners, etc....)

Table 2-2: Classification of defects, (Bevc, Mahut, Grefstad 1999, [11])

2.2 Actions

2.2.1 Loads

In general, loads can be considered to be primary or secondary. The sources of primary loading include the materials from which the structure was built, traffic, and various weather conditions, as well as unique loading conditions experienced during construction, extreme weather and natural catastrophes. Primary Loads are divided into two broad categories

according to the way in which they act upon the structure or structural element. These are dead loads and live loads.

Secondary loads are those loads due to temperature changes, construction eccentricities, shrinkage of structural materials, settlement of foundations, or other such loads.

2.2.1.1 Dead loads

Dead loads are those loads which are considered to act permanently; they are "dead," stationary, and unable to be removed. The self-weight of the structural members normally provides the largest portion of the dead load of a structure. Non-structural elements that are unlikely to vary during construction and use such as parapets, kerbs etc. must also be included in the calculation of the total dead load. Superimposed dead loads include the weight of non-structural elements that are likely to vary during construction and use (road surfacing, pipes and utility services, etc).

2.2.1.2 Live loads

Live loads are not permanent and can change in magnitude. They include loads due to the intended use of the structure and loads due to environmental effects caused by the sun, earth or weather. Wind and earthquake loads are put into the special category of lateral live loads due to the severity of their action upon a structure and their potential to cause failure. The load due to traffic is in most cases the dominating load in assessment of existing bridges and therefore plays an important role in the probabilistic-based assessment.

The magnitudes of live loads are difficult to determine with the same degree of accuracy that is possible with dead loads. The wind load used for the static design is estimated by a basic wind velocity, correction factors, aerodynamic coefficients, and projection areas of structures. Traffic data can be collected from weigh-in-motion systems (see Chapter 5.4.3), and a probability density function can be constructed to describe the actual measured loads.

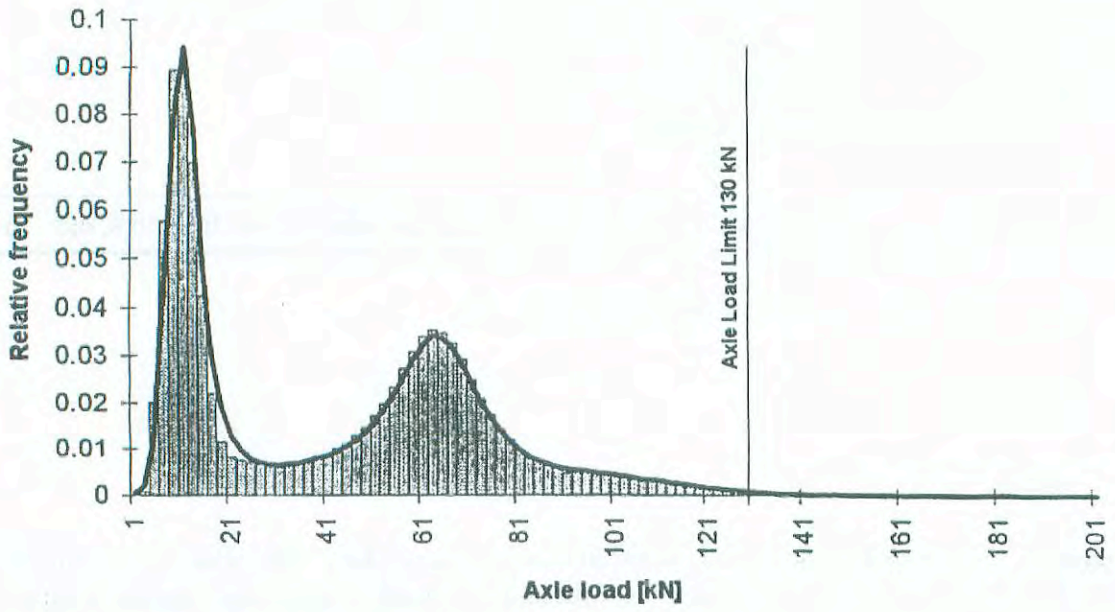

Fig. 2-4: Probability distribution of axle loads, (Bogath 1997, [12])

This probabilistic, site specific loading model is then used in place of the deterministic, general loading model provided in codes of practice, and gives a more accurate load rating for that specific bridge.

The traffic loads are often divided into populations such as, (Enevoldsen 2001, [38]):

- Ordinary traffic load with the main contribution from the largest loaded trucks with a weight of 40 – 60 t, depending on the regulations in the specific country
- Heavy transports with a special permission for passing over the bridge with a typical weight from 50 – 150 t

Based on these populations the load combinations are set up.

(1) Classes of loads for bridges:

- Dead loads:
  weight of the structure itself plus non-structural elements that are unlikely to vary during construction and use (parapets, kerbs, etc)

- Superimposed dead loads:
  weight of non-structural elements that are likely to vary during construction and use (road surfacing, pipes and utility services, etc)

- Traffic loads:
  load caused by vehicles, pedestrians, trams,..; dynamic loads caused by the movement of traffic on the bridge, centrifugal forces on curved bridges, braking forces, and collision loads

- Other live loads:
  wind load, earthquake, collision, forces due to flowing water and debris, impact load, etc.

- Secondary loads:
  thermal effects, friction forces in the bearings, shrinkage, creep and prestress forces in concrete bridges, differential settlement of the supports, error due to manufacturing and erection, etc.

Despite the fact that each and every load and loading combination should be considered in order to reduce the chance of structural failure, the determination of the loading remains a statistical exercise. Each and every load cannot be foreseen; thus, it is critical to determine the worst case that is reasonable to assume to act upon the structure.

The loads due to permanent actions are in general modeled by normal distributions with added contributions from model uncertainties. Variable loads are modeled by application of extreme distributions (e.g. a Gumbel distribution) obtained by a 1-year reference period (Enevoldsen 2001, [38]).

2.2.2 Traffic load model calibration

It has been possible to derive an average formula that gives an adjusting factor c, to be applied to the actual road traffic effects, in order to obtain the values corresponding to a mean return period of T years, (Calgaro 1997, [39]):

$c = 1.05 + 0.116 \log (T)$

This factor is equal to 1 for a mean return period of about 20 weeks. The formula shows that, when the return period goes from 100 years to 1000 years, the values increase by 9 % (Calgaro 1997, [39]).

According to EC1, for load-bearing capacity investigations, a simplified traffic load model in which the vibration coefficient (except for local effects at carriageway transitions) is already contained, is derived from and substantiated on the basis of the simulations, and the combination coefficients are determined (Merzenich, Sedlacek 1995, [89]).

Subsequently, probabilistic designs of bridges with the aid of the minimum values for β, which are interpreted as target values ($\beta = 4.7$) are executed and, from them, a required safety factor for the traffic loads of, $\gamma_0 = 1.35$ is determined (Merzenich, Sedlacek 1995, [89]).

2.3 Static load tests

Bridge deterioration with time and ever increasing traffic loads raise concerns about reliability of aging bridges. One of the ways to check reliability of aging bridges is proof load testing. A successful proof load test demonstrates immediately that the resistance of a bridge is greater than the proof load. Whereas analytical or predictive approaches used to determine load ratings may be overly conservative. For example, the actual load carrying capacity of a bridge is often higher than the predicted capacity, this may be due to system effects, load redistribution, etc. Thus a diagnostic or proof load test may be more appropriate if

- Analytical analyses produces an unsatisfactory load rating; or
- Analytical analysis is difficult to conduct due to deterioration or lack of documentation.

A diagnostic test may be used to verify or refine analytical or predictive structural models, whilst a proof load test is used to assess the actual load carrying capacity of a bridge. (Faber, Dimitri, Stewart 2000, [42])

The control of live load includes control of loads and load effects. Passive and active approaches have to be considered. The problem can be approached from two directions: (a) detection and control of overloaded vehicles, and (b) verification of the minimum load carrying capacity. Critical vehicles can be identified by way-in-motion monitoring (see Chapter 5.4.3). Minimum required load carrying capacity can be checked by proof loading [176]. Typical tests include torsional, bending, rotating bending, axial, and combined load testing.

2.3.1 Proof load testing

A loading test involves the process of loading and observation of the related reactions of an existing structure or a part of it for the purpose of assessment of it's load bearing safety and serviceability. It is characterized due to the fact that the testing load is increased following a fixed regime of loading and unloading cycles until the ultimate testing load F_u is reached. The ultimate testing load F_u is defined as the limit value of an acting load during the loading test, at which just no such damages occur that would affect the bearing capacity and serviceability for the future lifetime of the structure (Schwesinger, Bolle 2000, [128]). A reliability-based method may be used to determine the ultimate testing load. Such a method would be based on a probabilistic framework that considers bridge age, deterioration, magnitude of proof loads, test risk, updated bridge reliability (for prior service loading and

proof loading) and associated decision-making applications such as a risk-cost-benefit analysis. (Faber, Dimitri, Stewart 2000, [42])

Load tests are essentially designed to investigate structural response under short-term loading. Thus the selected instrumentation needs to respond accordingly and must provide sufficient sensitivity since strains from live loads are likely to be relatively small. Items that can be investigated with live load tests include impact factors, lateral load distribution, shear lag, and vertical deflections (U.S. Department of Transportation 1996, [147]). However, it should also be recognized that there is a risk that the bridge will be damaged or not survive a proof load test and so proof load testing may not always be cost-effective (Faber, Dimitri, Stewart 2000, [42]).

2.3.1.1 Loading methods

Load testing involves the application of physical test loads to a structure or parts of it, measurement of the response of the structure under the influence of the loads and interpretation of the results to make recommendations for future courses of action. Although a load test of a full-scale structural element or of a complete structure is a costly and time-consuming operation, it generally yields valuable results. A single loading case may not be able to provide the range of information required and it may be necessary to perform a series of tests to satisfy the technical requirements (Faber, Dimitri, Stewart 2000, [42]).

Loads may be applied using dead weight or by mechanical means and consideration need to be given to any effect the loading method may have on the observed behavior. Materials, which can be used, include building materials, water, cast-iron weights and loaded vehicles. Water is fairly easy to handle by pumping but it has the disadvantage in terms of its low density compared with other materials, see Fig. 2-8. In the event of sudden failure it is possible for the water to be dispersed by pumping or puncturing the water tanks (Faber, Dimitri, Stewart 2000, [42]).

Other forms of dead weight used for testing in buildings require labor for handling and consequently they can be slower and more expensive to use. Precise knowledge of applied load may be obtained by using cast-iron weights, but costs of hiring and transporting these may be substantial (Faber, Dimitri, Stewart 2000, [42]).

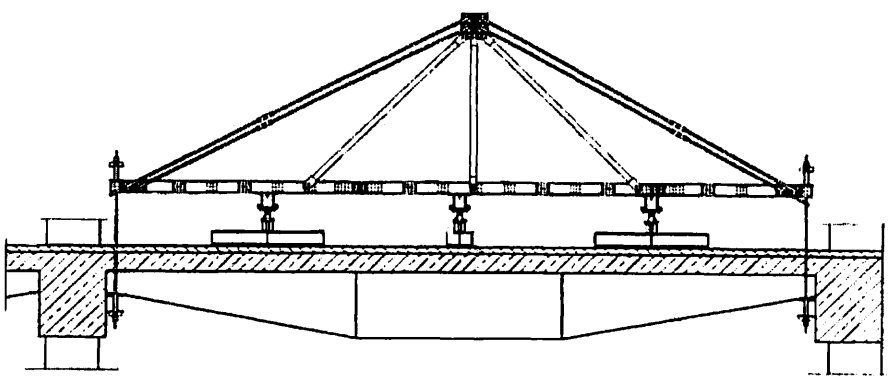

Fig. 2-5: Reaction frame, [135]

Where jacking systems are used, restraint provided to the structure by the system should be minimized by using ball seatings and rollers. Jacking systems require heavy steel girders to be connected on site to form a reaction frame. The load is applied to the structure by the use of hydraulic jacks and a dead load of concrete blocks. The framework supplies a steady reference platform from which the vertical deflection of the bridge can be measured. The

response can be measured with extensometers and strain-gages. The main problems with jacking systems is the requirement to provide a reaction and the difficulty in generating distributed loads unless spreader frames or large numbers of jacks are used (Faber, Dimitri, Stewart 2000, [42]).

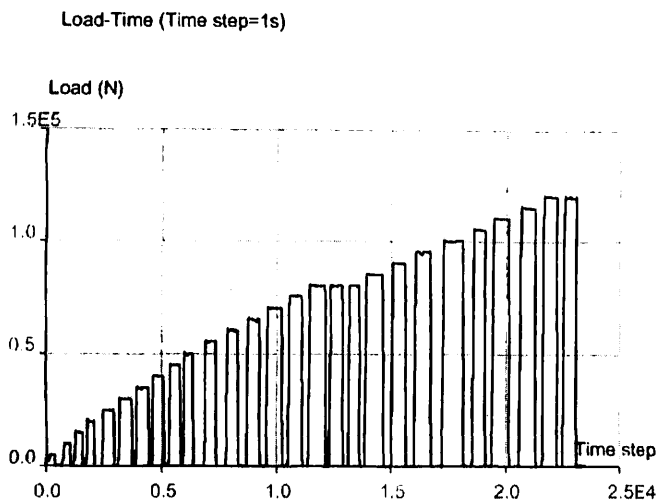

Fig. 2-6: Schedule for the static test force (Ebert, Zabel, Bucher 1999, [36])

Before applying any load, deformation measurements should be carried out to verify the test setup stability. In order to avoid unnecessary damage to the structure due to the proof load, it is recommended to increase the load gradually and to measure the deformations. Hence, the load is applied to the structure in accordance to a loading schedule, and held for a certain time period. The deflection is then noted and the next load increment applied. This is repeated for all the steps in the loading schedule. The results can then be portrayed graphically as a load / displacement graph. Measurements may also give a better insight into the behavior of the system. In general proof loads can not cover with long-term effects. These effects should be compensated by calculation.

For steel and reinforced concrete structures the proof load test often is considered successful if the eventual deformations of the structure are less than about 25 % of the maximum deformations, suggesting that inelastic behavior of this magnitude is tolerable for the types of steel used. For modern reinforced concrete using steels with less pronounced yield plateaus this may be optimistic. Importantly, the proof-load test says nothing about how close the proof-load might have been to the ultimate capacity of the structure, how much ductility remains, and whether there has not been some damage caused by the test itself. (Krämer, De Smet, Pecters 1999, [76])

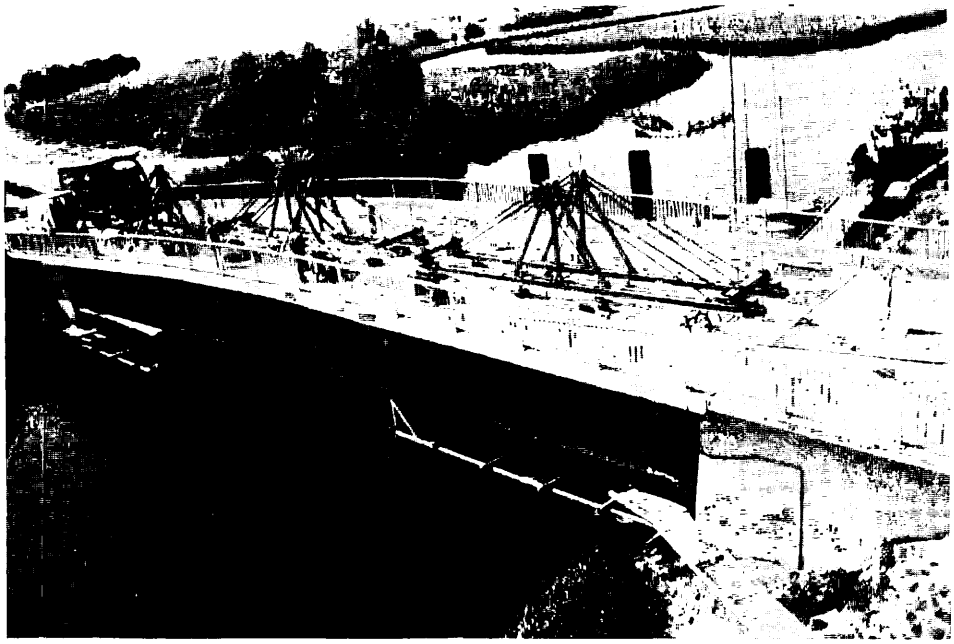

Fig. 2-7: Loading test of a bridge in Dassow, Germany

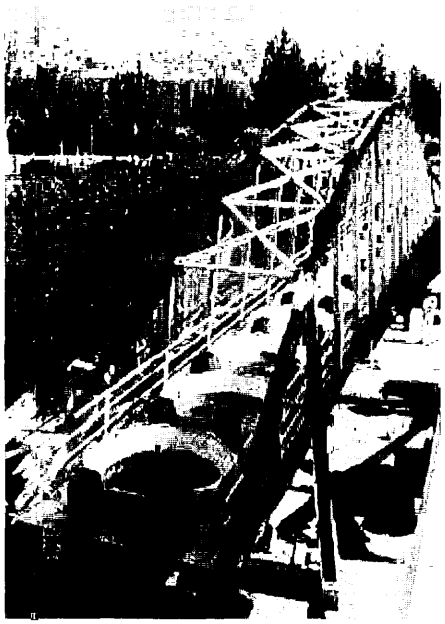

Fig. 2-8: Static load test using water tanks, (Sobrino, Pulido 2002, [135])

2.3.1.2 Loading truck, research project – BELFA

Conventional methods of proof loading tests are time-consuming and lead to long-term road closings. Furthermore, they result in a perforation of the bridge sealing, which protects the structure against water penetration. Another possibility to apply loads to the structure is by placing trucks or locomotives or even military tanks of known weights at various points of the

structure. These tests can also be one with incremental loads. Testing may also be carried out by passing the test vehicles over the bridge at incremental speeds starting from static position.

In order to provide a more efficient method for the in-situ loading tests, the Hochschule Bremen, TU Dresden, HTWK Leipzig and Bauhaus-University Weimar developed in cooperation with the companies EGGERS and WEMO a special loading vehicle BELFA. The layout of the operation mode of the loading vehicle is shown in Fig. 2-9.

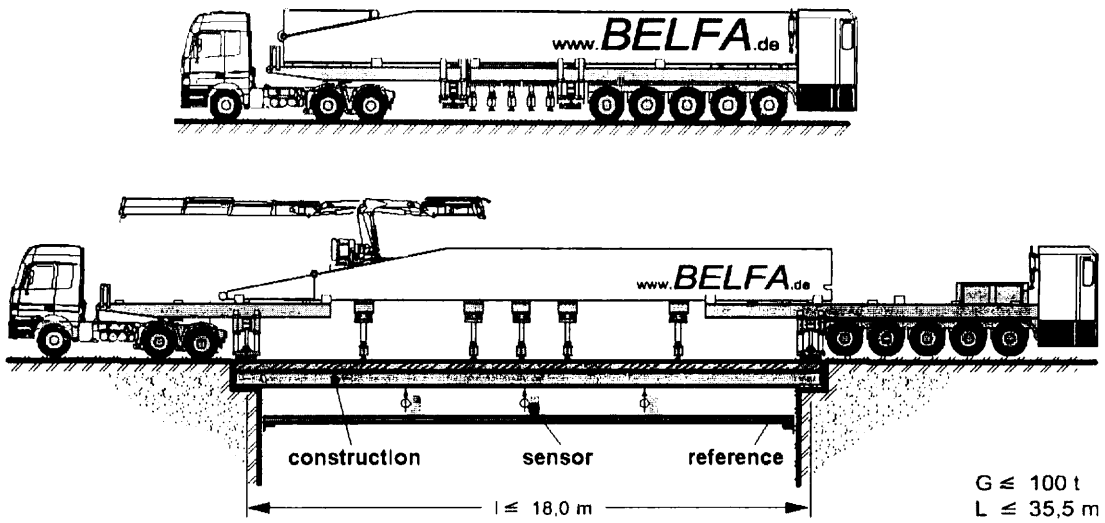

Fig. 2-9: Operation mode of loading vehicle BELFA, (Gutermann 2002 [51])

The loading vehicle BELFA is certified as a special vehicle and uses public roads (see Fig. 2-9: A). Before the tractor reaches the structure to be tested, the rear axles are locked and the tractor pulls out the front part (see Fig. 2-9: B). Additionally, the axle load of the tractor can be reduced by uploading the last three axles. Thus, a damage-free passage of the tractor over the structure is ensured. Before the wheels of the rear part approach the structure, they are locked again and the girder (yellow) is pulled away from the rear part. Having crossed the bridge, the tractor is fixed to the chassis and all axles are uploaded and fixed. Hydraulic jacks raise the vehicle and activate the entire mass for a loading test (see Fig. 2-9: C). Now, the crane, which is installed on the girder and can be moved in longitudinal direction is used for loading additional ballast. Water tanks can increase the total weight up to 100 t. Five hydraulic actuators with a maximum load of 500 kN each are moved to their test position and will perform load cycles controlled by on-board electronic systems. The reactions of the building are monitored by using an independently supported measuring base and are displayed on-line on a computer. After the test loading, the vehicle is converted into its transport mode and will be ready for a new application immediately. However it should be noted that the application of BELFA is limited to road bridges up to a span (total or individual) of 18 m [169].

2.3.2 Diagnostic load testing

Diagnostic load testing involves driving pre-weighed trucks across a bridge along various transverse paths at both a crawl speed (pseudo-static test) and at full speed (dynamic test). The weight of the trucks is chosen to not exceed the bridge's current rating level. Before testing starts, numerous fast-mounting strain transducers, and in some cases other instruments such as displacement gages are set up at predetermined locations on the bridge. Measurements

are recorded as the test vehicle is driven across the bridge. From the data collected during the diagnostic test, a number of significant properties that affect the bridge's actual load-carrying capacity can be determined. These properties, which are typically estimated in order to perform a traditional load rating, include

- load distribution,
- support restraint,
- flexural resistance of the superstructure elements (cross-sectional properties including the state of composite action), and
- effects of impact.

Furthermore, the recorded strain can also help indicate the level of other, more difficult to quantify, sources of strength. By gathering enough response data, a more accurate structural model of the bridge can be created and used in the final bridge rating.

It should be noted that diagnostic testing has the benefit of explaining why the bridge is performing differently than assumed. The disadvantage to this method, as opposed to proof load testing, is that the results are determined for service loads, and need to be extrapolated to ultimate load levels. (Chajes, Shenton, O'Shea 1999, [25])

2.4 Dynamic load tests

When the structural damage is small or it is in the interior of the system, its detection cannot be carried out visually. A useful more elaborate non-destructive evaluation tool is dynamic testing. It relies on the fact that the occurrence of damage or loss of integrity in a structural system leads to changes in the dynamic properties of the structure. For instance, the degradation of stiffness due to the cracking of the reinforced concrete, gives information on the position and severity of the damage that has occurred (Maeck, Wahab, Peeters, Roeck, Visscher, De Wilde, Ndambi, Vantomme 2000, [82]).

A simple view of dynamic testing is to consider it as a procedure for determining the resonance (natural) frequencies of a structure. The identified vibration mode shape for each natural frequency corresponds to the defected shape when the structure is vibrating at that frequency. Each vibration mode is associated with a damping value, which is a measure of energy dissipation (Salawu, Williams 1995, [116]). From the measured dynamic response, induced by ambient or forced excitation, modal parameters (natural frequencies, mode shapes and modal damping values) and system parameters (stiffness, mass and damping matrices) can be obtained. These identified parameters can then be used to characterize and monitor the performance of the structure (Salawu, Williams 1995, [116]).

Vibration testing can be used in a continuous or intermittent way. In a continuous monitoring system typically a few sensors are installed on the structure whereas a large number of sensors can be used in intermittent monitoring, for example to obtain detailed mode shape information (Peeters, Maeck, De Roeck 2001, [106]).

Unfortunately, it is not only the health of a structure that influences its measurable dynamics, but also the applied excitation and the changing temperature are important factors and may erode the damage detection potential (Peeters, Maeck, De Roeck 2001, [106]). Normal environmental changes like the thaw-freeze cycles of bridge supports may have a considerable influence on the changes in eigenfrequencies during the year and should thus be taken into consideration during analysis.

2.4.1 Ambient vibration testing

Dynamic testing methods without any control on the input are classified as ambient vibration testing. The popularity of this method is due to the convenience of measuring the vibration response while the structure is under service loading. The loading could be from either wind, waves, vehicular or pedestrian traffic or any other service loading. Thus, ambient sources represent the true excitation to which a structure is subjected during its lifetime.

Since the input is unknown, certain assumptions have to be made about its nature (Salawu, Williams 1995, [116]). The basic assumption of the method is that the excitation forces are a stationary random process (white noise), having an acceptably flat frequency spectrum (Taškov 1988, [140]). If this assumption holds, then the vibration response of any structure subjected to such effects will contain all the normal modes. Ambient vibration testing implicitly assumes response data alone could be used to estimate vibration parameters (Williams 1992, [158], Bendat, Piersol 1980, [6]).

The procedure of ambient vibration testing is straightforward. First a computational model of the structure under surveillance is carried out and its natural frequencies and corresponding mode shapes are determined. Location of measurement points is selected in accordance with the geometric layout of the structure, e.g. at the center and quarter points of a span. Accelerometers are used for the simultaneous measurement of vertical, lateral and longitudinal vibration of the structure. (Wenzel [156], Salawu, Williams 1995, [116])

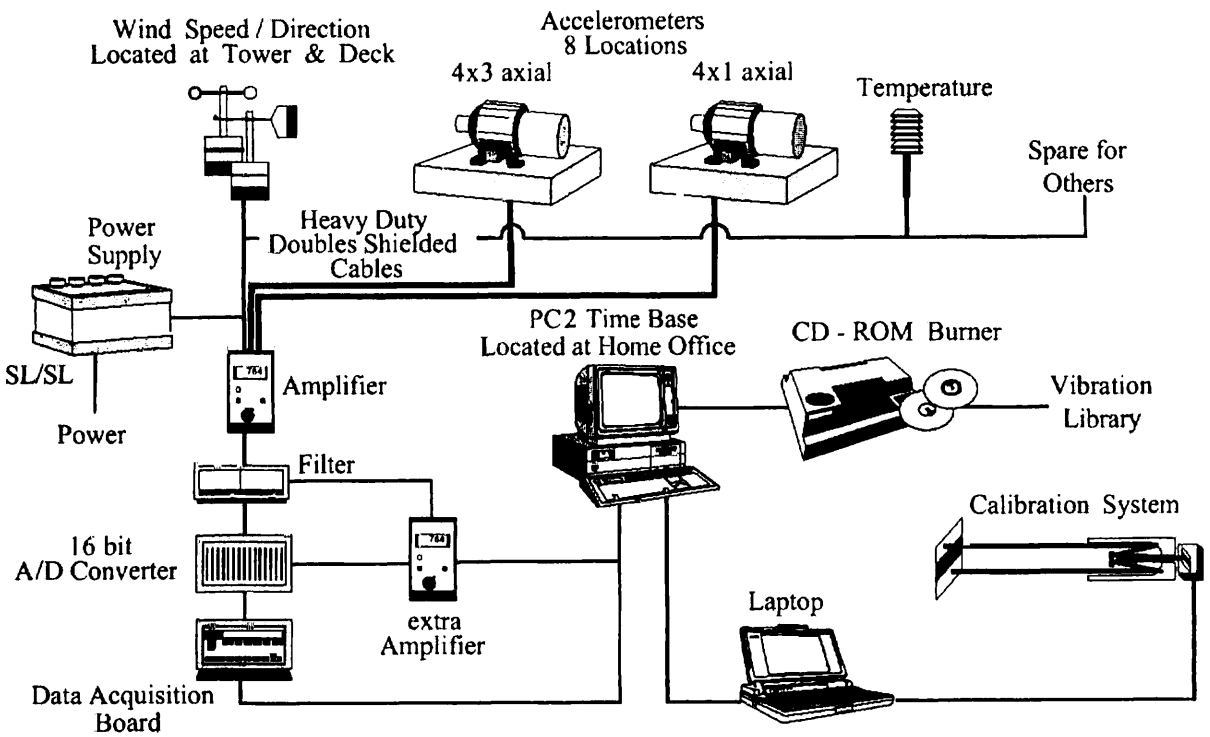

Fig. 2-10: Mobile monitoring system for ambient vibration testing [155]

The accelerations of a structure as a result of ambient excitation are typically very small and can vary considerably during acquisition: the signals have a large dynamic range as shown in Fig. 2-11. This causes challenges to the sensors, the acquisition system and the identification algorithms that need to extract weakly excited modes from sometimes noisy data. (Peeters, Maeck, De Roeck 2001, [106])

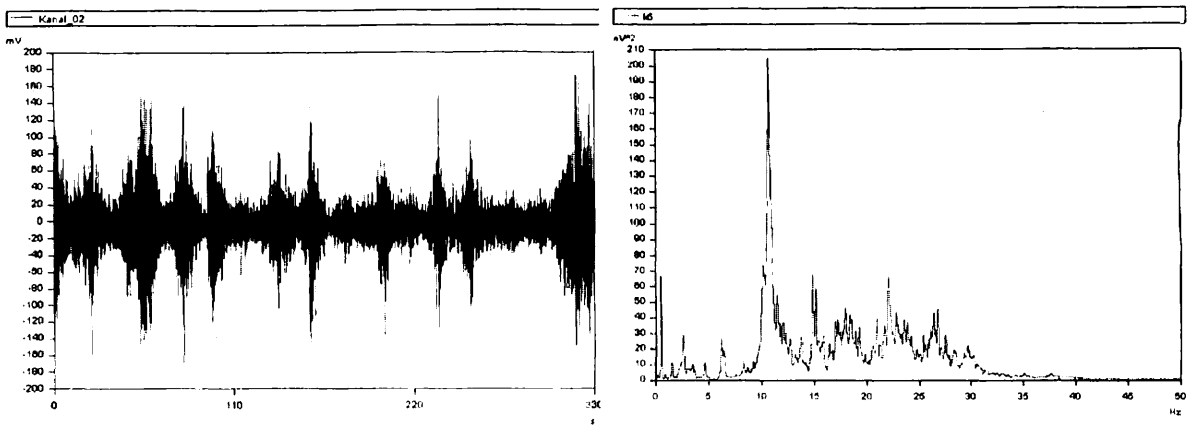

Fig. 2-11: Ambient response data, acceleration time signal (left) and power spectrum (right), (Wenzel [156])

The developments of the last few years both on the acquisition side and also on the identification side (e.g. the development of subspace identification methods) have greatly enhanced the use of ambient vibration testing as a non-destructive health monitoring technique. (Wenzel [156])

2.4.1.1 System identification for output-only measurements

Several methods are available to extract the modal parameters of the structure from measurements with unknown input. The detailed knowledge of the excitation is replaced by the assumption that the system is excited by white Gaussian noise.

A widely used method in civil engineering to determine the Eigenfrequencies of a structure is the rather simple peak-picking method. In this method, the measured time histories are converted to spectra by a discrete Fourier transform (DFT). The Eigenfrequencies are simply determined as the peaks of the spectra. Mode shapes can be determined by computing the transfer functions between all outputs and a reference sensor. The major advantage of the method is its speed: the identification can be done on-line allowing a quality check of the acquired data on site. Disadvantages are the subjective selection of Eigenfrequencies, the lack of accurate damping estimates and the determination of operational detection shapes instead of mode shapes, since no modal model is fitted to the data. (Peeters, De Roeck 1999, [107])

The simple and well-known frequency domain approach has been significantly improved, and a class of parametric techniques called Stochastic Subspace Identification (SSI) has been developed. These new techniques deal easily with noise contamination problems, closely spaced modes and complex-valued mode shapes. (Peeters, De Roeck 1999, [107])

The most general model of a linear time-invariant system excited by white noise is the so-called ARMAV-model: the autoregressive term of the outputs is related to a moving average term of the white noise inputs. Based on the measurements, the prediction error method is able to solve for the unknown matrix parameters. Unfortunately, this method results in a highly non-linear minimization problem with related problems such as: convergence not being guaranteed, local minima, sensitivity to initial values and especially in the case of multivariable systems, an almost unreasonable computational burden. One possible solution is to omit the moving average terms of an ARMAV-model that cause the non-linearity and to solve a linear least-squares problem to find the parameters of an ARV-model. A disadvantage is that since this model is less general, an over specification of the model order is needed which results in a number of spurious numerical modes. (Peeters, De Roeck 1999, [107])

The stochastic subspace system identification method shares the advantages of both the above-mentioned methods: the identified model is a stochastic state-space model which is in fact a transformed ARMAV-model, and as such more general than the ARV-model; the identification method does not involve any non-linear calculations and is therefore much faster and more robust than the prediction error method. (Peeters, De Roeck 1999, [107])

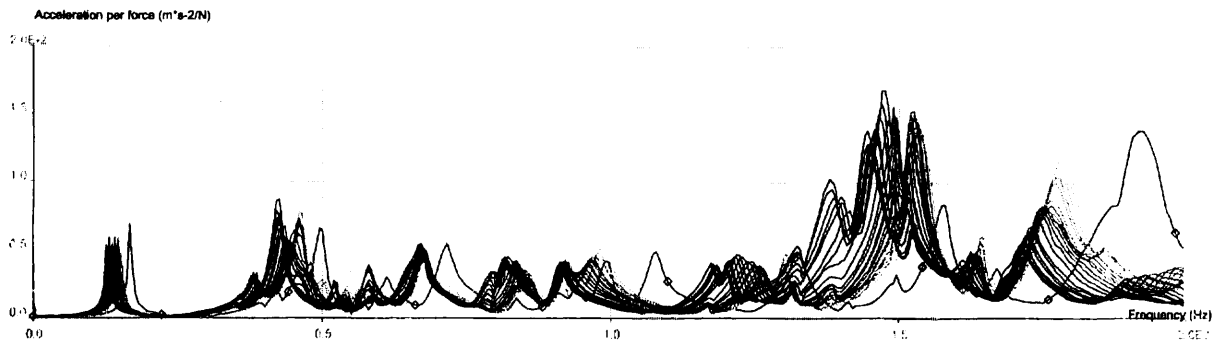

Fig. 2-12: Change of the frequency response function caused by increasing structural damage (Ebert, Zabel, Bucher 1999, [36])

2.4.1.2 Drawbacks of ambient vibration testing

In most cases, the nature of the input excitation can only be described by statistical parameters or by assuming the excitation spectrum to be concentrated within a frequency range. If the loading spectrum is limited to a narrow band of frequencies, only a limited picture of the dynamics of the structure can be monitored (Peeters, De Roeck 1999, [107]). Inadequate knowledge of the input force also implies generalized mass and stiffness cannot be derived. Anyhow in practice most structures show sufficient response, particular bridges.

Although reliable frequency and mode shape data can be obtained, estimated damping values are prone to errors. The errors in the damping estimates are due to a combination of factors such as the (possible) nonstationarity of the excitation process, signal processing and data analysis procedures necessary to extract modal parameters and the insufficient excitation of some modes. The frequency response function changes depending on the amplitude of the input excitation. This nonlinearity is sometimes helpful in the damage detection procedure. Hence, results from low level excitation might not be appropriate to predict the dynamic response to high level excitation. To achieve better results, it is necessary to use higher developed analysis techniques, which approximate the dynamic load levels likely to be encountered in the operating environment.

2.4.2 Forced Vibration Testing

Forced vibration testing incorporates those methods where the vibration is artificially induced. Amplitude and frequency of the applied input excitation are under control by the use of properly designed excitation systems. Forced vibration tests have the advantage of suppressing effects of extraneous noise in the measured structural response. Tests on offshore structures using both ambient and forced vibration methods have shown that damping and frequencies can be measured more accurately with forced vibration and that the higher modes can only be excited to measurable levels by forced excitation. (Salawu, Williams 1995, [116])

The physical means through which the excitation is realized may be termed a vibrator, exciter or shaker. It is a device used for transmitting a vibratory force into the structure. The

excitation device can be either of the contacting type, which means that the exciter stays in contact with the test structure throughout the testing procedure, or of the noncontacting type such as impactors. Physically mounted devices like vibrators are used for full-scale testing of large structures. Appropriate contacting vibrators are usually of the eccentric rotating mass or electrohydraulic type. (Salawu, Williams 1995, [116])

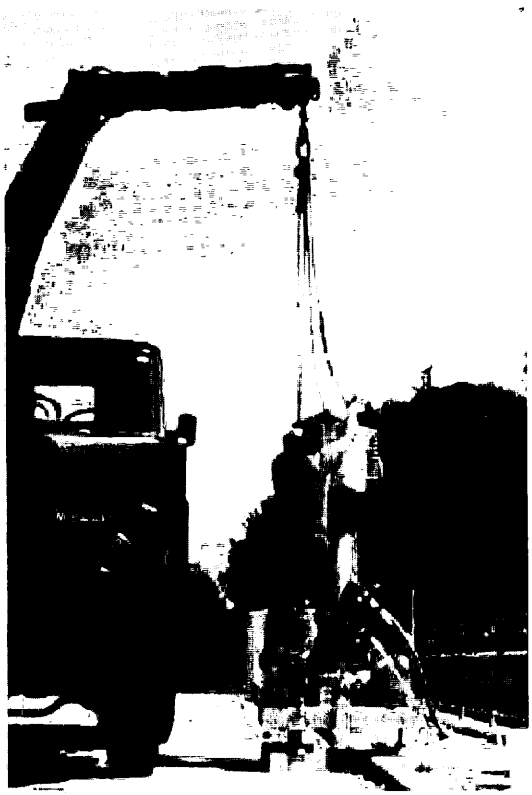

Fig. 2-13: Installation of a reaction mass shaker (EMPA)

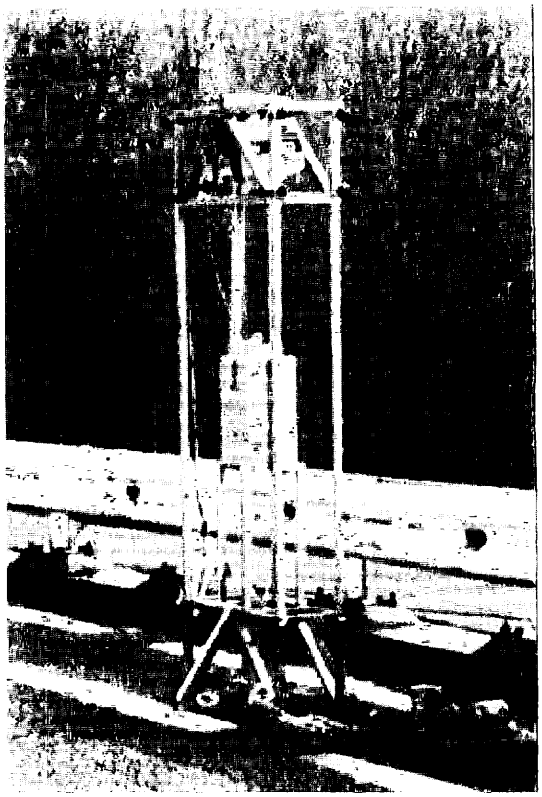

Fig. 2-14: Drop weight system, developed by K U Leuven (Peeters, Maeck, De Roeck 2001, [106])

2.4.2.1 Eccentric rotating mass vibrators

The eccentric mass vibrator generates vibratory force by using a rotating shaft carrying a mass whose center-of-mass is displaced from the center-of-rotation of the shaft. The vibrator can be operated at different frequencies by changing the rotational speed of the shaft. The simplest reaction type machine uses a single rotating mass. Machines with more than one rotating mass have the advantage of generating forces in more than one direction. However, rotating mass vibrators are capable of delivering only sinusoidally varying forces that are proportional to the square of the rotational speed so that reliable excitation can only be achieved above 1 Hz. (Salawu, Williams 1995, [116])

2.4.2.2 Electrohydraulic vibrators

The electrohydraulic vibrators can generate higher forces than the other types. The force is generated through the reciprocating motion induced by the high-pressure flow of a liquid. In operation, the system usually consists of a servocontrolled hydraulic actuator, which drives an attached mass. The weight of the mass can be varied to obtain varying force magnitudes. The vibrators provide relatively high vibration strokes and allow accurate excitation at different frequencies in bending or torsion. They also have the advantage of being able to apply a static preload and complex waveforms to the test structure. However, the attainable stroke reduces with increasing frequency. (Salawu, Williams 1995, [116])

2.4.2.3 Impactors

The simplest means of applying an impact to a structure is by using an instrumented hammer or suspended mass to deliver blows to the structure. The impulse delivered to the structure can be varied by changing the mass of the impact device. The impact frequency range can also be varied by changing the hammerhead type. The impulse function consists of a short duration broad-band spectrum. The width of the function determines the frequency content while the height and shape control the energy level of the spectrum. (Salawu, Williams 1995, [116])

Nevertheless, an instrumented hammer is rarely used on large structures because of the large mass of the latter and the risk of local damage, at the point of contact, to the structure when high force levels are applied. Other special impact devices have been developed to excite large structures, such methods include the use of a "bolt-gun" or dropping a weight onto the structure. Further possibilities to apply an impulsive force to a structure initially at rest include vehicle impact, driving a vehicle over an uneven surface, rocket impact or the controlled jumping of people. (Salawu, Williams 1995, [116])

In step relaxation testing, excitation is achieved by releasing the structure from a statically deformed position. The initial static deformation is obtained by either loading the structure with a wire or cable, hydraulic rams or by continuous thrust from rocket motors. The response of the structure to this form of excitation is strongly dominated by those modes whose deformed shapes resemble the statically deformed configuration of the structure. Although step relaxation is probably the simplest and most effective method of determining damping it is seldom used because of its difficulty in implementation. (Salawu, Williams 1995, [116])

2.4.2.4 Drawbacks of forced vibration testing

The number of reported forced vibration tests is less than that reported for ambient vibration testing. A factor contributing to this is the difficulty in constructing suitable excitation systems that can generate sufficient excitation forces at low frequencies (Salawu, Williams 1995, [116]). For very large structures, for example long span cable-stayed bridges, it becomes very difficult to apply sufficient artificial excitation to surpass the vibration levels from the ambient excitation, which is always present. If a structure has low-frequency (below 1 Hz) modes, it may be difficult to excite them with a shaker, whereas this is generally no problem for a drop weight or ambient sources (Peeters, Maeck, De Roeck 2001, [106]). It is also possible that not all the vibration modes of interest will be sufficiently manifested by transient excitation (Salawu, Williams 1995, [116]). Sometimes the excitation from natural sources (ambient vibration) exceeds the limit to be neglected.

The use of artificial shaker or impact excitation is not very practical: in most cases at least one lane has to be closed and secondary excitation sources, having a negative effect on the data quality, cannot be excluded: traffic under/on the bridge, wind, micro tremors. Furthermore impact testing has the disadvantage of potentially inducing localized damage on the test structure (Salawu, Williams 1995, [116]).

Eventually, if the cost of testing is a major concern, the use of shakers can be excluded. The price of a shaker and the additional manpower needed to install it on a structure makes it not very cost-effective (Krämer, De Smet, Peeters 1999, [76].

2.5 Material resistance

2.5.1 Concrete

Concrete is a highly versatile construction material, well suited for many applications. It is a mixture of Portland cement, water, aggregates, and in some cases, admixtures. Strength, durability, and many other factors depend on the relative amounts and properties of the individual components. However, even a perfect mix can result in poor quality concrete if correct placement, finishing, and curing techniques under the proper conditions of moisture and temperature are not used.

The following material properties affect the concrete resistance and are of importance for the safety evaluation of concrete structures and need to be determined experimentally:

- Compressive strength
- Carbonation depth
- Chloride content
- Permeability
- Porosity
- Existence of voids and inhomogeneities

In some cases the modulus of elasticity and the specific fracture energy are of additional interest. If the structure contains grouted tendon ducts the grouting mortar has to be investigated. For this material the carbonation level and the chloride content are of interest.

For the sake of completeness, the process of corrosion and associated deterioration mechanisms are shortly described in Chapter 5.7.1.

2.5.1.1 Compressive strength

High strength concrete requires a low w/c and strong aggregate. The water/cement ratio (w/c) of the mixture has the most control over the final properties of the concrete. Selection of a w/c ratio gives the engineer control over two opposing, yet desirable properties: strength and workability. A mixture with a high w/c will be more workable than a mixture with a low w/c.

The other important component for strength is the aggregate, the rock that is being bound by the hardened cement. Aggregate is what makes the difference between hardened cement and the structural material, concrete. Aggregate increases the strength of concrete.

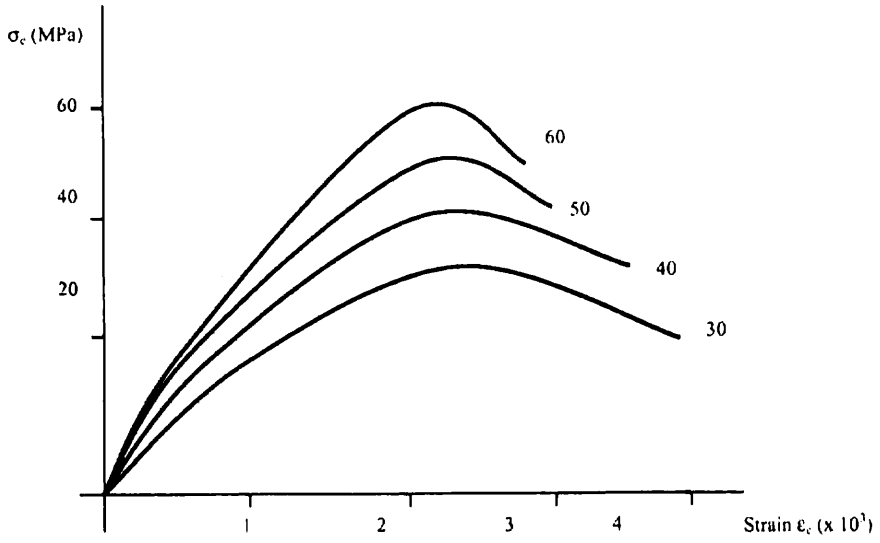

Fig. 2-15: : Stress-strain curves for concrete of various grades

The compression testing of cores cut from hardened concrete is a well-established method for strength estimation. Other physical properties, which can be examined from cores, include density, water absorption, indirect tensile strength and movement characteristics including expansion due to alkali-aggregate reactions. Cores are also frequently used as samples for chemical analysis following strength testing. [18]

2.5.1.2 Carbonation

During the hydration of the cement $Ca(OH)_2$ is formed resulting in the pH-value of the pore water being about 12.6. For preventing corrosion of the steel reinforcement a minimum pH-value of 11.5 is required. The $Ca(OH)_2$ reacts with the carbondioxide of the air resulting in a decrease of the pH-value:

$$Ca(OH)_2 + CO_2 \rightarrow CaCO_3 + H_2O$$

2.5.1.3 Chloride content

A high chloride content in concrete accelerates the corrosion process of the reinforcement. For the safety evaluation of existing reinforced concrete structures the determination of the chloride content, therefore, is an important part of the investigation. A high chloride content of the concrete in most of the cases is caused by the use of de-icing salts. Therefore, predominantly concrete bridges are affected.

2.5.1.4 Voids and inhomogeneities

Of special interest for the safety evaluation of concrete structures are poorly compacted spots in concrete members, so called honeycombs. In most cases, these imperfections are located at the concrete surface and can be found by visual inspection already. For finding voids inside the concrete member non-destructive methods have to be utilised (see Chapter 4).

2.5.2 Reinforcement

2.5.2.1 Metallic reinforcement

In construction, steel reinforcement is the most effective and cost efficient and therefore the most widely used reinforcing material in the world. However, it is well known that, under certain environments, the corrosion of steel reinforcement poses a serious problem. In the European Union countries alone, the annual cost of repair and maintenance of the infrastructure, as a result of problems associated with corrosion, is estimated to be around 30 billion €. [190]

There are several steps that can be undertaken at the design stage to overcome the problem of corrosion. The first step is to improve the standards of workmanship on site as many of the problems have been found to be associated with poor quality of construction. Workmanship plays a significant role in the long-term behavior of reinforced concrete. The correct location of the reinforcement, to give an adequate cover, is essential. The concrete must be adequately compacted, to give low permeability. Exposed surfaces must be well cured, to avoid excessive drying out at early ages, which leads to the development of cracks. However, in highly aggressive environments, improvements in workmanship alone may not be sufficient to ensure adequate durability. Further steps will then be necessary. There are many possible approaches, which may be outlined as follows (Clarke 1993, [30]):

- Improving the concrete, which may include reducing the porosity, by including admixtures to inhibit corrosion or by applying coatings to the surface to prohibit water ingress
- Cathodic protection of the reinforcement, either by means of an impressed current or by sacrificial anodes;
- Using a coated reinforcement, such as a fusion bonded epoxy coating or galvanizing;
- Using a stainless steel;
- Using a non-ferrous reinforcement.

(1) Fusion-bonded Epoxy-coated Reinforcement

This method of protecting reinforcement from corrosion in aggressive environments has been in use mainly in the US, since the early 1970s. The coating is an epoxy powder specially formulated to resist impact and abrasion, and to possess a sufficient degree of flexibility to bending stresses in the detailing of the bars, and to possess high bond to the surface of the rebars. The epoxy resin used is defined as a thermosetting epoxy powder coating material consisting mainly of epoxy resin plus curing agent and pigments. It is acknowledged that some damage will occur to the coating during transportation, and during fixing, placing and compacting the concrete around the bars (Perkins 1997, [108]).

(2) Galvanized Reinforcement

The object of galvanizing is to provide protection of the rebars in adverse conditions of exposure. Galvanizing consists of coating the steel with zinc by either dipping the steel into tanks of molten zinc or by electrodeposition from an aqueous solution. The corrosion protection provided by the zinc coating is mainly dependent on the thickness of the coating (Perkins 1997, [108]).

When concrete/mortar is placed around galvanized rebars there is a chemical reaction between the zinc coating and calcium hydroxide in the hydrating cement paste. The rebar

surface is passivated by the formation of a layer of zinc hydroxide. However the presence of very small concentration of chromate (about 0.002 % or 20 ppm) in the cement will inhibit the reaction between the cement paste and the zinc and thus limit the formation of hydrogen (Perkins 1997, [108]).

(3) Stainless Steel Reinforcement

Corrosion resistant stainless steel contains a minimum of 12 % chromium. On contact with air, the chromium forms a thin oxide layer on the surface of the steel. The addition of other elements such as nickel and molybdenum enhances the passivity and thus improves the corrosion resistance. This passivity layer has the advantage of being self-repairing. Thus, if damage occurs during handling and fixing, the passive oxide layer rapidly reforms and the corrosion resistance is not affected. However, physical contact between stainless steel reinforcement and other embedded metal like normal carbon steel reinforcing bars should be prevented. This is to avoid the phenomenon of bimetallic corrosion in which the less noble metal will act as a sacrificial anode and will corrode more rapidly (Clarke 1993, [30]).

A variety of stainless steels with different mechanical properties and degrees of corrosion resistance are available but with the addition of being significantly more expensive than standard reinforcement.

(4) Non-Metallic Reinforcement

In recent years, the use of fiber reinforced polymer (FRP) as structural reinforcement for concrete structures has become a novel technique in construction. These FRP materials are advanced composites made of continuous non-metallic fibers (glass, carbon,..) with high strength and stiffness embedded in a resin matrix. Due to excellent properties such as e.g. high strength, low weight and non susceptibility to galvanic corrosion, these FRP materials can be used for new structures (reinforced and prestressed concrete) as well as for the rehabilitation of existing structures (external FRP sheet bonding and FRP external post-tensioning) [167]. There is a large number of types and shapes of FRP reinforcement available and its use in construction is expanding rapidly. However, a major obstacle in adopting FRP widely in construction is the lack of accepted Standards for design. [190]

- **Woven fabric reinforcement systems**
  Fabrics consist of at least two independent fiber systems that might differ in material, strength and fiber content and are in most cases woven orthogonal. Fabrics in structural engineering are both impregnated and fixed on the concrete surface with epoxy resin. One field of application for woven sheets is the sheathing of axial compression columns where the stirrup reinforcement is already corrosive.
- **Grid reinforcement systems**
  In the manufacturing process two orthogonal winding heads deposit the continuous carbon fibers in a grid pattern. The lightweight and the environmental resistance of carbon grids make them an attractive reinforcing element for adverse conditions. Due to the non-magnetic properties, NEFMAC (New Fiber Composite Material for Reinforcing Concrete) grids have been applied as reinforcement for hospitals and in sensitive structures such as scientific laboratories, further in coastal areas where rapid corrosion of steel reinforcement is a problem.
- **Carbon lamella reinforcement system**
  Deterioration, misdesign or increased load-carrying requirements are some of the reasons why a steel reinforced structure might become deficient. Instead of replacing

the structure it can be strengthened with externally applied carbon lamellas. Both prestressed and non-prestressed carbon lamellas have proven to be successful in increasing the strength and stiffness of reinforced concrete beams.

- **Carbon fiber external and prestressed reinforcement elements**
  Due to their low weight, high tensile strength and good overall environmental durability, carbon fiber tendons, wires, strands, ropes and cables are increasingly being used for reinforcement of concrete structures like bridges and other large buildings. Carbon fiber tendons have shown their effectiveness as partial substitute for conventional steel tendons in external prestressed concrete bridges.
- **Fiber reinforced concrete**
  Fiber reinforcement consists of short pieces of various materials and shows no preferred reinforcing direction. The fibers reduce the shrinkage cracking, increase the stability of green concrete, and in case of glass and plastic fibers increase the fire resistance period. Applications can be found in industrial flooring, prefabricated concrete structures and air-placed concrete.

Increased initial material costs for composite structural elements are offset by reduced transportation and handling costs, reduced maintenance, and anticipated longer useful life of the entire structure. Compared to steel reinforcement, the advantages of non-metallic reinforcement can be found in

- low weight and easy handling
- reduced concrete cover
- corrosion resistance
- durability

2.5.3 Tendons

Most concrete bridges consist of prestressed concrete. The geometric cross sections and design/construction procedures used represent a broad range of possible structural design configurations. Common to all of these is the role of the prestressing reinforcement. In bridges, this reinforcement element provides the concrete structure with a means for counteracting tensile stress resulting from service loads and with the needed capacity for the strength limit state. Consequently, the prestressing reinforcement's quality and its protection against deterioration processes are paramount to attaining functional and safety requirements.

Due to their low weight, high tensile strength and good overall environmental durability, carbon fiber tendons, wires, strands, ropes and cables are increasingly being used for reinforcement of concrete structures like bridges and other large buildings. Carbon fiber tendons have shown their effectiveness as partial substitute for conventional steel tendons in external prestressed concrete bridges.

Problems regarding durability of post-tensioning tendons have been discussed in IABSE Working Commission 3 "Concrete Structures" and fib Commission 9 "Reinforcing and prestressing materials and systems". In this Chapter a short overview is given on tendon types and related defects.

2.5.3.1 Grouted tendons

The cementitious grout surrounds the tendon in an alkaline environment that will inhibit corrosion of the steel, and prevents the ingress and circulation of corrosive fluids. In case of break of a tendon, due to the bond with the grout, part of the prestress remains transmitted to

the concrete. Therefore grouted tendons are less vulnerable than ungrouted tendons to local damage. However, grouted tendons can not be visually inspected, mechanically tested or re-tensioned in the event of greater than expected loss of prestress [184].

2.5.3.2 Ungrouted tendons

Prestressing force is transmitted to the concrete, primarily, at the location of the anchorages. Corrosion is prevented by organic petroleum based greases or corrosion inhibiting compounds. These are either applied to the surface of the tendon prior to installation or injected into the tendon duct following completion of the stressing sequence. Some countries use a combination of both coating and injection. Tendons can be removed for visual inspection/replacement, mechanically tested in-situ, and retensioned to maintain prestress. Ungrouted tendons are more vulnerable than grouted tendons to local failure and corrosive fluids can circulate along the ducts. [184]

2.5.3.3 Tendon deterioration

The durability of post-tensioning systems is considerably influenced by the quality of execution, as for example the grouting for sufficient corrosion protection. Design defects are therefore mainly linked to construction defects or unsuitable techniques, or to the use o flow durability materials. Significant faults regarding the post-tensioning system in bridges are large or interconnected voids, leakage, water, chlorides and corrosion. Hence a management strategy is required for the control of such defects. Depending on the severity of the faults, this seems likely to include monitoring and further inspections but also regrouting. In the longer term some structures may be suitable for supplementary post-tensioning. Design details and measures to protect the post-tensioning systems of new bridges were described in Concrete Society Technical Report TR47, which was published in 1996 (Concrete Society 1996). New procedures to improve grouting will be helpful, as will additional protection systems (fib CEB-FIP 2001, [43]).

(1) Voids

Voids in grouted tendons that are sufficiently widespread to constitute an unbonded system or contain water, chlorides or both present a severe threat to the long-term durability of the structure. This risk is related to how well sealed voids are from the atmosphere i.e. where there is leakage this ay provide a path for water and chlorides to enter the ducts and corrode the tendons. Isolated voids in themselves are not a major problem. Where the ducts are well sealed from the atmosphere, the presence of even a thin layer of grout over the surface of the wires provides effective corrosion protection. (fib CEB-FIP 2001, [43])

(2) Tendon corrosion

The two principal construction defects responsible for corrosion are poor waterproofing and incomplete grouting of the prestressing ducts. Serious corrosion problems can occur where tendons are inadequately protected whether due to poor detailing or poor workmanship exacerbated by inadequate grouting. Corrosion is caused by the ingress of chlorides and other deleterious materials through vulnerable areas such as anchorages, joints or cracks. The

difficulty of detecting corrosion and the absence of visual evidence of deterioration in most cases means that visual inspection alone is not sufficient to determine the condition of these structures. Problems with externally bonded tendons have occurred where chlorides have gained access into the concrete box section. Further durability problems may occur with internal grouted tendons in the future as the corrosion protection provided t-date begins to break down and moisture and chlorides gain access over time. It is possible to improve the corrosion protection by using thick-walled ribbed PE-PP sheathings or more recently by electrically isolating the tendons. (fib CEB-FIP 2001, [43])

Due to delayed steel ruptures of quenched and tempered steel "Sigma" and "Neptun" the reputation of the prestressed concrete construction was damaged. However, today it is known that in bridge construction sufficient minimum ordinary reinforcement rather robustness reinforcement always exists and the nowadays-approved prestressing steels do not react oversensitive to stress corrosion. (fib CEB-FIP 2001, [43])

(3) Anchorage faults

In case of external post-tensioning the transfer of prestressing force is mostly performed via brackets/disks. National and international regulations as well as the optimizing of the multifunctional anchorage parts led to an approach of the different tensioning systems, see VSL, Freyssinet, SUSPA, DSI etc. Even a prestressing possibility in the free length is given by special intermediate anchors. For all systems a possibility of removal must be feasible and proven (fib CEB-FIP 2001, [43]).. In post-tensioned, ungrouted systems, the tendons and anchorage components are normally protected from corrosion by a layer of thick viscous grease, which is applied at the time of installation.

The presence of aggressive water in the ducts often results from bleeding. Bleeding is a separation of fresh concrete, where the solid content sinks down and the displaced water rises or penetrates in inner hollows. In the bleeding water significantly high contents of sulphates and increased quantities of chlorides may be accumulated by leaching of the construction materials cement, aggregates and water. The bleeding water penetrates into the ducts through poor sealed anchorages, couplings and defects in the sheet and accumulates at the deepest points (fib CEB-FIP 2001, [43]).. Thus consideration needs to be given to encapsulation of anchorages in corrosion resistant materials, use of corrosion inhibitors in surrounding concrete, and use of very low permeability, high performance concrete mixtures.

Inspection results today indicate that, outside the anchorage zone of the rebar (generally the end sections of the rebar), substantial loss of steel or bond do not necessarily reduce the element strength significantly; ductility and stiffness are affected to a greater extent. In the anchorage zone, all mechanical properties are more sensitive to corrosion damage.

2.5.3.4 Damage detection

A methodical, quantitative, field-applied engineering basis for evaluating and maintaining the prestressed concrete bridge infrastructure's reliability has long been pursued. Availability of a nondestructive testing or imaging technique could consolidate and simplify the application of periodic measurements and inspections of prestressed concrete bridges (Ciolko, Tabatabai 1999, [29]).

The NCHRP Web Document 23 (Ciolko, Tabatabai 1999, [29]) documents the feasibility of various NDT systems based on scientific examination of the state of the art. The report also presents an assessment of the technology horizon with respect to promising nondestructive

testing and evaluation concepts and documents the research team's recommendations for future research.

Overview of NDE Methods for Condition Evaluation of Prestressing Steel Strands in Concrete Bridges (Ciolko, Tabatabai 1999, [29]):

- Ultrasonic Defect Detection
- Pulsed Eddy Current
- Acoustic Emission (Prestressing Wire Break Monitoring)
- Surface Spectral Resistivity Method
- Nonlinear Vibro-acoustic Method
- Electrical Time Domain Reflectrometry (ETDR)
- X-Ray Diffraction for Direct Stress Measurements
- Strain Relief for Prestress Measurements
- Imaging and Tomographic Systems
- Magnetostrictive Sensors
- Magnetic Flux Leakage
- Power Focusing Ground Penetrating Radar

Fig. 2-16: Significant corrosion of tendon and ruptured strands (PE pipe and grout removed), (Evans, Bollmann 2000, [41])

Fig. 2-17: Tendon anchorage after removal of sheath, (Vollrath, Tathoff 1990, [152])

Fig. 2-18: Bridge inspection, (Vollrath, Tathoff 1990, [152])

3 Visual inspection & conventional in-situ material testing

The visual inspection is the first step necessary for the condition assessment of structures. By the means of visual inspection an overall impression should be obtained of all symptoms of deterioration including the identification of actual and potential sources of trouble. All the activities leading to the final choice of a rehabilitation strategy for a damaged bridge are initiated at this stage.

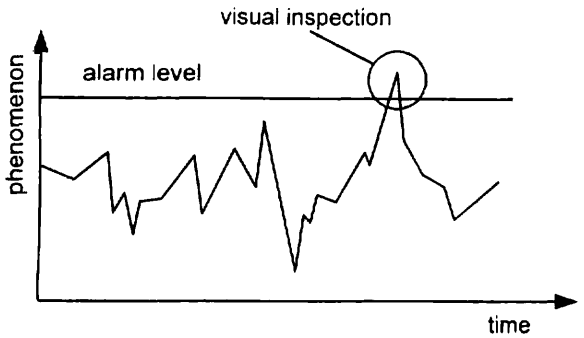

Fig. 3.1: Event triggering for visual inspection

In order to ensure an optimum collection of information an inspection concept is needed, including:

- Description of the structure
- Historical information, (including previous inspection reports)
- Access equipment needed (tower wagon or scaffold) – lane closure, necessary downtimes
- Possible removal of everything that prevents good visual access
- Inspection equipment
- Competences & responsibilities

When searching historical information of a construction special attention should be paid to all kinds of modification the construction may have suffered. It is obvious that the research of historical information does not only concern the time of construction, but its complete lifetime.

Inspections which may significantly interfere with normal traffic movement and which might affect the safety of the inspectors must be coordinated with district personnel in order that appropriate traffic control measures may be undertaken. Inspections of the underside of bridges that cannot be reached by conventional ladders may be performed by the use of vehicles with under-bridge platforms. (Texas Department of Transportation 2001, [141])

During the visual inspection special attention needs to be paid to various factors, including:

- Verification of information gathered during the planning of the assessment
- Old coatings, impregnations or protections
- The appearance of the original concrete surface
- Differences of the color of the concrete surface
- The presence of cracks, their appearance and pattern
- Superficial deterioration of the concrete skin
- Deterioration of the concrete itself

- Exposed rebars
- Deformations of the structure
- Presence of humidity or water, leakages, etc.
- Fouling (algae, moss, tresses)

The findings must be described in detail as they form the basis for any consequent measures. In addition, it may be useful to state the name of the inspector, as well as the names of all that may have been in attendance.

Visual inspection is a primary component of both routine and in-depth inspections.

3.1 Routine inspection

The routine inspection is a visual inspection of all visible parts of the structure. The inspection should be carried out by a highly experienced bridge engineer. The purpose is to maintain an overview of the general condition of the whole infrastructure stock, and to reveal significant damage in due time, so that rehabilitation works can be carried out in the optimum way and at the optimum time, taking safety and economic aspects into consideration.

One set of information generated during a routine inspection is a series of "condition ratings" assigned to the various structural components. These condition ratings give an overall measure of the condition of a structure by considering the severity of deterioration in the structure and the extent to which it is distributed throughout each component. The ratings assigned to each element are based on a standard set of definitions associated with numerical ratings.

The equipment needed for routine bridge inspections usually includes the following (Texas Department of Transportation 2001, [141]):

- Cleaning tools including wire brushes, screwdrivers, brushes, scrapers, etc.
- Inspection tools including pocketknife, ice pick, hand brace, bit, and increment borer for boring timber elements, chipping hammer, etc.
- Visual aid tools including binoculars, flashlight, magnifying glass, dye penetrant, mirror, etc.
- Basic measuring equipment including thermometer, center punch, simple surveying equipment, etc.
- Recording materials such as appropriate forms, field books, cameras, etc.
- Safety equipment including rigging, harnesses, scaffolds, ladders, bosun chairs, first-aid kit, etc.
- Miscellaneous equipment should include C-clamps, penetrating oil, insect repellant, wasp and hornet killer, stakes, flagging, markers, etc.

3.1.1 Inspection of concrete members

Common concrete member defects include cracking, scaling, delamination, spalling, efflorescence, popouts, wear or abrasion, collision damage, scour, and overload. The inspection of concrete should include both visual and physical examination. (Chen, Duan 2000, [27])

3.1.1.1 Crack detection

Two of the primary deteriorations noted by visual inspections are cracks and rust stains. Cracking in concrete is usually large enough to be seen with the bare eye, but it is recommended to use a crack gage to measure and classify the cracks. Cracks are classified as hairline, medium, or wide cracks. Hairline cracks cannot be measured by simple means such as pocket ruler, but simple means can be used for the medium and wide cracks. Hairline cracks are usually insignificant to the capacity of the structure, but it is advisable to document them. Medium and wide cracks are significant to the structural capacity and should be recorded and monitored in the inspection reports. Cracks can also be grouped into two types: structural cracks and nonstructural cracks. Structural cracks are caused by the dead- and live-load stresses. Structural cracks need immediate attention, since they affect the safety of the bridge. Nonstructural cracks are usually caused by thermal expansion and shrinkage of the concrete. These cracks are insignificant to the capacity, but these cracks may lead to serious maintenance problems. For example, thermal cracks in a deck surface may allow water to enter the deck concrete and corrode the reinforcing steel. The length, direction, and extent of the cracks and rust strains should be measured and reported in the inspection notes (Chen, Duan 2000, [27]).

(1) Measuring the crack width

Crack width measurements may occasionally be required, and these will normally be made with a microscope or similar instrument. The magnified crack widths may be measured directly by comparison with an internal graduated scale, which is visible through the eyepiece. A simple unmagnified comparator scale can also be used to assist in the estimation of crack widths. Measuring crack widths over a longer period might exhaust the inspector. Thus it is recommended to measure a crack's width three times over a distance of about 100 millimeters to avoid a high error rate (Bundesministerium für wirtschaftliche Angelegenheiten 1987, [18], Institut für Konstruktiven Ingenieurbau 1997, [64]).

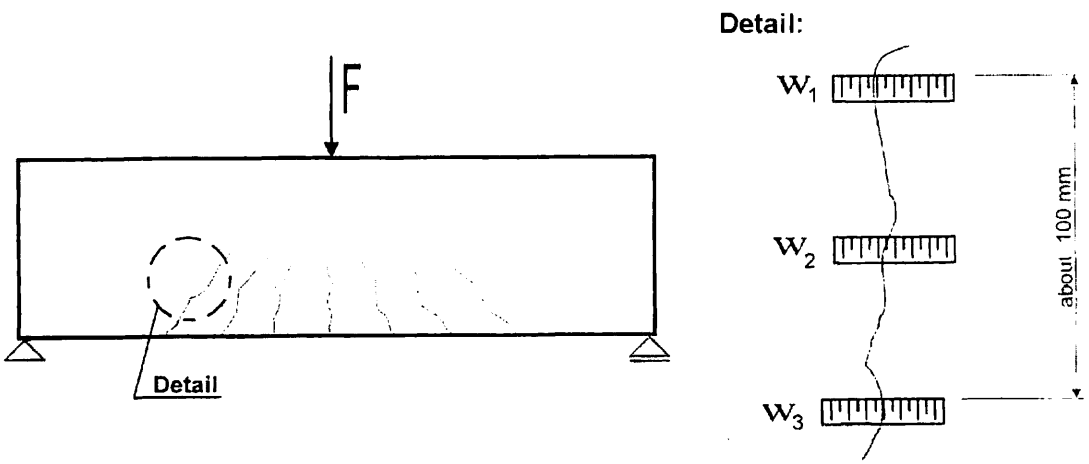

Fig. 3-2: Measuring the crack width, (Institut für Konstruktiven Ingenieurbau 1997, [64])

The average value of the three measurements can be calculated to obtain the final authoritative crack width ($\bar{\omega}$) for each crack, (Institut für Konstruktiven Ingenieurbau 1997, [64]):

$$\bar{\omega} = \sum_{i=1}^{3} \frac{\omega_i}{3}$$

3.1.1.2 Detection of delaminations

Delamination occurs when layers of concrete separate at or near the level of the top or outermost layer of reinforcing steel. The major cause of delaminations is the expansion or the corrosion of reinforcing steel due to the intrusion of chlorides or salts. Hammer sounding is used to detect areas of unsound concrete and usually used to detect delaminations. Tapping the surfaces of a concrete member with a hammer produces a resonant sound that can be used to indicate concrete integrity. Areas of delamination can be determined by listening for hollow sounds. The hammer sounding method is impractical for the evaluation of larger surface areas. For larger surface areas, chain drag can be used to evaluate the integrity of the concrete with reasonable accuracy. Chain drag surveys of deck are not totally accurate, but they are quick and inexpensive. There are other advanced techniques available for concrete inspection described in Chapter 4. (Chen, Duan 2000, [27])

3.1.2 Inspection of metallic members

Common steel and iron member defects include corrosion, crack, collision damage, and overstress. Cracks usually initiate at the connection detail, at the termination end of a weld, or at a corroded location of a member and then propagate across the section until the member fractures. Since all of the cracks may lead to failure, bridge inspectors need to look at each and every one of these potential crack locations carefully. (Chen, Duan 2000, [27])

The most recognizable type of steel deterioration is corrosion. The cause, location, and extent of the corrosion need to be recorded. This information can be used for rating analysis of the member and for taking preventive measures to minimize further deterioration. Section loss due to corrosion can be reported as a percentage of the original cross section of a component. The depth of the defect can be measured using a straightedge ruler or caliper. (Chen, Duan 2000, [27])

One of the important types of damage in steel members is fatigue cracking. Fatigue cracks develop in bridge structures due to repeated loadings. Since this type of cracking can lead to sudden and catastrophic failure, the bridge inspector should identify fatigue-prone details and should perform a thorough inspection of these details. For painted structures, breaks in the paint accompanied by rust staining indicate the possible existence of a fatigue crack. If a crack is suspected, the area should be cleaned and given a close-up visual inspection. Additionally, further testing such as dye penetrant (see Chapter 4.3) can be done to identify the crack and to determine its extent. If fatigue cracks are discovered, inspection of all similar fatigue details is recommended. (Chen, Duan 2000, [27])

Symptoms of damage due to overstress are inelastic elongation (yielding) or decrease in cross section in tension members, and buckling in compression members. The causes of the overstress should be investigated. The overstress of a member could be the result of several factors such as loss of composite action, loss of bracing, loss of proper load-carrying path, and failure or settlement of bearing details. (Chen, Duan 2000, [27])

Similar to concrete members, there are advanced destructive and nondestructive techniques available for steel inspection. Some of the nondestructive techniques are described in Chapter 4.

Visual inspection is not confined to the surface, but may also include examination of bearings, expansion of joints, drainage channels, post-tensioning ducts and similar features of a structure.

3.2 In-depth inspection

In-Depth Inspections are usually performed as a follow-up inspection to a Routine Inspection to better identify any deficiencies found (Texas Department of Transportation 2001, [141]). A testing program for reinforced concrete structures that supplements visual observations may include obtaining and testing cores and samples for compressive strength, chloride ion content, depth of carbonation, pH value, and petrographic examinations. Load testing may also sometimes be performed as part of an In-Depth Inspection. (Texas Department of Transportation 2001, [141])

3.2.1 Concrete strength

The compressive strength of concrete in existing structures can be determined efficiently by testing drill cores or non-destructively by performing sclerometer tests. Testing drill cores is the most direct and reliable way of concrete strength testing. However this method is labour-intensive and partially damaging the structure. After removing the drill core the remaining hole needs to be closed carefully in order to avoid further damage. It is recommended to use epoxy or cement mortar. Alternatively pull-out tests can be performed to estimate concrete strength.

3.2.1.1 Difference between prism and cube strengths

Compressive strength tests may be performed on cylindrical or cubical specimens. It is recommended to use either cylinders with a diameter of 150 mm and a height of 300 mm, or to use cubes with a side length of 150 mm for the tests. However strength properties of a concrete specimen depend on its size and shape. In order to compare the results obtained from different specimen shapes the following equations apply:

Low strength concrete, C 20/25: $f_{cyl150} = \frac{1}{1.25} f_{cube150}$

High strength concrete, C 50/60: $f_{cyl150} = \frac{1}{1.20} f_{cube150}$

Conversion factors for different cube sizes:

$$f_{cube100} = \frac{1}{0.95} f_{cube150}$$

$$f_{cube150} = \frac{1}{0.95} f_{cube200}$$

It is recommended to determine the compressive strength of aged concrete by taking the average of at least 3 individual tests. Further it has to be mentioned that concrete in specimens may differ from that in the actual structure as a result of different curing and compaction conditions. Results obtained from drill cores may be compared with cube specimens using the following equation.

$$f_{cube200} = 0.95 f_{cube150} \approx f_{core100} = f_{core150}$$

3.2.1.2 Testing drill cores

When testing the drill cores it has to be taken into account that the results are size and geometry dependent. The smaller the core the higher the compressive strength.

Fig. 3-3 shows the compressive strength versus the size of the specimen. By using empirical relationships like the one in Fig. 3-4 the compressive strength values obtained at different sizes can be compared to each other.

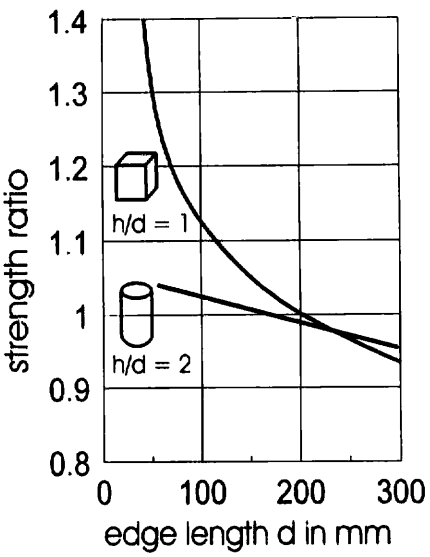

Fig. 3-3: Influence of specimen size on compressive strength (Schickert 1981)

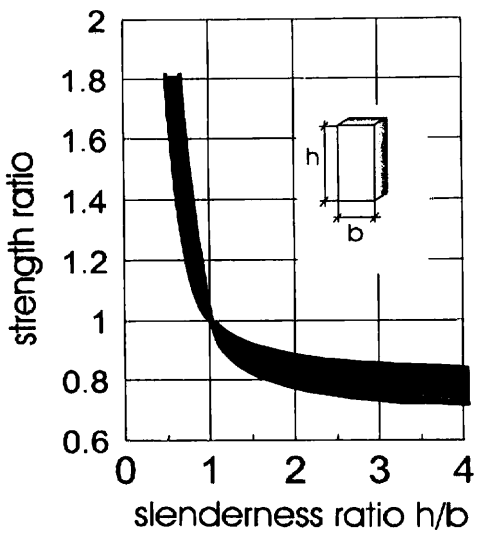

Fig. 3-4: Influence of the slenderness ratio on compressive strength (Schickert 1981)

In addition, the compressive strength depends on the slenderness of the specimen. Fig. 3-4 shows the compressive strength versus the specimen slenderness as obtained for different ratios of specimen height to specimen diameter (slenderness ratio). Such curves can be used for transforming the experimentally determined compressive strengths to a standard value for the slenderness ratio equal to one.

The drill cores can be used for determining the modulus of elasticity and other mechanical properties too.

3.2.1.3 Sclerometer method

A non-destructive technique for determining the compressive strength at concrete surfaces is the sclerometer method, see Fig. 3-5. The metal bolt at the tip of the sclerometer is adjusted normal to the concrete surface. Then, inside the device a certain weight is accelerated by a

spring and hits the metal bolt. The harder the concrete surface the more kinetic energy the bounced back weight will have. This energy is measured by recording the distance the weight is moving backward against the spring.

A combination of the drill core and the sclerometer method is in most of the practical cases an efficient way for determining the compressive strength. A small number of drill cores should be taken from the structure. In addition, by using a sclerometer at a large number of different spots the homogeneity of the material can be evaluated. In this way an overall information on the concrete strength is obtained.

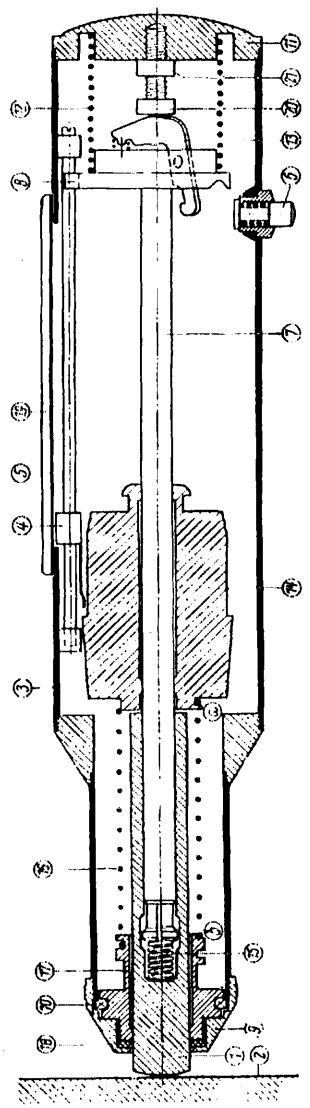

Fig. 3-5: Sclerometer (Hiese, Knoblauch 1988)

3.2.1.4 Pull-out test

The principle behind the test method is that the force required to pull a bolt or some similar device out of concrete can be correlated with the concrete's compressive strength. There are two basic categories of pull-out test; those which involve an insert already cast into the concrete, and those which offer the greater flexibility of an insert fixed into a hole drilled into the hardened concrete (Bundesministerium für wirtschaftliche Angelegenheiten 1987, [18]).

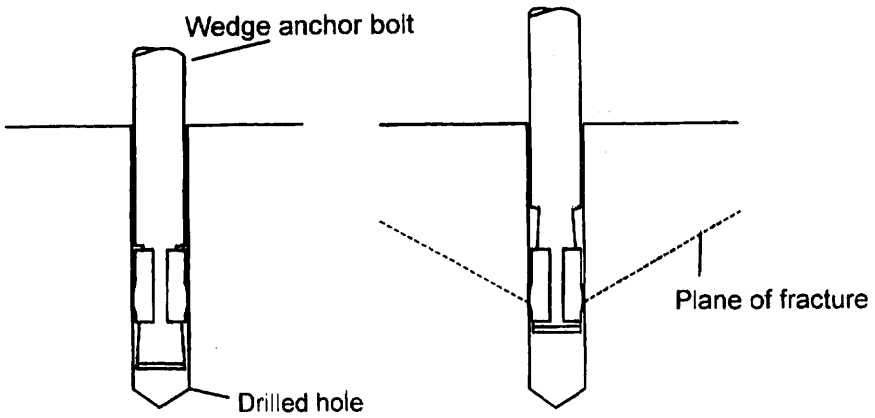

Fig. 3-6: Pull-out test (Bundesministerium für wirtschaftliche Angelegenheiten 1987, [18])

From the peak tensile force recorded by the loading equipment, and by using an empirical correlation chart, the equivalent concrete cube strength can be estimated. Although the results will relate to the surface zone only, the approach offers the advantage of providing a more direct measure of strength and at a greater depth than surface hardness testing by rebound methods, but still requires only one exposed surface (Bundesministerium für wirtschaftliche Angelegenheiten 1987, [18]).

Furthermore, the concrete strength can be estimated non-destructively by measuring the ultrasonic velocity (see Chapter 4.1.3).

3.2.1.5 Pull-off test

This approach has been developed to measure the in-situ tensile strength of concrete by applying a direct tensile force (Bundesministerium für wirtschaftliche Angelegenheiten 1987, [18]). The test can easily be executed on site. The choice of the test locations can be based on the results of the visual inspections or by the results of the concrete surface hardness test. The results of the hammer sounding may indicate areas in which spalling occurs. In these areas pull-off tests have no use at all. (CEB-FIP 1998, [22])

A circular steel disk is glued to the surface on which load is applied through a manually operated jack that bears against the concrete surface through a reaction ring. The fracture surface will be below the concrete surface and will thus leave some surface damage that must be repaired (Bundesministerium für wirtschaftliche Angelegenheiten 1987, [18]).

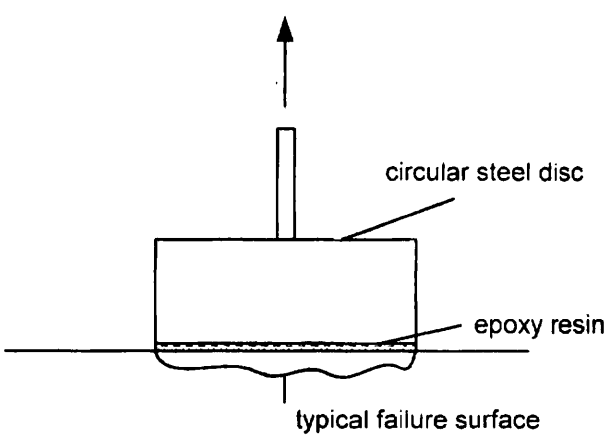

Fig. 3-7: Pull-off test(Bundesministerium für wirtschaftliche Angelegenheiten 1987, [18])

A nominal tensile strength for the concrete is calculated on the basis of the disk diameter, and this may be converted to compressive strength using a calibration chart appropriate to the concrete (Bundesministerium für wirtschaftliche Angelegenheiten 1987, [18]). One key feature of this method is that small changes in compressive strength are easily detected. Also concrete variables such as aggregate type do not significantly affect the correlation. In general, due to relative differences in curing and compaction, concrete at the top of a pour is less strong than that at the bottom, so strengths derived from testing the top surface may be considered to be conservative.

Different tests to determine concrete tensile strength are available, but most of these tests are executed in a laboratory.

3.2.2 Steel strength

The presentation of non-destructive evaluation and monitoring methods for mild and post-tensioning steels is the main purpose in this Chapter. In the following a very short overview on tests that can be performed if steel specimens from the actual structure are available is given. Of course these tests are only possible if pieces of the reinforcement of the structure can be extracted. For mild steels this is very often not a problem but it is much more difficult for post-tensioning tendons which are structural elements essential for the safety, serviceability and durability of a prestressed concrete structure. Thus, non-destructive techniques which allow for a reliable assessment of the properties of the post-tensioning steels without damaging the structure are very desirable.

If specimens from the structure are available the following tests can be performed to determine the main material properties of the steels:

- Static tensile tests: Yield and tensile strengths as well as strains, contraction values and Young's modulus can be determined by standard tensile tests. It has to be noticed that some minor corrosion does not effect the strength properties of the steels. Only if strong corrosion is present the ductility of the steel is influenced.
- Relaxation tests: Relaxation properties of steels can be determined according to ISO 15630-3 with a loading equivalent to 70 % of the effective tensile strength and a maximum allowable decrease in stress of 2.5%. These tests are especially important for high strength post-tensioning steels.
- Fatigue tests: To determine the fatigue strength of post-tensioning steels standard tests can be performed. This is especially important if dynamic loading is present on a structure as the strength of the steel is decreased as the number of load cycles increases. The results of fatigue test are visualized as Wöhler-lines or as Smith-diagrams. The influence of corrosion is clearly shown in the fatigue tests, as corrosion considerably decreases the fatigue strength. For mild steel reinforcement embedded in concrete the determination of the fatigue strength is of less importance.
- Corrosion tests: These tests are mainly used for post-tensioning steels if the sensitivity of the steels to hydrogen embrittlement is of interest. Two different types of corrosion tests exist. In the FIP test a concentrated ammoniumthiocyanate (NH_4SCN) solution is used and the specimens are loaded with a constant load equivalent to 80% of the tensile strength. The testing temperature is 50°C. The time until failure of the specimen is recorded, otherwise the test is stopped after 500 hours. The FIP test was developed for post-tensioning strands and due to the highly concentrated solution usually leads to a rather quick failure of the steel tested. The second test is the so-called DIBt test. These tests last up to 2000 hours and a thinned NH_4SCN solution is employed which should better reflect the chemical conditions in an actual structure. The other testing

parameters are the same as for the FIP test. If a steel lasts longer than 2000 hours in the testing solution the steel is not sensitive to hydrogen embrittlement.

3.2.3 Carbonation depth

For evaluating the possibility of corrosive damage to the surface it is necessary to measure the depth at which the carbonation has decreased the pH-value below the critical level. There are two ways for determining the carbonation depth:

1) A new fracture surface (perpendicular to the external concrete surface) is sprinkled by a liquid indicator, preferably Phenolphthalein. In the basic region the indicator changes its colour into a pink shade, see Fig. 3-8. The line between the colourless and the pink surface marks the carbonation depth. The fracture surface can be obtained by splitting a drill core. It is not advisable to use the surface of the drill core because the $Ca(OH)_2$ is being smeared over the core surface during the wet drilling process.
2) Using a standard drill bit some pulverised material is removed from the structure and preserved in distinct portions according to the drilling depth. Then the material is mixed with water and the mixtures pH-values are determined. The drill bit method is recommended for determining the pH-value of the grouting mortar in tendon ducts too.

3.2.4 Chloride determination

For determining the chloride content a pulverised sample is given into an acid solution and than a quantitative analysis is carried out. The acid solution is necessary for dissolving chlorides out of water resistant salts. By doing this a conservative value of the chloride content is determined which even after carbonation of the concrete will not be exceeded. The allowable value amounts 0.2% to 0.4% of the cement mass.

Fig. 3-8: Determination of carbonation depth with Phenolphthalein, (Vollrath, Tathoff 1990, [152])

Fig. 3-9: Qualitative determination of Chloride ingress, (Vollrath, Tathoff 1990, [152])

4 Non destructive evaluation (NDE)

Structures are checked for any sudden damage or deterioration such as signs of settlements or displacements, damage on slabs, girders, railings, columns or piers due to impact from traffic, erosion of slopes etc. For the registration of any kind of failure or damage observed, specially prepared forms are filled in, photos taken and the material handed over to the responsible engineer for further action.

Currently available methods for evaluating bridge decks include inspecting the deck condition visually, sounding a bare deck with a chain or hammer, measuring the half-cell potential of the deck, and taking cores. All these methods may require lane closure and have limited ability to determine the internal condition of the deck over the entire deck area. In addition, these methods are not effective in accurately determining the exact location and extent of delaminations in a bridge deck, and they are difficult to apply rapidly to a large number of bridge decks (Washer 2000, [155]).

Typical techniques used for bridge inspection include:

- Visual testing (VT)
- Penetrant testing (PT)
- Magnetic particle testing (MP)
- Radiographic testing (RT)
- Ultrasonic testing (UT)
- Impact echo (IE)
- Acoustic emission (AE)
- Eddy current testing (ET)
- Rebar locator (RL)

4.1 Concrete evaluation

4.1.1 Radiographic testing

Radiographic systems can be used for the detection of broken wires in cable-stayed bridges, imaging of post-tensioning strands in concrete beams, and the detection of voids in the grouted post-tensioning ducts (Washer 2000, [155]). The method may be used for detecting both surface and subsurface defects (Gosh 2000, [49]).

The system essentially consists of passing x-rays or gamma rays through the member being tested and creating an image on a photosensitive film. If there is a crack in the member or a void in the weld, less radiation is absorbed by the steel and more radiation passes through that area to the film. Thus the defects are shown on the film as dark lines or shaded areas, compared to the surrounding areas of sound material. This method has an advantage of providing a permanent record for every test carried out. However, it requires specialized knowledge in selecting the angles of exposure and also in interpreting the results recorded on the films. It also requires access from both sides of the test area, with the radiation source placed on one side and the film placed on the other side (Gosh 2000, [49]).

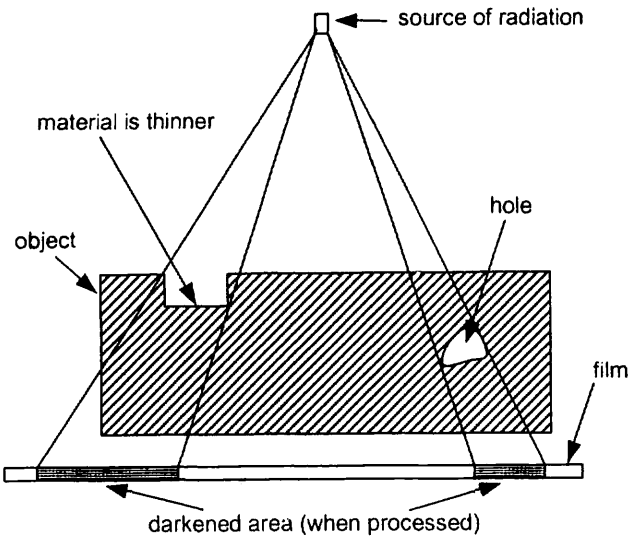

Fig. 4-1: Radiographic testing

4.1.2 Ultrasonic pulse echo

The ultrasonic Impulse-Echo-Method is based on measuring the time difference between sending of an impulse and receiving the echo, see Fig. 4-2. In addition, the intensity of the echo is measured. An electro-mechanical transducer is used to generate a short pulse of ultrasonic stress waves that propagates into the object being inspected. Reflection of the stress pulse occurs at boundaries separating materials with different densities and elastic properties. The reflected pulse travels back to the transducer that also acts as a receiver.

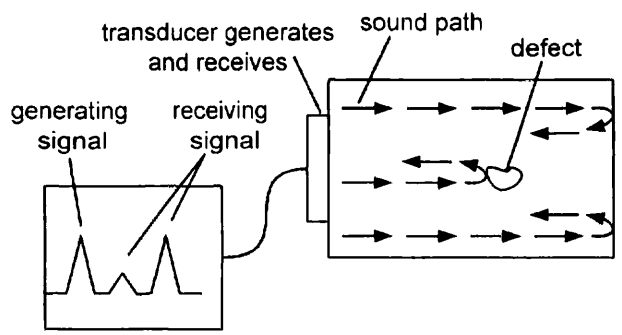

Fig. 4-2: Ultrasonic testing

The received signal is displayed on an oscilloscope, and the round trip travel time of the pulse is measured electronically. The results are displayed in a time-position-plot, see Fig. 4-3. If the ultrasonic velocity is known, the time can be related to the location of the flaw causing the echo.

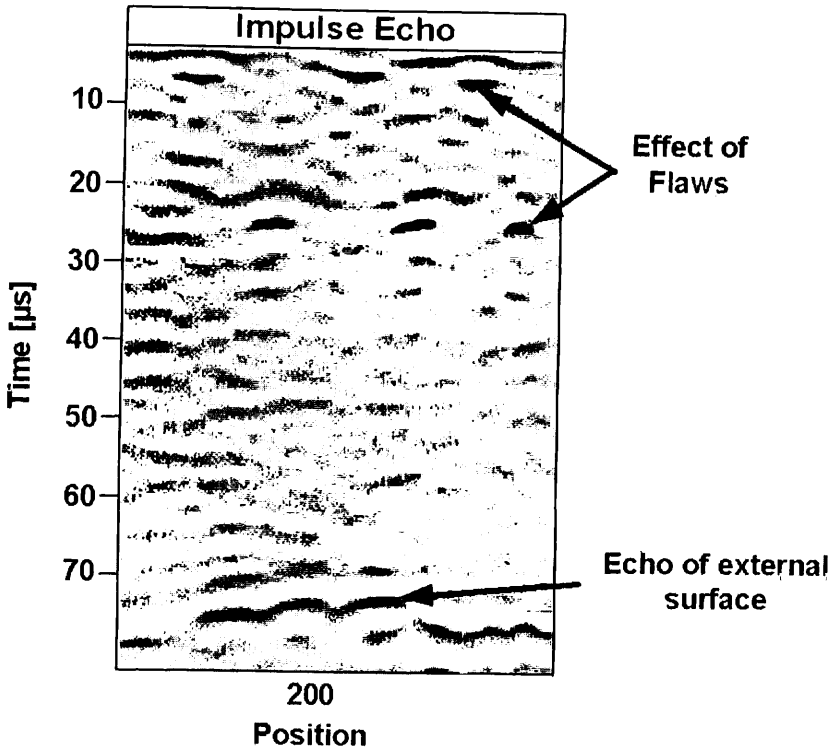

Fig. 4-3: Position-time plot obtained by using the Impulse-Echo-Method

The performance of the Impulse Echo-Method can be significantly increased by using an array of sensors instead of a single sensor (Jahnson, Kroggel, Ratmann 1995).

In nondestructive testing of metals, the ultrasonic pulse-echo (UP-E) technique has proven to be a reliable method for locating cracks and other internal defects. Attempts to use UP-E equipment designed for metal inspection to test concrete have been unsuccessful because of the heterogeneous nature of concrete (Carino and Sansalone, 1984). The presence of paste-aggregate interfaces, air voids, and reinforcing steel results in a multitude of echoes that obscure those from real defects (Carino 2001, [20]). However, for investigating the homogeneity in concrete walls or slabs with constant thickness the measurement of the ultrasonic velocity has proved to be an efficient method.

4.1.3 Ultrasonic pulse velocity method

Ultrasonic pulse velocity method measures the time of travel of an ultrasonic pulse passing through the concrete. The fundamental design features of all commercially available units are very similar, consisting of a pulse generator and a pulse receiver. Pulses are generated by shock-exciting piezo-electric crystals, with similar crystals used in the receiver. The time taken for the pulse to pass through the concrete is measured by electronic measuring circuits.

Pulse velocity tests can be carried out on both laboratory-sized specimens and completed concrete structures, but some factors affect measurement:

1) There must be smooth contact with the surface under test; a coupling medium such as a thin film of oil is mandatory.
2) It must be recognized that there is an increase in pulse velocity at below-freezing temperature owing to freezing of water; from 5 to 30°C (41 - 86°F) pulse velocities are not temperature dependent.

3) The presence of reinforcing steel in concrete has an appreciable effect on pulse velocity. It is therefore desirable and often mandatory to choose pulse paths that avoid the influence of reinforcing steel or to make corrections if steel is in the pulse path.

Ultrasonic pulse velocity tests have a great potential for concrete control, particularly for establishing uniformity and detecting cracks or defects. Its use for predicting strength is much more limited, owing to the large number of variables affecting the relation between strength and pulse velocity.

Fairly good correlation can be obtained between concrete compressive strength and pulse velocity. These relations enable the strength of structural concrete to be predicted within ±20%, provided the types of aggregate and mix proportions are constant.

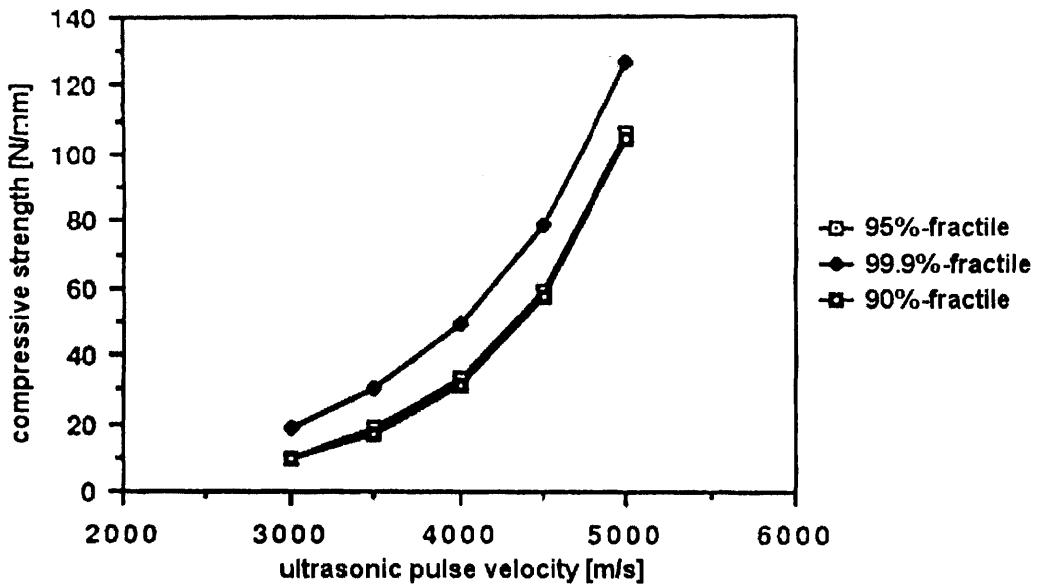

Fig. 4-4: Relation between compressive strength and pulse velocity (Bundesministerium für wirtschaftliche Angelegenheiten 1987, [18])

However, this method should be applied in combination with a destructive method only since it does not provide the required accuracy without calibration. The concrete member to be tested has to be accessible from two opposite sides. For high strength concrete the sensitivity of the method is comparatively small. The applicability of the ultrasonic strength evaluation is limited therefore to special cases only.

4.1.4 Impact echo testing

Another method for finding imperfections in concrete is the Impact-Echo-Method. It is based on using a short-duration mechanical impact to generate low frequency stress waves (2 to 20 kHz, typically) that propagate into the structure and are reflected by flaws and external surfaces (Sansalone, Sreet 1995). The impact can be produced by tapping a steel ball against the concrete surface or by hitting the surface by using a hammer, see Fig. 4-5.

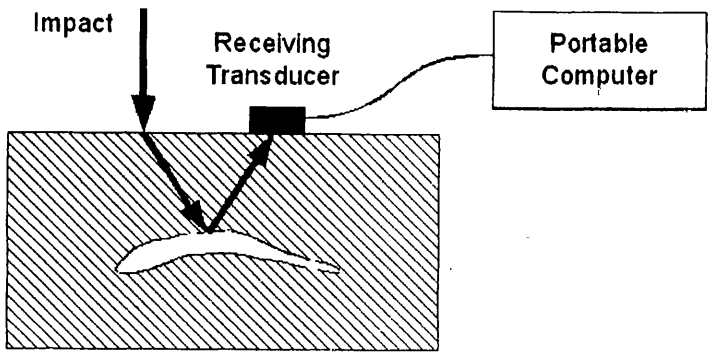

Fig. 4-5: Schematics of the Impact-Echo-Method (Sansalone, Street 1995)

As the low frequency stress waves propagate through the structure, they are reflected by air interfaces within the structure and the external surfaces of the structure. Possible air interfaces are: delaminations, voids, and cracks. Multiple reflections of the stress waves, between the impact surface, flaws, and/or other external surfaces, give rise to modes of vibration, which can be identified by frequency and used to determine the geometry of a structure or the location of flaws ([193], Jaeger, Sansalone, Poston 1997 [67], Carino 2001 [20]). A receiver, located on the surface near the location of impact, monitors the surface displacements caused by the arrival of the reflected waves (Jaeger, Sansalone, Poston 1997 [67]). The record of displacement versus time is transformed into the frequency domain for ease of signal analysis. The presence and nature of any internal flaws or external interfaces can be determined from analysis of the time-domain waveform and frequency spectrum. [193]

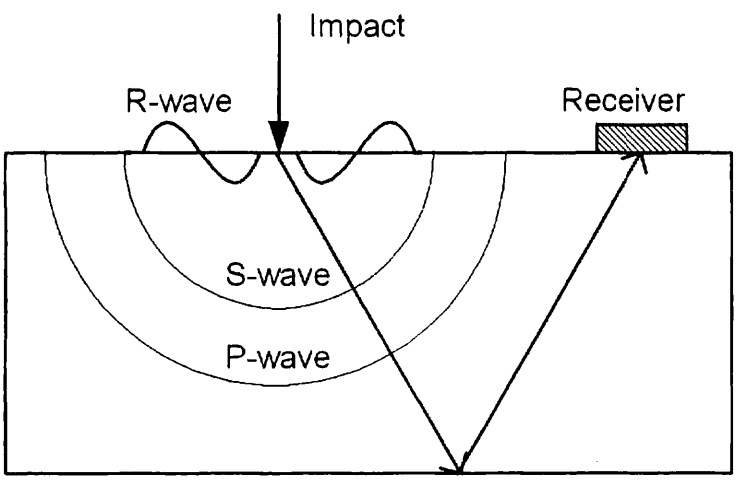

Fig. 4-6: Impact echo testing

Fig. 4-6 shows how the applied disturbance propagates through the solid as three different types of stress waves: a P-wave, an S-wave, and an R-wave. The P-wave, which is associated with the propagation of normal stress, and the S-wave, which is associated with shear stress, propagate into the solid along spherical wave fronts. In addition, there is an R-wave that travels away from the impact location along the surface (Carino 2001 [20]). Since stress wave propagation in a solid is affected directly by mechanical properties, wave speeds can be calculated based on the Young's modulus of elasticity, Poisson's ratio, and the density of the material.

When a stress wave traveling through material 1 is incident on the interface between a dissimilar material 2, a portion of the incident wave is reflected at an amplitude depending on the angle of incidence. The reflection coefficient, R, can be negative or positive depending on the relative values of the acoustic impedance of the two materials. For instance a negative reflection coefficient, such as would occur at a concrete-air interface, causes the sign of the stress in the reflected wave to be opposite the sign of the stress in the incident wave. Thus it is possible to distinguishing between reflection from a concrete-air interface and from a concrete-steel interface.

The P-wave produced by the impact undergoes multiple reflections between the test surface and the reflecting interface. Each time the P-wave arrives at the test surface, it causes a characteristic displacement. Thus the waveform has a periodic pattern that depends on the round-trip travel distance of the P-wave. In frequency analysis of impact-echo results, the objective is to determine the dominant frequencies in the recorded waveform. This is accomplished by using the fast Fourier transform technique to transform the recorded waveform into the frequency domain. The transformation results in an amplitude spectrum that shows the amplitudes of the various frequencies contained in the waveform. For plate-like structures, the thickness frequency will usually be the dominant peak in the spectrum. The value of the peak frequency in the amplitude spectrum can be used to determine the depth of the reflecting interface (Carino 2001 [20]).

Typical applications of impact-echo testing include [193]:

- Slab thickness measurements
- Detecting delaminations, cracks and voids
- Evaluating unconsolidated concrete
- Locating voids in grouted tendon ducts
- Locating subgrade voids beneath foundation slabs
- Evaluating mine shafts and tunnel liners
- Finding voids in grouted masonry
- Evaluating distributed damage in concrete

4.1.5 Infrared thermography

Infrared Thermography (IT) is a non-contact optical method, which utilizes differences in heat transfer through a structure to reveal the locations of hidden defects. Typical types of defects that can be located using IT include voids in the grout of masonry walls, delaminations in concrete slabs, and excessive moisture in wall & roof insulation. Infrared Thermography is used for the evaluation of bridge decks including the detection and quantification of delamination. However, infrared Thermography is limited by environmental conditions and has difficulty evaluating decks with asphalt overlays. The dual-band infrared Thermography using two different infrared wavelengths simultaneously overcomes some of the operational problems (primarily surface emissivity variations) encountered with standard infrared Thermography.

One of the methods selected for the bridge inspection is an active or transient Thermography. This method is dissimilar to the conventional thermographic methods in the utilization of time-dependent heating (or cooling) of the target. Depending on the type of defect and thermal characteristics of a target, an external heating or cooling is applied in the form of short energy pulses. The created thermal perturbation is then followed by a differential time-resolved infrared image analysis. (Shubinsky 1994, [133])

Coating defects, such as blistering and sub-surface corrosion spots, or excessive corrosion of the steel members can be detected in infrared images as a result of the differences in the

thermal diffusivity of the defective and nondefective areas. The temperature rise of the heated surface is governed by the amount of energy deposited and the speed of application, combined with the thermal properties of the surface material. As regards to the detection of defects, the amount of contrast observed at either surface is a function of the defect's dimensions and depth from the observed surface, the initial temperature rise and the material's thermal properties. (Shubinsky 1994, [133])

The physical phenomena behind active infrared inspection can be visualized by following propagation and detection of an induced thermal perturbation. An induced thermal "wavefront" can be imagined to flow from the exposed surface into the material. For a defect-free, homogenous material, the "wavefront" of heat passes through uniformly. However, where there are defects, such as delaminations or cracks (filled with air or an oxide), these create a higher thermal impedance to the passage of the "wavefront." Physically, when the defects are near to the surface, they restrict the cooling rate due to an insulation blocking effect, and thereby produce "hot spots." When this surface is viewed by a thermal imager, temperature differences arising from the defect's presence become clearly visible shortly after the deposition of the heat pulse. (Shubinsky 1994, [133])

The equipment required to perform active Thermography falls into tow separate areas: the heating source and the thermal imaging/analysis system. The typical heating sources utilized are pulsed quartz lamps. Thermographic analysis can be also performed by cooling the target instead of heating. The thermal/imaging analysis system typically includes IR thermographer integrated with PC-based image acquisition and processing hardware. Additional hardware can include video recorder, color printer and display monitor (Shubinsky 1994, [133]).

4.1.6 Ground-penetrating radar (GPR) systems

GPR is a pulse-echo method for measuring pavement layer thickness and other properties. It works like ultrasound, but uses radio waves rather than sound waves to penetrate the pavement. In a typical inspection application, GPR systems are used to locate structural components, like reinforcing bars embedded in concrete, to avoid wakening the structure while collecting core samples for detailed inspection. Advanced GPR, integrated with imaging technologies for use as a nondestructive evaluation tool, can provide the capability to quickly locate and characterize construction flaws and wear- or age-induced damage in these structures without the need for destructive techniques like coring. The bridge deck and its wearing surface are the most vulnerable parts of a bridge to damage from routine service, and they are particularly well suited for inspection using a vehicle-mounted inspection system (Warhus, Nelson, Mast, Johansson 1994, [154]). An advanced GPR system can reliably detect, quantify, and image delaminations in bridge decks. Such a system is designed to operate at normal highway speeds, eliminating the need for lane closure.

A mobile Ground Penetrating Imaging Radar (GPIR) gathers data for high-resolution image reconstruction of embedded defects and features. High quality image processing allows visualization of internal structure, permitting evaluation of deck conditions from the collected data using ultra-wide-bandwidth antennas and pulse generators (Warhus, Nelson, Mast, Johansson 1994, [154]). The GPR testing technique can determine pavement layer thickness as well as the presence of excessive moisture or excessive air voids in pavement layers.

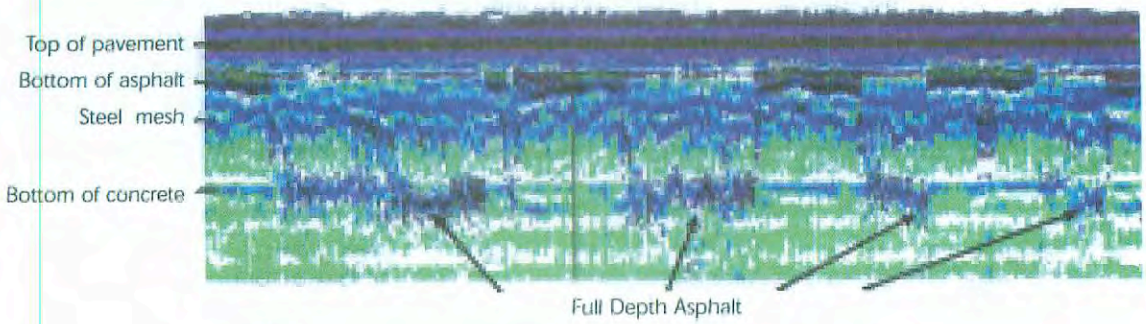

Fig. 4-7: GPR record of asphalt-overlaid concrete, showing evidence of full-depth patching in concrete [177]

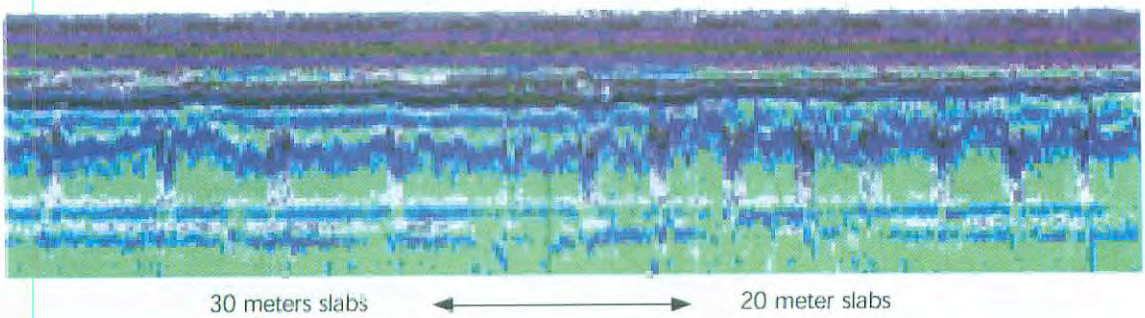

Fig. 4-8: GPR record showing transition in slab length from 30 to 20 meters [178]

The basic configuration of a mobile GPR equipment includes at least one radar antenna mounted on a GPR vehicle with a data acquisition unit. The antenna transmits pulses of radar energy into the pavement. These waves are reflected at significant layer interfaces and boundaries of dissimilar materials in the pavement. The reflected waves are captured by the system and displayed as a plot of reflection amplitude versus arrival time. The largest peak is the reflection from the pavement surface, the amplitudes before the surface reflection are internally generated noise and may be removed from the trace prior to signal processing. The reflections of significance to engineers are those that occur after the surface echo. These represent significant interfaces within the pavement, and the measured travel time is related to the thickness of the layer. Apart from determining the thickness of the surface layers from GPR data, dielectric values of surface and base layers are of particular interest as they indicate the presence of moisture and air voids in the pavement. Dielectric constants greater than 16 indicate layers saturated with water. Water has a dielectric constant of 81.

4.1.7 Acoustic Emission monitoring

Acoustic Emission (AE) refers to the generation of transient elastic waves during the rapid release of energy from localized sources within a material. The source of these emissions in metals is closely associated with the dislocation movement accompanying plastic deformation and the initiation and extension of cracks in a structure under stress. Other sources of Acoustic Emission are: melting, phase transformation, thermal stresses, cool down cracking and stress build up. [178]

The Acoustic Emission NDT technique is based on the detection and conversion of these high frequency elastic waves to electrical signals. High-frequency acoustic energy is emitted by an object when it is undergoing stress, such as when corrosion products formed on a corroding rebar push out on the concrete surrounding it. The primary advantage acoustic

emission monitoring offers over more conventional non-destructive evaluation techniques is that it results directly from the process of flaw growth. Slow crack growth in ductile materials produce few AE events, whereas rapid crack growth in brittle materials produces large quantities of high amplitude AE events. Corrosion product buildup and subsequent microcracking of the concrete represents the latter phenomenon. (Yuyama 1986, [161])

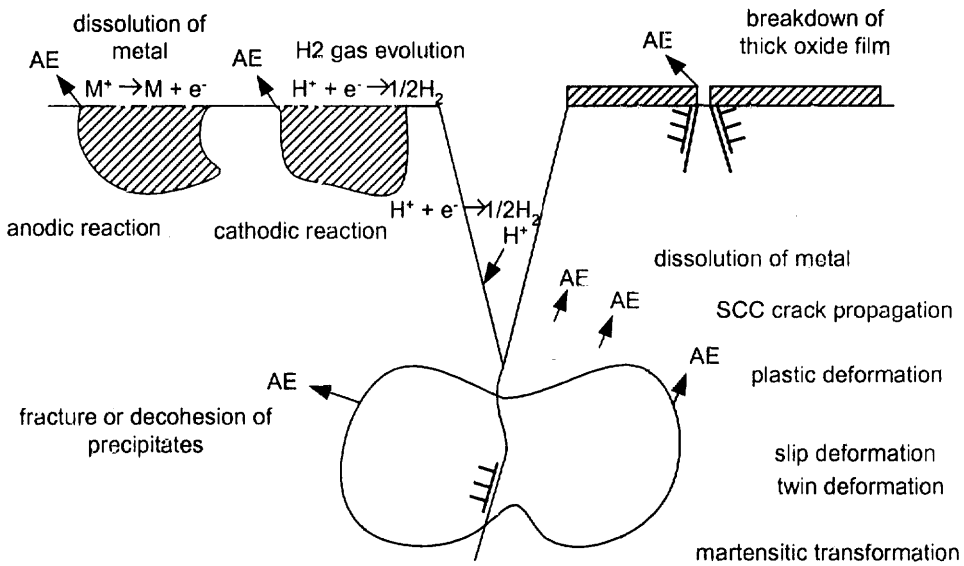

Fig. 4-9: Schematic AE sources during corrosion, stress-corrosion cracking (SCC), and corrosion-fatigue processes

A typical AE monitoring system uses piezoelectric sensors acoustically coupled to the test object with a suitable acoustic coupling medium, (grease or adhesive) and secured with tape, adhesive bonds or magnetic hold downs. The output of each piezoelectric sensor is amplified through a low-noise preamplifier, filtered to remove any extraneous noise and furthered processed by suitable electronic equipment. The AE signal is of a high frequency, as expected for rapid crack growth and is shifted between the transducers. Such a shift in the AE signals is due to the acoustic signal traversing down the rebar and should allow source location of the AE event and rebar corrosion to be calculated. (Yuyama 1986, [161])

In addition, AE monitoring detects corrosion earlier than the galvanic current and the half-cell potential measurements. (Yuyama 1986, [161])

Acoustic emission sensors [177]:

- Wideband Sensors
- High Hydrostatic Pressure Sensors
- Nuclear Radiation Resistant Sensors
- Variable Aperture Sensors
- Intrinsically Safe Sensors
- Miniature Sensors
- Water Tight and Underwater Sensors
- Rolling Sensors (Dry Contact)
- Airborne Sensors
- Unidirectional Sensors
- AE Integral Preamp Sensors

4.1.7.1 Application of AE for crack detection

The application of acoustic emission for the detection of fatigue or corrosion-fatigue cracks in steel bridge members has been under development for over a decade. Physical Acoustics of New Jersey, USA and DNL Technologies of Canada have tested their equipment on City bridges. In the early 90's NYC DOT Bridge Inspections purchased DNL AE equipment, which essentially scans for signals in the 300 KHz range under ambient excitations. The main purpose was to determine whether repairs of cracked components, such as bolted sandwich plates or drilled holes at crack tips, are effective in arresting the crack propagation. It has been recommended to combine acoustic emission with other types of monitoring, for instance, strain-gauging. Once crack locations are known, AE can monitor their activity. One major difficulty in this method's application is the inability of vehicular traffic to generate a meaningful response from the structure. (Yanev 2000, [160])

Monitoring lower frequency sound waves, such as those generated by wire breaks has become standard practice for investigating suspension and stay cables. (Yanev 2000, [160])

4.1.7.2 Electromagnetic acoustic transducers

This strain measurement technology uses electromagnetic acoustic transducers that generate and detect high-frequency stress waves in steel using electromagnetic fields. The system can measure the strain in steel members by detecting the change in travel time of stress waves. The advantages of this system are that it attaches magnetically to the steel member (very little surface preparation is required) and dynamic stress measurements can be quickly taken. (Turner-Fairbank Highway Research Center 1997, [14])

4.2 Reinforcement detection

Location and diameter of steel reinforcement can be determined destructively or non-destructively. As a result of the rapid development in non-destructive testing during the last decade several reliable methods have been proposed. Nevertheless, under certain circumstances a destructive investigation may be more efficient. In order to minimise the damage to a structure it is advisable to search for statically important and expected reinforcement only. In the case of a beam it is recommended that the concrete along a small path on the under side is removed, see Fig. 4-10. Number, diameter and concrete cover can be easily determined in this way. However, a possible second reinforcement layer in most practical cases will not be detected by using this technique.

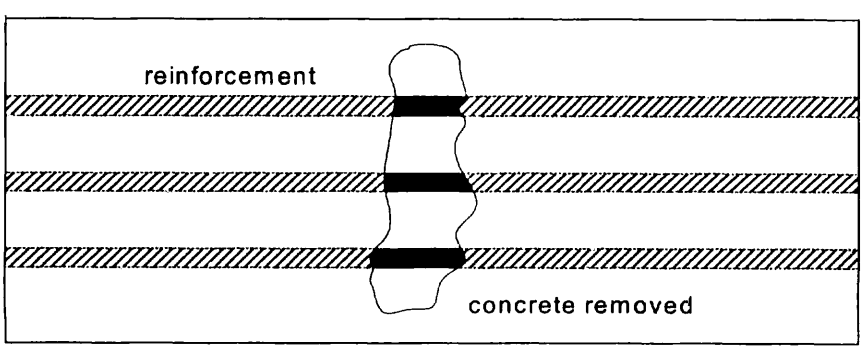

Fig. 4-10: Bottom view of a reinforced concrete beam

For detecting the steel reinforcement in concrete slabs a combined destructive and non-destructive procedure is recommended. First the position of steel bars in both directions is determined. This can be done by using a simple electro-magnetic steel detector. Then, the concrete is removed in three spots, according to Fig. 4-11. In this way it is possible to determine the steel diameters even if they are alternating.

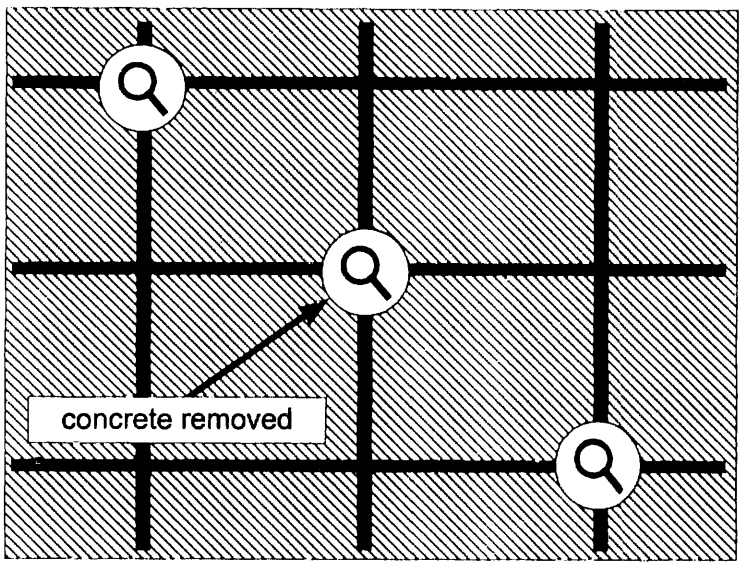

Fig. 4-11: Bottom view of a concrete slab

For the non-destructive determination of location and diameter of steel reinforcement three major groups of methods can be identified, see Table 4-1.

Methods based on	References
electro-magnetic fields	Flohrer 1995; Mehlhorn et al. 1995; Ricken et al. 1995; Alldred et al. 1995; Pöpel et al. 1995
radioactive radiation	Merkblatt B1 1990; Kapphahn 1996; Thiele 1978
Radar	Flohrer et al. 1993; Buyukozturk et al. 1995; Pöpel et al. 1995; Maierhofer et al. 1995

Table 4-1: Major non-destructive methods for the detection of steel reinforcement

4.2.1 Electro-magnetic methods

Several electro-magnetic effects have been exploited for detecting and localising steel reinforcement in concrete, see Table 4-2.

The effect of magnetic induction is the one which is predominantly used in commercial devices. State-of-the-art products allow an easy scanning of the concrete surface and generate the results in an image format, see Fig. 4-12.

Physical effect	What can be determined?	Explanation
permanent magnetism	location, concrete cover	The attractive power between the reinforcement and a permanent magnet on the concrete surface is measured.
Electro-magnetic induction	location, concrete cover, diameter	The magnetic flux is influenced by magnetic material in the electro-magnetic field.
Scattering of a magnetic field	location, concrete cover, diameter	First the reinforcement is magnetized by a permanent magnet. Then the magnetic field is measured by using a hall probe. The steel reinforcement causes a scattering of the field.

Table 4-2: Electro-magnetic methods for detecting steel reinforcement

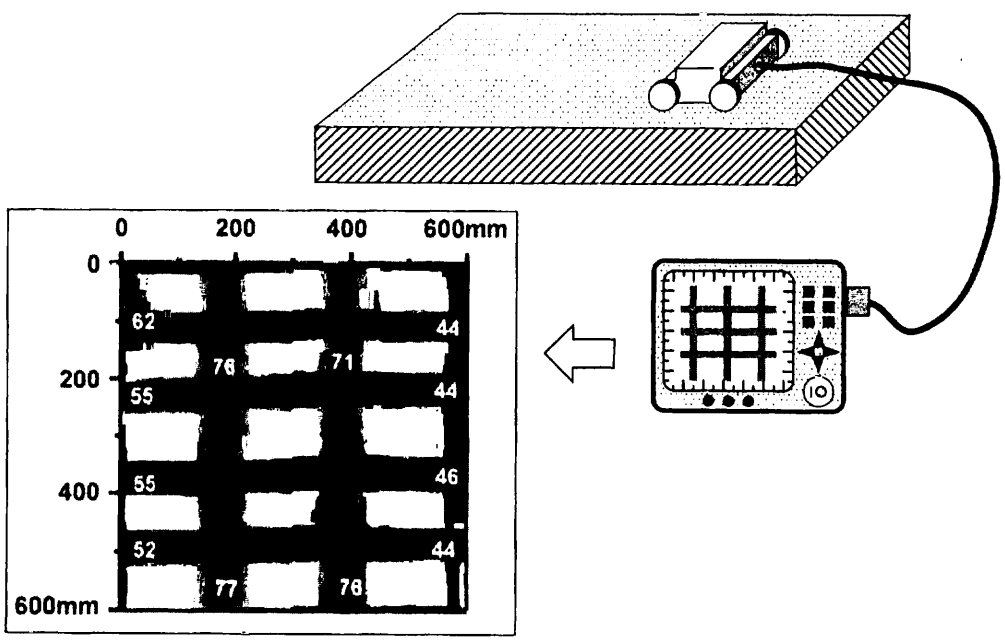

Fig. 4-12: Electro-magnetic scanning of a concrete surface

The advantages of the electro-magnetic methods are:

- The concrete cover can be determined reliably, whereas the determination of the bar diameters in practical cases sometimes causes problems.
- Results are obtained immediately. No time-consuming postprocessing is necessary.
- State-of-the art devices are cost-effective.

There are some limitations of the electro-magnetic methods:

- The methods work reliably only up to a concrete cover of about 100 mm.
- For high reinforcement ratios the resolution of the method might be not sufficient. (Bars located close to each other are detected as one bar.)

For most of the practical cases, however, the electromagnetic methods and the corresponding commercial devices are the most effective tools.

4.2.2 Radiography

If gamma or x-rays penetrate a solid sample, a portion of the radiation passes the sample, a portion will be absorbed and another part will be scattered in other directions. The absorbed portion depends on the thickness and on the density of the sample as well as on the atomic number of the material. Because of the large difference in density between concrete and steel the absorption of gamma or x-rays can be used for detecting the steel reinforcement. If the radioactive source is located on one side of the concrete member and a photographic film on the opposite side the projection of the reinforcement will appear on the film, see Fig. 4-13. If both the concrete cover and the bar diameter are unknown double exposure is a way for determining the unknowns.

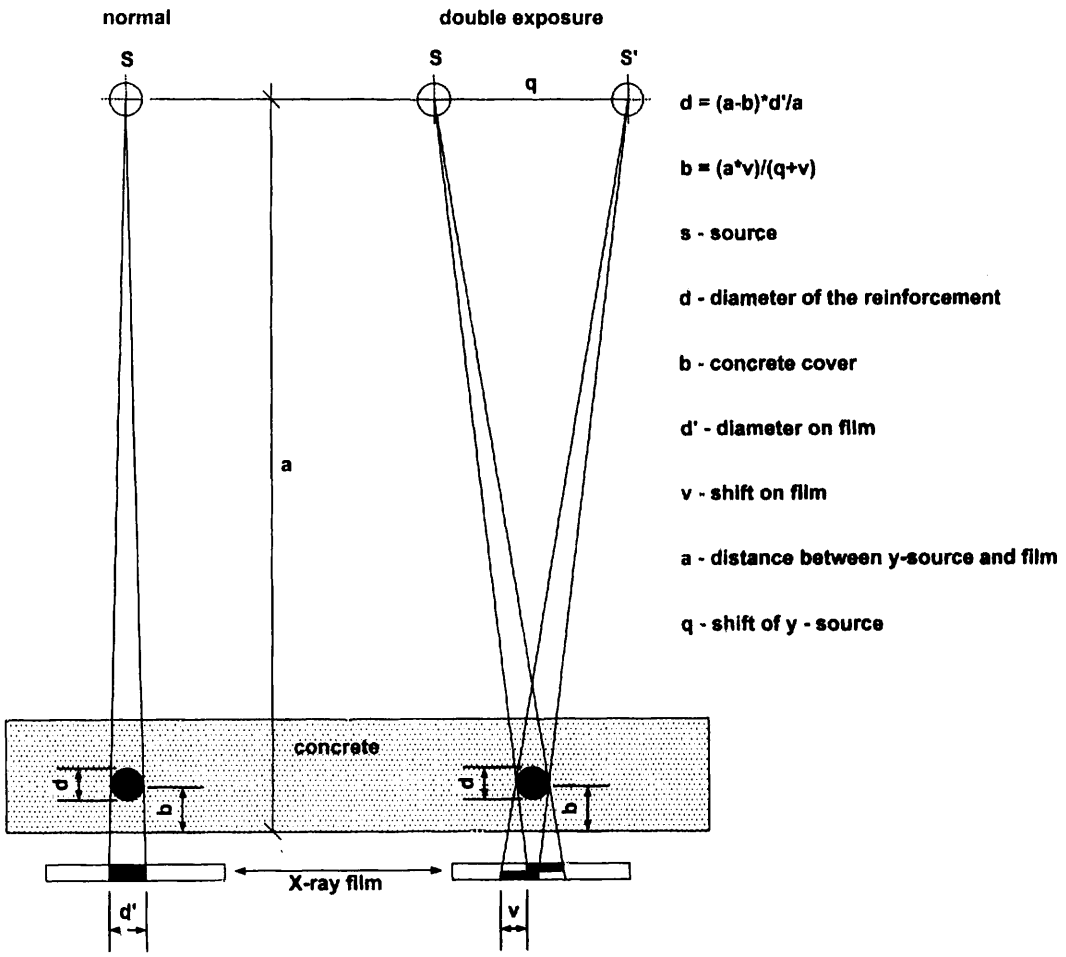

Fig. 4-13: Schematics of radiography

For x-rays (200kV) the maximum concrete thickness is about 25 cm and for Co-60 gamma radiation about 50 cm. The use of linear accelerators allows even larger concrete thickness to be studied. Practical exposure times range from 3 to 20 min. If the thickness is more than the maximum thickness mentioned above, the source can be placed in a drill hole, see Fig. 4-14. The same procedure is advisable if the structure is accessible from one side only. An additional effect of the drill hole radiography is an improvement of radiation protection.

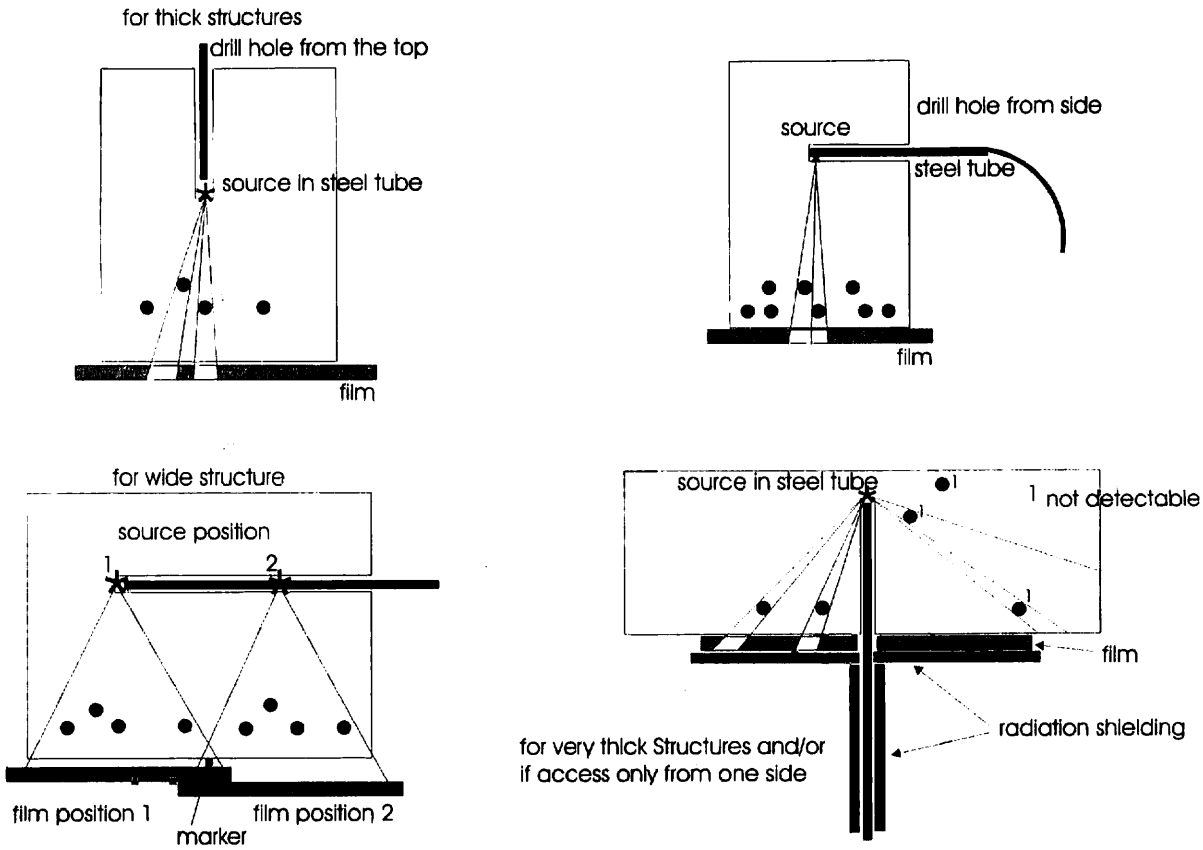

Fig.4-14: Drill hole radiography

The disadvantages of the radiography are the comparatively high costs, caused by the work of especially trained staff and the necessary radiation protection. In addition, no on-line information is provided because of the necessity of the film development. On the other hand, the results have an image format allowing an easy interpretation and documentation.

The radiography can be considered a possible option for detecting steel reinforcement, if no other methods can provide the needed information. This is especially the case at heavily reinforced parts of structures.

4.2.3 Radar methods

Electromagnetic waves are reflected at interfaces between materials having different electrical properties. This effect can be used for detecting steel reinforcement in concrete structures, see Fig. 4-15.

The advantage of the Radar principle is that the maximum inspection depth is about 50 cm, that means larger than for electro-magnetic methods. On the other hand, the interpretation of the data obtained appears to be difficult and reinforcement close to the concrete surface cannot be identified clearly. The Radar method, therefore, is beneficial in the case of large reinforcement diameters and high concrete covers. A useful application is the localization of prestressing cables. In this case the insensitivity against near surface reinforcement appears to be an advantage of the method. Usually prestressed cables are located deeper inside the concrete members than the not prestressed reinforcement.

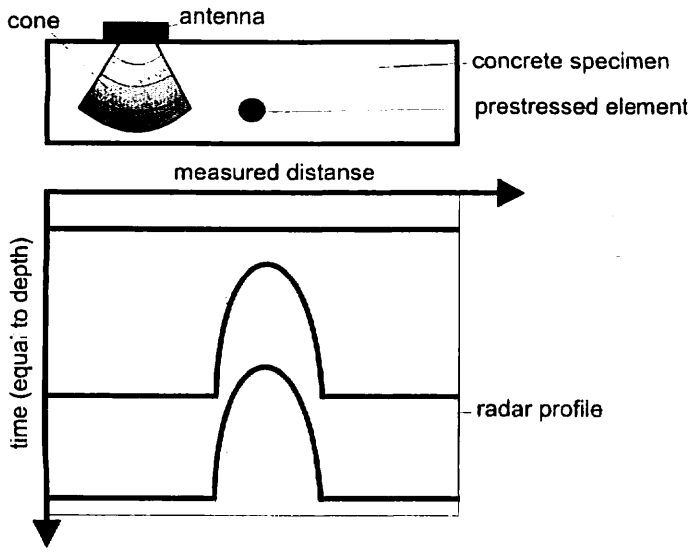

Fig.4-15: Radar method for detecting prestressed elements (Pöpel, Flohrer 1995)

4.2.4 Concluding remarks on the detection of reinforcement

For practical reasons, it is recommended that an in-situ investigation is started by using an electro-magnetic reinforcement detection device. The removal of the concrete cover at certain points allows the confirmation and completion of the information obtained non-destructively. Under certain circumstances this combination of electro-magnetic and destructive methods does not provide the required information. In these cases other, more costly methods can be used in addition:

- **Radiography** for heavily reinforced structures and large concrete thickness
- **Radar** for finding prestressed cables with large concrete cover

It should be mentioned that other techniques have been used for detecting reinforcement in concrete structures too, among them the ultrasonic Impulse-Echo-Method and the Infrared Thermography. However, these methods are more beneficial for solving other inspection problems and cannot be recommended for the practical reinforcement detection.

4.3 Steel evaluation

4.3.1 Penetrant testing

This method is used to locate and identify surface defects in nonporous materials. Further fields of application are:

- Detection of cracking and porosity in welded joints
- Detection of surface defects in castings
- Detection of fatigue cracking in stressed materials

The surface of the part under evaluation is coated with a penetrant in which a visible or fluorescent dye is dissolved or suspended. The penetrant is pulled into surface defects by capillary action. After a waiting period to insure the dye has penetrated into the narrowest

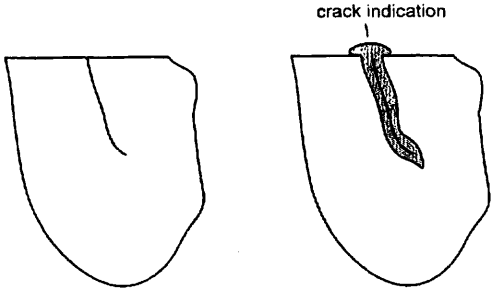

Fig.4-16: Liquid Penetrant Testing [171]

cracks, the excess penetrant is cleaned from the surface of the sample. A white powder, called developer, is then sprayed or dusted over the part. The developer lifts the penetrant out of the defect, and the dye stains the developer. Then by visual inspection under white or ultraviolet light, the visible or fluorescent dye indications, respectively, are identified and located, thereby defining the defect. [183]

4.3.2 Magnetic particle testing

Magnetic Particle Testing (MPT) is an NDT technique for crack identification that relies on local or complete magnetization of the component or surface being interrogated. It can only be applied to Ferromagnetic components. When a crack is present on the surface, then some magnetic flux will leak out from the sides of the crack (provided that the magnetic flow is in a suitable direction relative to the crack).

In Fig. 4-17 a magnetic field is established in a component made from ferromagnetic material. The magnetic lines of force or flux travel through the material, and exit and reenter the material at the poles. Defects such as cracks or voids are filled with air that cannot support as much flux, and force some of the flux outside of the part. Magnetic particles distributed over the component will be attracted to areas of flux leakage and produce a visible indication [171] If these particles are suitably coloured, or the background is suitably coloured, this concentration of particles will enhance the image of any cracks.

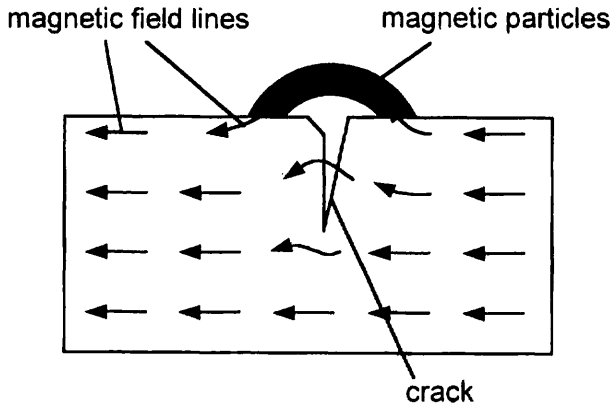

Fig.4-17: Magnetic particle testing

5 Measurement methods

The development of rational, cost effective strategies for the repair and rehabilitation of structural components necessitates the acquisition of reliable information on level and rate of deterioration. The relevant inspection techniques must show a reliable long-term performance, work in a non-destructive way and provide an overall condition assessment of the structure (CEB-FIP 1998, [22]). Many sensors available on the market or still being developed such as fiber optics, dielectric measurement sensors, piezoelectric materials, strain gages and others can be used for applications for health monitoring purposes (Chang 1997, [26]).

5.1 Geometry and dimensions

Geometry verification is an integral prerequisite for structural analysis and assessment. The real dimensions of structures and substructures may diverge from the design values even without forced deformation. However, as the measurement methodologies and instruments are essentially the same as for deformation monitoring, these techniques are treated in 5.2.

5.2 Deformations

Deformation refers to an internal shape change of a structure, which can be the result of a variety of direct or indirect agents. Examples include known forces applied to the structure to test it or unknown forces like traffic, wind, earthquakes or snow. Deformations can also be the result of changes in the materials constituting the structures like cracking, flow, relaxation or a change of temperature. A deformation is usually accompanied by a change of the strain field (Inaudi, Vurpillot, Casanova, Kronenberg 1998 [62], Inaudi, Vurpillot, Loret 1996 [63]).

The measurement of deformation can be approached either from the material or from the structural point of view. In the first case, monitoring will concentrate on the local properties of the materials used (e.g., concrete, steel, timber, composite materials, etc) and observe their behavior under load, temperature variations or aging. Given a sufficient number of sensors, the observations of local material properties made by short base-length strain sensors can be extrapolated to the global behavior of the whole structure.

In the structural approach, the structure is observed from a geometrical point of view. While strain sensors on a short base length are usually used for material monitoring rather than structural monitoring, long-gage sensors (with measurement bases much larger than the characteristic dimensions of the materials) give information on the behavior and response of the structure. However, material degradations like cracking or flow are only detected when they have an impact on the shape of the structure. Further, longer base-lengths help to reduce misleading measurements stemming from material non-homogeneities (Zimmermann, Kaouk 1994 ,[165]). Additionally, this approach usually requires a reduced number of sensors when compared to the material monitoring approach (Inaudi, Casanova, Vurpillot, Glisic, Kronenberg, Loret 2000, [61]).

A deformation measurement will however concentrate on the geometrical changes of the structure and not on the variation of its loading state. The measurement base could extend for many meters or even hundreds of meters for particular applications (e.g. geostructural monitoring or long suspended bridges). (Inaudi, Vurpillot, Casanova, Kronenberg 1998 [62], Inaudi, Vurpillot, Loret 1996 [63]).

The serviceability of a bridge is generally analyzed by a comparison between the vertical deflections expected by the engineer and those measured during a load test or in the long term (Vurpillot, Krueger, Benouaich, Clément, Inaudi 1998, [153]). Thus changes of camber with time can be determined. The measurement of vertical deflections of long-span girders is a task for which no simple method or sensing unit exists. Existing methods to measure deflections, such as e.g. triangulation, hydrostatic leveling, laser beams, or mechanical extensometers, etc., are often tedious to install and require an accurate elaboration. The determination of deflection by the use of displacement transducers requires a stable accessible reference location for each measurement and is, for most bridges, not practical. However, results can be achieved by measuring the deflection at various points along the span relative to the ends of the girder and by installing reference pins on the top of the girders (U.S. Department of Transportation 1996, [147]). The resulting complexity and costs limit the temporal frequency of these traditional measurements. The spatial resolution obtained is in general low, and only the presence of anomalies in the global structural behavior can be detected and warrant a deeper and more precise evaluation (Vurpillot, Krueger, Benouaich, Clément, Inaudi 1998, [153]).

Measurements of deflection must begin prior to detensioning and be obtained before and after every significant event that affects the girder. Frequency of readings after completion of the structure should be selected so that trends in the data are clearly discernable. Since changes in temperature gradients and live loads influence measured deflections, it is important to eliminate their influence. Taking readings early in the morning just before sunrise can minimize the effect of temperature gradients. Temperature gradients should be measured at the same time, and if necessary, a correction can be made for the temperature induced deflections. Life load effects on bridges can be eliminated or minimized by closing the bridge to traffic, if practical, or taking readings when the traffic volume is light. Failure to minimize these extraneous effects will increase scatter in the data. (U.S. Department of Transportation 1996, [147])

More recent measurement techniques applied for the detection of vertical displacement and curvature profile utilize a network of fiber optic deformation sensors and electrical inclinometers installed during concrete pouring or placed on the surface of the structure. Most embedded deformation sensors measure the relative displacement between two points inside the structure. The analysis of these measurements, generally obtained with sensors placed horizontally in a bridge, is not straightforward. In order to determine the overall displacement field of the structure from internal deformation measurements, an algorithm using the relation between the vertical and the curvature of a linear prismatic beam element is deployed. However to obtain information about rigid-body displacements in space, internal sensors are obviously useless and other measurements relative to fixed eternal points obtained using absolute sensors such as GPS, inclinometer, etc. should be carried out (Vurpillot, Krueger, Benouaich, Clément, Inaudi 1998, [153]).

The minimum number of sensors to be placed in the structure depends on the number of parameters needed to retrieve its curvature. One sensor is sufficient for the case of pure bending (constant bending moment diagram), a couple of sensors are necessary for the case of bending combined with axial force, and one additional sensor per section of beam is sufficient in the case of a linearly varying distributed load. In a real prestressed concrete bridge with varying moment of inertia, nonuniform load, etc., it is necessary to determine the form of the curvature diagram (for example, through finite element analysis). Generally, the curvature diagram can be approached by a second degree polynomial function. To obtain the best results, sensors must be placed in regions where the curvature values are the highest. The best suited length of sensors is determined by analyzing the behavior of a virtual sensor, placed in the finite element mesh of the model and stretched or deformed under the load present case. An increased number of sensors will enhance the measurement precision through a least

square fitting algorithm and add some redundancy useful in the case of sensor failures (Vurpillot, Krueger, Benouaich, Clément, Inaudi 1998, [153]).

5.2.1 Mechanical sensors

5.2.1.1 Wire and tape extensometers

Wire and tape extensometers are used to detect and monitor changes in the distance between two reference points. Typical applications include monitoring of deformations in underground openings as well as displacement monitoring of retaining structures, bridge supports, and other structures [191].

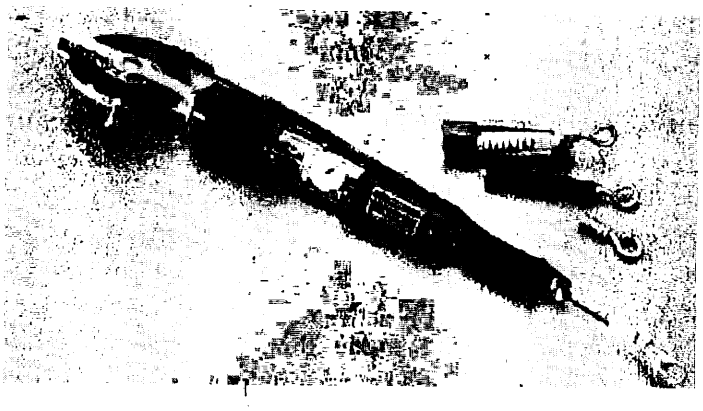

Fig. 5-1: Tape extensometer with reference points, developed by Slope Indicator

The reference points are permanently installed at measurement stations along the tunnel or structure. To obtain a measurement, the tape or wire is stretched between two reference points, hooking the free end of the tape/wire to one point and the instrument body to the other [191]. Maintaining a constant tension throughout the use of the wire or tape extensometer is very important. In some portable extensometers, the constant tensioning weight has been replaced by precision tensioning springs. One should be careful because there are several models of spring tensioned extensometers on the market, which do not provide any means of tension calibration. As the spring ages, these instruments may indicate false expansion results unless they are carefully calibrated on a baseline of constant length, before and after each measuring campaign.

If an extensometer is installed in the material with a homogeneous strain field, then the measured change Δl of the distance l gives directly the strain component $\varepsilon = \Delta l/l$ in the direction of the measurements. To determine the total strain tensor in a plane (two normal strains and one shearing), a minimum of three extensometers must be installed in three different directions.

Wire extensometers use invar wires and special constant tensioning devices which, if properly calibrated and used, can give accuracies of 0.05 mm or better in measurements of changes of distances over lengths from about 1 m to about 20 m. Invar is a capricious alloy and must be handled very carefully to avoid sudden changes in the length of the wire. When only small changes in temperature are expected or a smaller precision (0.1 mm to 1 mm) is required, then steel wires or steel tapes are more comfortable to use.

The actual accuracy depends on the temperature corrections and on the quality of the installation of the extensometer. When installing rods in plastic conduit (usually when installing in boreholes), the friction between the rod and the conduit may significantly distort the extensometer indications if the length of the extensometer exceeds a few tens of meters.

The dial indicator readout may be replaced by potentiometer or other transducers with digital readout systems.

5.2.2 Electrical sensors

Electrical displacement sensors are mechanical-electrical transducers for measuring the relative displacement between two points. To transform the displacement into any electrical quantity various physical effects are used. Furthermore, the displacement can be measured using contacting or non-contacting techniques depending on the prevailing conditions. Compared to other sensors for deformation measurements, e.g. electrical strain gages, the displacement sensors commonly have a sufficient long-term stability.

Length change measurements require a reference rod with a very low coefficient of thermal expansion. The rod must be fixed at one end and relative movement between the rod and the bridge measured at the other end with a dial gage, linear potentiometer, or linear variable differential transformer. Care must be taken to ensure that the rod is protected from damage or changes in alignment. When electrical transducers are used to measure length changes, they must be electrically stable over the duration and temperature range of the observation period.

Measurements of length changes are appropriate for long bridges without joints. However, little benefit will be obtained by measuring length changes of individual girders because of the complications of installing the reference rod (U.S. Department of Transportation 1996, [147]).

5.2.2.1 Inductive sensors

All inductive sensors use the modification of electromagnetic field of a coil as a result of the displacement of a ferromagnetic core. The main kinds of those sensors are the linear variable differential choke coil (LVDC) and the linear variable differential transformer (LVDT).

The LVDC-sensors consist of a movable magnetic rod surrounded by two symmetrically placed coils wound onto an insulating bobbin. The displacement of the rod relative to the coils changes the inductivity of the coils. By means of a special AC bridge the difference of the inductivities of the two coils is measured.

The LVDT-sensors are constructed by analogy with LVDC-sensors, but they comprise three coils (one primary coil and two secondary coils). The motion of the rod relative to the coils changes the magnetic coupling between the primary coil and the secondary coils. The primary coil is connected to an alternating voltage supply and the difference of the voltages induced in the secondary coils is measured (principle of transformer).

(1) Linear Variable Differential Transformer (LVDT)

An LVDT is a linear displacement transducer that works on the principle of mutual inductance, producing an electrical signal that is proportional to the position of a separate moving core. The transducer relates inductance to displacement by modifying the spatial distribution of an alternating magnetic field.

Basically, an LVDT consists of a primary winding, two secondary windings, and a separate, moveable, high-permeability core, as shown in Fig. 5-2. Driving the primary

winding with an oscillating excitation voltage creates an alternating magnetic field, which induces corresponding alternating voltages in the two secondary windings, in proportion to the position of the moveable core (Wheeler, Ganji 1996, [157]).

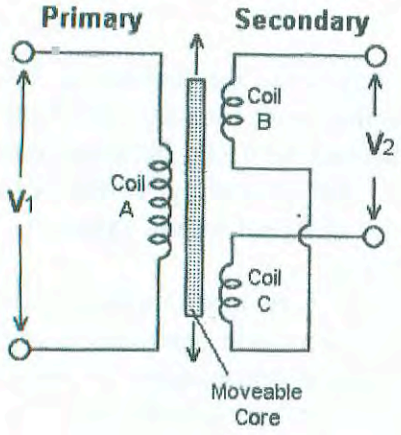

Fig. 5-2: Schematic LVDT, (Wheeler, Ganji 1996, [157])

When the core is displaced from this null position, the output amplitude on one secondary coil increases, while the output amplitude on the other coil decreases. These voltages can be used individually or combined to produce an output signal proportional to position, dependent upon the method of demodulation employed. The two main methods used are Ratiometric Operation and Differential Operation.

The fundamental advantages of LVDTs are their high degree of robustness, infinite resolution, and ability to operate at high temperatures and in extreme environments. They are available in ranges from a few thousandths of a centimeter up to several centimeters. In principle, they can be made to any size, but since the physical length is about three times the range, they are not the method of choice for measurement of larger displacements (Wheeler, Ganji 1996, [157]).

5.2.2.2 Potentiometer sensors

These sensors use the physical effect that the resistance of an electrical conductor is proportional to its length. A resistance potentiometer senses displacement by moving a variable contact through a distance that is proportional to the displacement. This movement causes a change in resistance.

A resistance potentiometer consists of a resistance element that is attached to the circuit by three contacts, or terminals. The ends of the resistance element are attached to two input voltage conductors of the circuit, and the third contact, attached to the output of the circuit, is usually a movable terminal that slides across the resistance element, effectively dividing it into two resistors. Since the position of the movable terminal determines what percentage of the input voltage will actually be applied to the circuit, the potentiometer can be used to vary the magnitude of the voltage; for this reason it is sometimes called a voltage divider.

The linear potentiometer is a device in which the resistance varies as a function of the position of a slider, as shown Fig. 5-3. With the supply voltage as shown, the output voltage will vary between zero and the supply voltage. Angular potentiometers (see Fig. 5-4) are designed to measure angular displacement of 3500° (multiple rotations) (Wheeler, Ganji 1996, [157]).

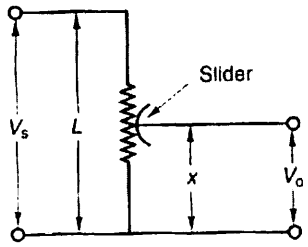

Fig. 5-3: Linear potentiometer, (Wheeler, Ganji 1996, [157])

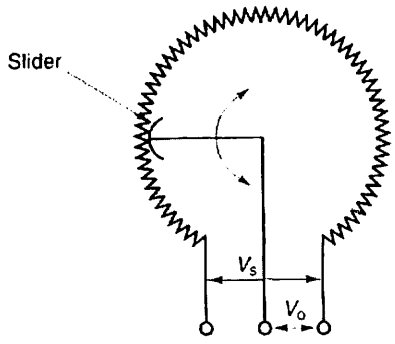

Fig. 5-4: Angular potentiometer, (Wheeler, Ganji 1996, [157])

The potentiometer sensors differ in the material of the potentiometer resistor (wire windings or conductive plastics) and in the kind of the variable contact. Initially, the resolution of potentiometer were limited to the diameter of the wire used, but conductive plastics have been developed to replace the wire windings so that there is a true linear relationship between displacement and output resistance.

Potentiometers are quite inexpensive, are readily available, and require no special signal conditioning. Both linear and rotary potentiometers can be constructed to have a non-linear relationship between displacement and output voltage for specialized applications. However potentiometer do have significant limitations. Because of the sliding contact, they are subject to wear and may have lifetimes of only a few million cycles. Furthermore, the output tends to be somewhat electrically noisy since the slider-resistor contact point has some resistance, and this can affect the output in a somewhat random manner (Wheeler, Ganji 1996, [157]).

In most practical circuits, a resistance measurement is replaced by a measurement of the voltage, which is directly proportional to the change in resistance. Conventional potentiometer sensors (PS) use a sliding contact to change the resistance. Compared with this, the inductive-potentiometer sensors (PSI) operate without a sliding contact and thus without any wear. A coil in the rod-shaped sensor housing is excited with an alternating current. A short aluminum collar is moved concentrically over the coil and influences the individual coil segments due to the eddy-currents generated in it. The aluminum collar has to be attached to the object to be measured.

5.2.2.3 Magnetostrictive sensors (MSS)

These long-stroke sensors employ a magnetostrictive phenomena called Wiedemann Effect. An ultrasonic wave is generated by a moving magnet operating near a magneto-strictive waveguide on which the sonic wave propagates up to the head of the transducer. The propagation time is measured and then the displacement of the moving magnet is operational. Usually the entire signal processing electronic is integrated into the transducer.

5.2.2.4 Capacitive sensors (NCS)

These sensors contain a guard ring capacitor and measure distances against any electrically conducting targets (e.g. metals). The distance between the sensor and the target determines the capacitance of the ring capacitor. The measurement of the capacitance-change provides the signal for the measuring displacement. Due to the use of the guard ring

capacitor-principle highly linear output characteristics can be realized without additional electronic linearity correction. These sensors are further characterized by their excellent resolution and stability, but they require a clean environment. Dirt, dust, water, or other dielectric media in the measuring gap can influence the measuring signal.

5.2.2.5 Technical parameters

Sensor type		**Technical**	**Parameters**	
(abbreviation)	Measuring ranges	Linearity	Resolution	Temperature range
LVDC	±1mm ... ±50mm	≥± 0.1 % FS [1)]	quasi infinite	-20°C ... +120°C
LVDT	±1mm ... ±50mm	≥± 0.1 % FS	quasi infinite	-20°C ... +120°C
PS	± 5mm ... ±200mm	≥± 0.5 % FS	0.5 % FS [1)]	-25°C ... +125°C
PSI	50mm ... 200mm	≥± 0.1 % FS	0.05 % FS	-40°C ... +60°C
MSS	100mm ... 1000mm	≥± 0.05 % FS	0.01 % FS	-20°C ... +80°C

Table 5-1: Technical parameters

[1)] FS Full scale

5.2.2.6 Application and selection criteria

The application of electrical displacement sensors considerably depends on the specific problem of investigation. In health monitoring they are used frequently for two main applications:

- Sensing of local displacements against an external fixed point what is known as measuring base (outside the investigated part of the structure), e.g. measurement of deflections or vibrations, settlement observation.
- Measurement of the relative displacement of two points on the structure, e.g. measurement of strains or of thermal expansions

The basic criteria for selection of displacement sensors are the following:

- Expected minimal change of displacement to identify the response of measuring object (resolution, linearity, accuracy)
- Expected maximum displacement (measuring range)
- Type of displacement measurement (static, dynamic etc.)
- Test duration (e.g. long-term stability)
- Operating temperature range
- Testing environment (moisture, dirt, vibration etc.)
- Installation environment (laboratory or field)
- Available financial resources (sensor costs, application costs)

5.2.2.7 Slope measurement

The tilting or deflection of concrete structures resulting from external loads, temperature changes, or deformation of the foundation is a vital piece of information for evaluating structural safety and stability. The changes in slope can be measured with tiltmeters or inclinometers. The measurement of tilt is usually understood as the determination of a deviation from the horizontal plane, while inclination is interpreted as a deviation from the vertical. Thus the same instrument that measures tilt at a point can be called either a tiltmeter or an inclinometer, depending on the interpretation of the results.

These instruments, most generally, are devices that are lowered through some sort of pipe, borehole, or channel that has been constructed in the structure. The casing is flexible enough to deform as the slope moves. The instrument is not fixed to the structure but moves through this channel taking readings at desired locations through the structure.

Applications:

- Deflection of bridge piers and abutments
- Monitoring of tilt on structures
- Slope stability
- Embankment and dam stability
- Heave/settlement and subsidence control
- Measuring mechanical response to applied loads

(1) Tiltmeter

The changes in slope can be measured with tiltmeters. There exist two types of tiltmeters. Biaxial tiltmeters measure rotations in two orthogonal directions, with an accuracy from < 0,00001° to < 0,01°. Uniaxial tiltmeters are sensitive to only one direction. Tiltmeters can be mounted on either vertical or horizontal surfaces and can be read either manually or with an automated data acquisition equipment. These sensing devices can be used for both short-term and long-term measurements. The tiltmeter consists of a reference plate, which is attached to the surface that is being monitored, and a sensing device. A tiltmeter, unlike an inclinometer, measures only at a discrete, accessible point. Thus deformation profiles of tall structures may be determined by placing a series of tiltmeters at different levels of the structure.

There are many reasonably priced models of various liquid, electrolytic, vibrating wire, and pendulum type tiltmeters that satisfy most of the needs of engineering surveys. Particularly popular are servo-accelerometer tiltmeters with a small horizontal pendulum. They offer ruggedness, durability, and low temperature operation. The output signal (volts) is proportional to the sine of the angle of tilt. The typical output voltage range for tiltmeters is 5 V, which corresponds to the maximum range of the tilt. Thus the angular resolution depends on the tilt range of the selected model of tiltmeter and the resolution of the voltmeter (typically 1 mV). There are many factors affecting the accuracy of tilt sensing. A temperature change produces dimensional changes of the mechanical components, changes in the viscosity of the liquid in the electrolytic tiltmeters, and changes of the damping oil in the pendulum tiltmeters. Drifts of tilt indications and fluctuations of the readout may also occur. Therefore, thorough testing and calibration are required even when the accuracy requirement is not very high.

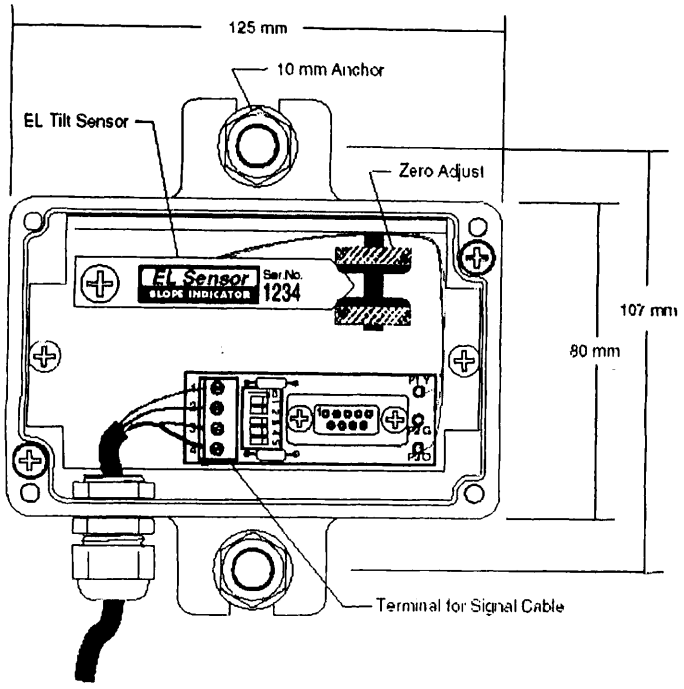

Fig. 5-5: Schematics of EL tiltmeter developed by Slope Indicator

Fig. 5-5 shows the EL tiltmeter developed by Slope Indicator. This tiltmeter consists of an electrolytic tilt sensor housed in a compact, weatherproof enclosure. The tilt sensor is a precision bubble-level that is sensed electrically as a resistance bridge. The bridge circuit outputs a voltage proportional to the tilt of the sensor. The housing is fixed to the structure using two anchors and a mounting bracket. The sensor is adjusted to near zero and then the initial reading is recorded. Changes in inclination are found by comparing the current reading to the initial reading. This operation can be performed in the data logger or in a spreadsheet [191].

(2) Inclinometer

Inclinometers are used for measuring the tilt over a certain length. Fig. 5-6 shows the in-place Inclinometer developed by Slope Indicator. The system consists of an inclinometer casing and a string of electrolytic inclinometer sensors. The inclinometer casing controls the orientation of the sensors. It is installed in a horizontal borehole, buried in a trench, or attached to a structure, with one set of grooves oriented vertically. The string of sensors is positioned within the casing. The sensors measure the inclination of the casing (tilt from horizontal). Changes in the inclination readings indicate that the casing has been displaced by ground movement. The amount of displacement is calculated by finding the difference between the current inclination reading and the initial reading and then converting the result to a vertical distance. In most in-place inclinometer applications, sensors are connected to a data acquisition system that continuously monitors movements and can trigger an alarm when it detects a change, or rate of change, that exceeds a preset value [191].

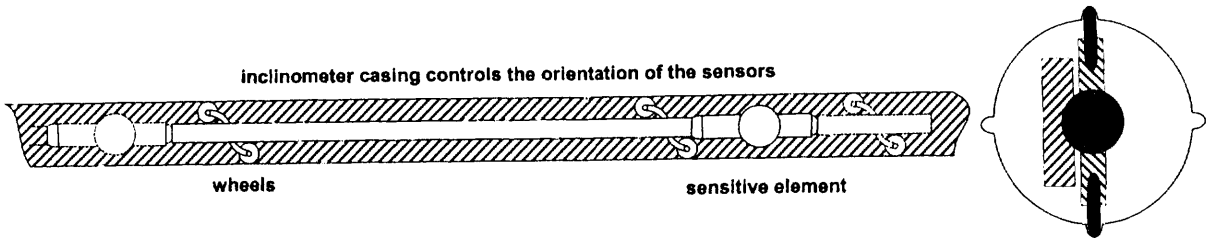

Fig. 5-6: Horizontal in-place inclinometer

(3) Time domain reflectometry (TDR)

Time domain reflectometry (TDR) is a new approach to monitor landslide and embankment stability. Originally developed to locate breaks and faults in communication and power lines, TDR can be used to monitor the movement of earth slopes. Data collection consists of simply attaching a TDR cable tester to a coaxial cable grouted in a borehole, and taking a reading.

The basic principle of TDR is similar to that of radar. An electrical pulse is sent down the coaxial cable grouted in a borehole. If the pulse encounters a change in the characteristic impedance of the cable, it is reflected. This can be caused by a break or deformation in the cable. The cable tester compares the returned pulse with the emitted pulse, and determines the reflection coefficient of the cable at that point. The reflection shows as a "spike" on the characteristic cable signature. The relative magnitude and rate of displacement, and the location of the zone of deformation can be determined immediately and accurately.

TDR has some advantages over traditional inclinometers:

- lower installation costs
- no limits on hole depth
- immediate determination of movement
- remote data acquisition capability

When combined with in-place tiltmeters and a datalogger, TDR can be used to determine the depth and direction of movement. Biaxial tiltmeters provide direction, while the TDR cable locates the depth at which movement is occurring.

5.2.3 Fiber optic sensors

Distributed fiber optic based sensing is a powerful sensing tool for monitoring and profiling a variety of parameters, or 'measurand' fields, such as strain, temperature, force, optical index, and chemical parameters along the length of a fiber cable.

An optical fiber, being a physical medium, is subjected to perturbation of one kind or the other at all times. It therefore experiences geometrical (size, shape) and optical (refractive index, mode conversion) changes to a larger or lesser extent depending upon the nature and the magnitude of the perturbation. In fiber optic sensing, the response to external influences is deliberately enhanced so that the resulting change in optical radiation can be used as a measure of the external perturbation. The optical fiber also serves as a transducer and converts measurands like temperature, stress, strain, rotation or electric and magnetic currents into a corresponding change in the optical radiation. Since light is characterized by amplitude, phase, frequency and polarization, any one or more of these parameters may undergo a

change. The usefulness of the fiber optic sensor therefore depends upon the magnitude of this change and our ability to measure and quantify the same reliably and accurately (Selvarajan, Asundi 1995, [129]).

Fiber optic instrumentation offers a number of benefits when compared to conventional electronic instrumentation. The following advantages provide compelling justification for using fiber optic sensors in various applications:

- Immune to EMI, RFI, and nuclear blast effects
- Immune to grounding problems and lightning strikes
- Inherently safe and suitable for use in highly explosive environments
- Tolerant of high temperatures and corrosive environments
- Wide Bandwidth
- Suitable for use in wet environments
- Geometric Versatility and Economy
- Lightweight and Compactness

In general, fiber optic sensors are characterized by high sensitivity when compared to other types of sensors. Specially prepared fibers can withstand high temperature and other harsh environments (Selvarajan, Asundi 1995, [129]).

Basically fiber optic sensors can be classed according to the light modulation mechanisms as an intensity, a phase, a frequency, or a polarization sensor (Selvarajan, Asundi 1995, [129]). Phase-modulated sensors compare the phase of light in a sensing fiber to a reference fiber in a device called interferometer, these sensors are also termed as interferometric sensors. In intensity-modulated sensors the perturbation causes a change in received light intensity, which is a function of the phenomenon being measured (Wheeler, Ganji 1996, [157]). From a detection point of view the interferometric technique implies heterodyne detection/coherent detection. Intensity sensors are basically incoherent in nature. Intensity or incoherent sensors are simple in construction, while coherent detection (interferometric) sensors are more complex in design but offer better sensitivity and resolution (Selvarajan, Asundi 1995, [129]).

A fiber optic sensor in general will consist of a light source, a sensing and transmission fiber, a photodetector, demodulator, processing and display optics and the required electronics.

5.2.3.1 Optical fiber

Optical fibers are thin, long cylindrical structures, which support light propagation through total internal reflection over several kilometers. A typical optical fiber consists of a glass core, a cladding layer that is typically made of silica glass or sometimes plastic, and an outer buffer layer of acrylate or other material. These layers are in turn protected by cables similar to those used for wires.

Three types of fibers are in common use for fiber optic sensors. Multimode fiber, single mode fiber and polarization preserving fiber are the three classes of fibers, which are used in the intensity type, the interferometric type and the polarimteric type of sensors, respectively (Selvarajan, Asundi 1995, [129]). Light in a single mode fiber essentially follows a single path to reach its destination, in multimode fiber applications light takes many paths, which leads to a spreading of the pulse called dispersion. The multiple paths limit the bandwidth of a signal traveling through a multimode link. The bandwidth can be increased by creating a fiber that has an index of refraction is not constant over the cross section, but varies with a maximum at the center and dropping off until it nearly reaches the index of refraction of the

cladding. The graded index core decreases dispersion, which increases bandwidth (LaBel, C.J. Marshall, P.W. Marshall, Luers, Reed, Ott, Seidleck, Andrucyk 1998, [77]).

5.2.3.2 Transmitter

Multimode fiber systems optical transmitters need only be a light emitting diode (LED); whereas for single mode applications a laser diode is necessary to achieve the wider bandwidth. LEDs are used as source emitters in multimode transmission systems that typically are no larger than 50 Mbps/s since they have large spectral width in comparison to laser diodes. Laser diodes and LEDs function by releasing photons via the recombination of electron-hole pairs within a p-n junction. The e-h pairs are separated in energy by an amount equal to the bandgap of the semiconductor at the p-n junction. The recombination event produces a photon with energy equal to bandgap energy. A current is applied to the device that drives this spontaneous emission. In laser diodes, the photons will then create other photons by stimulated emission and the result is a beam of coherent light, where in LEDs the light generated is incoherent (LaBel, C.J. Marshall, P.W. Marshall, Luers, Reed, Ott, Seidleck, Andrucyk 1998, [77]).

In comparison to laser diodes, LED's can generally be driven harder, are less expensive, have lower power, larger emitting regions, and longer lifetimes. Lasers, unlike LED's will not operate below a threshold current. Meaning, the diode will commence lasing (functioning) only when the threshold current is reached. Further, LEDs and laser diodes are temperature sensitive when considering overall lifetime (LaBel, C.J. Marshall, P.W. Marshall, Luers, Reed, Ott, Seidleck, Andrucyk 1998, [77]).

5.2.3.3 Receiver

The receiver of an optical measurement system is comprised of a photodiode, which converts optical energy into electrical energy (LaBel, C.J. Marshall, P.W. Marshall, Luers, Reed, Ott, Seidleck, Andrucyk 1998, [77]). Semiconductor photodiodes (PDs) and avalanche photodiodes (APDs) are the most suitable detectors in fiber optic measurement systems. APD can sense low light levels due to the inherent gain because of avalanche multiplication, but need large supply voltage typically about 100 V. The various noise mechanisms associated with the detector and electronic circuitry limit the ultimate detection capability. Thermal and shot noise are two main noise sources and need to be minimized for good sensor performance. Detector response varies as a function of wavelength. Silicon PD is good for visible and near IR wavelengths. Generally there is no bandwidth limitation due to the detector as such, although the associated electronic circuits can pose some limitations (Selvarajan, Asundi 1995, [129]).

5.2.3.4 Multiplexing capability

In most structures it is necessary to place a large number of strain and/or displacement sensors in order to gain a complete understanding of the structural behavior. If a fiber optic connection is necessary between the reading unit and each single sensor, the complexity of the monitoring system increases rapidly with the number of sensors. In-line multiplexing offers a simple way to increase the sensors that can be addressed along a single fiber line. In this case the sensors are paced in a chain one after the other and the reading unit can access all sensors at a single or at both ends of the chain. Even if the sensors are placed along a line, it is always

possible to arrange this chain in order to monitor a surface or even a volume with a single line. (Inaudi, Vurpillot, Loret 1996, [63])

The techniques that are most commonly employed are time (TDM), frequency (FDM), wavelength (WDM), coherence, polarization and spatial multiplexing (Udd, Schulz, Seim, Corones, Laylor 1998, [144]). Alternatively, it is more interesting to exploit the inherent ability of certain fiber sensors to create unique forms of distributed sensing. For example, optical time domain reflectometry (OTDR) and distributed Bragg gratins sensors are two such schemes in common use (Selvarajan, Asundi 1995, [129]).

Time division multiplexing employs a pulsed light source launching light into an optical fiber and analyzing the time delay to discriminate between sensors. This technique is commonly employed to support distributed sensors where measurements of strain, temperature or other parameters are collected.

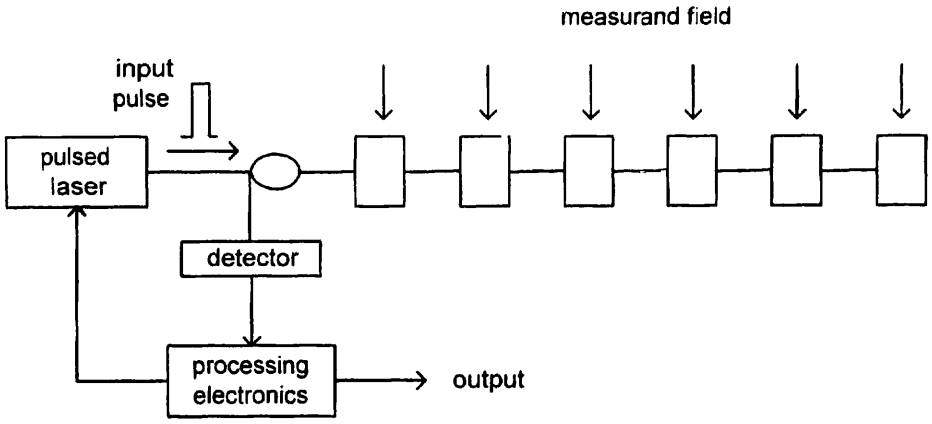

Fig. 5-7: Time division multiplexed sensor array using OTDR

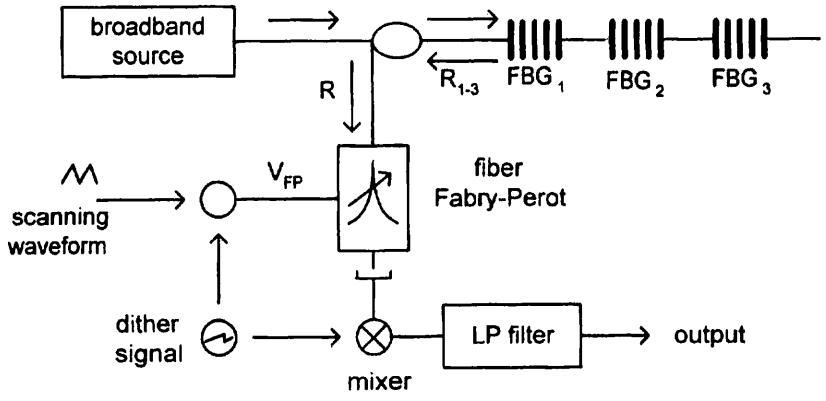

Fig. 5-8: Multiplexed sensor array using WDM / Bragg grating principles

5.2.3.5 Interferometric fiber optic sensors

In a typical inteferometric sensor, light from a source with high coherence, such as a laser diode, is split into two paths. One path (the reference leg) is isolated from the physical effect to be measured, while the other (the sensor leg) is subjected to the effect. The sensor is engineered so that the applied measurand effects a change in the optical path length of the sensor leg, either by elongation of the leg, or by a change in the refractive index of the leg. At the output of the sensor, the light in the two legs is combined. Since the light is coherent, the

two paths interfere, with the state of the interference depending on the relative phase difference between the interfering lightwaves; if the waves are in phase, they interfere constructively, producing strong optical power, and if they are out of phase, they interfere destructively, with a reduction in optical power.

Since the interferometer output changes dramatically for changes in optical path length of less than the wavelength of light (on the order of 10^{-6} meter), the interferometer yields highly sensitive measurements of fiber elongation or refractive index change. However, changes in optical path length longer than a wavelength yields periodic changes in the power output by the sensor. The term commonly used for each peak in intensity is a "fringe." The periodic output of the interferometer complicates the interpretation of the output, requiring additional equipment or algorithms to yield an output that is a monotonically varying function of the applied measurand. Some of the techniques used include counting of fringes, and use of more than one wavelength to derive an unambiguous measurement of the interference state.

Interferometric fiber optic sensors are by far the most commonly used fiber optic sensors since they offer the best performance. They have found application as acoustic, rotation, strain, temperature, chemical, biological and a host of other types of sensors (Selvarajan, Asundi 1995, [129]). Interferometric fiber optic sensors offer an interesting means of implementing structural monitoring with internal or embedded sensors (Inaudi, Vurpillot, Casanova, Kronenberg 1998, [62]). The precision requirements, the long gage lengths and the stability required by this application, point to the use of interferometric schemes. However, due to their incremental nature, most interferometric set-ups require continuous and uninterrupted monitoring, which is a major drawback for long-term applications. Low-coherence interferometry offers most of the advantages of interferometric sensors but features non-incremental operation allowing absolute measurements to be performed at any given time (Inaudi, Vurpillot, Casanova, Kronenberg 1998, [62]).

An interferometric sensor is based on the detection of changes in the phase of light emerging out of a single mode fiber (Selvarajan, Asundi 1995, [129]). Optical phase changes cannot be detected directly (optical waves have frequencies in the range of a few hundred THz). In order to detect a phase difference it is necessary to convert it into an optical intensity change (Donlagic 2000, [34]). This is achieved by using interferometric schemes like Mach-Zehnder, Michelson, Fabry-Perot or Sagnac forms.

(1) Mach-Zehnder interferometer

The fiber optic Mach-Zehnder interferometer is composed of two fiber beam splitters. In the first splitter the optical wave is split and directed into two separate fibers. One fiber is exposed to the measurand field, and is called measurement fiber. The other fiber is isolated from the surrounding and is called reference fiber. If the measurement fiber is unperturbed, then the two fibers have exactly the same length. The optical waves combined in the second splitter are therefore in phase and coherently add to give a maximum intensity output. If the measurement fiber experiences a mechanically or thermally applied strain, the optical length of the measurement fiber increases and the optical path difference changes. The intensity output decreases due to destructive interference. The optical intensity at the output of the interferometer is a function of the phase shift between the two optical waves (Donlagic 2000, [34]).

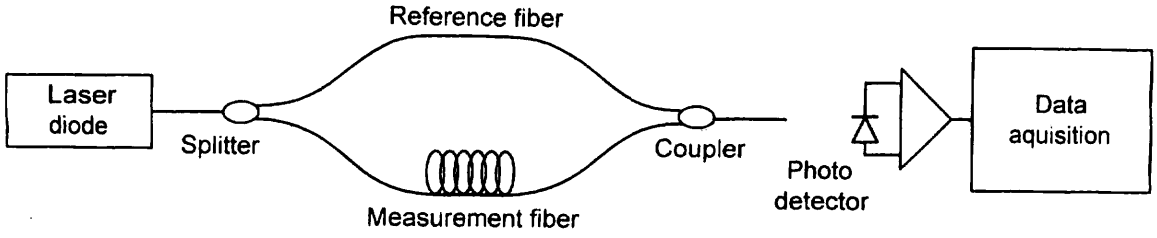

Fig. 5-9: Schematics of Mach-Zehnder interferometer

(2) Michelson interferometer

Another possible configuration of a two-beam interferometer is the Michelson Interferometer. In this configuration the radiation of a light emitting diode (LED) is launched into a single-mode fiber and split, by means of a monomode coupler (also used to recombine the waves), into a pair of fibers mounted on or embedded in the structure to be monitored. The measurement fiber is mechanically coupled to the structure and follows its deformations, while the reference fiber is installed freely inside a pipe and acts as a temperature reference. All deformations of the structure will then result in a change of the length difference between these two fibers. The light is reflected by mirrors at the end of the fibers or by a series of partial reflector pairs installed at different fiber locations, which allows the sensors to be multiplexed in-line [62]. The coupler recombines the two light beams and directs them towards the analyzer.

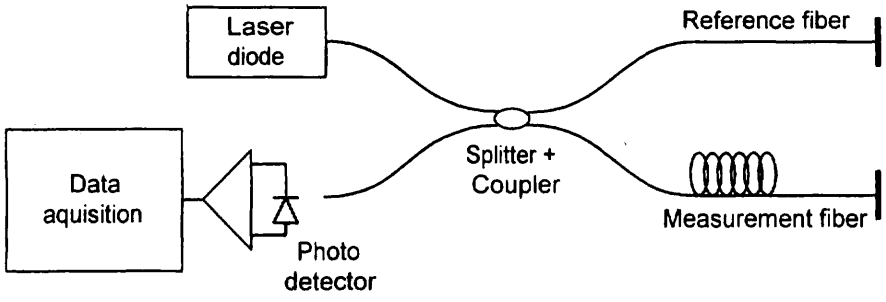

Fig. 5-10: Schematics of Michelson interferometer

A good representative of long base-length fiber optic deformation sensors is the SOFO measurement technique developed by Inaudi et Al. [62,63]. The measuring system shown in Fig. 5-11 consists of a double Michelson interferometer in a tandem configuration, based on the low-coherence interferometry principle. This configuration allows for absolute measurement of the path unbalance between measurement and reference fiber. Since the measurement fiber is pre-stressed to about 0.5% of the sensor length, it is able to measure deformations in both, elongation and shortening. The reflected light of these fibers is directed towards the analyzer interferometer. This second interferometer is also made of two fiber lines and can introduce a well-known path difference between them by means of a mobile mirror. On moving this mirror, a modulated signal is obtained on the photodiode only when the length difference between the fibers in the analyzer compensates the length difference between the fibers in the structure to better than the coherence length of the source. This type of sensor has resolution and sensitivity of 2 microns and is, like most fiber optic devices, insensitive to temperature, humidity, vibration, corrosion, and electromagnetic fields. Additionally, these sensors are easy and fast to install, embeddable in concrete, mortars, surface mountable on concrete, metallic or timber structures.

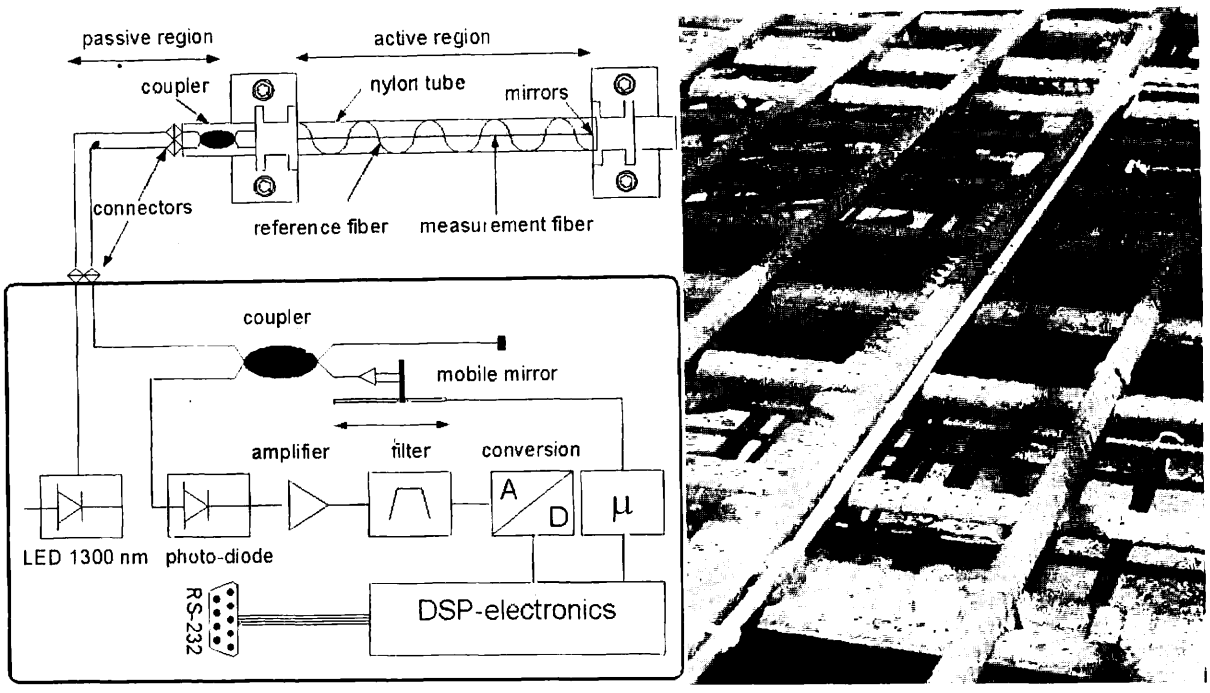

Fig. 5-11: Deformation sensor SOFO

Measurement resolution:	2/1000 mm RMS
Linearity / Accuracy:	< 2‰ of the measured deformation
Calibration:	None required
Gage length:	0.25 to 10m, up to 50 m with custom design
Cable length:	max 10 km
Dynamic range:	1.0% in elongation, 0.5% in shortening

Table 5-2: Technical parameters

SOFO Sensors offer the freedom to choose the length of the measurement basis according to the specific monitoring needs in a given structure. For concrete structures it is usually interesting to choose relatively long sensors in order to avoid false readings due to local variations in the material properties. In the case of bridges, the double-integration algorithm gives the most accurate results when long sensors are used. Ideally the whole length of the bridge should be spanned by a series of long sensors installed back to back. In most cases a coverage of 30-50% gives about the same level of accuracy. For most bridges, 4 to 6 sensor pairs per span are required to retrieve the vertical displacements of the structures.

The SOFO sensor can be embedded in new concrete for new and refurbished structures or mounted on the surface of existing ones. The sensors are immune to temperature variations, electromagnetic fields and showed no appreciable drift for use on at least 5 years.

The main care consists in protecting the sensors from degradations including direct UV exposure, highly corrosive sprays, rodents and birds, vandalism and careless manipulation.

(3) Fabry-Pérot interferometer (FPI)

Fabry-Perot interferometry is another approach to measuring displacement with high precision. Basically, an FPI consists of two reflective surfaces or mirrors facing each other, the space separating the mirrors being called the cavity length. When these surfaces are formed on facing ends of optical fibers they are referred to as extrinsic fiber etalons. Intrinsic fiber etalons have the reflective surfaces in a single fiber (Udd, Schulz, Seim, Corones, Laylor 1998, [144]). Light reflected in the FPI is wavelength-modulated in exact accordance with the cavity length. As the cavity length changes, the frequencies at which it transmits light change accordingly. By monitoring the optical transmission frequency, very small changes in the cavity length can be resolved.

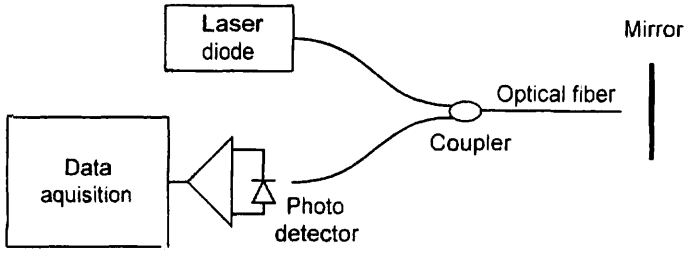

Fig. 5-12: Schematics of Fabry-Pérot interferometer

Fig. 5-12 shows the schematics of a Fabry-Pérot Interferometer. The radiation of the laser diode is coupled into the fiber and propagates through the coupler towards the end of the fiber. Then, one part of radiation is reflected from the end face of the optical fiber and the other part of radiation is flashed into the air, reflected from the mirror and returned back into the fiber. The optical beam reflected from the end face of the fiber interferes with the beam reflected from the mirror. As a result the intensity of the optical radiation at photodetector is periodically changed depending on the distance between the fiber and mirror.

Fabry-Pérot sensors are used to measure strain or temperature. When strain measurements are made in widely varying temperature conditions the temperature must be compensated for by taking an independent temperature measurements or packaging the sensor to be thermally insensitive. (Udd, Schulz, Seim, Corones, Laylor 1998, [144])

The intrinsic Fabry-Perot fiber etalon sensors are being used principally to support time varying strain measurement applications. This includes measuring strain on vibrating machinery and cylinder heads operating at elevated temperatures, as well as measuring dynamic loads on railway bridges. (Udd, Schulz, Seim, Corones, Laylor 1998, [144])

(4) Extrinsic Fabry-Perot interferometer (EFPI)

Extrinsic Fabry-Perot Interferometers (EFPIs) are constituted by a capillary silica tube containing two cleaved optical fibers facing each others, but leaving an air gap of a few microns or tens of microns between them. When light is launched into one of the fibers, a back-reflected interference signal is obtained. This is due to the reflection of the incoming light on the glass-to-air and on air-to-glass interfaces. This interference can be demodulated using coherent or low-coherence techniques to reconstruct the changes in the fiber spacing. Since the two fibers are attached to the capillary tube near its two extremities (with a typical spacing of 10 mm), the gap change will correspond to the average strain variation between the two attachment points.

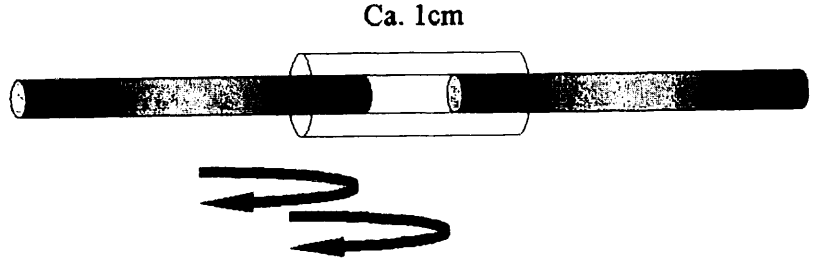

Fig. 5-13: Schematic representation of a extrinsic Fabry-Perot gauge

The extrinsic Fabry-Perot fiber etalon sensors are mainly being used to support single point static strain measurements. They have been used to support experiments on aircraft, to monitor manufacturing processes for structures and bridges, and to measure pressure. (Udd, Schulz, Seim, Corones, Laylor 1998, [144])

The use of these sensors is similar to the one of fiber Bragg gratings. The most notable differences are that EFPI's are not easily multiplexed along the same sensors line. Contrary to fiber Bragg gratings, temperature does not have a mayor influence on EFPI's. Temperature correction is only required for high resolution readings in the presence of large temperature variations. As for all strain gauges, it is important to select the proper packaging and bonding adhesive to obtain a reilable and drift-free strain reading.

(5) Sagnac interferometer

Another type of fiber interferometer is the Sagnac Interferometer, often called fiber-optic or laser gyroscope. This is probably the most developed interferometer. The Sagnac interferometer is primarily used for rotation rate measurement, though it can be used for other dynamic measurements as well (Donlagic 2000, [34]).

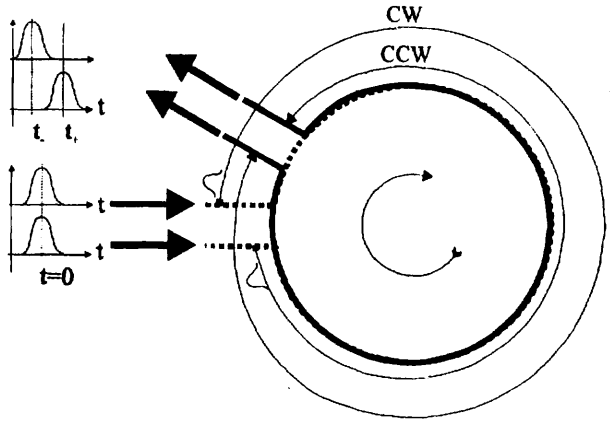

Fig. 5-14: Sagnac effect, (Donlagic 2000, [34])

Essentially, the Sagnac principle is a phase modulation technique and can be explained as follows: Two counter propagating beams, one clockwise (CW), and another counterclockwise (CCW), arising from the same source, propagate inside an interferometer along the same closed path. At the output of the interferometer the CW and CCW beams interfere to produce a fringe pattern, which shifts if a rotation rate is applied along an axis perpendicular to the plane of the path of the beam. Thus, the CW and CCW beams experience a relative phase difference, which is proportional to the rotation rate (Selvarajan, Asundi 1995, [129]). This

difference is again detected by combination of optical waves in the beam splitter to achieve maximum sensitivity of the system (Donlagic 2000, [34]).

5.2.3.6 Intensity modulated Fiber Optic Sensors

Intensity-based sensors are relatively simple to implement and widespread in application. In intensity modulated sensors the perturbation causes a change in received light intensity, which is a function of the phenomenon being measured (Wheeler, Ganji 1996, [157]). Low-cost light sources such as light emitting diodes (LEDs) can be used, and simple photodetectors may be employed to determine the intensity of the optical power in the sensor output.

The major problems associated with intensity sensors are random changes of transmissivity of optical path and variations of the output power of the optical source, which directly affects the accuracy of the sensor. Intensity sensors therefore need mechanisms that compensate for those changes.

(1) Microbend sensors

Microbend fiber sensors are configured so that an environmental effect results in an increase or decrease in loss through the transducer due to light loss resulting from small bends in the fiber. Light may be lost from an optical fiber when the bend radius of the fiber exceeds the critical angle necessary to confine the light to the core area and there is leakage into the cladding (Selvarajan & Asundi 1995 [129], Udd et al. 1998 [144]).

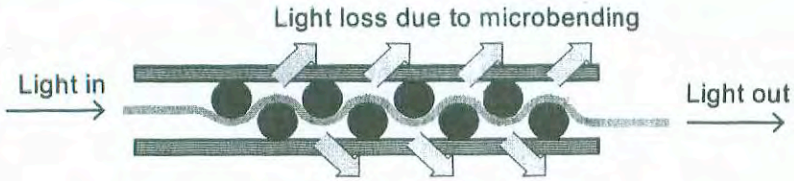

Fig. 5-15: Schematics of microbend fiber optic sensor

The typical layout of this sensor type consists of a light source, a section of optical fiber (multimode fiber) positioned in a microbend transducer designed to intensity modulate light in response to an environmental effect and a detector. In some cases the microbend transducer can be implemented by using special fiber cabling or optical fiber that is simply optimized to be sensitive to microbending loss. The Microbend sensor shown in Fig. 5-15 is designed using multimode fiber placed between two rigid plates having an optimum corrugation profile such that the fiber experiences multiple bends. Due to the microbending induced losses, the lower order guided modes are converted to higher order modes and are eventually lost by radiation into the outer layers resulting in a reduction of the optical intensity coming out of the fiber. A displacement of the plates causes a change in the amplitude of the bends and consequently an intensity modulated light emerges from the fiber core (Selvarajan & Asundi 1995 [129], Udd et al. 1998 [144]). A powermeter is used to measure the remaining light at the sensors output end and a calibration is developed between the measurand and the amount of output light.

Microbend based fiber sensors have been built to sense many different parameters including pressure, temperature, acceleration, flow, local strain, and speed. The microbend fiber-optic sensor technology is the least expensive of the fiber-optic sensor technologies

currently available. Microbend sensor systems are generally used when highly accurate measurements are not required and low cost is of paramount importance.

A microbend strip sensor might be designed that would withstand the temperatures and pressures encountered during paving with asphalt concrete. It could be put directly under the top mat during construction and take the place of traffic sensing loops that are used for controlling traffic signals. The same strip sensor could also be used to replace failed conventional loops. These applications would prevent the need to saw joints into the pavement for the placement of traditional loops, thereby decreasing pavement problems (Udd et al. 1998 [144]).

5.2.3.7 Frequency modulated fiber optic sensors

(1) Fiber Bragg grating sensors

Very popular for structural health monitoring applications are Fiber Bragg gratings. See Chapter 5.2.3, Fiber Bragg Grating (FBG) Sensors for a detailed description.

5.2.3.8 Raman sensors

Raman scattering is the result of a non-linear interaction between the light traveling in a fiber and silica. When an intense light signal is shined into the fiber, two frequency-shifted components called respectively Raman Stokes and Raman anti-Stokes, will appear in the back-scattered spectrum. The relative intensity of these two components depends on the local temperature of the fiber. If the light signal is pulsed and the back-scattered intensity is recorded as a function of the round-trip time, it becomes possible to obtain a temperature profile along the fiber (Inaudi et al. 2000 [61]). A system based on Raman scattering is commercialized by York Sensors in the UK. Typically a temperature resolution of the order of 1°C and a spatial resolution of less than 1 m over a measurement range up to 10 km is obtained for multi-mode fibers. A new system based on the use of singlemode fibers should extend the range to about 30 km with a spatial resolution of 8 m and a temperature resolution of 2°C. (Inaudi et al. 2000 [61])

5.2.3.9 Brillouin sensors

Brillouin scattering sensors show an interesting potential for distributed strain and temperature monitoring. For temperature measurements, the Brillouin sensor is a strong competitor to systems based on Raman scattering, while for strain measurements it has practically no rivals. (Inaudi et al. 2000 [60])

Brillouin scattering is the result of the interaction between optical and sound waves in optical fibers. Thermally excited acoustic waves (phonons) produce a periodic modulation of the refractive index. Brillouin scattering occurs when light propagating in the fiber is diffracted backward by this moving grating, giving rise to a frequency shifted component by a phenomenon similar to the Doppler shift. This process is called spontaneous Brillouin scattering. Acoustic waves can also be generated by injecting in the fiber two counter-propagating waves with a frequency difference equal to the Brillouin shift. Through electrostriction, these two waves will give rise to a traveling acoustic wave that reinforces the phonon population. This process is called stimulated Brillouin amplification (Inaudi et al. 2000 [60]).

The most interesting aspect of Brillouin scattering for sensing applications resides in the temperature and strain dependence of the Brillouin shift (Udd et al. 1991 [142]). This is the result of the change in acoustic velocity according to variation in the silica density. The measurement of the Brillouin shift can be approached using spontaneous or stimulated scattering. The main challenge in using spontaneous Brillouin scattering for sensing applications resides in the extremely low level of the detected signal. This requires sophisticated signal processing and relatively long integration times (Inaudi et al. 2000 [60]).

Systems based on the stimulated Brillouin amplification have the advantage of working with a relatively stronger signal but face another challenge. To produce a meaningful signal the two counter-propagating waves must maintain an extremely stable frequency difference. This usually requires the synchronization of two laser sources that must inject the two signals at the opposite ends of the fiber under test (Inaudi et al. 2000 [60]).

The MET (Metrology laboratory) group at Swiss Federal Institute of Technology in Lausanne (EPFL) proposed a more elegant approach (Udd et al. 1995 [143]). It consists in generating both waves from a single laser source using an integrated optics modulator. This arrangement offers the advantage of eliminating the need for two lasers and intrinsically insures that the frequency difference remains stable independently from the laser drift. Omnisens and SMARTEC (Switzerland) commercialize a system based on this setup. It features a measurement range of 10 km with a spatial resolution of 1 m or a range of 100 km with a resolution of 10 m. The strain resolution is 20 με and the temperature resolution 1°C (Inaudi et al. 2000 [60]).

Since the Brillouin frequency shift depends on both the local strain and temperature of the fiber, the sensor setup will determine the actual sensitivity of the system. For measuring temperatures it is sufficient to use a standard telecommunication cable. These cables are designed to shield the optical fibers from an elongation of the cable. The fiber will therefore remain in its unstrained state and the frequency shifts can be unambiguously assigned to temperature variations. If the frequency shift of the fiber is known at a reference temperature it will be possible to calculate the absolute temperature at any point along the fiber. Measuring distributed strains requires a specially designed sensor. A mechanical coupling between the sensor and the host structure along the whole length of the fiber has to be guaranteed. To resolve the cross-sensitivity to temperature variations, it is also necessary to install a reference fiber along the strain sensor. Similarly to the temperature case, knowing the frequency shift of the unstrained fiber will allow an absolute strain measurement (Inaudi et al. 2000 [60]).

5.2.4 Hydrostatic leveling systems (HLS)

The hydrostatic leveling system is based on the classical physical law of "connected vessels" (Vurpillot et al. 1998 [153]). The HLS consists of two or more interconnected fluid filled cells mounted on a structure at approximately the same elevation. One cell is designated to be the datum reference and is installed at a stable location outside the area affected by settlement. The other cells are fixed to the structure at selected locations. The fluid used for HLS is most often water (or water plus anti-freeze) due to the ease of its handling, environmental friendliness, well known properties, and low cost. Relative vertical movement of the cells causes fluid rearrangement in the circuit and consequently a level variation inside each cell. Cell elevations are related to the datum reference that can be checked by topographical survey if required.

Hydrostatic leveling is used in a wide variety of applications, but typically only as static installations on a very large scale (Imfeld et al. 1997 [59]). Hydrostatic levels are usually implemented using one of three approaches: the height-transfer method, which is the one

commonly associated with hydrostatic leveling, the pressure-transfer method, and the weight-comparison method. All three methods employ two vessels connected by a flexible tube. A tube that connects the air volumes over the cell water surfaces is necessary in the height-transfer and weight-comparison method. This ensures the atmospheric pressures over the cells are equal and the water is then free to flow between the cells. Any change in the elevation between the cells causes water to flow from one into the other, creating a new equilibrium surface. The surface of the water at each cell will conform to the same gravitational equipotential surface or "level" surface (Imfeld et al. 1997 [59]).

With the **height-transfer method**, changes in the water level height relative to the container are measured [58]. Since the water level within the connecting tubes always stays on a horizontal plane, vertical displacements can be deduced from the difference of the water levels between the deformed and the initial position of the structure. Vibration generated by the traffic does not influence measurements because of the great inertia of the HLS (Imfeld et al. 1997 [59]).

The **pressure-transfer method** implements the principle that equipotential surfaces within the fluid are at constant hydrostatic pressure to derive height difference information. Subsequent height variations occurring between the datum point and the measuring points cause proportional variations of the hydraulic pressure at each cell. A pressure transducer reads the fluid pressure at each cell. The measured pressure is referred to the liquid level in the reference cell (datum point) (Imfeld et al. 1997 [59]).

The **weight-comparison method** employs weight or load sensor cells, which accurately determines the weight of each cell. Since the height of the liquid column in each cell is a linear function of the measured weight, elevation changes can be measured very accurately (Imfeld et al. 1997 [59]).

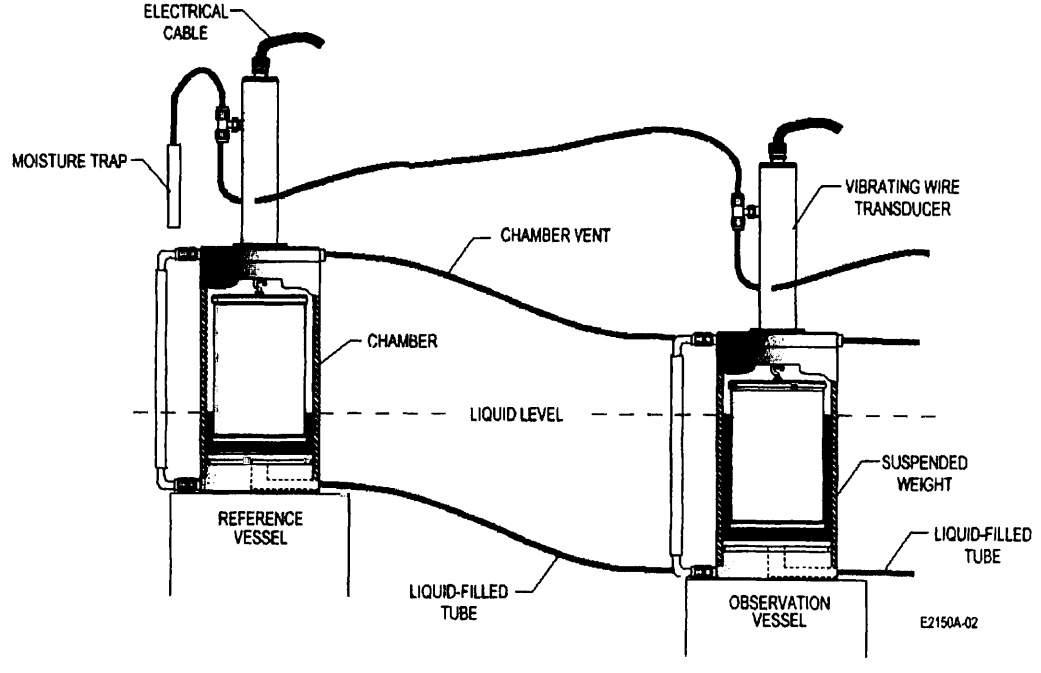

Fig. 5-16: Settlement gage developed by Roctest Telemac, [189]

The settlement gage shown in Fig. 5-16 is also a liquid level system that can be deployed in a multipoint measurement system consisting of a series of interconnected fluid filled cells. In each cell, a mass is suspended to a vibrating wire transducer. Changes in elevation of the water level in the cell modify the buoyancy force acting on the mass, thus modifying the resonant frequency of the vibration wire. [189]

Using conventional hydrostatic levels the error made on deflections for the overall system is of about ± 0,5 mm (Vurpillot et al. 1998 [153]). Pellissier developed a hydrostatic level, which can detect elevation differences even with an accuracy of +/- 5μm, the instrument incorporates several features that eliminate problems common with hydrostatic leveling. Typical error sources are: bubbles in the fluid line, temperature variations of the system, accelerations of the fluid, differing gas pressures above the cells, and observational. If bubbles are present in the fluid line they can cause two types of problems. Either they block the fluid tube if they are large or they can cause rapid variations of the fluid surface level due to their ability to expand at a greater rate than water when temperature changes. However, the largest source of error is due to thermal gradients in the fluid tube that cause the density of the fluid to be non-uniform. Hence, water of different temperature will form water columns of different heights. To alleviate these problems, a pump can be implemented in order to circulate the water throughout the entire system. Thereby a uniform temperature of the fluid can be forced and any bubbles will be pumped out of the fluid line. (Imfeld et al. 1997 [59])

Hydrostatic leveling systems are used for monitoring differential settlements in structures affected by nearby excavation and tunneling. Further applications include the measurement of settlement or heave of buildings, foundations, and other structures.

5.2.5 Geodetic measurements

Geodetic measurements are used to determine the geometrical configurations of a structure, this serves for monitoring geometrical variations due to permanent and long-term structural actions such as dead loads and super-imposed dead loads. Geodetic surveying cannot detect the structures' instant responses to transient and variable structural actions such as primary live loads.

5.2.5.1 Triangulation

Measurements of movements in large structures can be made very accurately, in two dimensions, by using triangulation and trilateration techniques. Inaccessible piers can be very accurately located by triangulation if a good base can be laid out and favorable intersection angles are obtained. In monitoring possible movements of structures, points on the structure must be related to points that have been selected for stability, usually at some distance from the structure itself. These will be called control points, and all movements of the structure will be related to one or more of them. It is important that the control points do not move, and for this reason, they should be placed in geological stable positions.

Triangulation and trilateration methods are similar in basic principle. In triangulation, the points are located at the apexes of triangles, and one base line and all angles are measured. Additional base lines are used when a chain of triangles, center point figures or quadrilaterals are required. All other sides are computed. Angles used in computation should exceed at least 15° or preferably 30° to avoid rapid change in sines for small angles. A trilateration system also consists of a series of joined or overlapped triangles, but contrary to a triangulated system, a trilaterated system measures the lengths of all the sides of the triangles and only enough angles and directions to establish azimuth.

Unless otherwise directed, measurement results established by triangulation and trilateration will be at least third-order accuracy for most applications. When measurements are made of lines exceeding 600 m, a major source of error is the inability to determine accurately the refractive index along the line. An error in temperature of 1 °C or in pressure of 2.5 mm (0.1 inch) of Hg will cause an error in length of 1 ppm. These errors may be

minimized by considering the ratio of two lines that have been measured within 30 minutes of each other. The errors of each line tend to be the same so that taking a ratio greatly reduces the magnitude of the error. The adjusted angles determined from corrected ratios are more accurate than the angles determined from the means of the lengths of the sides because ratios are more accurate than the lengths of which they are composed. As in the case of triangulation, a base line is necessary to determine the scale when ratios are used. The scale, however, is only as accurate as the mean of the two measurements of the baseline.

5.2.5.2 Global positioning system (GPS)

There are several different methods for obtaining a position using GPS. The method used depends on the accuracy required by the user and the type of GPS receiver available. Broadly speaking, the techniques can be broken down into three basic classes [181]:

- **Autonomous Navigation** using a single stand-alone receiver. Used by hikers, ships that are far out at sea and the military. Position Accuracy is better than 100m for civilian users and about 20m for military users.
- **Differentially corrected positioning**. More commonly known as DGPS, this gives an accuracy of between 0.5 - 5m. Used for inshore marine navigation, GIS data acquisition, precision farming etc.
- **Differential Phase position**. Gives an accuracy of 0.5 - 20mm. Used for many surveying tasks, machine control etc.

All GPS positions are based on measuring the distance from the satellites to the GPS receiver on the earth. This distance to each satellite can be determined by the GPS receiver. The basic idea is that of resection, which many surveyors use in their daily work. If you know the distance to three points relative to your own position, you can determine your own position relative to those three points. From the distance to one satellite we know that the position of the receiver must be at some point on the surface of an imaginary sphere, which has its origin at the satellite. By intersecting three imaginary spheres the receiver position can be determined. The problem with GPS is that only pseudo ranges and the time at which the signal arrived at the receiver can be determined. Thus there are four unknowns to determine; position (X, Y, Z) and time of travel of the signal. Observing to four satellites produces four equations, which can be solved, enabling these unknowns to be determined. [181]

There are several sources of error that degrade the GPS position from a theoretical few meters to tens of meters. These error sources are: [181]

4) Ionospheric and atmospheric delays
5) Satellite and Receiver Clock Errors
6) Multipath
7) Dilution of Precision
8) Selective Availability (S/A)
9) Anti Spoofing (A-S)

(1) Differential phase GPS, (DGPS)

Many of the errors affecting the measurement of satellite range can be completely eliminated or at least significantly reduced using differential measurement techniques. Differential Phase GPS is used mainly in surveying and related industries to achieve relative positioning accuracies of typically 5-50mm. It is a differential technique, which means that a

minimum of two GPS receivers is always used simultaneously. The Reference Receiver is always positioned at a point with fixed or known coordinates. The other receiver(s) are free to rove around. Thus they are known as Rover Receivers. [181]

Various components of the GPS signal:

- **Carrier Phase:** The sine wave of the L1 or L2 signal that is created by the satellite. The L1 carrier is generated at 1575.42MHz, the L2 carrier at 1227.6 MHz.
- **C/A code:** The Coarse Acquisition code. Modulated on the L1 Carrier at 1.023MHz.
- **P-code:** The precise code. Modulated on the L1 and L2 carriers at 10.23 MHz.

The carrier waves are designed to carry the binary C/A and P-codes in a process known as modulation. Modulation means the codes are superimposed on the carrier wave. The codes are binary codes. Each time the value changes, there is a change in the phase of the carrier. The carrier phase is used because it can provide a much more accurate measurement to the satellite than using the P-code or the C/A code. The L1 carrier wave has a wavelength of 19.4 cm. If you could measure the number of wavelengths (whole and fractional parts) there are between the satellite and receiver, you have a very accurate range to the satellite. The majority of the error incurred when making an autonomous position comes from imperfections in the receiver and satellite clocks. One way of bypassing this error is to use a technique known as Double Differencing. If two GPS receivers make a measurement to two different satellites, the clock offsets in the receivers and satellites cancel, removing any source of error that they may contribute to the equation. [181]

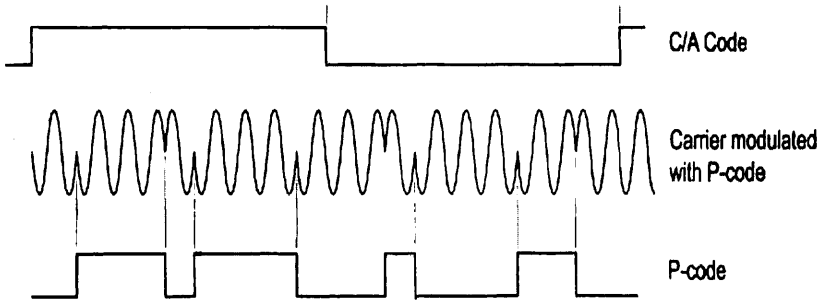

Fig. 5-17: Carrier Modulation [181]

The reference receiver

The Reference receiver antenna is mounted on a previously measured point with known coordinates. The receiver that is set at this point is known as the Reference Receiver or Base Station. The receiver is switched on and begins to track satellites. Because it is on a known point, the reference receiver can estimate very precisely what the ranges to the various satellites should be. The reference receiver can therefore work out the difference between the computed and measured range values. These differences are known as corrections. The reference receiver is usually attached to a radio data link, which is used to broadcast these corrections. The baseline(s) between the Reference and Rover receiver(s) are calculated. The basic technique consists of measuring distances to four satellites and computing a position from those ranges [181].

The rover receiver

The rover receiver is on the other end of these corrections. The rover receiver has a radio data link attached to it that enables it to receive the range corrections broadcast by the Reference Receiver. The Rover Receiver also calculates ranges to the satellites. It then applies the range corrections received from the Reference. This lets it calculate a much more accurate position than would be possible if the uncorrected range measurements were used. Using this technique, all of the error sources listed above are minimized, hence the more accurate position. It is also worthwhile to note that multiple Rover Receivers can receive corrections from one single Reference [181].

(2) Structural monitoring with GPS

The Global Positioning System (GPS) is especially suited for structural deformation monitoring of large structures like bridges. Satellite receivers are capable of determining positions to subcentimeter-level accuracies in near real-time under appropriate conditions. Thanks to this level of precision, the movement of structures can be monitored automatically and continuously. The technology exhibits no temperature or time-dependent drifts, and does not require a line-of-sight between individual points. Measurements can be relative in three dimensions, or referenced to a global coordinate frame. The falling tendency of GPS receiver equipment pricing and their miniaturization, along with their modest power requirements, allows building sizeable networks of autonomous measuring stations.

When planning to use GPS technology, several factors have to be taken into account to guarantee an effective result. In order to operate with GPS it is important that the GPS antenna has a clear view to at least 4 satellites. Sometimes, the satellite signals can be blocked by tall buildings, trees etc. Hence GPS cannot be used indoors. It is also difficult to use GPS in town centers or woodland.

There are two system architectures for structural monitoring with GPS, one based on a fixed network of sensors and the other based on mobile sensors.

Stationary GPS applications

Most conventional bridge monitoring systems rely on a fixed network of sensors that transmit their data back to a central site for processing and analysis. This is also a useful architecture for GPS-based systems. Sensor nodes are mounted on the structure at sites of interest. For measuring long-term movement, such as foundation settlement, creep, stress relaxation, and others the sensor nodes are mounted over the bridge piers. For measuring shorter term motion, such as that caused by wind or traffic loading, the sensors are mounted between piers. Each sensor node consists of a GPS receiver, microcontroller, and data radio. The GPS receiver tracks the satellite signals and computes the range and phase measurements. These measurements are transmitted to the central processing site by the data radios. The microcontrollers perform temporary data buffering, provide receiver control interfaces, and manage network communications flow control. The central processing site consists of a data radio and personal computer (PC) with software for system control, data communications and management, data-quality checking, position computation, and movement analysis. (Duff & Hyzak 1997 [35])

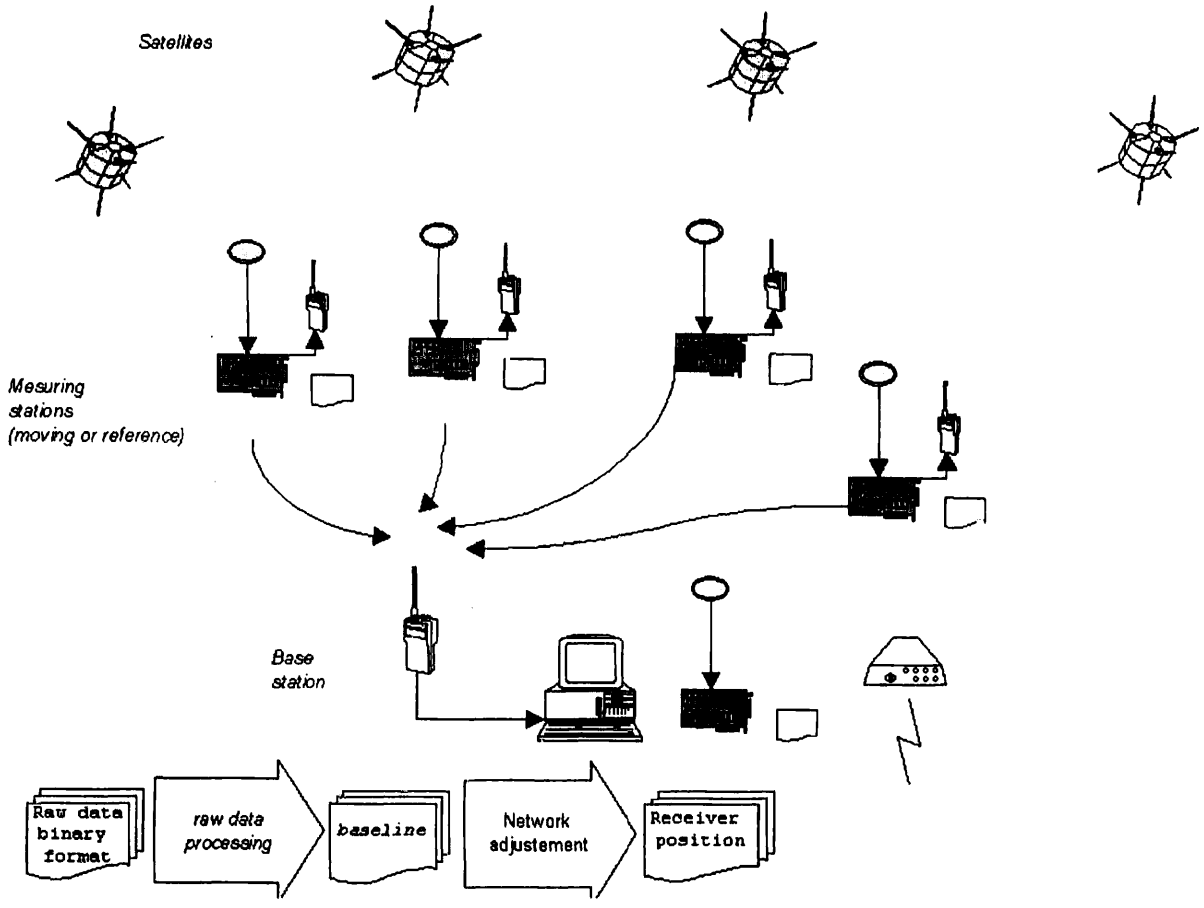

Fig. 5-18: Monitoring system and data processing chain

Mobile GPS applications

There is another implementation of GPS for bridge monitoring that does not apply to short-term motion but can provide a very cost-effective means of periodically measuring long-term deformations. This method consists of performing kinematic surveys of the bridge deck, using a combination of GPS and analog sensors. Achievable accuracies are in the centimeter range for each data point, and a very high spatial density of positions over the deck surface is produced. This allows for generation of three-dimensional surface profiles that will show pier settlement and vertical deformations of the superstructure (Duff & Hyzak 1997 [35]).

For this implementation, one or two GPS receivers are mounted on the side of a vehicle above its roof. A wheel is mounted directly below the GPS antenna with an LVDT inserted into the coupling between the wheel and the antenna. This will measure the effect of the vehicle's suspension system so it can be deleted from the position solutions. Inertial sensors such as accelerometers and gyros can be added to the GPS antenna assembly to further increase positioning accuracy (Duff & Hyzak 1997 [35]).

With the stationary reference GPS receiver collecting and storing its data, the instrumented vehicle is driven over the bridge several times in each traffic lane, collecting and storing its data for post-processing. Data from the GPS receivers and other sensors are combined for position computation and error analysis. The discrete positions are then filtered, and a three-dimensional surface profile is generated, representing the current shape of the bridge deck. Comparing successive profiles over time will show the extent and geometry of settlement or bending. This technique derives its high cost-effectiveness from the fact that a

few sensor packages can be used to monitor a large number of bridges. The GPS reference receiver and instrumented vehicle could periodically survey every bridge of interest in a wide region (Duff & Hyzak 1997 [35]).

(3) Application and selection criteria

There are many monitoring applications that can benefit from satellite surveying. The unique capabilities of this technique are best exploited where:

- the required precision is at sub-centimeter level
- the single stations are less than 20Km apart
- there is no line-of-sight between single stations
- there exists a good visibility of the open sky from all stations in the network
- the dynamics of the system under surveillance is low
- the area to be monitored is not easily accessible, requiring unattended operation for longer periods of time

GPS monitoring is currently a highly active field of research and development. It can be foreseen that as competition builds up and the system will be widely adopted, there will be many performance improvements while equipment prices will exhibit a falling tendency. Generally, the main components that influence the system cost are:

- receiver and antenna properties (GPS, GPS and GLONASS, number of frequencies)
- post-processing software
- communication channels used (GSM, radio link and possible repeaters)

longest baseline	20 km
accuracy	10..3mm
integration time	10..90 min
system dynamics, max.	10mm/h
mobile station size	20*20*20cm
mobile station weight	~5 Kg
operating temperature	-35..+70°C
antenna type	CRGP L1

Table 5-3: Technical parameters

(4) Limitations

Perhaps the most important limitation to the use of GPS technology to monitor structural deformation is that is requires the antenna to have a clear view of the sky. This limits its use to the top surface of structures. Small obstructions can be tolerated in many applications.

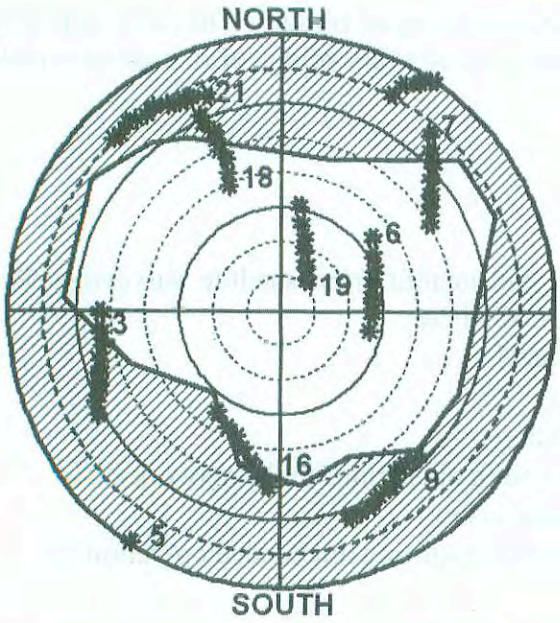

Fig. 5-19: Example of a satellite visibility plot; the grey area denotes obstructions (terrain, buildings, etc.)

Another limitation stems from the measuring principle itself, and excludes the use of GPS monitoring in heavily polluted electromagnetic environments.

Monitoring accurately with GPS requires averaging the measured data over a period of time. While instantaneous snapshots can provide an accuracy in the order of centimeters after the initial ambiguity problem is solved, integration times of up to 90 min may be required for millimeter level accuracy. Ongoing research combines the GPS sensor with three-dimensional accelerometers for accurate modal analysis.

(5) Accuracy of GPS

There are two primary attributes required of a GPS receiver system to produce subcentimeter-level positioning accuracy. First, the receiver itself must generate high-quality coherent phase data. Second, the GPS antenna assembly must have a precise electrical phase center and adequate multipath rejection capabilities. Because of imperfections in antenna element design and manufacturing processes, the range to satellites in different parts of the sky will be measured from slightly different points on the GPS antenna. The antenna's electrical phase center is the region to which satellite signals coming from different elevation and azimuth angles get referenced. A good survey-quality GPS antenna will have a phase center size of 5 millimeters or less. Structural monitoring applications involve relatively short GPS baselines, generally 2 kilometers or less. Under these conditions, multipath, or signal reflection from nearby objects into the GPS antenna, is the dominant source of error. Because phase multipath is zero mean (range multipath is not), its induced errors can be successfully reduced by averaging over time. However, if the antenna assembly does not provide a high degree of multipath rejection, averaging times of four to 24 hours may be needed to produce a single position with subcentimeter accuracy. The most effective device for multipath mitigation at the antenna is a choke ring. These groundplanes with concentric circular troughs reduce multipath through successive rounds of destructive interference as the signal nears the antenna element (Duff & Hyzak 1997 [35]).

For a typical bridge instrumentation scenario, the accuracy of each position computed lies at the centimeter level. Averaging positions for each site over time increases accuracy to the millimeter level. Under good tracking conditions, 1-millimeter accuracy is achievable.

Assuming that the GPS receivers produce high quality phase data and that distances between the reference GPS receiver and those on the bridge (baselines) are kept short, positioning accuracy is mainly a function of the averaging time used. This, in turn, depends on the type of motion that is being monitored. Foundation settlement, creep, and other movement generally occur over relatively long periods of time. Therefore, averaging times of a few hours can be used, producing positions with millimeter-level accuracy. Motion due to wind loading is cyclic with frequencies of a few hertz. Because, therefore, little or no averaging can be done, positioning accuracy is at the centimeter level. This restricts the utility of GPS for monitoring short-term motion to more flexible structures. Also, to measure short-term effects, sampling rates must be significantly increased, inducing heavier processing and data communication loads (Duff & Hyzak 1997 [35]).

5.2.5.3 Laser deflection measurements

With the advent of laser equipment, geodesic surveying has gained high accuracy and excellent field performance. Laser beam distance gauges have greatly facilitated and improved the essential bridge inspection task of measuring clearances (Yanev 2000 [160]).

(1) Coherent laser radar (CLR)

Bridge deflection measurement using coherent laser radar is an adaptation of a rapid inspection system developed for NASA. The portable laser scanning system deployed under a bridge is able to measure deflections at hundreds of individual points in a few minutes. The CLR is providing full field, three dimensional measurements of the bridge deflections under a variety of loading conditions. It also measures the vibration of the bridge and has the potential to facilitate the application of modal analysis (a branch of structural analysis that uses measurements of the vibrations of a bridge with respect to frequency, amplitude, shape, and decay with time to determine important structural properties of the bridge and to detect damage) as a bridge-inspection tool. The CLR can measure ranges from 2 To 30 meters, with sub-millimeter accuracy, and requires no special targets or surface preparation.

Conventional deflection measurement devices require time consuming preparation to properly install and often require access under the bridge structure, which in many cases means costly and inconvenient traffic control. The laser system has the ability to measure these bridge deflections quickly and with minimal setup time. A greater number of measurement locations can be obtained with the laser system as compared with conventional systems and, where needed, the laser system can make reliable measurements from a location, which would not require altering traffic.

The CLR directs a focused laser beam to a point on the structure to be measured and recaptures a portion of the reflected light. The single large-aperture optical path maximizes signal strength and stability. As the laser light travels to and from the target, it also travels through a reference path of calibrated optical fiber in an environmentally controlled module. Heterodyne detection of the return optical signal mixed coherently with the reference signal produces the most sensitive radar possible. Extensive signal processing extracts the range-dependent signal frequency with great accuracy. Measurement of the signal intensity and signal-to-noise ratio provides a built-in check that confirms measurement quality. The two paths are combined to determine the absolute range to the point.

Apart from deflection measurement, a potential application for laser-based position-sensitive measurement technology is measurement of the dynamics of large constructions like bridges, towers, buildings and masts and movement of other moving objects.

5.3 Strain measurements

The measurement of deformation from the material point of view includes the observation of local material properties made by a series of short-base length strain sensors.

Strain refers to the internal compressive and/or tensile state of a material and gives a measurement of the loading of the structure at a given point. Unfortunately there is no such thing as a real strain sensor (except for photoelasticity that is suited only for the study of some specific transparent materials). All other so-called strain sensors are actually deformation sensors with a very short measurement base. If it can be assumed that the strain state of the structure is almost constant along this short measurement path L, the measured deformation ΔL will be given by:

$$\Delta L = \varepsilon \cdot L$$

By measuring ΔL, it is therefore possible to obtain an indirect measurement of ε.

Strain sensors are best suited to monitor the local behavior of the materials rather than the global behavior of the structure. Strain sensors will therefore be placed at critical points of the structure where high strains are expected that could approach or surpass the material resistance (Inaudi et al. 1996 [63]).

When measuring deformations and strains it makes sense to differentiate short-term and long-term strains. Short-term strains are those changes that can be observed over a period of hours whereas long-term strains are those occurring over months or years. Short-term strains are generally caused by changes in dead and live loads, daily temperature cycles, or wind loading. Long-term strains are caused by seasonal temperature changes and creep and shrinkage in concrete structures. Both short-term and long-term surface strains can be measured using fiber optical, mechanical, and electrical resistance strain gages. Determining the changes in length between two points on the concrete surface can be achieved by comparison with the length of a standard invar reference bar. Other approaches use fiber optical sensors with comparable reference fibers or vibrating wires. Depending on the sensitivity of the measuring devices to changes in temperature it might be necessary to take into account the temperature of concrete surface and, e.g., standard reference bar temperatures when using a mechanical strain gage. Depending on the nature of the measurement, considerations regarding long-term stability, accuracy and reliability of the sensing device must be taken into account (U.S. Department for Transportation 1996 [147]).

5.3.1 Short-term strains

Short-term strains can be measured using electrical resistance strain gages. Although these gages can be attached directly to reinforcing steel in the field, this method requires attachment under field conditions and is very difficult. Consequently, the gages should be attached to separate lengths of reinforcement. This allows the gages to be attached to the bars under laboratory conditions and permits proper attachment of leads and waterproofing. The gaged bars can be tied directly to the reinforcement cage.

Independent of the type of used gage technology we will have to bring the lead wires to a readout unit or a data acquisition system located at a convenient position. Whenever possible, the wires should be protected from possible sources of damage by the use of appropriate sheathing. Electrical resistance strain gages can be applied to hardened concrete surfaces. Depending on the character of a material surface, special techniques are needed to prepare the surface prior to application of the gages. Weldable electrical resistance strain gages are available for use on steel structures and large size reinforcing bars. These gages are produced

with leads and waterproofing attached and only require spot welding to the steel. However, the installation issues as described in this section do not only apply to electrical resistance gages. The use of other types of sensors may prescribe other installation considerations.

5.3.2 Long-term strains

Measuring long-term strains should be done with gages designed specifically for this purpose. While electrical resistance gages may not be recommended for this purpose, there exist other gage technologies (fiber optical sensors, Carlson strain meters, vibrating wire gages, etc.) that are designed to have long-term stability, are robust for installation on site, and are provided with leads already attached. The gages can be either installed directly in the structure or by casting them in concrete blocks and then cast the blocks in the concrete structure. The latter method is discussed because doubts about the effect of differential creep and shrinkage between the block and the concrete. Long-term strain measurements are generally used to determine prestress losses. For this purpose, when positioning the gages, it is necessary to consider distribution of the prestressing forces. Gages should be placed at the center of gravity of the prestressing force close to midspan and parallel to the strand.

Measurements of long-term strains should begin as soon as the concrete is placed although readings in fresh concrete may not be appropriate for the "initial readings" for data reduction. Initial readings should be taken before and after every significant event that affects the stress in the structure. After completion of the structure, it may only be necessary to obtain data every few months. Sufficient readings should be obtained so that trends in the data are clearly discernable. (U.S. Department for Transportation 1996 [147])

5.3.3 Measurement of strain

Fundamentally, all strain gages are designed to convert mechanical motion into an electronic signal. A change in capacitance, inductance, or resistance is proportional to the strain experienced by the sensor. If a wire is held under tension, it gets slightly longer and its cross-sectional area is reduced. This changes its resistance (R) in proportion to the strain sensitivity (S) of the wire's resistance. When a strain is introduced, the strain sensitivity, which is also called the gage factor (GF), is given by:

$$GF = \frac{\frac{\Delta R}{R}}{\frac{\Delta L}{L}} = \frac{\frac{\Delta R}{R}}{Strain}$$

The ideal strain gage would change resistance only due to the deformations of the surface to which the sensor is attached. However, in real applications, temperature, material properties, the adhesive that bonds the gage to the surface, and the stability of the metal all affect the detected resistance.

For structural monitoring, the most important requirement that strain sensors should meet is the long-term stability of the output data, which can only be achieved by a quasi calibration free measuring system. Whereas electrical strain gages appear to be not suitable for long-term measurements due to the almost unavoidable "drift" of the strain readings, vibrating wire strain gages have proved to be applicable for structural monitoring. Several strain measuring techniques based on fiber optics have also been used for such purposes, however, not all of them have exhibited sufficient long-term stability. More recently, one of the most promising

new technologies in fiber optics, the fiber Bragg grating, has been employed for strain measurements.

5.3.3.1 Interpretation of strain measurements

Measurements of strains must be corrected for the coefficient of thermal expansion of the gages and the concrete if measurement of long-term strains is the objective. Determination of stresses from short-term strains requires a determination of the modulus of elasticity of the concrete or steel. Determination of stresses from long-term strains is considerably more complex and requires information about creep and shrinkage of the concrete. Consequently, accurate interpretation of the measured data requires information about the coefficients of thermal expansion of the gages and concrete, modules of elasticity of concrete and steel, and creep and shrinkage of concrete. These data can be calculated or may be available from previous projects. However, it is recommended that the properties be determined from measurements on the actual concretes used in the instrumented portions of the structure, which requires the manufacturing of separate test specimens. These specimens should be cured and stored as long as practical with the actual structure prior to test. (U.S. Department for Transportation 1996 [147])

5.3.3.2 Mechanical strain gages

Both short-term and long-term surface strains can be measured using mechanical strain gages. In this method, the distance between two points on the concrete surface is compared with the length of a standard invar reference bar. This approach requires the installation of special points on the concrete surface, is labor intensive, and cannot be used easily with an automated data acquisition system. It is particularly suitable for measurements of strand transfer length and as back up for long-term strain measurements by other means. Measurements of concrete surface temperatures and standard reference bar temperatures are also needed (U.S. Department for Transportation 1996 [147]).

5.3.3.3 Electrical strain gages

The strain measurement by means of electrical strain gages is the most commonly experimental method to identify the stress distribution of a structure or of a part of the structure. Therefore the electrical strain gages have obtained a high stage of development.

The gage is bonded to the part being studied, and the assumption is made that the strain in the gage is equal to the local strain in the part. This strain causes a modification of some electrical quantity of the gage.

Basically, the electrical strain gages may be classified by the physical effect of converting the strain into some electrical quantity. According to that, typical kinds of these gages are the metal resistance gage, the semiconductor gage and the capacitive gage.

(1) Metal resistance gage

The metal strain gages are the one most commonly used with the largest application field. Since the technology for this type of strain sensor is well established, there exists a vast

number of different configurations e.g.: single gages, rectangular rosettes, equiangular rosettes, quarter-, half- and full-bridge configuration, etc.

The physical principle of these gages is the following. When pulled or compressed, a metal wire changes its electrical resistance as a result of change of its length L, its cross-section and its specific resistivity ρ. The relative change of resistance ΔR referred to the basic resistance R is proportional to the strain ε:

$$\frac{\Delta R}{R} = \frac{\Delta \rho}{\rho} + (1 + 2\mu)\frac{\Delta L}{L} = k \cdot \varepsilon$$

μ = Poisson's ratio

That is, a strain can be detected by measurement of the change of electrical resistance. The sensitivity of metal resistance gages expressed by the gage factor k is about k = 2 ... 4 for all this gages and is determined by the geometrical share 1+2μ. Due to the small change of resistance a Wheatstone bridge and an additional amplifier are commonly used to obtain a voltage signal from the gage.

A resistance strain gage consists of a metal resistor element, which is formed as a meander-shaped measuring grid on a carrier matrix made of an isolating material such as plastics, see Fig. 5-20. When a load is applied to the surface, the resulting change in surface length is communicated to the resistor and the corresponding strain is measured in terms of the electrical resistance of the foil wire, which varies linearly with strain. The foil diaphragm and the adhesive bonding agent must work together in transmitting the strain, while the adhesive must also serve as an electrical insulator between the foil grid and the surface.

The material of metal resistor is a special alloy, e.g. constantan. Initially, the measuring grid was handmade by means of a thin wire, but these conventional wire gages were replaced by foil gages made by analogous with technology of printed circuits. The foil gages come in a wide variety of materials, sizes and types, from a large number of manufacturers. They have been designed for many special applications and operating conditions. Examples would include very large strains, very small strains, and elevated temperatures, on concrete and on reinforcing bars in use. They are also used as a basis for the design of transducers for measuring other parameters, such as force, pressure and acceleration.

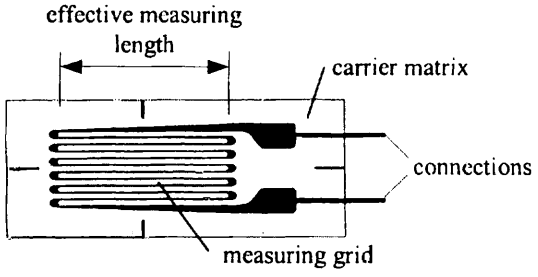

Fig. 5-20: Metal strain gage (foil gage)

Measuring circuit

Since dR/R is very small and difficult to measure directly, electronic circuits are used to measure the change in resistance rather than the resistance itself. Strain gage transducers usually employ four strain gage elements electrically connected to form a Wheatstone bridge circuit. The Wheatstone bridge is a divided bridge circuit used to measure very small changes

in static or dynamic electrical resistance. Fig. 5-21 shows a schematic diagram of a simple Wheatstone bridge circuit. (OMEGA 1998 [100])

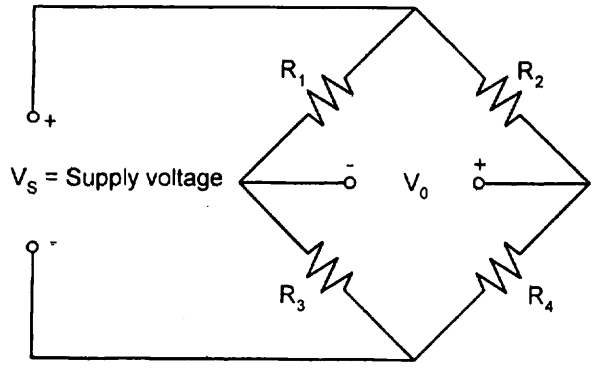

Fig. 5-21: Wheatstone bridge

As seen in the sketch, a supply voltage is provided across the bridge, which contains four resistors (two parallel legs of two resistors each in serics). The output voltage is measured across the legs in the middle of the bridge. In case the measuring device used to obtain the output voltage V_o has an infinite input impedance, and therefore has no effect on the circuit. The output voltage V_o can be calculated using Ohm's law, according to

$$V_o = V_s \frac{R_3 R_1 - R_4 R_2}{(R_2 + R_3) \cdot (R_1 + R_4)}$$

The output voltage of the Wheatstone bridge is expressed in millivolts output per volt input. The Wheatstone circuit is also well suited for temperature compensation. The total strain, or output voltage of the circuit (V_o) is equivalent to the difference between the voltage drop across R1 and R2. The bridge is considered balanced when R1/R4 = R2/R3 and, therefore, V_o equals zero. Any small change in the resistance of the sensing grid will throw the bridge out of balance, making it suitable for the detection of strain. (OMEGA 1998 [100])

When the bridge is set up so that R2 is the only active strain gage, a small change in R2 will result in an output voltage from the bridge. If the gage factor is GF, the strain measurement is related to the change in R2 as follows:

$$Strain = (\Delta R2 / R2) / GF$$

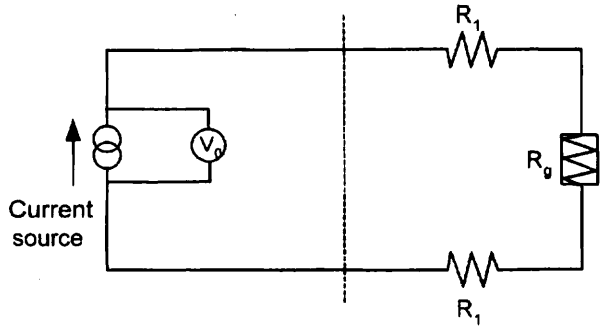

Fig. 5-22: Constant current circuit schematic

Resistance can be measured by exciting the bridge with either a constant voltage or a constant current source. Because R = V/I, if either V or I is held constant, the other will vary with the resistance. Both methods can be used. While there is no theoretical advantage to using a constant current source as compared to a constant voltage, in some cases the bridge output will be more linear in a constant current system. Also, if a constant current source is used, it eliminates the need to sense the voltage at the bridge; therefore, only two wires need to be connected to the strain gage element. The constant current circuit is most effective when dynamic strain is being measured. This is because, if a dynamic force is causing a change in the resistance of the strain gage (Rg), one would measure the time varying component of the output (V_o), whereas slowly changing effects such as changes in lead resistance due to temperature variations would be rejected. Using this configuration, temperature drifts become nearly negligible (OMEGA 1998 [100]).

The output of a strain gage circuit is a very low-level voltage signal requiring a sensitivity of 100 microvolts or better. The low level of the signal makes it particularly susceptible to unwanted noise from other electrical devices. Capacitive coupling caused by the lead wires' running too close to AC power cables or ground currents are potential error sources in strain measurement. Other error sources may include magnetically induced voltages when the lead wires pass through variable magnetic fields, unwanted contact resistances of lead wires, insulation failure, and thermocouple effects at the junction of dissimilar metals. The sum of such interferences can result in significant signal degradation.

Strain gage arrangement

The number of active strain gages that should be connected to the bridge depends on the application. For example, it may be useful to connect gages that are on opposite sides of a beam, one in compression and the other in tension. In this arrangement, one can effectively double the bridge output for the same strain. In installations where all of the arms are connected to strain gages, temperature compensation is automatic, as resistance change due to temperature variations will be the same for all arms of the bridge. In a four-element Wheatstone bridge, usually two gages are wired in compression and two in tension. For example, if R1 and R3 are in tension (positive) and R2 and R4 are in compression (negative), then the output will be proportional to the sum of all the strains measured separately. For gages located on adjacent legs, the bridge becomes unbalanced in proportion to the difference in strain. For gages on opposite legs, the bridge balances in proportion to the sum of the strains. Whether bending strain, axial strain, shear strain, or torsional strain is being measured, the strain gage arrangement will determine the relationship between the output and the type of strain being measured. (OMEGA 1998 [100])

(2) Semiconductor strain gages

The semiconductor gages apply the physical effect that the specific resistivity of a semiconductor is strongly depended on its strain (piecoresistive effect). Compared with the metal gages, therefore the part $\Delta\rho/\rho$ represents the essential share of the sensitivity. Gage factors of about k = 120 are typical for semiconductor gages. Due to this high factor the gages are predestined for micro strain measurements. In Fig. 5-23 a typical design of a semiconductor strain gage is shown. In these gages both p-type and n-type semiconductors are used. By using an n-type semiconductor in the grid, the gage comes with a negative gage factor and with a temperature coefficient of resistance controlled to match the coefficient of the thermal expansion of the measurement object. The combination of a p-type and an n-type

semiconductor formed as a half-bridge allows to generate gage factors up to about k = 220 respectively to enable a temperature compensation of the gage. The disadvantages of semiconductor gages are the strong dependence of the gage factor on the temperature, their small grid lengths and their sensitivity against mechanical influences. Therefore the application field of these gages is restricted to the measurement of micro strains and to the design of special transducers. Because of the rough environmental conditions they are not so significant in health monitoring.

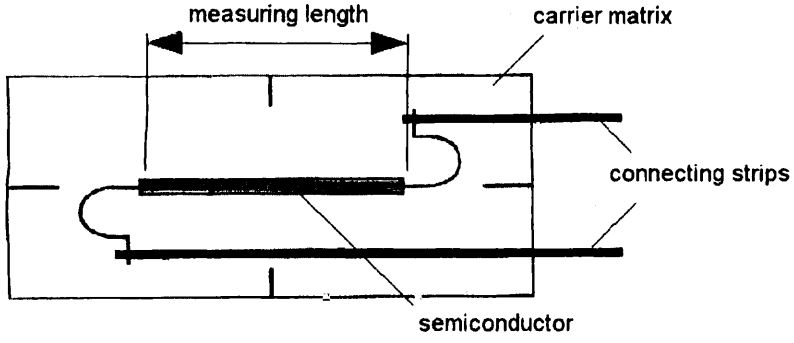

Fig. 5-23: : Semiconductor strain gage

(3) Capacitive gages

The electrical capacitance depends on the area of the capacitor plates, the distance between the plates and the dielectric constant of the material between the plates. For capacitive gages the dependence on the distance between the plates and on the area of the plates are especially used. The gages are so constructed that one parameter of the capacitance is changed as a result of the measuring strain. Fig. 5-24 shows a British development by the Central Electricity Research Laboratories (CERL) in cooperation with the company Planer. Here a plate capacitor is used where the plate distance is changed depending on the strain to be measured.

The advantages of capacitive gages are their insensitivity against high temperatures (up to 800°C) and their low zero-point drift. An adverse effect on their application meaning have the non-linear interdependence between strain and capacitance change as well as their high internal resistance, which require a special measuring circuit. The gages are usually fastened to the object studied by means of spot welding.

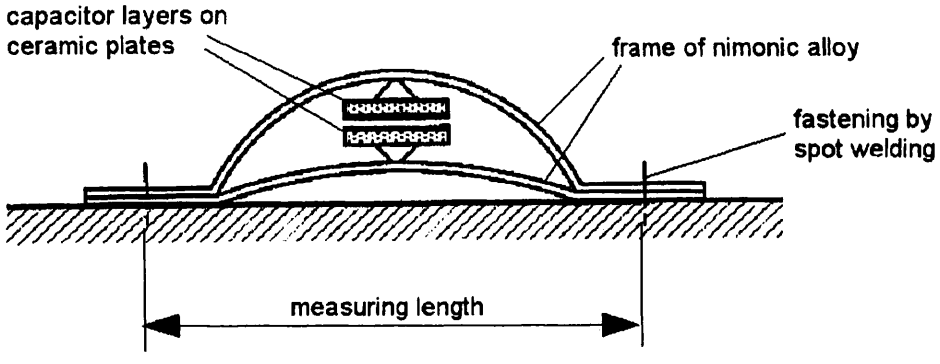

Fig. 5-24: Capacitive strain gage from CERL-Planer

(4) Technical parameters

The following parameters refer to the metal gages (foil gages) as the main kind of electrical gages, only.

Parameter	Value respectively design
Gage length [1]	0.5 ... 150 mm
Measurable strain range	≤50mm/m (normally); up to 200 mm/m (specially)
Resolution	≥1 μm/m (normally); up to 0.1 μm/m (specially)
Temperature range [2]	• – 200 ... + 200°C (non-zero referenced measurements; constantan grid) • – 20 ... + 70°C (high accuracy)
Gage factor k (average) [3]	2.05 ... 2.2 (usually), 4 (Platinum-tungsten)
Transverse sensitivity q [4]	– 0.9% ... + 2%
Gage resistance	120, 350, 500, 700, 1000 Ohms
Material of sensing grid	Alloys; e.g. Constantan, Karma, Nichrome V, Platinum-tungsten
Material of carrier matrix	e.g. epoxy-phenolic or polyester resin, polyamide, ceramics, stainless steel
Gage pattern	• 1 grid gages (linear gages); gages with 2, 3, 4 and more grids (gage chains) • gages with 2 or 3 measuring directions (rosettes) • special gages, e.g. gages for membranes or for the investigation of residual stress
Gage series	• gages with "Self-Temperature-Compensation" capability (S-T-C) • gages with creep adaptation • protected gages (e.g. waterproofed or shielded gages) • weldable gages
Fastening kind	with an adhesive, by (spot)welding or by embedding

Table 5-4: Technical parameters

[1] In civil engineering structures very small gages are rarely necessary. In concrete applications longer gage lengths are required to avoid anomalous local strain readings because of the effects of the aggregate size.

[2] The question of temperature limits in the application of strain gages is extremely difficult to answer. The reasons for this are the different influences of strain gage parameters at the relevant level, the influence duration of the temperature and also the tolerable measurement error. Measurements above 200 to 300°C give problems both with regard to zero-point stability and to the service life.

[3] The gage factor k is a proportional factor for the complete gage and depends on the grid material, the configuration of the grid and the strain transfer conditions into the grid. Therefore, the manufacturer using as test samples for each production lot defines the gage factor k. It is not possible to adjust the gage factor during manufacture in order to achieve a specific value.

[4] The transverse sensitivity q is defined as the ratio of the gage factor k_T (transverse to the direction of measurement) and the gage factor k_L (in the measurement direction). Whereas the gage factor k_L is measured in the uniaxial strain field, the gage factor k is made in the uniaxial stress field. Hence there is a difference between k_L and k, which depend on the strain gage's transverse sensitivity.

(5) Application and selection criteria

Fastening kinds

Strain gages are usually bonded to the investigated part with an adhesive. For special application weldable gages are available. These have a metal base, e.g. stainless steel and attachment is usually by spot welding. Use of weldable gages speeds up the installation process. Because of the steel base, these strain gages have very high strain rigidity. Therefore, they can only be used on thick-walled, strong objects, e.g. in steel constructions or at reinforcing rods in concrete structures. A third fastening method is to embed the strain gage in the material of the studied part. To this end special embedded gages are used. They include foil gages embedded in a special plastic cover, which allow both the waterproofing property and the adhesion quality. This fastening kind is restricted to some special applications and materials, e.g. to measure the internal strain (stress) in mortar or concrete.

Surface preparation for bonding with an adhesive

Strain gages can be satisfactorily bonded to almost any solid material if the material surface is prepared properly. However, this bonding requires a marked know how. The purpose of surface preparation is to develop a chemically clean surface having a roughness appropriate to the gage installation requirements, a surface alkalinity corresponding to a pH of 7 or so, and visible gage layout lines for locating and orienting the strain gage. Cleanliness is vital throughout the surface preparation process. It is also important to guard against recontamination of a once-cleaned surface. For applications at concrete you've got to be aware that concrete surfaces are usually uneven, rough, and porous. Therefore the surface must be prepared by a procedure, which accounts for these properties of concrete. For example, in order to develop a proper substrate for gage bonding, it is necessary to apply a leveling and sealing precoat of epoxy adhesive to the concrete.

Strain gage selection

The question that should be considered during the selection of a type of strain gage from the available gages arise due to the variety of strain gage applications and due to the conditions affecting the strain gage during service. There is no strain gage that meets all requirements. For this reason numerous different strain gages are available and are supplemented with special types when required.

Experience has shown that many users only have a vague idea of the process desired at the point of measurement. Therefore the fundamental part of selection procedure is to analyze the measuring problem. For example, the following aspects can be helpful to selection of a suitable type of strain gage:

- Fundamental object of the desired strain measurement (e.g. experimental stress analysis, manufacture of transducers, plant monitoring etc.)
- Mechanical conditions at the point of measurement
  Stress state (uniaxial or biaxial, direction of principal tension is known / unknown)
  Stress field topography (homogenous or inhomogeneous; determination of average or peek value)
  Type of loading (static or dynamic)
  Ratio of the useful part and the disturbance part of the measured strain, e.g. the wanted

(useful) strain is the one as the result of normal stress and is superimposed by a strain caused by bending stress as disturbance)

- Environmental conditions
  Duration of the measurement (once only, short term or long term etc.)
  Temperature (level, rate of change, one-sided radiation etc.)
  Other disturbance influences (humidity, moisture contents, chemicals, electric disturbing field etc.)
  Installation environment (laboratory or field)

The second requirement needed to select an optimum strain gage is the knowledge of the strain-gage's parameters. However, the determination of these parameters is not always carried out using the same method, so that the results may be interpreted differently. The purpose of national recommendations was to ease this situation and promote a universal measurement method. Work on international adaptation is in progress.

Strain gage material

When selecting a strain gage, one must consider not only the strain characteristics of the sensor, but also its stability and temperature sensitivity. Unfortunately, the most desirable strain gage materials are also sensitive to temperature variations and tend to change resistance as they age. Thus, when strains are measured with electrical resistance strain gages or mechanical strain gages, temperatures should be measured at the gage locations. Each strain gage wire material has its characteristic gage factor, resistance, temperature coefficient of gage factor, thermal coefficient of resistivity, and stability. Typical materials include Constantan (copper-nickel alloy), Nichrome V (nickel-chrome alloy), platinum alloys (usually tungsten), Isoelastic (nickel-iron alloy), or Karma-type alloy wires (nickel-chrome alloy), foils, or semiconductor materials. The most popular alloys used for strain gages are copper-nickel alloys and nickel-chromium alloys. Semiconductor materials like germanium and silicon show gage factors more than fifty times, and sensitivity more than a 100 times, that of metallic wire or foil strain gages. Silicon wafers are also more elastic than metallic ones. After being strained, they return more readily to their original shapes. However these materials exhibit substantial nonlinearity and temperature sensitivity. Semiconductor strain gages that depend on the piezoresistive effects of silicon or germanium measure the change in resistance with stress as opposed to strain. While the higher unit resistance and sensitivity of semiconductor wafer sensors are definite advantages, their greater sensitivity to temperature variations and tendency to drift are disadvantages in comparison to metallic foil sensors. Another disadvantage of semiconductor strain gages is that the resistance-to-strain relationship is nonlinear, varying 10-20% from a straight-line equation. With computer-controlled instrumentation, these limitations can be overcome through software compensation (OMEGA 1998 [100]).

Finally, it should be said, that due to their low-level outputs and the inherent sensitivity to electrical noise, these types of sensing elements require appropriate signal conditioning such as excitation, amplification, filtering, etc. (Sanayei & Saletnik 1995 [117])

(6) Disturbance influences and countermeasures

Temperature change

Civil engineering structures are subjected to changing thermal conditions, and this is a factor that must be considered for both short and long term installations. Any measured change in resistance would be interpreted as a change in strain, and the user usually wants the stress-induced strain. Changes in temperature cause a change in measuring signal of a strain gage from three distinct effects:

- The strain caused by the free thermal expansion of the part,
- the thermal expansion of the gage's measuring grid and
- the change of the specific resistivity of the gage's grid material.
- In addition the temperature response of the electrical resistance of the wiring, which is connected to the strain gage, can also cause a change in measuring signal.

The effects of these factors on stability of the measuring system may be reduced by proper design of the installation and the measuring circuit, calibration, and the data reduction process. These methods may be briefly described as:

1) Use of self-temperature-compensating gages (S-T-C), which reduce, but do not eliminate, some effects,
2) use of temperature compensating circuits, which require the use of a fully installed strain gage as a leg in the bridge circuit, and
3) use of a correction procedure in the data reduction process.

Moisture and drift

Civil engineering applications often require measurement of strain over long periods of time, and so stability of the measuring system becomes important. Factors, which affect stability, are the effects of time and moisture on the gage, the adhesive used, the circuit design, bridge completion resistors, etc. Gage manufacturers have developed materials and techniques to improve long term stability, to a point. For example, gage coatings are available for waterproofing installations, and encapsulated gages enclose the active resistor to reduce the effects of moisture.

Drift in the measuring circuit is a problem, which must be addressed using the requirements of a given application, because drift in the circuit must either be eliminated (to an acceptable degree) or corrected in the data reduction process.

5.3.3.4 Vibrating wire strain gages

(1) Functional principles

The vibrating wire gauges are based on the measurement of the vibration frequency of a metallic wire strained between two points undergoing a relative displacement. The wire is forced to vibrate by a coil excited by an electrical impulse. After a stabilization period, the wire frequency is recorded. Since this frequency depends on the wire tension and is therefore proportional to the displacement between the two attachment points, it becomes possible to measure the average strain in-between. The red-out unit is essentially a frequency meter. To obtain a more precise reading it is also possible to force the vibration at a single frequency and look for the maximum resonance point. Since the vibration frequency is also temperature

dependant, it is necessary to measure the temperature to correct for this cross-sensitivity. This can be done by measuring the coil resistance, which is also temperature dependant.

The following figure shows a typical packaging for vibrating wire sensors.

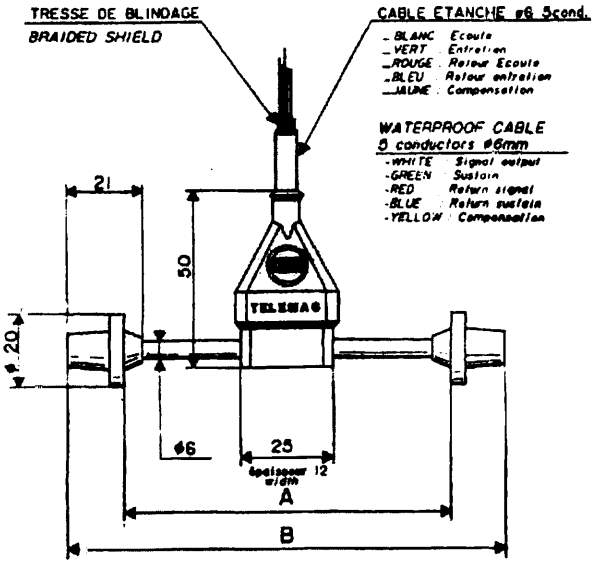

Fig. 5-25: Vibrating wire gauge for concrete embedding

A thin stainless steel wire is stretched between two contact points, if the wire is struck it vibrates at a frequency dependent on the wires length, mass per unit length, and tension. Since the length and wire properties are known, a change in frequency can be associated directly with a change in tension. The fundamental frequency (f) of vibration of a wire is related to its tension, length and mass by the following equation:

$$f = \frac{1}{2L}\sqrt{\frac{F}{m}}$$

L length of the wire
F wire tension
m wire's mass per unit length

A change in wire tension is related to a change in gage length (strain) and/or a change in temperature.

$$F = \varepsilon_w EA$$

ε_w wire strain
E Young's Modulus of the wire
A cross sectional area of the wire

Therefore strain can be calculated directly from the measurement of the wires fundamental frequency according to:

$$\varepsilon = \frac{4mL^2f^2}{EA}$$

Since the gage is sensitive to temperature each gage also contains a thermistor so that temperature corrections can be easily and accurately applied. With the temperatures recoded at each gage location, true strains can be calculated by the following relationship.

$$\varepsilon_T = \varepsilon_m + C(T - T_0)$$

ε_T true (temperature corrected) strain
ε_m measured strain
T temperature at the time of the strain reading
T_0 temperature at the time of the initial strain reading or some arbitrary base temperature
C coefficient of thermal expansion of the gage

In practice, the strain measurements from vibrating wire strain gages are made by causing the wire to vibrate with an electromagnetic pulse. The vibration of the wire is then monitored and converted to an electrical pulse by the same coil. The frequency or period of vibration is determined for the response pulse by counting the number of pulses within a specified time interval. When the frequency is determined, the value is squared and multiplied by the gage factor $(4mL^2/EA)x10^6$ to obtain a measurement in terms of micro-strain. Since the measurement is based strictly on the frequency of the pulse and not the magnitude, several thousand feet of cable can be used without effecting the measurements. Gage lengths from 50 to 250 mm are commercially available with a measurement range greater than 3000 με and a resolution better than 1 με. Since for large structures it can be considered that the strain is uniform over such a short length, vibrating wire can be used as localized strain sensors. Vibrating wires are among the most widely used strain sensors for the monitoring of concrete structures. They can be embedded in concrete of surface attached to existing structures. The vibrating wire principle can also be used to measure other parameters, in particular forces and pressures, when installed on an appropriate transducer.

(2) Technical parameters

Typical specifications for vibrating wire gauges are resumed in the following table:

Gage length:	60 mm to 300 mm
Measurement resolution:	0.2 μm/m
Linearity / Accuracy:	0.5 %
Dynamic range:	3'000 μm/m

Table 5-5: Technical parameters

(3) Application and selection criteria

Vibrating wires gauges exist in a number of different packages adapted to the installation in concrete or on the surface of existing structures. Some types of packaging are adapted for embedding in coarse aggregate concrete and are therefore particularly rugged. Other are more fragile and care must be taken during embedding. Operating temperature is limited to –20°C

to 50°C for some types, so models with wider temperature ratings must be selected for installation in structures undergoing higher temperature excursions.

Vibrating wire strain gages show an excellent stability over time. Other benefits of this type of gage are that cable length has virtually no effect on the measurements and the nature of the readings makes it nearly impervious to electronic/radio noise (Schiegg & Böhni 2000 [123]).

(4) Disturbance influences and countermeasures

The main disturbing influence are temperature changes. As mentioned it is possible to compensate for temperature effects by post-processing the data and using temperature reading for each measurement. Some read-our unit correct automatically for temperature variations. As the temperature correction depends on the thermal expansion coefficient and the modulus of the wire and of the host material, it is sometimes difficult to compensate the temperature influence completely.

Vibrating wires are generally not suitable for dynamic measurements and can be disturbed by strong vibrations in the structure during measurements. The process of "plucking" the wire and the measuring the period is relatively slow compared to other methods, such as a voltage measurement as with resistive type strain gages. Measurement of each gage requires approximately 1 second. Therefore this type of measurement is not suitable for dynamic applications where high frequency readings are required (Schiegg & Böhni 2000 [123]).

5.3.3.5 Fiber optic strain gages

Recent advances in fiber optic technologies led fiber optic strain sensors to become an alternative to classical resistance gages. These sensors are widely immune against rough environmental conditions and show good long term performance. Typical fiber optic strain sensors are fiber Bragg gratings and external Fabry-Perot interferometers (see Chapter 5.2.3) (Inaudi et al. 1996 [63]). A general overview of fiber optic sensor technology has been given in Chapter 5.2.3, where basic types and operation principles of these sensors are presented.

(1) Fiber Bragg grating (FBG) sensors

Fiber Bragg grating (FBG) sensors are characterized by a very good long-term stability and a high reliability. In addition, they have all the general advantages of glass fiber based sensors, such as electromagnetic insensitivity, small dimensions and the possibility of long distances between sensor and data acquisition device. Therefore, FBG based sensors are expected to be of significant influence on the development of structural monitoring techniques. Furthermore, the small dimensions of fiber Bragg gratings allow their utilization for "microsensors". By using them, new fields of application in material science can be found.

Functionality of FBG sensors

Initially, in-line fiber Bragg gratings (FBG) were developed as frequency filters for optical telecommunication systems. Their usability for measuring strains appeared to be a by-product. In 1989, Meltz et al. [88] produced fiber Bragg gratings by "burning" a series of equidistant lines into the glass core of a standard single-mode telecommunication fiber by using an excimer laser, see Fig. 5-26. These lines comprising the Bragg grating are characterized by a

refraction index different from the one of the regular fiber core. Light propagating in the glass fiber core will be reflected by the interfaces between the regions having different refraction indices. The reflected light is generally out of phase and tends to cancel. However, for a certain wavelength, the Bragg wavelength, the light reflected by the periodically varying refraction index will be in equal phase and amplified, (Melle et al. 1993 [87]).

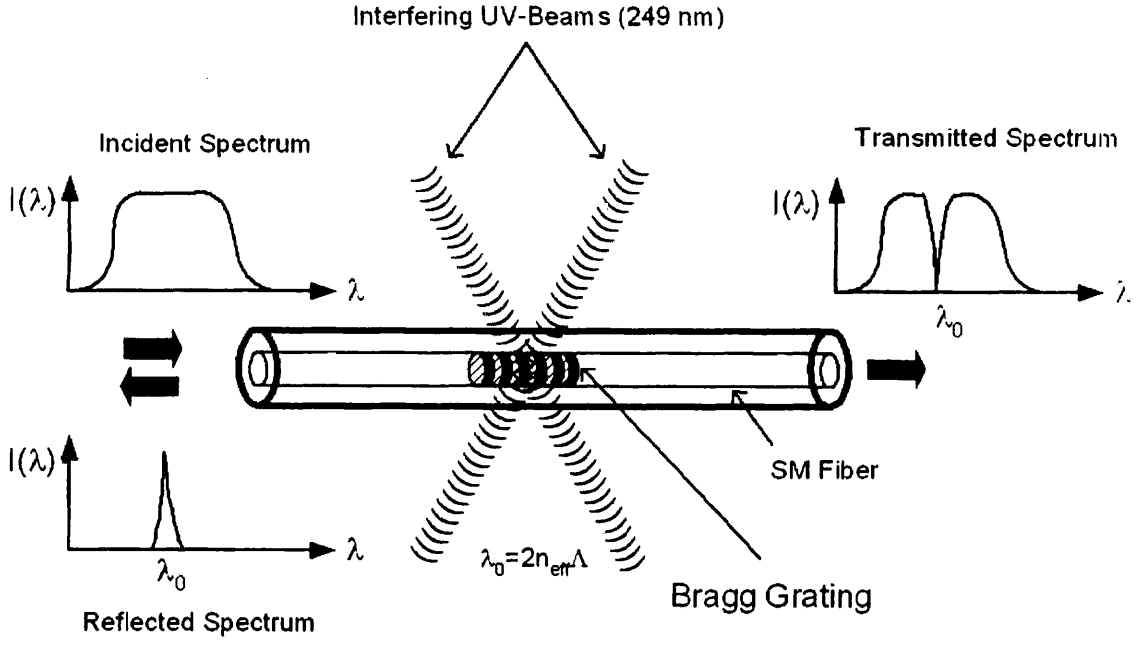

Fig. 5-26: "Writing" of a fiber Bragg grating

This results in a characteristic peak at this wavelength in the transmission as well as in the reflection spectrum, see Fig. 5-27. Since the peak wavelength depends on the spacing between the lines forming the gratings (grating pitch), the latter can be used for measuring strains. If the optical fiber is stretched, the Bragg wavelength increases.

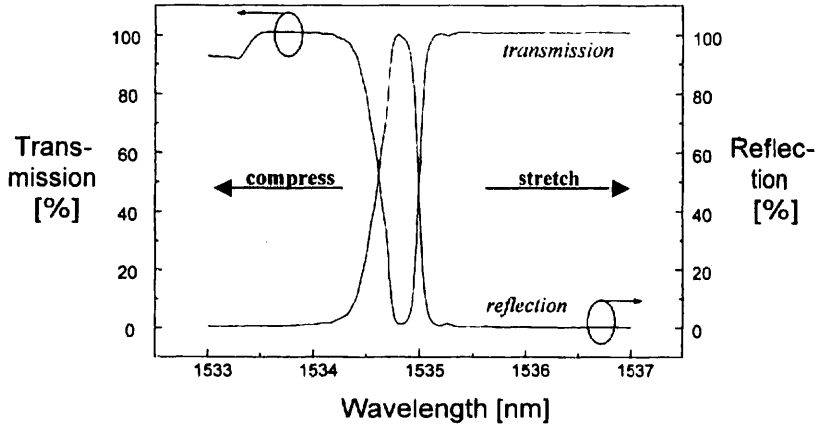

Fig. 5-27: Transmission and reflection spectrum of a fiber Bragg grating

The length of a fiber Bragg grating, i.e. of the sensitive fiber part, amounts to approximately 0.5 mm.

It has to be taken into account that the Bragg wavelength depends on the temperature too. The Bragg wavelength shift $\Delta\lambda$ is related to the strain ε and to the temperature change ΔT by

$$\frac{\Delta\lambda}{\lambda} = (1 - p_e)\varepsilon + \zeta\Delta T$$

where p_e and ζ are the strain-optic and the thermo-optic coefficient, respectively. Once these coefficients are known for a specific type of FBG sensor, the method is quasi calibration free and allows long-term measurements without a "drift" of the strain readings.

For measuring the Bragg wavelength shift a spectrum analyzer might be used. Whereas such devices are suitable for laboratory experiments they are in most cases not designed for field applications. However, an increasing number of special data acquisition systems for fiber Bragg grating sensors utilizing different measuring principles is being developed and offered on the market.

The interest in using FBG sensors for structural monitoring is growing rapidly. In a number of cases, structures were instrumented with strain sensors of this type. Saouma et al. (1998 [121]) instrumented beams and columns of a concrete frame structure. The predominant field of application for FBG sensors, however, are bridges. Sennhauser et al. (1998 [130]), Maaskant et al. (1997 [81]), Vohra et al. (1998 [150]), Idriss et al. (1998 [58]), Klink et al. (1999 [74]) as well as Measures (1994 [85]) reported on bridge monitoring utilizing FBG sensors.

Fiber Bragg grating sensors for structural monitoring

Sensors to be used for structural monitoring are expected to work reliably for the entire lifetime of the structure. Therefore, special attention has been paid to the development of an appropriate technique of sensor application. Basically there are three different ways of applying fiber Bragg grating sensors to reinforced concrete structures:

- Application of the sensor fiber directly to the steel reinforcement
- Application of the sensor fiber directly to the concrete surface
- Usage of a sensor holder to be placed in fresh concrete and covering the sensor fiber

Whereas the first and the third application mode are applicable for newly built structures the second one is of importance for the instrumentation of existing structures. When applying a sensor fiber directly to steel reinforcement or to the concrete surface a glue showing extremely low creep deformations and having a low reaction heat is needed. High temperatures during hardening of the glue might result in varying strains along the sensitive part of the fiber and consequently in a smeared wavelength spectrum not showing a distinctive peak at the Bragg wavelength. Furthermore, the sensor fiber has to be protected in order to prevent mechanical damage and corrosive attack by the alkaline environment. Fig. 5-28 shows the strains measured at a reinforced concrete beam under increasing load. Two glass fibers containing FBG sensors were glued directly to the steel reinforcement. For measuring compressive strains, at the top face of the beam 3 mm deep slits were cut into the concrete surface. Afterwards, glass fibers were glued into these slits. For comparison, electrical strain gages were also attached to the reinforcement as well as to the top face of the beam. An excellent accordance between the results obtained electrically and optically, respectively, could be achieved.

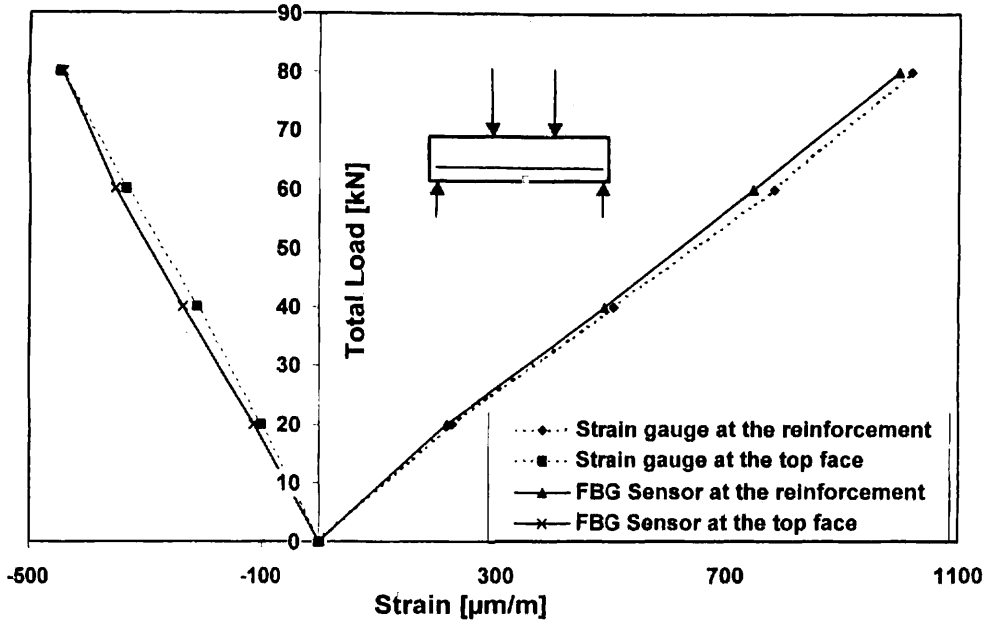

Fig. 5-28: Load-strain curve obtained at a R/C beam by using FBG sensors and electrical strain gages

For the instrumentation of new structures the use of sensor holders is recommended. They can be embedded in the concrete allowing an internal strain measurement. Sensor holders are supposed to protect the glass fiber against mechanical damage during casting and against chemical attack. In addition, they should provide sufficient bond to the surrounding concrete. Their stiffening effect on the strain distribution in the concrete should be minimized in order to ensure a quasi feedback-free strain measurement. Fig. 5-29 shows an example for a sensor holder, which has been designed, quite similar to vibrating wire gages. It consists of a 150 mm long steel tube. The glass fiber is longitudinally spanned inside. Outside the steel tube, a concrete-proof plastic hose protects the fiber and is attached to the sensor holder by the connectors at each end. The profile of the steel tube and the end plates provide sufficient bond with the surrounding concrete. By means of Finite-Element analyses, the dimensions of the sensor holder were optimized for allowing a feedback-free strain measurement in concrete having typical elastic properties.

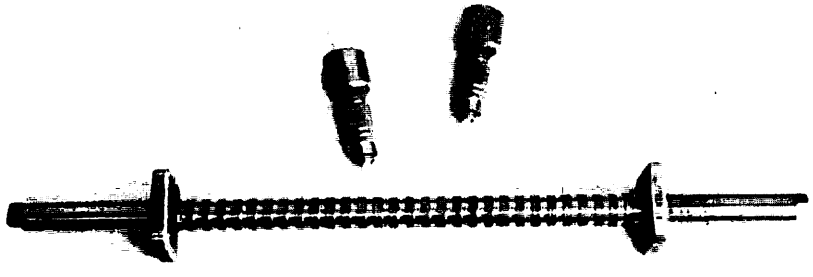

Fig. 5 29: FBG sensor holder made of a steel tube

The placement of a FBG-Sensor with sensor holder can be seen in Fig. 5-30. Before casting it is fixed to the steel reinforcement.

Fig. 5-30: Placement of a FBG-Sensor

Fiber Bragg grating (FBG) sensors work quasi calibration free and are therefore suitable especially for the long-term strain monitoring of concrete structures. The procedures and techniques for the sensor application as well as for the data acquisition require still more development. From the economical point of view, the strain measurement by using FBG-sensors is generally more expensive than the use of electric strain gages. This will probably limit the field of application for FBG-Sensors to long-term measurements only.

5.4 Force measurements

A major contributing factor to the deterioration of bridges are overloads. These overloads could be caused by heavy trucks or a seismic event (Turner-Fairbank Highway Research Center 1997 [14]). In the evaluation of structures, it is critical to determine the distribution of loading and to evaluate the stress levels in load-carrying members of the structure.

Transformation induced plasticity (TRIP) steel sensors can be used as a passive device to detect and measure the maximum load experienced by a structure. This steel undergoes a permanent change in crystal structure in proportion to peak strain. It changes from a nonmagnetic to a magnetic steel. This change can be easily measured. (Turner-Fairbank Highway Research Center 1997 [14])

5.4.1 Load cells

Load cell designs can be distinguished according to the type of output signal generated (pneumatic, hydraulic, electric) or according to the way they detect weight (bending, shear, compression, tension, etc.) [185].

5.4.1.1 Measurement principle

Hydraulic load cells are force-balance devices, measuring weight as a change in pressure of the internal filling fluid. In a rolling diaphragm type hydraulic load cell, a load or force acting on a loading head is transferred to a piston that in turn compresses a filling fluid confined within an elastomeric diaphragm chamber. As force increases, the pressure of the hydraulic fluid rises [185]. Hydraulic load cells may be used to measure compressive loads between structural members, e.g. at the junction between a beam and the top of a pile, or can be applied to the measurement of tensile forces in ground anchors, rock bolts and tie backs.

Two types of Hydraulic Load Cell are available:

- Solid cells for measurement of compressive forces
- Annular cells for monitoring tensile forces

Pneumatic load cells also operate on the force-balance principle. These devices use multiple dampener chambers to provide higher accuracy than can a hydraulic device. In some designs, the first dampener chamber is used as a tare weight chamber. Pneumatic load cells are often used to measure relatively small weights in industries where cleanliness and safety are of prime concern. The advantages of this type of load cell include their being inherently explosion proof and insensitive to temperature variations. Disadvantages include relatively slow speed of response and the need for clean, dry, regulated air or nitrogen. [185]

The **Vibrating Wire Load Cell** comprises a cylinder of high strength steel with several vibrating wire strain gauges located around the circumference of the cell. Loads applied to the cell are measured by the vibrating wire gauges and readings averaged to minimize the effects of uneven eccentric loading. Vibrating wire load cells provide excellent long-term stability and can be used with long cables without adversely affecting the output frequency. Further they are waterproof and have low temperature coefficients. However, they are not able to measure dynamic loading.

Strain-gage load cells convert the load acting on them into electrical signals. The gauges themselves are bonded onto a beam or structural member that deforms when weight is applied. In most cases, four strain gages are used to obtain maximum sensitivity and temperature compensation. Two of the gauges are usually in tension, and two in compression, and are wired with compensation adjustments. When weight is applied, the strain changes the electrical resistance of the gauges in proportion to the load. [185] High resistance strain gages are used to minimize cable effects.

In the area of new sensor developments, **fiber optic load cells** are gaining attention because of their immunity to electromagnetic and radio frequency interference (EMI/RFI), suitability for use at elevated temperatures, and intrinsically safe nature. Two techniques are showing promise: measuring the micro-bending loss effect of single-mode optical fiber and measuring forces using the Fiber Bragg Grating (FBG) effect. [185]

5.4.1.2 Load cell applications

Custom load cells, either solid or annular are available to suit any application or range. Various versions are available such as S type, shear, bending, shear pin, tension, donut (annular), diaphragm, column and compression. Shear and bending load cells are commonly used in weighing systems. Tension and S types can also be used in weight applications and to measure force.

The determination of prestressing forces prior to transfer can be measured with load cells by positioning them on strand at either the dead end or jacking end in the prestressing bed. Although calibrated hydraulic jacks are used to stress strands, they only provide the force before their release. For pretensioned members, load cells provide the force after release of the jack, during curing, and immediately prior to detensioning of the strand. Load cells may also be used on the ends of unbonded post-tensioning tendons and stay cables to measure the changes of force with time. In this context the verification of the zero-position of the load cell has to be considered. As a minimum, readings should be taken before and after stressing every strand and before and after detensioning every strand. Readings at other times will indicate

how the forces vary during concrete placement and curing. (U.S. Department of Transportation 1996 [147])

5.4.2 Cable stay force measurement

The forces in the stay cables are an excellent indicator of overall structural health for these types of bridges. The knowledge of the actual tensile forces in the ropes or cables of cable-stayed bridges, in the suspenders of arched bridges or in external tendons is required for the assessment of these elements themselves but also for the examination of the global stress of the structure. The determination of these forces by lift-off tests is connected with considerable expenditures as well as the danger of damages. The mounting works at the anchorages can unfavorably influence the durability of these critical elements.

Therefore fast and non-destructive methods for the determination of the forces are required. The measurement of the vibration characteristic is an approach for a solution because there is a simple, quasi linear relation between the eigenfrequencies and the rope and cable forces.

The behavior of ropes and cables greatly differs from the theoretical concept. This practical behavior is caused by numerous external conditions which give rise to pressure. The dynamic measurement gives information on the actual behavior of these elements and quantifies the deviation from the target value at the same time. Consequently a quick check is possible.

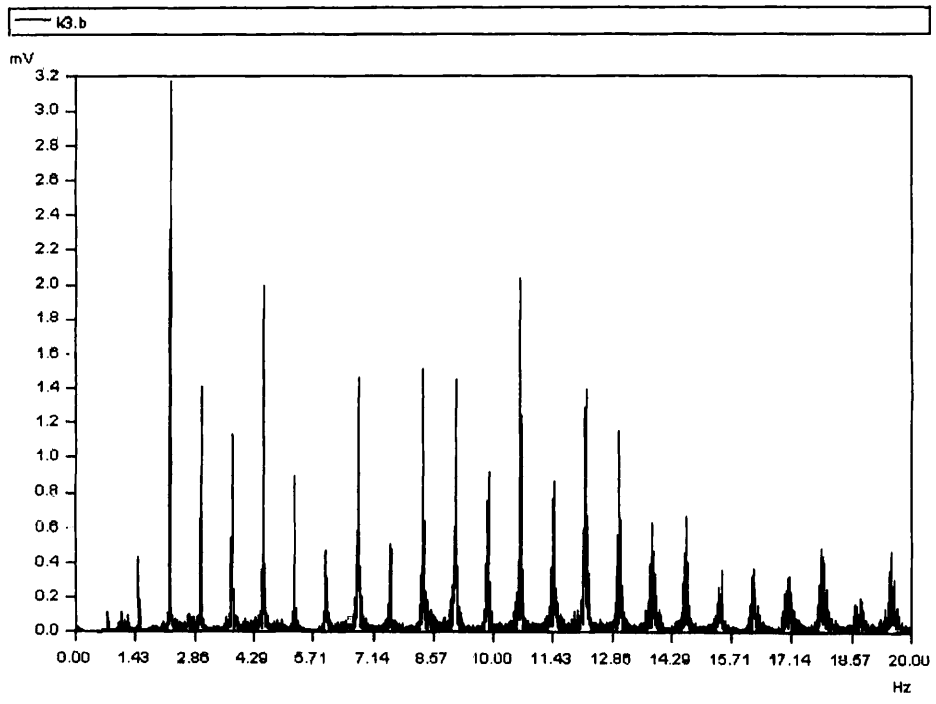

Fig. 5-31: Spectrum of a typical cable in civil engineering

Principally a control of the force with a new application of the pre-stressing jack is possible, but this check is connected with a great logistic, time and therefore also financial expenditure. Furthermore there is the danger that unintended damages at the cables are caused. For this reason modern, non-destructive procedures present itself, which are based on the dynamic characteristic. In addition, this has the great advantage that the AVM enables a quick, flexible and safe determination of the cable force.

5.4.2.1 Acceleration sensors

A useful, very accurate and at the same time economical determination of the cable force can be carried out by means of the measurement of the eigenfrequencies of the basic and harmonic oscillations. The cables are stimulated to oscillate by traffic or other environmental (ambient) reasons. By recording the effective acceleration a subsequent conversion of the signals into frequency spectra is possible, a simple Fourier Transformation (FFT) is applied here.

The spectrum, which represents the reaction (structural response) of the cable, very clearly shows the individual frequencies of the basic and harmonic oscillations. As the higher frequencies always show a multiple of the basic frequency, a determination of the cable force is exactly possible. The identified eigenfrequency (f) is a function of the effective cable force (N), the length (l), the mass (m) of the cable per meter and the marginal conditions.

$$N = 4 \cdot l^2 \cdot f^2 \cdot m + P_{n1} + P_{n2} \quad \text{... is valid for the basic oscillation} \qquad (5\text{-}1)$$

An extension of the equation by influence parameters (P_{nx}) enables the application of this method under varied conditions. For stay cables with great lengths it has proved that the flexural stiffness of the cables can be neglected.

(1) Acceleration sensors – identificaton of cable force

For the secure identification of the cable force an acceleration sensor has to be placed horizontally on the cable to be checked if possible and to be connected with the data-logger via the cable. After recording the measured data they are read in a special program, which automatically carries out the evaluation of the eigenfrequencies. By applying eq. (5-1), a determination of the effective cable force can be very quickly executed. The measuring interval usually amounts to approximately five and a half minutes.

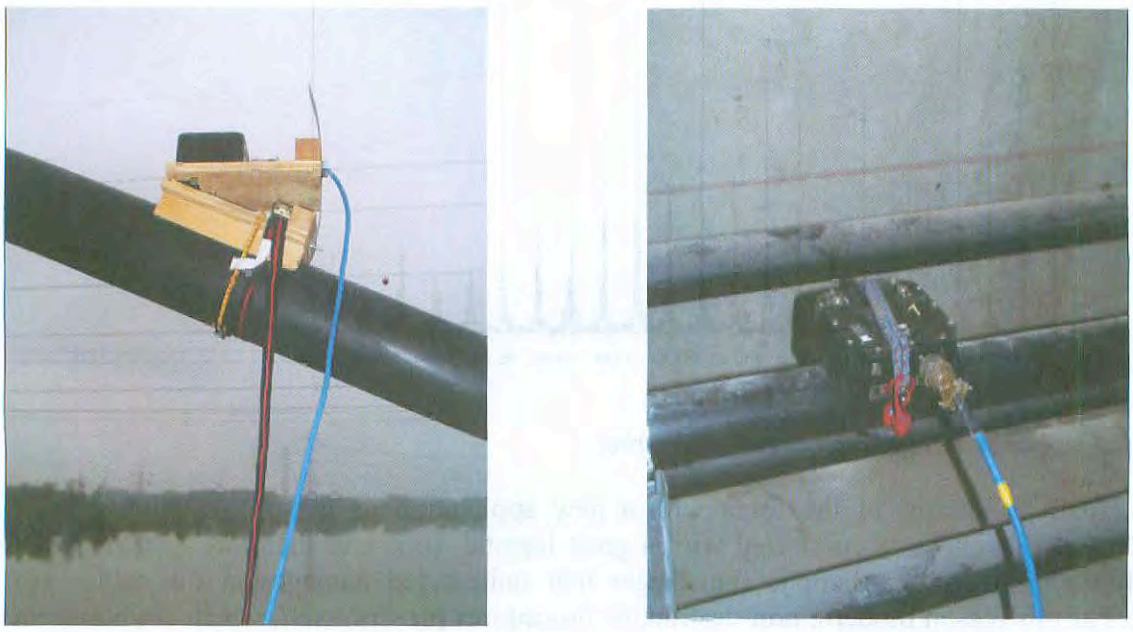

Fig. 5-32: Sensors at stay cables and external cables

A usual measuring interval of the BRIMOS® technology lasts for about five and a half minutes, in addition the time for mounting the acceleration sensor and the initializing of the system has to be considered. Periods of about 15 to 20 minutes (incl. evaluation of the cable force) have to be estimated for the check of a cable, which is a further advantage of this system.

In this context it should be mentioned that no closure or interruption of the traffic flow is necessary in order to perform the dynamic tests. The equipment is small and easy to handle close to the bridge cables. In fact, the main advantage of the measurement using accceleration sensors directly on the cable is the high accuracy of the results up to the high frequency band (all modes of interest acquired) as well as the possibility to obtain additional modal parameters such as modal damping and vibration intensity for example. The assessment of modal damping is from major interest for calculation of proneness of vibration from each cable concerning Galloping and Wind-Rain-Induced Vibrations.

Up to now numerous projects were completed with AVM where special questions concerning cables had to be answered. Standing out examples for this are the bridge over the Danube in Tulln where all cables were checked for the effective cable force and the susceptibility to vibrations. Furthermore the Donaustadt bridge in Vienna has to be mentioned where inspections due to the vibration susceptibility of a cable were ordered. A check of the cable forces of external pre-stressing elements was carried out at the Mur bridge St. Michael at the Phyrn motorway.

5.4.2.2 Laser vibrometer

Dynamic analysis is the basis for a new approach to the quantitative measurement of forces in stay cables. This innovative technique uses non-contact laser vibrometers to provide a rapid, low cost, yet accurate method for force measurement.

A single laser vibrometer is used to measure low- level cable vibrations due to ambient (wind and traffic) excitation. Laser vibrometers use optical interferometry to measure surface velocities ranging from 0 to 125 mm/s/V and from 0 to 30 MHz depending on equipment arrangements. The vibrating surface orthogonal to the laser causes the frequency of a laser beam to be shifted due to the Doppler effect. The shift in signal beam frequency is related to the velocity of the vibrating surface and the wavelength (λ) of the laser through the equation

$$f_s = \frac{2v}{\lambda}$$

where f_s is the frequency shift of the beam and v is the vibrating surface velocity. The signal beam and a known frequency reference beam are then combined to create an interference signal. This signal contains the velocity of the measured system.

The force evaluation method is based on an algorithm relating the measured cable frequency to its force. This formulation includes the effects of cable sag-extensibility, bending stiffness, various boundary conditions, intermediate springs or dampers, etc.

Since the need for contact measurement is eliminated, the evaluation personnel, as well as the device, can be stationed on the deck of the bridge, simply pointing the device to the cable. In addition to the safety advantages associated with that, the vibrometer allows the evaluators to target more than one cable from a single setup location. Contact sensors instead are more appropriate when long-term remote monitoring is desired.

5.4.3 Weight in motion (WIM)

While the dead load (see alo Chapter 2.2.1 Loads) can be considered constant over the whole lifetime of a bridge, the traffic load may vary over this period. The weight in motion method is used to register all vehicles in movement passing the measuring device located in the roadway. A complete WIM study under normal traffic would result in a count of total vehicles that cross the bridge, the lane traveled by each vehicle, the time of arrival, the vehicle speed, the axle configuration and axle weights, and strains/stresses at gauge locations. Thus one obtains a representative overview of the traffic occurring over a longer time period. The registrated axle loads are dynamic values, because the vibrations of the vehicles are included. The continuous collection of traffic loads on bridges by a state of the art equipment enables us to classify load events into various categories (e.g. vehicle classes) and to compare them with available regulations and requirements.

The measurement of the vertical forces is complicated by a number of factors, including the following (U.S. Department of Transportation 1996 [147]):

- Each sensor "feels" the vertical force of each axle for only a brief time.
- The "weight" applied to the sensor during that time period is normally not equal to the static weight of that axle. This is because while the vehicle is in motion, the truck and its components bounce up and down. If the truck mass is moving upward when an axle crosses the WIM sensor, the weight applied by that axle is lower than the static value. If the truck mass is landing, the weight applied is greater than the static value.
- Some sensors (strip) feel only a portion of the tire weight at any given time. Because the sensor is smaller than the footprint of the tire, the pavement surrounding the sensor physically supports some portion of the axle weight throughout the axle weight measurement.
- The tread on some tires is so well defined that very high concentrations of force are generated under those portions of the tread that are actually in contact with the ground. This is also mostly a problem for strip sensors.
- Sensors must be capable of weighing more than one axle in quick succession. That is, the scale must be able to "recover" quickly enough so that one axle weight does not affect the measurement of the following axle.
- Roadway geometry (horizontal and vertical curves) can cause shifts in vehicle weight from one axle to another.
- Vehicle acceleration or braking, torque from the drive axles, wind, the style and condition of vehicle's suspension system, and a variety of other factors can also cause shifts of weight from one axle to another.

The effects of many of these factors can be minimized through careful design of the WIM site. The site should be selected and designed to reduce the dynamic motion of passing vehicles. However, achieving these design controls requires restrictions on site selection, which means that WIM systems cannot be placed as easily or as universally as other traffic monitoring equipment. (U.S. Department of Transportation 1996 [147])

WIM scales work most accurately when they are placed flush with the roadway. Sensors that sit on top of the roadway cause two problems with WIM system accuracy: 1) They induce additional dynamic motion in the vehicle, and 2) they can cause the sensor to measure the force of tire deformation (which includes a horizontal component not related to the weight of the axle) in addition to the axle weight. This means that permanent installation of the sensors and/or frames that hold the sensors is normally better for consistent, accurate weighing results. The use of permanently installed WIM sensors is recommended as a means of improving the quality of the data. (U.S. Department of Transportation 1996 [147])

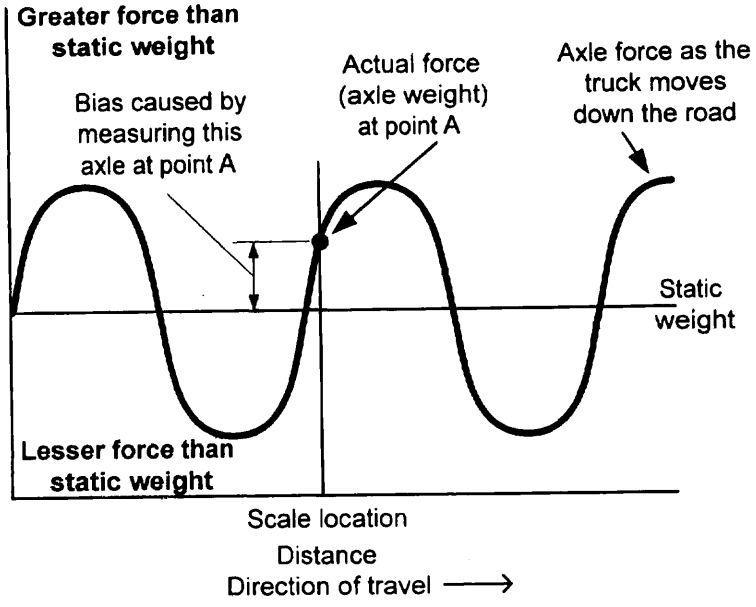

Fig. 5-33: Variation of axle forces with distance and the consequential effect on WIM Scale calibration

5.4.3.1 WIM monitoring equipment

Choosing a weigh-in-motion system for a specific application or use can be a difficult task because there are a number of technologies and systems available today. Each has its own set of advantages and limitations. For example, not all WIM systems can operate at high speeds, some can be installed in a few hours with relatively unskilled labor while others require several days of labor-intensive site preparation, and some work great for traffic data collection purposes but are not recommended for weight enforcement. (U.S. Department of Transportation 2001 [148])

(1) Bending plate WIM systems

Bending Plate WIM systems utilize plates with strain gages bonded to the underside. As a vehicle passes over the bending plate, the system records the strain measured by the strain gage and calculates the dynamic load. Bending plate scales can be portable or installed permanently with some minor excavation into the road structure and consist of either one or two scales. The scale or pair of scales is placed in the travel lane perpendicular to the direction of travel. When two scales are used in a lane, one scale is placed in each wheelpath of the traffic lane so that the left and right wheels can be weighed individually. The pair of scales is placed in the lane either side-by-side or staggered by five meters. Bending plate systems with one scale placed in either the left or right wheelpath are usually used in low volume lanes. (U.S. Department of Transportation 2001 [148])

Bending Plate WIM systems consist of at least one scale and two inductive loops. The scales are placed in the travel lane perpendicular to the direction of travel. The inductive loops are placed upstream and downstream from the scales. The upstream loop is used to detect vehicles and alert the system of an approaching vehicle. The vehicle speed, which is used to determine the axle spacing, can be determined by three methods: weigh pad to inductive loop, weigh pad to axle sensor, and weigh pad to weigh pad, if the weigh pads are staggered. If an

axle sensor is used to determine the vehicle speed, it is placed downstream of the weigh pad. (U.S. Department of Transportation 2001 [148])

There are two basic installation methods for a Bending Plate scale. In concrete roadways of sufficient depth, a shallow excavation is made in the surface of the road (Quick Installation). The scale frame is anchored into place using anchoring bars and epoxy. In asphalt roads or thin concrete roads, it is necessary to install a concrete foundation for support of the frame (Vault Installation). (International Road Dynamics Inc. 2001 [65])

Installing a complete lane of scales, loops and axle sensor can be accomplished in a day using the shallow excavation method and in 3 days using the concrete vault. (International Road Dynamics Inc. 2001 [65])

When properly installed and calibrated, the Bending Plate WIM system should be expected to provide gross vehicle weights that are within 10% of the actual vehicle weight for 95% of the trucks measured. (International Road Dynamics Inc. 2001 [65])

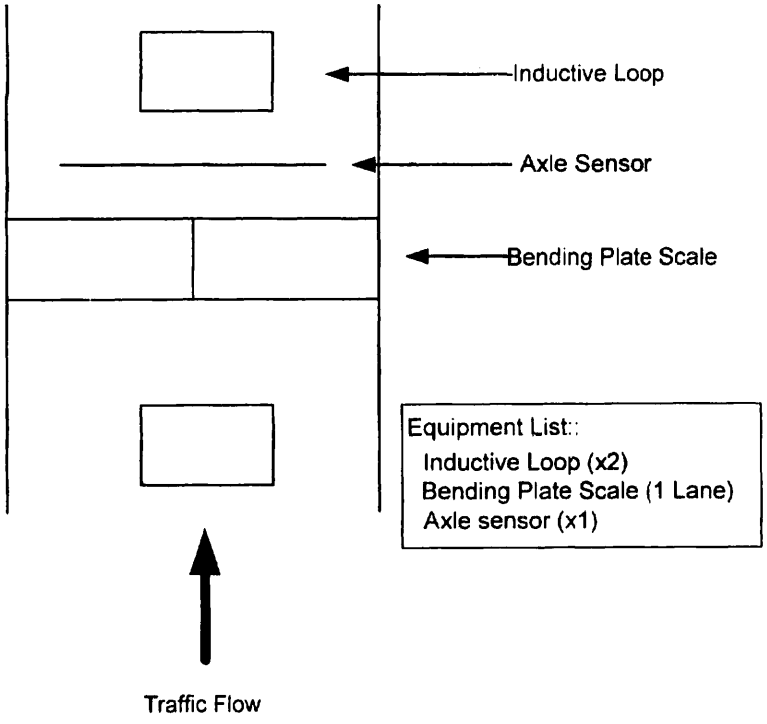

Fig. 5-34: Common configuration – bending plate

At six month intervals the following scheduled maintenance should be performed to ensure continued scale operation (International Road Dynamics Inc. 2001 [65]).

- Visually inspect the scale installation.
- Maintain installation of the epoxy material / concrete vault.
- Re-torque and/or replace stainless steel cap screws.
- Replace frost plugs as required.
- Maintain installation of the silicon seal.
- Maintain all splices in the junction boxes as required.
- Measure signal cable resistance of scale.
- Recalibrate the scales.
- In case of a Vault Installation maintain the slot between the concrete vault and the existing roadway with loop sealant.

(2) Piezoelectric WIM systems

Piezoelectric WIM systems utilize piezo sensors to detect a change in voltage caused by pressure exerted on the sensor by an axle and measure the axles weight. As a vehicle passes over the piezo sensor, the system records the electrical charge created by the sensor and calculates the dynamic load (U.S. Department of Transportation 2001 [148]).

The basic construction of the typical piezo sensor consists of a copper strand, surrounded by a piezoelectric material, which is covered by a copper sheath. When pressure is applied to the piezoelectric material an electrical charge is produced. The sensor is actually embedded in the pavement and the load is transferred through the pavement. The characteristics of the pavement will therefore affect the output signal (International Road Dynamics Inc. 2001 [65]).

For a complete data collection system, it is common to install two inductive loops and two piezoelectric sensors in each lane, which is being monitored. Installation begins by making a relatively small cut in the road into which the sensor will be installed perpendicular to the direction of travel. The sensor is placed in the sawcut and secured in place by a fast curing grout. The piezo sensors may or may not be encapsulated in an epoxy-filled metal channel, usually aluminum. The inductive loops are placed upstream and downstream from the sensor. The upstream loop is used to detect vehicles and alert the system of an approaching vehicle. The downstream loop is used to determine speed and axle spacings based on timing. (U.S. Department of Transportation 2001 [148], International Road Dynamics Inc. 2001 [65])

A complete lane installation consisting of two sensors and two loops can be accomplished in less than a full day, including curing time (International Road Dynamics Inc. 2001 [65]).

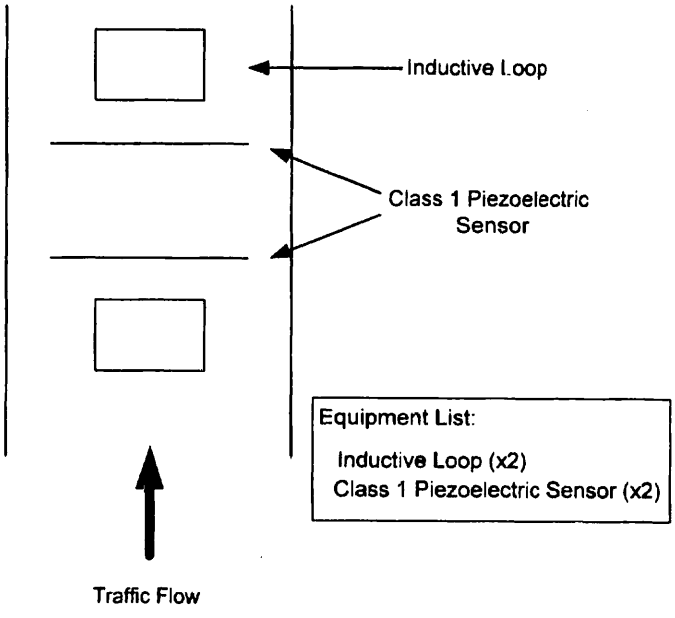

Fig. 5-35: Common configuration – piezoelectric WIM system

When properly installed and calibrated, a piezoelectric WIM system should be expected to provide gross vehicle weights that are within 15% of the actual vehicle weight for 95% of the trucks measured (International Road Dynamics Inc. 2001 [65]).

At six Month intervals the following Scheduled Maintenance should be performed to ensure continual sensor operation (International Road Dynamics Inc. 2001 [65]).

- Visually inspect the piezo installation.
- Maintain the installation of the grout.

- Maintain all piezo cable splices as required.
- Visually inspect the BNC connector and replace if required.
- Measure the resistance and voltage output of the sensor.

(3) Load cell WIM systems

Load cell WIM systems utilize a single load cell with two scales to detect an axle and weigh both the right and left side of the axle simultaneously. As a vehicle passes over the load cell, the system records the weights measured by each scale and sums them to obtain the axle weight.

The typical load cell WIM systems consist of a single load cell and at least one inductive loop and one axle sensor. The load cell is placed in the travel lane perpendicular to the direction of travel. The single load cell has two in-line scales that operate independently. Off-scale detectors are integrated into the scale assembly to sense any vehicles off the weighing surface. The inductive loop is placed upstream of the load cell to detect vehicles and alert the system of an approaching vehicle. If a second inductive loop is used, it is placed downstream of the load cell to determine axle spacings, which is used to determine the vehicle speed. The axle sensor is placed downstream of the load cell to determine axle spacings and vehicle speed. (U.S. Department of Transportation 2001 [148])

The installation of a single load cell scale requires the use of a concrete vault. The roadway is cut and excavated to form a pit. The frame is positioned in place and then is cast into the concrete to form a secure and durable foundation for the scale. Installing a complete lane of scales, loops and axle sensor can be accomplished in 3 days (International Road Dynamics Inc. 2001 [65]).

When properly installed and calibrated, the Single Load Cell WIM system should be expected to provide gross vehicle weights that are within 6% of the actual vehicle weight for 95% of the trucks measured (International Road Dynamics Inc. 2001 [65]).

At six month intervals the following scheduled maintenance should be performed to ensure continued scale operation.

- Visually inspect the scale installation.
- Maintain installation of the concrete vault.
- Maintain the slot between the concrete vault and the existing roadway with loop sealant.
- Remove the load cell from the load cell cavity, retorque the four (4) mounting bolts in the load cell cavity, check the splice, replace the antifreeze in the load cell cavity, replace the load cell, load cell hatch, secure and reseal load cell hatch.
- Retorque and/or replace the eight (8) mounting bolts as required.
- Replace all frost plugs as required.
- Maintain the installation of the silicon sealant between the scale and frame.
- Maintain all splices in junction boxes as required.
- Measure the signal cable resistance of the scale.

Recalibrate the scale.

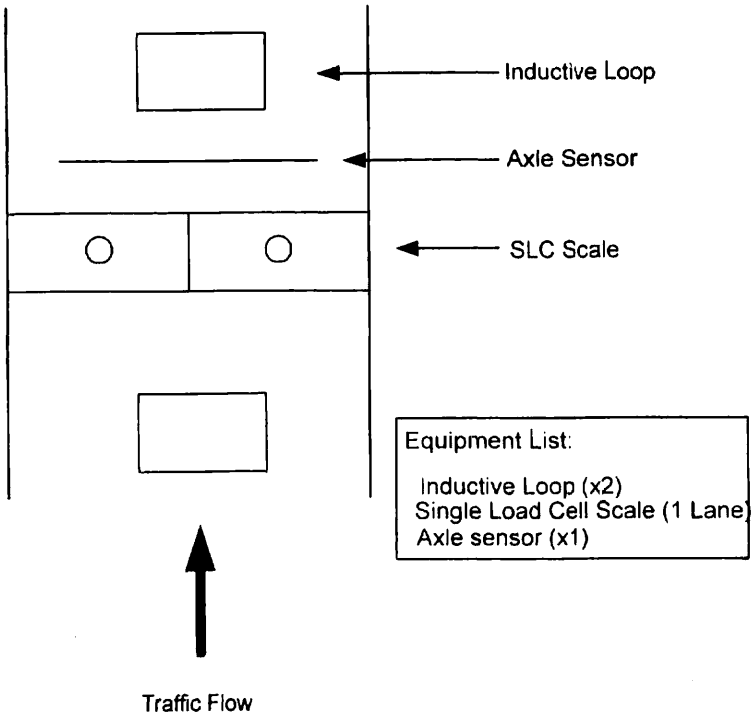

Fig. 5-36: Common configuration

(4) Capacitive systems

A capacitive-based WIM system basically consists of two or more metal plates. When force is applied, the bending action of the plates results in a change in the capacitance that is measured by sensors mounted on the underside of the plate. Capacitive mat system layouts typically consist of two inductive loops and one capacitive weight sensor per lane to cover a maximum of four traffic lanes. In a portable setup, the inductive stick-on loops and the capacitive weight sensor are placed on top of the road pavement and are meant to be used temporarily, sometimes up to 30 days. In a permanent setup the sensors are placed in stainless steel pans, flush-mounted with the pavement. The mat is installed perpendicular to the direction of the vehicle in the traffic lane. (U.S. Department of Transportation 2001 [148])

(5) Fiber optic sensor for WIM measurements

A probabilistic concept to describe traffic loads and their effects to a bridge from acquired axle-load data on the Brenner highway can be found in (Bogath 1997 [12]). The measuring device used at the Brenner highway is based on a monomer optical fiber. This fiber is double refractive, uncovered and lies between two metal strips which are weld together. If the sensor is loaded with a transversal force, the optical quality changes. The reason is the photoelastic characteristic of the fiber core and the surrounding material. Fig. 5-37 and Fig. 5-38 show the layer structure of the sensor.

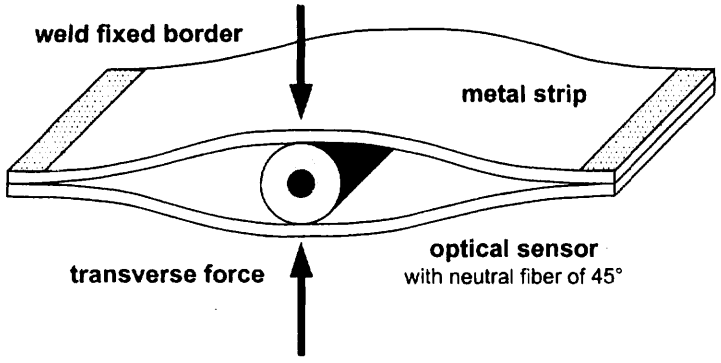

Fig. 5-37: Cross section of fiber optic WIM sensor, (Bogath 1997 [12])

A light beam generated by a laser diode travels along in a transfer optical fiber. Between the laser diode and the transfer fiber a polarization filter is situated, which converts the light into a linear polarized light beam. After the light beam has passed the sensor input it is reflected by a mirror at the end of the fiber. The reflected light beam travels back to the polarization filter where it is analyzed by a photo diode. The weight acting on the sensor is changed in a series of polarimetric maximums and minimums. By simply counting the maximums and minimums, the modification of the double refraction is found out, which in turn can be related to the axle load. The layout of the measuring device is shown in Fig. 5-38.

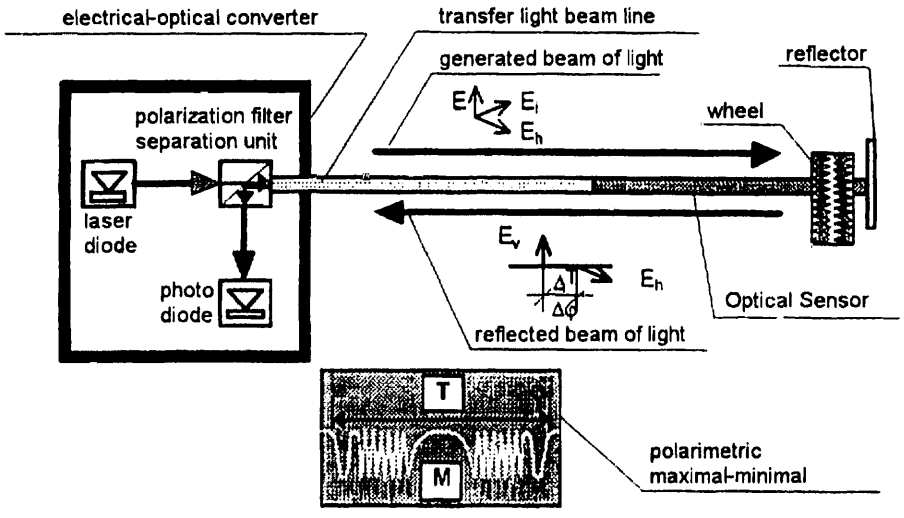

Fig. 5-38: Simplified architecture of the fiber optic measurement device, (Bogath 1997 [12])

When a wheel passes the sensor a characteristic signature is recorded (Bogath 1997 [12]):

- The first maxima-minima oscillation is equal to the increase of load
- The continuous signal refers to the pressure applied by the wheel in on the sensor
- The second maxima-minima oscillation is equal to the reduction of load

Measurements at the Brenner highway gave the following results (Bogath 1997 [12]):

- The period of the signal is inversely proportional to the vehicle velocity
- The number of maximal-minima raises with the wheel-weight
- Dual tire have a characteristic signal
- The system is insensitive against electric shocks and electromagnetic radiation

In combination with measurement software the following data was recorded at the Brenner Highway:

- Weight of the moving vehicle – per wheel
- Weight of the moving vehicle – per axle
- Sum of the weights in motion –per vehicle
- Velocity of the vehicle
- Distance between the axles

In a first utilization this registered axles are classified into vehicles and vehicles themselves are classified into twelve vehicle groups according to Fig. 5-39.

For each registered vehicle the following data was recorded:

- Record time
- Distance to next vehicle
- Velocity of the vehicle
- Length of the vehicle
- Number of axles
- Vehicle group
- Single axle load
- Total load of the vehicle

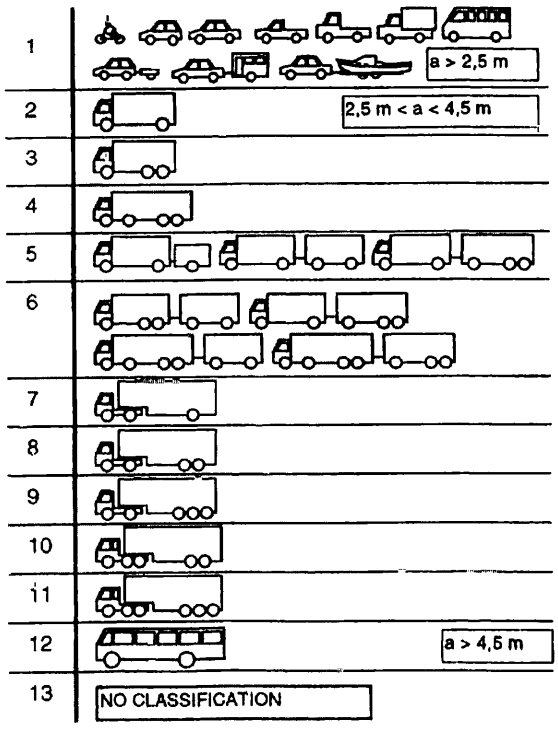

Fig. 5-39: Example for vehicle classification, (Bogath 1997 [12])

WIM scale calibration must account for the vehicle dynamics at the data collection site. Because vehicle dynamics are affected by pavement roughness, the "correct" calibration value for a scale is a function of the pavement condition and the sensor installation at each site. Because pavement conditions change over time, and because those changes affect WIM scale performance, even permanently installed WIM sensors need to be periodically calibrated.

5.4.4 Direct stress measurement

Stress measurement is typically accomplished through the use of foil strain gages. However, these gages require some surface preparation to install and are unable to measure the distribution of dead load within the structure (Washer 2000 [155]). Alternatively, a few direct stress measurement techniques will be described in this section.

5.4.4.1 Ultrasonic measurement of stress

Since stress modifies the velocity of ultrasonic waves, it has often been suggested that an accurate measurement of the velocity of sound in a component could be used to infer or even measure stress. However, ultrasonic wave velocities can be affected by microstructural inhomogeneities and temperature variations. Further there are difficulties in separating the effects of multiaxial stresses.

Changes in ultrasonic speed can be observed when a material is subjected to a stress, the changes providing a measure of the stress averaged along the wave path. The acoustoelastic coefficients necessary for the analysis are usually calculated using calibration tests. Different types of wave can be employed but the commonly used technique is the critically refracted longitudinal wave method.

Ultrasonic stress measurement techniques are based on the relationship of wave speed in various directions with stress. The most significant variation in travel-time with the strain was found for longitudinal waves, followed by the shear waves when the particles vibrate in the direction of the load. The other waves do not show significant sensitivity to the deformation [184].

The relationship of measured L_{CR} wave travel-time change and the corresponding uniaxial stress is given by [184]:

$$\Delta\sigma = \frac{E}{Lt_0}(t - t_0 - \Delta t_T)$$

$\Delta\sigma$ change in stress
E Young's modulus
L acoustoelastic constant for longitudinal waves
t measured travel time
t_0 reference travel time
Δt_T temperature effect on travel time

For stress measurement work, the LCR probes are arranged in a tandem fashion, with one probe acting as the transmitter and the other as a receiver. In some cases, dual receivers are used. Distance between the probes is kept constant by the rigid space bar, assuring that any change in travel-time between the two probes is due to stress or material variations, and not a change in probe spacing. The effects of stress, texture and temperature on the wave speed all contribute to the aggregate changes in data collected [184].

A possible alternative to common NDE techniques for making the applied stress measurements is ultrasonic techniques using noncontact electromagnetic acoustic transducers (EMATs). This method requires no time consuming surface preparation and is therefore easy to install. The bending stress in the outer fibers of a bridge girder is a primary contributor to fatigue damage. Therefore, the EMATs generate and detect Rayleigh waves (RW), which travel along the surface of the specimen. The acoustoelastic effect will cause a change in time-of-flight of the RW as a result of applied stress due to vehicle traffic. These stress

fluctuations are relatively low, usually less than 14 MPa, and occur at frequencies in the order of several Hertz.

With the use of ultrasonic measurement techniques, the state of stress in a steel bridge member and the stress level in high-strength steel strand used in pre-stressed and post-tensioned concrete can be evaluated (Washer 2000 [155]). More specific applications include rolled and welded steel and aluminum plate, pressure vessels, turbine rotors, discs and blades and railroad rail and wheels [184].

5.4.4.2 X-ray diffraction

X-ray diffraction is a known method for the determination of surface stress in steel elements. When the stress distribution across the section of a structural member is relatively uniform or well known, this method can be useful in obtaining estimates of the stress in a loaded structure.

In this method, strains are estimated by measuring the elastic atomic lattice spacing (distance between atomic planes). Using Bragg's law of diffraction the value of surface residual stress can be found by measuring the angle at which an X-ray beam diffracts from the surface of an analyzed component. The method can be very helpful in detecting redistribution of stresses, designed to be uniform. Then it is of value to obtain a relative stress reading even if the absolute value may be questioned. A reliable calibration of a stress-free sample, comparable to the "in-situ" tested material, is highly desirable, but not always possible. A good understanding of the elastic and plastic stress-strain relationships in steel is indispensable. (Yanev 2000 [160])

This method is a relatively simple and effective technique for measurement of prestressing levels in wires. Brauss et al. (1998) present tests on bridge suspender cables and wire ropes (in the laboratory and in the field) using the X-ray diffraction equipment. The authors conclude that this technique provides quantifiable results, is nondestructive, and provides a measure of total stresses (applied plus residual stresses). However, in case of enclosed elements such as PT tendons and stay cables, this method would be partially destructive. In any case, if one needs to subtract residual stresses from measured values, then a sample must be cut out from the cable. Also, in a multi-strand or multi-wire cable, there may be significant variations between absolute strain values in different elements. Therefore, a large number of tests may be required to obtain an average value as an estimate of total force.

5.4.4.3 Magneto-elastic stress measurement

In contrast to the direct stress measurement methods a couple of magneto-elastic techniques are in practical use. Especially, methods using the change of magnetic material properties by stress resulting a high sensitivity.

(1) Eddy-current sensoring

As a possibility for the long-term monitoring of bridge constructions the impedance measurement of reinforcing steel with eddy current sensors. With this method arising damage is promptly recognisable. Costs can be thus effectively reduced. Each kind of steel possesses individual stress distributions in its, as well as a certain pre-magnetisation with preferred direction. Mechanical forces cause direction-controlled changes of the structure and magnetic moment generated by the electron spins. The latter changes the magnetisation of the ferrous-

magnetic steel. The magnetic measuring depends on the magnetic permeability and thus on the magnetisation of steel.

$$\Delta L \sim \Delta\mu_r = \frac{J_s^2}{3 \cdot \mu_0 \cdot \lambda_s \cdot E \cdot \varepsilon}$$

E Young's Modulus
ε Strain
J_s Magnetic Polarisation
ΔL Variation of Inductivity
λ_s Saturation Magnetostriction
$\Delta\mu_r$ Variation of magnetical permeability
μ_0 Permeability of Vacuum

Thus the strength in amount and direction can be measured. The principle of the eddy current sensor technology is based on the measurement of the complex impedance of the eddy current coil. This measuring effect be based on the electromagnetic reciprocal effect between the field of eddy currents produced in the structural steel and the exciting coil. The measured impedance depend on the magnetostrictive characteristics of the material, which admits for an exact stress measurement [192].

(2) 3MA method

3MA is a multiple parameter modelling of mechanical and technological material properties. It is based on multiple regression and neural network algorithms which are calibrated by non-destructively (nd) determined data. These are selected from well-defined calibration specimens and by the use of different micro-magnetic nd-techniques (ndt). Magnetic domain walls (Bloch walls) move in the ferromagnetic materials under dynamic magnetisation. They strongly interact with microstructure parameters like dissolved atoms (C, N, Cu), dislocations, precipitates, second phases and grain boundaries. All of the micro-magnetic techniques and derived parameters are based on these Bloch wall interactions. Therefore, they show interrelationships to mechanical parameters characterising strengthening or softening of the materials. The same type of microstructures ('lattice defects') impeding dislocation movement under mechanical load impedes Bloch wall movement under magnetic load. These mechanical parameters are hardness and those derived from the standard tensile test, like yield strength and tensile strength but also toughness-sensitive. 3MA is the official acronym for the development of ndt-techniques for materials property determination and prediction under the framework of the German Nuclear Safety-Research Programme [180].

(3) Transformer measuring technique

This measuring method gives a possibility to determine stress changes in pre-stressing steel with high accuracy. For a simultaneous measurement of several magnetic characteristics, eg saturation magnetisation, coercivity, remanence and permeability, under utilisation of the magneto-elastical effect the sensors for stress measurement were built for minimised space requirements, high measuring accuracy, small costs and large insensitivity to humidity and dust. The measuring system was tested and improved by calibrations of pre-stressing steels in the test equipment and comparative investigations. A computer-controlled recording of

measurements is realised, in which the calibration curves can be put down by examined pre-stressing steels [179,182].

A similar measurement method is already existing for 15 years in Slovakia. The magnetic characteristics of amplitude permeability and incremental permeability at a properly chosen operating point are about 100 times more stress-sensitive than the electrical resistance effect. The relative change of the magnetic incremental permeability of steel is up to 10^(-3) / MPa, while the relative change of strain gauge electrical resistance is about 10^(-5) / MPa. The magneto-elastic method, therefore, enables the measurement of stress under 1 MPa in noisy industrial environments and over wide temperature range [170,175,188].

(4) Conclusion

The introduced magnetic stress measurements are based on the magneto-elastic effect. They differ fundamentally in the measurement of characteristic magnetic and electric values, eg remanence and inductance. According to the measuring procedure this requires a calibration on the magnetostrictive coefficient of a respective steel. As the magnetic state (residual stress and pre-magnetisation) is generally unknown, intensive research in this area is absolutely necessary. However, devices are practical in use which consider only partly a complete parameter dependence.

5.5 Dynamic parameters

The dynamic response of a structure concerning ambient vibrations (state of the art technology) can be assessed by use of different methods, which could be measurements of motion, deformation or forces along the points of interest. Concerning measurement of motion the most important methods are acquisition of displacements, velocities or accelerations. Basically it does not play any role which of these parameters is measured, because an integration respectively a differentiation can transform one of these signals to each other. The current practice is the use of accelerometers for dynamic testing, because very accurate results can be obtained with this type of transducer. The following section relates only to accelerometers, basically the same things are applicable also for velocity sensors.

5.5.1 Acceleration sensors

It can be differentiated between absolute and relative acceleration sensors, which do not need a measuring basis. Generally, the functioning of acceleration sensors is based on certain physical (piezo electrical, inductive, capacitive, piezoresistive, electric dynamically) principles (Serridge and Licht 1990), (Tränkler and Obermeier 1998).

In principal accelerometers are devices constituted by mass-spring-damper-systems that produce signals proportional to the acceleration in a frequency band below their own resonance. Different systems and working principles can be distinguished in the construction of an accelerometer, the following main groups can be identified:

- Piezoelectric sensors
- Piezoresistive and capacitive sensors
- Force-balanced accelerometers

In the following section a short description of each sensor principle is given according to the technical descriptions from sensor providers.

5.5.1.1 Piezoelectric sensors

The following figure presents schematically the mechanical components of a piezoelectric accelerometer for a configuration known as delta-shear. There are also some other configurations possible such as planar-shear, compression and annular construction. The active part of the accelerometer are the piezoelectric elements, which act as springs and connect the seismic masses to the base of the accelerometer through a rigid center, suffering therefore slight shear deformations when vibrating with the structure. These vibrations originate a charge which is proportional to the acceleration of the seismic masses and consequently, proportional to the acceleration of the surface where the sensor is located.

Compared to other types of accelerometers, piezoelectric accelerometers have several advantages, such as (i) no external power source required (the accelerometers are designated as self-generating), (ii) are very robust and stable in the long term and relatively insensitive to temperature changes and (iii) characterized by high signal-to-noise ratios and finally (iv) are linear over a wide frequency and dynamic range.

In contrast to these advantages the piezo elements have the disadvantage of aging. Thus it is necessary to (re)calibrate the acceleration sensor at regular intervals in order to ensure accuracy of measurement. Because of their very good properties the acceleration sensors based on the piezo electrical principle are the most widely used sensors in the vibration measurement practice. However, these transducers present a serious inconvenience in applications involving large and flexible structures with low level frequency response, which is due to their limitation in the lower frequency range. Piezoelectric transducers are not capable of a true DC (0 Hz) response, as the piezoelectric elements only produce charge when acted by dynamic forces. The actual low frequency limit is determined by the preamplifier to which the sensor is connected and is in general > 1 Hz.

5.5.1.2 Piezoresistive and capacitive accelerometers

Piezoelectric sensors shown before have been defined as self-generating transducers, in the sense that they generate an electrical charge proportional to the mechanical energy, which is then conveniently amplified and transformed into an electrical energy. These devices can also be designated as active transducers.

Piezoresistive and capacitive sensors are defined as passive sensors (compare to piezoelectric sensors), requiring the supply of electrical energy. This energy modifies with the change of mechanical energy, the difference to the input energy being proportional to the structural acceleration.

Piezoresistive accelerometers are composed of a bending beam with bonded strain-gages forming part or all of an active Wheatstone bridge. The beam supports a seismic mass. As the beam deforms under acceleration of the seismic mass, the Wheatstone bridge is unbalanced and the differential output (proportional to the beam strain) is a measure of acceleration.

Capacitive accelerometers comprehend a bending beam supporting a seismic mass in a scheme similar to piezoresistive transducers. In this case, the seismic mass moves from its central support between two electrodes. The measuring elements form a half-capacitive bridge, which is unbalanced whenever the seismic mass moves, the differential output measured being proportional to the structural acceleration.

Piezoresistive and capacitive accelerometers basically are adequate for Civil Engineering applications for flexible structures since they can measure accelerations from DC level.

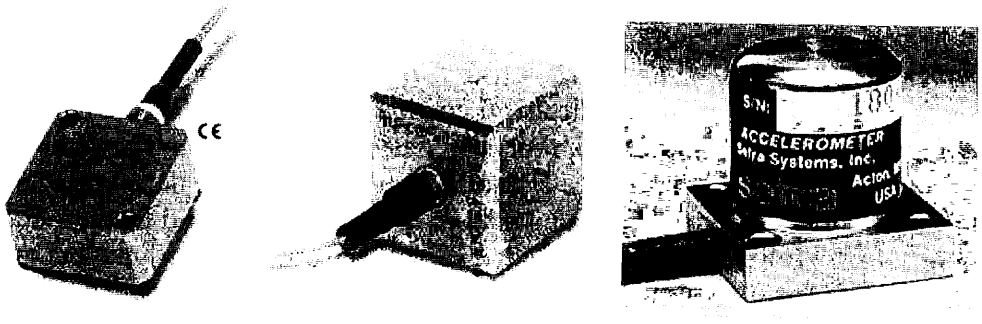

Fig. 5-40: Accelerometers

5.5.1.3 Force-balance accelerometers

These sensors belong to the category of passive transducers and are composed, similar to the piezoresistive and capacitive accelerometers, by mass-spring systems whose motion generates modification of the DC voltage fed as input. Usually a central plate (mass) is supported on four suspension beams that are anchored on their tips and acting like a spring. When the transducer experiences acceleration, the central plate moves causing unequal capacitances between the central multi-plate electrode and two fixed electrodes. The changes in capacitance are sensed and conditioned to generate a DC voltage that is fed back to the capacitor plates and electro statically forces the central plate back to the equilibrium position. The voltage required to hold the central plate in equilibrium provides the output signal. This signal is proportional to the structural acceleration.

Force-balance accelerometers have been available for a long time and constitute at present one of the most employed types of transducers for Civil Engineering applications to large flexible structures. These transducers have a set of characteristics that fit well the requirements for ambient vibration testing of flexible structures, such as robustness, the high sensitivity, the operation in the low frequency range (from DC to as much as 100 Hz) and a significant dynamic range.

5.6 Environmental measurements

5.6.1 Temperature

Most basic instrumentation programs include measurements of temperatures. Temperature measurements are generally required for the correction of other measurements. Other applications of temperature measurements are the determination of temperature gradients for superstructures or for investigations on the effect of heat of hydration on concrete. Measurements of temperature to determine the effects of the heat of hydration must be made during the concrete curing period.

Data acquisition for heat of hydration requires that measurements must begin as soon as the concrete is placed and continue until the concrete temperatures fall to near ambient. Temperatures should be recorded at 30-minute intervals during the first 24 hours to ensure measurement of the maximum temperature. Data acquisition for temperature gradients need not begin until the bridge is complete and need only be made in summer and winter. Temperature readings at hourly intervals will provide sufficient information. Data acquisitions for freeze-thaw cycles need only be made from late fall to early spring depending on geographic location. Temperature readings at 30-minute intervals should provide sufficient information. (U.S. Department of Transportation 1996 [147])

5.6.1.1 Thermocouples

Thermocouples are the most widely used sensors for measuring temperature. They are based on the Seebeck effect that occurs in electrical conductors that experience a temperature gradient along their length. A Thermocouple basically consists of two dissimilar metals joined together at one end (junction), which produce a small unique voltage. The developed Seebeck voltage is a function of the temperature of the junction. In fact, it was found that the Seebeck voltage is the sum of two voltage effects: the Peltier effect, generated at the junction, and the Thompson effect, which results from the temperature gradient in the wires. Thus, the net thermoelectric voltage generated between the open ends depends on the temperature difference between junction ($T_{junction}$) and reference end (T_{ref}), the relative Seebeck coefficient of the wire pair and the uniformity of the wire-pair relative Seebeck coefficient. The reference temperature at the measurement junction can be established using ice baths, electronically controlled reference temperature devices, compensated reference temperature systems or zone boxes.

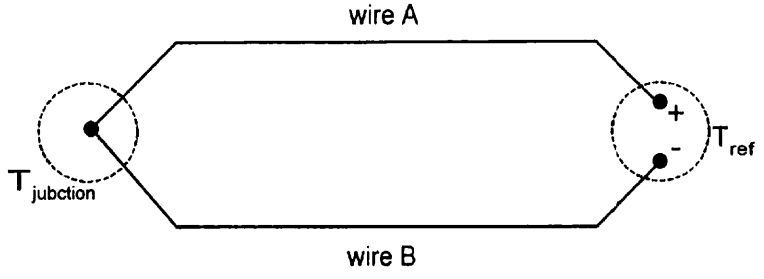

Fig. 5-41: Schematics of simplest thermocouple

The simplest thermocouple probe shown in Fig. 5-41 is simply a pair of wires twisted together at one end with the other end connected to the terminals of a voltmeter.

Thermocouples are available in a variety of forms including different combinations of metals and calibrations. It is possible to either purchase bulk thermocouple wires bought as spools of insulated pairs and form a thermocouple junction by welding or soldering them together or to obtain wires with a junction already formed by the manufacturer. The three most common thermocouple alloys for moderate temperatures are Iron-Constantan (Type J), Copper-Constantan (Type T), and Chromel-Alumel (Type K). Each alloy has a different temperature range and environment, although the maximum temperature varies with the diameter of the wire used in the thermocouple. Chromel-Alumel thermocouples generate electrical signals, while the wires are being bent, and should not be used on vibrating systems, unless strain relief loops can be provided. Type T thermocouples are inexpensive and very sensitive but corrode rapidly at temperatures over 400 °C. Type K thermocouples are popular for general use since they are moderately priced, reasonably corrosion resistant, and usable at temperatures up to 1372 °C. They also have a relatively linear output, which means that for applications in which accuracy requirements are not too severe, the temperature can be computed by assuming a linear relationship between temperature and voltage.

Prefabricated sheathed thermocouple probes are available with one of three junction types: grounded, ungrounded or exposed. At the tip of a grounded junction probe, the thermocouple wires are physically attached to the inside of the probe wall. This results in good heat transfer from the outside, through the probe wall to the measurement junction. In an underground probe, the measurement junction is detached from the probe wall. Response time is slowed down from the grounded style, but the ungrounded type offers the advantage of electrical isolation. Ungrounded junction is used for measuring in corrosive conditions. In the exposed junction style, the thermocouple protrudes out of the tip of the sheath and is exposed to the

surrounding environment. This type offers the fastest response time, but is limited in use to non-corrosive and non-pressurized applications.

Fig. 5-42 shows a circuit for handling multiple thermocouples, in which each voltage is read separately, including the reference temperature signal. If a dedicated temperature indicator is being used, the reference temperature branch of the circuit need not be used, since the internal electronics of the system will always add a correction to the thermocouple signal based on the thermocouple connection panel temperature.

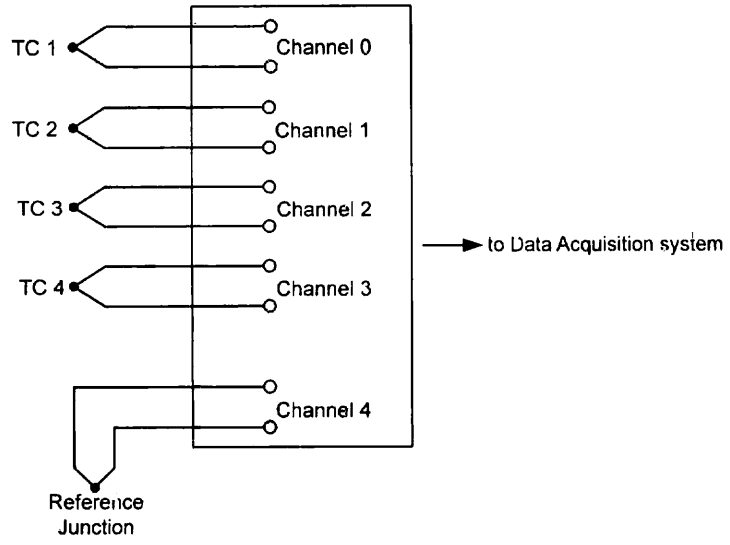

Fig. 5-42: Multiple thermocouples

When good spatial resolution or good transient response is required, a thermocouple is to be preferred over other common temperature sensors. (Omega 1998 [100], Wheeler 1996 [157])

5.6.1.2 Resistance temperature detectors (RTD)

RTDs are wire wound and thin film devices that work on the physical principle of the temperature coefficient of electrical resistance of metals. Materials for RTDs can be gold, silver, copper or platinum. Platinum, however, has become the most-used metal for RTDs due to its linearity with temperature. Its desirable characteristics include chemical stability, availability in a pure form, and electrical properties that are highly reproducible. The electrical resistance of the RTD material changes as a function of temperature. In this way, by measuring the resistance of the element, the temperature of the element can be determined form tables, calculations or instrumentation. The relationship between resistance and temperature can be approximated by the Callendar-Van Dusen equation:

$$\frac{R}{R_0} = 1 + \alpha \cdot \left[T - \delta \cdot \left(\frac{T}{100} - 1 \right) \cdot \left(\frac{T}{100} \right) - \beta \cdot \left(\frac{T}{100} - 1 \right) \cdot \left(\frac{T}{100} \right)^3 \right]$$

T Temperature
R Resistance at temperature T
R_0 Resistance at the ice point
α, β, δ Constants, dependent on the purity of the metal, which are determined by calibration

RTDs are generally more accurate and more stable over time than thermocouples. They are nearly linear over a wide range of temperatures and can be made small enough to have response times of a fraction of a second. They can be used to measure temperature directly, not simply relative temperature as with thermocouples. On the other hand, RTD probes require an electrical current to produce a voltage drop across the sensor that can be then measured by a calibrated read-out device. Unavoidably, the measuring current generates heat in the RTD. A self-heating factor, "S", gives the measurement error for the element in °C per milliwatt.

Basically, an RTD probe is an assembly composed of a resistance element, a sheath, lead wire and a termination or connection. The sheath, a closed end tube, protects the resistance element against moisture and the environment to be measured.

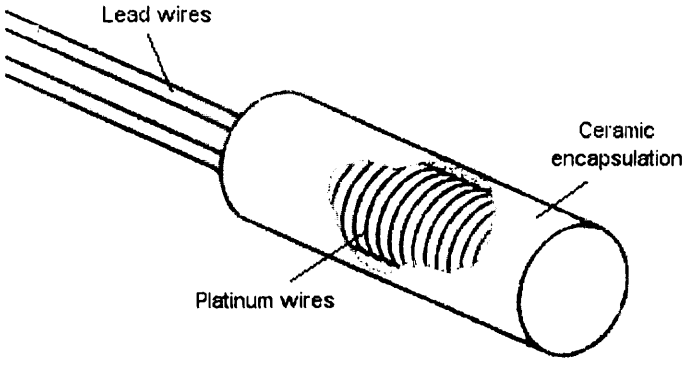

Fig. 5-43: RTD, wire wound sensing element

There are a large number of configurations of RTD sensing elements. Wire wound elements (see Fig. 5-43) are made primarily by winding a very fine strand of platinum wire onto a glass or ceramic coil. The coil is then inserted into a mandrel and powder is packed around it to prevent the sensor from shorting and to provide vibration resistance. The outer coating prevents damage or contamination. RTD elements can also be made by depositing platinum as a thin film on a ceramic substrate and then encapsulating it with ceramic or glass. An advantage of the thin film sensor, shown in Fig. 5-44, is that a greater resistance can be placed in a smaller area. The thin-film design is a newer technology and is gaining favor due to lower cost. It is important in the design of RTD probes to minimize strain on the platinum due to thermal expansion since strain also causes changes in resistance.

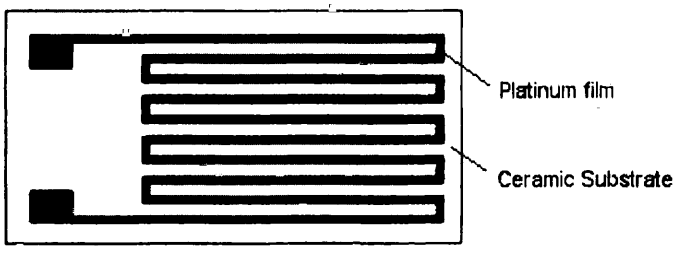

Fig. 5-44: RTD, thin film sensing element

As with strain gages, the Wheatstone bridge is an appropriate circuit to measure the resistance change for an RTD. However, the lead wire used between the resistance element and the measuring instrument has a resistance itself, this inaccuracy must be compensated. Thus, the optimum form of connection for RTDs is a four-wire circuit (see Fig. 5-45). It removes the error caused by mismatched resistance of the lead wires. A constant current is

passed through A and C; between B and D the voltage drop across the RTD is measured. With a constant current, the voltage is strictly a function of the resistance and a true measurement is achieved. This design is slightly more expensive than two- or three-wire configurations, but is the best choice when a high degree of accuracy is required. (Omega 1998 [100],Wheeler 1996 [157])

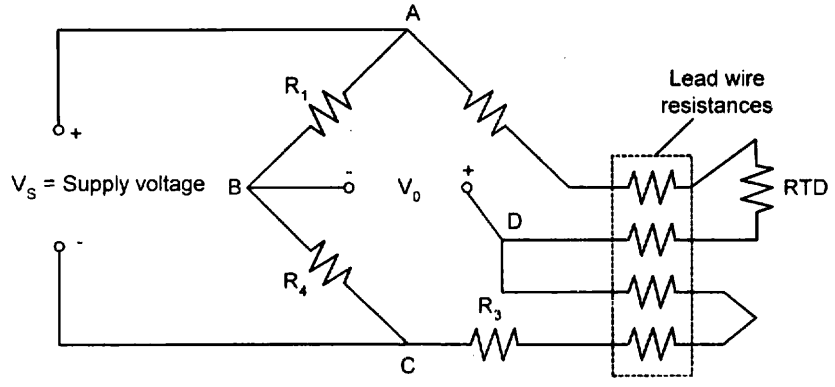

Fig. 5-45: Four-wire RTD circuit

5.6.1.3 Fiber optic temperature sensors

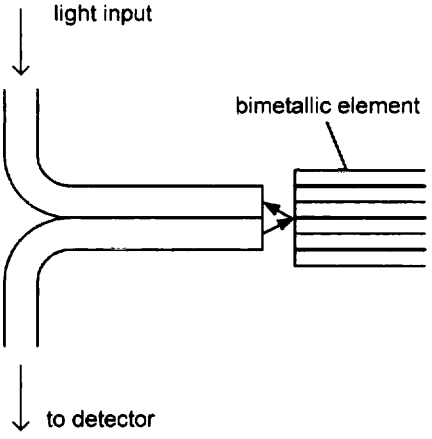

Fig. 5-46: Reflective fiber optic temperature transducer

Several fiber optic sensing concepts have been used in measurement of temperature. These include reflective, microbending, intrinsic, and other intensity- and phase-modulated concepts. (Wheeler 1996 [157])

One type of fiber optic temperature sensor based on the reflective concept measures the displacement of a bimetallic element used as an indication of temperature variation.

Another type of fiber optic temperature sensor consists of a temperature sensing component being placed on the tip of the fiber optic's "free end". The other end is attached to a measuring system that collects the desired radiation and processes it into a temperature value. The sensing component can be made of liquid crystals, semiconductor materials, materials that fluoresce, and other materials that can change spectral response.

The effects of temperature variations on a semiconducting crystal are well known and predictable. When the crystal's temperature increases, its transmission spectrum shifts to

higher wavelengths. The relationship between the temperature and the specific wavelength at which the absorption shift takes place is very predictable. The position of the absorption shift is then analyzed and correlated back to temperature.

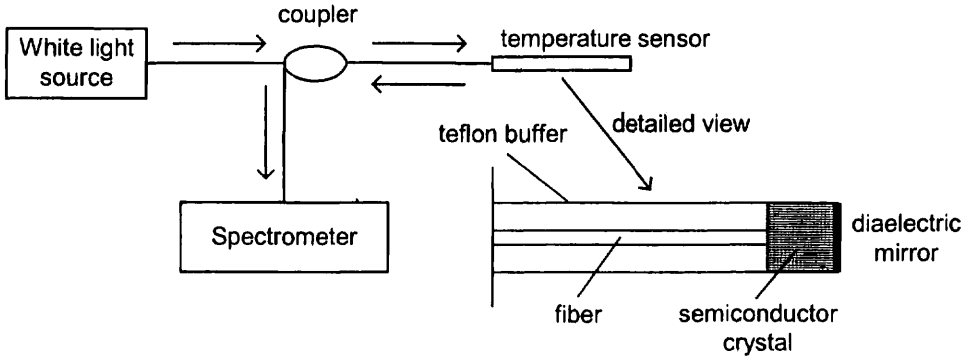

Fig. 5-47: Schematics of fiber optic temperature measurement using a semiconductor crystal

In Fig. 5-47 a white light source injects light into one of the branches of the coupler. This light travels down the probe's optical fiber to the semiconducting crystal, which absorbs some of it. Unabsorbed light is reflected by the dielectric mirror and returned down the fiber to the coupler, where it is directed to a spectrometer.

The concept of microbending is also used for temperature measurement. Using thermal expansion of a component structure, the sensor can measure the temperature by altering the fiber bend radius with temperature. (Wheeler 1996 [157])

5.7 Durability monitoring

Beside the solid mechanical quantities described above, there exist a variety of other physical and chemical processes that take place. Thus, it might be necessary to measure temperatures, humidity and other electrochemical phenomena to ensure a holistic surveillance concept.

5.7.1 Corrosion

Corrosion of reinforcing bars induces an early deterioration of concrete structures and reduces their service life (Pruckner 2001 [111]). In particular the increased use of deicing salts in the northern climates and the attack from sea salt in coastal areas has exacerbated concrete rebar corrosion (Zdunek 1995 [162]). It causes the reduction of reinforcing bar section, the cracking of concrete cover produced by the expansion of corrosion products, and the loss of composite interaction between steel and concrete due to bond deterioration (Pruckner 2001 [111]). The ability to detect this deterioration in its early stages is critical in directing repairs to the most at-risk bridges and will help optimize the use of limited funds.

The surface of the corroding metal acts as a mixed electrode upon which coupled anodic and cathodic reactions take place. At anodic sites, metal ions pass into solution as positively charged ions (anodic oxidation) and the excess of electrons flow through the metal to cathodic sites where an electron acceptor like dissolved oxygen is available to consume them (cathodic reduction). The electrons created in the anodic reaction must be consumed elsewhere on the steel surface establishing the corrosion reaction. The process is completed by the transport of

ions through the aqueous phase, leading to the formation of corrosion products at the anodic sites either soluble (e.g. ferrous chloride) or insoluble (e.g. rust, hydrated ferric oxide). If the current caused by the electron flow could be measured at all, the measured quantity, I_{net} would represent a net effect of the partial currents resulting from oxidation and reduction. (Pruckner 2001 [111])

$$I_{net} = \sum I_{ox} - \sum |I_{red}|$$

The corrosion rate CR is proportional to the sum of the partial anodic currents (corrosion current) causing metal dissolution. CR is defined as the loss of the corroding metal in micrometers per year [µm/a] and can be calculated by (Pruckner 2001 [111]):

$$CR = \frac{i_{corr} \cdot t_a \cdot M_{Me}}{zF \cdot d_{Me}} \cdot 10^6 [\mu m/a]$$

i_{corr} corrosion current density [A/m^2]
t_a year in seconds (31557600 s/a)
M_{Me} molar weight of the metal (for iron 0.055847 kg/mol)
z number of electrons (for Fe z = 2)
F Faraday constant (96485 C/mol)
d_{Me} density of the metal (for iron d_{Me} = 7860 kg/m^3)

The ferroconcrete system comprises reinforcing bars or reinforcement embedded in concrete, a medium in which the high alkalinity of the concrete (pH value of 12-14) when cast produces a stable film of passive oxides on the steel surface, which if maintained prevents any form of active corrosion from ensuing. However, penetration of aggressive ions, as e.g. chloride from deicing salt or carbonate from acid rain, will destroy the passivation of the embedded steel. In the presence of oxygen and a concrete humidity of about 60 – 80%, corrosion of the steel will start and develop continuously (Rodríguez 1996 [114]).

Corrosion in either carbonated or chloride contaminated concrete reduces the reinforcing bar section. When steel corrodes it forms rust that occupies a volume much greater than the steel itself. This exerts large expansive stresses on the surrounding concrete. Because the concrete is low in tensile strength, these stresses can cause cracking and spalling, which, in turn, permits faster ingress of water, oxygen and chlorides, accelerating corrosion further. Whereas homogenous attack penetration at the bars occurs in carbonated concrete, chlorides usually produce localized attack and cause a significant section decrease. (Pruckner 2001 [111])

5.7.1.1 Chloride contamination

Chloride ions are by far the most common contributor to premature corrosion in reinforced concrete structures. Chloride contamination is mostly due to the penetration of chloride ions from the outside (Breit 1998 [13]). Chloride is common in nature and may be introduced in concrete through admixtures, deicing salts, industrial chemicals, seawater or contamination of concrete mix water or aggregates.

Chloride induced corrosion of steel in concrete is – at least at the beginning – characterized by a very localized attack with the development of active/passive macrocells (Elsener & Böhni 1990 [37]). The coexistence of unattacked (passive) and corroding areas on

the same rebar network form a short circuited galvanic element with a high corrosion current on the active area. This macrocell corrosion is by nature very much more aggressive than the microcell corrosion that occurs in the case of carbonation leading to depassivation. This is essentially because in macrocell corrosion the anode area is very small in relation to the total cathode area available, which leads to intense localized corrosion. In the fullness of time the small pits will merge to form larger anodic sites, but there will always be alternating areas of anode and cathode along the rebar. These most often exist with an excess of cathode over anode and the attendant higher rates of corrosion that are so typical in the chloride environment. (van Es & Bennnett 2001 [40])

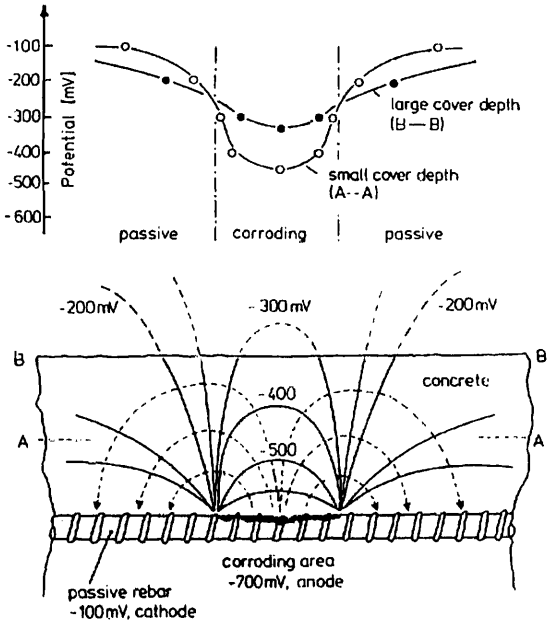

Fig. 5-48: Schematic representation of a corrosion marco cell(Elsener & Böhni 1990 [37])

Apart from the dominating influence of the concrete porosity and the pore size distribution the water and chloride uptake is also strongly related to the humidity gradients present in the cover part of the concrete structures (Zimmermann et al. 1998 [166]). The process of chloride ions building up until a corrosion-inducing limit has been reached depends on one hand on the supply of chloride from the ambient conditions outside and, to a substantial degree, on the concrete technology parameters influencing chloride transport and the binding of chloride taking place. The cement type and the water cement ratio are the essential influencing parameters in this context. As chloride corrosion of the reinforcement can only be caused by free chloride ions, the decisive factor in connection to corrosion of the reinforcement is actually not the total chloride content, but rather the fraction of uncombined, free chloride. (Breit 1998 [13])

Up till now the free chloride content could only be determined from expressed pore water of cores, a highly destructive and costly technique. In contrast to that, the quantitative determination of the total chloride content of concrete, which is carried out by decomposition of the concrete powder in acid and subsequent potentiometric titration using silver nitrate solution, is a relatively simple and safe determination method. This is the reason why national and international sets of rules relate the critical limit to the total chloride content relative to cement. Evaluation of the literature on the critical chloride content has shown that a lower corrosion-inducing critical total chloride content ranges at around 0.2 % by mass relative to cement content (Breit 1998 [13]).

5.7.1.2 Carbonation

Carbonation reduces the alkalinity of concrete thereby permitting corrosion. Carbonation occurs when carbon dioxide from the air reacts with the concrete to reduce the pH of concrete. This process involves a chemical change in the concrete in which the calcium hydroxide hydration compounds are converted into calcium carbonate compounds, hence the term carbonation. As a consequence reinforcement steel is not protected any longer by passivity in high alkalinity. Carbonation of concrete also induces additional shrinkage, which may cause crack formation.

The natural weathering process of carbonation should by design never be able to reach the reinforcement during the expected lifetime of the structure. In practice perhaps the concrete cover or quality can be compromised in construction and situations can arise in which the carbonation front has reached the steel, resulting in cracking and spalling (van Es & Bennnett 2001 [40]). Carbonation is normally a slow process, but can be accelerated by concrete cracking or inadequate concrete cover.

5.7.1.3 Corrosion measurement

Several methods have been developed for detecting and evaluating the effects of steel corrosion in concrete. These methods include visual inspection, chaining or sounding for delamination, pH level determination, potential measurements, polarization techniques, and x-ray spectroscopy. However, many of these methods require concrete cores to be brought into the laboratory for testing. In addition, the laboratory methods require significant technical expertise. Additionally, the evaluation of the results from many of the tests rely on subjective or statistical interpretations from previously reported tests. Further, different researchers use different methods of testing and evaluating. Due to the high complexity of the phenomenon, reliable methods of corrosion detection and evaluation have developed slowly (Elsener & Böhni 1990 [37]).

The easiest and most straightforward method for detecting steel corrosion in reinforced and prestressed concrete structures is the visual inspection for rust staining and cracking (Rodríguez et al. 1996 [114]). Rust stains that follow the line of reinforcement clearly indicate steel corrosion. When corrosion progresses further, cracking of the steel concrete cover occurs. Direct or remote inspection techniques are used to detect obvious signs of corrosion, such as physical damage in the form of spalling or cracking. Visual observation can range from coarse examination to detailed mapping of the surface. Core sampling is often performed if the visual observation suggests that further evidence is needed. However, visual observation is subjective and provides corrosion detection only after significant corrosion has occurred. Core sampling is destructive and requires repair of the concrete. (Yuyama 1986 [161])

Another approach is the chloride determination, a method that establishes the likelihood as to whether or not corrosion is occurring. The significance of a chloride analysis lies within the spectrum of simply determining that the concentration is sufficient to cause steel to change from a passive to an active corrosion state. Beyond the threshold value of chloride concentration necessary to cause corrosion, the rate of corrosion is a function of many variables, but in particular of moisture content. Therefore, even though a bridge slab may have more chlorides than the threshold value, it may not be in an active state when considering ambient and environmental factors, which are necessary for corrosion. Likewise, if a bridge deck is in an active corrosion state, additional amounts of chlorides may have little effect on the corrosion (Bungey & Millard 1996 [19]).

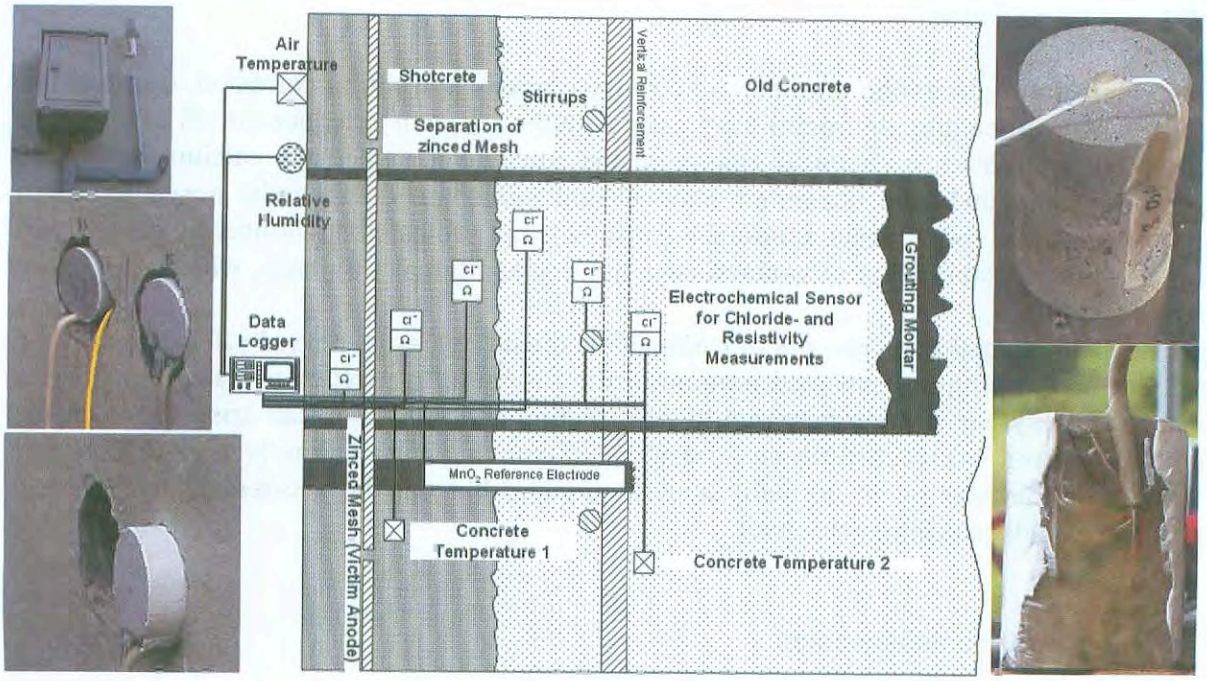

Fig. 5-49: Corrosion sensor unit developed by Zimmermann, Schiegg, Elsener and Böhni (Elsener & Böhni 1990 [37], Zimmermann et al. 1998 [166])

Environmental factors such as the humidity content of the concrete, the chloride concentration or the oxygen content of the adjacent pore solution are decisive for the rate of corrosion propagation. Therefore the conductivity of the concrete cover, the chloride concentration or the pore water solution and the corrosion current of rebars as well as the temperature are important parameters to be monitored over an extended period of time (Schiegg & Böhni 2000 [123]). Additional information about humidity gradients occurring in the concrete cover and the extent of the humidity exchange zone (transport zone) would be highly desirable to improve the prediction of the corrosion behavior of reinforced concrete structures (Zimmermann et al. 1998 [166]).

ELECTROCHEMICAL METHODS	NON-ELECTROCHEMICAL METHODS
Corrosion Measurements on the Actual Rebar: Half-cell potential measurements Galvanostatic pulse method	Visual inspection Seismic method Infrared Thermography Acoustic emission Radiography and radiometry Radar Electrical resistivity of concrete Electrical resistance method Optical fiber sensors Magnetic technique Microwave based Thermoreflectometry
Corrosion Measurements on Embedded Probes: Potentiodynamic polarization methods *Localized electrochemical impedance spectroscopy* *Electrochemical impedance spectroscopy* Corrosion macrocell current measuring Electrochemical noise	

Table 5-6: Methods for corrosion measurement [184]

(1) Half-cell potential measurements

For an electrochemical mechanism such as galvanic corrosion to occur, there must be a potential difference. Potential methods such as the half-cell potential method rely on this known condition for corrosion detection. In particular, the half-cell potential method measures voltage gradients or drops by use of a high-impedance voltmeter and a constant voltage reference cell. The half-cell consists of a metal rod immersed in a solution of its own ions. The metal rod is connected with the reinforcement steel by a voltmeter, and the ion solution is connected to the pore water via a moist porous plug.

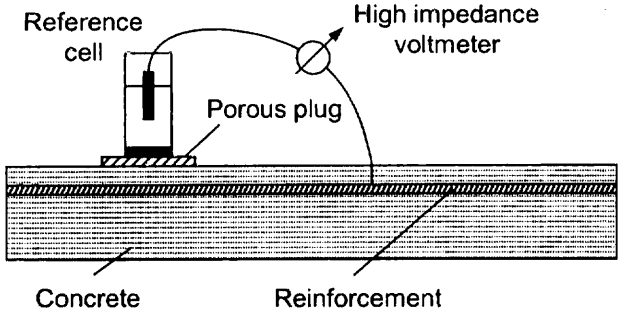

Fig. 5-50: Principle of half-cell potential measurement

The reference cell possesses a constant internal voltage, which allows voltage changes existing on the reinforcement to be measured. The measuring method is based on many measurements of potential and correlation of measured potentials with observed corrosion rate at reinforcement. This method provides both an effective means for determining if corrosion is occurring and the extent of corrosion distress. However, if corrosion has occurred and then was stopped by some means, the method proves ineffective (Rostam 1992 [115]). Another limitation of applying this method is that corrosion in rebars embedded in concrete decks is usually localized in certain areas, while other areas remain free of it. This highly non-uniform condition is difficult to evaluate. The erratic nature of the results may cause (sometimes unduly) doubt on the procedure. (Wright 1995 [159])

Nevertheless, this method is applicable regardless of the size or the depth of cover over the reinforcing steel. It can be used in structures which show no visible signs of distress to determine when corrosion initiates, or in a structure which shows severe corrosion distress to determine the extent of corrosion (Rostam 1992 [115]). As a tool used in initial characterization, it is required to examine as much of the structure as possible.

Hand held equipment

The half-cell is moved across the concrete surface to be investigated, and the electrode potentials are measured at many points [184]. The measured potential is drawn as equipotential lines to identify the corrosion areas (Moller 1992 [91]). Extra devices are constructed to accelerate measuring (Broomfield et al. 1990 [16]).

Embedded reference electrodes

Results obtained by means of the hand held equipment are not accurate, because there is a concrete layer between half-cell and steel with variations in resistance and thickness. To avoid

negative effects of the concrete layer, half-cells can be embedded in concrete close to the reinforcing steel. Different reference electrodes are commercially available. A potential between the steel and electrode can be measured by using the half-cell. The advantage of the method is its great sensitivity, which makes the method suitable for measurements of pitting corrosion at large concrete structures. [184]

(2) Galvanostatic pulse technique

In this technique a short time anodic pulse is applied galvanostaticially on the reinforcement, from a counter electrode positioned on the surface of the concrete. The resultant rebar potential change is monitored by means of a reference electrode, also located on the concrete surface, and the high impedance voltmeter [174].

The slope of the potential vs. time curve, measured during the current pulse, has been used to provide information on the rebar corrosion state. Passive rebar has reportedly a relatively steep slope, while rebar undergoing localized corrosion has a very slow slope. In the latter case, the rebar potential only shifts by a few millivolts below the applied current pulse (Elsener & Böhni 1990 [37]). The potential data has also been used to obtain a measure of the concrete resistivity (for a given depth of cover) (Elsener & Böhni 1990 [37]). The technique is reportedly very rapid and may facilitate more unambiguous information on the rebar corrosion state than is possible by simple potential mapping (Elsener & Böhni 1990 [37]).

(3) Measurements with embedded sensors

Measuring with embedded probes may have several purposes. The type and number of probes will depend on these aims. Examples of applications are to:

- Follow the effectiveness of a repaired structure or of a surface treatment.
- Monitor the advance of the carbonation front or of the chloride threshold.
- Detect the beginning of reinforcement corrosion.
- Control a cathodic protection installation.

Following parameters can be measured by suitable embedded electrochemical sensors:

- Electrochemical potential
- Corrosion rate
- Electrical resistance
- Oxygen availability
- Corrosion Macrocell current
- Chloride content
- pH-value
- Humidity variations

Potentiodynamic polarization methods

Polarization methods involve changing the potential of the working electrode and monitoring the current, which is produced as a function of time or potential. Several methods may be used in polarization of specimens for corrosion testing. Potentiodynamic polarization is a technique where the potential of the electrode is varied at a selected rate by application of a current through the electrolyte. It is probably the most commonly used polarization testing method for measuring corrosion resistance and is used for a wide variety of functions [173]:

- Cyclic polarization tests
- Cyclic voltammetry
- Potentiostaircase method
- Electrochemical potentiodynamic reactivation (EPR)
- Linear polarization resistance (LPR)

In the **Linear Polarization Resistance (LPR) technique**, a potential (typically of the order of 5-50 mV) is applied to a freely corroding sensor element and the resulting ("linear") current response is measured. This small potential perturbation is usually applied step-wise, starting below the free corrosion potential and terminating above the free corrosion potential [172]. The polarization resistance of a material is defined as the slope of the potential-current density ($\Delta E/\Delta i$) curve at the free corrosion potential, yielding the polarization resistance R_p that can be itself related to the corrosion current, according to:

$$R_p = \frac{\Delta E}{\Delta i} = \frac{B}{i_{corr}}$$

R_p Polarization resistance (kΩ)
ΔE Potential response (mV)
Δi Applied current (mA)
I_{corr} Corrosion intensity (μA/cm²)
B Empirical polarization resistance constant, it can be related to the anodic/cathodic Tafel slopes

The measurement of polarization resistance has very similar requirements to the measurement of full polarization curves. There are essentially four different methods of making the measurement according to whether the current or the potential is controlled and whether the current (or potential) is swept smoothly from one value to another, or simply switched between two values. In addition the measurement may be made between two nominally identical electrodes (a two-electrode system), or a conventional three-electrode system (working, reference and counter) may be used [173].

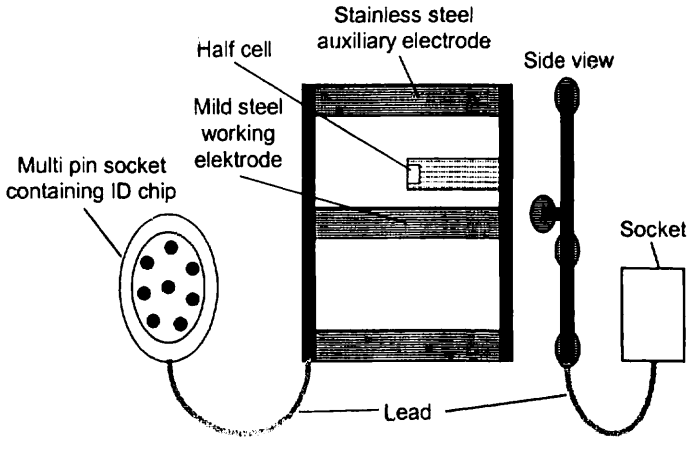

Fig. 5-51: Half cell embedded in concrete

If linear polarization is used in corrosion monitoring then in new construction the measurement can be made with an embedded half cell against a mild steel "working

electrode" with one or more stainless steel auxiliary electrodes, as shown in Fig. 5-51. The system has been designed to fit into the rebar cage. A cable runs from the unit to a multipin socket fixed to the formwork. After casting and curing the concrete, the formwork is removed, leaving the socket exposed for connection to a hand held or permanently wired monitoring system [173].

Electrochemical impedance spectroscopy (EIS) uses polarization with alternating current. Instrumentation for measurements is more sophisticated than for other polarization measurements, consisting of a potentiostat and spectrum analyzer. Reinforcement is maintained at its corrosion potential E_{corr} by the potentiostat, with application of a sinusoidal potential (10 to 20 mV) in a wide frequency range. The response at input signal is also sinusoidal with phase shift relative to the input signal. The EIS method in its basic formulation is very attractive because it can determine polarization resistance and add extra information about the corrosion process. The high frequency range can give information about dielectric properties of concrete, and the low frequency range information about dielectric properties of passivity film on the steel [184]. However, EIS data generation and analysis generally requires specialist electrochemical knowledge and can be rather lengthy, making it unsuitable for rapid evaluation of corrosion rates [174].

Data obtained by the conventional EIS technique are averaged across the entire area of the sample, and this technique is not suitable for application for chloride induced pitting corrosion. To avoid problems, localized electrochemical impedance spectroscopy (LEIS) is developed. The principles of LEIS are similar to those in conventional EIS, but LEIS combines both established direct current scanning probe methods with alternating current impedance techniques [184].

Electrochemical sensor for Chloride- and resistivity measurements

In Fig. 5-52 a chloride sensitive sensor element based on a solid AgCl (silver chloride) electrode for use in cement paste, mortar and concrete is shown. The chloride sensor is mounted in a stainless steel tube, which also allows to observe simultaneously the humidity conditions by measuring the resistivity between different sensors. The central chloride sensitive element is a silver wire coated with electrochemical deposited silver chloride (AgCl). The electrical insulation between the AgCl coated wire and the stainless steel tube is obtained by a small, flexible Teflon tube. Finally an epoxy resin is used as sealer to prevent ingress of solution into the stainless steel or Teflon tube. Each sensor has two electrical connections, one to the silver wire (chloride sensor) and one to the stainless steel tube for resistivity measurements. (Zimmermann et al. 1998 [166])

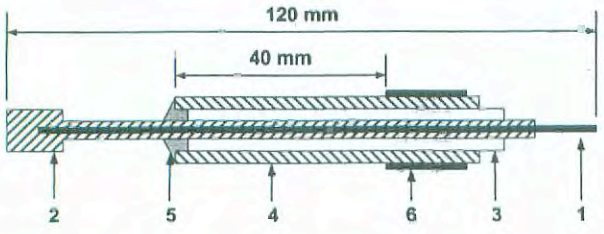

1 silver wire
2 AgCl coating
3 teflon tube
4 stainless steel tube
5 epoxy sealing
6 insulation

Fig. 5-52: Chloride sensitive sensor element

For field applications the sensors are casted into mortar cores or mounted in concrete cores taken from the structure. The sensor element shall be placed at the same level as the steel

rebar and oriented parallel to it. The potential of the chloride sensors and the rebars are measured versus an MnO_2 – reference electrode embedded in the surrounding concrete. (Zimmermann et al. 1998 [166])

This chloride and resistivity sensor for use in cement based materials has been developed and tested at the Swiss Federal Institute of Technology Zürich in Switzerland. The results show (Zimmermann et al. 1998 [166]):

- The potential depends linearly on the logarithm of the chloride concentration in the pore water solutions and follows Nernst law with a good linearity in a large concentration range. The sensors show an excellent stability and reproducibility.
- The chloride sensor allows to determine the free chloride concentration in pore water of mortars. Depassivation of rebars in bulk pore water solution occurs when the Cl^-/OH^- - ratio is > 1. In mortars depassivation takes already place at lower ratios most probably due to crevice effect, therefore no critical threshold value exits.
- With resistance measurements between neighboring sensors the water uptake can continuously be monitored in the cover zone. The water and chloride ingress occurs differently. There is a significant time lag between the water and chloride front.
- Sensor arrays in mortar and concrete cores for field application have been developed. Further experiments to test the reliability of the sensor arrays and the electronic instrumentation of the monitoring units have to be carried out.

Corrosion macrocell current measurement

During the corrosion process, corrosion macrocells are formed with a distribution of anodic and cathodic areas. The voltage in a macrocell element is equal to the potential difference between active and passive steel and drives the corrosion current [184]. The macro cell current measured between embedded rebar probes can serve as an indication of the severity of corrosion [174].

Interestingly, the concept of measuring a macro cell current as indicator of corrosion severity can also be applied to probe elements of identical materials and exposed to the same environment. It may be somewhat surprising that a significant current will flow between nominally identical probe elements but this principle has been used in commercial corrosion monitoring and surveillance systems for many years. It can be argued that such measurements are mainly relevant to detecting the breakdown of passivity and the early stages of corrosion damage. If extensive corrosion damage is occurring on both the probe elements, the macro cell current measured will not accurately reflect the severity of attack [174].

Electrochemical noise

Fluctuations of potential and current, generated spontaneously by the corrosion process, lead to electrochemical noise. Analysis of fluctuations after spectral decomposition gives not only finding of corrosion, but also characterization of the corrosion process [184]. For these measurements, three nominally identical rebar probe elements can be conveniently embedded in the concrete [174].

Advantage of the electrochemical noise method is the small external current or voltage needed for the measurement. Measured signals can be analyzed by mathematical analysis. In the case of complicated kinds of corrosion, like metastabile pitting corrosion or corrosion inhibitor induced by unstable passivation, mathematical analysis becomes unsuccessful, and some researchers suggest application of chaos theory at corrosion electrochemistry (Katwan et al. 1996 [72], [184]).

6 Implementation issues and data acquisition

The next Chapters will focus on techniques for the acquisition, the modeling, and the interpretation of knowledge, which are common to most monitoring and measurement systems, regardless, the specific testing and instrumentation methods which may be employed. This starts with the selection of appropriate sensing elements and suitable data acquisition components and ends up with the archiving and representation of the acquired data in well organized databases. Finally the system modeling (see Chapter 8.1) and its linkage to measured data closes the loop of monitoring and provides the basis for any analysis and decision making. (Santa & Bergmeister 2000 [119])

A prerequisite for any efficient structural monitoring system is an elaborate conceptualization of the object to instrument and a careful planning in order to guarantee the validity and accuracy of the monitoring procedure. The definition of the objective of the instrumentation program usually follows the realization that something about the structure is not known well enough and that measurements of a number of quantities at a certain location would be desirable for the sake of economy or safety. The first step is to reflect on all possible ways the construction might respond to externally induced actions and to choose which quantities to measure, where to measure them, and to select adequate instruments to do so. This requires an estimation of the magnitudes of changes in the quantities to be measured, which allows the definition of the range, resolution, accuracy, and sensitivity of the instruments selected to measure them. In much the same way, the temporal behavior of the observed phenomena might be a criterion for the dynamic requirements for both the instruments and the data acquisition and recording equipment. As next the instrument positions and the number of instrumented sections have to be determined. Instruments can be installed in trouble spots, such as points where it is expected that there will be large stress concentrations or points where it is supposed that deficiencies have already initiated. Alternatively, the instruments can be placed at a number of representative points or zones of the structure. Nevertheless, the phenomena that occur on a structure like a bridge and resulting failures are not always the same and depend on the function and type of structure of the bridge as well as on the used materials. Additionally, there exist a lot of different sensors and testing methods each of them having its advantages and each of them requiring different application considerations. The instrumentation and testing layout is finally strongly governed by the expected problem and the specific interests of the executing engineers. (Santa & Bergmeister 2000 [119])

6.1 Measurement and sensor characteristics

Generally speaking, instrument characteristics can be divided into two categories, static and dynamic ones. The first one describes the parameters of an instrument when the output has settled to a steady reading. These static characteristics have a fundamental effect on the quality of measurements. Dynamic characteristics describe the dynamic response of an instrument between the time that a measured quantity changes and the time when the instrument output attains a constant value. This section gives a short overview of the most common characteristics that apply to most instruments and have to be considered in this context (Morris 1996 [92], Wheeler & Ganji 1996 [157], Wright 1995 [159]).

A measuring system must be designed to reflect accurately the sensed measurand within the transducer. Accuracy quantifies the degree of correctness of a measurement. A highly accurate measurement will have a very small error. However, accuracy does not necessarily include validity, which represents a degree of faithful reproduction of the measurand as if the measurement system was not there. The tolerance of an instrument is closely related to the

term accuracy. It describes the maximum deviation of an instrument to its specifications given by the manufacturer. Precision describes a degree of random variations of an instrument when measuring a constant quantity. In this sense, we identify an instrument to be precise, if the spread of a large number of readings is very small. Precision is not to be intended as a synonym for accuracy. Highly precise instruments may have low accuracy due to a bias, which is usually removable by recalibration of the instrument. In this context we can frequently find the terms repeatability and reproducibility. They describe the closeness of output readings when the same input is applied repetitively over a short period of time, they are an alternative way to express the precision of an instrument. The sensitivity of measurement is a measure of the change in the instrument output, which occurs when the quantity being measured changes by a given amount. Resolution is a term that is closely related to the measurement sensitivity of an instrument. The resolution is the lower limit on the magnitude of the change in the input quantity that produces an observable change in the instrument output. Resolution is governed by the granularity of the output scale, i.e. how finely its output scale is divided into subdivisions (Wheeler & Ganji 1996 [157]). Beside the first type of sensitivity there exists a second type of sensitivity, the sensitivity to disturbance that usually occurs due to environmental changes that affect an instrument in two main ways, the zero drift and the sensitivity drift. The latter defines the amount by which the measuring sensitivity varies as ambient conditions change. The zero drift is the effect where the zero reading of an instrument drifts by a change in ambient conditions, resulting e.g. in an erroneous offset of the measurement from the measurand. The term bias describes a constant error over the full range of measurement of an instrument and is usually removable by recalibration. Usually, measurement devices are calibrated to behave according to the characteristics and specifications by the manufacturer. However, when using the instrument over a certain period, the behavior of the instrument can diverge from these specifications for a variety of different reasons, such as harsh environmental conditions. In this case it is necessary to recalibrate the instrument back to the given specifications. This is usually done by a second reference instrument that is assumed to meet the standard specifications. Calibration ensures that the measuring accuracy of all instruments is known over the whole measurement range, provided that the instruments are used in environmental conditions that are the same as those under which they were calibrated. For evidence it is desirable, that the output reading of an instrument is linearly proportional to the quantity being observed. The degree of non-linearity can be seen as the maximum deviation of a single measurement to the theoretical linear relation between physical phenomenon and the output of the measurement. Non-linearity is usually expressed as a percentage of full scale readings. The hysteresis is an output characteristic of an instrument, where the output paths for cyclic steadily increasing and decreasing do not coincide. It is usually caused by such effects as friction and electrical capacitance. Instruments that suffer significant hysteresis exhibit a so called dead space, which is defined as the range of different input values over which no change in the output value can be observed. A similar characteristic of an instrument is the threshold, the minimum level of an inputs magnitude before a change on the instruments output can be detected.

When measuring we want the instruments to truly state the actual value of a measurand. In any measurement system it is important to minimize errors in instrument readings to the minimum possible level and to quantify the maximum error, which may exist. The deviation of a systems output and the actual value of a system must be small enough so that the result can be used for the intended purposes. Simply stated, all errors mentioned in the previous paragraphs are defined as the difference between the measured value and the true value of the measurand (Morris 1996 [92], Wright 1995 [159]). Systematic errors describe errors in the output readings that affect consistently only on one side of the correct reading. Common sources of systematic errors are non-calibrated instruments, poor cabling and shielding practice, not considering thermal effects, etc. Sometimes even the measurement itself can be a

source of system disturbance by influencing the measured quantity. Random errors are perturbations of the measurement caused by random and unpredictable effects. Different from systematic error, random errors affect the measurement in a non constant way and therefore detection and treatment might be difficult. Errors that occur randomly can usually be eliminated by statistical methods. The examination whether an observed error is systematic or random is important to identify and isolate the source of an error and to apply the appropriate treatment. Finally, the overall behavior of a measurement system and the total measurement system error are of interest. Measurement systems often consist of several components, each of which is subject to systematic and random errors. Once the different sources of errors are identified and quantified, we can calculate the total error of the measuring system by the aggregation of the single error sources. To get a total error calculation it remains to investigate how the errors associated with each component of a measurement system combine together.

6.1.1 Electrical signal measurements

Most of today's state-of-the-art systems for monitoring and process control are based upon our most effective productivity machine - the computer. Even if these machines are offering a wide range of capabilities, most real-world signals cannot be read directly by digital computers, they are represented by analog signals distinguished by their continuum of levels, while computers recognize only digital levels. Therefore, additional equipment is required, that translates real-world signals in a format that digital computers can accept. The variety of sensors, measuring procedures and the underlying physical realities leads to the necessity for a signal modification subsystem. The sensing element has a significant physical characteristic that changes in response to changes in the measurand. The signal modification subsystem changes the output of the sensing element in some way to make it more suitable for the used indicating or recording devices. These three subsystems are quite obvious in most measuring and monitoring systems. (Santa & Bergmeister 2000 [119])

The most common way of implementing engineering measurement and monitoring applications is based on sensing and data acquisition devices that use electrical signals to transmit information between the components. The electrical properties of a device or one of its components are caused to change by the measurand, either directly or indirectly. This is usually achieved by changes in a resistance, capacitance, current or voltage. Even if the measurement principle of a sensor is not an electrical one, the measurand value is usually mapped to and accessible by a standard electrical interface. In this case we speak of a signal conditioning unit that prepares the measuring output for further use. Many transducers are based on a two stage architecture. In one stage, the measurand causes a physical but not necessarily electrical change in a sensor. The second stage then converts that physical change into an electrical signal. In this context we could define the first stage device as the sensor, while the whole system could be defined as a transmitter. But signal conditioning does not only mean the conversion of a non-electrical signal into an electrical one, there are many possible functions for the signal conditioning stage (Wheeler & Ganji 1996 [157]).

6.1.2 Signal conditioning

Transducer outputs must often be conditioned to provide a signal suitable for the following data acquisition hardware. Amplification is the most common type of conditioning. The amplitude of analog input signals can vary over a very wide range, but most sensing elements originally deliver almost low-level outputs. On the one hand it is difficult to transmit

such signals over wires of great length, on the other hand most processing hardware is designed to work best when their inputs are in the range of ±10V or 0 to 20 mA. For the highest possible accuracy, the signal must be amplified so that the maximum voltage range of the conditioned signal equals the maximum input range of the A/D converter. Very high resolution of the latter reduces the need for high amplification and provides wide dynamic ranges. Ideally, an amplifier would have several choices of gain that is applied to the low-level signals. The amplifier units should preferably be located close to the transducers, sending only high-level signals to the A/D-converter, to minimize the effects of noise on the readings. In some cases the output of a measuring unit will provide a voltage output with an amplitude that is higher than the input range of the next component. In this case the signal must be reduced to a suitable level for further elaboration. One method of attenuating signals by analog means is to use a potentiometer connected in a voltage-dividing circuit. Nevertheless, dividing networks of this type might be affected by some potential loading problems and attenuation can be frequency dependent (Wheeler & Ganji 1996 [157]). Another issue in signal conditioning is to isolate the transducer signals from the data acquisition and elaboration hardware for safety purposes. The system that is subject to monitoring activities may contain high-voltage transients that could damage a component of the measuring system. Another important reason for needing isolation is to make sure that the readings are not affected by differences in ground potentials or common-mode voltages. Signal filtering removes unwanted noise from a signal by processing the signal so that a certain band of frequencies within the signal cannot pass. The band of frequencies removed can be at the low-frequency end of the spectrum (lowpass), at high frequency end (highpass), at both ends (bandpass), or in the middle of the frequency spectrum (bandstop). There are two common reasons for filtering. The first one is the situation in which there is parasitic noise (such as 50 Hz power-line noise) imposed on the signal. The second occurs when a data acquisition system samples the signal at discrete times. In this case, filtering is necessary to avoid the aliasing problem. Like the noise filter, the antialiasing filter is a lowpass filter. However, it has a very steep cutoff rate, so that it almost completely removes all frequency components higher than the input bandwidth of the data acquisition board. If these signals are not removed, they erroneously appear as signals within the bandwidth of the acquisition board. Although filtering is usually achieved by the use of hardware filters, they can be equally realized as software filters.

If the output of a transducer has a non-linear relationship to the measured input quantity, a process called linearization can convert this signal to a linear one by special operational amplifier configurations. Many transducers, such as thermocouples, have a nonlinear response to changes in the phenomenon being measured. To linearize the signal, the amplifier must be configured with an equal and opposite non-linear relationship between the amplifier input and output terminals.

Many transducers, such as e.g. electrical resistance strain gages, require external voltage or current excitation. Signal conditioning modules usually provide these signals. Additionally, many transducers are resistance devices in a Wheatstone bridge configuration, which often require bridge completion circuitry and well defined excitation sources.

Finally, signal conditioning includes processing techniques to manipulate signals. For instance, many monitoring and control processes use current to transmit signals rather than voltage. Hence, a voltage to current conversion is important. On the other side there exist a variety of transducers that produce frequency-modulated signals. In this case converting a frequency signal to a voltage, current, or resistance signal might be useful.

6.1.3 Wiring and noise considerations

Signals entering a data acquisition system include unwanted noise. Whether this noise is troublesome depends on the signal-to-noise ratio and the specific application. In general, it is desirable to minimize noise to achieve high accuracy. Digital signals are relatively immune to noise because of their discrete and high-level nature. In contrast, analog signals are directly influenced by relatively low-level disturbances. Unfortunately, measuring analog signals with a data acquisition circuitry is not always as simple as wiring the signal source leads to the data acquisition board. Therefore, considerations with regard to an accurate wiring, grounding, and shielding should help to reduce interference noise pick up mechanisms. Signals come in two forms: referenced and non-referenced signal sources, or in other terms, grounded and floating signal sources. Depending on the signal to be measured and the available connecting possibilities (non referenced single ended, referenced single ended, differential) offered by the data acquisition hardware, a convenient grounding and connecting solution has to be selected so that different chassis- and grounding-potentials cannot affect the measurement.

One method of reducing errors due to capacitive coupling is to use a shield. The shield blocks the interfering current and directs it to the ground. When using shielded wires, it is very important to connect only one end of the shield to ground. The connection should be made at the data acquisition system-end of the cable. Connecting both ends of the shield can generate significant errors by inducing ground-loop currents. A shield can work in three different ways: bypass capacitively coupled electric fields, absorb magnetic fields, and reflect radiated electromagnetic fields. Another approach is to use twisted pairs. These cables offer several advantages. Twisting of the wires ensures a homogeneous distribution of capacitances. Capacitances both to ground and to extraneous sources are balanced. This is effective in reducing capacitive coupling while maintaining high common-mode rejection. From the perspective of both capacitive and magnetic interferences, errors are induced equally into both wires. The result is a significant error cancellation. The use of shielded or twisted-pair wires is suggested whenever low-level signals are involved. With low impedance sensors, the largest gage-connecting wires that are practical should be used to reduce lead-wire resistance effects. On the other hand, large connecting wires that are physically near thermal sensing elements tend to carry heat away from the source, generating measurement errors. This is known as thermal shunting, and it can be very significant in some applications. There is no direct answer to the question, what the maximum allowable cable length should be. Signal source type, signal level, cable type, noise source types, noise intensity, distance between noise source and cable, noise frequency, signal frequency range and requested accuracy are just some of the variables to consider.

6.2 Instrumentation issues

Although there are a variety of sensors available in the market, they may not be readily applicable to monitoring the condition of large continuous structures. A network of distributed reliable and economical sensors is required. Accordingly, key technology issues in the sensing are as follows (Chang 1997 [26]):

- Distributed sensors: Techniques will need to be developed to distribute a large array of sensors in a network economically and effectively. This area is particular important for civil infrastructures, because these structures are typically large.
- Remote sensing: Wireless communication between local sensors and a controller is needed. As the number of sensors increases with the size of the structures, so does the number of communication wires. The management and handling of hundreds and

thousands of wires can be difficult and challenging. With remote sensing capability, data could be gathered locally, but the structures could be monitored remotely.

- Sensor reliability and integrity: The failure of sensors or actuators may result in fault signals or make the systems useless. The integrity of sensors and actuators under various loading conditions and environments for particular applications needs to be studied. The long-term behavior of sensors and actuators and the interfacial strength between the sensors/actuators and the host structures need also to be considered.

6.3 Data acquisition hardware

Data acquisition systems need to be selected based on the types and quantity of sensors. Output from the sensing elements can generally be measured using manual-read-out boxes or automated data-acquisition systems (ADAS). ADAS requires an investment in equipment and installation time but greatly facilitates data acquisition particularly where a lot of readings are required in a short time. Data reduction is also a lot easier and more timely. Manual readings are labor intensive to obtain and still require input into a computer for data reduction and analysis. (U.S. Department of Transportation 1996 [147])

In the past, automatic data loggers were the accepted form of automation. Data loggers include strip-chart recorders, printers, and tape or disk recorders. However, in an increasing number of applications, data loggers and programmable controllers could not do everything that was desired. The continually improving price/performance ratio of today's computers makes it convenient for scientists and engineers to use computer-based instrumentation technologies in monitoring and process control environments. Unlike traditional instrumentation technologies that are often inflexible and cost intensive, computers and appropriate peripheral accessories are a suitable tool for a very broad spectrum of applications. Computers manage the acquisition of data from multiple sensors with high sampling rates, save the data, manipulate and display the data, and, if required, make use of the results to perform control functions (Wheeler & Ganji 1996 [157]). Additionally, modern computer architectures support good man-machine-interaction and are highly connective and flexible with regard to extensions, while common "black box"–solutions are very often limited in functionality and interactivity. Nevertheless, additional data acquisition hardware is necessary to gap the bridge between the computer and the signals delivered by the transducers or the signal conditioning modules as mentioned in 6.1.2. In spite of the significant degree of standardization among PC and data acquisition hardware manufacturers, there exists a wide variety of products of different architecture, performance, and levels of cost (Morris 1996 [92], (Wheeler & Ganji 1996 [157]). This starts from the number of supported channels, the types of inputs and outputs, conversion accuracy, sampling rates, amplification and filtering, transmission protocols, and ends up with the degree of spatial distribution of the inputs and outputs. In this sense, the right choice of suitable peripherals depends on the requirements of the application and is one of the basic factors for a successful implementation. When selecting the architecture and the components of an automated data acquisition system, first the type of sensors and I/O signal types that should be used must be defined. This selection is strongly related to the physical phenomenon to be measured. In much the same way, the used data acquisition hardware must be designed to have the necessary channel count, input range, resolution, and sampling rate. In this section we would like to address the most decisive properties that characterize a data acquisition equipment (Santa & Bergmeister 2000 [119]).

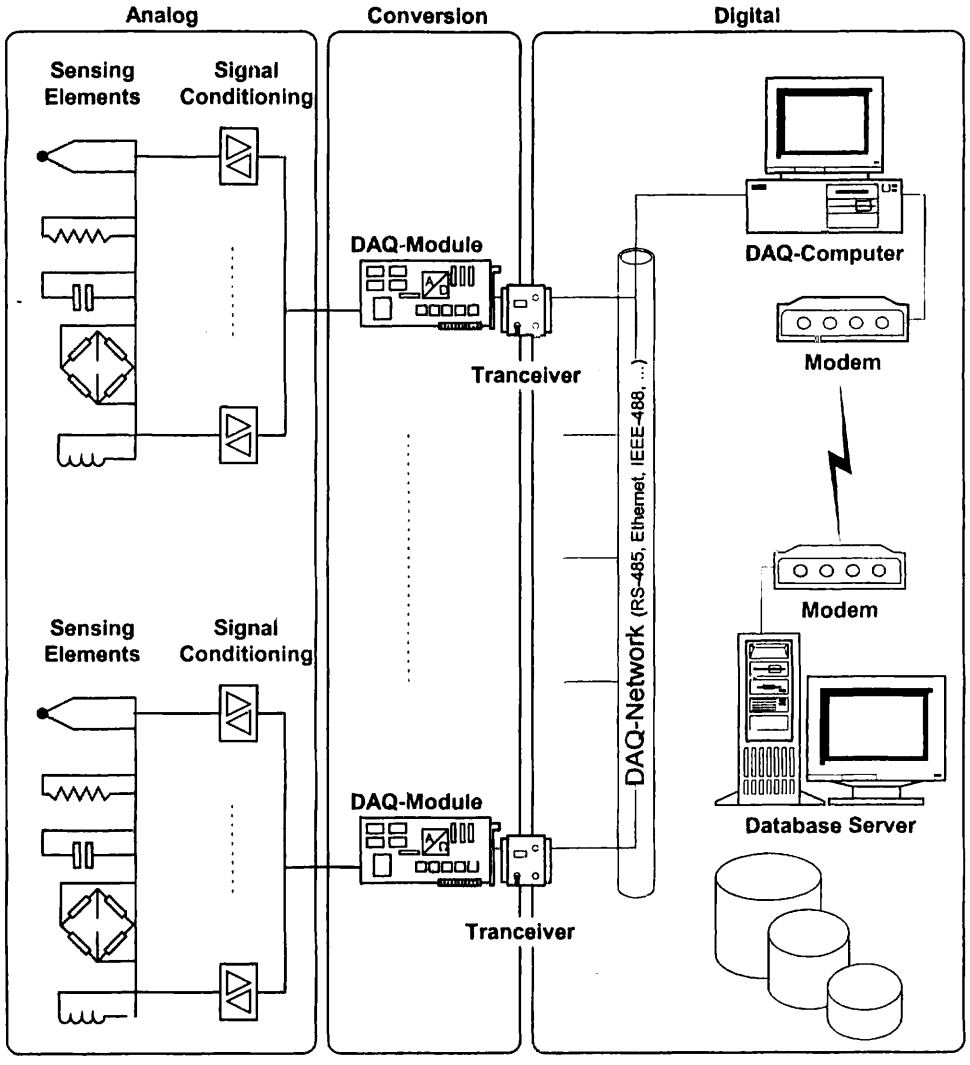

Fig. 6-1: Components of a distributed data acquisition network

The sampling rate specifies how often an A/D-conversion per channel can take place. Higher sampling rates obviously lead to more points in a given acquisition time, providing a better representation of the original signal. If the measurand is changing faster than the DAQ-System is digitizing, errors are introduced into the measured data. In fact, data that is sampled too slowly can appear to be at a completely different frequency. This distortion is referred to as aliasing. According to the Nyquist theorem the sampling rate must be at least twice the rate of maximum frequency component in the signal to measure. When using a multiplexing device, switching delays and settling times have to be considered when selecting the desired sampling frequency. A multiplexer selects and routes one channel to the A/D-converter for digitizing, then switches to another channel and repeats. Because the same converter is sampling many channels, the effective rate of each individual channel is reduced in proportion to the number of channels sampled. For measuring highly dynamic physical phenomena data acquisition boards with sampling rates beyond 1 MS/s are available as stock items. (Santa & Bergmeister 2000 [119])

The number of bits that the A/D-converter uses to represent the analog signal is the resolution. The higher the resolution of the converter, the higher the number of divisions the voltage range is broken into, and therefore, the smaller the detectable voltage changes. A typical conversion resolution of 16 bit divides the analog range into 2^{16} divisions. Closely related to this topic is term of input range, which refers to the minimum and maximum

voltage levels that the converter can span. Most DAQ-boards offer selectable ranges so that the converter is able to handle a variety of different voltage levels. (Santa & Bergmeister 2000 [119])

An important aspect of creating DAQ-based systems is high-speed data throughput coupled with simultaneous data processing. To carry out system level tasks, the processor should not be tied up with the task of transferring data into RAM. The ISA bus uses special circuitry to perform direct memory access (DMA). This feature is not available on PCI-bus based products, they can instead make use of the improved mechanism of bus mastering. (Santa & Bergmeister 2000 [119])

Due to the geometry and size of most civil infrastructures and the resulting spacing between measurement locations of interest, monitoring applications usually introduce the need to distribute the measurement functionality out into the field. It is almost difficult and inefficient to wire all signals to one central connection box located somewhere on the structure. A more suitable approach is the employment of a series of distributed DAQ-Modules that communicate via robust industrial network technology. The most obvious benefit of such systems is the saving in signal wiring. In addition, noise corruption problems that may occur when using long-distance analog signal wiring can be avoided by local A/D-conversion and the transmission of digital signals, which are quite robust against noise on the network links. The developments in industrial automation have resulted in a range of different networking technologies and open industry standards such as Ethernet, RS-232, RS-485, RS-422, IEEE-488, and a series of Fieldbus-specifications. Nevertheless, the transfer rates of the network communication may limit the available dynamic range in terms of sampling rates. (Santa & Bergmeister 2000 [119])

DAQ-hardware without software is of little use, therefore the majority of products comes with a dedicated driver software. This is a software layer located between hardware, operating system and application software. It allows comfortable access to the functionality of the hardware by programming its registers, managing its operation and its integration with the computer resources, such as processor interrupts, DMA, and memory. The driver software hides the low-level, complicated details of hardware programming while preserving high performance. However, a driver does not perform any measurement campaigns by its own, but it provides the interface to the application software where the application logic is realized.

6.4 Data acquisition and organization

After installing and wiring the sensing elements with the DAQ-hardware, the taking of the readings and their processing must be carried out in a systematic, organized way. The first issue that comes up is the scheduling of the data acquisition, a process that is strongly related to the nature of the physical phenomena and the capabilities of the acquisition system. This is usually done by defining the acquisition speed and setting the time schedule for the collection of data from each sensor. However, beside this synchronous type of data acquisition there exists another method of collecting data, the event-driven acquisition. Depending on the nature of the monitored system it can often be of interest to measure a series of quantities only when one critical measurand has gained a certain threshold value. In this context phenomena of diverse nature may be measured at different speeds with different time schedules. For the same reason a combination of various data acquisition subsystems may be used to measure these phenomena. As these subsystems can significantly differ with respect to data formats and functionality, the readings of all components have to be synchronized and integrated in a global repository for raw data. Therefore it is essential to perform a clock synchronization for all subsystems and to complete the measurements with a time stamp. An accurate structure and hierarchical organization of this repository is indispensable for the further use of the raw

data. Equally important is an intuitive nomenclature for both the channel and file descriptions. It is usually not recommended to integrate the raw data of all measurements directly into one database. On the one hand, different phenomena need different post-processing and analysis methods. On the other hand, the volume of the acquired data can usually be drastically reduced by appropriate post-processing methods without any significant loss of information (e.g. statistical methods, mean values, variation, maximum and minimum values, etc.). For the same reason it is recommended to archive raw data in a compressed format. We can, e.g., imagine, that a digital sample of a time varying signal can be analyzed in the frequency domain to obtain some modal data. The description of these modal parameters requires disproportional less space than archiving the whole sample of data in the time domain. Once a certain revision of data has been performed, it makes sense to integrate this reduced stock of data in one or more central databases with a uniform and well specified data format. The technical basis for this data organization are relational database concepts. This leads us to the next requisition.

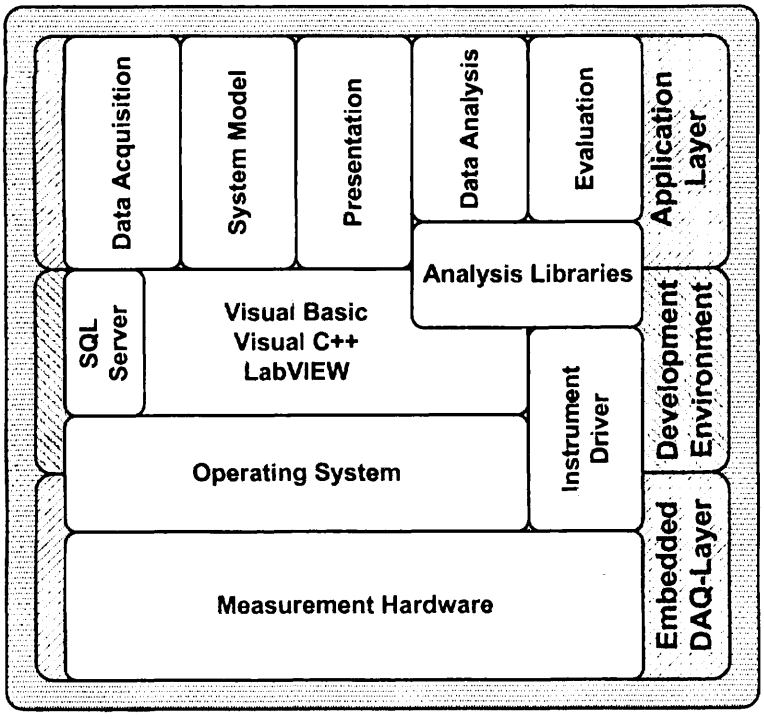

Fig. 6-2: Software engineering layers

The monitored data usually is of interest for a series of different addressees each of them requiring dedicated means of representation and different levels of detail. Depending on how critical the yielded data proves to be for the operational system, the outcome of the data evaluation may address different recipients, following e.g. a hierarchical flow chart classified by the hazardousness, urgency, responsibility, and other criteria. This situation demands different means of data representation and user interfaces. Client-Server database systems like Microsoft SQL Server or Oracle offer the advantage of central data administration by preventing inconsistency and redundancy of the archived data. Different client applications can communicate with the relational database over the network by being offered different rights of access, views and manipulation features. Beside the access to the data from different machines in the Intranet, it might be of interest to have an additional interface for the monitored data on the Internet. Web technologies with graphical browsers and high multimedia capabilities have become more and more powerful recently. The technical basis for such an implementation is currently the Microsoft Information Server, Active Server Page

technology and ActiveX Data Objects. In this context a variety of data presentation techniques may be implemented, starting form simple data tables, enhanced reports, and ending up with sophisticated animations.

Beside this type of networking and remote data access, it is usually important to have also remote access to the computer that actually performs the data acquisition. Civil infrastructures are usually difficult to access and not located in the immediate neighborhood of the supervising engineers. Therefore the DAQ-computer should be controllable remotely and has therefore to be approachable via wireless or traditional line access. A prerequisite is therefore the presence of a modem and a network protocol for controlling the data acquisition and for the file transfer. There exist several products on the market which provide the functionality for this tasks, starting from classical FTP and ending up with sophisticated programs for remote control such as pcAnywhere from Symantec, a program which provides you complete control of the remote machine as if you were on site.

Moreover a PC-based implementation offers the platform for the integration of further functionality beyond the narrower range for measurements of deformations, loads, and material deterioration. Considering the case of highway infrastructures, the installation of visual traffic surveillance through a network of video cameras could be one example for such extensions. Other candidates would be road weather stations for visibility measurements, detection of precipitation, fog and black ice, and an according control of variable message and traffic signs on the highway. Therefore, whenever a monitoring system is planned to match the actual requirements, it should anyhow be designed for easy expandability and wide flexibility to extensions.

7 Evaluation and statistical interpretation of data

Installation of sensing elements and data acquisition is only the start of monitoring field performance. Interpretation of data is equally important (U.S. Department of Transportation 1996 [147]). A quality network of sensors equipping the structure does not increase by itself its safety if not accompanied by a comprehensive analysis of the measurements.

The data retrieved directly from sensors contain a lot of information, most of which are unusable and irrelevant to the interest of the particular concern. Furthermore, the data can be highly corrupted by the environment and noise, resulting in difficulties in interpretation (Chang 1997 [26]). These interferences may be overcome by using signal processing techniques to filter and process sensor measurements.

The accuracy and reliability of the monitoring system strongly rely upon the accuracy and reliability of the analysis for relating the sensor measurements to the physical changes in the structures. Sensor measurements are point-wise in the continuous structures. Damage or an abnormal condition may not appear at the location where the sensor is located. Therefore, sensor information needs to be extrapolated for prediction of damage that appears at a distance away from the sensor locations. Mathematically speaking, determination of the physical condition of a structure based on sensor measurements is a nonlinear inverse problem. (Chang 1997 [26])

7.1 Statistical evaluation of data

A series of values can be described by a few characteristic numerical values, so called statistical parameters. Parameters may, alternatively, be replaced by so-called moments. The main moments of a sample are the mean and the standard deviation.

7.1.1 Modeling of uncertainties

All measurements include some random variations, often called noise. Hence there may be a substantial variability between individual measurements. In order to reduce noise, and get closer to a reliable value, multiple measurements can be combined.

Uncertainties exist in both field measurements and in the models that incorporate these data. These uncertainties in data arise in multiple ways. In the field of measurement they can emerge as random measurement error, systematic errors from imperfectly calibrated instruments, and recording and other transmission errors. There are several different methods for calculating measurement uncertainty but they are beyond the scope of this Chapter.

Statistical uncertainty arises from the lack of information due to e.g. a limited number of samples in tests (Enevoldsen 2001 [38]). The greater the number of samples that are available, the greater is the confidence in respective statements (Schneider 1997 [126]). All measurement results made on populations will have an average value and a standard deviation. The sample of experimental results can be replaced by a suitable distribution (see Fig. 7-1).

The uncertain variables related to load, resistance and modeling are modeled as stochastic variables with corresponding statistical distributions including parameters according to the specific project material and level of knowledge concerning materials, loads and mechanical modeling. (Enevoldsen 2001 [38])

(1) Resistance variables

The basic resistance variables for e.g. concrete strength or steel yield stress are often modeled as Log-normal distributed stochastic variables for which the statistical parameters (mean and standard deviation) are obtained from the project information, including information from as-built information (drawings, specifications of materials etc.) and later material testing. (Enevoldsen 2001 [38])

- *Concrete:* Compressive strength, tensile strength, modulus of elasticity, fracture energy, poison rate. Distribution type: normal, log-normal, Weibull. Parameters of influence: compaction, curing hardening, aggregate types, specimen sizes, geometrical uncertainties, and degradation of concrete
- *Reinforcement Steel, Structural Steel, Prestressing Steel:* Yield strength, ultimate strength, modulus of elasticity, R5 strain, Poisson ratio. Distribution type: normal, log-normal, Weibull. Parameters of Influence: steel type, geometries of steel, and diameter of steel bars
- *Geometrical Dimensions:* Concrete cover, effective depth, dimensions of columns, slabs and beams. Distribution Type: normal, Gumbel

(2) Load variables

Actions are as a rule stochastic processes in time, which can be represented by two stochastic variables. From the histograms derived from the observed data, two different kinds of variables are defined. The leading action is determined essentially by analyzing the relative stochastic process with respect to its extreme values. Usually these exhibit an extreme value distribution, such as a Gumbel distribution. Accompanying actions are essentially derived from the average-point-in-time values of the stochastic process. Accompanying actions in many cases exhibit a more or less symmetrical distribution with respect to the mean and are normally modeled by normal or log-normal distributions. (Schneider 1997 [126])

In general, the loads due to permanent actions are modeled by normal distributions with added contributions from model uncertainties. Variable loads are modeled by application of extreme distributions (e.g. a Gumbel distribution) obtained by a 1-year reference period (Enevoldsen 2001 [38]).

7.1.2 Estimation of standard deviation and mean

The expected value $\bar{x}$ can be estimated by the arithmetic mean, which is calculated from n observed values $x_1, \ldots x_n$

$$\bar{x} = \frac{1}{n}\sum_{i=1}^{n} x_i$$

The standard deviation is calculated from the differences of individual results from the average. The standard deviation s is estimated by

$$s = \frac{1}{n-1}\sum_{i=1}^{n} (x_i - \bar{x})^2$$

In the case that $\bar{x}$ is known, s is estimated unbiasedly by

$$s_x = \frac{1}{n}\sum_{i=1}^{n}(x_i - \bar{x})^2$$

7.1.3 Determination of characteristic values

The characteristic resistance x_k is calculated by

$$x_k = \bar{x} - ks$$

whereby

$$k = \frac{1.282}{\sqrt{n}} + 1.645$$

if the standard deviation is known.

In case that the standard deviation is not known, k can be calculated according to Owen for a desired confidence level 1-α.

Number of tests	k
2	13.090
3	5.311
4	3.957
5	3.401
10	2.568
50	1.965
∞	1.645

Table 7-1: k-factors for the 5% quantile and a confidence level of 90% (Owen)

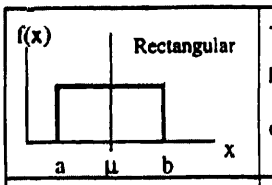	$-\infty < a < b < +\infty$ $\mu = \frac{a+b}{2}$ $\sigma = \frac{b-a}{\sqrt{12}}$	$a \le x \le b$ $f(x) = \frac{1}{b-a}$ $F(x) = \frac{x-a}{b-a}$	
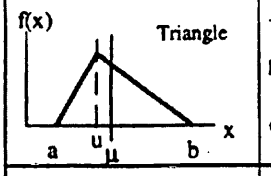	$-\infty < a < b < +\infty$ $\mu = \frac{1}{3}(a+b+u)$ $\sigma = \sqrt{\frac{1}{18}\left(a^2+b^2+u^2-ab-au-bu\right)}$	$a \le x \le u$ $f(x) = \frac{2}{b-a}\left(\frac{x-a}{u-a}\right)$ $F(x) = \frac{x^2-2ax+a^2}{(b-a)(u-a)}$	$u \le x \le b$ $f(x) = \frac{2}{b-a}\left(\frac{b-x}{b-u}\right)$ $F(x) = 1-\frac{x^2-2bx+b^2}{(b-a)(b-u)}$
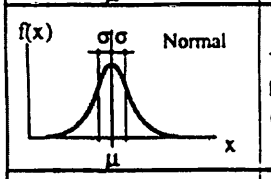	$-\infty < \mu < +\infty \qquad \sigma > 0$ μ σ	$f(x) = \frac{1}{\sigma\sqrt{2\pi}}\exp\left(-\frac{1}{2}\left(\frac{x-\mu}{\sigma}\right)^2\right)$ $F(x) = \frac{1}{\sigma\sqrt{2\pi}}\int_{-\infty}^{x}\exp\left(-\frac{1}{2}\left(\frac{x-\mu}{\sigma}\right)^2\right)dx$	
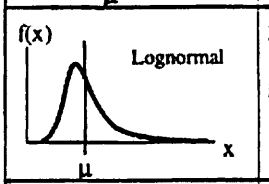	λ, ζ $\mu = \exp\left(\lambda + \frac{\zeta^2}{2}\right)$ $\sigma = \mu\sqrt{\exp(\zeta^2)-1}$	$f(x) = \frac{1}{\zeta x\sqrt{2\pi}}\exp\left(-\frac{1}{2}\left(\frac{\ln x-\lambda}{\zeta}\right)^2\right)$ $F(x) = \int_0^x \frac{1}{\zeta x\sqrt{2\pi}}\exp\left(-\frac{1}{2}\left(\frac{\ln x-\lambda}{\zeta}\right)^2\right)dx$	
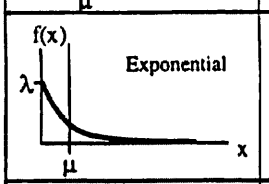	$\lambda > 0$ $\mu = \frac{1}{\lambda}$ $\sigma = \frac{1}{\lambda}$	$x \ge 0$ $f(x) = \lambda\exp(-\lambda x)$ $F(x) = 1-\exp(-\lambda x)$	
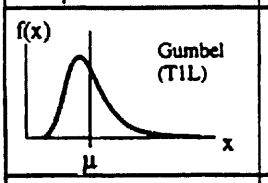	$u, \alpha \qquad \gamma \approx 0.577216$ $\mu = u + \frac{\gamma}{\alpha}$ $\sigma = \frac{\pi}{\alpha\sqrt{6}}$	$f(x) = \alpha\cdot\exp(-\alpha(x-u)-\exp(-\alpha(x-u)))$ $F(x) = \exp(-\exp(-\alpha(x-u)))$	
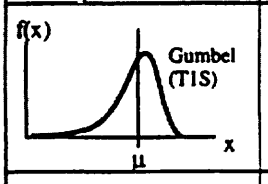	$\mu = u - \frac{\gamma}{\alpha}$ $\sigma = \frac{\pi}{\alpha\sqrt{6}}$	$f(x) = \alpha\cdot\exp(\alpha(x-u)-\exp(\alpha(x-u)))$ $F(x) = 1-\exp(-\exp(\alpha(x-u)))$	
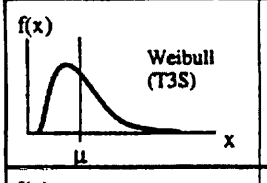	$\varepsilon \le x < +\infty \qquad k > 0$ $\mu = \varepsilon + (u-\varepsilon)\Gamma\left(1+\frac{1}{k}\right)$ $\sigma^2 = (u-\varepsilon)^2\left[\Gamma\left(1+\frac{2}{k}\right)-\Gamma^2\left(1+\frac{1}{k}\right)\right]$	$f(x) = \frac{k}{u-\varepsilon}\left(\frac{x-\varepsilon}{u-\varepsilon}\right)^{k-1}\cdot\exp\left(-\left(\frac{x-\varepsilon}{u-\varepsilon}\right)^k\right)$ $F(x) = 1-\exp\left(-\left(\frac{x-\varepsilon}{u-\varepsilon}\right)^k\right)$	
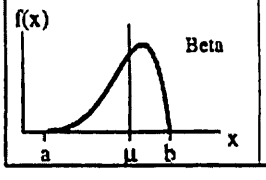	$-\infty < a < b < +\infty \qquad r, s \ge 1$ $\mu = a + (b-a)\cdot\frac{r}{r+1}$ $\sigma = \frac{b-a}{r+s}\cdot\sqrt{\frac{r\cdot s}{r+s+1}}$	$f(x) = \frac{\Gamma(r+s)}{\Gamma(r)\cdot\Gamma(s)}\cdot\frac{(x-a)^{r-1}(b-x)^{s-1}}{(b-a)^{r+s-1}}$ $F(x) = \frac{\Gamma(r+s)}{\Gamma(r)\cdot\Gamma(s)}\cdot\int_a^u\frac{(u-a)^{r-1}(b-u)^{s-1}}{(b-a)^{r+s-1}}du$	

Fig. 7-1: Frequently used distribution types (Schneider 1997 [126])

7.2 Optimization procedures

In order to solve an underdetermined system of equations optimization procedures can be used.

Available optimization procedures may be classified according to two categories. One class is based on gradients of the objective function (or the Lagrangian), the other one is based on gradient-free search strategies. In the following, representative methods are discussed with respect to the potential merits in system identification.

7.2.1 Optimization by sequential quadratic programming (NLPQL)

The mathematical background of the NLPQL-algorithm is described in detail in (Schittkowski 1981 [124,125]). The optimization aims at solving the following problem

$$f(x_1,x_2,...,x_n) \rightarrow \min$$

where the objective function $f:\mathbf{R}^N \rightarrow \mathbf{R}$ is subjected to the equality and inequality constraints

$$\begin{cases} g_k(x_1,x_2,...,x_N) = 0 & k = 1,m_e \\ h_l(x_1,x_2,...,x_N) \geq 0 & k = 1,m_e \end{cases}$$

The range of each of the variables $x_1, x_2,...,x_N$ is limited by upper and lower bounds. The algorithm solves the optimization problem by a sequential quadratic approximation of both the objective function and the augmented Lagrangian. The quadratic subproblems are solved exactly. The Hessian of the Lagrangian is updated from the gradients during the iteration process. The gradients themselves have to be provided by the user. If available on closed form (e.g. by analytical differentiation of the Lagrangian) the method is extremely effective. However, in the context of finite-element based system identification the gradients are usually evaluated by numerical differentiation. The handling of constraints can be controlled by an active set-strategy.

The solution obtained by gradient-based search methods satisfies local optimality criteria. For situations in which multiple local optima exist, this may be unsatisfactory. Restarting the procedure with different (e.g. randomly chosen) starting values can improve the chances of locating the global optimum.

7.2.1.1 Application and discussion

The following example shows an application of the NLPQL algorithm to a problem with a large number of local optima.

$$f(x,y) = x\sin(2\pi x) + y\sin(5\pi y) \tag{7-1}$$

The maximum f(x,y) is to be located within the boundaries:

for $8.0 \leq x \leq 12.1 \wedge 2.1 \leq y \leq 5.8$.

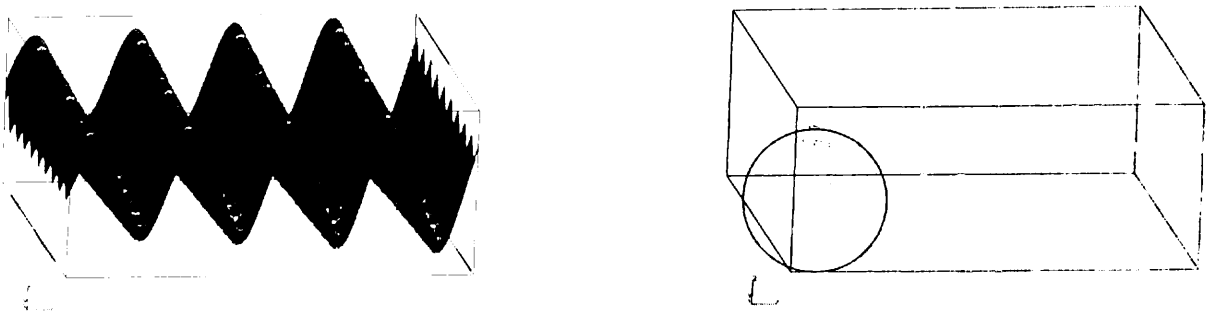

Fig. 7-2: Quality function and the optimization path

Fig. 7-2 shows the objective function and the search path of the NLPQL-algorithm. Within a small number of steps, a local optimum is found. However, it is virtually impossible to reach the global optimum. Hence the need for a procedure, which can "leave" local optima during the iteration becomes apparent.

7.2.2 Evolution strategy and genetic algorithms

Evolution strategy and genetic algorithms are both search procedures that use the mechanics of natural selection and natural genetics. The algorithm design can start from an existing measurement database or from randomly generated potential solutions. First a population of possible solutions to a problem is developed. Next, the better solutions are recombined with each other to form some new solutions. Finally the new solutions are used to replace the poorer of the original solutions and the process is repeated. The methods used thereby are the same for both evolutionary and genetic algorithms.

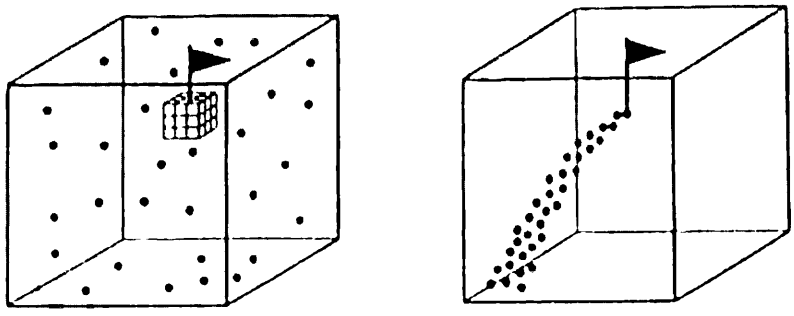

Fig. 7-3: Search procedures, Monte Carlo (left), Evolutionary Algorithm (right), (Rechenberg 1973)

To evolve towards the next "generation" of generally better solutions, the EA selects the highest performing candidates from the current generation using "survival-of-the-fittest" learning. It then exchanges some parameter values or search coordinates between candidates through an operation called "crossover" and introduces new values or coordinates through an operation called "mutation".

Evolution strategies imitate, in contrast to the genetic algorithms, the effects of genetic procedures on the phenotype. Both techniques make use of past trial information for global optimality in a similarly "intelligent" manner to a human designer.

7.2.3 Genetic algorithms

The class of Genetic Algorithms (GA) represents a first order strategy and is suitable for obtaining the global optimum in a high dimensional non convex objective function space. The search strategy is based on stochastics and objective-oriented elements, which are loosely based on concepts of evolution in biology. It appears to be quite well suited for identification tasks. The GAs have the following advantages in contrast to conventional gradient-based optimization procedures:

- A higher degree of independence from the starting point. This is a consequence of the population approach combined with stochastic components.
- It is not necessary, that the objective function is continuously differentiable, since gradients are not required.

The GAs have the following disadvantages:

- A proof of convergence to the global optimum is not available.
- The computational effort is considerably higher This disadvantage can reduced by suitable computational implementation (parallelization) of the optimization problem.

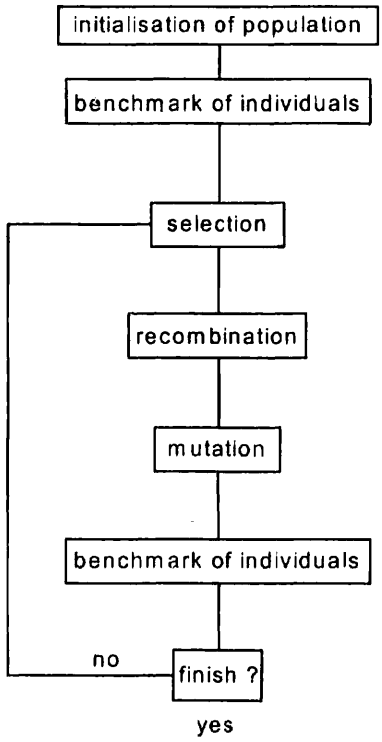

Fig. 7-4: Flow chart of the genetic algorithm

(1) Presentation of solution

The chromosomes can be coded in two different ways: either as binary vectors (Genetic Algorithm) or as real vectors (Evolutionary Algorithm). Binary values take only two values, so of course it is not possible to represent a real valued search variable by one bit. In dependence of number range and needed precision of variable several bits are necessary.

for instance: number of range: 0..5; precision: 0.01; possible values: 5/0.01 = 500; needed bits:

$2^8 = 256 < 500 < 2^9 = 512 \Rightarrow 9$ bits

The sum of all bits, which represent one search variables, is called "Gen". The sum of all genes collected in a binary vector is called "chromosome". The binary code has disadvantages if in high dimensional problems real variables are coded in high precision. This leads to very long binary vectors combined with large search spaces. By application of the real coding it is possible to avoid the mentioned disadvantages. The search variables (gene) are saved as real numbers and subsequently are collected in vectors (chromosomes). The disadvantage from this coding is that the classical evolutionary procedure of crossover cannot be performed.

(2) Initialization

In this phase a starting population P(t = 0) of *n* individuals is stochastically generated based on uniform probability within the given bounds. This ensures that the search for the optimum begins from different points in the search space. In the binary coding the values get zero or one, in the real coding the variables get a value between the upper or lower bound of the predefined variable range.

(3) Fitness

The evaluation and interpretation of the objective function value (and the constraint conditions) provides a measure for the "fitness value". By means of the fitness value the selection probability p_s for the recombination is calculated.

(4) Selection

For the recombination *n* individuals are chosen from the current population. Two different kinds of selection can be used: stochastic and deterministic selection. The possibility of choosing a single individual more than once is given by the random selection. The selection probability p_s is dependent from the fitness value of an individual and from an additional selection pressure. The deterministic selection is strictly based on the rank of an individual within the population.

(5) Recombination (Crossover)

Crossover presents an important operator with the aim to generate descendants based on proved individuals from the last generation. Generally two steps are performed. At first individuals chosen for the recombination are mixed and then two by two individuals are chosen as parents. In the second step the parents' chromosomes are recombined according to different crossover schemes (Single-, Point-, Multipoint-, Shuffle-Crossover).

(6) Mutation

The main task consists therein to find a new region of the search space and to avoid the convergence to a suboptimum. Generally the selection of individuals leads to a homogenous population, in other words the variety of genes is reduced. Hence the procedure of crossover has no influences on the population. For the mutation a mutation rate is used, mostly by 3-5%.

- Binary Coding: Each bit is mutated and subsequently inverted with probability 0.5.
- Real Coding: Each gene is mutated according to a uniform distribution.

(7) Substitutions

In general the population size is kept constant. Therefore it is necessary to decide which individuals should survive or be substituted for the next generation. There are different kinds of substitutions scheme (substitutions of complete generation, elitism, slight elitism, cancellation of n worst individuals, cancellation of n stochastically chosen individuals, etc.).

(8) Boundary Conditions

In all practical optimization problems boundary conditions have to be considered, such as bounds for the search variables or equality and inequality restraints. It is therefore necessary to provide a concept for the treatment of invalid solutions in bounded search spaces. One direct method is to reprobate all invalid solutions with the disadvantage of increased computation time. An alternative concept is the implementation of so-called "reparation functions" or "penalty functions".

(9) Application and Discussion

For the function eq. (7-1) the maximum $f(x,y)$ is searched using genetic algorithms within the bounds: for $8.0 \leq x \leq 12.1 \wedge 2.1 \leq y \leq 5.8$. The maximum value is found in the upper corner. It is noticed that the GA can easily locate the global optimum, quite in contrast to the NLPQL-algorithm.

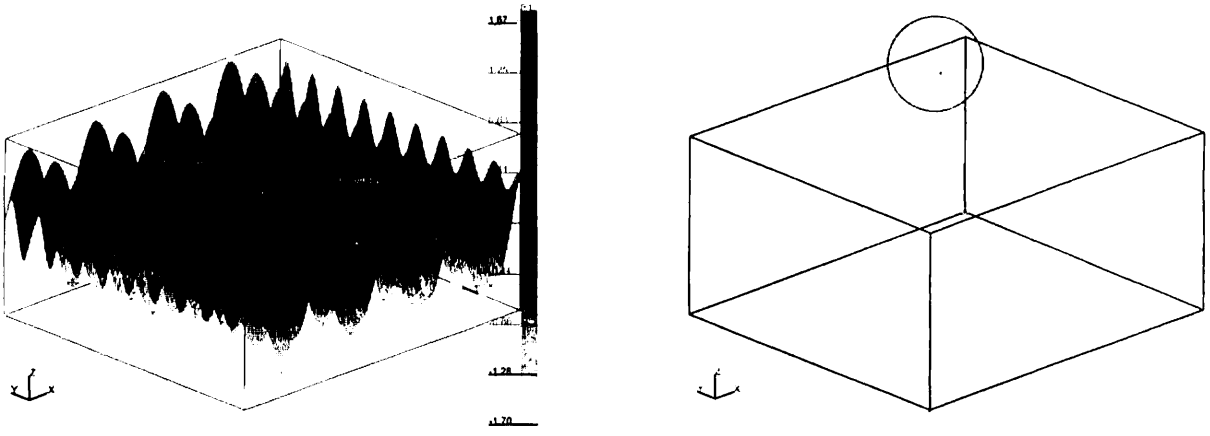

Fig. 7-5: Quality function and location of optimum

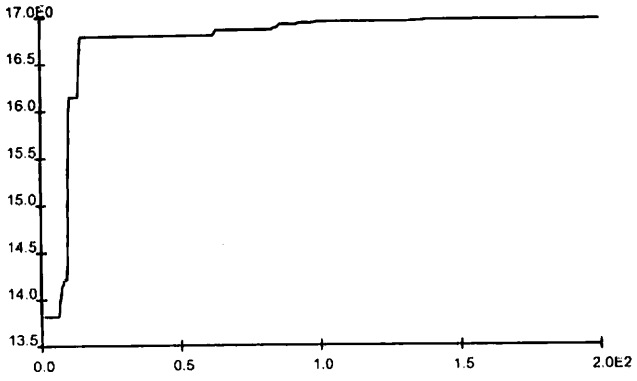

Fig. 7-6: History of best fitness during the optimization process

7.2.4 Monte Carlo method

The Monte Carlo method provides approximate solutions to a variety of mathematical problems by performing statistical sampling experiments on a computer. The method applies to problems with no probabilistic content as well as to those with inherent probabilistic structure. Among all numerical methods that rely on N-point evaluations in M-dimensional space to produce an approximate solution, the Monte Carlo method has absolute error of estimate that decreases as N superscript -1/2 whereas, in the absence of exploitable special structure all others have errors that decrease as N superscript -1/M at best.

With the Monte-Carlo method the approximate calculation of the probability density and of the parameters of an arbitrary limit state function is replaced by statistically analyzing a large number of individual evaluation of the function using random realizations x_{ik} of the underlying distributions X_i. The index k stands for the k-th simulation (k=1,2...z) of a set of x_i. Each set of the k realizations gives a value (Schneider 1997 [126]):

$$g_k = G(x_{1k}, x_{2k}, \ldots x_{ik}, \ldots x_{nk})$$

The heart of the method is a random number generator that produces random numbers a_{ik} between 0 and 1. Such a number is interpreted as a value of the cumulative distribution function $F_{Xi}(x_i)$ and delivers the associated realization x_{ik} of the variable X_i (Schneider 1997 [126]).

The number of all realizations for which $g_k < 0$, is counted. Thereby p_f can be calculated according to the frequency definition of probability as, (Schneider 1997 [126]):

$$p_f = \frac{z_0}{z}$$

where z is the total number of all realizations of G.

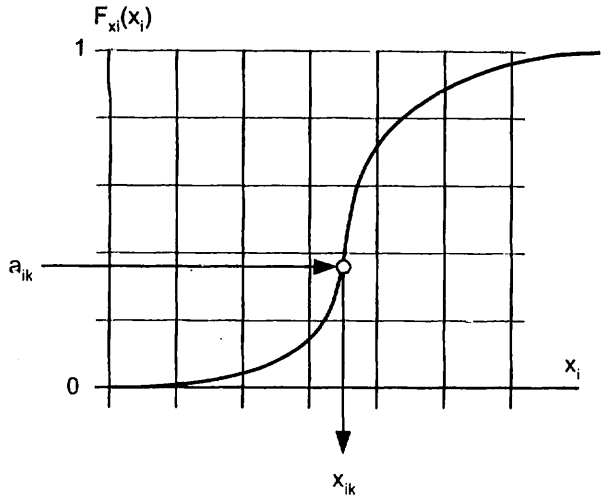

Fig. 7-7: Monte Carlo technique, (Schneider 1997 [126])

In addition to counting z_0 and z, g_k could be analyzed statistically, by determining the mean value m_G and the standard deviation s_G and, if of interest, higher moments too. From these two values the safety index β can be determined, and from it an estimated value for the probability of failure p_f, (Schneider 1997 [126]):

$$\beta \approx \frac{m_G}{s_G} \qquad p_f \approx \Phi(u = -\beta)$$

As can be seen, in this estimate it is assumed that the density of G is normally distributed.

In some computer programs the resulting values g_k are continuously presented in a histogram, thus giving immediately an idea of the probability density of the variable G (Schneider 1997 [126]).

In order to reduce the computational effort, a number of sampling methods have been developed, such as importance sampling, adaptive sampling and Latin Hypercube sampling.

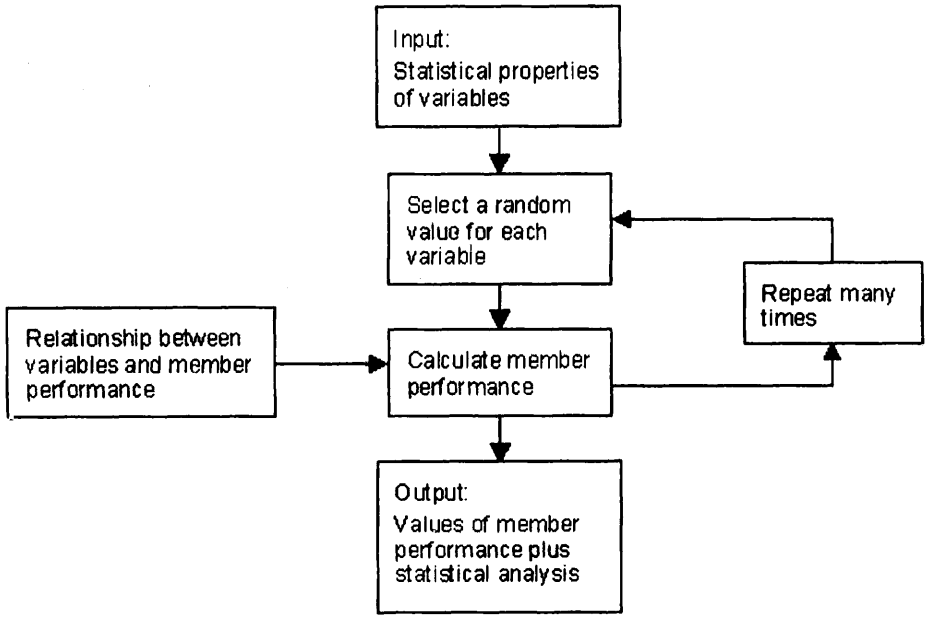

Fig. 7-8: Simulation procedure for member strength statistical properties, (Melchers 1999 [86])

7.2.4.1 Latin hypercube sampling (LHS)

The Stratified Monte Carlo simulation called Latin Hypercube Sampling is a highly recommended technique. It allows a small number of simulations under achieving of an acceptable accuracy. This technique belongs to the category of advanced simulation methods [97]. Briefly, it is a special type of Monte Carlo numerical simulation methods, which uses the stratification of the theoretical probability distribution functions of input random variables.

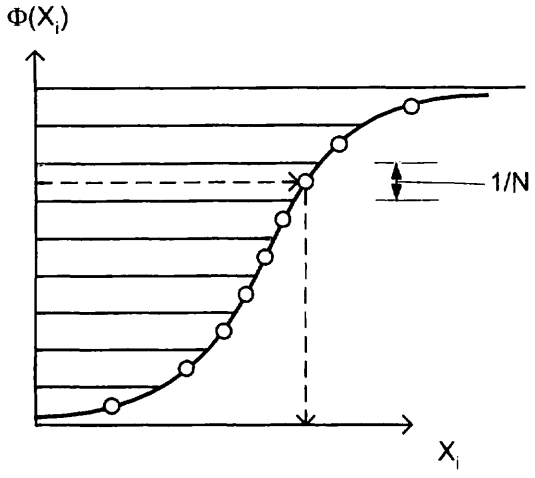

Fig. 7-9: LHS technique

The idea of LHS is quite simple: The range (0;1) of the probability distribution function of each random variable is divided into N_{sim} different non- overlapping intervals of equal probability $1/N_{sim}$. The centroids of these intervals are then usually used in a simulation process – representative values are obtained via the inverse transformation of a probability distribution function. The centroids are selected randomly based on random permutations of integers 1,2,..., j,..., N_{sim}. The basic concept of LHS is sketched in Fig. 7-9.

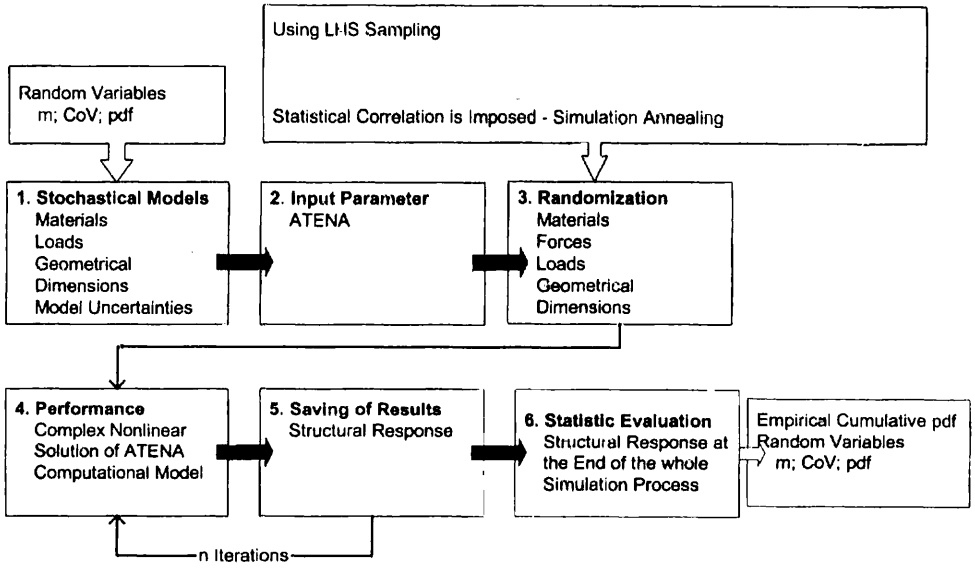

Fig. 7-10: Structure of statistical analysis software package SARA (Strauss 2002 [138])

Every interval of each variable is used only once during the simulation process. By repetitive calculations of the response function a set of response variables is obtained and evaluated by simple statistics. In case of crude MCS such a process can be quite time consuming as thousands of simulations are needed for acceptable good estimations. Using a smaller number of simulations (e.g. less than hundred); LHS results in satisfactory estimates of basic statistical parameters of response. It is valid mainly for the first and the second statistical moment, but quite good results can also be obtained for the third moment (skewness) (Strauss 2002 [138]).

7.3 Database

Concepts of probability calculation and design based on FEM need suitable basic variables. We can distinguish three types of basic variables: *Environmental variables*; like wind, snow, earthquake, temperature, etc. they are stationary, time dependent stochastic processes. *Structural variables;* structural-like dimensions, structural materials, etc. they are amenable to checking and can, if necessary, be improved by being replaced. *Utilization variables:* Live loads, traffic loads, crane loads etc. can be controlled by supervision, they are generally time-dependent stochastic processes. Sometimes it is more suitable to subdivide the basic variables in R variables and S variables.

Generally a resistance model for concrete structures m_R can be described by the basic variables of concrete strength $f_{c,ij}$, steel strength $f_{y,ij}$, the steel section area A_s and geometrical dimensions of cross sections b, h. All these characteristic numerical values obtained from experiments may be collected and stored in a material database, so that an easy selection of material models and load models (type of concrete, type of steel etc. and additionally the age of the materials) for probability based analysis is possible. The basic variables of the database are parameters of a random sample and an associated histogram and can be described by a few characteristic numerical values, such as the means, the variance (reps. the standard deviation) and the type of distribution suffice.

Within the scope of the research project SARA (see Chapter 11.3) an extensive database was created. In addition to the statistical data and material models obtained from the literature, an exhausting investigation was performed to get more detailed information about the hardening and curing terms of concrete, (recommended by JCSS 2000 [69] and Melchers 1999 [86] for example), to get more detailed information about the statistical scatter of the stress strain behavior of concrete and to get statistical information about the time-dependent behavior of concrete (Strauss 2002 [138]).

Topics of the investigations were first, the influence of the curing, the placing, the hardening conditions and the testing conditions on the compressive strength of concrete. Secondly, the description of the stress and strain scatter along the stress-strain line of concrete and finally the influence of the changes of cement and the shape of aggregates on the compressive strength of concrete (Strauss 2002 [138]).

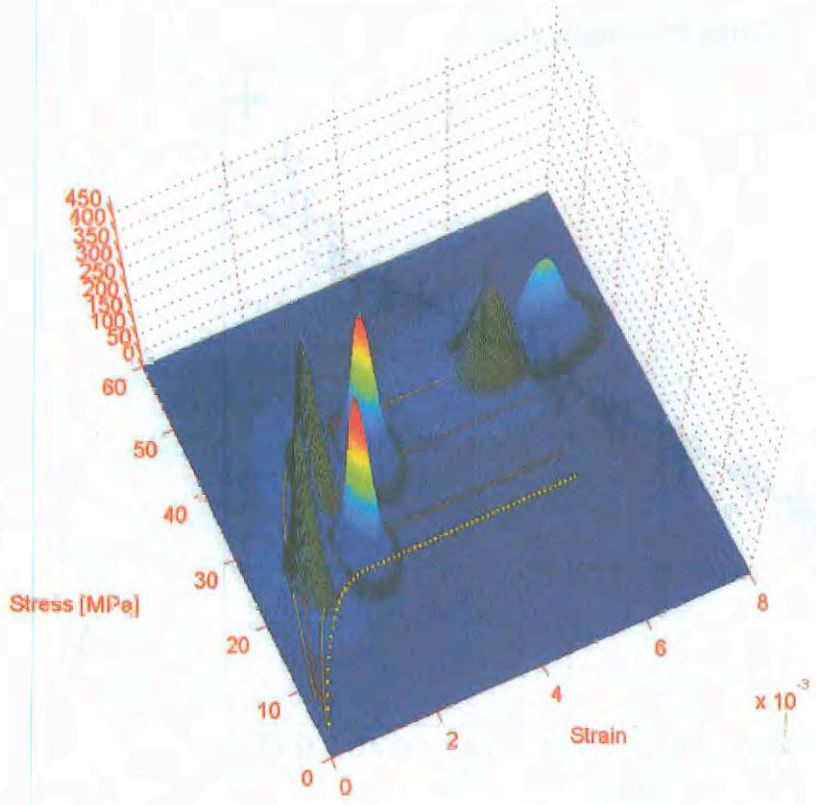

Fig. 7-11: Comparison of the compressive strength recommended by EC2 and the experimental results

For most of the data, fitting procedures, as the Kolmogorov – Smirnov – Test, are employed to get the best describing distribution type. Chosen distribution types for fitting the resistance are the Beta, the Exponential, the Log–Normal, the Gamma, the Normal and the Weibull distribution. The user interface is designed with Delphi and can be seen in Fig. 7-14. (Strauss 2002 [138]).

	Ho	P	k
Beta	0	0.910	0.168
Expo	1	0.001	0.600
Log-N	0	0.915	0.168
Gamma	0	0.800	0.300
Norm	0	0.937	0.161
Weibull	0	0.995	0.127
Kolmogorov Smirnov Test			

Table 7-2: Estimating of the statistical parameters along the stress-strain line for C25/30, (Strauss 2002 [138])

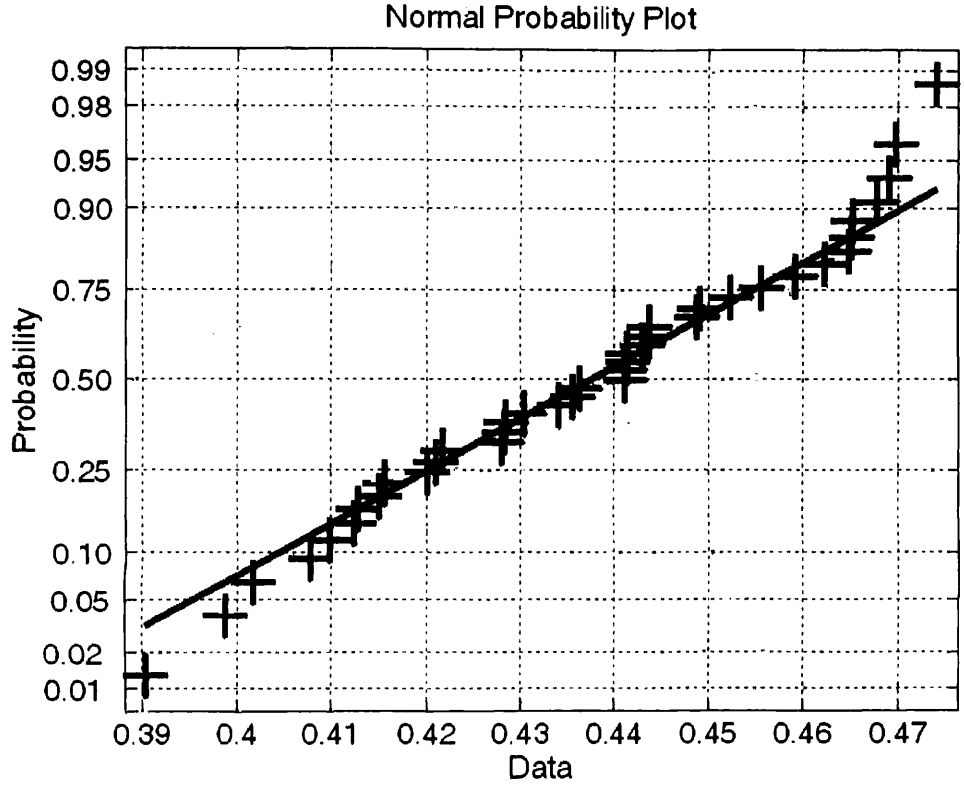

Fig. 7-12: Norm distibution plot

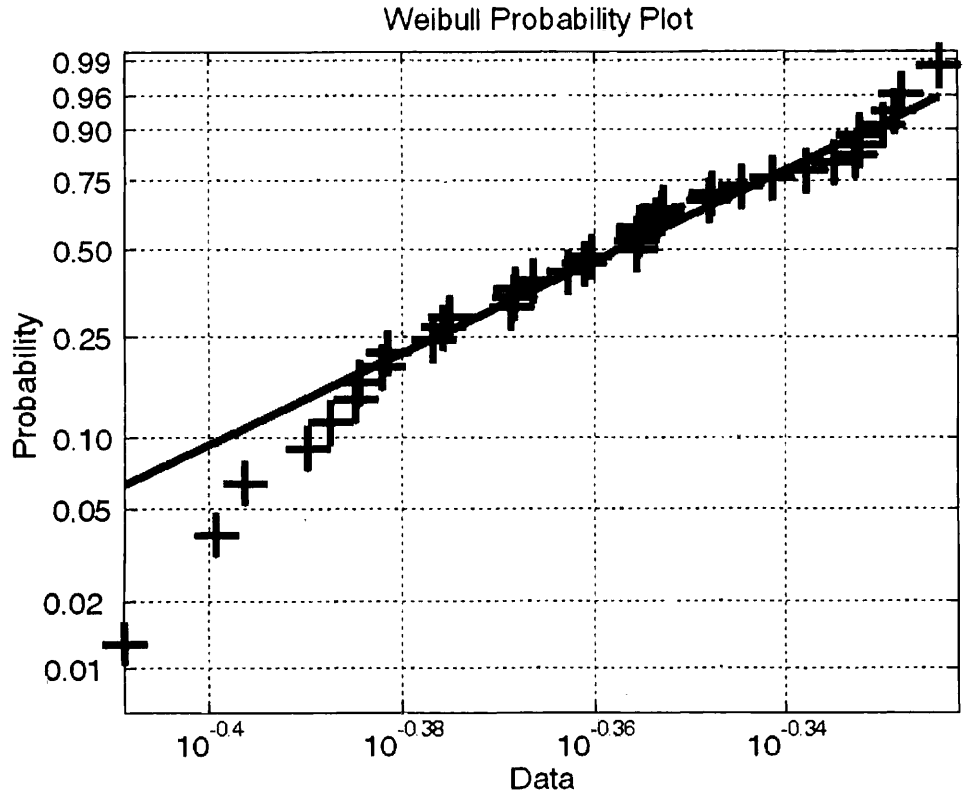

Fig. 7-13: Weibull distibution plot

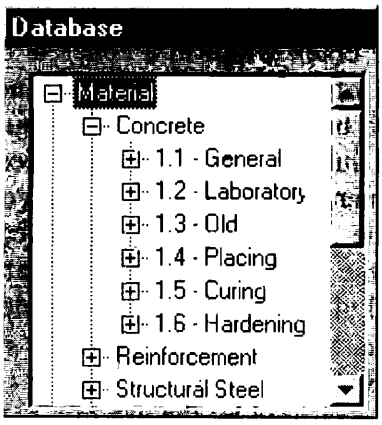

Fig. 7-14 a: Example of a database interface

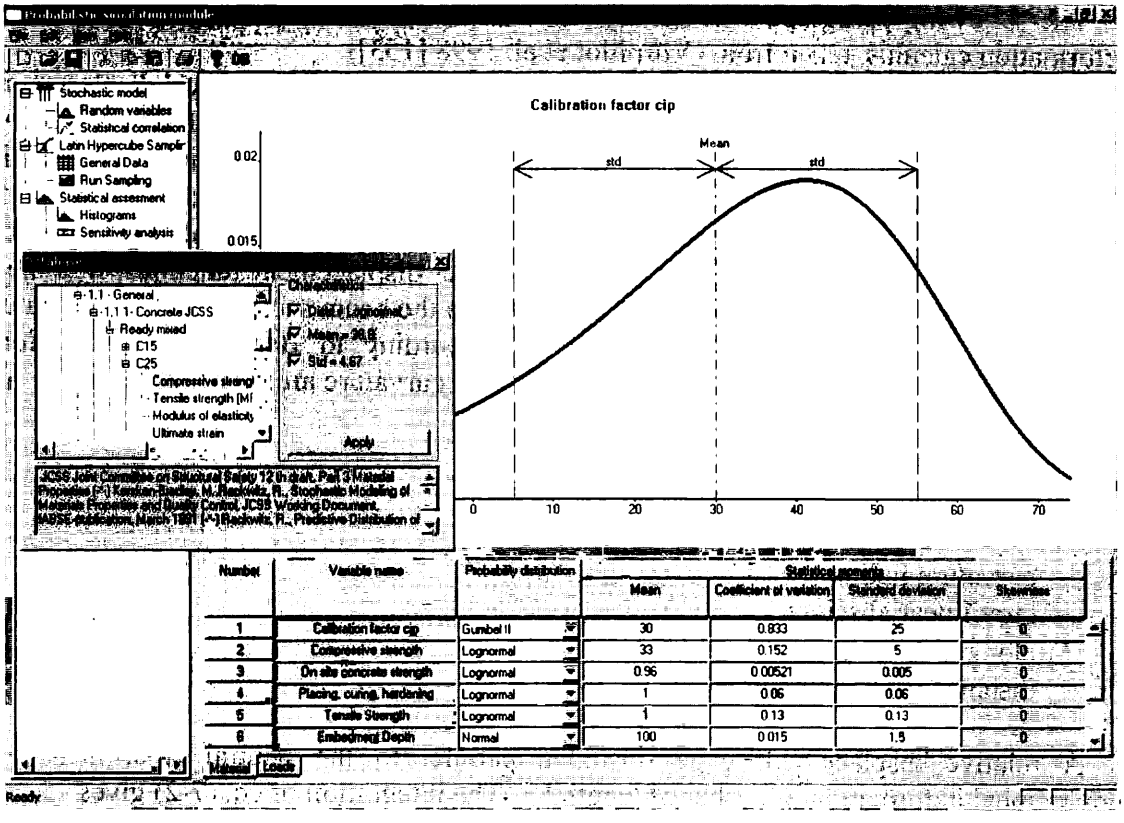

Fig. 7-14 b: Example of a database interface

7.4 Evaluation of relative deformation measurements

In a structure undergoing complex deformations, it is often necessary to install a large number of sensors to obtain useful information. This presents two major difficulties: it is first necessary to decide the number, size and position of the sensors to be installed and then to analyze the huge data flow that results from the measurements. The deformations measured by each single sensor rarely give useful information. Only an appropriate correlation between the values obtained by several sensors generates data that can be correlated to observable

quantities like the vertical displacement of a bridge or the crack width in a concrete beam. Thus it is useful to subdivide a structure into a number of macro-elements that undergo relatively simple deformations. Each section is supposed to have a constant or continuously varying inertia, a constant load across its length and the introduction of local forces and supports only at its ends. These sections can be further segmented into cells containing only a few sensors or even a single one. If the behavior of the materials in a section can be considered as homogeneous (e.g., no local cracking), the polynomial degree that best approximates its deformation is determined either analytically or using finite-element programs. If a degree N + 2 is found to approximate satisfactorily the deformation of the section, it will be subdivided into N cells. (Inaudi et al. 1998 [62])

The vertical displacement and curvature profile can be measured by the use of a network of fiber optic deformation sensors placed on the structure. In the method presented by Inaudi et Al. (1998 [62]), the structure is first subdivided into sections that undergo simple deformations and then further segmented into cells that contain only a few sensors and where the structural behavior is assumed to be linear. Information about the local and global behavior of the structure under test is obtained by combining the measurements from the sensors of each cell section and finally of the whole structure (Inaudi et al. 1998 [62]).

The following paragraph will shortly line out the fundamentals of the algorithm for the deformation calculus, taken from (Vurpillot et al. 1998 [153]).

Considering the plane section conservation law of Bernoulli, the vertical displacement of a uniformly loaded beam on *n* spans is expressed as a sequence of n fourth degree polynomial with a C_1 continuity at their border. Each polynomial $P_i^4(x)$ domain includes a section of beam, which has a constant inertia, a constant uniform load, and an introduction of end forces and moments only at its extremities. The second derivative of the vertical displacement gives n second degree polynomials. To determine the exact displacement functions, it is therefore necessary to retrieve the curvature functions $P_i^2(x)$ on the beam sections and to integrate them twice guaranteeing the border continuity C_1. According to Bernoulli's assumption, the elongational strain at any material fiber and the beam curvature are related as

$$\frac{1}{r(x)} = -\frac{\varepsilon(x)}{y} \tag{7-2}$$

r curvature radius
x curvilinear abscissa
ε elongational strain
y distance from the neutral axis

A relative displacement gage, installed parallel to the neutral axis, measures the elongational deformation of a fiber of length L1. The integration of eq. (7-2) gives

$$\int_0^{l_1} \frac{dx}{r(x)} = -\int_0^{l_1} \frac{\varepsilon(x)dx}{y} \Rightarrow \frac{1}{l_1}\int_0^{l_1} \frac{dx}{r(x)} = \frac{1}{l_1}\frac{\int_0^{l_1}\varepsilon(x)dx}{y} \Rightarrow \frac{1}{r_m} = -\frac{-(l_2 - l_1)}{y \cdot l_1} \tag{7-3}$$

where:
r_m mean radius of curvature
l_1 initial sensor fiber length
l_2 final sensor fiber length

Eq. (7-3) shows that a relative displacement gage, placed parallel to the neutral axis measures the mean curvature r_m^{-1} of the element of the beam. In the case of combined bending and axial load and temperature variations, it can be shown that a pair of relative displacement gages, placed at different distances parallel to the neutral axis are required to measure the mean curvature of a beam element.

The curvature function of each beam is a second degree polynomial of the form

$$P^2(x) = ax^2 + bx + c \tag{7-4}$$

Since the polynomial $P^2(x)$ has three unknowns, only three independent measurements are necessary to determine these three coefficients for a single beam section. With three relative displacement sensors, we obtain

$$\frac{1}{ri}: \quad mean \quad curvature \quad on \quad [x_i' : x_i''] \quad i \in \{1,2,3\}$$

where x_i' and x_i'' denote the left and right limit of sensor i. The coefficients a, b, c are solutions of the following linear system of equations:

$$\frac{\int_{x_i'}^{x_i''} (ax^2 + bx + c)dx}{x_i'' - x_i'} = \frac{1}{r_i}, i \in \{1,2,3\}$$

Eq. (7-4) gives the curvature function of the adjacent beam sections. We retrieve the displacement functions by integrating them twice. Furthermore, the C_1 continuity of the displacement functions must be guaranteed at the borders. The displacement functions are expressed as

$$P_i^4(x) = \iint P_i^2(x)dx' + \alpha_i x + \beta_i \qquad i \in \{1,2,...,n\}$$

Where the constants of integration α_i and β_i are obtained by enforcing the following continuity conditions for displacement and slope of adjacent beam sections and zero displacement boundary conditions at both ends of the beam: There are two unknowns for the displacement field of each of the n beam sections. The above continuity and boundary conditions give $2n$ equations from which the $([n-1]+[n-1])+2 = 2n$ unknowns can be obtained.

$$P_i^4(X = L_i) = P_{i+1}^4(X = 0)\Big|_{i \in [1;n-1]}$$

$$P_i^{4\prime}(X = L_i) = P_{i+1}^{4\prime}(X = 0)\Big|_{i \in [1;n-1]}$$

$$P_1^4(X = 0) = 0$$

$$P_i^4(X = L_n) = 0$$

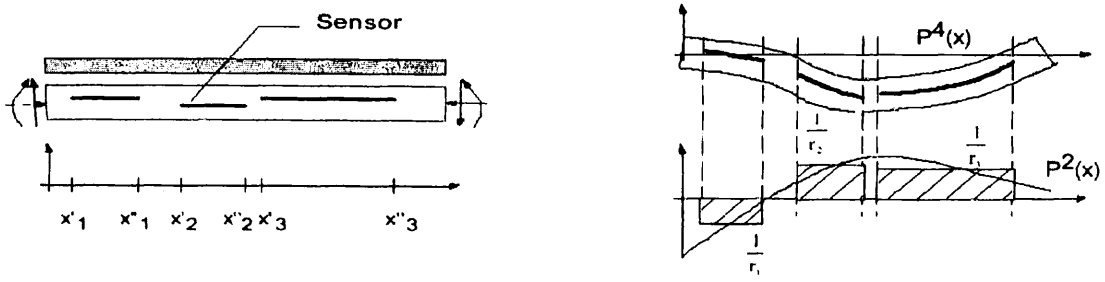

Fig. 7-15: Strain, curvature and deflection for a beam section

The above general hypotheses follow Bernoulli-Navier beam theory and require the knowledge of the boundary conditions of the whole beam. The Bernoulli hypothesis is usually satisfied under serviceability condition, while the boundary conditions are known in general. Engineers are interested in the beam's internal forces. These forces are induced only by the relative displacements of the beam with respect to its chord. This means that the above methodology is able to extract the deformation of the beam but not its rigid-body displacements in space. To obtain information about these displacements, internal sensors are obviously useless and other measurements relative to fixed external points obtained using absolute sensors should be carried out. (Vurpillot et al. 1998 [153])

7.5 Evaluation and interpretation of vibration measurements

7.5.1 Overview

System identification including model updating and damage detection presents a key topic in monitoring of mechanical systems. In order to perform this task many algorithms for interpretation of vibration data were developed in recent decades.

Most methods work either in the time- or frequency domain. The disadvantages of the frequency domain methods (problems with frequency solution, leakage effects and closely spaced modes) have led to a more intensive development of time domain methods. However time domain methods are more sensitive against influences of measurement noise. They cannot estimate residual effects of modes, which lie outside the frequency range of analysis. The frequency domain methods tend to provide better results when the frequency range of interest is limited and the number of modes is relatively small. Time domain methods deliver the complementary part. The best results can be obtained when a great frequency range connected with many modes exist in the data set (McGowan 1991 [84]).

Many dynamic system identification procedures are based on extracted modal parameters (indirect methods) and few procedures use vibration data directly (Natke 1992 [94]). In general a preprocessing (filtering, data decimation) seems very useful to reduce measurement noise, computation time and the order of the model (Unbehauen 1993 [145]).

The algorithms are dependent on the chosen equipment, which encloses questions about the kind of excitations (forced vibration, ambient vibration). The techniques can be divided into single-input-output (SISO), single-input-multi-output (SIMO), multi-input-multi-output (MIMO) methods. An excellent overview of different techniques is given in (McGowan 1991 [84]). The tendency in recent years is going from single (multi) input-output methods to multi output-only data sets with more than one reference-sensor (Peeters 2000 [105]) based on ambient vibration. Including special mathematical features like (generalized) singular value decomposition (GSVD), (SVD) more accurate results can be obtain (Lenzen 1994 [78], Huth 2002 [54]).

In the following Chapter a basic tool in the frequency domain to extract modal parameters is presented.

7.5.2 The complex transfer function

The theory of the complex transfer function is described in detail e.g. in (Clough 1993 [31], (Unbehauen 1993 [145]). There exists a basic relation between the input and the output signals of a linear continuous system, which can be described by the transfer function. In addition to the jump and impulse response functions in the time domain the transfer function characterizes the system in the frequency domain.

7.5.2.1 Time domain

A linear and time invariant continuous system with an input and output signal can be described by its response to a unit impulse force F(t) =δ(t)

$$\delta(t) = \begin{cases} 0 & t \neq 0 \\ \infty & t = 0 \end{cases} \qquad \int_{-\infty}^{\infty} \delta(t) = 1$$

The response is called "impulse response function" h(t) of the system

$$y(t) = \int_{-\infty}^{\infty} F(\tau) h(t-\tau) d\tau \tag{7-5}$$

τ: start time of impulse

The following equation applies for a harmonic input signal F(t)

$$F(t) = F_0 e^{-jwt} \tag{7-6}$$

and the output signal becomes

$$y(t) = y_0 e^{-j(wt+\phi)} + e^{-\xi wt}(A \sin \omega_d t + B \cos \omega_d t) \tag{7-7}$$

ω circular frequency
ω_d damped circular frequency
A, B constants to be determined from initial conditions

Here y(t) can be physically interpreted as displacement and F(t) as applied force.

7.5.2.2 Frequency domain

To develop the complex transfer function H(ω), it is necessary to carry out the Fourier transformation of the time signals y(t) and F(t). If eq. (7-6) is Fourier transformed, we obtain

$$F(\omega) = \int_{-\infty}^{\infty} F(t)e^{-jwt}dt \tag{7-8}$$

and from eq. (7-7)

$$y(\omega) = \int_{-\infty}^{\infty}\left[\int_{-\infty}^{\infty} F(\tau)h(t-\tau)d\tau\right] \tag{7-9}$$

Under the condition of stationarity in the system the homogeneous part in eq. (7-7) vanishes. Eq. (7-9) can be described easier after transformation, which is derived in [31].

$$y(\omega) = F(\omega)\int_{-\infty}^{\infty} h(t)e^{-jwt}dt \tag{7-10}$$

In this equation, the integral is the complex transfer function, which depends on the circular frequency ω.

$$H(\omega) = \int_{-\infty}^{\infty} h(t)e^{-jwt}dt \tag{7-11}$$

Since digitized measured data is used, H(ω) is not a continuous function but a discrete function with a finite number of values resulting from the finite length of the time series N Δt. Assume that the force is applied at t = 0. Substituting $e^{jwt} = \cos\omega t + \sin\omega t$ eq. (7-8) has the following form

$$F(\omega) = \int_{t_0}^{t_n} F(t)(\cos(\omega t) + \sin(\omega t))dt \tag{7-12}$$

and eq. (7-10)

$$y(\omega) = \int_{t_0}^{t_n} y(t)(\cos(\omega t) + \sin(\omega t))dt \tag{7-13}$$

F_0 maximum amplitude of half sine impulse
τ_{imp} length of impulse

For example, if the input signal is described by a half sine impulse, eq. (7-6) is given by

$$F(t) = F_0 \sin\frac{\pi}{\tau_{imp}} t \tag{7-14}$$

and eq. (7-5) for phase I (forced damped vibration) becomes

$$y(t) = \frac{F_0}{k - m\frac{\pi^2}{\tau_{imp}^2} + c^2\frac{\pi^2}{\tau_{imp}^2}} \left[\left(k - m\frac{\pi^2}{\tau_{imp}^2} \right) \sin\frac{\pi}{\tau_{imp}} t - c\frac{\pi^2}{\tau_{imp}^2} \cos\frac{\pi}{\tau_{imp}} t \right]$$
$$+ e^{-\xi\omega t} \left(\frac{v_1 + \xi\omega y_1}{\omega_d} \sin\omega_d t + y_1 \cos\omega_d t \right)$$

k stiffness of system
c coulomb friction

In the phase II (free damped vibration) there exists only the homogenous solution

$$y(t) = e^{-\xi\omega t} \left(\frac{v_1 + \xi\omega y_1}{\omega_d} \sin\omega_d t + y_1 \cos\omega_d t \right) \tag{7-15}$$

Analogous to eq. (7-12), eq. (7-13) the eq. (7-14), eq. (7-15) can be transformed into the frequency domain. For the analysis of the complex transfer function the complex division of eq. (7-11) is carried out.

$$H(\omega) = \Re[H(\omega)] + \Im[H(\omega)] = \frac{\Re y(\omega)\Re F(\omega) + \Im y(\omega)\Im F(\omega)}{(\Re F(\omega))^2 (\Im F(\omega))^2} + j\frac{\Re y(\omega)\Im F(\omega) + \Re y(\omega)\Im F(\omega)}{(\Re F(\omega))^2 ((\Im F(\omega))^2}$$

By taking the real part $\Re[H(\omega)]$ and imaginary part $\Im[H(\omega)]$ the magnitude $M[H(\omega)]$ is calculated by

$$M[H(\omega)] = \sqrt{(\Re[H(\omega)])^2 + (\Im[H(\omega)])^2}$$

and the phase angle Θ, Chopra [28]

$$\Theta(\omega) = \tan^{-1}\frac{\Im(\omega)}{\Re(\omega)} = \tan^{-1}\left[\frac{2\xi\beta}{1-\beta^2} \right] \tag{7-16}$$

$\beta = \frac{\omega}{\omega_0}$ ratio between the circular frequency of input signal and the natural circular frequency of the system.

The first derivative of eq. (7-16) at the resonance point ($\omega = \omega_0$) is calculated as

$$\frac{d\Theta(\omega)}{d\omega} = -\frac{1}{\xi\omega}$$

from which the damping ratio ξ is obtained according to

$$\xi = \left[-\omega_0 \frac{d\Theta(\omega = \omega_0)}{d\omega} \right]^{-1}$$

If the natural frequencies of the system are well separated, then they can be located at the points where the phase angle is equal $\pm \pi/2$ and the real part $\Re[H(\omega)]$ equals zero.

8 System analysis

8.1 System modeling

In most fields of research, a good solution often depends on a good representation. The readings of the single sensors do not immediately provide useful information on the behavior and the performance of the system. Depending on the process of interest, it is usually necessary to combine and transform a series of measurements to obtain the desired output. A simple example should illustrate this problem.

If we are interested in determining the deflection of a beam, we can do this by installing different types of sensing elements. One approach could be to use a series of pairs of strain gauges installed parallel to the neutral axis of this beam. The elongational strain at any material fiber and the beam curvature are related according to the Bernoulli-Navier beam theory, the curvature function of each beam section is a second degree polynomial. The displacement functions can then be obtained by double integration of the curvature functions for each instrumented section. Another approach would be to install multiple tiltmeters on the beam. The rotation θ_i at each sensor caused by load application reveals vertical deflections by the formula $h_i = l_i \sin \theta_i$, l_i denoting the length of one instrumented segment.

As we can see from these examples, the used sensing technology strongly governs the method of modeling and analysis. Additionally, the combination of both methods could improve the measurement system (in this case the determination of the rigid body motion). Further we can see, that a reading from one single sensor is not valuable for the determination of the global behavior, accordingly we differentiate the terms of data and information. Therefore an accurate modeling of the system and its linkage to the measurements are a central issue in any monitoring system. For structural evaluation, the most accepted mode for modeling and comparing measured and calculated data is the finite element approach. According to the evaluation of the measured data, the finite element model is subsequently improved to match as best the actual situation of the monitored structure. Once the finite element model has gained a certain level of completeness and validity, it provides the basis for analytical prediction and simulation.

However, for some instrumented processes it might not always be possible to formulate a well defined analytical evaluation model. Corrosion processes on reinforced concrete structures are a complex function of different variables like moisture, chloride concentration, oxygen content of the pore solution, conductivity of the concrete cover, and many others (Zimmermann 1998 [166]). The interpretation of these parameters may be in part based on empirical experience and expert knowledge. Such systems are therefore good candidates to be modeled and evaluated by knowledge based systems and inference mechanisms. Again, the process of system modeling might underlie several steps of revision in order to improve and validate the model assumptions or to verify the effectiveness and efficiency of the monitoring system.

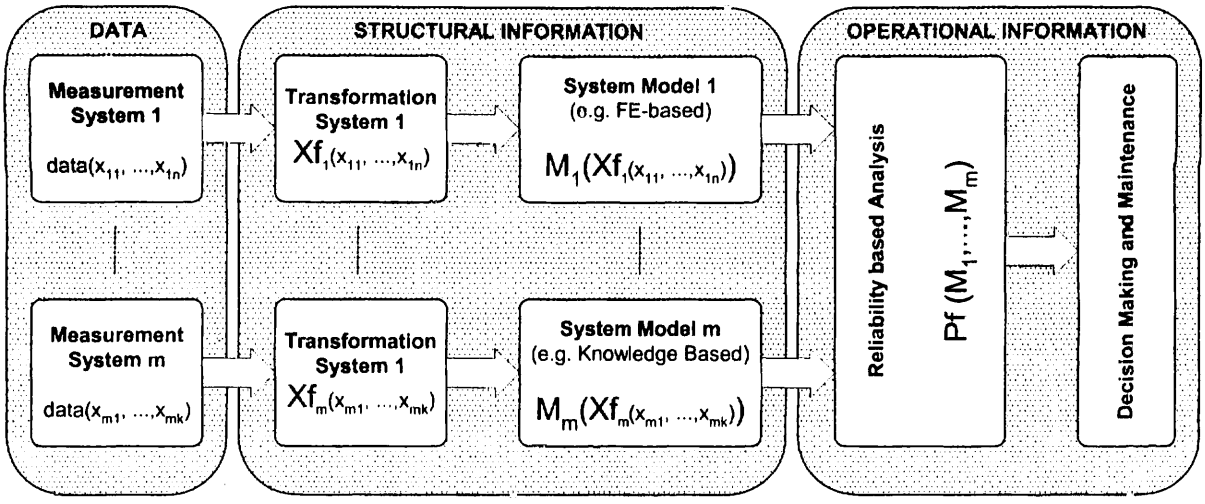

Fig. 8-1: System modeling and data evaluation

An ultimate objective of any monitoring procedure is the decision making support for the assessment and maintenance of the operational system. Probabilistic reasoning and reliability-based methodologies are very powerful approaches enhancing the treatment of the different types of randomness in the monitored processes.

8.1.1 Linear and non-linear structural analysis

The installation of sensing elements and of an automated data acquisition system to collect measured data is only the start of monitoring field performance. Interpretation of the acquired data is equally important, namely the comparison of measured and calculated data in order to validate the model assumptions or to verify the effectiveness and efficiency of the monitoring system. For this purpose a finite element model of the monitored structure based on a linear or non-linear approach might be build. Comparing measured and calculated data helps to analyze the causes of discrepancies. (Bergmeister 2000 [8])

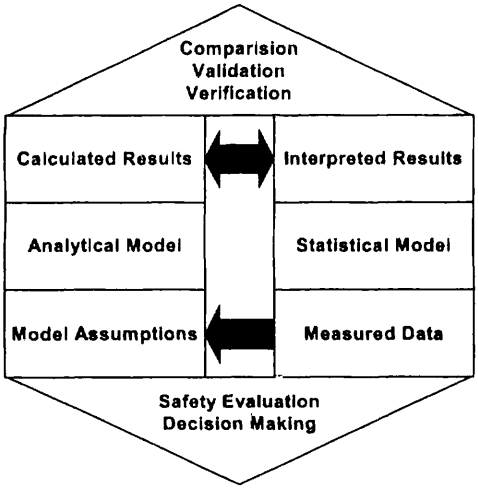

Fig. 8-2: Comparison of analytical and measured behavior

To calibrate the analytical state determination model (called mechanical model), the response of a virgin bridge structure is first traced by the filament beam element to the

ultimate load range. The initial stiffness of the service load level can be estimated by the fundamental frequency of the bridge structure obtained from vibration tests, static loading tests, and the major experimental information collected by the continuous monitoring system. The calibration of the analytical model is then adapted to the load-deflection response of the existing bridge structure. Once a calibration has gained a certain level of completeness, analytical prediction provides a quantitative knowledge and hence is a useful tool to support structural evaluation, decision making, and maintenance strategies. (Aktan et al. 1997 [2])

8.1.1.1 Non-linear analysis of concrete structures

Fracture analysis of concrete and reinforced concrete structures can be successfully applied to practical engineering problems. A constitutive model of crack propagation suitable for finite element calculation is based on fracture mechanics. Recent work in the field of fracture mechanics of concrete structures has resulted in the development of new concepts, which have found the way in design standards and tools such as computer programs.

Fracture is one of the most important features of concrete behavior with a significant non-linear effect. For its modeling the smeared crack concept has been adopted, in which the crack propagation is based on the idea of a crack band within the finite element continuum, see Bazant and Oh (1983), book of Bazant and Planas (1998), Rots (1988). The model was further enhanced by a refined definition of the crack band, Cervenka et al. (1995) and is used for example in the program SBETA (1997). The advantage of this formulation is that it can solve a problem of discontinuity due to cracks by the standard finite element method, without re-meshing. In the smeared crack model a real discrete crack is simulated by a strain localization in continuous displacement field. This localization is caused by the negative stiffness of material softening (Cervenka 1998 [24]).

The behavior of crack in concrete is idealized by the model of cohesive fictitious crack according to Hillerborg et al. (1976) where crack opening law is governed by three parameters: tensile strength f_t, G_f and the shape of the softening curve, see Fig. 8-3.

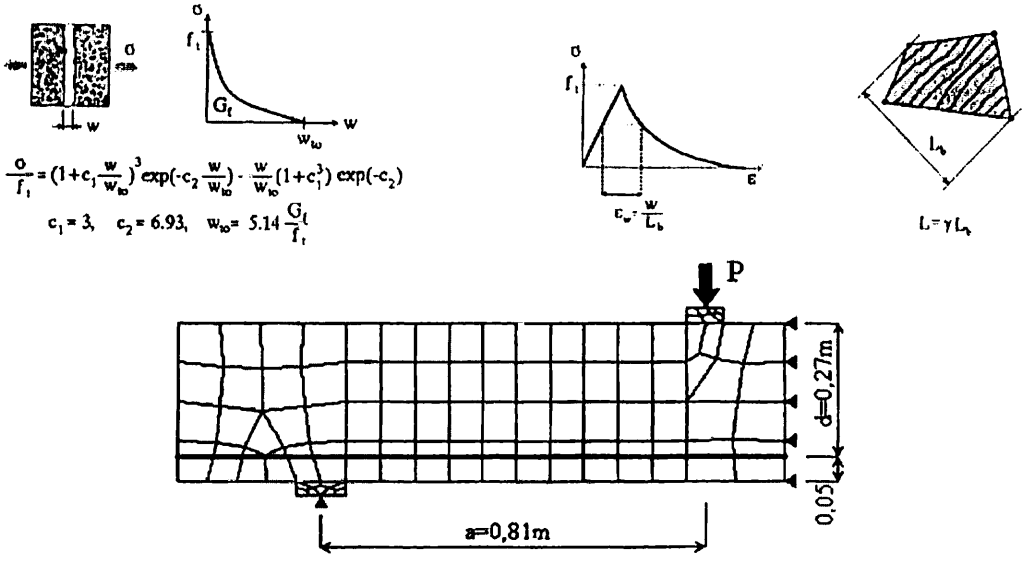

Fig. 8-3: Crack stress-crack opening law, crack stress-strain law, (Cervenka 1998 [24])

In the smeared crack model the crack width w is transformed into crack strains ε_w using the crack band size L, Fig. 8-3. This transformations assure, that the same fracture energy is used regardless the size of the finite element. Details of the crack band model can be found in

Chapter 8 of the book by Bazant and Planas (1998). A refined relation of the crack band size introduces the orientation factor γ, which is a function of the crack angle with respect to element sides and changes linearly between 1 to 1.5 (Cervenka 1998 [24]).

In a general algorithm of concrete behavior the above described model of fracture is combined with a model of compressive failure. For this purpose a damage-based model is used, Cervenka V. and Pukl (1992), in case of plane stress analysis and the plasticity-based model, Cervenka J. et al. (1998), in case of three-dimensional analysis with confinement effects. It should be realized that in many cases a compression failure is as important as a tensile failure. Both compression and tension can exhibit softening and their combination represents a significant theoretical and algorithmic problem (Cervenka 1998 [24]).

8.1.2 Structural identification

The integration of analytical modeling, followed by experiment for the calibration and verification of the analytical model for reliable simulation is termed structural identification (Aktan et al. 1998 [1], Aktan et al. 1997 [2], Aktan et al. 2000 [3]).

Structural identification serves the starting point and core of health monitoring. Applications of the structural identification principle provide the most reliable manner of characterizing a bridge for analysis and decision-making as it goes through its lifecycle. The structural identification principle therefore is what should guide bridge engineers in the determination of minimum required amount of the best possible measurements to be collected so that a structure may be accurately and completely characterized in order to reliably establish its health at the serviceability and safety limit states. (Catbas et al. [21])

Possible analytical models include: (a) smeared macro models representing only the basic behavior mechanisms, such as a single-degree-of-freedom model representing an entire bridge; (b) smeared and distorted element-level models such as a simple beam or a grillage representing the entire superstructure system; (c) element-level models where each structural element, such as a girder, diaphragm, or truss-member is represented by a corresponding analytical element and the resulting model correctly represents the 3D geometry of the entire bridge system; (d) microscopic-level finite element models representing every detail of the elements, connections, supports and boundaries of the entire bridge system or just a subassembly of the bridge; (e) a mixture of (c) and (d). (Catbas et al. [21])

There are many experimental techniques for capturing the geometry, material properties and their distribution, deterioration and damage and transforming this information to a reliable characterization of a bridge. A detailed discussion of the technologies that are available for structural identification is presented in the following Sections. (Catbas et al. [21])

The six steps that are critical in a structural identification application are (Catbas et al. [21]):

1) Collecting information, conceptualizing and a-priori modeling to best represent the knowledge about the bridge. Since our goal is to refine an initial and often incomplete and coarse representation of the structure and reach one that is capable of simulating the system's true behavior at even the local member/material level, this initial model must be adaptable. The level of detail of the model, (a) to (e) as discussed earlier will depend on the exact purpose of structural identification.
2) Experiment design based on analytical and preliminary experimental studies. Sensitivity analysis by the a-priori model is required to determine optimal excitations and responses, and to select an acceptable range of measurements. Selection of excitation and response measurements depends on the type, number, and location of sensors required to quantify the parameters used for simulating the bridge. An optimal data set or sets must be defined which consider response type, number of sensors, and

locations. Error sensitivity analyses are required to determine the acceptable level of noise for the measurements and the required confidence bounds for the structural parameter estimates. The optimization procedure based on both the experimental and analytical points of view will ensure that the data obtained from the full scale tests is valid and useful for structural identification.

3) Full-scale tests follow. Modal tests can be performed in conjunction with measurement grids of various resolutions, with various numbers and positions of reference sensors, and with impact loads and forced excitations. The results from modal tests can be used to verify global system behavior and the critical mechanisms that affect the global modes of vibration. Static or crawl tests by loaded trucks in conjunction with properly designed instrumentation provide data for more refined modeling of localized behavior. Careful in-depth visual inspection in conjunction with various localized probes and material sampling and testing permit to capture deterioration and damage.
4) Processing of the experimental data is a distinct step for error mitigation and quality assurance. A rigorous full-scale test program will produce large volumes of data sets. This data must be processed and "conditioned" for use in the parameter estimation step such that errors in the data due to measurement system errors, as well as friction or freezing in movement mechanisms, nonlinearities or a lack of stationarity (random changes with time) in the structure during the experiment are identified, accounted for and data is corrected. Measurement data that has a higher level of confidence due to the type of loading, excitation and sensing, or due to the signal/noise of the measurement, should be identified for a greater weighing.
5) Model calibration is conducted first by understanding the physical implications of the experimental data related to the load distribution and especially the movements and deformations at the interfaces of the various structural systems. The mechanical properties and the boundary and continuity conditions of the analytical model are adjusted so that the model configuration agrees with the physical insight observed during the experiment and by processing the experimental data. Otherwise, most parameter identification processes that are based on linearity, idealized boundaries, supports and release conditions cannot converge to meaningful results. Calibration is conducted by progressively adjusting the numerical values of the groups of parameters that define the material, geometry, boundary and continuity conditions until the discrepancies between the measured data and simulated behaviors of the analytical model are minimized with respect to an objective function (Ghanem & Shinozuka 1995 [148], Shinozuka & Ghanem 1995 [132], Sanayei & Saletnik 1995 [117]). The resulting "calibrated" analytical model must be tested for both completeness and uniqueness and it must be confirmed and validated. One approach is to use some data sets for calibration and others for validation.
6) Utilization of the calibrated models for decision making and management follows as the most relevant and critical step. The field-calibrated analytical model serves as the best measure of the as-is conditions of the bridge; this may be used for load-capacity rating, permit-loading, evaluating the actual levels of internal forces, stresses and deformations under operating conditions, and how any existing and/or future local deterioration or damage may impact the system-reliability and load capacity rating. The field-calibrated linear model also serves as the best possible starting point for simulations by a nonlinear finite-element analysis software package in order to predict the nonlinear behaviors and possible failure modes of the bridge in the context of failure-mode analyses. The insight gained from the modeling and experiments, and the results of analytical simulations with the field-calibrated model should provide interpretations that should be useful to practitioners and bridge owners. It is important to recognize that a field-calibrated model represents the bridge conditions and health

only in a snapshot of time, and as loading and bridge conditions change, certain experiments should be repeated to monitor the changes in at least selected "critical" properties.

The relation between structural identification and health monitoring may be therefore summarized as follows: In the case of structural serviceability and safety, health monitoring consists of a series of structural identification applications providing snapshots along the lifecycle of a bridge, these snapshots may be connected along time by continuously monitoring the critical loading effects and the corresponding bridge responses. In this manner, any event that may slowly or abruptly create a significant change in the force and deformation states and that may cause damage to the bridge is recognized in a timely manner and appropriate management decisions may be taken. (Catbas et al. [21])

8.1.2.1 Damage detection algorithms by using vibration measurements

(1) Introduction

Damage detection, localization and damage extent are tasks concerning monitoring of mechanical systems. These investigations should be performed several times during the whole lifetime of such systems. Thereby the personal and technical costs for the life time management can be reduced.

Damage detection based on interpretation of vibration data sets presents a so called nondestructive technique (NDT). This is a reason why many researchers in the last two decades have focused their efforts on this field. Damage detection represents a related part of dynamic system identification. An overview of existing techniques, their derivation and validation by experiments, is given in (Doebling 1998 [33], Friswell & Mottershead 1995 [47], Natke & Cempel 1997 [95]).

Damage detection techniques can be model- or non-model (indicator) based. In the first case a valid mathematical model must be updated using a set of vibration data measured on a real structure. In the second case only the data set is needed. This encloses the disadvantage that the information about the mechanical systems is strongly focused on one aspect of damage detection (in most cases location and extent of damage). For both cases several techniques are presented in this Chapter.

(2) Minimum rank update theory

In the paper by Zimmermann & Kaouk a lot of references to the development of localization and damage detection are given. Here emphasis is put on two aspects, i.e. location and extent of damage.

Damage detection: location

It is assumed that an n-DOF finite element model of the undamaged structure exists and the equation of motion is given as

$$M\ddot{x} + C\dot{x} + Kx = 0 \tag{8-1}$$

where M,C,K are the $n * n$ analytical mass-, damping- and stiffness matrices and x is a displacement vector of dimension n. FE-model and measured structure must be consistent,

which requires the dimension of both measured and analytical mode shapes to be equal. That is fulfilled, if either all FEM degrees of freedom are measured (in practice this is not possible), or if algorithms for expansion (Berman & Nagy 1983 [10], Smith & Beattie 1990 [134], Zimmermann & Widengren 1990 [164]) or reduction (McGowan 1991 [84], O'Callahan 1989 [98]) of dimensions of mode shapes can be used. The basic approach of Hurty-Transformation also allows for the reduction of modal measured degrees of freedom (Zheng 1996 [163]). In these cases the additional error may become significant as the ratio of measured to unmeasured degrees of freedom decreases.

It is assumed that ΔM, ΔC, ΔK are the exact perturbation matrices, which reflect the structural damage. The eigenvalue problem can now be written as

$$[\lambda_{di}{}^2(M-\Delta M)+\lambda_{di}(C-\Delta C)+(K-\Delta K)]v_{di}=0 \tag{8-2}$$

For the localization of system changes it is sufficient, if p of n ($p<<n$) eigenvalues and mode shapes are measured. The perturbation matrices on the right hand side are grouped, which defines a damage vector d_i.

$$d_i = Z_{di}v_{di} = \lambda_{di}^2(\Delta M)+\lambda_{di}(\Delta C)+(-\Delta K)v_{di} \tag{8-3}$$

where

$$Z_{di} \equiv (\lambda_{di}^2 M+\lambda_{di}C+K) \tag{8-4}$$

The inspection of d_i reveals that the j element of d_i will be zero when the j rows of the perturbation matrices are zero. The finite element model for the j degree of freedom is not directly affected by damage or on the other side the degrees of freedom, which are affected by damage, can be determined by inspecting the elements of d_i. It is noticed, that eq. (8-3) is the Modal Force Criterion as proposed by Ojalvo (1988 [101]). In specific cases, the damage vector defined by eq. (8-3) can lead to incorrect conclusions concerning the location of damage Gysin (1990 [52]). In an alternate view eq. (8-3) can be written as

$$d_i^j \equiv z_{di}^j v_{di} = \left\| z_{di}^j \right\| \left\| v_{di} \right\| \cos\theta_i^j \tag{8-5}$$

where d_i^j is the j component (j DOF) of the i damage vector, z_{di}^j is the j row of the matrix Z_{di} and θ_i^j is the angle between the vectors z_{di}^j and v_{di}. In the case when the measurements are free of error, a zero d_i^j corresponds to an θ_i^j of ninety degrees, whereas a nonzero d_i^j corresponds to an 0_i^j different than ninety degrees. It is possible to use the deviation of the angle from ninety degrees as an indicator of damage.

$$\alpha_i^j = \theta_i^j\left(\frac{180°}{\pi}\right)-90° \tag{8-6}$$

It is remarked by using eq. (8-6) that only the damaged DOF's take values substantially different from zero degrees.

Damage detection: extent

For the necessary determination of the extent of structural damage Zimmermann & Kaouk have proposed the following procedure based on the assumptions of an undamped system and negligible effect of damage on the mass properties.

The extent algorithm can be summarized succinctly in two steps. At first the matrix B is calculated by

$$MV_d\Lambda_d + KV_d = \Delta K_d V_d \equiv B \tag{8-7}$$

Second, the perturbation matrices are calculated as follows

$$\Delta K_d = B(B^T V_d)^{-1} B^T \tag{8-8}$$

$$\Delta M_d = B(B^T \Lambda_d V_d)^{-1} B^T \tag{8-9}$$

The extent algorithm defined by eq. (8-7), eq. (8-8) assumes that B is of full column rank. For the case that the experimental measurements produce not a full column rank of B it follows

$$MV_d^p \Lambda_d^p + KV_d = \Delta K_d^p V_d^p \equiv B^p \tag{8-10}$$

(3) Projected input residuals

In [99] the Projected Input Residual Method (PIRM) is presented for identification of mass-, damping- and stiffness matrices. The PIRM aim functional can be formulated in dependence of parameter a as

$$J(a) = \left\| P(a)(P^m - S_\omega(a)C^T C U^m \right\|_2^2 \tag{8-11}$$

where

S_ω the dynamic stiffness matrix, C the measurement matrix, U^m the output vector or matrix and P^m as the input vector or matrix. The following equation

$$P(a) = I_n - \left[S_\omega(a)\bar{C}^T \right]\left[S_\omega(a)\bar{C}^T \right]^+ \tag{8-12}$$

with $\bar{C}$ as to C complementary measurement matrix ensures the projection into a measured m-dimensional space. The aim functional $J(a)$ is minimized by solving a convex optimization problem. However the direct identification of parameter matrices is time consuming. Another possibility to locate the damage is the indicator (non-model-based) analysis, which can be applied by the following definition

$$\tau_{\upsilon} = \frac{\left\| v^{(\upsilon)}(1) \right\|}{\left\| v_D^{(\upsilon)}(1) \right\|} \geq 0 \quad \text{für} \quad \upsilon = 1,\ldots,n_p \tag{8-13}$$

where $v_D^{(\upsilon)}$ are the PIRM-residuals for the measurements U_D^m of the possible damaged structure. The system is excited by the same input-vector (matrix) P^m as used for the undamaged case U^m.

(4) Changes in the curvature of mode shape

In the paper by Pandey et al. (1991 [104]) the authors have proposed the changes in the curvature mode shapes for localization of system changes (here: mass or stiffness of the system). Based on the displacement DOF of the mode shapes the curvature of the i-th element can be approximated using the central difference method

$$\ddot{\upsilon}_i = \frac{(\upsilon_{i+1} - 2\upsilon_i + \upsilon_{i-1})}{h^2}$$

where h is the length of the elements or the distance between two measurement points. However the direct calculation of the curvatures from measured mode shapes results in oscillating and inaccurate values. In this context Maeck et al. (2000 [82]) have suggested a smooth procedure of the Curvatures. Therefore a weighted residual penalty-based technique is adopted.

(5) Changes of flexibility matrix

Another technique presents the changing of the flexibility matrix (Pandey et al. 1991 [104]) between the damaged and undamaged system. The calculation of the flexibility matrix is based on the mass-normalized modal matrix Φ and on the matrix of eigenvalues Λ

$$F_x = \Phi \Lambda^{-1} \Phi^T = \sum_{i=1}^{n} \frac{1}{\omega^2} \phi_i \phi_i^T$$

Each column of the flexibility matrix F_x contains the vector of node displacements (rotations) concerning a unity load on a degree of freedom.

(6) Modal assurance criterion

An important requirement is to be able to compare experimental results with corresponding results obtained for the finite element model. If a unique assignment is not possible, additional information has to be obtained from the eigenvectors. The so-called MAC-value (Modal Assurance Criterion) in eq. (8-14) (Friswell & Mottershead 1995 [47]) allows a judgment of the comparability of the modal data (Jahn 1997 [68]):

$$MAC = \frac{(\phi_X^T \cdot \phi_A)^2}{(\phi_X^T \cdot \phi_X) \cdot (\phi_A^T \cdot \phi_A)} \tag{8-14}$$

ϕ_X eigenvector of the test model
ϕ_A eigenvector of the analytical model

The value of the MAC varies between 0 and 1. A value of 1 indicates that the modes correspond exactly. As a rule the accordance of the compared vectors is acceptable, if MAC ≥ 0.8. (Jahn 1997 [68])

(7) Coordinated modal assurance criterion

The coordinated modal assurance criterion (COMAC) is closely related to the well known modal assurance criterion (MAC) (Friswell & Mottershead 1995 [47]), which gives a measure of the accordance between mode shapes of the damaged and undamaged system. With the COMAC the j-th component of mathematical model or undamaged experimental state can compared with damaged state concerning all l determined mode shapes

$$COMAC(i) = \frac{\left(\sum_{i=1}^{l} |\phi_a(i,j)\phi_x(i,j)| \right)^2}{\sum_{i=1}^{l} |\phi_a(i,j)|^2 \sum_{j=1}^{l} |\phi_x(i,j)|^2}$$

A COMAC value of 1 means that there are no differences between the mode shapes. Additional and more sensitive information for locating damage can be gained by changing the position of the excitation [69].

(8) Multiple damage location assurance criterion

In (Shi et al. 2000 [131]) the multiple damage location assurance criterion (MDLAC) is proposed, it is based on a comparison of the differences between the calculated and the measured mode shapes in respect to the sensitivity of mode shapes concerning one parameter a (for example: stiffness). These differences are collected in the vector $\Delta\phi$

$$MDLAC(k) = \frac{\left|(\Delta\phi)^T (\delta\phi(a))\right|^2}{(\Delta\phi)^T (\Delta\phi)(\delta\phi(a))^T (\delta\phi(a))}$$

The vector $(\delta\phi(a))$ corresponds to a column of the sensitivity matrix S

$$S = \begin{bmatrix} \frac{\partial\{\phi_1\}}{\partial a_1} & \frac{\partial\{\phi_1\}}{\partial a_2} & \cdots & \frac{\partial\{\phi_1\}}{\partial a_k} \\ \frac{\partial\{\phi_2\}}{\partial a_1} & \frac{\partial\{\phi_2\}}{\partial a_2} & \cdots & \frac{\partial\{\phi_2\}}{\partial a_k} \\ & \vdots & & \\ \frac{\partial\{\phi_m\}}{\partial a_1} & \frac{\partial\{\phi_m\}}{\partial a_2} & \cdots & \frac{\partial\{\phi_m\}}{\partial a_k} \end{bmatrix}$$

(9) Dynamic influence coefficients

The dynamic influence coefficients $F_{dyn,i}$ represent the inverse of the stiffness matrix. They must be determined before and after damage is introduced into a mechanical system.

By transformation of the well known equation of motion

$$M\ddot{w} + D\dot{w} + Kw = f$$

where

M the mass matrix, D the damping matrix, K stiffness matrix, f excitation forces into a state space formulation the following equation by introducing the velocity as additional variable $\dot{w} = v$ can be found

$$\begin{bmatrix} \dot{w} \\ v \end{bmatrix} = \begin{bmatrix} 0 & I \\ -M^{-1}K & -M^{-1}K \end{bmatrix} \begin{bmatrix} w \\ v \end{bmatrix} + \begin{bmatrix} 0 \\ M^{-1}f \end{bmatrix}$$

and with $z^T = [w \ \mathrm{v}]$

$$\dot{z} = Az + Bx$$
$$y = Cz$$

The input and output vectors y and x can be directly measured.

$$y(t) = \sum_{i=1}^{n} F_{dyn,i} \int_0^t e^{\lambda_i (t-\tau)} x(\tau) d\tau$$

By performing the Laplace transformation it follows

$$Y(s) = \sum_{i=1}^{n} F_{dyn,i} \frac{1}{s - \lambda_i} X(s) = R(s)X(s)$$

and the dynamic influence coefficients can be derived from

$$R(s) = \sum_{i=1}^{n} F_{dyn,i} \frac{1}{s - \lambda_i}$$

to

$$F_{dyn,i} = \lim_{s \to \lambda_i} (s - \lambda_i) R(s)$$

More detailed information concerning the closed derivation and some applications can be found in (Lenzen 1994 [78]).

8.2 Decision support for multiple mechanical models

A good model is important for finding answers to questions that arise during the life of a structure. For example, the following questions may be relevant (Robert-Nicoud et al. 2000 [113]):

- Is something wrong with the structure? (damage detection)
- What might be the most critical problem in a particular situation? (damage prediction)
- What is the state of the structure (cracks, creep, support displacement, etc.)? (serviceability problem)
- What might be the state of the structure after several years? (prediction)
- Is it better to repair now or to delay it? (management)
- What kind of new observations or measurements are necessary for making good decisions? (monitoring)
- Is the repair plan successful? (monitoring)
- What is the risk of failure of a structure? (structural safety)
- etc.

Models provide information that is employed for design as well as during other activities through out its life cycle, such as monitoring, diagnosis, intervention and prediction. Tasks of modern engineers are not only found in design and construction, as it has been in the past, but are now increasingly present throughout the entire structural life cycle. (Robert-Nicoud et al. 2000 [113])

Typical weaknesses of current modeling approaches include (Robert-Nicoud et al. 2000 [113]):

- Modeling assumptions are made without adequate justifications and verifications.
- Simple models are often not compared with more complex ones in order to determine whether or not more complex models are more appropriate.

Most work on theoretical modeling does not make use of measurement data. Techniques that do make use of measurement data, for example (Kabe 1985 [70], Sohn and Law 1997 [136]), often aim only to correct parameters such as stiffness coefficients. Characteristics of behavioral models that explain the change in stiffness coefficients are not explicitly available using these techniques (Robert-Nicoud et al. 2000 [113]).

In the numerical modeling community, there is a tendency to aim at very high levels of sophistication of models. At the same time, there is usually a significant level of uncertainty in measurement data. Uncertainties in measurement data as well as the effect of uncertainty of model parameters on model accuracy are not often considered simultaneously. An outline of software, which supports engineers for such tasks, is presented in the next section. (Robert-Nicoud et al. 2000 [113])

8.2.1 Combining models and observations for decision support

Models are often numerous and observations usually contain much information. It is important to combine them to arrive at feasible models for better decision making related to monitoring, diagnosis, repair and prediction (Robert-Nicoud et al. 2000 [113]).

8.2.1.1 Percentage deviation approach

(1) MODULES:

- **Model library:** The model library contains a set of models with explicit assumptions and methods for computation of behavior.
- **Model retrieval/ calibration:** This module compares measurement data with model results. Models are initially selected by examining trends in measurement data. Each of the selected models is then analyzed to find out how the predicted behavior matches with measurements. Global search techniques such as PGSL (Raphael and Smith 2000 [112]) are used to calibrate parameters when only ranges of values of parameters are known.
- **Qualitative evaluation:** This module assists engineers when comparing data with calibrated models to identify suitable candidate models.

(2) RELATIONSHIPS:

- **Engineer-model interaction (Link A,** Fig. 8-4**):** Users either define models manually or models are generated automatically through the technique of model composition (Raphael and Smith 1998 [112]) by selecting a set of assumptions. For each model that is generated, parameters related to behavior such as deformations, curvatures, slopes, etc. are automatically calculated. The term model does not refer to a point solution, but a set of solutions defined by a range of values for its parameters.
- **Model library-measurement system interaction (Links D, E, C,** Fig. 8-4**):** Results of models may be used to help define the most appropriate measurement that is required. An important consideration is that the measurement should provide enough information to identify candidate models from among the set of all possible models. This is possible only if the measurement data is able to discriminate between features of behavior of different models. The information about the sensitivity of instruments along with the model precision is also used to choose the best measurement system.
- **Engineer-data interaction (Link F,** Fig. 8-4**):** Users provide visual information about the structure such as cracks, deformations, general aspects, etc.
- **Engineer-model retrieval module interaction (Link B,** Fig. 8-4**):** Users define rules for retrieval and for comparing measurement data with model results. A common method of comparison is by computing the root mean square difference. Many other techniques may also be appropriate. Users are also able to select subsets of measurement data for sensitivity analysis.

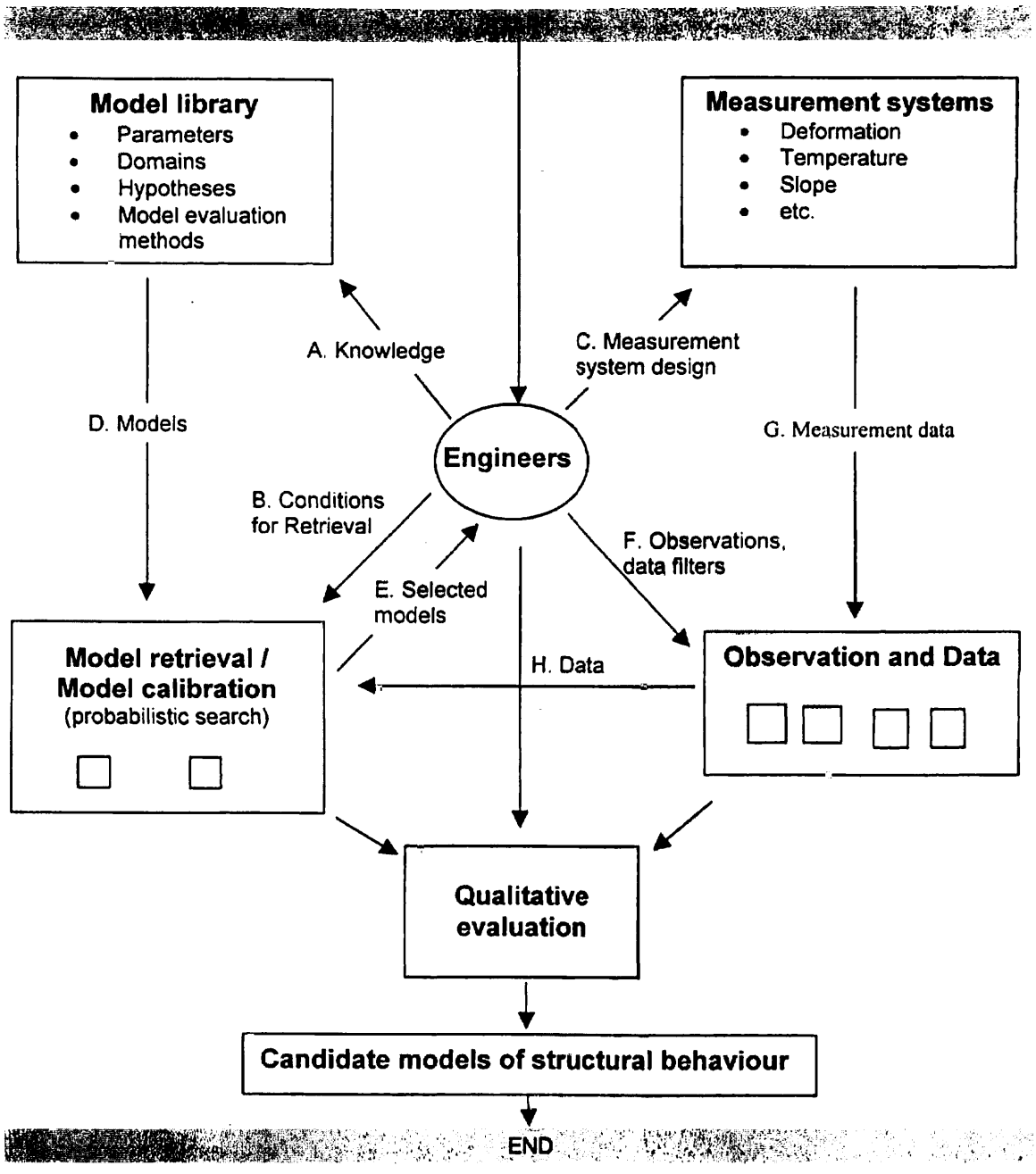

Fig. 8-4: Entities and relationships in the decision support system. Flow of information between modules is shown with arrows. Engineers compare models with data and observations in order to identify the most appropriate models (Robert-Nicoud et al. 2000 [113]).

According to Robert-Nicoud et al. (2000 [113]) the following observations and conclusions can be made from their study presented in Chapter 11.2:

- Selecting models through referring to only one type of observation is not sufficient. Displacement observations are not sensitive enough for evaluating candidate models.
- Although finite element modeling is useful, it must be defined carefully. For example, a small change in boundary conditions greatly affects the results.
- The process of identifying models that match measurements leads to examining models that have large numbers of parameters. The number of observation points must be greater than the number of parameters.
- Quantitative information related to values of parameters is more difficult to verify.

Difficulties in finding the best combination of values using probabilistic search are illustrated in Fig. 8-5

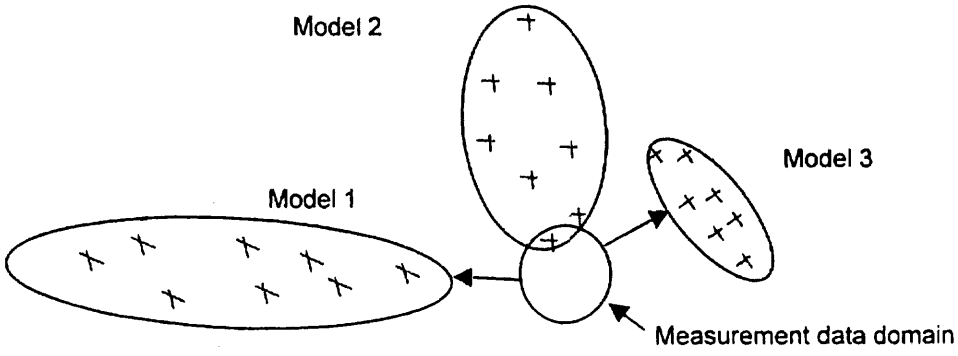

Fig. 8-5: Domain defined by models (each cross expresses a set of values for parameters), (Robert-Nicoud et al. 2000 [113])

- **Measurement data domain:** The set of data points representing the variations due to uncertainties in the measurement system and the operating environment (temperature, humidity, traffic, etc.)
- **Domain of a model:** space defined by the range of values of parameters in a model

Two situations are of interest (Robert-Nicoud et al. 2000 [113]):

- **Situation 1:** The measurement data domain intersects the domain of a model (for example, Model 2 in Fig. 8-5). Here, it is interesting to find out the characteristics of the intersecting sub-domain.
- **Situation 2:** The domain of a model does not intersect the measurement data domain. Instead of identifying individual points having least error, it is interesting to consider the overall behavior of the model. For example, the domain of Model 1 in Fig. 8-5 contains some points close to the measurement data. However, this might be the case because the model covers a large space of possibilities due to a large number of parameters that can be tuned. On the contrary, Model 3 gives an overall close match to the measurement data and its behavior is less sensitive to change in values of parameters.

Probability density functions denoting the quality of solution points may be used for identifying interesting model sub-domains. The percentage deviation (PD) is computed by dividing the root mean square difference by the mean value of data points. The optimization algorithm examines different possibilities and chooses the best one according to a user defined criteria. The classification of the various models is done in the following way:

- $PD \geq 50\%$ bad
- $25\% < PD < 50\%$ reasonable
- $PD \leq 25\%$ good

Through combining measurement data with models it is hoped that better decision support for diagnosis and maintenance of bridges will be made possible (Robert-Nicoud et al. 2000 [113]).

8.2.1.2 Probabilistic deviation approach

(1) Safety aspects

In this section a possible approach will be discussed in order to link the measured data to limits given by thy design. The limit state function for monitoring is described by the following method:

$$F_M\left[\text{Monitoring data} \le \text{Limits}\left\{\begin{array}{lll}\text{Ultimate Limit State} & \text{ULS} & \text{(loads)}\\ \text{Serviceability Limit State} & \text{SLS} & \text{(deformations)}\\ \text{Durability Limit State} & \text{DLS} & \text{(chlorides)}\end{array}\right\}\right]$$

$$P_f = P[\, F_M(X_1, X_2, ..., X_n, a, b)]$$

$$\frac{L_i \pm m_i}{S_i} \ge \beta$$

Li Limits given at the ultimate limit state, serviceability or durability limit states
mi mean values of monitoring data
Si standard deviation of monitoring data

As the ULS-, SLS- and DLS-limits have already been applied in the design phase, we have to guarantee that the measured data are in a safe range. Therefore some acceptance indices will be proposed in the following table:

β	P_f	
1.3	$1 \cdot 10^{-1}$	Good
1.8	$3.5 \cdot 10^{-2}$	Medium
2	$1 \cdot 10^{-2}$	Bad

Table 8-1: Acceptance index β

8.3 Reliability states

Recently, Frangopol and Das (1999) and Thoft-Christensen (1999) proposed five bridge reliability states. These states are indicated in

Table 8-2 along with the associated reliability indices. The service life of bridges is a progression of reliability states from excellent ($\beta \ge 9.0$) to unacceptable ($\beta < 4.6$). As indicated in Wallbank et al. (1999), Das (1999), and Frangopol et al. (1999), the justification for carrying out essential maintenance (such as major repairs) is that without it the element will be unsafe, and the justification for preventive maintenance (such as painting, silane treatment) is that if it is not done at the time it will cost more at a later stage to keep the element from becoming critical. The attributes for reliability and associated maintenance actions are also indicated in

Table 8-2. It should be mentioned that preventive maintenance work should be considered as a package of actions (such as silane treatment, deck waterproofing, expansion joint replacement, extraction of contaminants). It is expected that the cost of these packages (called options in Table 8-2) should increase with the decrease in the reliability state of the bridge. (Frangopol et al. 2001 [46])

Reliability State				
5	4	3	2	1
Reliability Index				
$\beta \geq 9.0$	$9.0 > \beta \geq 8.0$	$8.0 > \beta \geq 6.0$	$6.0 > \beta \geq 4.6$	$4.6 > \beta$
Attribute for Reliability				
excellent	very good	good	Fair	unacceptable
Maintenance Action				
Preventive 5	Preventive 4	Preventive 3	Preventive 2	Essential 1
Option 5a Option 5b Option 5c . .	Option 4a Option 4b Option 4c . .	Option 3a Option 3b Option 3c . .	Option 2a Option 2b Option 2c . .	Option 1a Option 1b Option 1c . .

Table 8-2: Definition of reliability states, attributes, and maintenance actions, [46]

Using this approach, maintenance actions are selected in response to distinct changes in the reliability states. In this manner, bridge reliability is directly incorporated in bridge management and all limitations associated with current Markovian-based bridge management systems can be relaxed (Frangopol et al. 2001 [46]).

8.3.1 First rehabilitation time

The random variables associated with no maintenance action scenario are: initial target reliability index B_0, time of damage initiation T_I, and reliability index deterioration rate A. Five additional random variables have to be introduced in order to characterize the preventive maintenance scenario: time of first application of preventive maintenance T_{PI}, time of reapplication of preventive maintenance T_P, duration of preventive maintenance effect on reliability T_{PD}, deterioration rate of reliability index during preventive maintenance effect Θ, and improvement in reliability index (if any) immediately after the application of preventive maintenance Γ. The assumed PDFs of all the eight random variables for steel/concrete composite bridges are indicated in Kong and Frangopol (2001 [46])

8.3.2 First rehabilitation time after no maintenance

Using Monte-Carlo simulation it is possible to generate the PDF of the reliability index of a group of steel/concrete composite bridges at any point in time Fig. 8-6 compares the PDFs

of the first rehabilitation time (i.e., rehabilitation rate) for steel/concrete composite bridges provided by experts in 1997 [i.e., triangular distribution (20,35,50) where 20, 35, and 50 represent the lowest, mode, and highest age (in years), respectively, Maunsell Ltd. And Transport Research Laboratory 1998], in 1998 (i.e., the logistic distribution characterized by the parameters 35.9 years and 6.2 years, Maunsell Ltd. And Transport Research Laboratory 1999), and the one obtained through complex reliability analysis computations using Monte-Carlo simulation and quadrate fitting. It is interesting to note that: (a) the target reliability index was not specified in 1997 and 1998; (b) in the reliability analysis carried out in 1999 the target reliability index was specified as 4.6; (c) the modes of the three distributions in Fig. 8-6 are approximately the same (Frangopol et al. 2001 [46]).

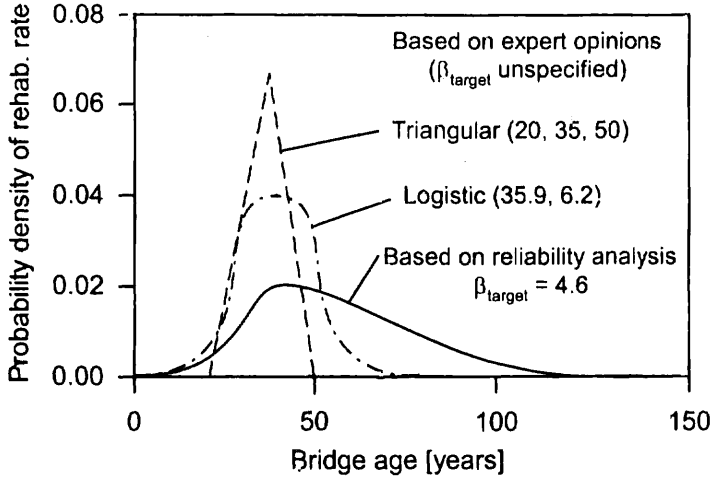

Fig. 8-6: Probability density of first rehabilitation time for steel/concrete composite bridges assuming no maintenance, (Frangopol et al. 2001 [46])

8.4 Structural reliability analysis

Procedures used in assessment of existing structures are in many aspects different from that taken in designing new structures. In general assessment requires application of advanced methods, as a rule beyond the scope of common design codes. The effects of the construction process and subsequent life of the structure, during which it may have undergone alteration, deterioration, misuse, and other changes to its original state, must be taken into account. (Holický 2000 [53])

Two approaches for the assessment of existing structures are known at present. The first approach means the immediate evaluation of a structure based on results obtained during inspections by using various types of classification methods. The second approach is "reliability-based evaluation". This evaluation method depends on the ability to express the influence of defects and deterioration on the global reliability of the whole structure (Nad 2000 [93]). Reliability theory provides a method for allowing for variability in the major parameters governing the behavior of a structure. For example, a bridge may be designed for a concrete strength of 40 MPa whereas in practice the actual strength of concrete within a bridge is likely to have a range of values between say 35 and 50 M Pa. Similarly most other parameters of strength, dimension and load can be more realistically modeled by a statistical distribution of specified mean, standard deviation and type.

Uncertainties in the various mechanical models are described as random variables using their probability density function (PDF). In the optimal case, all random variables are

measured and real data are available. Then a statistical assessment of this experimental data (e.g. data on strength of concrete, modulus of elasticity, loads) is based on the selection of the most appropriate density functions. In the case of some input parameters with no experimental evidence a decision based on professional judgment and empirical knowledge should be accepted. With a sensitivity analysis (α-factors) the most appropriate mechanical model may be defined. Important is also that the most influencing random variable can likely be identified using a probabilistic approach (e.g. deformation). After this identification the measured data has to be compared with the most appropriate mechanical model (Bergmeister 2000 [8]).

The limit state function for probabilistic based structural identification may be described as follows:

Limit State function: $g(x) = F_{MM} - F_{BM}$

Mechanical Model: $F_{MM}X(1), X(2), X(i-1)$ $\quad P_f = P[\, F_M(X_1, X_2, ..., X_i, a, b)]$

Behavioural Model (measured data): $F_{BM}X(i)$

8.4.1 Basic variables

Checking for structural safety, e.g., traditionally follows deterministic patterns. In principle, a defined value R_d of the resistance of a structural component is derived from a number of characteristic values. In a similar manner a defined value S_d representing the action effects is derived from a number of characteristic values of actions. In order to check for safety or failure these two single values R_d and S_d are then compared. (Schneider 1997 [126])

The deterministic form of the safety condition reads:

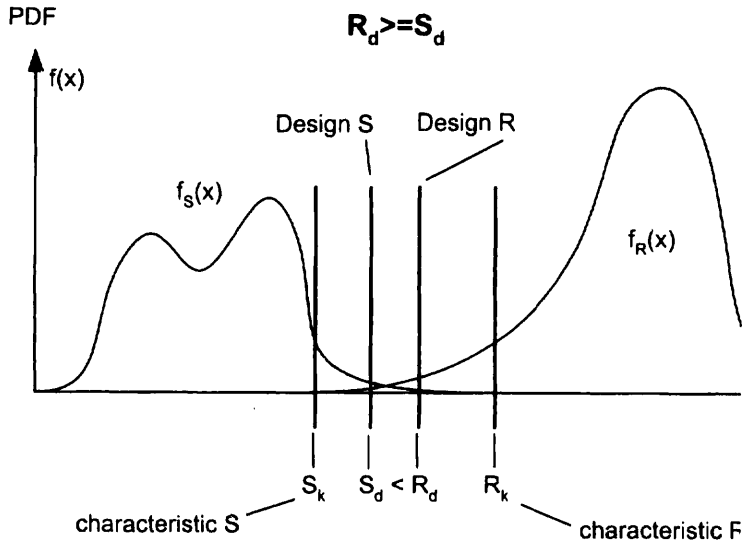

Fig. 8-7: The safety condition

However R and S depend on a number of quantities. Naturally, all these quantities depend in turn on others. In many cases a comparison on the basis of R and S alone is possibly too inaccurate. On the other hand, a fine division into many basic variables is more "accurate" but also more complicated and cumbersome. Choosing the optimal basis of assessment therefore is always an issue to be addressed. (Schneider 1997 [126])

Since the majority of input data involved in such situations are of random nature a probabilistic approach inevitably should be developed (Vokroj et al. 1997 [151]). Reliability (or probabilistic) analysis includes information from all resistance and loading variables influencing the assessment process (not just point estimates) and so provides a rational criterion for the comparison of the likely consequences of decisions taken under uncertainty.

To describe adequately the resistance properties of structural elements, (Melchers 1999 [86]) suggests to collect information about the following:

- Statistical properties for material strength and stiffness
- Statistical properties for dimensions
- Rules for the combination of various properties
- Correlation effects between different properties and between different locations of members and structure
- Influence of time (e.g. size changes, strength changes, deterioration mechanisms such as fatigue, corrosion, erosion, weathering, marine growth effects)
- Influence of fabrication methods on element and structural strength and stiffness
- Influence of quality control measures such as construction inspection and in-service inspection
- Effect of proof loading, i.e. the increase in confidence resulting from prior successful loading

The totality of observations of a quantity under the same conditions is termed a population. The concrete in a building, e.g., is a population. Each arbitrarily selected zone is an element of this population. Observations are necessarily limited to a number of cylindrical specimens drilled out randomly form the concrete. This is the random sample. The observed property is, for example, the compressive strength of the cylindrical specimen. (Schneider 1997 [126])

The results drawn from a sample are then summarized in histograms or presented by the cumulative frequency.

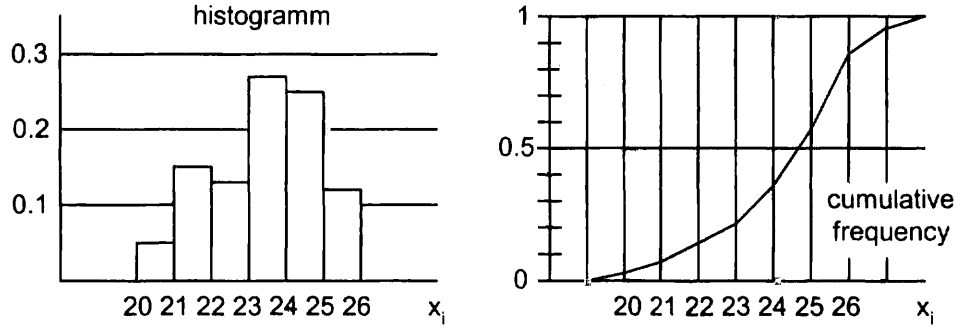

Fig. 8-8: Presentation of sample data, histogram (left), cumulative frequency (right)

The sample of experimental results is then replaced by a suitable distribution function. Typical resistance variables for example are best represented with a log-normal distribution, since they appear as a product of variables. Besides, negative resistances are hardly possible (Schneider 1997 [126]). Detailed information on R variables can be gathered from extensive material databases.

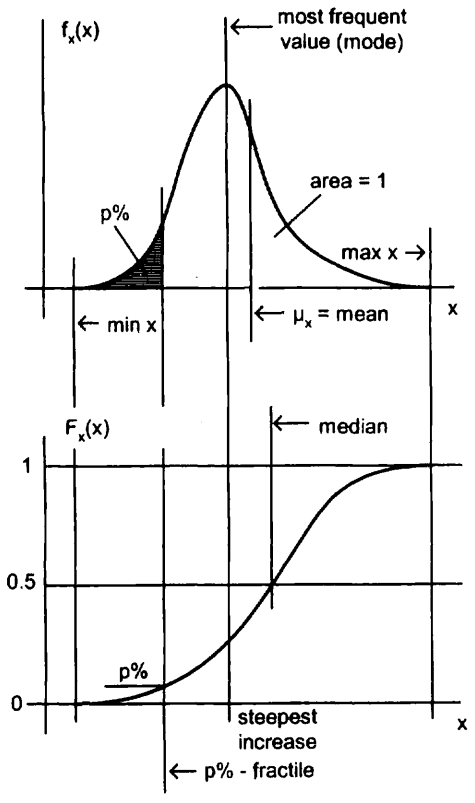

Fig. 8-9: Distribution functions, top: probability density function (PDF), bottom: cumulative distribution function (CDF)

The advantage to replace the sample data with mathematically defined distribution functions lies in the fact that further computations will be easier. The sampling data and the associated histograms can be described by a few characteristic numerical values, so-called parameters. Parameters may, alternatively, be replaced by so-called moments. The main moments of a sample are the mean, the variance, the skewness, and the kurtosis (Schneider 1997 [126]). The parameters of the corresponding continuous distribution functions include the median, the mode, the skewness and the kurtosis depending on the type of distribution. A variety of techniques are available for the approximate determination of the different parameters.

Measurement processes usually introduce a certain amount of variability or randomness into the results, and this randomness can affect the conclusions drawn from measurements. In the next Chapter we shortly discuss this problem.

8.4.2 Classical approach for a limited quality of data

$R_k = m_R \pm k_n \cdot s_R$

where:

m_R	is the mean value of the sample results
k_n	is the coefficient depending on the number of results n
s_R	is the standard deviation of the results
R_k	is the characteristic value of measurement data

For the classical approach for a limited quality of data the characteristic value may be based on the 5% fractile. If there is a complete lack of knowledge about the standard deviation, the value k_n has to be taken from Table 8-3 for the case that the standard deviation is unknown. If on the other hand the standard deviation is fully known from prior knowledge, the value of k_n has to be taken from Table 8-3 for the case that the standard deviation is known. In the given procedure a normal distribution of the test results is assumed.

Standard deviation	N							
	3	4	6	8	10	20	30	∞
Unknown	3,15	2,68	2,34	2,19	2,10	1,93	1,87	1,64
Known	2,03	1,98	1,92	1,88	1,86	1,79	1,77	1,64

Table 8-3: Values of kn based on a 5% fractile

8.4.3 Bayesian approach including prior knowledge

According to the Bayesian approach, the characteristic value in the case that a normal distribution of the test results is assumed, equal to:

$$R_d = \eta\left(m_R \pm t_\nu \cdot s_R\sqrt{1+\frac{1}{n}}\right)$$

where t_ν is the coefficient of the Student distribution

The value of t_ν, follows from Table 8-4, where $\nu = n-1$. The product $\alpha\beta$ corresponds to a fractile $P(\Phi)$ as indicated in Table 8-4. It is known that the Bayesian approach is sensitive for the value of the standard deviation, especially if only a small number of test results are available. Too small or too large standard deviations might result into unsafe or uneconomic design values. An advantage of the Bayesian theory is that the prior knowledge can avoid unrealistic design values.

αβ	**P(Φ)**	**ν**							
		2	3	5	7	9	19	29	∞
1,64	0,05	2,92	2,35	2,02	1,89	1,83	1,73	1,70	1,64

Table 8-4: Values of t_ν

8.4.4 Creation of density function

In order to find the density function of continuous measured data, the so called evaluation strategy or other parameter identification techniques may be applied (see Chapter 7.2.2). Essentially data is classified into groups and subsequently the combined density functions are fitted by the use of evolution strategies such as mutation, recombination, and selection. The idea is, that small variations of the determining variables must lead to small changes in the evaluation of the fitness function. An example for the fitting of measured load data is given in Fig. 8-10.

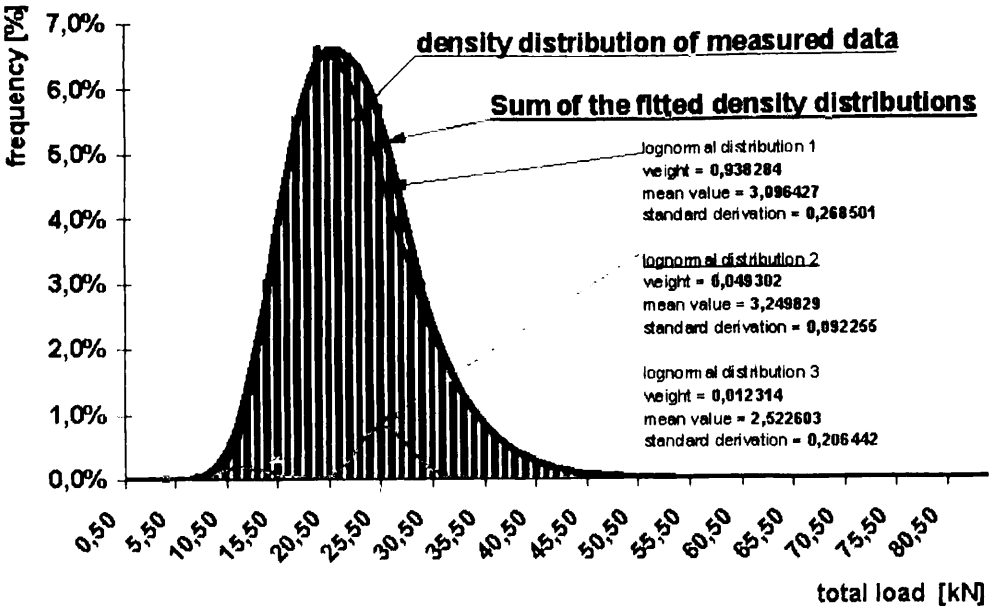

Fig. 8-10: Real axle-load and fitted density function

8.4.5 Overview of target reliabilities for ultimate limit state design

The values presented in this section were obtained from the IABSE Working Commission 1, (IABSE WC1 2001 [56]). The intention of this international working group is to get an idea of the use of probabilistic methods all over the world and the target reliabilities involved in such analyses. This was accomplished by the means of an international enquiry to collect the necessary information.

One may imagine that some codes officially allow for probabilistic design and prescribe some value for the target failure probability or reliability index. For other codes the probabilistic method may only be an explicit or implicit background. Some codes may even still be on a completely non-probabilistic basis. Thus it is interesting to get an idea of the present situation related to this topic (IABSE WC1 2001 [56]).

The main results from the enquiry representing the present state of affairs in 16 countries are summarized in the following tables. From Table 8-5 it can be concluded that partial factor design has become more or less the standard in most countries. Note that some countries have two systems, bringing the total number in Table 8-5 above 16. (IABSE WC1 2001 [56])

Safety format	No. of countries
partial factors	4
partial factors + load combination factors (e.g. PSI-factors in the Eurocode I)	12
allowable stress	1
Otherwise	1

Table 8-5: Safety formats used

Table 8-6 gives the results as far as the status of the probabilistic methodology is concerned. The result is an almost uniform distribution as far as the various alternatives are concerned, varying from the allowance to do a full probabilistic analysis to a complete neglect of probabilistic thinking (IABSE WC1 2001 [56]).

1	Official alternative for partial factors	5
2	Official background (in the code)	5
3	information background (in the code)	3
4	information background (outside the code)	3
5	background notion	2
6	not at all	4

Table 8-6: Failure probability or reliability index mentioned as:

Table 8-7 gives an overview of target reliabilities for countries that have the probabilistic method as an alternative design method or at least as a background to their partial factor method. More detailed information may be found in (IABSE WC1 2001 [56]). For convenience in Table 8-7 only the ranges have been indicated, rather than the individual values. All values in Table 8-7 have been converted to values for a reference period of one year. The corresponding failure probabilities can be found from $P_F = \Phi(-\beta)$, where F is the distribution function of the standard normal distribution. The central value seems to be about $\beta = 4$, as could be expected (IABSE WC1 2001 [56]).

BETA	**3.1**				**3.5**					**4.0**					**4.5**						**5.0**	
Austria												X										
Argentina	X	X	X	X	X	X	X	X	X	X	X	X	X	X	X	X	X	X	X	X	X	X
Canada	X	X	X	X	X	X	X	X	X	X	X	X	X	X								
China	X	X	X	X	X	X	X	X	X	X	X											
Denmark							X	X	X	X	X	X	X	X	X	X	X					
Estonia												X										
Germany												X										
Holland						X	X	X	X	X	X											
Italy												X										
South Africa				X	X	X	X	X	X	X	X	X	X	X	X	X	X	X				
Spain												X										
Sweden							X	X	X	X	X	X	X	X	X	X	X	X				
UK																		X				
USA										X												

Table 8-7: Overview of target reliability indices β for a one year reference period (IABSE WC1 2001 [56])

8.4.6 Reliability analysis methods

With all the known statistical properties for each of the variables, simulation methods are used to generate sample distributions of resistance and action values describing the structural reliability problem.

The classical reliability theory introduced the form of a response variable or safety margin as the function of basic random variables X_i (Novak [96]).

$$Z = G(X_1, X_2, \ldots, X_i)$$

The Xi represent the random variables, which describe both the problem and the requirements for a particular basis of assessment. These variables are geometrical and material parameters, load, environmental factors etc., generally uncertainties (random variables or random fields). These quantities can be also statistically correlated (Schneider 1997 [126], (Novak [96]).

In case that Z is a safety margin, G(.) is called a limit state function and can generally be written as:

$$G(X) = G(X_1, X_2, \ldots, X_i) \geq 0$$

Of interest in the present connection is the probability of failure p_f. It can be defined as follows (Novak [96]):

$$p_f = \int_{D_f} f(X_1, X_2, \ldots, X_i) dX_1, dX_2, \ldots, dX_i \tag{8-15}$$

where D_f represents failure region where $G(X) < 0$ and $f(X_1, X_2, \ldots X_i)$ is the function of marginal probability density or random variables $X = X_1, X_2, \ldots, X_i$. Equality $Z = 0$ divides the multidimensional space of basic random variables X_i into safe and failure region. Probability of failure is the probability that the limit state function is negative (Novak [96]).

The methods for determining theses probabilities or the corresponding indices are classified according to their degree of complexity, (Schneider 1997 [126]):

- **Level I:** The variables X_i are introduced by one single value only, e.g., by the mean value or some other characteristic value. This is the level of the current codes. Statements about the failure probability are not possible.
- **Level II:** The variables X_i are introduced by two moments or parameters, e.g., by the mean value and the standard deviation. Statements about the probability of failure obtained on this basis have a nominal character and can be used for comparison purposes.
- **Level III:** If the variables X_i are introduced using suitable distribution functions, then the results obtained can, given the adequacy of the input values, lead to results which, for all but rather small probabilities, can be used in an extended context.

Proposal for target reliability indices for existing concrete structures:

- Minimum acceptable value with a yearly inspection:
  ULS: $\beta_f = 3.8$
  SLS: $\beta_f = 2.5$

9 Concluding remarks

The continued use of existing structures is of great importance because the built environment is a huge economic and political asset, growing larger every year. The assessment of existing structures is now a major engineering task. The need to monitor the structural performance of our infrastructure inventory has become an international issue that transcends national boundaries. Both public safety and for maintenance and repair planning, structural monitoring is becoming increasingly important to both authorities and owners of structures around the globe. Since civil infrastructures are huge in size compared to any other structures and are exposed to harsh environments at all times, maintenance and damage inspection of civil infrastructures can be costly and time-consuming. Any downtime could cause a much more significant economic impact on the society than downtime with any other types of structures. Regular inspection and condition assessment of engineering structures are necessary so that early detection of any defect can be made and the structure's updated safety and reliability can be determined. Early damage detection and location allows maintenance and repair works to be properly programmed and thereby minimizing the overall costs of ownership and maintenance.

Structural monitoring of civil infrastructure systems is cost-effective and necessary since infrastructures are generally the most expensive investments/assets in any country. Recent advances in sensing technologies and material/structural damage characterization combined with current developments in computations and communications have resulted in a significant interest in developing new diagnostic technologies for monitoring the integrity of and for the detection of damage of both existing and new structures in real time with minimum human involvement. Using distributed sensors to monitor the "health" condition of in-service structures becomes feasible if sensor signals can be interpreted accurately to reflect the in-situ condition of the structures through real-time data processing. The entire system might be integrated and automated to perform real time inspection and damage detection. Therefore, the essence of structural health monitoring technology is to develop autonomous systems for the continuous monitoring, inspection, and damage detection of structures with minimum labor involvement. The results of structural conditions might be reported through a local network or to a remote center automatically by addressing different classes of recipients responsible for decision-making. Clearly, the development of such systems involves many disciplines such as structures, materials, computations, signal processing, etc.

The major benefits of monitoring systems are:

- real-time monitoring and reporting
- structural information on a continuous time basis (structural history)
- early detection of deteriorations and initializing deficiencies
- information for reliability based preventive maintenance operations
- saving in maintenance cost
- reducing labor, visual inspection, downtime, and human error
- automation – improving safety and reliability
- calibration data for analytical models for validation and verification

The safety evaluation remains difficult and must be based on engineering judgement supported by monitoring.

10 References

1. A.E. Aktan, N. Catbas, A. Turer, Z.F. Zhang, *Structural identification: Analytical aspects*, *Journal of Structural Engineering*, ASCE, 124(7), 817-829, 1998
2. A.E. Aktan, D.N. Farhey, A.J. Helmicki, D.L Brown, V.J. Hunt , K.L. Lee, A. Levi, *Structural identification for condition assessment: experimental arts*, Journal of Structural Engineering, 1997
3. A.E. Aktan, K.A. Grimmelsman, R.A. Barrish, N. Catbas, and C.J. Tsikos, *Structural Identification of a Long Span Bridge*, Proceedings of the Fifth International Bridge Engineering Conference, April 3-5, Tampa, Florida, Transportation Research Board, Volume 1, pp. 210-218, 2000
4. ATENA, Nonlinear Finite Element Analysis of Reinforced Concrete Structures, Cervenka Consulting, Revision 05/2001
5. V. Bayer, C. Bucher, M. Ebert, O. Huth, G. Purkert, J. Riedel, D. Roos, Y. Schorling, V. Zabel, *SLang - The Structural Language*, Institut für Strukturmechanik, Bauhaus Universität Weimar, 1998
6. J.S. Bendat, A.G. Piersol, *Engineering applications of correlation and spectral analysis*, John Wiley, New York USA, 1980
7. K. Bergmeister, *Safety evaluation on existing concrete structures in combination with an inspection*, CEB Commission 1 Task-Group 1.4 - Workshop, 16.-27.09.1996
8. K. Bergmeister, *Integrated Monitoring of Bridges*, Colloquium of SFB 477, Technical University Braunschweig, Germany, 22.06.2000
9. K. Bergmeister, U. Santa, A. Strauss, *Monitoring and Evaluation of Civil Infrastructure Systems*, Third world congress of monitoring 04-2002
10. A. Berman, E.J. Nagy, *Improvements of a Large Analytical Model Using Test Data*, AIAA Journal, Vol.21, No. 8, pp. 1481-1487, 1983
11. L. Bevc, B. Mahut, K. Grefstad, *Review of current practice for assessment of structural condition and classification of defects*, BRIME PL97-2220, March 1999
12. H. Bogath, *Verkehrslastmodelle für Straßenbrücken*, Institute of Structural Engineering, PhD Dissertation, 1997
13. W. Breit, *Critical Corrosion Inducing Chloride Content – State of the Art (Part 1)*, Betontechnische Berichte, Beton 7/98
14. Bridge and Structures Related Research – Summary, *Nondestructive Evaluation (NDE) of Highway Bridges*, Turner-Fairbank Highway Research Center, published by FHWA Office of Engineering Research and Development, June 1997
15. BRITE/EuRam BE96-3157, SIMCES, Synthesis Report, 1999-07-13
16. J.P. Broomfield, P.E. Langford, A.J. Ewins, *The Use of Potential Wheel to Survey Reinforced Concrete Structures*, Corrosion Rates of Steel in Concrete, ASTM STP 1065, N.S. Berke, V., Chaker, D. Whiting, EDS, American Society for Testing and Materials, Philadelphia,1990, pp.157-173
17. D.L. Brown, R.J. Allemang, R. Zimmermann, M. Mergay, *Parameter Estimation Technique for Modal Analysis* , S.A.E. paper number 790221, 1979
18. Budesministerium für Wirtschaftliche Angelegenheiten, Straßenforschung Heft 338, *Verfahren zur Vorhersage des Umfanges von Brückensanierungen*, Wien 1987
19. J.H. Bungey, S.G. Millard, *Testing of Concrete in Structures*, Chapman & Hall, 1996
20. N.J. Carino, *The Impact-Echo Method: An Overview*, Proceedings of the 2001 Structures Congress & Exposition, May 21- 23, 2001, Washington D.C., ASCE
21. Catbas F.N., M. Pervizpour, K.A. Grimmelsman, A. E. Aktan, *Health Monitoring of Bridges: Definitions, Scenarios and Possible Benefits*, Drexel Intelligent Infrastructure Institute (www.di3.drexel.edu), Drexel University

22. CEB-FIP, *Strategies for Testing and Assessment of Concrete Structures*, Bulletin 243, May 1998
23. CEB Task Group 1/4, Y. Schiegg, B. Elsener, H. Böhni, *Potential mapping on reinforced concrete bridges*, Workshop on the Evaluation and Monitoring of Existing Concrete Structures
24. V. Cervenka, *Applied Brittle Analysis of Concrete Structures*, ACI Fall Convention in Los Angeles, October 26 1998, Finite Element Fracture Analysis of Concrete Structures, ACI Committee 446/447
25. M.J. Chajes, H.W. Shenton, D. O'Shea, *Use of Field Testing in Delaware's Bridge management Program*, 8th International Bridge Management Conference, TRB, National Research Council, Denver, Colorado, Vol I, B-4, 1-6, 1999
26. F-K. Chang, *Structural Health Monitoring: A Summary Report on the First Stanford Workshop on Structural Health Monitoring*, Sept. 18 – 20, 1997
27. W.-F. Chen, L. Duan, *Bridge Engineering Handbook*, CRC Press, 2000
28. A.K. Chopra, *Dynamics of structures: theory and applications to earthquake engineering*, Englewood Cliffs, New Jersey: Prentice Hall
29. A.T. Ciolko, H. Tabatabai, *Nondestructive Methods for Condition Evaluation of Prestressing Steel Strands in Concrete Bridges*, Final Report, Phase I: Technology Review, NCHRP Web Document 23 (Project 10-53), March 1999
30. J.L. Clarke, *Alternative Materials for the Reinforcement and Prestressing of Concrete*, Blackie Academic & Professional, 1993
31. R.W. Clough, *Dynamics of Structures*, McGraw-Hill, Inc. 1993
32. F. Deblauwe, D.L. Brown, R.J. Allemang, *The Polyreference Time Domain Technique*, proceedings of the IMAC 1987, 832-845
33. S.W. Doebling, C.R. Farrar, M.B. Prime, *A Summary Review of Vibration-Based Damage Identification Methods*, The Shock and Vibration Digest 30 (1998), pp. 91-105
34. D. Donlagi´c, *Fiber optic sensors: An introduction and overview*, 2000
35. K. Duff, M. Hyzak, *Structural Monitoring with GPS*, Public Roads, 1997
36. M. Ebert, V. Zabel, C. Bucher, *Changes of dynamic structural parameters with progressive structural damage*, Proceedings of 13th ASCE Engineering Mechanics Division Conference, Baltimore, USA, 13-16th June 1999
37. B. Elsener, H. Böhni, *Potential mapping and corrosion of steel in concrete, Corrosion rate of steel in concrete*, ASTM STP 1065, Berke, N. S., Chaker, V., Whiting D., eds., American Society for Testing and Materials, Philadelphia, pp. 143-156, (1990)
38. I. Enevoldsen, *Experience with Probabilistic-based Assessment of Bridges*, Structural Engineering International 4/2001, IABSE Journal, Vol. 11 No. 4, pp. 251-260
39. ENV 1991-3, J.A. Calgaro, Traffic Loads on Bridges, *Road traffic loads calibration of the main loading system, Background Studies*, February 1997
40. R. van Es, J. Bennett, *Galvanic Cathodic Protection*, The Galvance System, July 2001
41. J.O. Evans, H.T. Bollmann, *Detensioning an external prestressing tendon*, web publications at http://www11.myflorida.com/structures/, September 2000
42. M.H. Faber, V.V. Dimitri, M.G. Stewart, *Proof load testing for bridge assessment and upgrading*, Engineering Structures 22 (2000), pp 1677-1689
43. fib CEB-FIP, *Durability of post-tensioning tendons*, bulletin 15, Workshop 15-16 November 2001, Ghent (Belgium)
44. FIP, Commission 10, Management, *Maintenance and Strengthening of Concrete Structures (Maintenance, Operation and Use)*, Technical Report, April 2000
45. D.M. Frangopol, 2000:*Bridge Health Monitoring and Life Prediction based on Reliability and Economy*, International Workshop on the Present and Future in Health Monitoring, September 3rd-6th, 2000, Bauhaus-University Weimar, Germany

46. D.M. Frangopol, J.S. Kong, E.S. Gharaibeh, *Maintenance Strategies for Bridge Stocks: Cost-Reliability Interaction*, Current and future trends in bridge design, construction and maintenance 2, Thomas Telford, London, 2001, pp 13 – 22
47. M.I. Friswell, J.E. Mottershead, *Finite Element Model Updating in Structural Dynamics*, Kluwer Academic Publishers, Dordrecht, 1995
48. Ghanem, R., Shinozuka, M., *Structural-System Identification. I: Theory, J. Engineering Mechanics*, ASCE, 121(2), 255-264, 1995
49. U.K. Ghosh, *Repair and Rehabilitation of Steel Bridges*, A.A. Balkema Publishers, 2000
50. A. Guggenberger, *Carbon Fiber Reinforcement in Structural Engineering*, PhD Dissertation, Institute for Structural Engineering, University of Applied Sciences, Vienna, Austria, 2001
51. M. Gutermann, *Entwicklung, Bau und Erprobung eines Belastungsfahrzeuges (BELFA) – Abschlußbericht, Abschnitt: Allgemeine Einführung*, Hochschule Bremen, Eigenverlag 2002
52. H. Gysin, *Comparison of Expansion Methods for FE Modeling Error Localization*, Proceedings of the 8th International Modal Analysis Conference, Kissimmee, Fl. pp 195-204, 1990
53. M. Holický, *Advanced Methods of Structural Assessment*, Proceedings of the 6th International Workshop on Material Properties and Design, Freiburg, Germany, Sept. 2000, pp 21-38
54. O. Huth, *Ein adaptiertes Polyreferenz-Verfahren und seine Anwendung in der Systemidentifikation,* for Ph.D.Thesis handed in Institute of Structural Mechanics, Bauhaus-University Weimar, 2002
55. O. Huth, J. Riedel, C. Bucher, *Finite Element Optimierung einer Stahlbetonbrücke auf der Grundlage von in-situ Experimenten,* Proceedings of the DACH-Tagung Berlin November, 1999
56. IABSE WC1, *Enquiry into Target Reliabilities for Ultimate Limit State Design*, Interim report March 2001
57. S.R. Ibrahim, E.C. Mikulcik, *A Method for the direct identification of Vibration Parameters from the Free Response*, Shock and Vibration Bulletin 47, No.4, 1977, pp 183-198
58. R. Idriss, K.R. White, J.W. Pate, S.T. Vohra, C.C. Chang, B.A. Danver, M.A. Davis, *Monitoring and evaluation of an interstate highway bridge using a network of optical fiber sensors*, International Workshop on Fiber Optic Sensors for Construction Materials and Bridges, Newark, New Jersey (USA), May 3-6, 1998, Technomic Publishing Company, Lancaster, pp 159-167
59. H.L. Imfeld, D. Plouffe, R. Ruland, *Pellissier H5 Hydrostatic Level*, Proceedings of the 5th International Workshop on Accelerator Alignment, 1997
60. D. Inaudi, *Fiber optic smart sensing*, Optical Measurement techniques and applications, P.K. Rastogi editor, Artech House, 1997, pp. 255-275
61. D. Inaudi, N. Casanova, S. Vurpillot, B. Glisic, P. Kronenberg, S.L. Loret, *Lessons Learned in the Use of Fiber Optic Sensor for Civil Structural Monitoring*, 6th International Workshop on Material Properties and Design, Present and Future of Health Monitoring, Bauhaus University , September 2000, pp 79 – 92, AEDIFICATIO Publishers, D-79104 Freiburg
62. D. Inaudi, S. Vurpillot, N. Casanova, P. Kronenberg, *Structural monitoring by curvature analysis using interferometric fiber optic sensors*, Smart Mater. Struct. 7 (1998), 199-208
63. D. Inaudi, S. Vurpillot, S. Loret, *In-line coherence multiplexing of displacement sensors: a fiber optic extensometer*, SPIE, Smart Structures and Materials, 1996, San Diego, USA

64. Institut für Konstruktiven Ingenieurbau, *Fachberichte aus dem Konstruktiven Ingenieurbau 1995-1996*, Heft 32/Jänner 1997
65. International Road Dynamics Inc., *Weigh-In-Motion Technology Comparisons*, Technical Brief, January 2001
66. International Standard, ISO 13822, *Bases for design of structures – Assessment of existing structures*, first edition 2001-12-15
67. B. Jaeger, M. Sansalone, R. Poston, *Using Impact-Echo to Assess Tendon Ducts*, Concrete International, Vol. 19' No. 2, February 1997
68. T. Jahn, *Identification of damage in reinforced concrete structures*, Proceedings of the Second International Symposium on Mathematical Modelling, Editors: I. Troch, F. Breitenecker, Technical University Vienna, Austria, February 1997, pp. 259-264
69. JOINT COMMITTEE ON STRUCTURAL SAFETY, Probabilistic Model Code, 12th draft, 10-11-2000
70. A.M. Kabe, *Stiffness matrix adjustment using mode data*, AIAA 23, 1985, pp. 1431 – 1436
71. D. Kamarys, *Detektion von Strukturveränderungen durch neue Identifikationsverfahren in der experimentellen Modalanalyse*, Ruhr-Universität Bochum, Dissertation, Institut für Mechanik, Mitteilung Nr. 119, 1999
72. M. J. Katwan, T. Hodgkiess, P.D. Arthur, *Electrochemical Noise Technique for the Prediction of Corrosion Rate of Steel in Concrete Materials and Structures*, Vol.29, June 1996, pp. 286-294
73. Z. Keršner, D. Novák, B. Teplý, R. Rusina, *Modelling of Deterioration of Concrete Structures by Stochastic Finite Element Method*, 7th International Conference on Structural Safety and Reliability, Kyoto, Japan, November 24 – 28, 1997
74. T. Klink, J. Meißner, V. Slowik, *Dehnungsmessung an einer Spannbetonbrücke mit Faser-Bragg-Gitter-Sensoren*, *Bautechnik*, 74 (1997) 6, 401-405C. Krämer, C.A.M. De Smet, B. Peeters, *Comparison of Ambient and Forced Vibration Testing of Civil Engineering Structures*, Proceedings of the International Modal Analysis Conference, IMAC XVII, Kissimmee, FL, USA, 1999
75. T. Krawzyk, *Volumenoptimierung von Stahlprofilen unter Beachtung von Stabilitätskriterien*, Diplomarbeit, Bauhaus-Universität Weimar 1998
76. C. Krämer, C.A.M. De Smet, B. Peeters, *Comparison of Ambient and Forced Vibration Testing of Civil Engineering Structures*, Proceedings of the International Modal Analysis Conference, IMAC XVII, Kissimmee, FL, USA, 1999
77. K.A. LaBel, C.J. Marshall, P.W. Marshall, P.J. Luers, R.A. Reed, M.N. Ott, C.M. Seidleck, D.J Andrucyk, *On the Suitability of Fiber Optic Data Links in the Space Radiation Environment: A Historical and Scaling Technology Perspective*, NSREC98 July, 1998
78. A. Lenzen, *Untersuchung von dynamischen Systemen mit der Singulärwertzerlegung. Erfassung von Strukturveränderungen*, Dissertation, Institut für Mechanik, Ruhr Universität Bochum 1994
79. A. Lenzen, H. Waller, *Numerische Modellierung von dynamischen Systemen aus Messignalen mit der verallgemeinerten Singulärwertzerlegung*, 5. Tagung über Dynamische Probleme - Modellierung und Wirklichkeit am 10. und 11. Oktober 1996, Curt-Risch-Institut für Dynamik, Schall und Me¡technik, Universität Hannover
80. A. Lenzen, H. Waller, *Anwendung der Singulärwertzerlegung zur Schadenserkennung und –lokalisation,* IV. Kolloquium Technische Diagnostik, Dresden,März 1996.
81. R. Maaskant, A.T. Alavie, R.M. Measures, G. Tadros, S.H. Rizkalla, A. Guha-Thakurta, *Fiber optic Bragg grating sensors for bridge monitoring*, Cement and Concrete Composites, 19(1997), 21-33

82. J. Maeck, M. Abdel Wahab, B. Peeters, G. De Roeck, J. De Visscher, W.P. De Wilde, J.-M. Ndambi, J. Vantomme, *Damage identification in reinforced concrete structures by dynamic stiffness determination*, Engineering Structures 22, Elsevier Science Ltd, 2000, p 1339 – 1349
83. N.M.M. Maia (editor), J.M.M. Silva (editor), J. He, N.A.J. Lieven, R.M. Lin, G.W. Skingle, W.-M. To, A.P.V. Urgueira, *Theoretical and Experimental Modal Analysis*, Research Studies Press LTD. Baldock, Hertfordshire, England, 1997
84. P.E. McGowan, *Dynamic Test/Analysis Correlation Using Reduced Analytical Models*, M.S. Thesis, Engineering Mechanics, Old Dominion University, 1991
85. R.M. Measures, *Bragg grating fibre optic sensing for bridges and other structures*, Second European Conference on Smart Structures and Materials, Oct. 12-14, 1994, Glasgow/UK, SPIE Vol. 2361, 162-167
86. R.E. Melchers, *Structural Reliability Analysis and Prediction*, John Wiley, 1999.- XVIII, 437 pages ISBN 0-471-98324-1
87. S. Melle ,M., K. Liu, R. Measures, *Practical fiber-optic Bragg grating strain gage system, Applied Optics*, 32(1993)19, 3601-3609
88. G. Meltz, W.W. Morey, W.H. Glenn, *Formation of Bragg-Gratings in Optical Fibers by a Transverse Holographic Method*, Optics Letters, 14(1989)15, 823-825
89. G. Merzenich, G. Sedlacek, *Hintergrundbericht zum Eurocode 1 – Teil 3.2: "Verkehrslasten auf Straßenbrücken"*, Bundesministerium für Verkehr Abteilung Straßenbau, Bonn-Bad Godesberg, August 1995
90. Z. Michalewicz, *Genetic Algorithms + Data Structures= Evolutionary Programs*, Springer Verlag 1994
91. P.H. Moller, *Potential Mapping - an Important Method of Measuring R.C. Structures*, Construction Maintenance & Repair, June 1992, pp. 21-23.
92. A.S. Morris, *The essence of measurement*, Prentice Hall, Englewood Cliffs, New Jersey, 1996
93. L. Nad, *Corrosion Monitoring – Possibility or Necessity?*, Proceedings of the 6th International Workshop on Material Properties and Design, Freiburg, Germany, Sept. 2000, pp 21-38
94. H.G. Natke, *Einführung in Theorie und Praxis der Zeitreihen- und Modalanalyse*, 3. überarbeitete Auflage, Vieweg Verlag, Braunschweig/Wiesbaden, 1992
95. H.G. Natke, C. Cempel, *Model-Aided Diagnosis of Mechanical Systems*, Springer Verlag Berlin Heidelberg 1997
96. D. Novak, *SARA: Structural Analysis and Reliability Assessment*, General proposals for development and implementation of efficient and feasible reliability tools into ATENA software
97. D. Novak, B. Teply, Z. Kersner, *The Role of Latin Hypercube Sampling Method in Reliability Engineering*, Strucrural Safety and Reliability (ICOSSAR-97), Balkema, Rotterdam, The Netherlands, 1988
98. J.C. O'Callahan, *A Procedure for an Improved Reduced System (IRS) Model*, Proceedings of the Seventh International Modal Analysis Conference Williamsburg, VA, pp. 1174-1186, 1989
99. M. Oeljeklaus, H.G. Natke, *The Use of Projected Input Residuals in Damage Identification*, 3rd International Workshop on Structural Health Monitoring, Stanford CA, USA, 2001
100. OMEGA, *Transactions in Measurement and Control: Force Related Measurements*, OMEGA Handbook Vol. 3, 1998
101. I.U. Ojalvo, D. Pilon, *Diagnostics for geometrically Locating Structural Math Errors From Modal Test Data*, Proceedings of the 29th AIAA Structures, Structural Dynamics and Materials Conference, Williamsburg, VA, pp. 1174-1186, 1988

102. C.C. Paige, *Computing the generalized Singular Value Decomposition*, SIAMJ. Num. Anal. Vol. 18 No. 3, June 1981
103. A.K. Pandey, M.Biswas, *Damage Detection in Structures Using Changes in Flexibility*, Journal of Sound and Vibration, 1994, 169(1), pp. 3-17
104. A.K. Pandey, M. Biswas, M.M. Samman, *Damage Detection from Changes in Curvature Mode Shapes*, Journal of Sound and Vibration, 1991, 145(2), pp. 312-332
105. B. Peeters, *System Identification and Damage Detection in Civil Engineering*, Ph.D.Thesis, Katholike Universiteit Leuven, Faculteit Toegepaste Wetenschappen, 2000
106. B. Peeters, J. Maeck, G. De Roeck, *Vibration-based damage detection in civil engineering: excitation sources and temperature effects*, Smart Materials and Structures 10, 2001, pp. 518-527
107. B. Peeters, G. De Roeck, *Reference-based stochastic subspace identification for output-only modal analysis*, Mechanical Systems and Signal Processing, V.6(3), 1999, p 855-878
108. P.H. Perkins, *Repair, Protection and Waterproofing of Concrete Structures*, E & FN SPON, 1997
109. R.T. Prince, *Evaluation of Field Tests performed on an Aluminum Deck Bridge*, Master Thesis, Virginia Polytechnic Institute and State University, 1998
110. R. Prony, Essai Experimental et analytique suer les Lois dc la Dilabilte des Fluides Elastique et sur Celles de la Force Expansisive de la Vapeur dc l'eau ct de la Vapeur de l'alkool, a Differentes Temperatures, Journal de l'ecole Polytechnique, Paris, Vol 1,Cahier 2, Floreal et Prairial an III (1795) p. 24-76
111. F. Pruckner, Corrosion and Protection of Reinforcement in Concrete – Measurements and Interpretation, PhD Thesis, May 2001
112. B. Raphael, I. Smith, *A probabilistic search algorithm for finding optimally directed solutions*, In proceedings of Construction Information Technology 2000, Iceland building Research Institute, Reykjavik, 2000
113. Y.Robert-Nicoud, B. Raphael, I.F.C. Smith, *Decision support through multiple models and probabilistic search*, Proceedings of Construction Information Technology 2000, Icelandic Building Research Institute, Reykjavik, 2000, pp 765-779
114. J. Rodríguez, L.M. Ortega, J. Casal, J.M. Díez, *Assessing Structural Conditions of Concrete Structures with Corroded Reinforcement*, International Congress: Concrete in the Service of Mankind, Conference No. 5 Concrete Repair Rehabilitation and Protection, Dundee, UK, June 1996
115. S. Rostam, *Assessment and repair strategies for deteriorating concrete bridges*, 3rd International Workshop on Bridge Rehabilitation, Darmstadt, (1992)
116. O.S. Salawu, C. Williams, Review of full-scale dynamic testing of bridge structures, Engineering Structures, Elsevier Science Ltd, 1995
117. Sanayei, M., Saletnik, M. J., *Parameter Estimation of Structures from Static Strain Measurements; Part I: Formulation,* Journal of Structural Engineering, ASCE, (In Press, July 1995)
118. U. Santa, K. Bergmeister, Instrumentation and Data Acquisition Techniques in Structural Health Monitoring, Proceedings of the Sixth International Workshop on Material Properties and Design, Bauhaus University Weimar, Sept. 2000, AEDIFICATIO Publishers
119. U. Santa, K. Bergmeister, Techniques for the Acquisition, Modeling and Interpretation of Knowledge in Monitoring Applications, Proceedings of the 6th International Workshop on Material Properties and Design, Bauhaus University Weimar, September 2000
120. U. Santa, K. Bergmeister, A. Strauss, Guaranteeing Structural Service Life Through Monitoring, 1st fib congress in Osaka 13-19 October 2002, Japan

121. V.E. Saouma, D.Z. Anderson, K. Ostrander, B. Lee, V. Slowik, Application of fiber Bragg grating in local and remote infrastructure health monitoring, Materials and Structures, 31(1998), 259-266Y.
122. V. Saouma, Bridge Diagnostic Inc., Boulder, Colorado, ITLL Structural Monitoring System, January 1997
123. Schiegg, H. Böhni, Online-Monitoring der Korrosion an Stahlbetonbauwerken, Beton- und Stahlbetonbau 95, 2000, Heft 2, Ernst & Sohn
124. K. Schittkowski, *The Nonlinear Programming Method of Wilson, Han, and Powell with an Augmented Lagrangian Type Line Search Function, Part 1: Convergence Analysis*, Numer. Math 38 1981, pp. 83-114
125. K. Schittkowski, *The Nonlinear Programming Method of Wilson, Han, and Powell with an Augmented Lagrangian Type Line Search Function, Part 2: An Efficient Implementation with Linear Least Squares Subproblem*, Numer. Math 38 1981, pp. 115-127
126. J. Schneider, *Introduction to Safety and Reliability of Structures*, Structural Engineering Documents, IABSE, 1997
127. E. Schoeneburg, F. Heinzmann, S. Feddersen, *Genetische Algorithmen und Evolutionsstrategien*, Addisson-Wesley (Deutschland) GmbH, 1994
128. P. Schwesinger, G. Bolle, *EXTRA – a new Experiment Supported Condition Assessment Method for Concrete Bridges*, SPIE's 5th International Symposium on Nondestructive Evaluation and Health Monitoring of Aging Infrastructure, Newport Beach, California USA, 5-9 March 2000
129. A. Selvarajan, A. Asundi, *Photonics, Fiber Optic Sensors and their Applications in Smart Structures*, Journal of Non-destructive Evaluation, Vol. 15(2), pp. 41-56. 1995
130. U. Sennhauser, P. Brönnimann, P. Mauron, P.M. Nellen, *Reliability of optical fibers and Bragg grating sensors for bridge monitoring*, International Workshop on Fiber Optic Sensors for Construction Materials and Bridges, Newark, New Jersey (USA), May 3-6, 1998, Technomic Publishing Company, Lancaster, 117-128
131. Z.Y. Shi, S.S. Law, L.M. Zhang, *Damage Localization by Directly Using Incomplete Mode Shapes*, Journal of Engineering Mechanics, 2000, 6, pp. 485-500
132. Shinozuka, M. and Ghanem R., *Structural System Identification II: Experimental Verification*, Journal of Engineering Mechanics, ASCE, Vol. 121, No. 2, pp. 265-273, 1995.
133. G. Shubinsky, *Visual & Infrared Imaging for Bridge Inspection*, 1994
134. S.W. Smith, C.A. Beattie, *Simultaneous Expansion and Orthogonalization of measured Modes for Structure Identification*, Proceedings of the AIAA dynamic Spezialist Conference, Long Beach, CA, pp. 261-270, 1990
135. J.A. Sobrino, M.D.G. Pulido, *Towards Advanced Composite Material Footbridges*, Structural Engineering International 2/2002, IABSE Journal, Vol. 12 No. 2, pp 84-86
136. H. Sohn, K.H. Law, *A Bayesian probabilistic approach for structure damage detection*, Earthquake engineering and structural dynamics, Vol. 26, 1997, pp. 1259 – 1281
137. K. Steffens, *Experimentelle Tragsicherheitsbewertung von Bauwerken, Grundlagen und Anwendungsbeispiele*, Ernst & Sohn, September 2001
138. A. Strauss, *Optimisation of non-linear FE – Analysis and Reliability Assessment, Numerical concepts and material models for existing concrete structure*, submitted to the PhD symposium in Munich 2002
139. STRAUSS Modell ISARCO Bridge
140. L.A. Taškov, *Dynamic testing of bridge structures applying forced and ambient vibration methods*, Proc. Conf. On Civil Engineering Dynamics, Society for Earthquakes and Civil Engineering Dynamics, London, UK, 1988, Paper 6
141. Texas Department of Transportation, *Bridge Inspection Manual*, December 2001

142. E. Udd, Fiber Optic Sensors, Wiley, 1991
143. E. Udd, Fiber Optic Smart Structures, Wiley, New York, 1995
144. E. Udd, W. Schulz, J. Seim, J. Corones, H.M. Laylor, *Fiber Optic Sensors for Infrastructure Applications*, SPR 374, Report No. FHWA-OR-RD-98-18, February 1998
145. R. Unbehauen, *Systemtheorie*, R. Oldenburg Verlag München Wien 1993
146. U.S. Army Corps of Engineers, *Engineering and Design - Deformation Monitoring and Control Surveying*, Engineer Manual 1110-1-1004, 1994
147. U.S. Department of Transportation, Federal Highway Administration, *Implementation Program on High Performance Concrete, Guidelines for Instrumentation of Bridges*, August 1996
148. U.S. Department of Transportation, Federal Highway Administration, Office of Highway Policy Information, *Traffic Monitoring Guide*, Executive Summary, May 1, 2001
149. U.S. Department of Transportation, Federal Highway Administration, *States' Successful Practices Weigh-in-Motion Handbook*, Dec. 1997
150. S.T. Vohra, C.C. Chang, B.A. Danver, B. Althouse, M.A. Davis, R. Irdiss, *Preliminary results on the monitoring of an in-service bridge using a 32-channel fiber Bragg grating sensor*, International Workshop on Fiber Optic Sensors for Construction Materials and Bridges, Newark, New Jersey (USA), May 3-6, 1998, Technomic Publishing Company, Lancaster, 148-158
151. P. Vokroj, B. Teplý, D. Novák, Z. Keršner, *Corrosion and life-time prediction of a steel storage tank*, International Conference on Carrying Capacity of Steel Shell Structures, 1 - 3 October 1997, Brno, Czech Republic
152. Vollrath, Tathoff, *Handbuch der Brückeninstandhaltung*, Beton-Verlag, 1990
153. S. Vurpillot, G. Krueger, D. Benouaich, D. Clément, D. Inaudi, *Vertical Deflection of a Pre-Stressed Concrete Bridge Obtained Using Deformation Sensors and Inclinometer Measurements*, ACI Structural Journal, V. 95, No. 5, September-October 1998
154. J.P. Warhus, S.D. Nelson, J.E. Mast, E. M. Johansson, *Advanced Ground-Penetrating, Imaging Radar for Bridge Inspection*, UCRL-JC 113707, 1994
155. G. A. Washer, *Developing NDE Technologies for Infrastructure Assessment*, Public Roads Magazine, 2000
156. H. Wenzel, *Quality Assessment and Damage Detection by Monitoring*, http://www.vce.at
157. A. J. Wheeler, A. R. Ganji, *Introduction to Engineering Experimentation*, Prentice-Hall Inc., 1996
158. C. Williams, *Testing of large structures using vibration techniques*, Structural Integrity Assessment, Elsevier Applied Science, London UK, 1992, p 290-229
159. C.P. Wright, *Applied measurement engineering – How to design effective mechanical measurement systems*, Prentice Hall, Englewood Cliffs, New Jersey, 1995
160. B. Yanev, *Past Experience and Future Needs for Bridge Monitoring in New York City*, 6th International Workshop on Material Properties and Design, Present and Future of Health Monitoring, Bauhaus University, Sept. 2000, pp 93 – 108, AEDIFICATIO Publishers
161. S. Yuyama, *Fundamental Aspects of Acoustic Emission Applications to the Problems Caused by Corrosion*, Corrosion Monitoring in Industrial Plants Using Nondestructive Testing and Electrochemical Methods, ASTM STP 908, ASTM STP 908, eds. G.C. Moran and P. Labine (Philadelphia, PA: ASTM, 1986), pp. 43–74.
162. A.D. Zdunek, D. Prine, Z. Li, E. Landis, S. Shah, *Early Detection of Steel Rebar Corrosion by Acoustic Emission Monitoring*, CORROSION95, the NACE International Annual Conference and Corrosion Show, 1995

163. Zheng, M.Sc.Qian, *Identifikation struktureller Parameter von Rechenmodellen mit Hilfe der Schwingungsversuchsdaten von Teilstrukturen*, Dissertation, Universität Gesamthochschule Kassel 1996
164. D.C. Zimmermann, W. Widengren, 1990, *Model Correction Using a Symmetric Eigenstructure Assignment Technique*, AIAA Journal, Vol. 28, No.9, pp. 1670-1676
165. D.C. Zimmermann, M. Kaouk, *Structural Damage Detection Using a Minimum Rank Updating Theory*, J. of Vibration and Acoustics, 116, 1994, pp. 1110-1115
166. L. Zimmermann, Y. Schiegg, B. Elsener, H. Böhni, *Electrochemical Techniques for Monitoring the Conditions of Concrete Bridge Structures,* 1998
167. http://allserv.rug.ac.be/~smatthys/fibTG9.3/About.html
168. http://
169. www.belfa.de
170. http://www.cedrat.com
171. http://www.cnde.iastate.edu/faa-casr/Inspection_methods.htm
172. http://www.corrosion-club.com
173. http://www.corrosion-doctors.org
174. http://www.corrosionsource.com
175. http://www.dynamag.sk
176. http://www.engin.umich.edu/dept/cee/sme/controlbridge.html
177. http://www.envirocoustics.gr/
178. http://www.fhwa.dot.gov
179. http://www.ibmb.tu-bs.de
180. http://www.izfp.fraunhofer.de
181. http://www.leica-geosystems.com/
182. http://www.mpa.tu-bs.de
183. http://www.nde.lanl.gov/
184. http://www.ndt.net
185. http://www.nea.fr
186. http://www.omega.com
187. http://www.ornl.gov/dp121/
188. http://www.projstar.sk
189. http://www.roctest.com
190. http://www.shef.ac.uk/~tmrnet/background.html
191. http://www.slopeindicator.com
192. http://www.uni-kassel.de/fb16/ipm/mt/de/Welcome.ghk
193. http://www.wdpa.com

11 Annex – case studies

Table 11-1. Overview of case studies presented in this Chapter

11.1 Road bridge Tuckhude

Christian Bucher

Institute of Structural Mechanics
Bauhaus University Weimar, Germany

11.1.1 Task

In context with non-destructive tests of existing structures a basic task is a realistic description of load carrying and deformation behavior of structures. The solution of this task is a necessary condition for the assessment of the effect of existing damage or reconstruction measures. In this case study the example of a road bridge with small band width is used to show one possible procedure of adaptation of FE-model based on dynamic experiments. The optimization is performed by Genetic Algorithm and the identified parameters are presented.

11.1.2 Structure of the bridge

The investigated road bridge Tuckhude (Mecklenburg-Vorpommern, Germany) with 7:24m span width is built from 28 prefabricated reinforced concrete beams. The concrete has a quality corresponding to B25 (according to DIN 1045) and a reinforcement steel quality category ST A-I with a statically effective area $A = 15{:}97\text{cm}^2$ per beam. The static system of the complete bridge is a hinge supported slab.

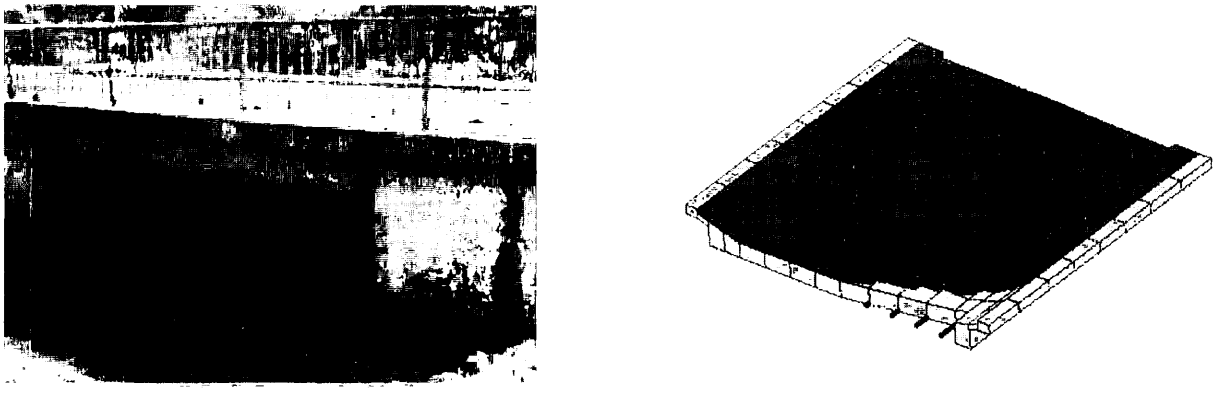

Fig. 11-1: Photograph and FE-model of the road bridge

This system is modeled with finite elements using volume elements with 20 nodes for the concrete and beam elements with 2 nodes for the steel bars. The model has two layers, one for the structure and one for the road pavement.

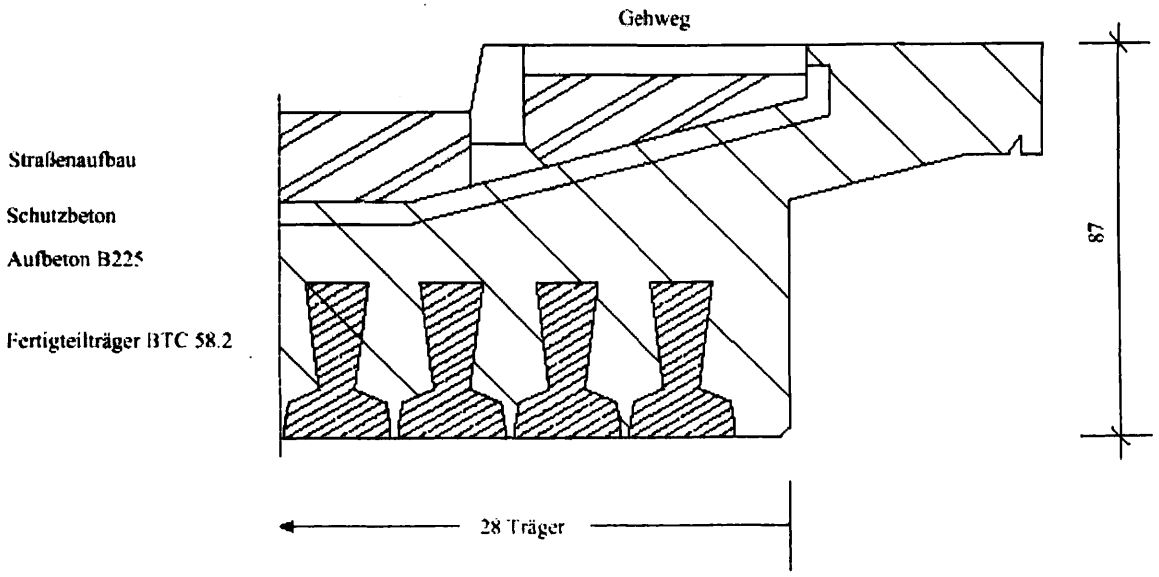

Fig. 11-2: Cross section of the road bridge

11.1.3 Realization of experiments

An impact system (see Fig. 11-3) was chosen to excite the bridge. Its advantage is its technical simplicity and speed of measurement. For the measurements piezo-electrical accelerometers and three dynamic PCB force transducer with a measure range $0.225 < f < 100 * 10^3$ Hz were used.

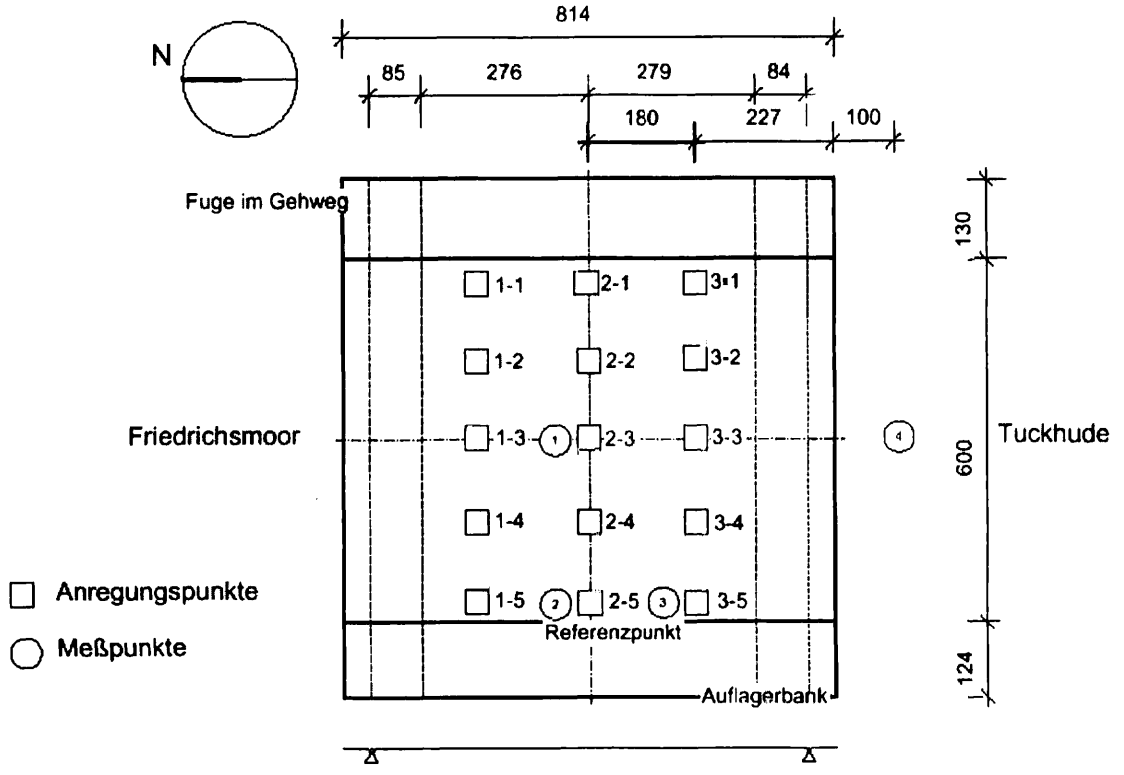

Fig. 11-3: Position of the excitation and measurement points

The measurement data were recorded with a sampling interval $\Delta t = 0.977ms$. For the improvement of the signal/noise ratio the experiments were repeated and averaged. During impact a maximum excitation force of approximately $F = 50kN$ and a maximum response acceleration $a = 0.43m/s^2$ were measured.

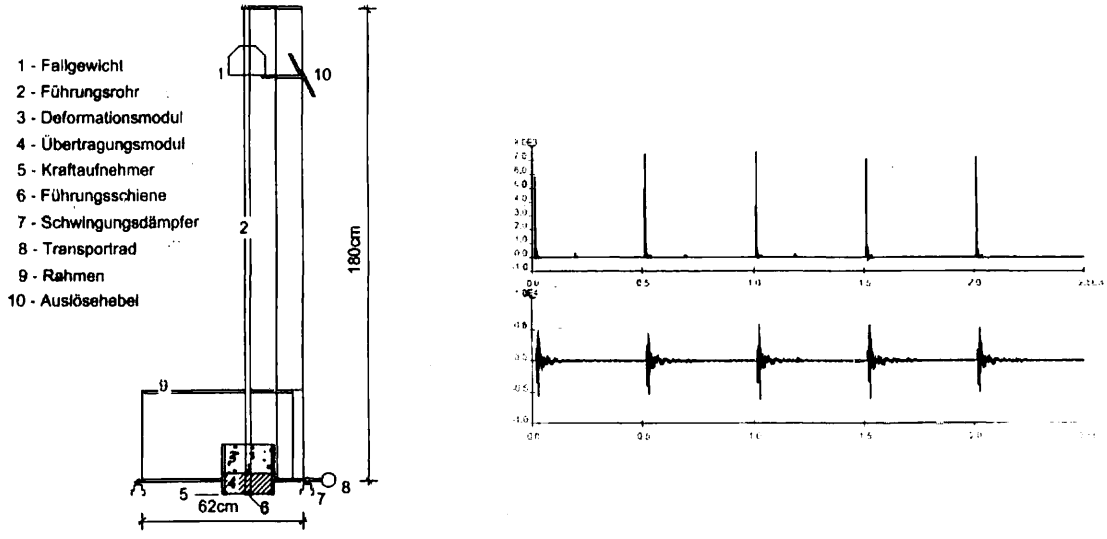

Fig. 11-4: Impact weight system and records of force time and acceleration-time functions, excitation 2-2, force transducer 3, acceleration transducer 2

11.1.4 Interpretation of time series

The complex transfer function is detailed derived in Chapter 7.5.2. Here the results are presented from the interpretation of the complex transfer function. Altogether 6 resonance frequencies with the corresponding mode shapes could be identified, Table 11-2.

Nr.	f_m[Hz]	f_v[Hz]	D_m[%]	D_v[%]
1	24.23	23.65-24.89	7.67	6.06-9.92
2	31.87	30.61-32.43	6.40	5.81-8.24
3	39.70	36.10-38.95	2.51	1.03-5.26
4	41.96	41.10-43.64	3.59	2.16-5.33
5	47.36	45.66-47.91	4.61	3.87-5.92
6	52.95	52.88-53.00	3.20	1.15-4.32

Table 11-2: Identified resonance frequencies and damping ratios

f_m mean value of natural frequency
f_v scatter range of natural frequency
D_m mean value of the damping ratio
D_v scatter range of the damping ratio

For the visualization of mode shapes (Fig. 11-5) the FE-model is statically condensed at the measured degrees of freedom. The visualization is based on the spectral magnitudes together with the phase angles. The mode shapes 1 (24.23 Hz), 2 (31.87 Hz), 5 (47.36 Hz) show a good agreement with the of FE-model, so these mode shapes and their corresponding natural frequencies are considered in the computation of the complex transfer function.

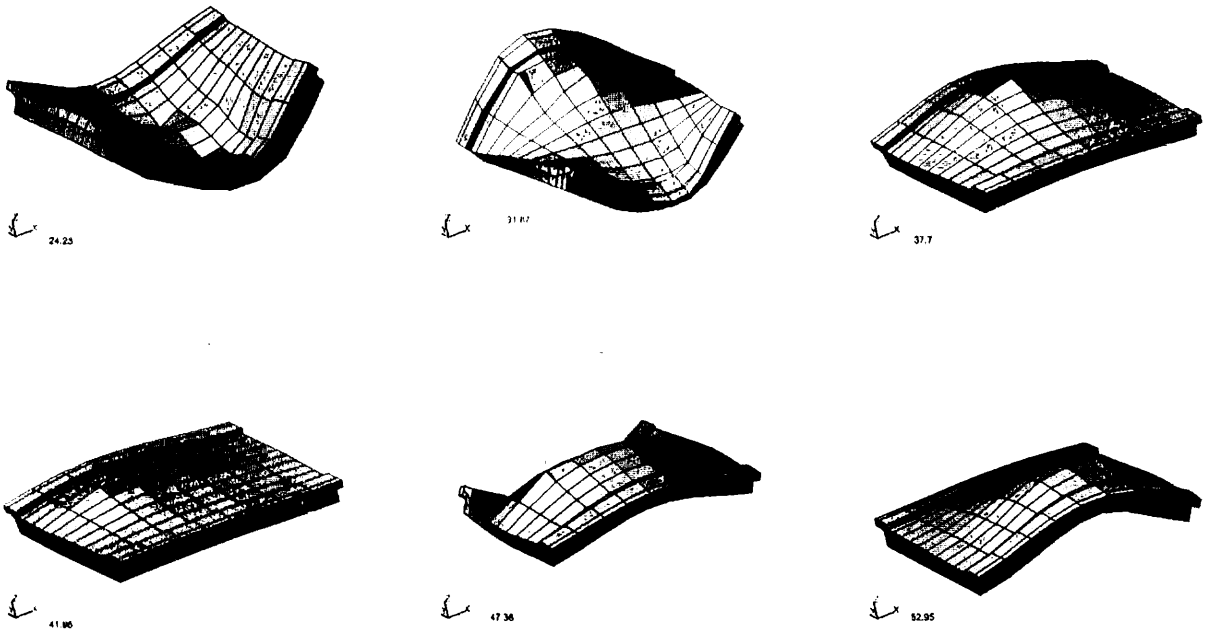

Fig. 11-5: Visualized mode shapes

11.1.5 Optimization

The optimization task consists in the minimization of the differences from measured and calculated transfer functions. This leads to the determination of the free FE-model parameters. For the objective function the differences are between the experimentally determined (H_M) and the calculated (H_{MO}) complex transfer functions at all measured degrees of freedom are calculated. The sum of second vector norm of the difference vectors results in the objective function value J.

$$J = \sum_{n=1}^{F_n} \left\| H_{MO} - H_M \right\|_2$$

The free parameters of the FE-model describe material date (elastic modulus) and modal damping ratios. The optimization is realized by using Genetic Algorithms. This procedure is shortly explained with the correspondent references in Chapter 7.2.2.

11.1.6 Free parameter

The dynamic parameters of the FE-model are assembled in a chromosom. Some of these parameters describe the elastic-modulus of steel and concrete elements. For reducing the dimensions of search space, several elements are collected in groups (see Fig. 11-6). The concrete is described by 8, the steel by 3 parameters. For the calculation of complex transfer function from model shapes 1, 2, 5 the corresponding 3 modal damping ratios are included in the chromosom.

11.1.7 Results

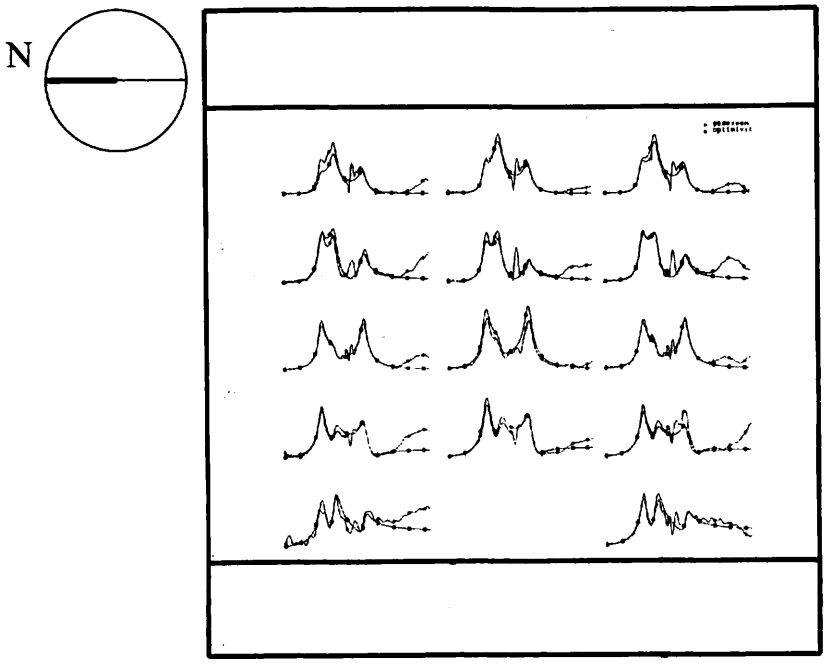

Fig. 11-6: Comparison between measured and calculated complex transfer functions for all measured degrees of freedom

After the optimization there is a very good agreement of complex transfer functions as shown in Fig. 11-6. The modal damping ratios show a good agreement between measurement

Nr.	f_m[Hz]	D_m[%]	D_{ident}[%]
1	24.23	7.67	7.61
2	31.87	6.40	6.41
5	47.36	4.61	4.01

Table 11-3: Experimentally obtained and numerically identified damping ratios

and computation as well (see Table 11-3). However, the determined material parameters are so different in value that a physical interpretation appears not to be possible. One reason may be that only few local material parameters describe the global dynamic behavior of structure. A different (global) formulation of the free parameters, which allows a more realistic description of the structural behavior is part of future research work.

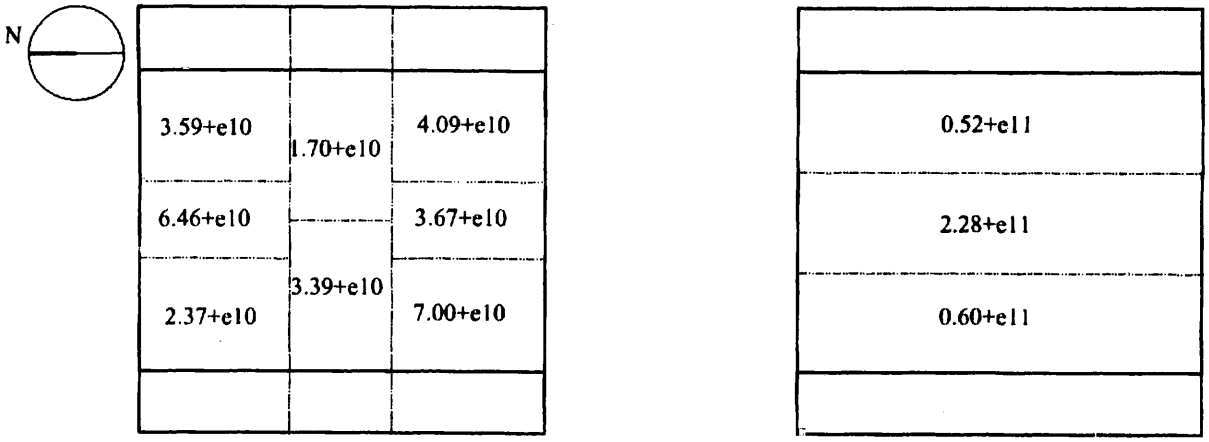

Fig. 11-7: Distribution of elastic modulus for concrete and steel after the optimization process (values in N/m²)

11.1.8 Acknowledgements

The investigations are supported in part by the German Research Council (DFG) within the Collaborative Research Center SFB 524 "Materials and constructions for the revitalization of buildings" at the Bauhaus-Universität Weimar and by the Ministry of Research (BMB+F) within the cooperative research project EXTRA II. The contribution of the laboratory for experimental static's, Hochschule Bremen, to the measurements of the road bridge Tuckhude is acknowledged.

11.2 Optimization approach for identifying good mechanical models

Yvan Robert-Nicoud (Research Assisstant)
Benny Raphael (Research Associate)
Ian F.C. Smith (Professor)

IMAC-DGC, EPFL
CH-1015 Lausanne, Switzerland

11.2.1 Description of the bridge

The Lutrive highway bridge was constructed in 1972 using the cantilever method with central hinges. Two bridges were built (one for each direction of traffic) with a length of 395 m. each and a maximum span of approximately 130 m. The longitudinal section is shown in Fig. 11-8:

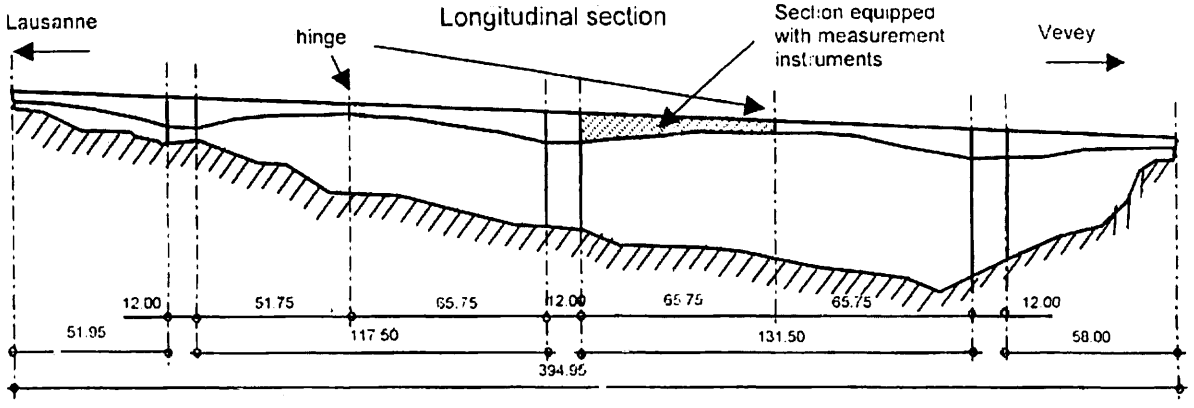

Fig. 11-8: Longitudinal section of Lutrive Bridge (values in meters)

The cross-section of the bridge is a pre-stressed box-girder with variable inertia. The maximum height is 8.50 m. at the column and 2.50 m. in the mid-span, at the hinges. More information about the bridge can be found in (Burdet and Badoux 1999 [1]). A brief history of the bridge is given below:

1971-1972:	Construction of the bridge
1973, 77, 78, 80, 85, 86:	Annual optical level meter measurements
1986:	An engineering office was given the contract to survey the bridge after large deformations were observed at mid-span
December 1988:	External pre-stress added to the two bridges
1988-1999:	Displacement on the south bridge increases. New measurement systems are installed on the bridge, including a hydrostatic levelling system (1988)*, and fibre optical sensors (1996)**
November 1997:	Load tests with fibre optic sensors **, inclinometers*, and optical level meter *

December 1999:	New additional external pre-stress added to the south bridge
	*(Burdet and Fleury 1997 [4])
	**(Perregeaux 1998 [2], Perregeaux et al. 1998 [3])

Table 11-4: Bridge history

11.2.2 Models of Lutrive bridge

Finding a good model for Lutive bridge and the right explanations for abnormal increases in displacements have remained a challenge for several years. Various hypotheses involving parameters such as creep, pre-stress and joint characteristics at mid-span have been made. New external pre-stress has been added twice on this structure in less than 30 years in order to correct serviceability deficiencies.

For this example, model changes over time have not been analysed. Only the task of defining a good model for a particular point in time is studied. The situation that is analysed is a load test that was conducted in 1997. The advantage of this case is that knowledge of the loading including positions on the structure is available.

One section of the bridge was equipped with instruments placed symmetrically on both sides of the box-girder. Measurements systems, part of measurement data and a sample of models are presented below:

11.2.2.1 Measurement systems

- Fibre optic sensors at the following five longitudinal positions (Perregeaux 1998 [2]) from the column in the Lausanne direction:
  8.4m., 20.4 m., 32.5 m., 44.5 m., 56.8 m.
- Inclinometers at four positions from the same column (Burdet and Fleury 1997 [4]):
  16.1 m., 29.5 m., 49.3 m., 65.75 m.
- Optical level meters at four positions from the same column (Burdet and Fleury 1997 [4]):
  11.9 m., 29.9 m., 47.8 m., 65.75 m.

11.2.2.2 Measurement data

Each measurement system provide the following measurement data:

- Two fibre optical sensors placed on the upper part and lower part of an element define the curvature by the relations derived from simple beam theory:

$$\frac{1}{r_m} = \frac{l_{inf,2} - l_{sup,2}}{Y \cdot l_1}$$

r_m : *mean radius of curvature*
l_1 : *initial length of upper and lower sensors*
$l_{sup,2}$: *final length of upper sensor*
$l_{inf,2}$: *final length of lower sensor*
Y: : *distance between upper and lower sensors*

- Inclinometers give the slope of the cross-section. (Burdet and Fleury 1997 [4])

- Optical level meters give the vertical displacement of cross-sections. (Burdet and Fleury 1997 [4])

11.2.2.3 A sample set of models

A sample set of models has been defined for the Lutrive Bridge. The following points are relevant to the section of the bridge which is examined:

- Only the section that is limited from the column to the mid-span has been analysed with models M1, M2, M3, M4, M5 and M6.
- The complete structure has been analysed using models M7 and M8.

Characteristics of each model are presented in Fig. 11-9 a-h.

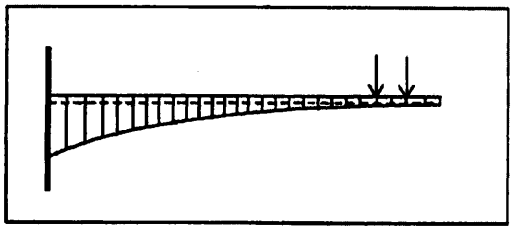

Fig. 11-9 a: Model M1

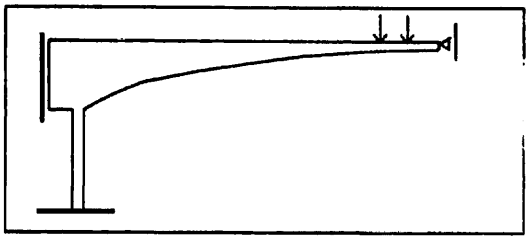

Fig. 11-9 b: Model M2

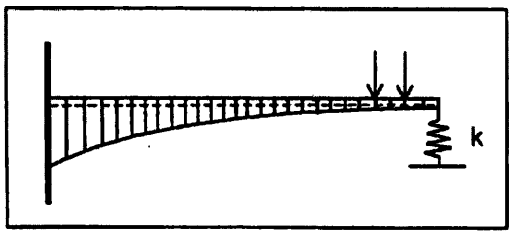

Fig. 11-9 c: Model M3

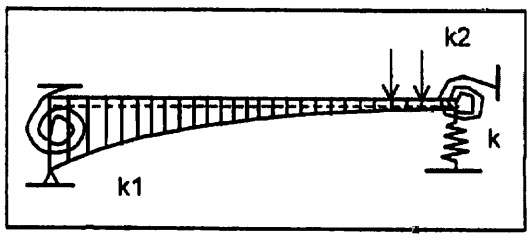

Fig. 11-9 d: Model M4

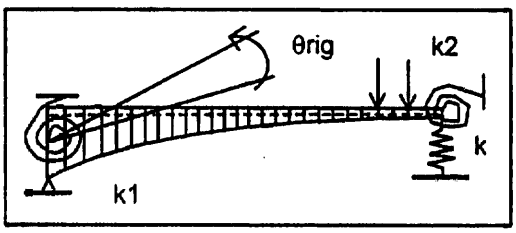

Fig. 11-9 e: Model M5

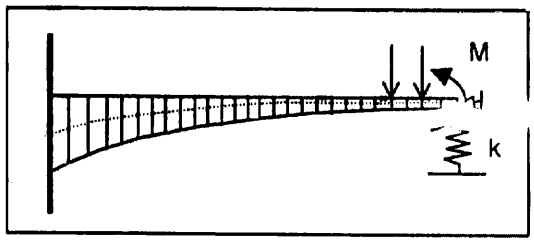

Fig. 11-9 f: Model M6

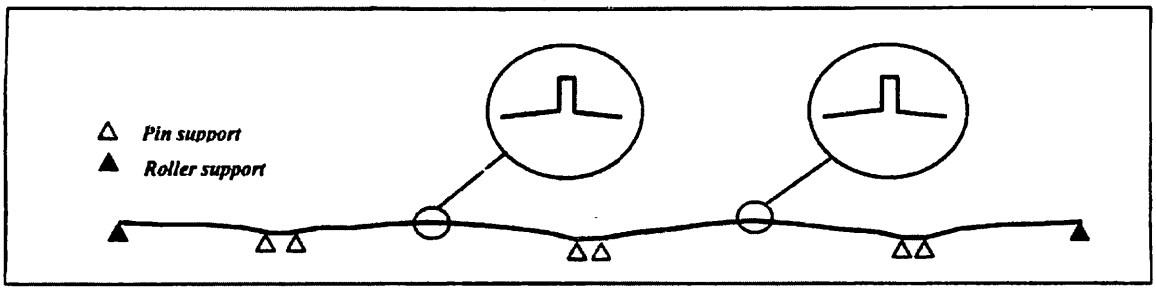

Fig. 11-9 g: Model M7

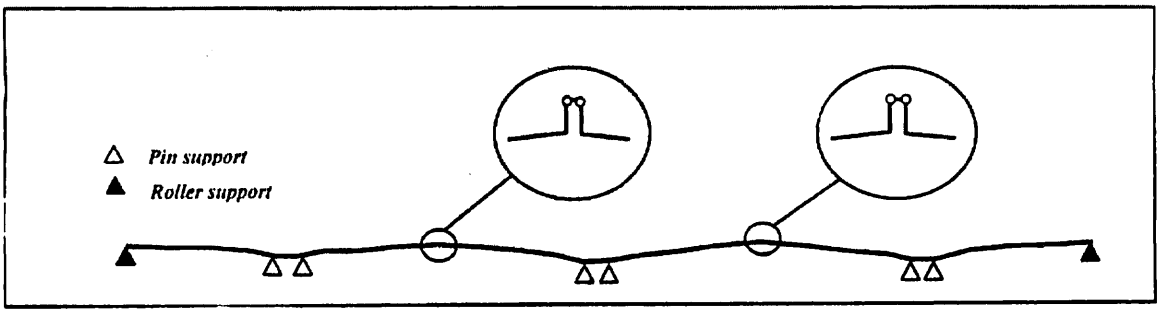

Fig. 11-9 h: Model M8

M1: Design model (Perregeaux 1998 [2]) **Description:** • Cantilever bridge with parabolic section profile (variable moment of inertia) • Evaluated analytically **Parameters:** • E: 38e6 [kN/m^2]	***M2: Design model*** (Perregeaux 1998 [2]) **Description:** • Cantilever bridge with parabolic section profile (variable moment of inertia) • Evaluated through finite elements modelling (MAPS) **Parameters:** • E: 32e6 [kN/m^2]
M3: Propped cantilever model **Description:** • Propped cantilever bridge supported on a spring at the propped end • Parabolic section profile • Evaluated analytically (force method, virtual work) **Parameters:** • E: 38e6 [kN/m^2] • I: from 5.129 to 138.89 m^4 • k: 17'114 [kN/m]	***M4: Beam with rotational and vertical springs*** **Description:** • Simply supported beam with rotational springs at both ends • Supported on a spring at one end • Parabolic section profile • Evaluated analytically (force method, virtual work) • Use of GPSL algorithm for calibrating value of parameters **Defined Parameters:** • I: from 5.129 to 138.89 m^4 **Undefined Parameters:** • E, k, k1, k2

M5: Beam with rigid body rotation **Description:** • Simply supported beam with rotational springs at both ends • Supported on a spring at one end • Parabolic section profile • Evaluated analytically (force method, virtual work) • Rigid body rotation at supported point • Use of GPSL algorithm for calibrating parameters values **Undefined Parameters:** • E, k, k1, k2, θrig **Defined Parameters:** • I: from 5.129 to 138.89 m^4	***M6: Finite element modelling with arch effect*** **Description:** • Propped cantilever bridge supported on a spring at the propped end • Arch effect with compression force • Parabolic section profile • Finite element model (MAPS) with beams • Bending moment at the end **Parameters:** • I: from 5.129 to 138.89 m^4 • E: 30e6 [kN/m^2] • M: 1000 [kNm] • k: 16'300 [kN/m]
M7: Complete finite element modelling of the entire structure **Description:** • Parabolic section profile • Finite element model (MAPS) with beams • Change of neutral axis position at mid-span • Features of sections provided by the civil engineer office that was commissioned to study the bridge (Realini & Bader) **Parameters:** • E: 30e-6 [kN/m^2] • I: from 5.501 to 151.543 m^4	***M8: Complete finite element modelling of the entire structure*** **Description:** • Parabolic section profile • Finite element model (MAPS) with beams • Change of neutral axis position at mid-span • Features of sections provided by the civil engineer office that was commissioned to study the bridge (Realini & Bader) • Hinges at mid-span **Parameters:** • E: 30e-6 [kN/m^2] • I: from 5.501 to 151.543 m^4

Table 11-5: Model description

11.2.3 An algorithm for finding best solutions in solution spaces

For models that include parameters which may have a range of values, we employ an algorithm called PGSL (Raphael and Smith 2000 [5]) for finding the best combination of values of parameters. The algorithm consists of minimising the root mean square difference which is calculated as the difference between the computed and measured values of parameters. For the Lutrive Bridge, this difference was minimised in separate runs for displacement, slope and curvature.

PGSL is a stochastic search algorithm based on the assumption that better points are more likely to be found in the neighbourhood of good ones. Points are generated randomly in the search space according to a probability density function (PDF) and they are evaluated using a user defined objective function. The user specifies the initial range of values of parameters.

The algorithm dynamically updates the PDF such that more intensive search is carried out in regions containing good solutions.

Results with PGSL algorithm for finding good solutions for Models 4 and 5 are shown below, Table 11-6.

Model No	**Parameters used in optimisation**	**Results with PGSL algorithm**				
		E [kN/m^2]	k [kN/m]	k1 [kNm/rad]	k2 [kNm/rad]	θ_{rig} [mrad]
4	displacement	50.00e6	28'076	9.99e19	2.8e-8	-
4	slope	28.34e6	15'625	9.96e19	2.64e-4	-
4	curvature	48.64e6	16'300	9.81e19	5.48 e5	-
5	curvature	48.64e6	16'300	9.81e19	5.48 e5	0.072

Table 11-6: Model calibration with PGSL algorithm (model calibration module, Fig. 8-4)

11.2.3.1 Results

Results for displacement, slope and curvature for the different models and for data measurement are shown in Fig. 11-10 and Fig. 11-11. Only displacement and curvature has been calculated for numerical models.

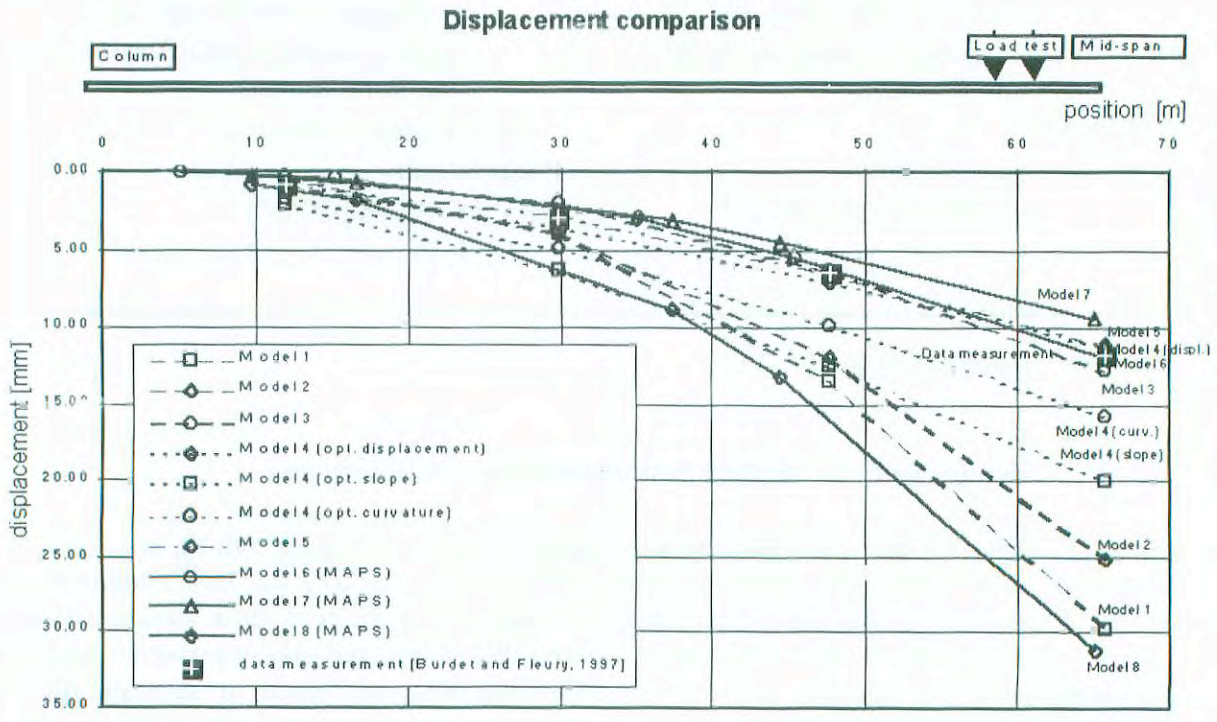

Fig. 11-10: Displacement comparison

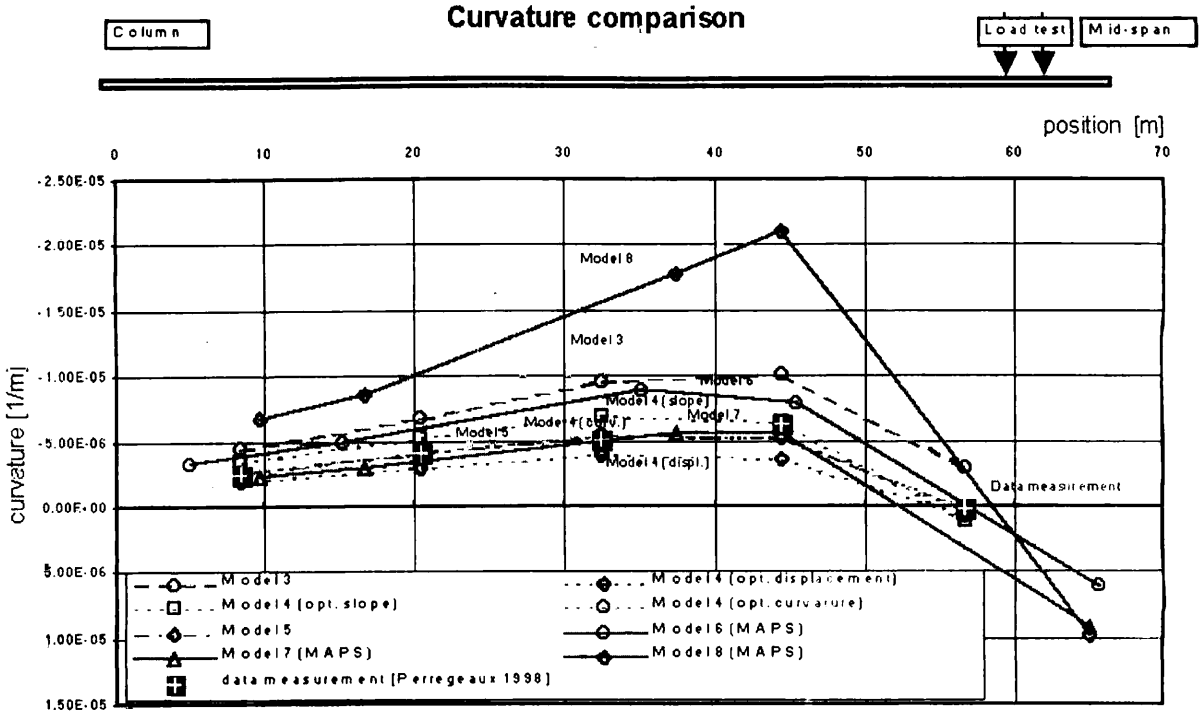

Fig. 11-11: Curvature comparison

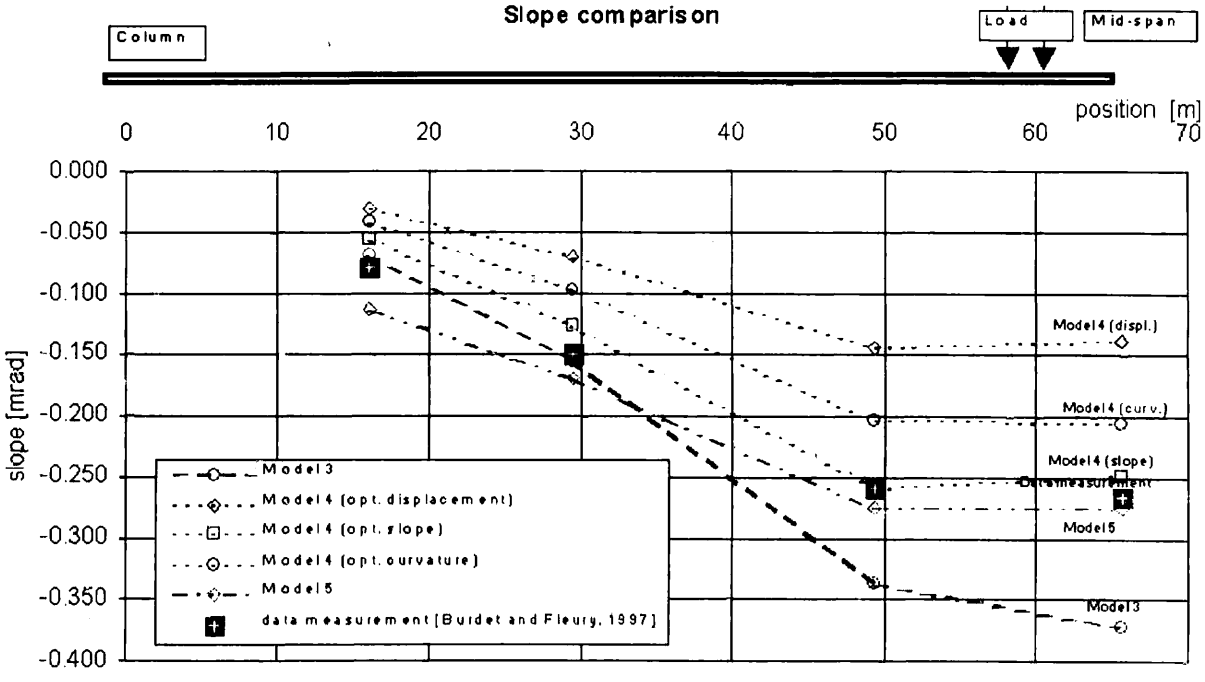

Fig. 11-12: Slope comparison

11.2.4 Analysis of results

The three figures are used to classify models based on the percentage deviation (PD) which is computed by dividing the root mean square difference by the mean value of data points. Models are classified as good (PD <25%), reasonable (PD 25-50 %) and bad (PD > 50 %) as shown in Table 11-7.

Model No optimisation criteria is given in brackets	**Criteria**		
	Displacement	Slope	Curvature
1	Bad	-	-
2	Bad	-	-
3	Good	Reasonable	Bad
4 (displacement)	Good	Bad	Reasonable
4 (slope)	Bad	Good	Reasonable
4 (curvature)	Bad	Reasonable	Good
5 (curvature)	Good	Good	Good
6	Good	-	Bad
7	Good	-	Reasonable
8	Bad	-	Bad

Table 11-7: Evaluation of models (Qualitative evaluation Module, Fig. 8-4)

11.2.5 References

1. O. Burdet, M. Badoux, *Long-term Deflection Monitoring of Prestressed Concrete Bridges Retrofitted by External Post-Tensioning – Examples from Switzerland*, IABSE Symposium "Structures for the Future – The Search for Quality", International Association for Bridge and Structural Engineering, Report Vol 83, 1999, pp. 112 - 114
2. N. Perregeaux, Pont de la Lutrive-N9, *Equipement et analyse du comportement au moyen du système de mesure à fibre optique SOFO*, Diploma Thesis, EPF-Lausanne, 1998
3. N. Perregaux, S. Vurpillot, J-S. Tosco, D. Inaudi, O. Burdet, *Vertical Displacement of Bridges Using the SOFO System: a Fiber Optic Monitoring Method for Structures*, ASCE-12th Engineering Mechanics. Conference Proceedings: A force for the 21st Century, 791-794, San Diego, USA, 1998
4. O. Burdet, B. Fleury, *Pont sur la Lutrive aval (VD)- Rapport d'essai de charge statique complémentaire*, EPFL-IBAP, 1997
5. B. Raphael, I. Smith, *A probabilistic search algorithm for finding optimally directed solutions*, in proceedings of Construction Information Technology 2000, Iceland building Research Institute, Reykjavik.

11.3 Structural analysis and safety assessment of existing concrete structures

Konrad Bergmeister (Professor) and Alfred Strauss (University Assistant)

Institute of Structural Engineering
University of Applied Sciences, Vienna, Austria

Vladimir Cervenka (Project Manager) and Radomir Pukl (Project Manager)

Cervenka Consulting, Prague, Czech Republic

Johann Kollegger (Professor) and Eva M. Eichinger (Research Assistant)

Institute for Structural Concrete
Vienna University of Technology, Vienna, Austria

Drahomir Novak (Professor)

Institute of Mechanics
Technical University, Brno, Czech Republic

11.3.1 Stochastic nonlinear analysis of a prestressed concrete bridge

In the following an example dealing with the probabilistic approach to nonlinear analysis of concrete structures is presented. The nonlinear finite element software ATENA developed by Cervenka Consulting in Prague is used for the simulation of damage and failure in concrete and reinforced concrete structures. It is based on advanced material models including damage concept, smeared crack approach and crack band theory with fracture energy-related softening. The uncertainties of the material properties as well as the loads, which form the input for the computational model, can sometimes be large. I order to get realistic results it is desirable to consider these variables not as deterministic values but as random variables taking into account their mean value, standard deviation and distribution type. Thus, the programs FREET and ATENA were integrated in order to randomize the fracture analysis of engineering structures as described in section 3 of this paper. The basic aim of statistical nonlinear fracture analysis is to obtain an estimation of the structural response statistics (failure load, deflections, cracks, stresses, etc.). Sensitivity and reliability analysis can be consequently performed. The applicability of this advanced engineering method is shown by the stochastic assessment of an existing pre-stressed bridge structure (Fig. 11-13).

The single span bridge to be assessed is located in Vienna, Austria and was built in 1977. It is a fully post-tensioned box-girder bridge made of 18 segments each with a length of 2,485 m. The total length of the bridge is 44.60 m, the width 6.40 m and the height 2.10 m (Fig. 11-14). The segmental joints are filled with epoxy resin. Due to an ongoing construction project the bridge has to be demolished. Before the demolition a range of non-destructive tests as well as a final a full-scale destructive load test will be performed. The presented stochastic simulation is part of the predictive numerical study for planning and optimizing the test setup. The segments were cast from concrete B500 and are reinforced with mild steel St 50. The post-tensioning tendons consist of 20 strands St 160/180. The bridge structure was analyzed using the stochastic nonlinear simulation package described above.

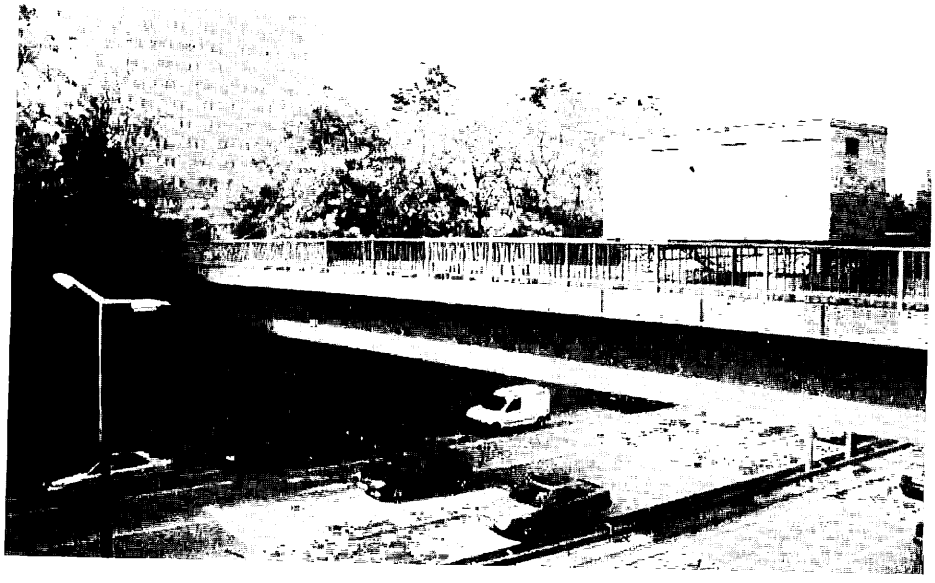

Fig. 11-13: Single-span box-girder bridge in Vienna, Austria

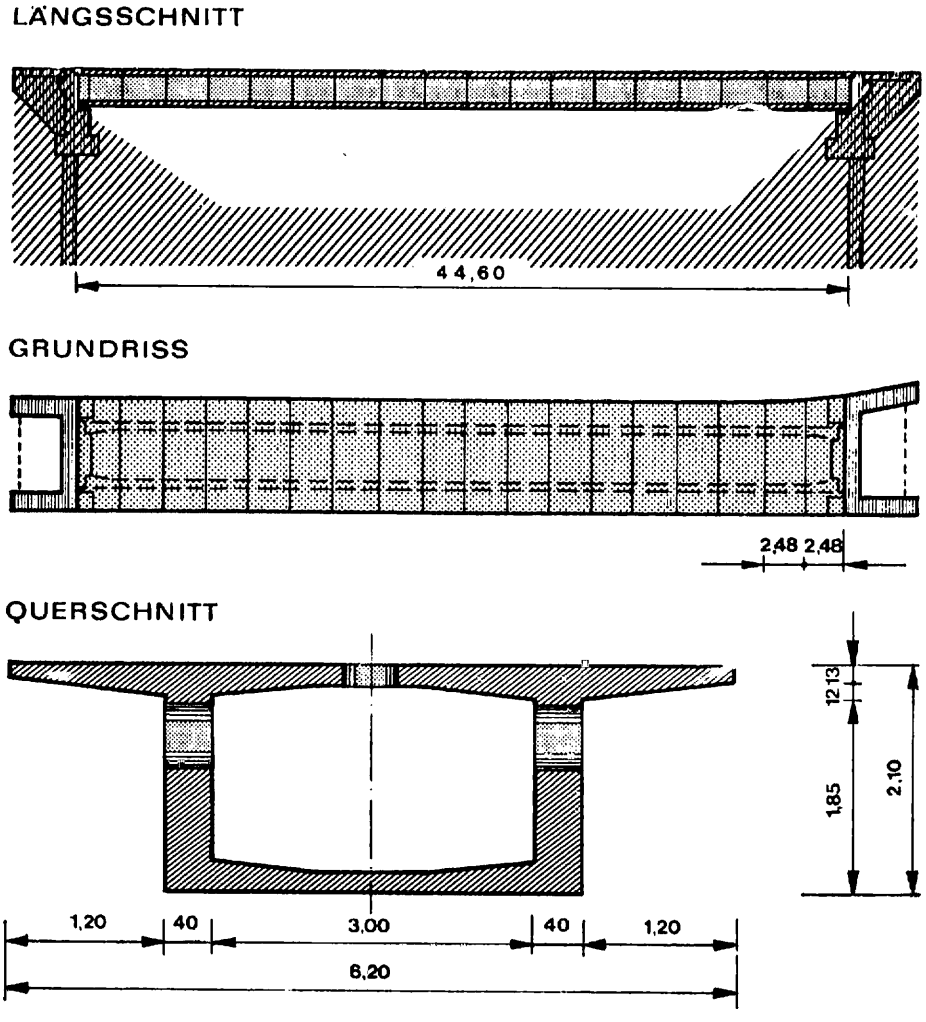

Fig. 11-14: Box-girder bridge in Vienna

11.3.1.1 Material properties for the stochastic analysis

Mean values of the material parameters for concrete B500 were generated using ATENA defaults (based on recommendations by CEB, fib, RILEM etc.).

Random variable description	Symbol	Units	Mean value	COV	Distribution type	Reference
Concrete grade B500						
Modulus of elasticity	E_c	GPa	36.95	0.15	Lognormal	Database
Poisson's ratio	μ	-	0.2	0.05	Lognormal	Estimation
Tensile strength	f_t	MPa	3.257	0.18	Weibull	Database
Compressive strength	f_c	MPa	42.5	0.10	Lognormal	Database, [9]
Specific fracture energy	G_f	N/m	81.43	0.20	Weibull	[10]
Uniaxial compressive strain	ε_c	-	0.0023	0.15	Lognormal	Database
Reduction of strength	c_{Red}	-	0.8	0.06	Rectangular	Estimation
Critical comp displacement	w_d	m	0.0005	0.10	Lognormal	Estimation
Specific material weight	ρ	MN/ m3	0.023	0.10	Normal	[11]
Prestressing strands						
Modulus of elasticity	E_s	GPa	200.0	0.03	Lognormal	[1]
Yield stress	f_y	MPa	1600.0	0.07	Lognormal	[1]
Prestressing force	F	MN	21.85	0.04	Normal	[11]
Area of strands	A_s	m^2	0.0237	0.001	Normal	[11]

Table 11-8: Statistical properties of random variables

The statistical properties of selected random variables considered in the study were collected from several sources (Joint Committee on Structural Safety 2000 [1], Mirza et al. 1997 [9], Wittmann 1994 [10], Al-Harthy and Frangopol 1994 [11]) including the database described in section 2 of this paper. The parameters are summarized in Table 11-8.

Statistical correlation among random variables was considered. Information on correlation of the variables can e.g. be found in references (Joint Committee on Structural Safety 2000 [1], Mirza et al. 1997 [9]). The prescribed correlation matrix for concrete material is in the upper triangle of Table 11-9. The correlation matrix generated by simulated annealing for 8 samples is shown in the lower triangle of Table 11-9. The correlation matrix generated for 32 samples contained almost the prescribed values.

Variable	E_c	f_t	f_c	G_f	ε_c
E_c	1	0.7	0.9	0.5	0.9
f_t	0.77	1	0.8	0.9	0.6
f_c	0.83	0.82	1	0.6	0.9
G_f	0.69	0.83	0.75	1	0.5
ε_c	0.84	0.77	0.83	0.69	1

Table 11-9: Correlation matrix for concrete properties

11.3.1.2 Nonlinear Finite Element analysis and selected results

The finite element model of symmetrical half of the box-girder is shown in Fig. 11-15. The bridge was pre-stressed and then loaded with prescribed displacement in the middle of the span. The ultimate failure load and the descending branch were obtained.

Fig. 11-15: Finite element model of the box-girder bridge

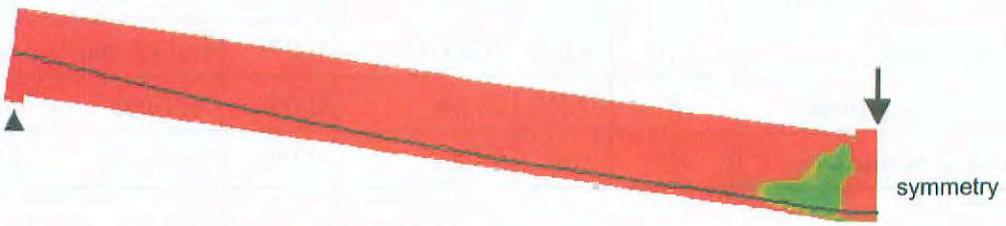

Fig. 11-16: Distribution of principal strains before failure

The bridge girder failed typically in the middle of the span. First the prestressing tendons yielded, tensile cracks developed, and the concrete in the compression flange of the box girder crushed and split. Fig. 11-16 shows a typical distribution of the principal strains shortly before failure on the deformed structure. The deformations are enlarged by a factor of 10.

Two stochastic simulations - with 8 and 32 samples - were performed and the structural response was evaluated (Fig. 11-17). The simulations resulted in an estimation of statistical characteristics of the ultimate load (Table 11-10), i.e. resistance of the structure R.

For reliability analysis a proper analysis of the load S has to be done in order to work with the limit state function $g = R - S$. If g is normally distributed, the reliability index can be estimated from mean value and standard deviation of g as $\beta = \mu_g / \sigma_g$.

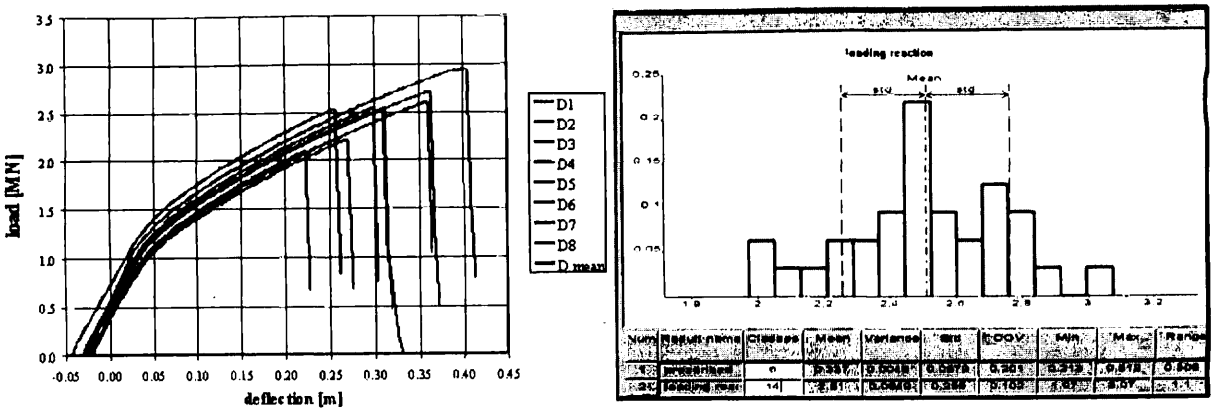

Fig. 11-17: left - load-deflection curves (8 samples), right - histogram of ultimate loads (32 samples

Number of samples	Mean value	Variance	Standard deviation	Coeff. of variation
	[MN]	[MN]	[MN]	-
8	2.52	0.0707	0.266	0.105
32	2.51	0.0649	0.255	0.102

Table 11-10: Estimation of basic statistical parameters of the ultimate load

Under assumption of normal probability distribution for both R and S a simple possibility of utilization of obtained statistical characteristics of ultimate load for reliability calculation can be drawn. Considering different levels of load S (mean values) and two alternatives of variability (coefficient of variation 0.1 and 0.2), reliability index is plotted in Fig. 11-18. The horizontal line represents target reliability index as specified by Eurocode (2001 [12]) (4.7 for 1 year).

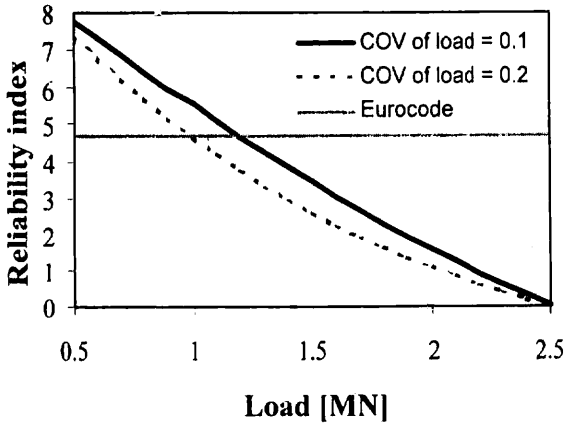

Fig. 11-18: Reliability assessment

11.3.2 Conclusions

Considering realistic material parameters as well as load parameters allows the design engineer to be much more precisely in the analysis of the overall behavior on an ultimate limit state. It can be concluded that the reliability index for existing structures is not only dependent on the material and load parameters but depends also on the mechanical model and the nonlinearity of the geometry and the material. This innovative concept allows us to analyze the safety of a structure including material, structural and stochastic nonlinearity. For the future a flexible safety margin of ß equal 2.5 – 4.7 for existing structures may be proposed (Ishida [14]).

11.3.3 References

1. Joint Committee on Structural Safety: *Probabilistic Model Code*, 12th draft, 10-11-2000
2. Ch. Petersen, *Der wahrscheinlichkeitstheoretische Aspekt der Bauwerkssicherheit im Stahlbau*; Deutscher Ausschuss für Stahlbau, Deutscher Stahlbautag, 1977
3. S.A. Mirza and J.G. MacGregor, *Variations in Dimensions of Reinforced Concrete Members*, Proc.ASCE, Journal of the Structural Division, Vol, No.ST4,1979
4. A.C.W.M. Vrouwenvelder and A.J.M. Siemens, *Probabilistic calibration procedures for the derivation of partial safety factors for the Netherlands Building Code*; HERON, Vol.32, No. 4, Stevin-Laboratory of the Faculty of Civil Engineering, Delft University of Technology, 1987
5. A. Hordijk, *Local approach to fatigue of concrete*, Thesis Technische Universiteit Delft.- With ref. With summary in Dutch, ISBN 90-9004519-8, NUGI 833
6. V. Cervenka, J. Cervenka, and R. Pukl, *ATENA – an Advanced Tool for Engineering Analysis of Connections*, *Connections between Steel and Concrete*, ed. R. Eligehausen, RILEM Publications, Ens, France, pp. 658-667, 2001
7. D. Novák et al., *FREET – Feasible Reliability Engineering Efficient Tool*, Program documentation, Brno University of Technology, Faculty of Civil Engineering, Institute of Structural Mechanics / Červenka Consulting, Prague, Czech Republic, 2002
8. D. Novák, B. Teplý, and Z. Keršner, *The Role of Latin Hypercube Sampling Method in Reliability Engineering*, Structural Safety and Reliability (ICOSSAR-97), Balkema, Rotterdam, The Netherlands, 1998
9. S.A. Mirza, M. Hatzinikolas, and J.G. McGregor, *Statistical descriptions of strength of concrete*, Journal of Structural Division, ASCE, Vol. 105, N. 6, pp. 1021-1037, 1979
10. F.H. Wittmann, V. Slowik, and A.M. Alvaredo, *Probabilistic aspects of fracture energy of concrete*, Materials and Structures, N. 27, pp. 499-504, 1994
11. A.S. Al-Harthy, and D.M. Frangopol, *Reliability assessment of prestressed concrete beams*, Journal of Structural Engineering, ASCE, Vol. 120, N. 1, pp. 180-199, 1994
12. Eurocode – Basis of structural design, CEN, Brussels, Belgium, (2001)
13. D. Novák, M. Vorechovský, V. Cervenka, and R. Pukl, *Statistical Nonlinear Analysis – Size Effect of Concrete Beams*, *Fracture Mechanics of Concrete Structures (FraMCoS 4)*, Eds. R. de Borst, Balkema, The Netherlands, pp. 823-830, 2001
14. T. Ishida, Documentation report on the achievements in the Ph.D. thesis entitled, *An integrated computational system of mass/energy generation, transport and mechanics of materials and structures*

11.4 Whole lifespan monitoring of the Versoix Bridge

Branko Glišic, Daniele Inaudi and Samuel Vurpillot

SMARTEC SA, Switzerland

11.4.1 Abstract

Civil structures are omnipresent in every society, regardless of culture, religion, geographical location and economical development. They affect human, social, ecological, economical, cultural and aesthetic aspects of societies. Therefore, no only good design and quality construction, but also a durable and safe exploitation of civil structures are imperative goals of structural engineering. The most safe and durable structures are usually those that are well managed. Measurement and monitoring have an essential role in structural management. In this paper, the importance and the benefits of monitoring during the whole lifespan of concrete bridges are presented.

The lifespan of a concrete bridge starts with construction – pouring of concrete. Follow curing of concrete, testing of the bridge and most importantly the service period. During service, the structure may be refurbished, strengthened or enlarged, according to necessities. Finally, at the end of exploitation, the bridge can be dismantled. Monitoring during each period of the bridge lifespan is important and can give rich information allowing a better understanding of structural behaviour and consequently better planned and less expensive management. In this paper, the importance of monitoring of each period of a concrete bridge's life is examined step by step, and illustrated an on-site example.

The benefits of the information obtained by monitoring are apparent in several domains. First, it helps to improve and enlarge the knowledge concerning structural behaviour and makes accurate calibration of numerical models describing and predicting this behaviour possible. Thus, project and construction can be optimised in structural and economical aspects. Second, permanent monitoring can give early indications of structural malfunctioning. In this way, safety measures can be considered in time, and intervention on the structure can be performed immediately and with minimal economic looses.

The design, installation and use of a monitoring system for lifespan monitoring of the Versoix concrete bridge in Switzerland, is presented in this case study.

11.4.2 Introduction

Monitoring (or auscultation) of structures involves recording of time dependent parameters during certain periods. These parameters are related to the construction material (concrete, steel, timber, etc.) and to the structure itself. In both cases they can be physical, mechanical or chemical.

The life of a concrete bridge starts with construction – pouring of concrete. Follow curing of concrete, testing of the bridge and most importantly the service period. During service, the structure may be refurbished, strengthened or enlarged, according to necessities. Finally, at the end of exploitation, the bridge can be dismantled. Monitoring during each period of the bridge lifespan is important and can give rich information allowing a better understanding of structural behaviour and consequently better planned and less expensive management.

In the next paragraphs we will explain generally and through examples, importance and benefits of monitoring performed during each phase of the structure life.

11.4.3 Whole lifespan monitoring of bridges

The importance of whole lifespan monitoring is highlighted in this section.

11.4.3.1 Monitoring during construction of a new bridge

Construction is a very delicate phase in the life of structures. For concrete structures, material properties change through ageing. It is important to know whether or not the required values are achieved and maintained. Defects (e.g. premature cracking) that arise during construction may have serious consequences on structural performance. Monitoring data help engineers to understand the real behaviour of the structure and this leads to better estimates of real performance and more appropriate remedial actions.

Important information obtained through monitoring during construction includes the following: Estimation of hardening time of concrete in order to estimate when shrinkage stresses begin to be generated (Glisic 2000 [4]); Deformation measurements during early age of concrete in order to estimate self-stressing and risk of premature cracking (Frangopol et al. 1998 [3]); When structures are constructed in successive phases, measurement can help to improve the composition of concrete when necessary. In case of pre-fabricated structures, sensors may be useful for quality control; Optimisation between two successive phases of pouring due to evaluation of cure in previous phases; For prestressed structure, deformation monitoring of cables helps to adjust prestressing forces and determine the relaxation (Idriss 2002 [6]); Monitoring of foundation settlement helps to understand the origins of built-in stresses; Damage caused by unusual loads such as thunderstorm or earthquakes during construction may influence the ultimate performance of structures; Optimal regulation of structural position during erection (Vohra 1998 [7]); Knowledge improvement and recalibration of models (Bernard 2000 [8]).

The installation of a monitoring system during the construction phases allows monitoring to be carried out during the whole life of the structure. Since most structures have to be inspected several times during service (SIA [9]), the best way to decrease the costs of monitoring and inspection is to install the monitoring system from the beginning.

11.4.3.2 Monitoring after refurbishing, strengthening or enlargement of bridge

Material degradation and/or damage are often the reasons for refurbishing existing structures (Inaudi et al. 2000 [10]). Also, new functional requirements for the bridge (e.g. enlarging) lead to requirements for strengthening (Inaudi et al. 1999 [11]). If strengthening elements are made of new concrete, a good interaction of new concrete with the existing structure has to be assured. Early age deformation of new concrete creates built-in stresses and bad cohesion causes delamination of the new concrete, thereby erasing the beneficial effects of the repair or strengthening efforts.

Since new concrete elements observed separately represent new structures, the reasons for monitoring them are the same as for new structures, presented in previous subsection. The determination of the success of refurbishment or strengthening is an additional justification (Inaudi et al. 1999 [11]).

11.4.3.3 Monitoring during bridge testing

Bridges have to be tested before service for safety reasons (Inaudi et al. 1999 [11]). At this stage, the required performance levels of structures have to be reached. Typical monitored parameters (such as deformation, strain, displacement, rotation of section and cracks opening) are measured. Tests are performed in order to understand the real behaviour of the structure and to compare it with theoretical estimates (Hassan 1994 [12]). Monitoring during this phase can be used to calibrate numerical models describing the behaviour of structures (Bernard 2000 [8]).

11.4.3.4 Monitoring during service

The service phase is the most important period in the life of a structure. During this phase, construction materials are subjected to degradation by ageing. Concrete cracks and creeps, steel oxidises and may crack due to fatigue loading. The degradation of materials is caused by mechanical (loads higher then theoretically assumed) and physico-chemical factors (corrosion of steel, penetration of salts and chlorides in concrete, freezing of concrete etc.). As a consequence of material degradation, the capacity, durability and safety of structure decrease.

Monitoring during service provides information on structural behaviour under predicted loads (Inaudi et al. 1999 [11]), and also registers the effects of unpredicted overloading. Data obtained by monitoring are useful for damage detection, evaluation of safety and determination of the residual capacity of structures. Early damage detection is particularly important because it leads to appropriate and timely interventions. If the damage is not detected, it continues to propagate and the structure no longer guarantees required performance levels. Late detection of damage results in either very elevated refurbishment costs[1] or, in some cases, the structure has to be closed and dismantled. In seismic areas the importance of monitoring is most critical.

Subsequent auscultation of a structure that has not been monitored during its construction can serve as a basis for understanding of present and for prediction of future structural behaviour (Hassan 1994 [12]). This is discussed next.

11.4.3.5 Monitoring during dismantling of bridge

When the structure does no longer respond to the required performances and the costs of reparation or strengthening are excessively high, the ultimate lifespan of the structure is attained and the structure should be dismantled. Monitoring helps to dismantle structures safely and successfully.

11.4.4 Example of whole lifetime monitoring: the Versoix Bridge

The North and South Versoix bridges are two parallel twin bridges (Inaudi et al. 1999 [11]). Each one supported two lanes of the Swiss national highway A9 between Geneva and Lausanne. In order to support a third traffic lane and a new emergency lane, the exterior beams were widened and the overhangs extended (see Fig. 11-19).

Because of the added weight and pre-stressing, as well as the differential shrinkage between new and old concrete, the bridge bends (both horizontally and vertically) and twists during the construction phases. In order to increase the knowledge on the bridge behaviour and performance and to optimise the concrete mix, the engineer decide to monitor strain,

displacement and temperature over whole lifespan of the bridge. The SOFO monitoring system (www.smartec.ch [14], Inaudi 1997 [15]) (see Fig. 11-20), based on low-coherence interferometry in the optical fibres (Inaudi 1997 [15]), was selected for this purpose, since its performances meet the requirements for whole lifespan monitoring.

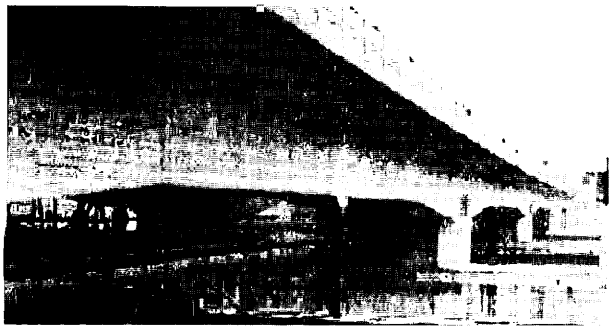

Fig. 11-19: View to Versoix Bridge before enlargement

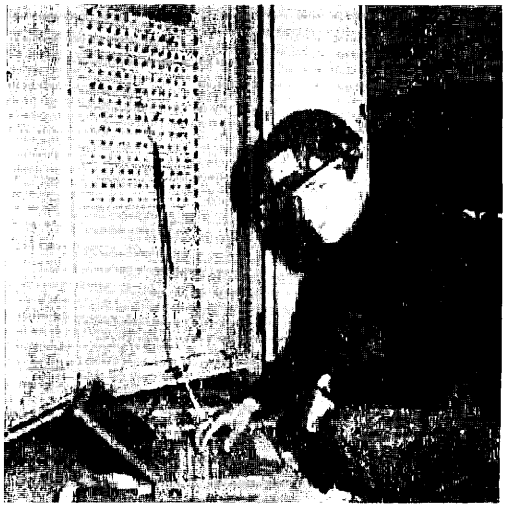

Fig. 11-20: SOFO system reading unit

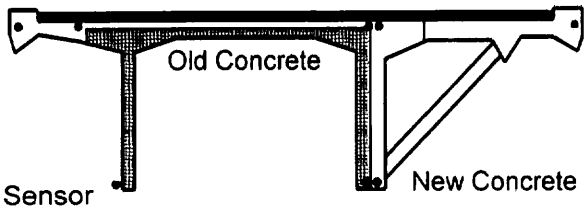

Fig. 11-21: Position of sensors in cross-section

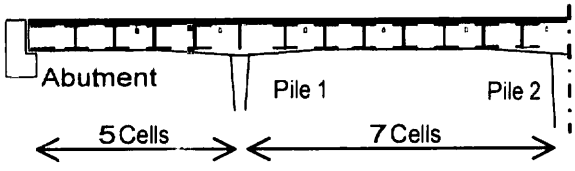

Fig. 11-22: Longitudinal position of sensors

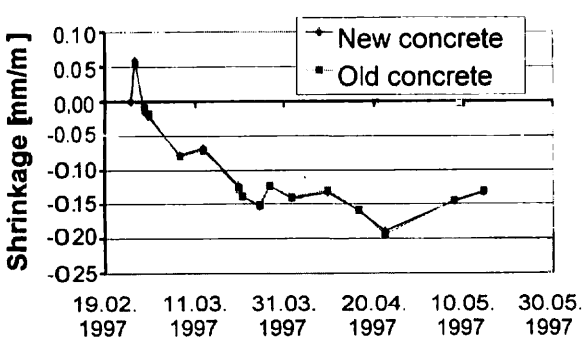

Fig. 11-23: Old-new concrete interaction monitoring

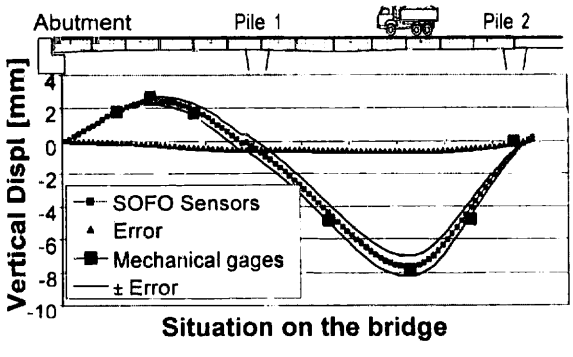

Fig. 11-24: Monitoring during the load test

The sensors ware surface mounted onto the existing (old) part of the bridge and embedded into the fresh concrete of the new part of the bridge. Eight sensors per cross-section were installed as shown in *Fig. 11-21*, and total of 12 sections is equipped as shown in *Fig. 11-22*. The

sensors are connected to reading unit by means of intermediate connection boxes and multi-fibre extension cables. The central measurement point with the reading unit is situated near the abutment and is shown in Fig. 11-20.

11.4.4.1 Monitoring during and after enlargement

The main concern during the construction was to ensure good interaction between old and new concrete. In order to control the interaction, the sensors are installed side-by-side in new and old concrete (see Fig. 11-20). Monitoring performed during more than two months after the pouring shown that both sensors measured the same deformation and thus the interaction between the old and new concrete is estimated as a very good. In addition horizontal deflection due to unequal heat on left and right side of the cross-section and different pouring times is detected (see Fig. 11-25). An example of measurements is presented in Fig. 11-23.

11.4.4.2 Monitoring during testing of bridge

During a load test, performed in Mai 1998 after the end of construction works, the vertical displacement of the bridge was also monitored using the same fibre optic sensors. Fig. 11-24 shows an example of the measurement taken during the load test of the bridge. Values obtained with SOFO sensors are calculated using double integration of curvature [16]. Measurements were also performed using dial gages (invar wires installed and measured by IBAP-EPFL under the bridge) and are presented in the same figure. Results of test confirmed the design performances of enlarged bridge.

11.4.4.3 Monitoring during service of bridge

Long-term monitoring of the Versoix Bridge continues. Monthly quasi-static measurements are performed in order to monitor strain and displacement evolution of the bridge. Five years strain evolution of a cross-section is presented in Fig. 11-25. After the cross-section is bended horizontally due to unequal heat and different time of concrete pouring, all sensors measures approximately same deformation confirming that the cross-section is not exposed to unexpected bending due to damage or delamination.

In Fig. 11-26 diagrams of strain obtained by measurements (sensor A11) are compared with the models (Strain – calc. Shrinkage + temperature) and very good accordance is observed confirming good design and realisation of the bridge. The evolution of shrinkage is not finished but it is stabilised (see Fig. 11-26). The seasonal temperature variation influenced behaviour of the bridge and can also be seen in Fig. 11-26.

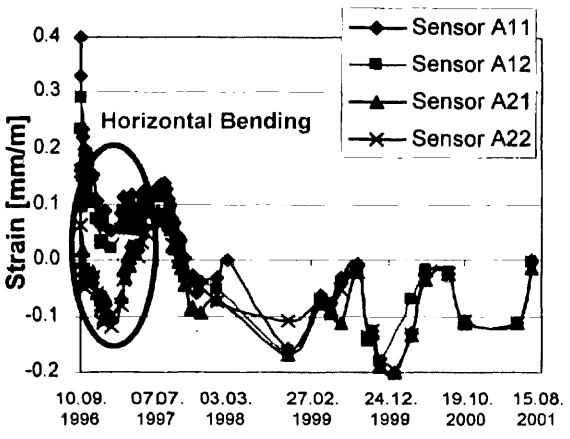

Fig. 11-25: Versoix bridge five-years strain evolution

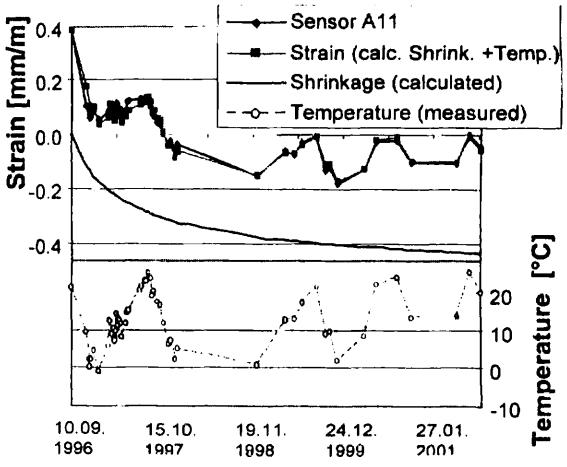

Fig. 11-26: Uncoupling of shrinkage and temperature

11.4.5 Conclusions

The whole lifespan monitoring comprehends continuous or periodical registering of parameters including all phases of the structure life. The benefits of whole lifespan monitoring of bridges are presented in this paper. They reflect through better planned and less costly structural management, increase of safety and improvement of knowledge concerning real structural behaviour. The whole lifespan monitoring calls for sophisticated monitoring systems, which performances satisfy safety, technological, economical and esthetical aspects, being easy to use, fast to install, durable, reliable, stable, independent from human intervention and insensitive to external influences.

The advantages of whole lifespan monitoring are illustrated by real on-site example, carried out using SOFO monitoring system installed onto the Versoix Bridge in Switzerland. The benefits gathered the each phase of the bridge's life are presented and they fully justify the whole lifespan-monitoring concept.

11.4.6 References

1. S. Radojicic, E. Bailey, E. Brühwiler, *Consideration of the Serviceability Limit State in a Time Dependant Probabilistic Cost Model*, in Application of Statistics and Probability, Vol. 2, pp 605-612, Balkema, Rotterdam, Netherlands,1999
2. I. F. Markey, Enseignements tirés d'observations des déformations de ponts en béton et d'analyses non linéaires, Ph.D. Thesis N° 1194, EPFL, Lausanne, Switzerland (1993)
3. D. M. Frangopol, A. C. Estes, G. Augusti, M. Ciampoli, *Optimal bridge management based on lifetime reliability and life-cycle cost*, Short course on the Safety of Existing Bridges, ICOM&MCS, pp 112-120, EPFL, Lausanne, Switzerland (1998)
4. B. Glisic, *Fibre optic sensors and behaviour in concrete at early age*, Ph.D. Thesis N° 2186, EPFL, Lausanne, Switzerland (2000)
5. S. Vurpillot, D. Inaudi, J.-M. Ducret, *Bridge monitoring by fiber optic deformation sensors: design, emplacement and results*, SPIE, Smart Structures and materials, Vol 2719, pp. 141 - 149, San Diego, USA, (1996)
6. R. L. Idriss, *Nondestructive Evaluation for Lifetime Bridge Assessment: From Construction to Service*, 81st Annual Meeting of the Transportation Research Board (TRB), Washington DC, USA (2002)

7. S.T. Vohra, B. Althouse, G. Johnson, S. Vurpillot, D. Inaudi, *Quasi-Static Strain Monitoring During the "Push" Phase of a Box-Grider Bridge Using Fiber Bragg Grating Sensors*, European Workshop on Fiber Optic Sensors, Peebles, Scotland, (1998)
8. O. Bernard, *Comportement à long terme des éléments de structures formés de bétons d'âges différents*, Ph.D. Thesis N° 2283, EPFL, Lausanne, Switzerland (2000)
9. SIA 462, Swiss norms
10. D. Inaudi, N. Casanova, S. Vurpillot, B. Glisic, P. Kronenberg, S. Lloret, *Deformation monitoring during bridge refurbishment under traffic*, 16th Congress of IABSE, Luzern, Switzerland, on CD,(2000)
11. D. Inaudi, P. Kronenberg, S. Vurpillot, B. Glisic, S. Lloret, *Long-term monitoring of a concrete bridge with 100+ fiberoptic long-gage sensors*, SPIE, Conf. Nondestructive Evaluation Techniques for Aging Infrastructure & Manufacturing, Vol 3587-07, Newport Beach, USA (1999)
12. M. Hassan, *Critères découlant d'essais de charge pour l'évaluation du comportement des ponts en béton et pour le choix de la précontrainte*, Ph.D. Thesis N° 1296, EPFL, Lausanne, Switzerland (1994)
13. S. Vurpillot, G. Krueger, D. Benouaich, D. Clément, D. Inaudi, *Vertical Deflection of a Pre-Stressed Concrete Bridge Obtained Using Deformation Sensors and Inclinometer Measurements*, ACI Structural Journal, Vol. 95, No. 5, Sptember-October 1998
14. www.smartec.ch
15. D. Inaudi, *Fiber Optic Sensor Network for the Monitoring of Civil Structures*, Ph.D. Thesis N° 1612, EPFL, Lausanne, Switzerland (1997)
16. S. Vurpillot, Analyse automatisée des systèmes de mesure de déformation pour l'auscultation des structures, Ph.D. Thesis N° 1982, EPFL, Lausanne, Switzerland (1999)

11.5 Structural monitoring and evaluation of the Colle Isarco Viaduct (A22, Italy)

Konrad Bergmeister, Ulrich Santa, Alfred Strauss

Institute of Structural Engineering, Vienna, AUSTRIA

11.5.1 Introduction

The condition assessment of aged structures is becoming a more and more important issue for civil infrastructure management systems. The continued use of existing systems is, due to environmental, economical and socio-political assets, of great significance growing larger every year. The performance of many of these in-service structures has decayed over the years of utilization and the inherent level of safety might be inadequate relative to current design documents. Structural integrity has to be guaranteed by the structural safety under ultimate and serviceability conditions in order to ensure the safety of the structure and its users. For the purpose of developing adequate life extension and replacement strategies, issues such as whole-life performance assessment rules, target safety levels and optimum maintenance strategies must be formulated and resolved from a lifetime reliability viewpoint and lifecycle cost perspective (Frangopol 2000 [12]).

In front of this background we find the necessity to identify the key parameters and procedures to verify and update the knowledge about the present condition of a structure with respect to a number of aspects. A visual inspection may yield a first qualitative, maybe purely intuitive impression. A better judgment would be based on the evaluation of acquired quantitative information. Recent progress in the development of sensing technologies and material/structure damage characterization combined with current data processing techniques have resulted in a significant interest in diagnostic tools to monitor structural integrity and to detect structural degradation. Adequate monitoring techniques provide qualitative and quantitative knowledge that facilitates more precise condition assessments and resulting maintenance interventions. This includes the observation of mechanical parameters such as loads, strains, displacements and deformations as well as environmentally induced processes such as corrosion. Therefore, the development of monitoring concepts on a continuous time basis for structural components and for the global behavior is fundamental for guaranteeing structural integrity.

11.5.2 Instrumentation

The definition of the objective of the instrumentation program usually follows the realization that something about the structure is not known well enough and that measurements of a number of quantities at a certain location would be desirable for the sake of economy or safety. The first step is to reflect on all possible ways the construction might respond to externally induced actions and to choose which quantities to measure, where to measure them, and to select adequate instruments to do so. This requires an estimation of the magnitudes of changes in the quantities to be measured, which allows the definition of the range, resolution, accuracy, and sensitivity of the instruments selected to measure them. As next the instrument positions and the number of instrumented sections have to be determined. Instruments can be installed in trouble spots, such as points where it is e.g. expected that there will be large stress concentrations or points where it is supposed that deficiencies have already initiated. Alternatively, the instruments can be placed at a number of representative points or zones of the structure (Inaudi 1999 [3]). After testing, the taking of the readings and

their processing and analysis must be carried out in a systematic, organized way (Aktan et al. 1997 [11]). In the following sections we will describe the monitoring equipment that was installed on Colle Isarco viaduct on the Italian Brennero-Highway A22 (Fig. 11-27). The overall length of the instrumented section is 378 m. The maximum height of the box girders near the supports number 8 and 9 is 11 m, having a uniform width of 6 m. the arrangement for each roadbed is approximately 11 m wide. The height of the 4 supporting piles No. 7, 8, 9 and 10 is 33m, 75m, 60m and 60m respectively. The bridge was built in 1969 and was upgraded through an essential rehabilitation and maintenance intervention in 1999.

11.5.3 Deformation and displacement

When forces are applied to a structure, the components of the structure change slightly in their dimensions and are said to be strained and they may even underlie a certain translational or rotational displacement. Creep, shrinkage, and seasonal temperature changes may result in overall length changes of a bridge or components of a bridge. The measurement of deformation can be approached either from the material or from the structural point of view (Inaudi 1999 [3]). On the one hand, observation of local material properties made by a series of short base-length strain sensors can be extrapolated to the global behavior of the whole structure. While strain sensors on a short base length are usually used for material monitoring rather than structural monitoring, long-gauge sensors give information on the behavior and response of structure. However, material degradations like cracking are only detected when they have an impact on the shape of the structure. Further, longer base-lengths help to reduce misleading measurements stemming from material non-homogeneities.

A good representative of long base-length fiber optic deformation sensors is the SOFO measurement technique developed by Inaudi et Al. [2,3,4]. This measuring system is based on the principle of low-coherence interferometry (Fig. 11-29). The infrared emission of a light emitting diode is launched into a standard single mode fiber and directed, through a coupler, towards two fibers mounted on or embedded in the structure to be monitored. The measurement fiber is in mechanical contact with the structure itself and will therefore follow its deformations in both elongation and shortening. The second fiber, called reference fiber, is installed free in the same pipe. Mirrors, placed at the end of both fibers, reflect the light back to the coupler, which recombines the two beams and directs them towards the analyzer. This is also made of two fiber lines and can introduce a well-known path difference between them by means of a mobile mirror. On moving this mirror, a modulated signal is obtained on the photodiode only when the length difference between the fibers in the analyzer compensates the length difference between the fibers in the structure to better than the coherence length of the source. This type of sensor has resolution and sensitivity of 2 microns and is, like most fiber optic devices, insensitive to temperature, humidity, vibration, corrosion, and electromagnetic fields. Additionally, these sensors are easy and fast to install, embeddable in concrete, mortars, surface mountable on concrete, metallic or timber structures.

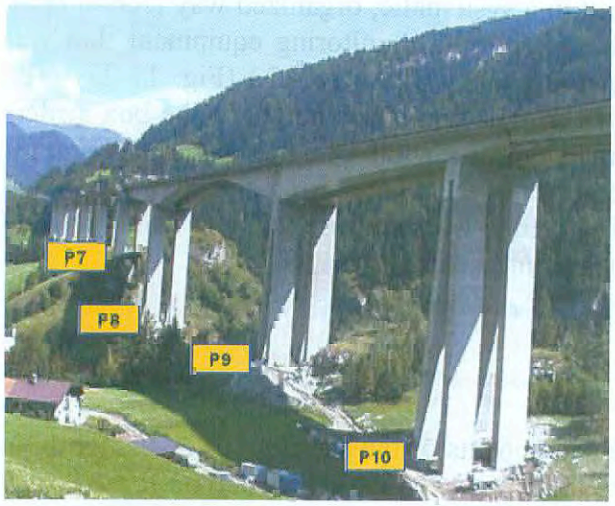

Fig. 11-27: Monitored section of the Colle Isarco Viaduct

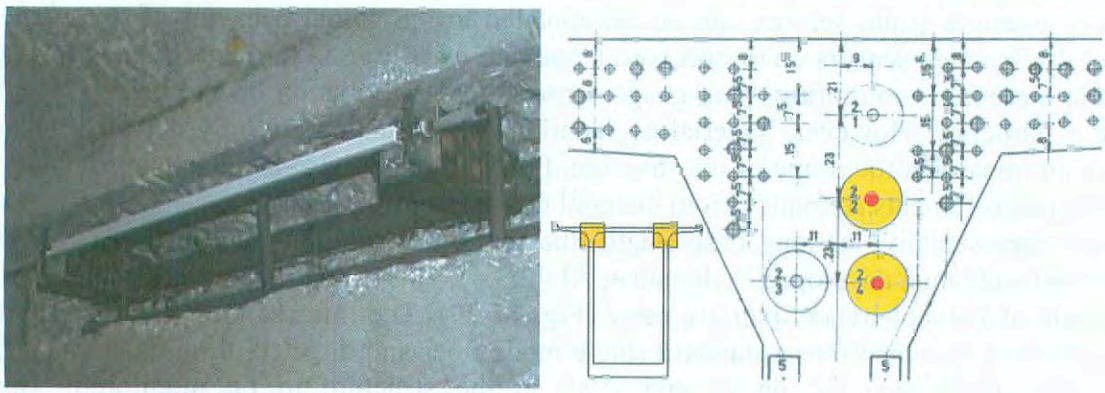

Fig. 11-28: Instrumentation setup of prestessing steel Dywidag ∅32 ST 85/105

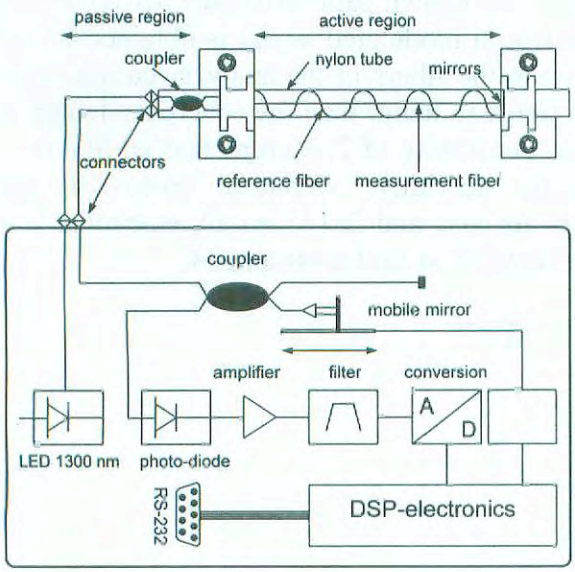

Fig. 11-29: Deformation sensor SOFO

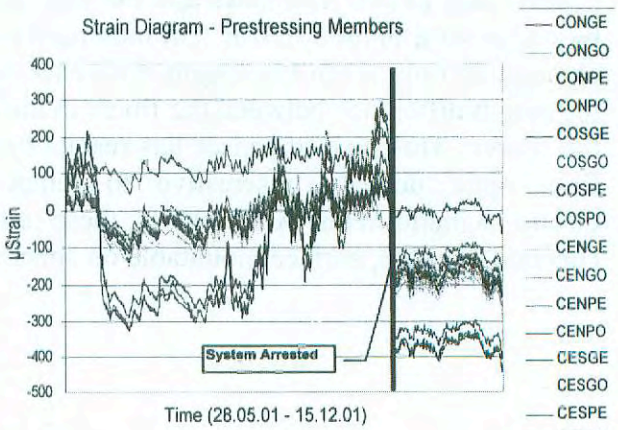

Fig. 11-30: Strain evolution of prestessing members Dywidag ∅32 ST 85/105

In the present monitoring system, a network of this type of sensor was installed for strain and deformation measurements. 96 fiber optical SOFO-Sensors with a base length of 10 m were installed on the concrete surface parallel to the neutral axis of the box girders in order to determine the vertical, horizontal, and torsional deformations. Sensors with a base length of 0,5 m were used to measure the strains of 16 selected prestressing members (Dywidag ∅32 ST 85/105, Fig. 11-28, Fig. 11-30). Another 24 sensors with a base length of 8 and 10 m were installed on the piles P7 and P8 (Fig. 11-27).

The Fig. 11-30 shows the strain evolution for the period of approximately 6 months. By a continuous observation of the strain evolution, eventual prestressing losses and associated failures should be detectable in the domains of both short and long-term stresses. Due to a stroke of lightning the system was out of order for a couple of weeks, as indicated by the vertical red line in Fig. 11-30. Nevertheless, the strain values beyond this hazard refer to the reference measurement campaign performed on the 28.05.01, 10:00 am.

The same evaluation of strain can be made for the 96 sensors installed parallel to the neutral axis on the concrete surface of the box girders as well as for the 24 sensors installed on the piles P7 and P8. In order to separate the influence of thermal gradients in the structure and other agents (traffic, snow, wind), 60 thermocouples (T-Type, embedment depth 200 mm) have been installed in the girders and on the piles P7 and P8. Further, 10 LVDTs have been installed to instrument movements on the bearings (Fig. 11-34).

The measurement of vertical deflections of long-span girders is a task for which no simple method or sensing unit exists. Current methods to measure deflections, such as e.g. triangulation, hydrostatic leveling, laser-based leveling, differential GPS, etc., are often tedious to install and require an accurate elaboration. The determination of deflection by the use of displacement transducers requires a stable accessible reference location for each measurement and is, for most bridges, not practical.

A more suitable method was developed by Inaudi et Al. [2,3,4], where the vertical displacement and curvature profile can be measured by the use of a network of fiber optic deformation sensors placed on the structure. This method is described in more detail in Chapter 7.4

Evaluation of relative deformation measurements.

By applying this approach to the measurements taken on the box girders of the Colle Isarco Viaduct, we obtain e.g. the 24 hour deflection behavior (07.06.01) for the cantilever beam ESP (Fig. 11-32):

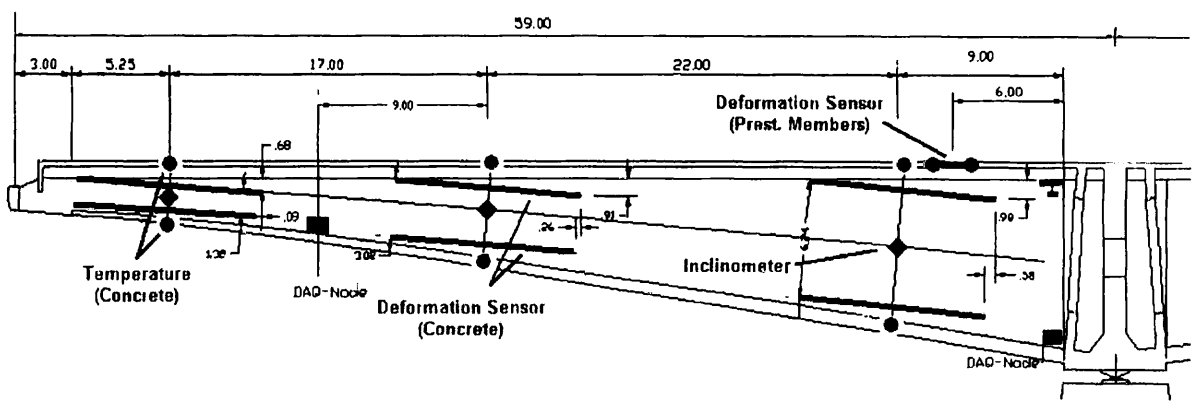

Fig. 11-31: Instrumentation detail of girder ESP

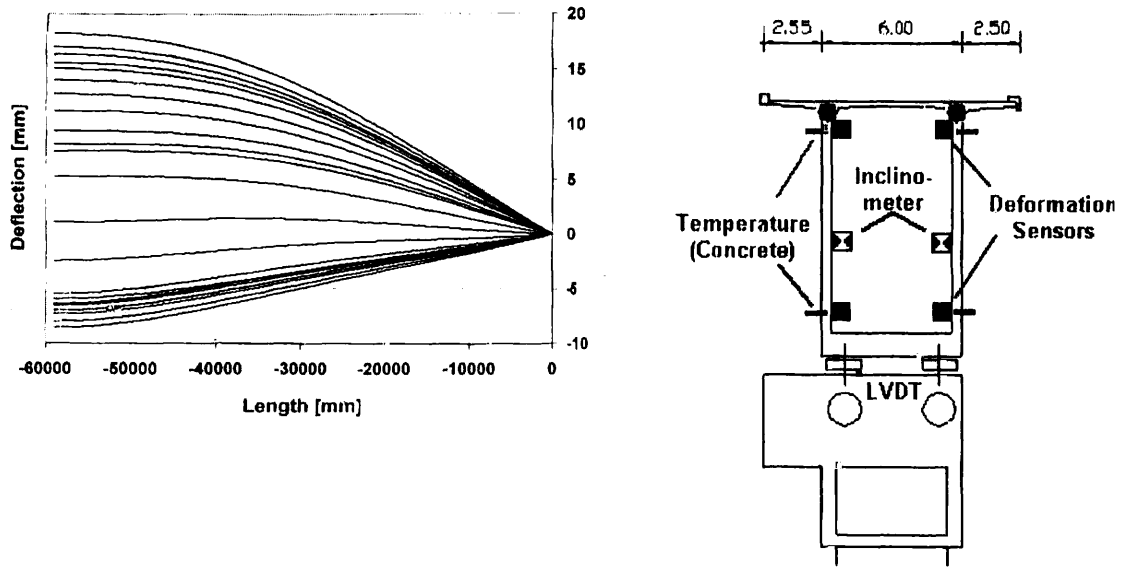

Fig. 11-32: Vertical deflection – 24h behavior of cantilever ESP on 07.06.2001

Another approach that found application on the Colle Isarco Viaduct was the installation of 36 highly accurate (resolution and threshold: 0.00005°) LCF-100 inclinometers from WPI Instruments. These sensing devices can be used for both short-term and long-term measurements (Burdet 1993 [10]). On the one hand, these inclinometers complete the fiber optical network with information on the rigid body displacements of the structure. On the other hand, given a sufficient number of sensors, vertical deflections can immediately be determined by the simplified relation $h_i = \sin(\tau_i) * l_i$, where h_i denotes the vertical deflection of a section i with length l_i, where a rotation of τ_i was measured. Alternatively, a similar algorithm as described above (Vurpillot et al. 1998 [1]) might find application for a more precise representation.

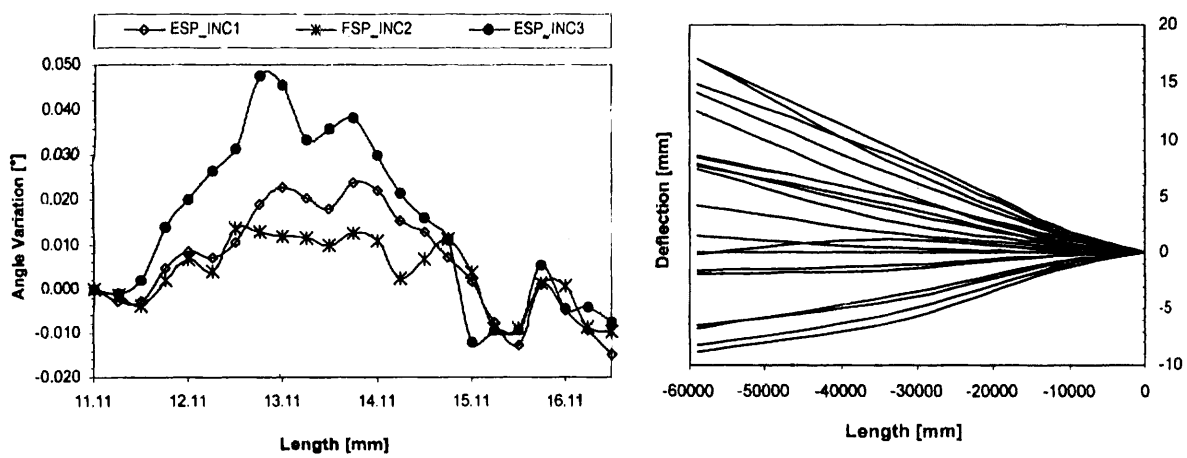

Fig. 11-33: Inclinometer measurements: 1 week behavior of cantilever ESP (11.11.01 – 17.11.01)

11.5.4 Durability monitoring

Steel embedded in good quality concrete is protected by the alkalinity of the concrete pore water. However, penetration of aggressive ions, as e.g. chloride from deicing salt or carbonate from acid rain, will destroy the passivation of the embedded steel. In the presence of oxygen and the right humidity level in the concrete, corrosion of the steel will start and develop continuously (Rostam 1992 [9]). This category of measurements is based on the electrochemical nature of corrosive processes that is comparable to the anode and cathode principle (Zimmermann et al. 1997 [5]).

Several methods have been developed for detecting and evaluating the effects of steel corrosion in concrete. These methods include visual inspection, chaining or sounding for delamination, pH level determination, potential measurements, polarization techniques, and x-ray spectography. The easiest and most straightforward method for detecting steel corrosion in reinforced and prestressed concrete structures is the visual inspection for rust staining and cracking (Rostam 1992 [9]). Rust stains that follow the line of reinforcement clearly indicate steel corrosion. When corrosion progresses further, cracking of the steel concrete cover occurs.

Another approach is the chloride determination, a method that establishes the likelihood as to whether or not corrosion is occurring. The significance of a chloride analysis lies within the spectrum of simply determining that the concentration is sufficient to cause steel to change from a passive to an active corrosion state. Beyond the threshold value of chloride concentration necessary to cause corrosion, the rate of corrosion is a function of many variables, but in particular of moisture content. Therefore, even though a bridge slab may have more chlorides than the threshold value, it may not be in an active state when considering ambient and environmental factors which are necessary for corrosion. Likewise, if a bridge deck is in an active corrosion state, additional amounts of chlorides may have little effect on the corrosion (CEB TG 5.4 1998 [7]).

For an electrochemical mechanism such as galvanic corrosion to occur, there must be a potential difference. Potential methods such as the half cell potential method rely on this known condition for corrosion detection. In particular, the half cell potential method measures voltage gradients or drops by use of a high-impedance voltmeter and a constant voltage reference cell. The reference cell possesses a constant internal voltage, which allows voltage changes existing on the reinforcement to be measured. This method provides both an effective means for determining if corrosion is occurring and the extent of corrosion distress. However, if corrosion has occurred and then was arrested by some means, the method proves ineffective in detecting this. Nevertheless, this method is applicable for members regardless their size or the depth of cover over the reinforcing steel. It can be used in structures that show no visible signs of distress to determine when corrosion initiates, or in a structure which shows sever corrosion distress to determine the extent of corrosion.

On 4 selected columns of the Colle Isarco viaduct 12 electrochemical multiprobes have been installed to determine the concentration of free chlorides, corrosion current and the electrochemical potentials at different embedding levels (Fig. 11-35, Fig. 11-39). These multiprobes have been developed at the IBWK/ETHZ by Zimmermann, Schiegg, Elsener, and Böhni [5,6]. After 18 month of measurements, the results show, that the applied rehabilitation concept (cathodic protection through installation of a zinced mesh) proves to work in the expected way.

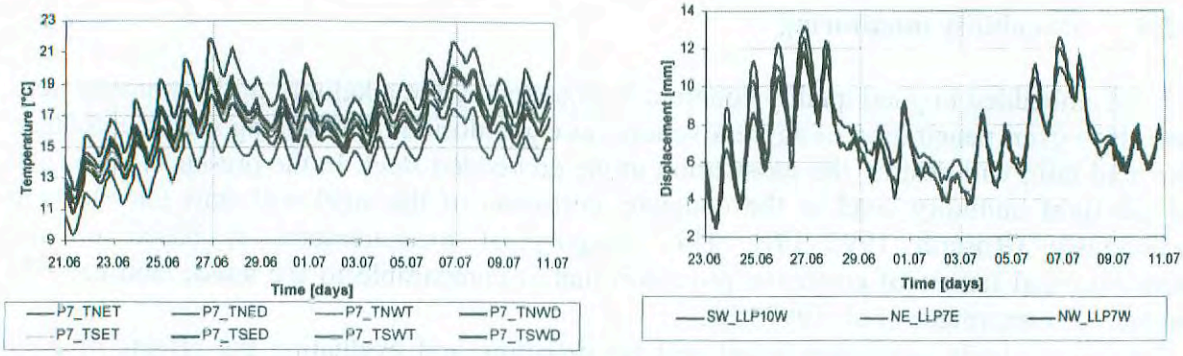

Fig. 11-34: Temperature distribution and horizontal bearing movements on Pile P7

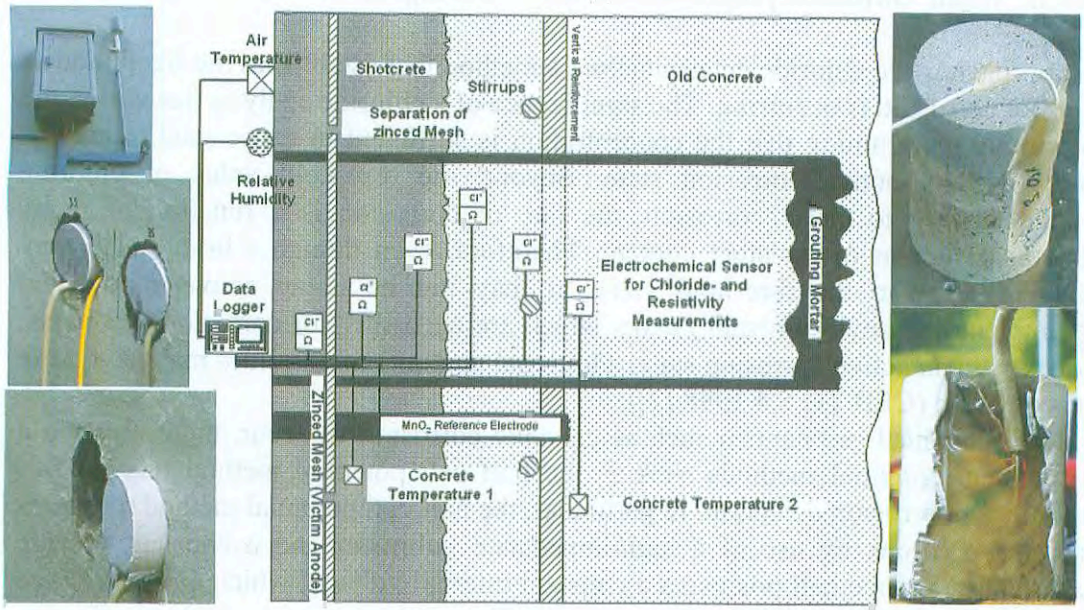

Fig. 11-35: Corrosion sensor unit developed by Zimmermann, Schiegg, Elsener and Böhni [5,6]

Fig. 11-36: Potential field map (column 1)

First of all, potential field measurements were performed by the use of a CSE reference electrode to determine, whether the reinforcement of the columns is in an active or passive state (Fig. 11-36). This and a laboratory chloride analysis led to the identification of good

installation locations for the sensing elements. The central chloride sensitive element in the electrochemical sensor shown in Fig. 11-39 is a silver wire coated with electrochemically deposited silver chloride (AgCl). This coat wire is mounted in a stainless steel tube. Each sensor has two electrical connections, one to the silver wire (chloride sensor) and one to the steel tube for resistivity measurements.

Arrays of these sensors were installed in concrete cores (Fig. 11-35) taken from the structure, allowing measurements at different embedding depths. Fig. 11-37 shows a sample of measured concrete temperature, corrosion current and potentials. A chloride concentration measurement [mol/l] of a selected region on column 2 can be seen in Fig. 11-38.

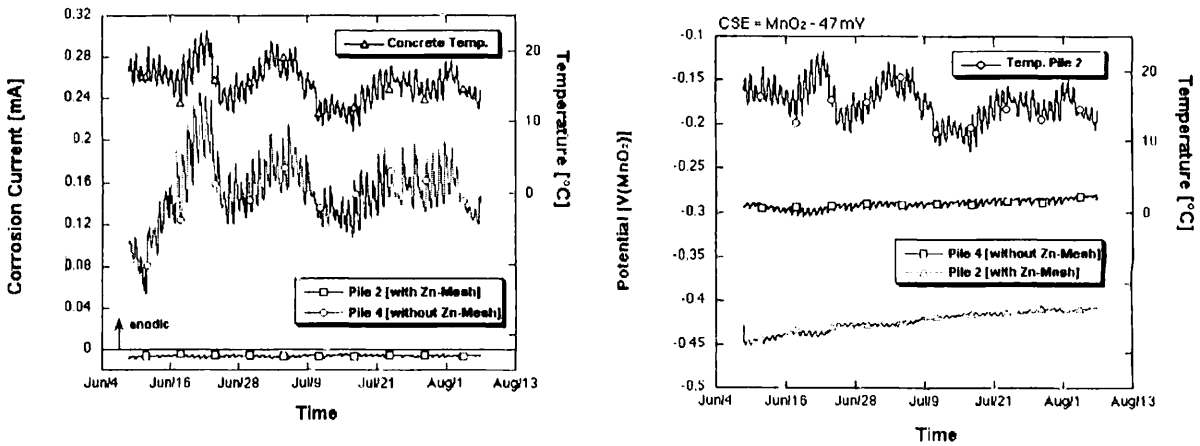

Fig. 11-37: Measured concrete temperature, corrosion current and potential

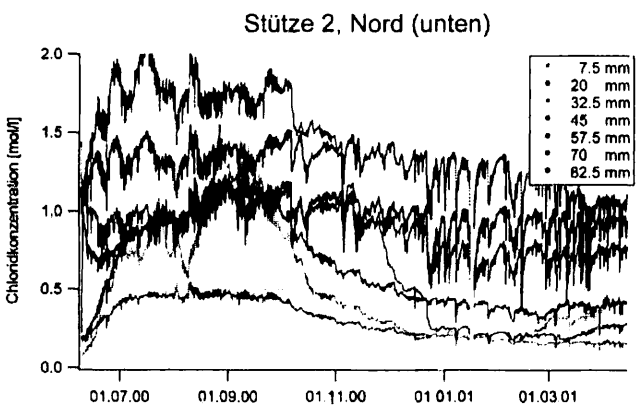

Fig. 11-38: Chloride concentration measurement [mol/l]

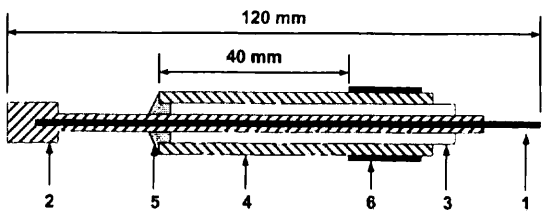

1 silver wire
2 AgCl coating
3 teflon tube
4 stainless steel tube
5 epoxy sealing
6 insulation

Fig. 11-39: Chloride sensitive sensor element

11.5.5 Data acquisition

When selecting the architecture and the components of an automated data acquisition system, first the types of sensors and I/O signal types that should be used must be defined (Santa and Bergmeister 2000 [13]). Many types of sensors and signals must be conditioned before connecting them to a data acquisition device (DAQ). This includes the amplification of low-level signals, the isolation to avoid effects from environmental potentials, and filtering to

remove unwanted noise from signals. Additionally, certain sensors often need external excitation. Finally, a linearization due to nonlinear responses of sensors to changes of a physical phenomenon might be necessary. In this context some considerations about the used sensors and their characteristics might be useful for an adequate selection. Criteria, such as accuracy, acquisition rates, number of channels, flexibility, reliability, expandability, ruggedness, and computer platform are used to determine the best DAQ-devices for the specific application. Finally, the choice of appropriate device drivers and application and/or programming software closes the cycle of selecting DAQ-components. Due to the geometry and size of most civil infrastructures and the resulting spacing between measurement locations of interest, monitoring applications usually introduce the need to distribute the measurement functionality out into the field. As in our case, it would have been almost difficult and inefficient to wire all signals to one central connection box located somewhere on the structure. A more suitable approach is the employment of a series of distributed DAQ-modules that communicate via robust industrial network technology. Noise corruption problems that may occur when using long-distance analog signal wiring can be avoided by local A/D-conversion and the transmission of digital signals which are quite robust against noise on the network links. The developments in industrial automation have resulted in a range of different networking technologies and open industry standards such as Ethernet, RS-232, RS-485, RS-422, IEEE-488, USB, and a series of Fieldbus-specifications. Nevertheless, the transfer rates of the network communication may limit the available dynamic range in terms of sampling rates. Finally, the readout-units that control transducers delivering non-standard signals, as e.g., fiber optic devices, vibrating wires, etc., have to be integrated in the data acquisition network via the specified hard- and software interfaces.

11.5.6 Data interpretation and system modeling

The installation of sensing elements and a data acquisition system to collect measured data is only the start of monitoring field performance. Interpretation of the acquired data is equally important, namely the comparison of measured and calculated data in order to validate the model assumptions (Aktan et al. 1997 [11]).

Most available simulation packages are purely deterministic, and all geometrical, material and load parameters are bound to crisp deterministic values. Consequently, simulation results such as deflections, stresses, failure loads etc. are also deterministic. Explicit modeling of uncertainty is therefore highly desirable for a proper reliability assessment. SARA (Structural Analysis and Reliability Assessment) , a project related to the present monitoring program, is based on the 2D/3D nonlinear analysis program ATENA developed by Cervenka Consulting. The fundamental FEM functionality is enhanced by probabilistic analysis concepts.

The necessary handling and treatment of the statistical data of structures – loading and resistance in general – needs special sampling methods. The probability distribution functions for the basic input variables to these advanced simulation techniques can be obtained from stochastically models of materials (with and without degradation of strength), stochastic models for proof loading (permanent load variable and traffic load) and, related to the present monitoring program, from the comparison of recorded structural monitoring data. The structural monitoring data is used to suit the stochastically models, for example with Bayesian updating, or for the derivation and validation of the numerical model assumptions.

Once this tuning has led to a certain level of completeness and validity, analytical prediction provides a quantitative knowledge and hence is a useful tool to support structural evaluation, decision making, and maintenance strategies.

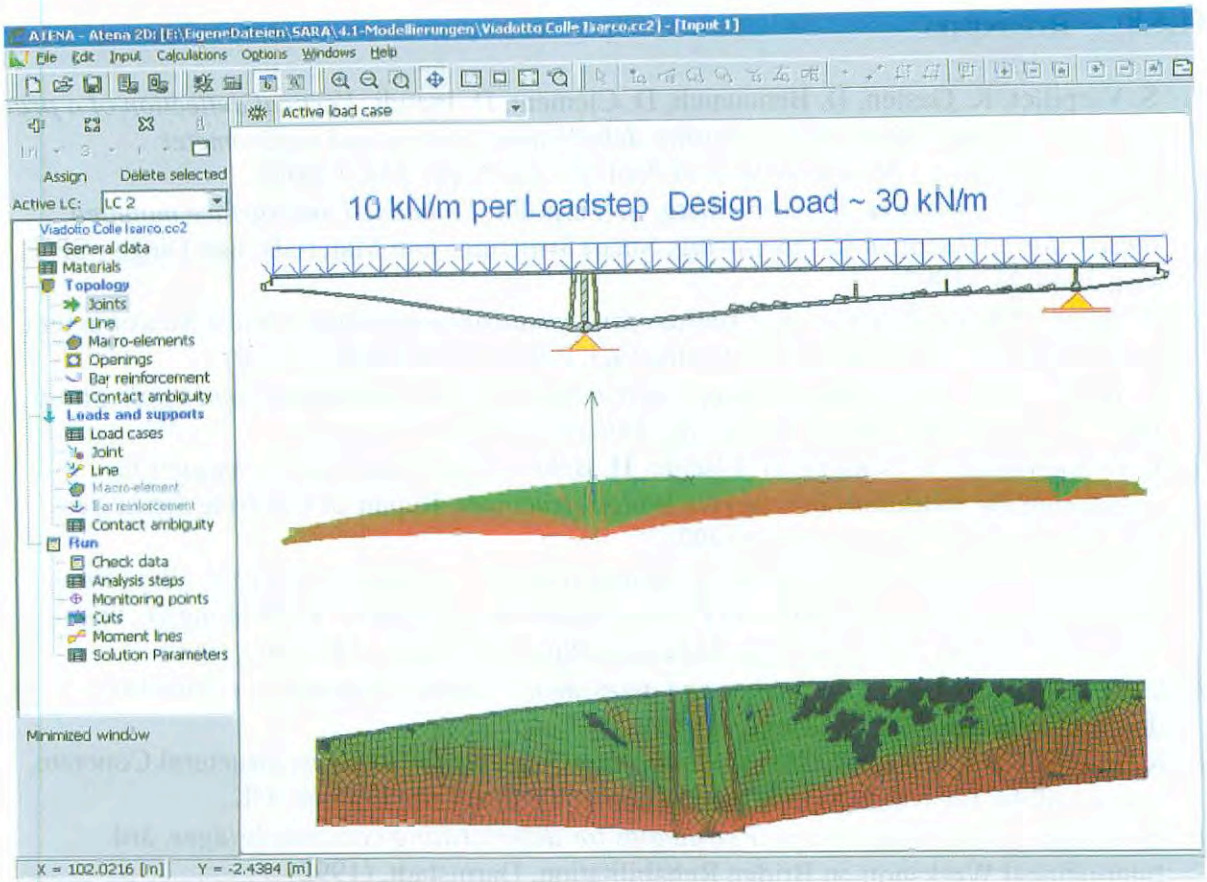

Fig. 11-40: Non-linear analysis of the Colle Isarco Viaduct – ATENA interface

However, for some instrumented processes it might not always be possible to formulate a well-defined analytical evaluation model. Corrosion processes on reinforced concrete structures are a complex function of different variables like moisture, chloride concentration, oxygen content of the pore solution, conductivity of the concrete cover, and many others (Zimmermann et al. 1997 [5], Elsener and Böhni 1990 [6], Rostam 1992 [9]). The interpretation of these parameters may be in part based on empirical experience and expert knowledge. Such systems are therefore good candidates to be modeled and evaluated by knowledge based systems and inference mechanisms.

11.5.7 Concluding remarks

Monitoring continuously the decisive parameters of an existing structure provides the quantitative basis for the condition assessment in order to ensure the safety of highway bridges with regard to life extension and replacement strategies. In this paper we presented the instrumentation program installed on the Colle Isarco viaduct. We have illustrated the performed deformation and displacement measurements as well as first interpretations of the results. A special focus is given to the monitoring of durability performance such as corrosion parameters. The output of the presented monitoring activities serves as a basis for SARA, a project based on a probabilistic nonlinear FE analysis concept. Comparison and combination of measured and analytically modeled behavior is useful to calibrate and tune the mechanical and numerical model assumptions in order to facilitate analytical prediction. Finally, structural monitoring and analysis should be the basis for decision-making support in order to aid maintenance and repair interventions.

11.5.8 References

1. S. Vurpillot, K. Gaston, D. Benouaich, D. Clément, D. Inaudi, *Vertical deflection of a pre-stressed concrete bridge obtained using deformation sensors and inclinometer measurements*, ACI Structural Journal, Vol. 95, No. 5, pp. 518, (1998)
2. D. Inaudi, N. Casanova, P. Kronenberg, S. Vurpillot, *Embedded and surface mounted sensors for civil structural monitoring*, Smart Structures and Materials, San Diego , SPIE Vol. 3044-23, (1997)
3. D. Inaudi, *Long-gage fiber optic sensors for structural monitoring*, Optical Measurement Techniques and Applications, Editor Rastogi, P.K., Artech House, (1999)
4. D. Inaudi, *Fiber optic smart sensing, Optical Measurement Techniques and Applications*, Editor Rastogi, P.K., Artech House, pp. 255-275, (1997)
5. L. Zimmermann, Y. Schiegg, B. Elsener, H. Böhni, *Electrochemical techniques for monitoring the conditions of concrete bridge structures*, Repair of Concrete Structures, Proceedings of Int. Conference, (1997)
6. B. Elsener, H. Böhni, *Potential mapping and corrosion of steel in concrete, Corrosion rate of steel in concrete*, ASTM STP 1065, Berke, N. S., Chaker, V., Whiting D., eds., American Society for Testing and Materials, Philadelphia, pp. 143-156, (1990)
7. CEB TG 5.4, *Strategies for testing and assessment of concrete structures*, Bulletin d'information No. 234, Lausanne, (1998)
8. K. Bergmeister, U. Santa, *Global Monitoring Concepts for Bridges*, Structural Concrete, Journal of the fib, No. 2, March 2001, Thomas Telford Ltd., London, UK.
9. S. Rostam, *Assessment an repair strategies for deteriorating concrete bridges*, 3rd International Workshop on Bridge Rehabilitation, Darmstadt, (1992)
10. O. Burdet, *Load testing and monitoring of Swiss bridges*, CEB Information Bulletin No. 219, Safety and Performance Concepts, Lausanne, (1993)
11. A.E. Aktan, D.N. Farhey, A.J. Helmicki, D.L. Brown, V.J. Hunt, K.L. Lee, A. Levi, *Structural identification for condition assessment: experimental arts*, Journal of Structural Engineering, (1997)
12. D.M. Frangopol, *Bridge Health Monitoring and Life Prediction based on Reliability and Economy*. International Workshop on the Present and Future in Health Monitoring, September 3rd-6th, 2000, Bauhaus-University Weimar, Germany.
13. U. Santa, K. Bergmeister, *Instrumentation and Data Acquisition Techniques in Structural Health Monitoring*. International Workshop on the Present and Future in Health Monitoring, September 3rd-6th, 2000, Bauhaus-University Weimar, Germany.

11.6 Assessment of old post-tensioning wires

Eva M. Eichinger (Research Assistant) and Johann Kolleger (Professor)

Institute for Structural Concrete
Vienna University of Technology, Austria

This paper presents results of tensile, relaxation, fatigue and corrosion tests on quenched and tempered as well as cold-drawn post-tensioning wires from bridges more than 30 years old. The main properties of these steels are summarised and are helpful when assessing similar structures.

11.6.1 Introduction

When an existing bridge is assessed using probabilistic methods detailed knowledge of the actual material properties is of utmost importance to guarantee accurate and realistic models of the variables on the resistance side. In case of a post-tensioned bridge detailed information on the properties and the condition of the post-tensioning steels is therefore crucial.

To identify the properties of the post-tensioning wires the chemical properties of the wires were determined and tensile, fatigue, relaxation and corrosion tests were performed. Thus, realistic estimates of the material parameters in comparable existing bridge structures could be derived. Detailed results of this study are given in (Eichinger et al. 2002 [1]).

11.6.2 Bridges examined

In the years 2000 and 2001 several post-tensioned concrete bridges from the 1950's to 70's were demolished and rebuilt in Austria because concerns about their durability and ultimate strength were raised. Three of the bridges were post-tensioned with quenched and tempered wires of the "old" type produced before 1965 which are quite sensitive to hydrogen embrittlement. One bridge used cold-drawn steel. In the following sections the bridges are described a little more detailed.

11.6.2.1 Autobahnüberführung Regau, Upper Austria

This bridge consists of two independent post-tensioned concrete structures and has a curved plan view. The total length is 34.3 m, the span is 33.5 m. The bridge has a box girder cross-section with a width of 8.0 m and transverse beams at the ends. The main girders are post-tensioned in five layers with 16 tendons, which were tensioned either from the transverse end beams or the bridge deck. Each tendon consists of 24 post-tensioning wires of steel type NEPTUN N 40 St 1420/1570.

11.6.2.2 Melkflussbrücke Winden, Lower Austria

This bridge also consists of two independent post-tensioned concrete structures. The main girders have T-cross-sections and are continuous beams over three fields. The width of the structure is 14.05 m, the total length 68.4 m with single spans of 21.96 m + 25.57 m + 19.41 m. Transverse beams are situated at the supports and at mid-span. The post-tensioning tendons consist of 16 oval wires of steel type SIGMA oval St 145/160.

11.6.2.3 Murbrücke Thalheim, Styria

This bridge is a continuous beam over three fields with a box girder cross-section. The total length is 182.0 m and the single spans are 56.0 m + 70.0 m + 56.0 m. The bridge has a total width of 9.80 m. At the supports transverse beams are situated. The post-tensioning tendons consist of 34 oval wires of steel type SIGMA oval St 145/160.

11.6.2.4 Steinerbachbrücke Mondsee, Upper Austria

The main girders of this bridge are prefabricated and carry the cast-in-place bridge deck. The total width of the bridge is 14.05 m. The prefabricated girders have lengths of 27.20 m and 30.30 m, respectively. At the supports and at mid-span transverse beams are situated. The main girders are prestressed and the tendons consist of 12 round wires of steel type DELTA 100 St 150/170.

11.6.3 Performed tests and major test results

Three different types of post-tensioning wires from four different bridges were examined. The steels from the bridges in Regau (NEPTUN N 40 St1420/1570) as well as Thalheim and Winden (SIGMA oval St 145/160) are quenched and tempered and are said to be quite sensitive to hydrogen embrittlement. For comparison also the cold-drawn steel from a bridge in Mondsee (Delta 100 St 150/170) was examined. It has to be noticed that - except some of the wires from the bridge in Regau – all specimens examined showed no or only negligible visible corrosion.

11.6.3.1 Chemical properties and metallography

The chemical properties of the post-tensioning wires were examined using emission spectrometry. The composition of the quenched and tempered steel wires shows quite high contents of silicon and manganese and matches the so-called "old" type of SIGMA steel produced before 1965. The chemical properties of the steel DELTA 100 match those for cold-drawn steels produced today with a slightly higher content in copper.

On longitudinal and transversal grindings the structure, the degree of cold-drawing and the percentage of non-metallic inclusion according to DIN 50602 were examined by microscope. Two typical longitudinal grindings are shown in Fig. 11-41. On the left side a structure without cold-drawing is presented (steel type SIGMA oval from the bridge in Winden), on the right the typical cold-drawn structure of a steel wire is given (steel type DELTA 100 from the bridge in Mondsee).

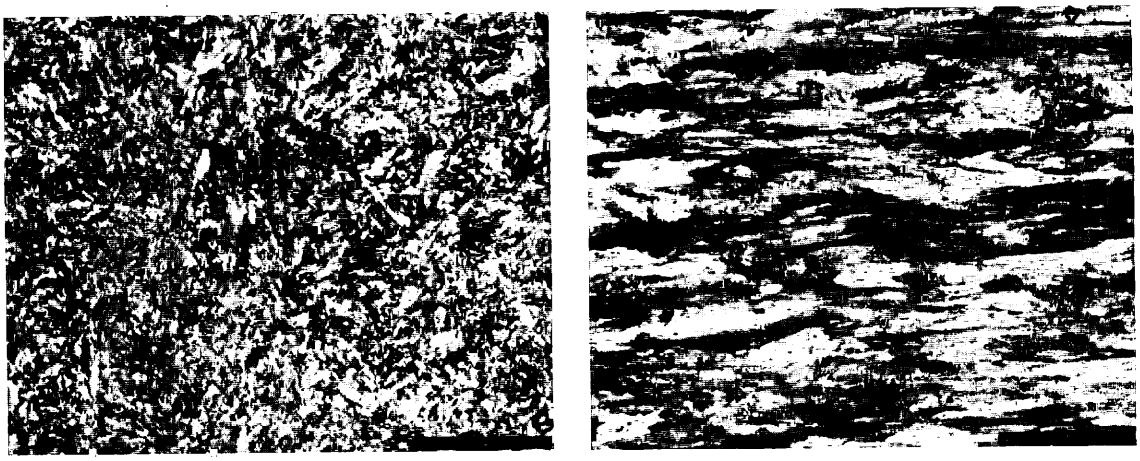

Fig. 11-41: Structure of quenched/tempered steel (left) and cold-drawn steel (right), 1000 x enlarged

11.6.3.2 Tensile tests

As suspected some minor corrosion does not effect the strength properties of the steels. Only if strong corrosion is present the ductility of the steel is influenced. As the tests showed strain and contraction values are reduced, while yield and tensile strength are not effected.

11.6.3.3 Relaxation tests

The relaxation tests were performed according to ISO 15630-3 with a loading equivalent to 70 % of the effective tensile strength and a maximum allowable decrease in stress of 2.5%. The results are shown in Fig. 11-42.

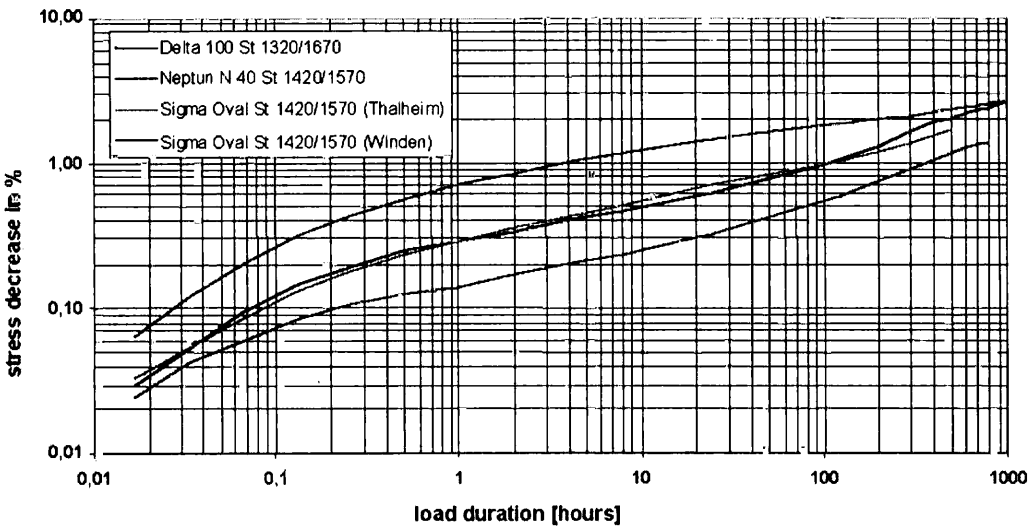

Fig. 11-42: Results of relaxation tests

All wires examined passed the test. This indicates that the relaxation properties of the tested steels were much higher at the time of production as the steels have been in use in the bridge structures for more than 30 years.

11.6.3.4 Fatigue tests

The influence of corrosion is clearly shown in the fatigue tests, as corrosion considerably decreases the fatigue strength. The results of the fatigue tests in form of trend lines for the different types of steels examined are presented in Fig. 11-43.

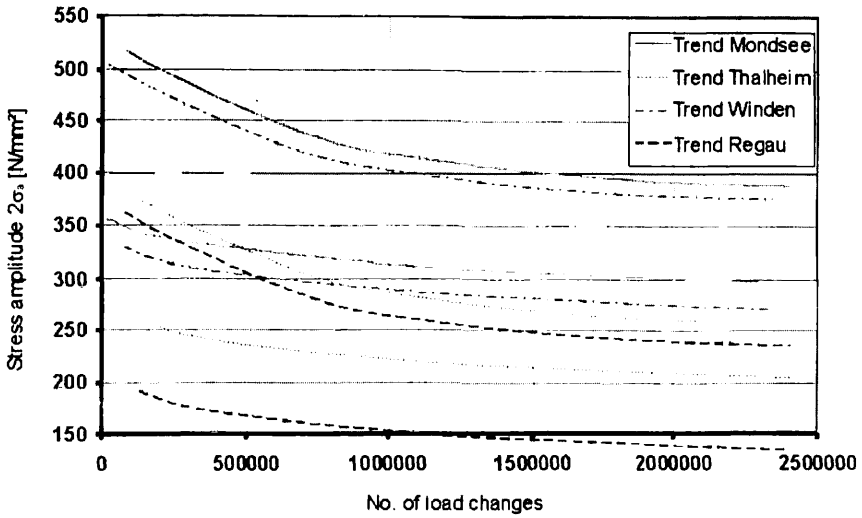

Fig. 11-43: Results of fatigue tests

In the fatigue test the cold-drawn wires DELTA 100 showed far better results than the quenched and tempered steels, but their fatigue strengths still are under the values allowable for new steels.

11.6.3.5 Corrosion tests

To show whether the steels were sensible to hydrogen embrittlement two different types of corrosion tests were performed. In the FIP test a concentrated ammoniumthiocyanate (NH_4SCN) solution was used and the specimens were loaded with a constant load equivalent to 80% of the tensile strength. The testing temperature was 50°C. The time until failure of the specimen was recorded, after 500 hours the test was stopped. The FIP test was developed for post-tensioning strands and due to the highly concentrated solution usually leads to a rather quick failure of the steel tested. Furthermore, DIBt tests were performed. These tests last up to 2000 hours and a thinned NH_4SCN solution is employed.

The results of the FIP tests are given shown in Fig. 11-44 and compared to values which are common for steels produced today. The higher sensitivity of quenched and tempered wires in comparison to cold-drawn steel is clearly visible. Only the cold-drawn steel Delta 100 gives satisfying results comparable to those for new steels.

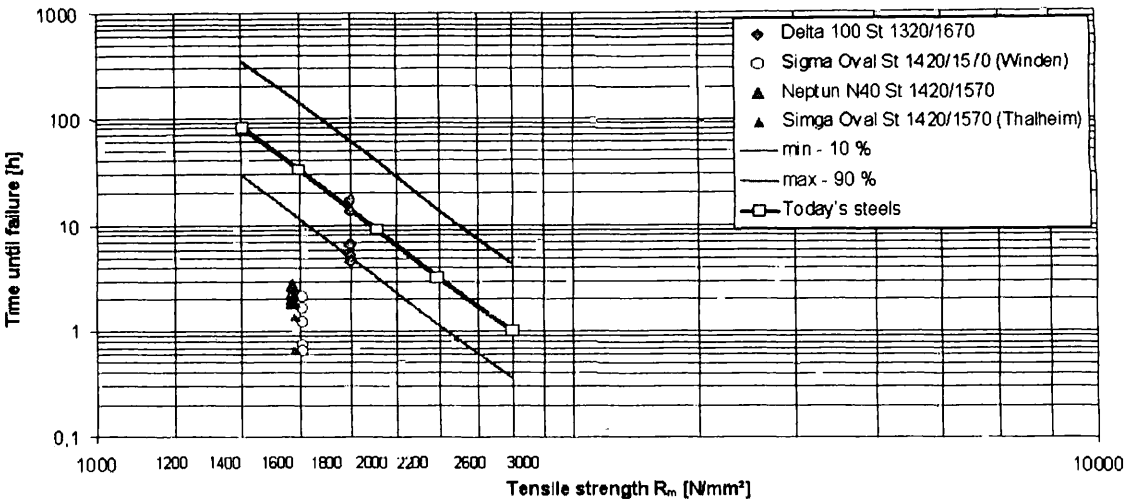

Fig. 11-44: Results of corrosion tests according to ISO 15630-3

11.6.4 Conclusions and outlook

This paper presented test results on quenched and tempered as well as cold-drawn steel wires from four bridges more than 30 years old. With the results of this study more realistic models of the properties of post-tensioning steels can be derived and used for the assessment of similar bridge structures.

Currently tensile tests are performed on post-tensioning tendons which were built using the wires of the discarded bridges. Wire breakage is included in the tendon at specified patterns. Therefore, the ultimate load of these damaged tendons heavily depends on bond action between wires, grout and surrounding concrete. In combination with the test results presented above the measured ultimate tensile strength of the damaged tendons will be evaluated using probabilistic methods, in order to come up with a realistic estimate of the tendon strength and the reliability of a comparable existing bridge structure in case that damage to the tendons is likely to be present. For reinforced concrete bridges such reliability calculations have already been performed (Eichinger et al. 2002 [2], Enevoldsen and Eichinger 2001 [3], Pukl et al. 2002 [4]). Based on the results presented above a probabilistic assessment of post-tensioned structures and the calculation of the probability of failure of an old bridge with defects in the post-tensioning tendons will also be possible.

11.6.5 References

1. E.M. Eichinger, H. Winter, J. Kollegger, *Untersuchungen an Spannstählen des Typs Neptun N40, Sigma Oval und Delta 100*, Publications of the Inst. for Structural Concrete No. 2/2002, Univ. of Technology, Vienna, 2002
2. E.M. Eichinger, W. Wenighofer, J. Kollegger, *Reliability Assessment of Two Concrete Bridges*, Research Report No. 01/10, Inst. for Structural Concrete, Univ. of Technology, Vienna, 2002
3. I. Enevoldsen, E.M. Eichinger, *Practical Experience with Probabilistic-Based Assessment of Bridge Structures*, Publications of the Austrian Society of Concrete and Construction Technology, No. 47, Vienna, November 2001
4. R. Pukl, D. Novak, E.M. Eichinger, Stochastic Nonlinear Fracture Analysis, Proceedings IABMAS 2002, Barcelona, July 2002

11.7 Bridge classification based upon ambient vibration monitoring

Helmut Wenzel (Managing Director) and Roman Geier (Project Manager)

VCE Holding GmbH
Diesterweggasse 1
A-1140 Vienna, Austria

11.7.1 Abstract

Bridges are essential for the transportation infrastructure of any country. The peak of construction of the European Transportation Infrastructure happened in the 1970s. It is estimated that nowadays 760,000 bridges are serving within the Trans-European Network (TEN) and the primary and secondary road network. Owners of bridges expect that the critical age where rehabilitation and retrofit works at bridges become essential starts after 30 years of service. Considering the time of construction a huge peak of repair and retrofit investment is expected for the years starting from 2005 onwards. Studies carried out show that the required effort could be more than tripled compared to present values. In times of shrinking budgets, as prevailing now, alternative methods to deal with this problem are required.

Therefore different monitoring systems based on the analysis of the dynamic characteristic have been developed recently. Owners of concrete bridges require assessment tools for those components which cannot be inspected visually. BRIMOS provides additional information for the bridge inspector to carry out an accurate assessment of the condition and the remaining lifetime of the bridge.

In the scope of the dynamic tests a classification system is established. This classification was drawn up on the basis of experience gathered from more than 80 assessed bridge structures. The results of artificial damages on real prestressed concrete and reinforced concrete bridges were integrated as an important basis for the establishment of the system. From this classification system the urgency of any required rehabilitation measures can be derived, which enables an optimum control of the existing financial sources with simultaneous maintenance of a maximum safety level for the users.

11.7.2 Summary

Owners of structures realize the need for quality control tools to be applied for maintenance and rehabilitation planning as well as lifetime assessment. Practicing engineers highly desire quality control of construction and feedback from structures for more economic design and better understanding of the performance. Researcher were always fascinated by the potential of full scale dynamic tests of structures. These common aspects triggered the development of structural monitoring. It is recently well-known that each structure has its typical dynamic behavior which may be addressed as vibrational signature. Any changes in a structure, such as all kinds of damages leading to decrease of the load carrying capacity have an impact on the dynamic response. This suggests the use of the dynamic response characteristic for the evaluation of quality and structural integrity. Monitoring of the dynamic response of structures makes it possible to get very quick knowledge of the actual conditions and helps in planning of rehabilitation budgets.

11.7.3 General

Monitoring the quality of structures comprises a wide field of engineering tasks. The most promising recent developments has been achieved with Ambient Vibration Testing and dynamic System Identification (SI) tools. Ambient Vibration Testing does not require a controlled excitation of the structure. The structural response to ambient excitation is recorded in a large number of points. From these ambient measurements the condition of the structure is derived.

As already mentioned, a huge peak of bridge construction happened in the 1970s, which are reaching their critical age currently. Thus, an enormous maintenance and rehabilitation effort is coming towards the road and bridge authorities (Fig. 11-45). To manage this problem, advanced technologies in bridge priority ranking concerning maintenance actions are urgently required.

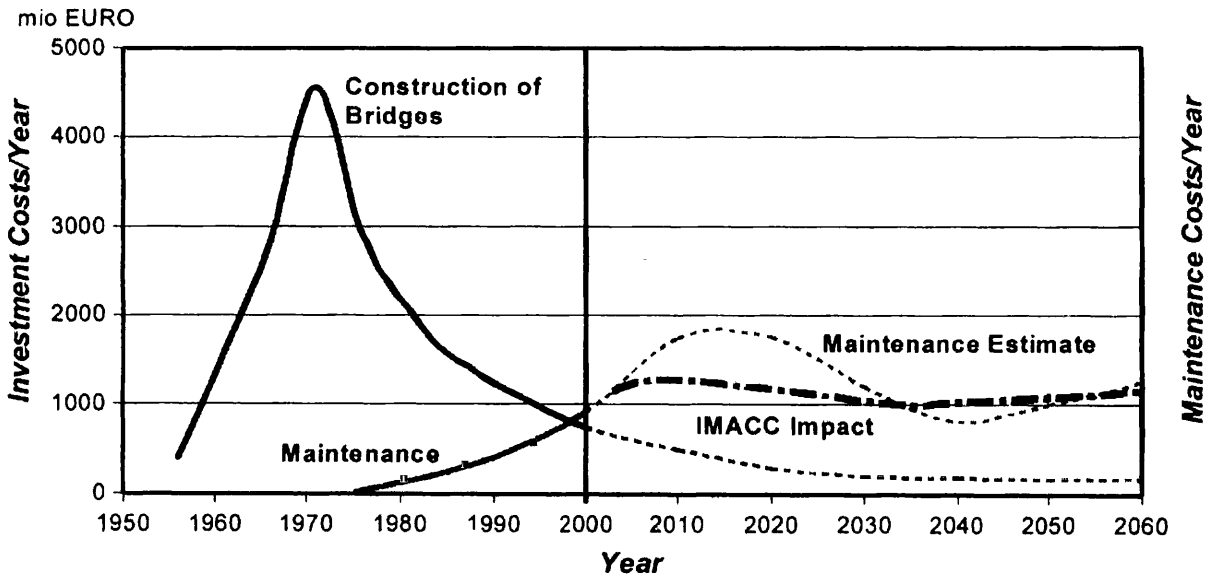

Fig. 11-45: Construction of bridges vs. maintenance costs estimated

11.7.4 Benchmark tests

Prestressing steel with a yield strength of 145/160 kP/mm² was used in early post-tensioned bridges until the year 1965 in Germany and Austria. These tendons were called "Sigma Oval" and "Neptun N40". Tests performed on this steel quality raise doubts that specific early charges show a proneness to stress-crack-corrosion. After a sudden spectacular failure of a prestressed beam of an industrial building in Germany in 1993 detailed investigations have been done.

Due to an additional damage on a highway bridge in Austria in 2000 all structures built with the specific type of prestressing steel were assessed very carefully. During these tests on 28 bridges in Austria, 5 of them turned out to be in a critical condition. In the framework of an Austrian research project VCE had the chance to introduce artificial damages to this 5 structures and study the effects to the dynamic response.

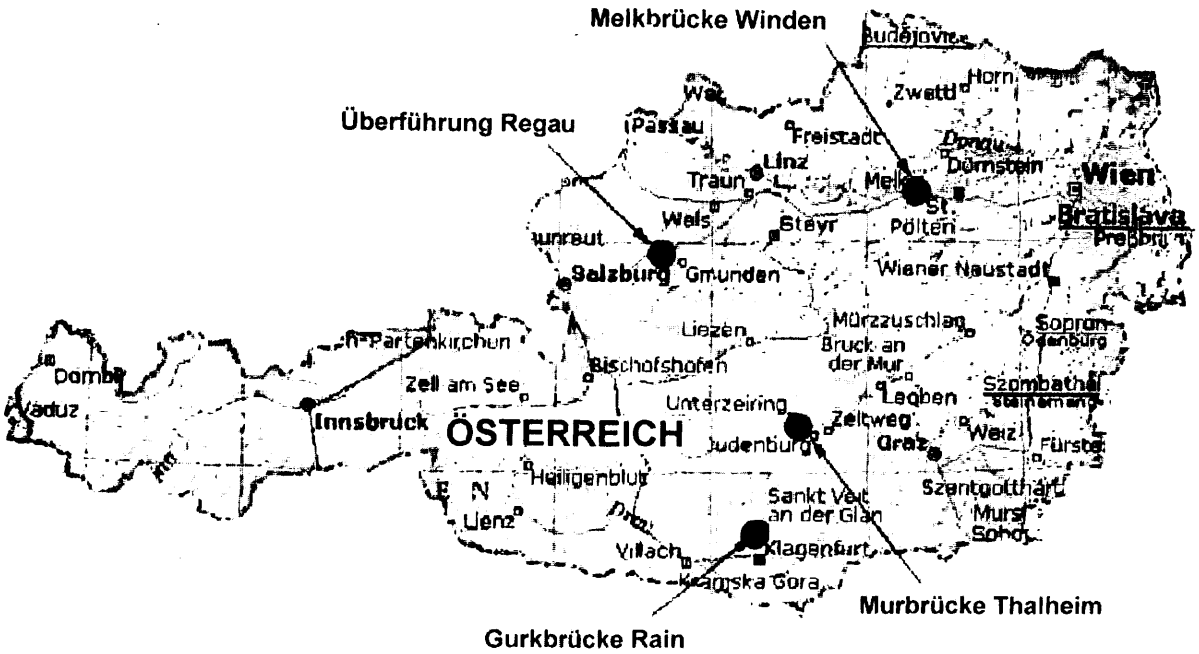

Fig. 11-46: Location of test structures in Austria

It was decided to replace the 5 critical structures because rehabilitation would have been to costly and therefore not desired. The experience from the BRITE-EURAM project SIMCES was studied in detail before the field tests have been planned. Such a possibility to apply artificial damages to 5 post-tensioned structures in real scale is unique in the world until now. Thus, all tests have been planned very carefully. Main focus was put to the identification of damages in prestressing tendons, which are currently assessed by visual and very local inspection techniques, only.

A global assessment of a structure, pointing out prospective damages and damage locations, is therefore urgently required. Before the structures were damaged an initial vibration test was performed, using a sensor setup with high density. A second measurement sequence was performed after removing the pavement in order to quantify the effect caused by the additional load. The pavement only has influence on the natural frequency due to the additional load. There was no stiffening effect recognizable.

Fig. 11-47: Structural assessment of a bridge

Fig. 11-48: Cutting of prestressing tendons

The assessment of the capabilities of dynamic methods was done by introducing artificial damages to the embedded tendons. This was performed by cutting the tendons which turned out to be a very complicated and time-consuming task. Later on, the damages of the other projects were induced by drilling cores to the structure. This was a very sensitive method for damaging tendons in a sequence.

11.7.5 Damage assessment

System identification (SI) means extracting the dynamic characteristic of bridges or other civil engineering structures from vibration data. The vibrational characteristic serves as input to modal calibration and damage identification algorithms. Technical development work is carried out all over the world on this subject. One of the recent projects was the BRITE-EURAM project SIMCES (System Identification Methods for Civil Engineering Structures) which focuses on the subject of damage identification based upon ambient vibration measurements.

The major tools of the damage assessment are the natural frequencies, the mode shapes, damping values, vibration intensities due to traffic as well as trend cards indicating the structural behavior over time.

11.7.6 Trend cards

The development of so-called trend cards is a major outcome of the real scale damage tests performed in 2001 in Austria. These cards represent the signal in a frequency-time diagram. Fig. 11-49 shows typical trend cards as they are obtained from several ambient vibration measurements.

In order to distinguish the individual frequency peaks, a coloring of the card is required so that the energy content of the oscillation and therefore the respective intensity can be determined. By this type of representation, damages are already visible in their beginning phase in the frequency spectra. What has to be mentioned, however, is that the basic frequencies with their long-wave vibration forms are insensitive to local damage. Therefore the assessment and interpretation of the whole measured frequency spectrum assumes greater significance.

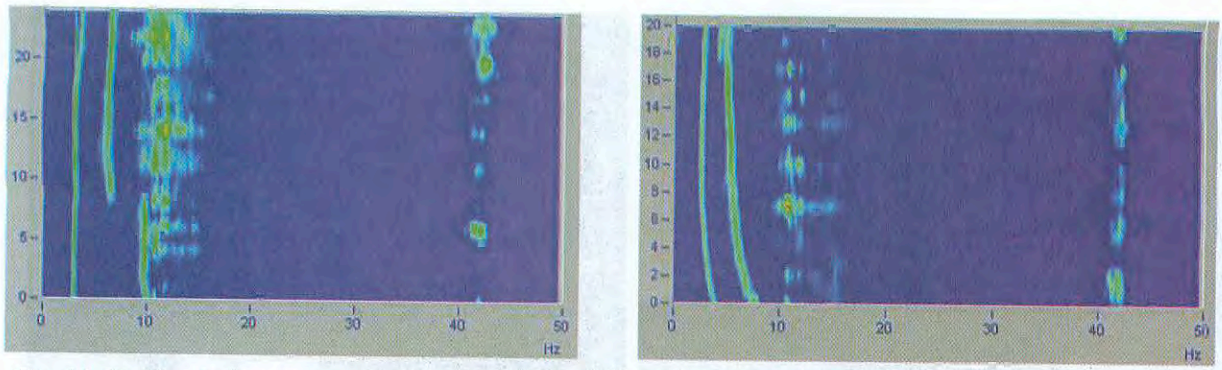

Fig. 11-49: Trend of a structure in a good condition (left) and a damaged structure (right)

11.7.7 BRIMOS recorder

One major result of the artificial damages is the knowledge that only one sensor, located at a specific point of the structure, leads to a good impression about the structural performance. Using these results a priority ranking of bridges can be done, leading to the classification if more detailed investigations are necessary. For this purpose a compact monitoring and assessment system, the so-called BRIMOS-Recorder, was developed which should give a first estimation about the structural condition. Main assumption for design was, that a use of the system is possible for the bridge owners and local authorities by themselves. Interpretation and assessment of the measurements has still to be done by experts. This method makes the investigation of a large number of bridges in short time possible, which leads to a higher safety level for the users. Locating the sensor is one of the major tasks for a correct assessment and classification of the investigated structure. The best location was found by assessing the results from the artificial damage tests. The following rule was defined for placing the BRIMOS recorder to the structure.

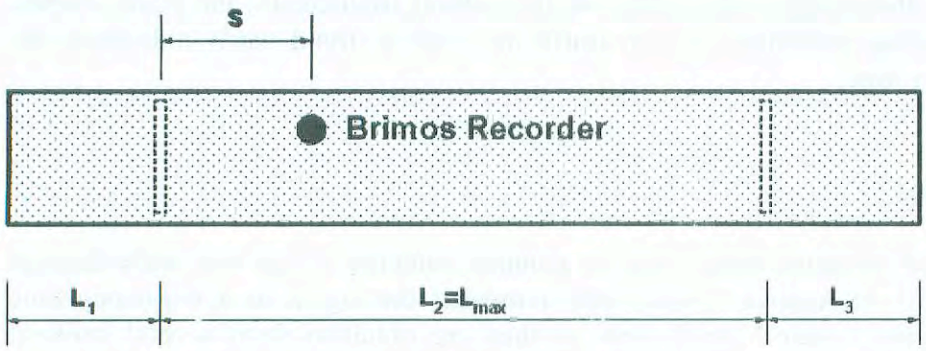

Fig. 11-50: Location of the BRIMOS recorder on the structure

$$S = 0.4 \cdot L_{\max}$$

A generalization with regard to the assessment of the respective frequency band is, however, not admissible, as the behavior is strongly dependent on the respective structure type. Consequently also local damages, for example at bigger structures, could bring about clear changes in natural frequencies and the respective basic vibration forms. In order to assess the chronological development of the structural condition it is required to carry out

dynamic measurements of the structure at periodic intervals. In this context a 6-monthly examination interval seems useful but at the beginning of the measuring series a sufficient number of basic values has to be collected over a shortened interval. Based on these basic values the chronological development of the condition can be represented graphically by trend cards.

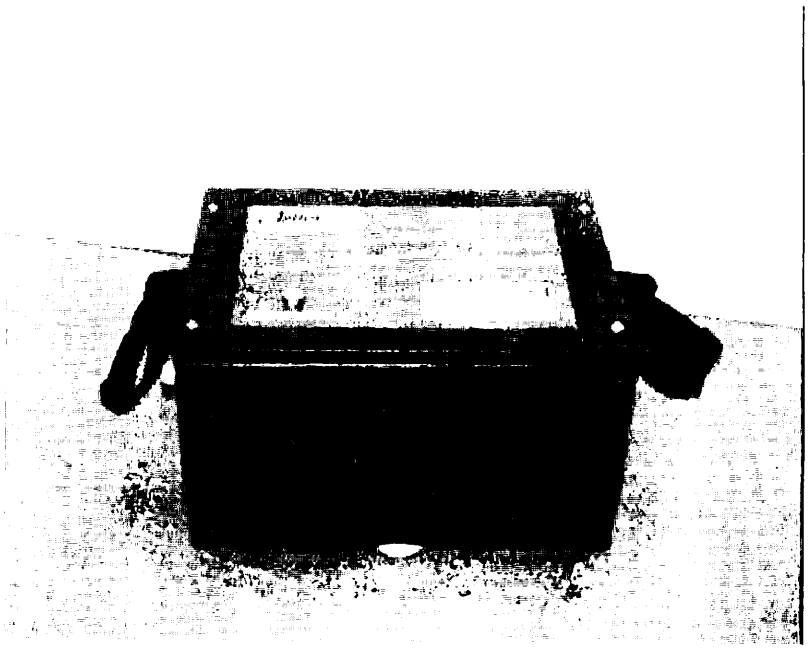

Fig. 11-51: BRIMOS recorder developed by VCE

11.7.8 Classification scheme

Classification is used to identify structures which show distinct problems and urgently require maintenance and rehabilitation efforts. A proper budget planning of the responsible bridge authority can be done according to the time schedule set up based upon the measured results of the ambient vibration system. A classification of structures is possible and can be used as a basis for priorities. In the following illustration the measuring results of 35 prestressed concrete bridges, which were built between 1955 and 1965, are shown. The condition of the structures is reflected in the measuring values and therefore clearly shows the 0need for any action required.

Class A represents bridges which are in a very good condition and do not have any problems. Bridges assigned to group B basically show a good condition, however some local problems and small damages may be possible. These bridges are usually exposed to high traffic loads. Bridges classified into C show a critical structural condition and urgently need rehabilitation measures or a total replacement.

From the practical point of view a combined assessment should consists of a rough check using the BRIMOS-Recorder technology in order to classify the specific structure. This classification should be the starting point for further detailed and costly assessment. In this way only the structures classified as critical should be investigated in detail.

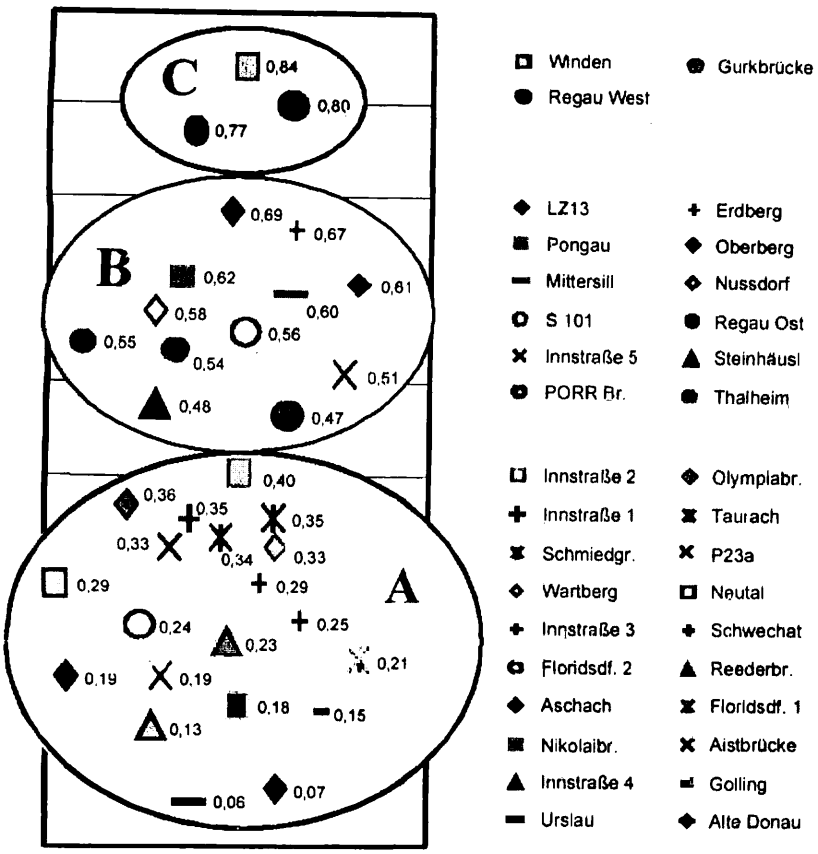

Fig. 11-52: Classification of structure according BRIMOS

11.7.9 Conclusions

From the results it was derived that the failure of only few prestressing tendons can be found by the use of the ambient vibration method. Recent assessment procedures failed because only the basic frequencies and corresponding mode shapes had been observed. The tests showed that small changes very often do not lead to a change of the fundamental frequencies in the range up to 10 Hz. The frequencies in the high range as well as the damping values are very sensitive to changes or damages of the prestressing tendons.

The problems and failures with the assessment using the ambient vibration method in the last few years could be caused by the circumstance that a numerical simulation of these effects is nearly impossible. The infected mode shapes in reality are in a frequency range where the calculation results in rough estimations of the frequency.

Bridge classification using the modal parameters natural frequencies, mode shapes, damping values, vibration intensities as well as trend cards is a very effective tool for assessment and priority ranking of the structures. It should be noted in this context that the assessment of all modal parameters together as well as the assessment of the total frequency band of interest is very important. The Brimos Recorder thus can help to increase safety in the traffic network considerably, at the same time reducing the inspection and maintenance costs.

11.7.10 References

1. www.vce.at
2. www.samco.org
3. R. Geier, H. Wenzel, D. Pichler, *BRIMOS – Beurteilungsmethode für den Brückenbau*, Publication for the Austrian Ministery of Infrastructure, 2001
4. B. Peeters, *System Identification and Damage Detection in Civil Engineering*, PhD Thesis, Katholieke Universiteit Leuven, 2001
5. H. Bachmann, *Vibration Problems in Structures – Practical Guidelines*, Birkhäuser Verlag, ETH Zürich, 1996
6. R. Geier, H. Wenzel, E. Eichinger, *Untersuchungen anlässlich des Abbruches ausgewählter Tragwerke*, Publication for the Austrian Ministery of Infrastructure, 2001
7. S. Agrati, *Estimation of Structural Parameters form Ambient Vibration Test*, Master Thesis, Danish Technical University, 1994
8. C.P. Beards, *Strucutral Vibration, Analysis and Damping*, Halsted Press, ISBN 0 470 23586 1
9. A. Felber, *An Introduction to Ambient Vibration Testing – Course Manual*, EMPA Report-No. 155'715 Dübendorf
10. A. Felber, R. Cantieni, *Introduction of a new Ambient Vibration Testing System – Seven Bridge Test*, EMPA Report-No. 156'521 Dübendorf.
11. H. Wenzel, R. Geier, *Dynamic tests of real bridges till failure*, Symposium Health Monitoring and Retrofitting of Large Civil Engineering Structures, San Diego, 2001
12. J. Maeck, G. De Roeck, *Damage assessment using vibration analysis of the Z24-bridge*, Symposium Health Monitoring and Retrofitting of Large Civil Engineering Structures, San Diego, 2001

11.8 Enhancing performance of major bridges by integrating advanced technologies

A. E. Aktan, F. N. Catbas, K.A. Grimmelsman, M. Pervizpour

Drexel Intelligent Infrastructure Institute, Drexel University
3001 Market Street, Suite 50, Philadelphia, PA 19104

11.8.1 Motivations

There is evidence that visual biannual inspections of major bridges cost significantly while restricting operations for many months. Yet these inspections may miss many of the early initial signs of deterioration and damage even when these may be visible, as there are natural limitations to the ability of even experienced human eyes to scan hundreds of members and connections that may have dimensions in the order of a hundred feet.

If we characterize a bridge by a field-calibrated replica finite element model by integrating experimental, analytical and information technologies, this would serve as an excellent vehicle complementing and enhancing visual inspection. The process of constructing an analytical model and the process of collecting experimental data for ist calibration, if performed by experienced structural engineers, provide a conceptual understanding of the structure and its behavior under load. The calibration of the analytical model and subsequent simulations by the calibrated finite element model provide an excellent understanding of the most critical elements and mechanisms that deserve the attention of an experienced bridge engineer-inspector. By the same token, if the measurements and analyses indicate various redundant sub-systems of a bridge to be negligably stressed, these systems may not require an indepth inspection.

Applications to existing major bridges that exhibit premature aging, distresses and performance problems and/or to bridges that have aged beyond their anticipated design lifecycles offer exceptional payoff. Whether the conventional approaches to the maintenance management of such bridges are effective, especially after their aging, is a valid question. Many bridge engineers concur that there are too many limitations and shortcomings to the current approaches to inspection, evaluation, maintenance, rehab and retrofit design and construction of existing major bridges. Moreover, the cost and operational impacts of the common inspection and maintenance practices have also reached quite high and objectionable levels, and given the lack of assurance of their effectiveness, we should expect the bridge owners, consultants and contractors to be ready to embrace innovative paradigms that promise cost-effective and measurement-based objective approaches to solving performance problems with aging major bridges.

We note that the single most pressing challenge in solving performance problems such as objectionable movements and geometry changes, displacements, vibrations and visible signs of aging, deterioration, distress and damage to materials, elements and connections is to first clearly identify any root causes and determine the most effective and compatible renewal technique based on mitigating the root cause. In most cases, monitoring over an extended time may be necessary for definitively identifying the root cause(s) and mechanisms leading to symptoms of deterioration or damage.

In the case of major bridges identified as lacking sufficient system reliability due to the construction details or techniques that have been recognized as undesirable, the challenge would be in designing a retrofit that would indeed provide a significant enhancement of the system reliability while not adversely impacting any of the existing elements, and one that can be safely and feasibly constructed.

Most retrofits are designed and constructed with great uncertainty regarding the as-is condition of a structure and how the retrofit would be affecting the performance of existing systems that will remain in place. There is a conspicuous lack of established and/or codified guidelines for retrofit design, and most designers design retrofit by following exactly the same analysis methods and thought processes that are followed in desig ning a new structure. Health monitoring of a retrofit candidate for a sufficient period before the design of retrofit and continued monitoring through and following retrofit offers especially important advantages and benefits to the owners of bridges that require retrofit.

The application to the Commodore John Barry Bridge over the Delaware River has been intended to serve as a demonstration describe further in the following.

11.8.2 Demonstration on the Commodore Barry Bridge

Di3 conducted a technology demonstration project on the Commodore John Barry Bridge (CBB) which is one of the four major long-span bridges owned and operated by the DRPA of PA and NJ and further described in the following. The general motivations behind the demonstration were:

(a) Is it possible to characterize the through-truss structure of the main spans of the bridge in terms of a fieldcalibrated finite element model such that the movements, deformations, forces and stresses caused by live loads, wind and temperature at the critical regions may be reliably estimated (say within a confidence interval of 75%);

(b) What is the current state and future projections of the safety and serviceability performance of the bridge? Can we answer this question with technology integration in a manner that will convince the owner and consultants? For example, there were previous experiences with wind-induced vibrations damaging the truss members. Given these experiences, can we measure how wind is currently affecting the bridge? Is there a concern for fatigue? Are the vibrations of the deck of concern? Does the condition of the concrete deck warrant a concern?

11.8.2.1 The Commodore John Barry Bridge

The Commodore John Barry Bridge (CBB) (Fig. 11-53) spans the Delaware River between Chester, Pennsylvania and Brid geport, New Jersey. The bridge has five traffic lanes and currently serves more than six million vehicles annually, a significant percentage of which is heavy truck traffic. It was opened to traffic in 1974 as the longest cantilever steel truss bridge in the world with a main span length of 1,644 feet and a total bridge length of 13,912 feet. The focus of the study and subsequent discussions are directed to the principal long-span through-truss component shown in Fig. 11-53.

The sub-structures of the through -truss comprised of four reinforced concrete piers that are shown in the photo in Fig. 11-53. The piers were constructed on pile foundations. The two principal trusses of the through-truss are spaced 72.5 feet apart. Each truss has 73 panel points spaced at 45.7 feet intervals. The top and bottom chords of the trusses are constructed from welded box sections. A combination of welded box and I-sections are used for the vertical and diagonal truss members.

Lateral "wind" bracing is provided by K-bracing at the top and bottom chord levels, and by portal and sway frames located at various panel points throughout the structure. The suspended span of the bridge is connected to the cantilever arms via vertical hangers, which are pinned at their upper and lower extremities . Truss members with axial and rotational releases transition the top and bottom chords between the suspended span and the adjacent

cantilever arms. The floor system of the bridge is an 8-inch thick lightweight reinforced concrete deck that is composite with 9 steel beams laterally spaced at 6.9 feet. The beams are continuous over the floor beams in either four span or five span increments. Fig. 11-54 further illustrates various aspects of the structure.

(1) Objectives

The specific objectives of the study follow from the motivations presented earlier. The through-truss segment of the bridge was constructed with two principal truss systems as shown in the photo in Fig. 11-53.

As a result of the cantilever-truss construction of the structural system of CBB, the suspended 822 feet-long central component of the main span is hung from the cantilever arms by four tension elements (Fig. 11-54, also showing the "dummy" upper-chord element that is equipped with a movement system at the hanger connection). This rendered the suspended central portion of the structure to be non-redundantly supported by the four pin-ended hangers. The hangers, therefore, should certainly be considered as "fracture critical elements" due to a lack of any other primary or secondary mechanism for maintaining equilibrium should a failure of any one of the hangers took place.

A further area of concern in the evaluation of safety related to load-capacity rating. The stringers carrying the floor-system were considered to be the critical elements for live-load stresses and governed permit-rating. Given this background, the specific objectives of the study were established as:

(a) Evaluation of the actual stresses of the critical elements that governed the structural safety performance, i.e. the four hangers and the stringers within the floor system;
(b) Evaluation of the condition of the deck that exhibited widespread cracking and deterioration, and the causes of vibration of the walkway railing along each side of the deck that required frequent repairs and replacement because of vibration related damage. Fig. 11-55 shows typical deck damage initiating from cracks traversing the entire width of the deck at frequent intervals and deterioration of concrete around the crack mainly due to traffic-induced abrasion;
(c) Evaluation of the stresses of the truss elements that were constructed with an electro - slag welding process that was subsequently discovered to be highly susceptible to cracking, as well as the soundness of the electro –slag welds. An earlier study of the electro -slag welds a decade ago had recommended checking the welds in ten years;
(d) Evaluate the effectiveness and the conditions of approximately 1000 vibration dampers installed on the unbraced truss elements (some dampers are visible in Fig. 11-55) following damage caused by wind-induced vibrations to welded member connections during the erection of the bridge. These dampers had reached the end of their initially predicted useful lives of 20 years; At 28 years of age as a "young" bridge, the CBB has been inspected more a dozen times, with a half of these "in-depth". Although the inspections are valuable, whether any one of the above areas of specific performance concern could have been effectively and conclusively addressed by visual inspection is questionable.

(2) Work-Plan

(a) Conceptualizing the structural systems of the bridge, including the full recognition of the natural-environmental and the socio-technical systems that impact the bridge performance.

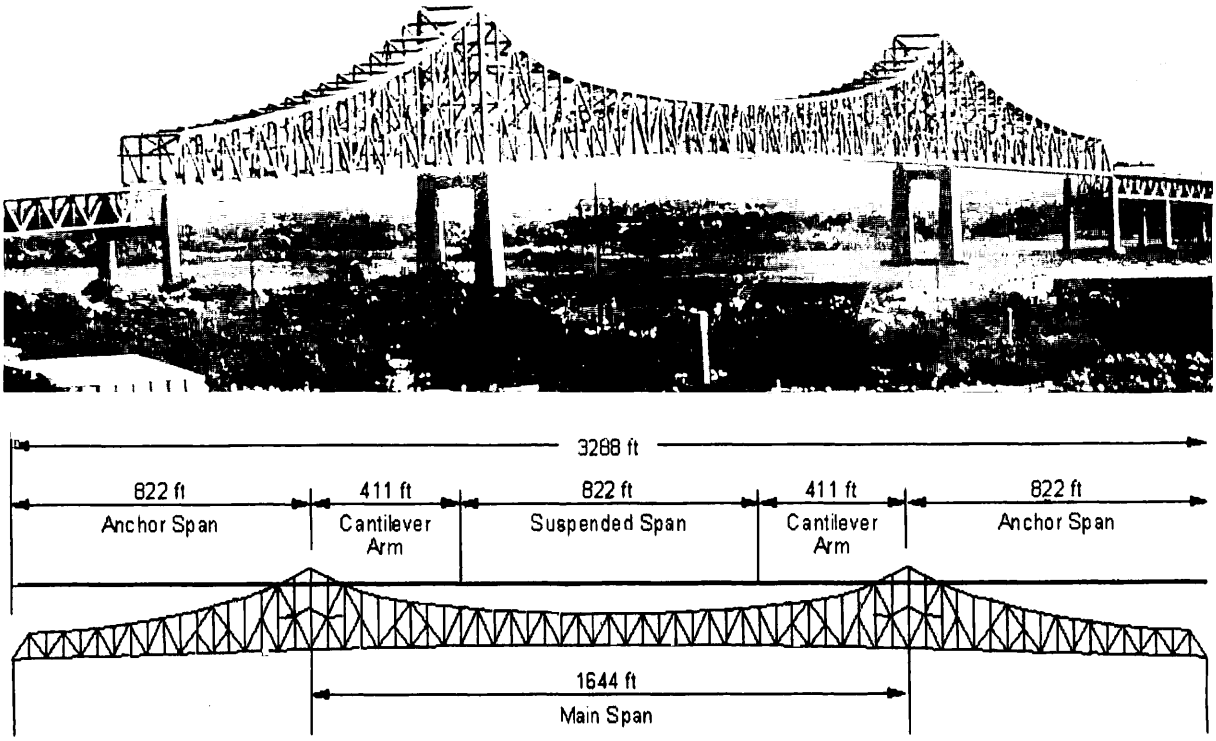

Fig. 11-53: Commodore Barry Bridge through-truss structure

The 3D geometry of the piers, supports, structural systems and components, connections, force-releases and the movement mechanisms were conceptualized by virtually reconstructing the entire structure in 3D CAD. At the culmination of this stage, the 3D CAD was transformed into a finite element model of the bridge and numerous analyses were conducted. Analysis results were correlated with the results from the initial design calculations and load-rating calculations.

As an example, Fig. 11-56 shows how the global geometric attributes of the structure and of the floor system (the shell elements modeling the concrete deck are not shown) were modeled by reconciling the 2D plans, photographs taken during visits to the bridge and 3D CAD. Similar comparisons of drawings, photographs, 3D CAD and the FE model were prepared for every critical region and detail of the structure such as the typical connections, bearings, member force releases, the movement systems, etc. In this manner, the FE model was developed and verified to represent all the critical physical details of the as constructed structure as completely and accurately as possible.

(b) Various experimental studies were conducted on the bridge:

- The operating vibrations were monitored at the tower regions, the mid-span and in the vicinity of the hangers.

Fig. 11-54: View of truss elements including a closeup view of a pin-and-hanger

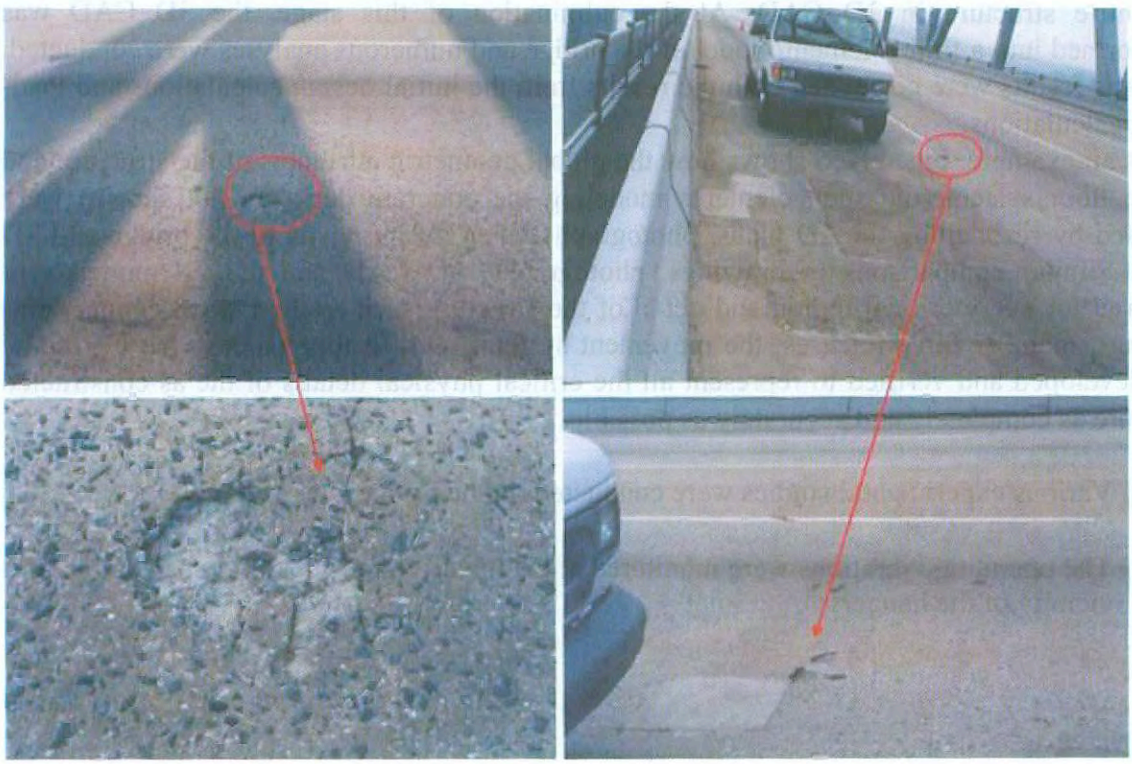

Fig. 11-55: Deterioration of lightweight concrete deck and view of railing

Approximately 16 accelerometers were used to simultaneously capture the traffic-induced vibrations and their attenuations or amplification through the deck, the railing, the floor system and the trusses. Frequency-domain transformations and cross-correlations revealed the dominant input vibrations occurred at a frequency band of 5-15 Hz and with an amplitude of about 0.25 g at the deck, attenuating to an amplitude of 0.15 g at the truss lowerchord. Impact-modal analysis of several railing elements revealed that the railing fundamental frequency in the lateral and vertical directions was about the same, 10 Hz, and this coincided with the frequency of the input excitation. The coupled lateral-vertical resonance of the railing elements caused extensive damage to the railing;

In conjunction with the ambient monitoring of the vibrations, various stringers and the girders of the floor system were instrumented and the operating strains were monitored under traffic. The stringers were observed to experience the largest tensile strains under traffic, corresponding to about 3-6 Ksi peak stresses at various locations. A composite behavior of the stringers with the lightweight concrete deck was evident from the measured strain profiles along the depth of the stringer sections under staffic.

Although it is certain that many interacting mechanisms are involved in causing the observed cracking and deterioration of the lightweight concrete deck, the traffic- induced vibrations were considered sufficiently critical as these aggravated the distress and at leas negatively impacted the effectiveness of any local patch repair. Various options for controlling deck vibrations exist. Increasing the mass of the deck and separating its frequency band from that of the input excitation, or making modifications to the structural connection details between the stringers and the floor girders, or adding artificial damping material to the stringers, as well as possible combinations of all of these options are promising alternatives. Naturally, simulations by a field-calibrated analytical model would be critical for evaluating these alternative solutions to the problem of deck vibration. Further, when the Authority considers it appropriate to replace the deck in the future, it is recommended to consider prefabricated posttensioned reinforced concrete segments as opposed to cast-in-place concrete. Recent applications of prefabricated segmental post-tensioned deck elements on the Van Der Zee Bridge in New York have enabled replacement with almost no impact on traffic.

- Various vibration dampers on truss members were tested in the field by monitoring the vibrations of the dampers and of the truss members before and after removing the dampers.

Some of the dampers on the bridge were replaced by spares and the removed dampers were brought from the field into the laboratory for in-depth testing of their mechanical, materials and dynamic characteristics. Dampers were found to have been well-tuned to the member frequencies for optimum energy dissipation. The chemical and physical properties of the neoprene material was investigated further by cutting samples for chemical analysis. Results did not reveal any deterioration.

Fig. 11-57 shows the photograph of a truss member equipped with several dampers. Note that the protective cover has been removed from one damper. A second photograph shows a close up view of the damper instrumented by two accelerometers. The time -histograms of member and damper acceleration responses in the same figure indicate that acceleration amplitudes that were about 0.15 g without the dampers are being reduced to about 0.06 g with the dampers. The importance of the dampers in controlling operating vibrations was therefore clear from these results from monitoring. Although the damper and member vibrations are yet to be monitored under sufficiently high wind that would cause wind-induced excitation of a member, it is clear that the dampers are highly effective and critical for controlling truss vibrations.

Results of material tests conducted on the damper material and experiences of the earliest users of similar material indicated that the dampers should have a useful life of at least 50 years if controlled by the durability of neoprene. Five different dampers representing different damper mass configurations were identified for continuous monitoring of their acceleration responses together with the truss elements, and a visual inspection schedule was designed so that the mechanical conditions of every damper and its attachment to the truss would have been evaluated at least once a decade.

- Nondestructive evaluation of the critical welds.

Electro -slag welds that were identified as critical and were previously tested in 1997 were re -evaluated by ultra-sonic and dye-penetration testing. No changes were observed in the conditions of any of the defects that were identified a decade ago. In addition, the welds on the critical hangers fabricated from A514 steel were tested and these were established to be in excellent shape. Monitoring of the traffic-induced strains of the truss members by strain gages intermittently over several months indicated live load stress amplitudes were within only 1 Ksi in the members with critical electro -slag welds and within 3 Ksi in the hangers.

- Instrumentation and continuous monitoring of both the intrinsic and transient (live - load) strains in the hangers, various chord elements and of the wind linkages for more than a year in conjunction with video images of traffic, wind and temperature.

Wind was measured at the tower and midspan of the bridge by four ultrasonic sensors. The data permitted an understanding and quantification of the loading influences creating intrinsic and transient stresses along with the stresses. Such an extensive and long-term data collection about the wind, temperature and live-load environment together with the corresponding strains provided a unique insight into the relative significance of the load effects and the challenges of health monitoring based on continuous and long-term data collection.

For example, unless wind speed and all of the three perpendicular wind directions are measured at a sufficient number of locations within the bridge, it is not possible to correctly characterize the wind environment. Many incidents of high wind were observed within the year. However, the measurements revealed that the mean windspeed during durations of consistent wind direction for an hour was significantly less than the peak wind speed measured on the bridge during the same duration. Therefore, even when wind speeds of 50-60 mph were measured, the "effective" wind speed was in fact 20 mph or less, and often such an

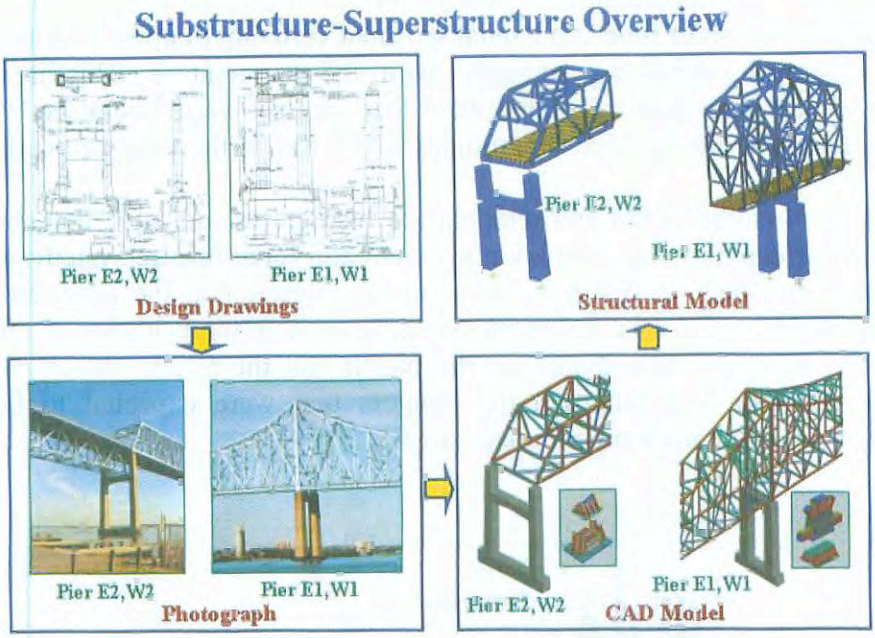

Fig. 11-56: Conceptualizing and 3D analytical modeling of the through truss structure

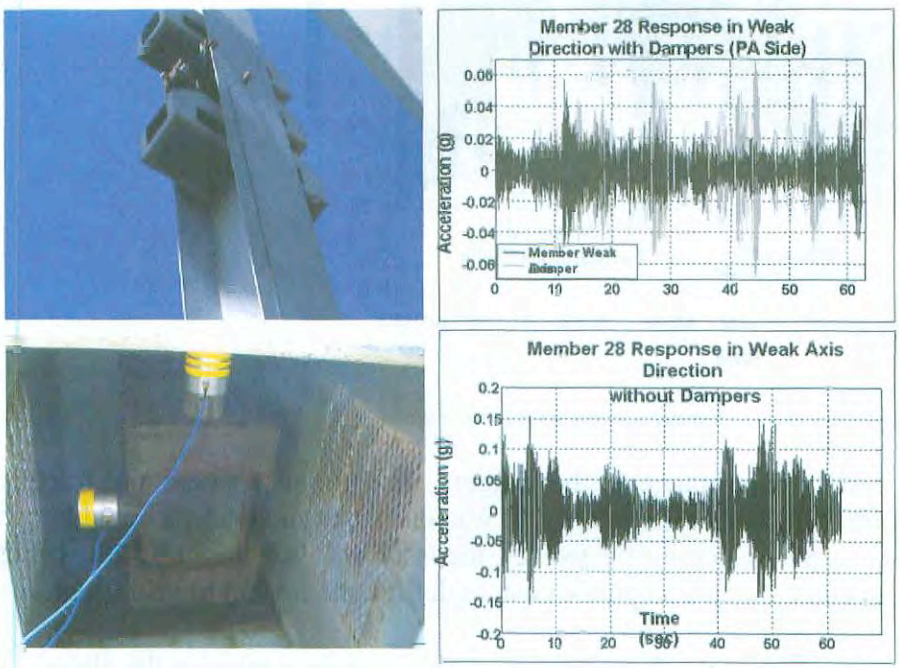

Fig. 11-57: Monitoring truss members with and without the vibration dampers

"effective" wind with a consistent direction may not occur at all throughout the entire length of the bridge. At the same time, although such "sporadic" high wind with changing directionality had little impact on the structural stresses and vibrations, it had significant impacts on the operations at the bridge. One conclusion was that a time window of an hour when high speed wind (exceeding 40 mph) may occur consistently in a given direction and throughout the entire length of the bridge may have a return period of a decade or longer.

Temperature changes and solar radiation were observed to be the most significant load effect on the trusses. For example, Fig. 6 shows the annual change in the intrinsic strains of one of the hangers, together with the temperatures recorded during the year. Strains are

observed to vary significantly in the order of 6 Ksi or more during days when large temperature changes occur within a short time. An annual seasonal variation of up to 10 Ksi is observed in the intrinsic strains correlating perfectly with the temperature. This is a considerable stress when we consider that calculated dead load stresses varied between 20 Ksi-30 Ksi at most truss members and reached magnitudes of 50 Ksi at the most critically stressed elements.

A closer scrutiny of the measured strain and temperature histograms indicated that the hanger intrinsic strains were affected by the complex movement and force-release systems at and in the vicinity of these members. A distincly unsymmetric behavior at the long-term strains of the two instrumented hangers was attributed to a difference in the behavior of the movement systems at their respective boundaries on the North and the South trusses. In addition, an out-of-plane behavior was noted in the hangers that were expected to be concentrically loaded due to radiation and temperature changes.

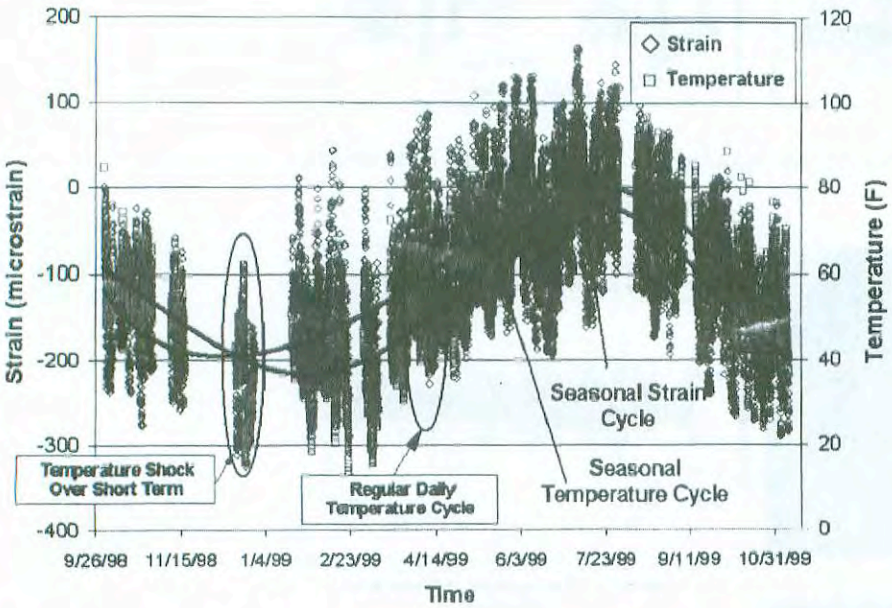

Fig. 11-58: Long-term changes in intrinsic hanger strains with temperature

Such observations were of importance as the hangers are the most critical and fracture-critical elements that control the system-reliability. It was clear that the bridge should benefit from a retrofit to enhance system-reliability, however, the issue was how to retrofit the bridge in an effective and safe manner and at acceptable cost, including the impact to operations.

- Ambient monitoring of the through-trusses was carried out for capturing the global dynamic characteristics of the proncipal structural system.

Ambient monitoring of long-span bridges has been attempted for many years, and it has been demonstrated that it is possible to extract some information about frequencies and mode shapes. However, there has not been any results revealing data on the dynamic properties of a major bridge with a desirable accuracy and completeness within their entire frequency band of interest, especially when the frequencies are less than 1 Hz. Recent work at Tokyo University demonstrated that it is possible to greatly improve the reliability of operating frequencies and mode shapes extracted from ambient vibration monitoring of long-span bridges by using a large number of sensors for simultaneously recording data throughout a bridge at a fine spatial resolution.

The frequencies and mode shapes, if they are reliably captured with a sufficiently fine spatial resolution along a bridge are invaluable for calibrating a finite element model.The dynamic characteristics may also be directly interpreted to gain insight about the boundary and continuity conditions under operating conditions. In most cases an ambient monitoring test may be the only means for objective measurements to gain insight on the actual global structural mass, stiffness and damping properties of a major bridge.

- Controlled load testing

Fig. 11-59 shows the cranes that were positioned in static configurations as well as crawled along the bridge for this test that required closure of the bridge. The through-truss and two typical approach spans were tested during the two consecutive nights on Nov 16 and 17.

Two 108 Kip cranes were used for loading and 52 high-speed strain gages were used for recording critical member strains during the tests. Both the floor system and the truss responses were captured as the cranes were statically positioned at critical locations. Following this a crane crawled on each of the five lanes throughout the bridge. By conducting the tests between midnight and 4 AM, it was possible to maintain reasonably constant ambient conditions. *Fig. 11-59* shows the influence coefficients obtained for one of the hangers and a lower-chord member at mid-span by crawling the crane along each lane. These influence coefficients may be further normalized by decomposing them into single-axle loads, and these may serve as an excellent index capturing the as -is structural behavior.

Even if different vehicles are used for repeating controlled load tests every several years or after a change in bridge conditions is suspected, changes in the influence coefficients for critical member responses can be detected, serving as an objective condition index. Both the relative values of the influence coefficients obtained for the loading of different lanes , and those obtained as the load resided at different locations along the bridge serve as valuable indicators of the stiffness and load distribution. The load versus strain relations at each location of the load(s) may serve as an independent test for checking the reliability of the finite element model in simulating local strains and therefore member forces under live load. Finally, the stress states that would be measured at critical member crossections by appropriate instrumentation provide an important understanding of local behavior, such as the level o f composite action and the amount of flexure in truss members. For example, measurements by the hanger instrumentation during the loading test indicated unsymmetric bending in these members.

(c) The calibration of the finite element model:

There are many practical uses of detailed 3D finite element models that are true to the actual geometry of the structure and capable of simulating local behaviors at the element and connection levels. Both hardware and software for analyzing large structural models have recently become readily available and feasible.

Before calibration, any human errors in input were eliminated by reviewing the results of diagnostic analyses and by systematically checking input data after transforming the input file into a spreadsheet format. In this manner various patterns represented within the data based on symmetry or anti-symmetry could be checked as a means of validating its accuracy. It is important to note that many errors in element properties and connectivity that were not recognized by reviewing the output of the diagnostic analyses were discovered by such a scrutiny of the patterns in the input data.

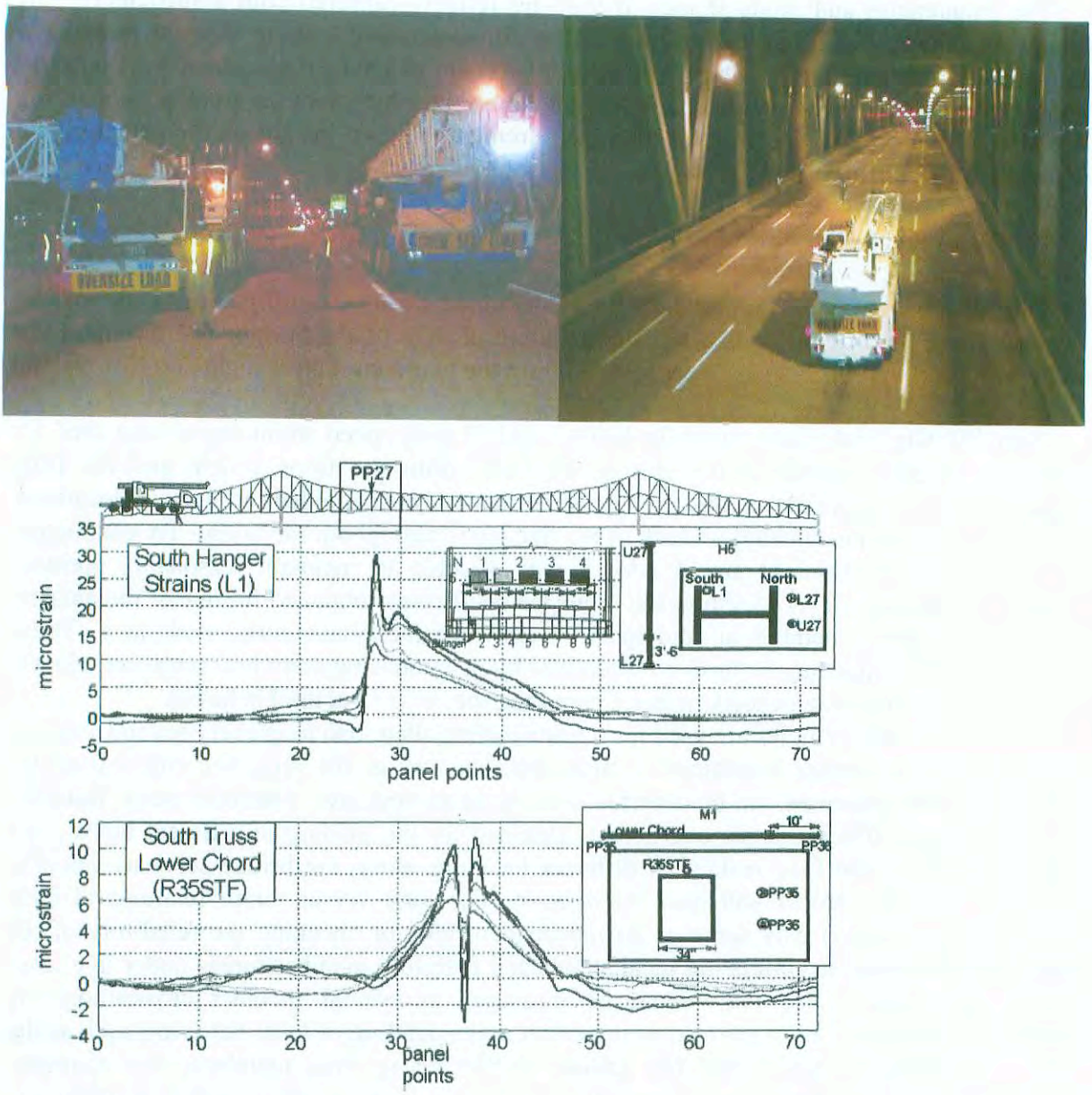

Fig. 11-59: Loading cranes and sample influence lines from controlled testing

Calibration process started by a careful analysis of mass and inertia modeling in order to eliminate the uncertainty in this parameter, and leaving only the stiffness-related parameters for adjustment. The impacts of substructure stiffness, boundary conditions of the superstructure, and the assumptions of continuity or lack of continuity at each of the movement mechanisms at the windlinkages, hangers and between the cantilevers and the suspended span on the calculated frequencies and mode shapes were investigated.

After understanding the impact of various assumptions on boundary and continuity conditions on the dynamic properties, the pier stiffnesses were increased substantially, and all the movement mechanisms were fixed before the model dynamic properties approached the measured properties. After a sufficiently c lose correlation was obtained between the measured and simulated global dynamic properties, the strains at the critical elements obtained during the controlled load testing were used for local calibration of the floor system element and connection s tiffnes ses . When a fully -composite behavior of the deck and the stringers, and full continuity between the stringers and the deck were simulated, the root-

mean-square (RMS) of the error between measured and simulated strains at 20 measurement locations were reduced from 55% to 24%. The assumptions on global and local stiffness and continuity brought the RMS of the errors in the first six frequencies from 28% to 1.5%. Hence, the model was considered to be sufficiently calibrated. This model can now reliably serve for condition evaluation, load-rating, vulnerability evaluation, evaluation of any retrofit scheme, etc.

11.8.3 Conclusions and recommendations

The two areas of special concern for the bridge owner have been the deterioration of the deck concrete and the lack of system-reliability due to the fracture critical hangers. Data collected on vibration levels of the deck, of the truss, and how dampers on truss elements are effectively reducing the vibration of these elements should be useful for making decisions regarding the serviceability of the deck. This data, in conjunction with the calibrated finite element model of the bridge representing the deck and the floor system and their relation with the truss in detail, are sufficient for evaluating alternatives for the replacement or modification of the deck.

About a year ago, t he Authority has issued a contract for hydro -demolition of the deteriorated areas and patching these with a new material that is claimed to have excellent bonding characteristics. This operation, as would be expected, has had a significant impact on the operations as two of the five lanes at a time are blocked for maintenance. However, once this operation is complete, it may be an excellent time to add a sealant membrane and a 2 inch riding surface on the deck for both reducing the vibrations and for helping confine the patches. At this time, the hangers would have been retrofit as discussed in the following, and there should not be a concern in relation to adding to the dead load.

The Authority has issued a contract for the design and installation of retrofit on the four hangers. The retrofit concept is simply "post-tensioning" each of the hangers by four rods, tensioning the rods in increments and in sequence so that about half the tension carried by the hanger is taken over by the rods. Naturally, there are many installation and long-term maintenance issues that require careful analysis, however, the system has already been applied to a number of major cantilever truss bridges in the area without any incident. At the same time, given the significant levels of intrinsic force variation in the hangers, their state of unsymmetric bending, and the complexity of their boundary conditions at the truss connections, it is prudent that a careful monitoring of the state-of-stress in the hangers and in the post-tensioning rods be carried out during and following installation.

11.9 Evaluation of historic concrete structure

Jerome P. O'Connor, James M. Cutts, Grefory R. Yates, and Carlton A. Olson

Concrete International, Volume 19 Number 8, August 1997

11.9.1 George Rogers Clark Memorial

1) Vincennes, Indiana, is the home of a memorial built to commemorate the evolutionary War victory of George Rogers Clark over the British at Fort Sackville, which opened up the westward expansion of the United States (Fig. 11-60). Built in the early 1930s, the facility includes a colonnaded monument building and a terrace approximately 52 m square. Below the memorial and terrace are reinforced concrete support slabs, beams, and columns. The facility is owned and managed by the NPS.
Shortly after completion of the facility, the terrace began to lead. Though many different attempts have been made to stop the leaks, no repair has been successful in providing a long-term solution to the problem. Water leakage has resulted in concrete deterioration as well as damage to finishes in service areas, while rendering other areas under the terrace unsuitable for storage.

2) The evaluation revealed that the majority of the deterioration of the concrete support structure and leakage through the terrace was adjacent to construction joints running through the structural elements (Fig. 11-61). Deterioration in these areas of the structure included corrosion damage to concrete beams and slabs. Away form the construction joints, damage was much less extensive. To assess the condition of the terrace waterproofing systems, areas of topping concrete and stone work were removed. A waterproofing membrane present on top of the structural slab was found to be brittle and discontinuous.

   Results of the evaluation showed the following:
   (a) Deterioration of the concrete was present in the terrace structure in the form of corroded reinforcement with subsequent delamination and spalling of cover concrete.
   (b) Deterioration was concentrated along construction joints that were present at regular intervals throughout slabs and beams.
   (c) Leakage through the terrace occurred at random cracks in the support slabs but was especially severe at construction joints. Stalactites had formed at cracks and joints.
   (d) Covermeter surveys verified reinforcement to be generally as specified. Cover over reinforcement was generally 13 mm in slabs and 38 mm in beams, with some localized areas less than 6 mm. Diagonal cracks were observed on the sides of "stepped" girders framing between the terrace and columns supporting the memorial building. Computer analysis verified that the cracks were caused by thermal expansion and contraction of the structure.
   (e) Half-cell potential tests verified a low probability of active corrosion of embedded reinforcement in areas away from locations of visible corrosion damage.
   (f) Concrete cores were tested in compression and for chloride ion content and were subjected to petrohgraphic examination. The compressive strength of concrete averaged 57.9 MPa. Chloride ion contents were lower than the threshold generally

regarded as the level at which corrosion of reinforcement would occur. The microscopic evaluation verified good quality.

3) Water leakage through the terrace occurred at random cracks in the support slabs but especially severe at construction joints has resulted in corrosion of the reinforcement with subsequent delamination and spalling of cover concrete.
4) Recommended repairs to the structural elements included conventional repairs to corrosion-damaged members. Also recommended were repairs to the terrace waterproofing system, including the removal of concrete and stone surfaces to allow for the installation of new waterproofing and drainage materials. The evaluation also recommended that only non-chloride-based deicing chemicals be used on the terrace surfaces.

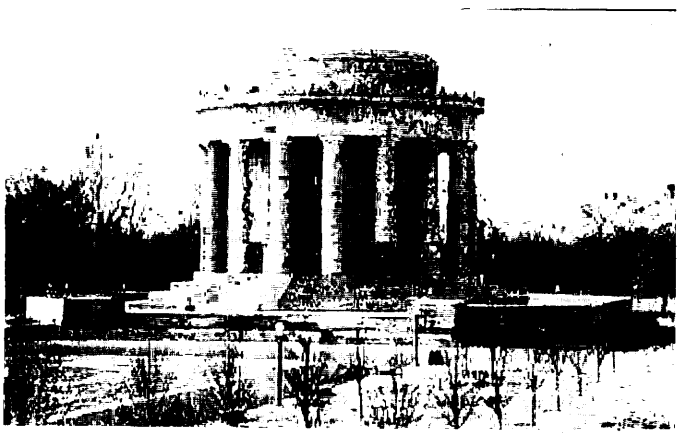

Fig. 11-60: Overall view of the gorge Rogers Clark Memorial

Fig. 11-61: Concrete deterioration at a joint in the Clark Memorial terrace

11.10 Condition assessment of a 50 year old reinforced concrete bridge

Johannes E. Maier

Züricher Hochschule Winterthur, Switzerland

11.10.1 Structural description

The Langensand Bridge, a two span concrete box girder bridge, is located near the railway station of Luzern. Constructed by the end of the 1930's it replaced an existing steel truss bridge. The bridge traverses the rail tracks, connecting Luzern's city center with the industrial area located near the railway station. Apart from several public bus services the bridge serves mainly the heavy traffic to the nearby industrial area. The low traffic capacity of the connecting roads causes repeatedly a tailback of vehicles on the bridge. The average daily traffic volume passing the bridge consists of 1350 busses and 22000 passenger cars.

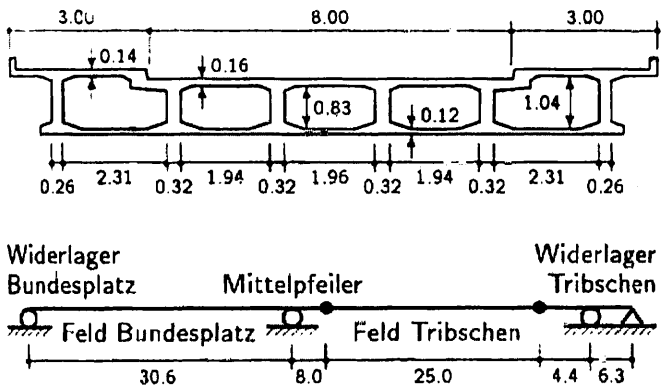

Fig. 11-62: Cross section and structural system of Langensand Bridge

The box girder consists of 5 continuous variable-depth (1.0 – 1.4 m) concrete box sections, the depth being increased over the two abutments and internal support. There are two internal hinges located at the second span (Tribschen) changing the structural system to a cantilever beam. In longitudinal direction the bridge deck is divided into chambers by transverse cantilevers, see Fig. 11-63.

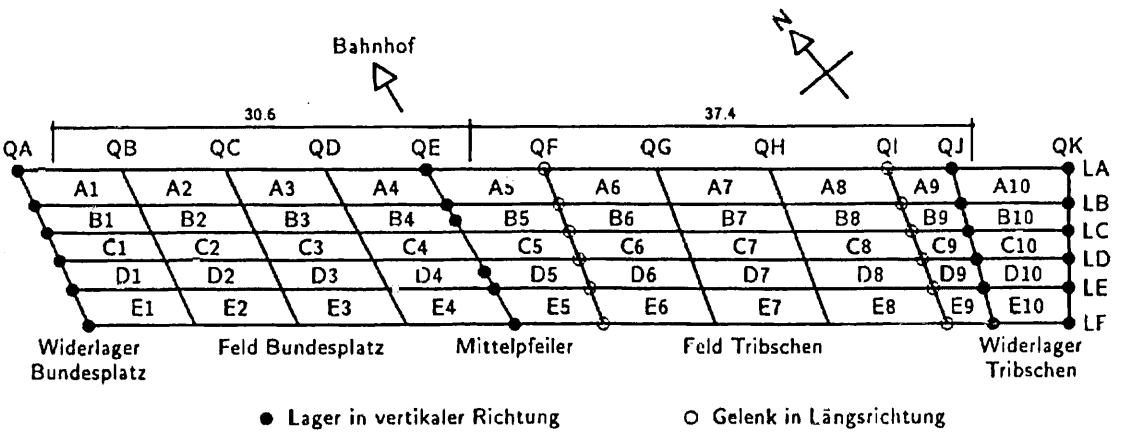

Fig. 11-63: Plan view of bridge deck, showing girder arrangement, hinges and supports

11.10.2 Objectives

In 1991 the Swiss federal railway authority commissioned the Dr. P. Ritz & Dr. B. Zimmerli Engineering Inc. to evaluate the structural integrity and verify possible restoration needs. The condition assessment procedure comprises the following steps:

- Visual inspection
- Mapping of corrosion potentials on the bottom side of the bridge deck
- Core sampling for material testing purposes
- Static recalculation
- Bridge restoration concept
- Cost estimate

This segmental approach for condition assessment provides a maximum efficiency and allows for continuing adjustment of the procedure according to the actual condition of the structure. With the aid of potential mapping, critical areas within the structure could be identified at an early stage. Thereby it was possible to select suitable locations for core sampling.

11.10.3 Visual inspection

Within the visual inspection that was carried out in spring 1991 the total surface area and the accessible spaces inside the bridge were examined. The following results were concluded:

- Spalling and rust stains at edge beams; corroded reinforcement is partly visible
- Spalling and heavy corrosion of deck slab beneath the sidewalks at box girder access holes
- Accumulations of mud, sand and water in box girder chambers due to damaged joint sealings
- Active hairline cracks in the driveway slab and webs at the middle pier
- Localized increased concrete porosity and voids with exposed reinforcement along the girder
- Exhausts from steam and diesel locomotives have blackened the bottom view of the bridge girder; lime scums can be found at various points and in particular at hinge joints
- Deterioration of concrete surface at the pier and abutments
- Trucks and busses can easily excite the bridge structure, this might be due to unevenness of the roadway joint at the abutment Bundesplatz

11.10.4 Mapping of corrosion potential

Surveys conducted by the Swiss Society for Corrosion Protection [0], have shown that potential measurements carried out at the bottom side of the driveway slab provide reliable information on the rebar corrosion state of the upper reinforcement layer. This is of viable importance for economical structural inspection. Since if the measurements have to be carried out at the deck surface all coating and sealing layers would need to be removed. However, in case the lower reinforcement layer is subjected to corrosion but the concrete surface shows no signs of corrosion wrong result might be obtained with this method.

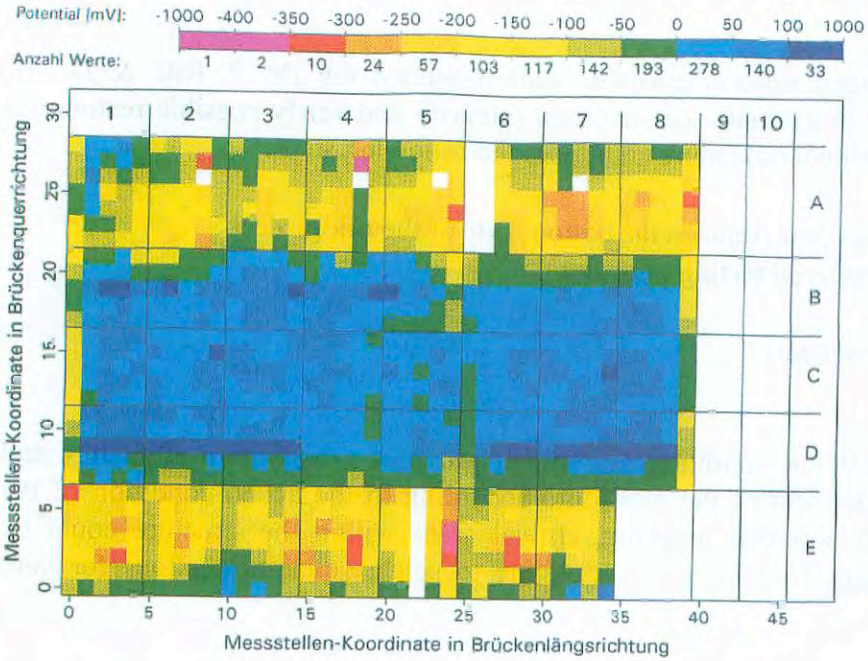

Fig. 11-64: Potential measurements carried out at bottom side of driveway slab (A to E = Cells, 1 to 10 = Chambers)

At the Langensand Bridge the corrosion potential was measured at 1100 points. The spacing between measurement points in the longitudinal direction was 1.3 to 2.0 m, and in transversal direction an average distance of 0.4 m was chosen. Fig. 11-64 shows the results obtained.

The following conclusions were drawn from measurements:

- High possibility of corrosion near box girder access holes (measured potential ≤ -275 mV, active state)
- Corrosion is likely to occur at the inner edge of sidewalks, hinges, and the roadway joint near abutment Bundesplatz (measured potential ranging between –250 and 0 mV)
- Corrosion can be excluded in the driveway area (measured potential ≥ 0 mV, passive state)

In order to confirm these results, surface layers were removed at 4 locations on the north end of the bridge and additional potential measurements on the deck surface were performed. Further, the condition of rebars was examined and the chloride content determined. Since no signs of active corrosion were found at these locations, a low possibility of corrosion can be assumed for the whole deck reinforcement apart from the area near the box girder access holes.

11.10.5 Material testing

For laboratory testing concrete cores of 50 mm diameter were drilled and additional inspection openings were cut for reinforcement examination.

11.10.5.1 Measurement of concrete cover

The use of a concrete cover meter for this task was impossible due to electro-magnetic fields induced by overhead contact lines. Thus the concrete cover thickness could only be determined at core holes or separate openings where reinforcement was visible. Apart from the bottom slab where a value of 11 mm was observed, the minimum concrete cover measured corresponds to 17 mm.

11.10.5.2 Concrete texture and porosity

The concrete texture and porosity was examined on thin sections. The results showed that porosity is mainly caused by single voids and cavities. Regarding admixtures, a considerable mica content but low content of powder materials like fine sand and cement were observed, which results in poor embedding of coarse grains. Porosity measurements showed a total pore volume of 12% and an air filled pore volume of 1%. The frost resistance determined by an empirical relationship is found to be medium to high.

11.10.5.3 Carbonation

The carbonation depth was measured by sprinkling the fracture surface of both the splitted drill cores and the inspection openings on the structure with Phenolphthalein.

Maximum carbonation depth:	
Abutment Tribschen	31 mm
Abutment Bundesplatz	40 mm
Bottom slab	30 mm
Girder LA	25 mm
Girder LC and LD	60 mm
Girder LF	20 mm
Middle pier – truss	20 mm
Middle pier - slab	40 mm

11.10.5.4 Chloride content

Chloride measurements where carried out on 12 drill cores obtained from the inspection openings used for potential measurements. The first 10 cm of the cores showed values between 0.032 and 0.096% of the cement mass. These values lie far below the critical value of 0.4 of the cement mass, which accounts for the good concrete protection by the asphalt coating. The locations for the inspection openings were chosen in areas that showed low corrosion potentials, indicating that corrosion is likely to occur. Due to the low Chloride content encountered at these inspection openings it can be concluded that no salt-water intrusions have occurred anywhere else on the bridge deck.

11.10.5.5 Concrete compressive and tensile strength

The concrete specimens obtained from longitudinal girders and the bottom slab showed compressive test values between 46 and 125 MPa, which result in an average compressive strength of 88 MPa. The statistical analysis performed in accordance with the SIA norm 162 classifies the test results into concrete category B50/40.

The test results for concrete tensile strength were obtained in the range of 2.7 to 5.0 MPa, also complying with concrete category B50/40.

The results for the Young's modulus range between 31 GPa and 54 GPa, lying within the scatter range of concrete category B50/40.

11.10.5.6 Steel strength

Test results using steel specimens, extracted from the actual structure showed the appropriate steel quality (St37 and St52), as it was specified during bridge design.

11.10.6 Static recalculation

During planning and construction of the Langensand Bridge the SIA norm 112 (published 1935) was effective. It was used for the definition of loads but also contained design guidelines. The recalculation task was carried out in accordance with today's SIA norm 160 (published 1989) for load definitions and SIA norm 162 (published 1989) containing design guidelines.

Based on experimental test results the following material constants were assumed:

- **Concrete B50/40:**
  Compressive strength = 26 MPa
  Shear stress limit = 1.2 MPa
  Young's modulus = 35 GPa

- **Reinforcement St37:**
  Yield point = 240 MPa

- **Reinforcement St52:**
  Yield point = 350 Mpa

For analysis of the complete structural system the box girder was modeled as a grid with torsional flexibility. Thereby neglecting the flexural strength of the upper and lower deck slab as well as the torsional stiffness of longitudinal and transversal girders results in an underestimation of the overall load capacity. For the recalculation of the bridge deck in transversal direction a continuous beam with two cantilevers was considered. A dynamic load factor of 1.8 was used.

11.10.6.1 Ultimate limit state

The SIA norm 162 requires a minimum resistance factor of 1.2 for reinforced concrete structures.

Load factors used for structural analysis:

- Self-weight of the structure = 0.8 / 1.3
- Additional dead loads= 1.0 to 1.3
- Traffic loads = 1.5

The structural analysis yielded unsatisfactory resistance factors in bending mode for the edge girders LA and LF at the center of both spans (minimum value 0.98). However, none of the longitudinal girders fell below the requested shear resistance. The bending resistance was proven to be insufficient (minimum bending resistance value 0.51) for the transversal girders QC, QE, and QG in contrast to their shear resistance capacity. Due to the reduced loading and dimensions of the other transversal girders no analysis was carried out for these members.

In a second approach the transversal stiffness was reduced by a factor of 10. Consequently, the reduced load distribution of the transversal members resulted in lower bending resistance factors in longitudinal direction (minimum value 0.94 at girder LA) and a marginal sufficient load bearing capacity in transversal direction.

According to these results the driveway slab does not provide sufficient bending resistance. This is especially valid for the sidewalks with a minimum bending resistance of 0.38, where the slab thickness amounts only 0.14 instead of 0.16 m. In the area of the roadway local plastic deformation leading to stress redistribution can help to mobilize the required load bearing capacity. Furthermore the punching shear check yields inadequate resistance values for the sidewalk area. Whereas the structural analysis of the four truss elements and two slabs located at the pier showed satisfactory results.

11.10.6.2 Serviceability limit state

Due to the structures dead load and with consideration of creep effects a maximum deflection of 95 mm at the second span (Tribschen) of girder LA was calculated. This value exceeds the allowable deflection of l/700 = 57 mm by 67%. At the first span (Bundesplatz) of girder LF the maximum long-term deflection is reached exceeding the threshold value by 64%.

In contrast to the long-term deflections, short-term deflections due to traffic loads remain below threshold. The maximum short-term deflection amounts 27% of the threshold value (l/600), it was obtained at the first span (Bundesplatz) of girder LC.

11.10.6.3 Vehicle Impact

A collapse of the Langensand Bridge due to head-on train collision would cause considerable economical damage and certainly have an impact on railway operation. The risk evaluation of a possible train impact showed that the bride abutments and middle pier are located in a potential danger zone.

The SBB guidelines for site layout and design of structures located in collision risky areas stipulates a front impact design load of 3.0 MN and a lateral impact design load of 1.0 MN. Recalculation according to these values showed insufficient structural resistance.

11.10.7 Restoration concept

Based on investigation results the cost for the necessary maintenance work amounts to 0.94 or 1.05 Million Swiss Francs, depending on the construction method. The following work tasks were suggested:

- Installation of guard rails to separate roadway from sidewalks
- Renewal of driveway slab near box girder access holes

- Replacement of curbs and banister
- Drainage of girder cells
- Replacement of roadway joints at hinges and at the abutment Bundesplatz
- Sealing of bridge deck and pavement renewal
- Repair spalling concrete
- Fixing of cracks at the middle section of outer longitudinal girders by injection

Absence of cracking and a high concrete tensile strength indicate that no bridge deck enhancement is necessary. Cleaning of the highly polluted concrete surface and impregnation with a hydrophobic coating would prevent water from penetrating into the concrete and improve the overall appearance of the structure. The required impact resistance for the abutments can be achieved by filling the interior with concrete. With regard to the middle pier, a cost-risk analysis showed that replacement is the best solution. All the repair work needs to be carried out in 3 steps in order to minimize traffic interference, except for the work at the bottom side where rail traffic affects working conditions.

11.10.8 References

1) F. Hunkeler, *Grundlagen der Korrosion und der Potentialmessung bei Stahlbetonbauten*, Vereinigung Schweizerischer Strassenfachleute, Zürich, 1994

11.11 Static and dynamic monitoring of concrete structures by means of fiber optic Bragg grating sensors

S. Matthys, W. Moerman, L. Taerwe

Magnel Lab. for Concrete Research, Ghent Univ., Belgium

W. De Waele, J. Degrieck

Dept. Mechanics of Materials and Structures, Ghent Univ., Belgium

G. De Roeck, S. Jacobs

Dept. of Civil Engineering, K.U.Leuven, Belgium

11.11.1 Abstract

The integration of Bragg grating sensors in concrete structures in order to measure deformations has proven to be successful in several applications. Examples of monitored structures by the Magnel Laboratory for Concrete Research are a concrete girder bridge over the Ring Canal by Ghent, a Quay wall at the Ring Canal and a trough girder containing a railway track of a bridge. Currently a joint research project investigates the feasibility of integrating Bragg grating sensors in concrete in order to dynamically monitor a 17.6 m long prestressed concrete girder. Also, a Bragg grating based deformation amplifier which can be attached externally to the concrete surface is under development. During the project 3 post-tensioned concrete girders will be submitted to static and dynamic loading conditions and monitored with several types of measuring devices, including accelerometers, Bragg gratings, deformeters, crack microscopes, etc. Although, only the first test stage has been completed the use of Bragg gratings looks feasible and promising for dynamic monitoring.

11.11.2 Introduction

The interest to monitor the structural behaviour of infrastructure in a more detailed way, has grown considerably over the last 15 year. This interest relates to several (deterioration) problems which have been reported and demonstrate that the service life of infrastructure is often shorter than planned for or that unforeseen problems may occur. With respect to periodic inspections, monitoring in a more continuous way offers an important contribution to the safety, economical benefit (reducing repair and disrupt costs) and feedback for design guidelines.

Existing monitoring techniques, not based on fibre optic sensing, are limited in number and application possibilities. The use of fibre optic sensors offers a enhancement, resulting in a better and wider use of monitoring techniques. At the Magnel Laboratory for Concrete Research of Ghent University, monitoring of concrete structures with Bragg sensors has been investigated (Moerman, Taerwe, Waele, Degrieck, Baets 2001 [13], Moerman 2001 [14]). Given the multidisciplinary character, this research has often been executed in collaboration with other research groups. As a result of this research during the last years several practical applications of monitoring of newly built concrete structures have been initiated (see next section).

Furthermore, a strong research interest exist on dynamic monitoring of civil engineering structures, to detect damage by changes of the dynamic characteristics of the structure (Wahab, De Roeck 1998, [15]). In a recently started research project "Enhanced Performance

of Dynamic Monitoring of Civil Engineering Structures by Integration of Optical Fibre Sensors", several research groups from different universities in Belgium investigate together the feasibility and application possibilities of dynamic monitoring of prestressed girders by means of fibre optic Bragg gratings. To cover both newly built and existing concrete structures, also the feasibility of a Bragg grating based deformation amplifier which can be applied externally, is under development.

11.11.3 Structures monitored by the Magnel Laboratory

11.11.3.1 Box girder of road bridge

At the south of the city of Ghent a prestressed concrete girder bridge, with a total length of 147 m, was built in 2001. The bridge has two side spans with a length of 40 m each and a central span of 67 m, crossing the Ring Canal. The bridge consists of two identical box girders placed next to each other. After tensioning the cables of the first box girder, it was pushed aside in order to enable the contractor to use the same scaffolding for the second girder without having to displace it. Three cross sections of the first girder (midspan of a bridge side span, section above an intermediate support and midspan of the central span) were instrumented with 6 fibre Bragg grating (FBG) strain sensors (see section below) each. In each sections one sensor is integrated at the top and the bottom of the 3 webs (Fig. 11-65). For verification, at the level of the FBG strain sensors additional strain measurements are performed at the concrete surface with mechanical deformeters (Demec).

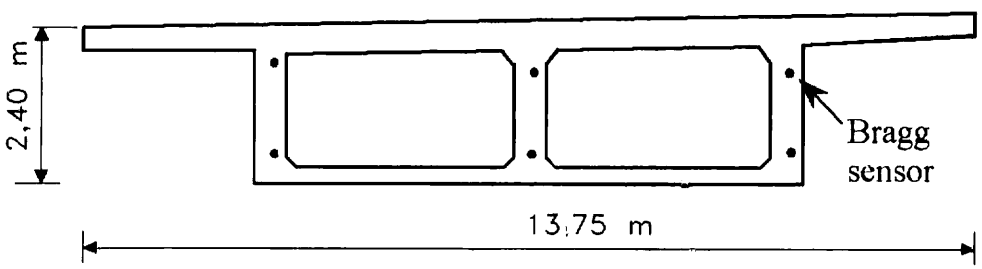

Fig. 11-65: Position of the FBG strain sensors in a cross section

The purpose of the project was to monitor the girder during the tensioning of the prestressing cables, the push aside phase, the proof load testing and afterwards during service. An example of the measurements during tensioning is given in Fig. 11-66, which shows the strains measured in the middle web at midspan of the central span. The results obtained from the FBG strain sensors correspond well with the results obtained by using the mechanical deformeters. The correspondence was also good with respect to the calculated strains. In comparison with the deformeter measurements, the FBG readings gave a much clearer indication of the sequence at which the different cables were tensioned in the cross-section. During the push aside phase, data readings indicated no significant changes in the stress state of the girder.

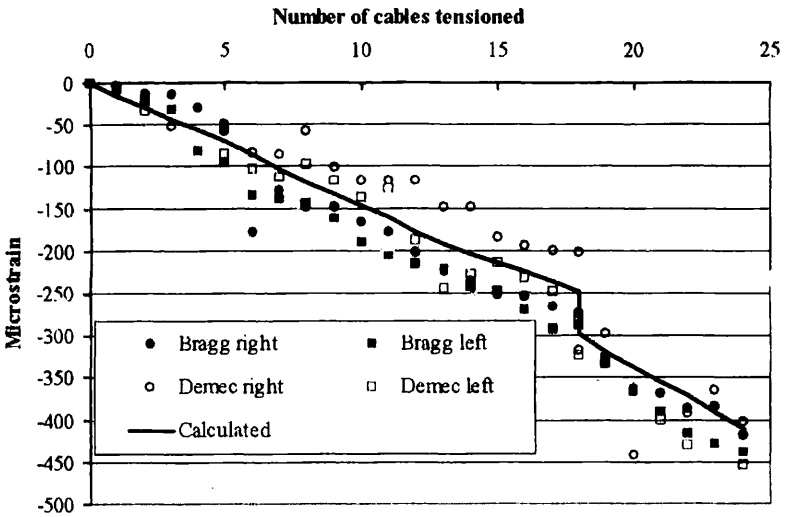

Fig. 11-66: Strains measured in the middle web at the mid-section of the central span

11.11.3.2 Quay wall

In order to measure the forces in 3 ground anchors of a 175 m long quay wall (Fig. 11-67) a load cell based on Bragg sensors was developed. In order to exclude the influence of the eccentricity of the applied load, each load cell contains 3 Bragg sensors placed every 120°. The load cells could easily be integrated in the quay wall and allowed a determination of the force in the ground anchor during the test phase (up to 2 times service load), during final tensioning and afterwards. Comparison with the loads derived from the oil pressure of the hydraulic jack used to tension the anchors showed a very good agreement, as demonstrated in Fig. 11-68.

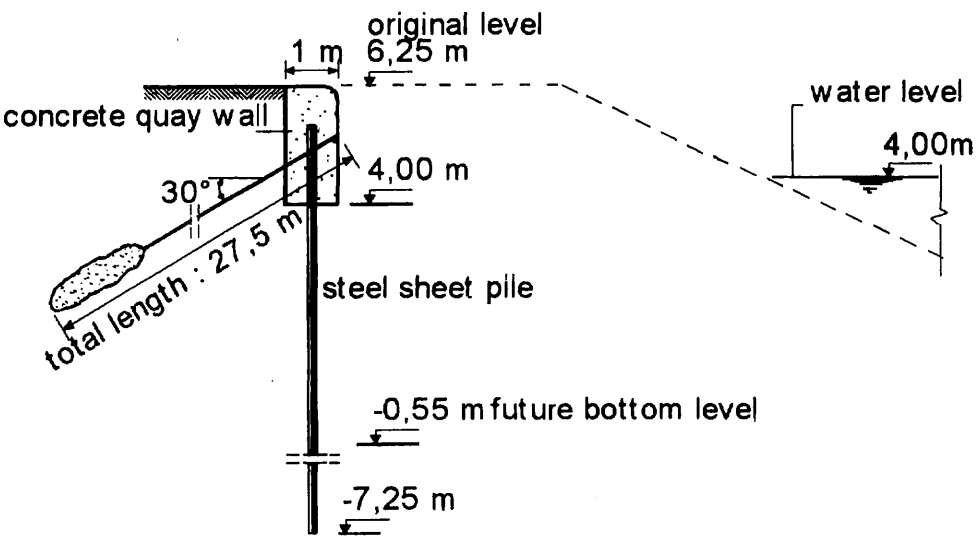

Fig. 11-67: Cross-section of the quay wall

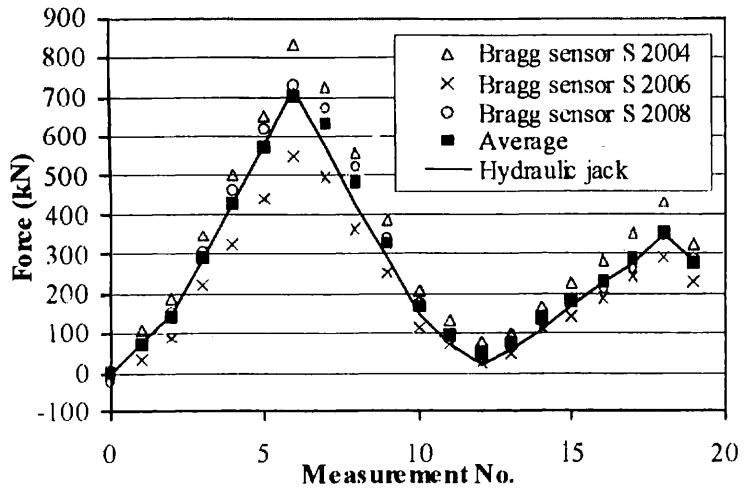

Fig. 11-68: Bragg grating monitoring of force in ground anchor

11.11.3.3 Trough Girder of Railway Bridge

For the replacement of the steel deck of a railway bridge along the rail track Gent-Moeskroen, the national railway company (NMBS) decided to use two prefabricated prestressed trough girders, of one which has been equipped with 10 FBG strain sensors at different locations and directions. Each trough girder is 4 m wide and 16.4 m long. A view of the installation of the FBG strain sensors during manufacturing of the reinforcement cage of the girders is given in Fig. 11-70. The installation of the girders is scheduled for the end of May, beginning of June 2002.

11.11.4 Dynamic monitoring

Whereas the above mentioned projects basically focus on quasi-static monitoring of concrete structures so far, there is also a considerable interest in dynamic monitoring. For this reason, a research project "Enhanced Performance of Dynamic Monitoring of Civil Engineering Structures by Integration of Optical Fibre Sensors" has recently been started. Some details of this project and the first test results obtained, are discussed in the following sections.

11.11.4.1 Aim of the project

Bringing together expertise from different research groups, it is aimed to develop a monitoring technique for civil engineering structures able to detect damage by changes in the dynamic response (dynamic system characteristics). The application of such a dynamic monitoring technique can lead to early detection of damage which eg. may result in significant savings of maintenance and 'disrupt of use' costs. Also, for the evaluation of the effectiveness of rehabilitation and strengthening interventions, dynamic monitoring tests before and after may be useful. Furthermore, with the dynamic monitoring technique it is aimed to increase the monitoring performance with respect to localization and quantification of damage.

11.11.4.2 Outline

As the available information of the dynamic behaviour of prestressed concrete is scarce and as the relation between strength and stiffness of prestressed concrete is less clear (due to the prestress, damage initiates less easily cracks or cracks tend to close again) than for reinforced concrete, it has been decided to focus the project on prestressed concrete. For the dynamic monitoring tests accelerometers as well as optical fibre strain sensors are used. The latter are based on Bragg gratings.

The project, which is scheduled to run from 2001 till 2004, is multidisciplinary bringing together expertise of 5 research groups coming from the universities of Ghent, Leuven and Brussels and the Royal Military Academy. The following tasks are defined:

- Characterization of damage, for correlation and comparison with damage prediction from the dynamic monitoring tests. Among other aspects, emphasis will go to the study of the cracking behaviour using visual inspection and (video)microscopy, ultrasonic measurements, strain measurements and digital image correlation techniques.
- Determination of modal strains as these are sensitive damage indicators. For the measurement of modal strains, the feasibility and performance of optical fiber sensors are studied. Exploratory research has already demonstrated that the Bragg grating is an excellent sensor for dynamic measurements.
- Development of numerical models for (cracked) reinforced and prestressed concrete, to correlate results of dynamic monitoring tests with predictions.
- Optimization of damage identification algorithms for dynamic monitoring data.
- Investigation of the statistical uncertainty of the measured changes in dynamic system characteristics, which is important to assess the accuracy in localizing and quantifying damage based on dynamic monitoring.

11.11.4.3 Test parameters and configuration

Tests are conducted on 3 prestressed (post-tensioned) large scale concrete beams with a total length of 17.6 m and a total depth of 0.8 m, produced and tested at the Magnel Laboratory for Concrete Research. The dimensions and test set-up are given in Fig. 11-69. A first beam is subjected to both dynamic and quasi-static loading. After dynamic monitoring tests of the yet unloaded beam, several quasi-static load/unloading steps will be executed, each time followed by a dynamic (monitoring) test. The load steps are gradually increased until failure. The two other beams will be subjected to simulations of real damage scenarios.

During quasi-static loading the beams are tested in 6-point bending (Fig. 11-69). For the dynamic monitoring tests the beam is each time placed on 4 air spring bellows at a certain distance of the beam ends and subjected to an impact of 120 kg at one beam end. The impact is excentrically with respect to the longitudinal beam axis, in order to initiate both bending and torsion modes. For a good characterization of the degree of damage, modal strains need to be measured for a sufficient number of eigenmodes (experiments are aimed to be conducted in the frequency range of 0 till 200 Hz).

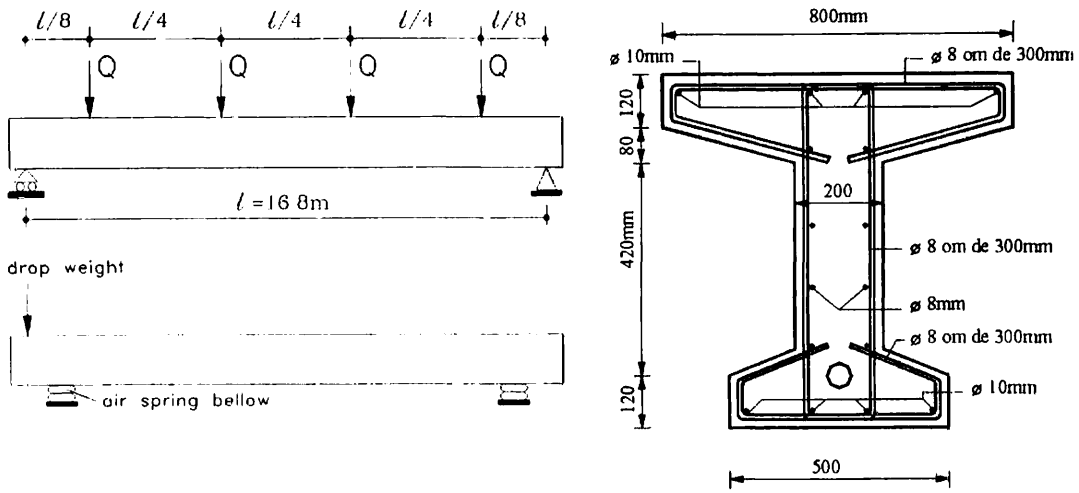

Fig. 11-69: Test set up and beam cross-section at midspan

A first beam has been produced, containing 8 internal FBG strain sensors, 4 sensors at the midspan section and 4 at a distance of 5.2 m from the beam end. These locations correspond with those sections for which maximum deformations are obtained for respectively the first 2 eigenmodes. After post-tensioning the beam was moved on his static supports and preparations for the dynamic monitoring tests were executed. First dynamic monitoring tests were performed, basically to verify the test set-up, measuring equipment and data acquisition. To stabilize the beam position at the dynamic supports when floating the air cushions (so that the beam is lifted from its static supports) and during dynamic monitoring, cross-shape installed tensile chords are used. With this configuration it is avoided that the beam shifts away from its dynamic supports, yet allowing a sufficient degree of freedom to move (vibrate) during the impact test.

11.11.4.4 FBG strain sensors

In this research programme, two types of strain sensors are used, both based on fibre Bragg gratings (FBG strain sensors). A first type, used as internal sensor, has been developed at the Magnel Laboratory for Concrete Research and has already been implemented in several cases (see section 'Structures Monitored by Magnel Laboratory'). The strain sensor consists of a deformed steel rebar with a diameter of 14 mm and a length of 1.2 m (Fig. 11-71). At the middle of the bar a Bragg grating is glued into a narrow groove, with a specially selected and tested adhesive. At the opposite side a thermocouple is attached to allow temperature compensation. This internal FBG strain sensor, which has been extensively tested in laboratory conditions (Moerman 2001 [14]), can be implemented in newly built structures, to measure the concrete deformation.

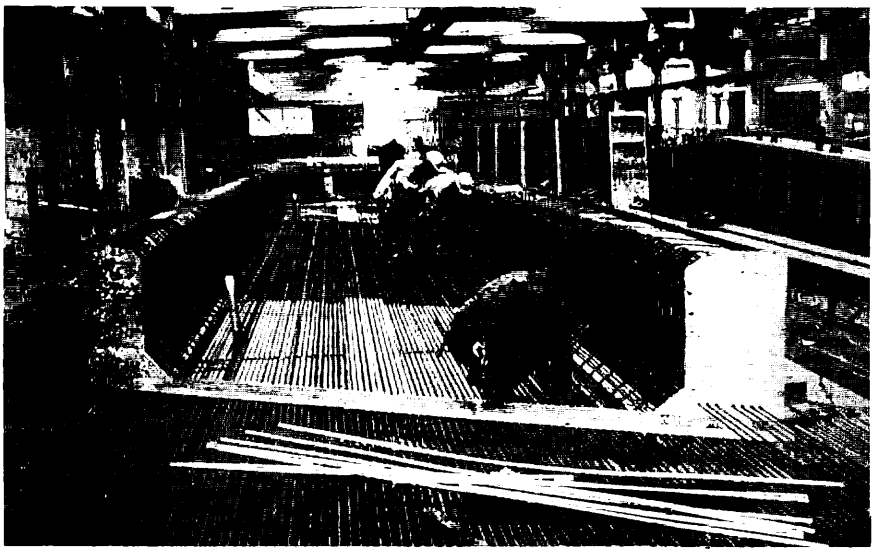

Fig. 11-70: View on the production of the girder and installation of the FBG sensors

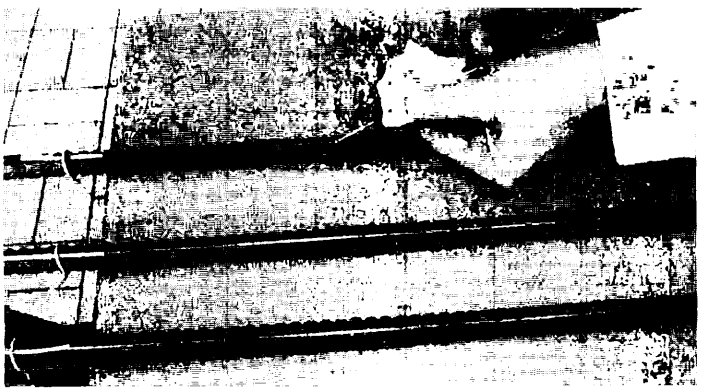

Fig. 11-71: Preparation of internal FBG strain sensor

A second sensor type, developed in the framework of this dynamic monitoring project by the Department of Mechanics of Materials and Structures of Ghent University, deals with an external FBG strain sensor. This sensor is a deformation amplifier with a gauge length of 500 mm and consists of two concentric aluminum tubes (Fig. 11-72). At one end, both tubes are fixed to an end-piece. At the opposite end only the outer tube is fixed to a similar end-piece, while the shorter inner tube is freely suspended inside the larger tube. An optical fibre is glued between the free end of the inner tube and the end-piece of the external tube. For protection against possible buckling under compressive loading, the optical fibre part with the Bragg sensor is positioned in a glass capillary filled with epoxy resin. With this configuration the deformation over a gauge length of 500 mm is transferred to a sensing gauge length of about 20 mm long, so that the Bragg sensor measures strains that are roughly 25 times larger than the real strains. Static and dynamic laboratory experiments show the feasibility and good performance of this FBG sensor. With these experiments it has been demonstrated that the magnification ratio of the extensometer equals 19.3. The first eigenfrequency of the external FBG strain sensor equals 288 Hz, which is considerably higher then the frequency range of the lower eigenmodes of the beam: so the behaviour of the sensor is static.

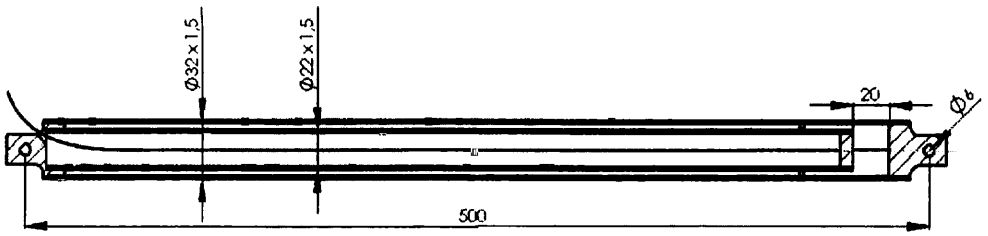

Fig. 11-72: External FBG strain sensor

11.11.4.5 First test results

Regarding the static monitoring, only test results are available so far with respect to the post-tensioning of the beam and the time dependent deformations. For example in Fig. 11-73 the strain measured by one of the internal FBG strain sensors is given during the post-tensioning stage and compared with mechanical deformeter measurements after post-tensioning.

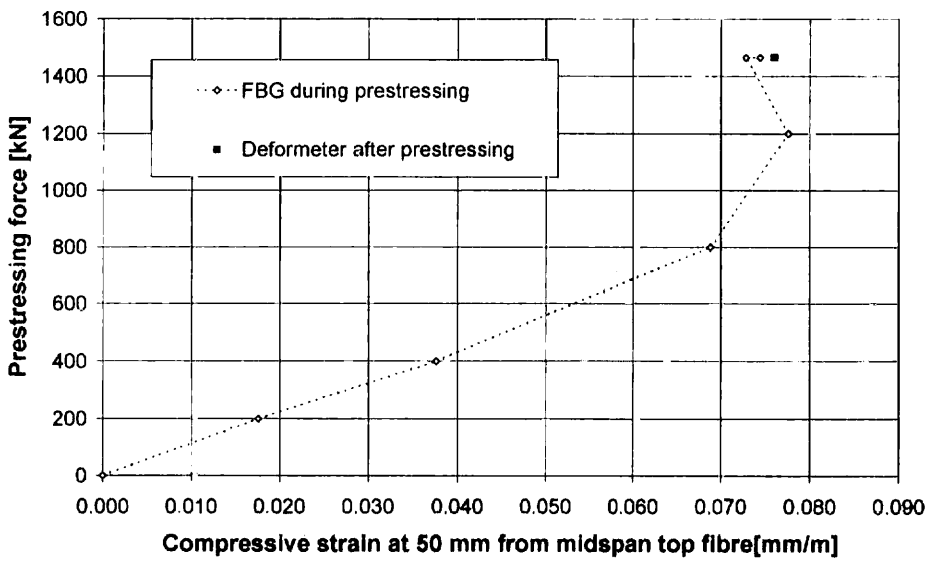

Fig. 11-73: FBG strain readings before and after post-tensioning

With respect to the dynamic monitoring, a first test sequence to verify the testing configuration and the use of FBG strain sensors for dynamic monitoring, indicatively confirmed the good behaviour of the FBG sensors during dynamic monitoring. The measurements were showing a good signal to noise ratio. In Table 11-11 for example, for the first 2 bending modes, the results are shown of the modal strains measured by the internal FBG sensors in the section at a distance of 5.2 m from the beam end, compared to computer analysis.

To study the dynamic system characteristics of the test beam (not yet subjected to any static loading) into more detail, a second sequence of dynamic monitoring tests has been executed. The analysis of the measurements is ongoing and will be correlated with a third sequence of dynamic monitoring tests, with the dynamic supports moved at a distance closer to the static supports (that is 1.5 m in stead of 3.5 m). Indeed, during these first dynamic monitoring tests small tensile stresses (less than the concrete tensile strength) are induced at the midspan top fibre of the beam. It was noted that due to these tensile stresses, small

shrinkage cracks present in the top flange increased in length. By moving the dynamic supports outwards, the complete cross-section will remain in compression during the dynamic monitoring.

Distance from bottom fibre	Internal FBG Mode B1 at 10.5 Hz	Internal FBG Mode B2 at 29.6 Hz	Predicted by FEM
750 mm	-0.835	-0.810	-0.737
280 mm	0.321	0.335	0.421
50 mm	1.000	1.000	1.000

Table 11-11: Modal strains relative to the strain near the bottom

11.11.5 Conclusions

In Belgium, fibre Bragg grating (FBG) strains sensors are actually used for the monitoring of 3 concrete structures: a post-tensioned concrete box girder of a 147 m long road bridge, a concrete quay wall with a length of 175 m and a prestressed prefabricated concrete trough girder of a 16.4 m long railway bridge.

To study the enhanced performance of dynamic monitoring of civil engineering structures by means of the integration of optical fibre sensors, a research project has been initiated, bringing together expertise of 5 research groups. In the framework of this project also an external FBG strain sensor in the form of a deformation amplifier has been developed. Dynamic monitoring tests are executed on 3 prestressed concrete beams with a span of 16.8 m and a total depth of 0.8 m. First test results obtained, demonstrate the feasibility of using FBG strain sensors for dynamic monitoring.

11.11.6 Acknowledgements

The authors wish to acknowledge the financial support by the Ministry of the Flemish Community, Department of Environment and Infrastructure, the contractors Cinec and Herbosch-Kiere, the Belgian National Railway Company (NMBS) and the Fund for Scientific Research - Flanders.

11.11.7 References

13. W. Moerman, L. Taerwe, W. De Waele, J Degrieck, R. Baets, *Application of Optical Fibre Sensors for Monitoring Civil Engineering Structures*, Structural Concrete, Vol. 2, No. 2, 2001, pp. 63-71.
14. W. Moerman, *Geïntegreerde optische sensoren voor de opvolging van bouwkundige constructies* (in Dutch), Doctoral thesis, Ghent University, Faculty of Engineering, Department of Structural Engineering, Magnel Laboratory for Concrete Research, Belgium, 2001, 305 pp.
15. M.M. Abdel Wahab, G. De Roeck, *Dynamic Testing of Prestressed Concrete bridges and Numerical Verification*, J. of Bridge Eng., ASCE, Vol. 3, No. 4, 1998, pp. 159-169.

ISSN 1562-3610
ISBN 2-88394-062-2

Monitoring and safety evaluation of existing concrete structures

Contents

fib CEB-FIP

fédération internationale du béton
the international federation for structural concrete
created from the merger of CEB and FIP